The Eurasia Proceedings of Science, Technology, Engineering & Mathematics

EPSTEM

VOLUME 35 ICRETS CONFERENCE

ISSN: 2602-3199
ISBN: 978-625-6959-77-4

ICRETS 2025: 7th International Conference on Research in Engineering, Technology and Science
July 10- 13, 2025 Peja, Kosovo
Edited by: Prof.Dr. Mehmet Ozaslan - Gaziantep University, Türkiye

The Eurasia Proceedings of Science, Technology, Engineering & Mathematics (EPSTEM)
ISSN: 2602-3199

ICRETS 2025

International Conference on Research in Engineering, Technology and Science (ICRETS)

Proceedings Book

Editor

Mehmet Ozaslan

Gaziantep University, Türkiye

ISBN: 978-625-6959-77-4

Published by the ISRES Publishing

Address: Askan Mah. Akinbey Sok. No: 5-A/Konya/TÜRKİYE
Web: www.isres.org
Contact: isrespublishing@gmail.com

Dates: July 10- 13, 2025
Location: Peja, Kosovo
https://2025.icrets.net

About Editor

Prof Dr. Mehmet Ozaslan
Department of Biology, Gaziantep University, Türkiye
Website: mehmetozaslan.com
E-mail: ozaslanmd@gantep.edu.tr

Language Editor

Lecturer Ceren Dogan
School of Foreign Languages, Necmettin Erbakan University, Türkiye
Email: cerendogan@erbakan.edu.tr

Editorial Policies

ISRES Publishing follows the steps below in the procedings book publishing process.
In the first stage, the papers sent to the conferences organized by ISRES are subject to editorial oversight. In the second stage, the papers that pass the first step are reviewed by at least two international field experts in the conference committee in terms of suitability for the content and subject area. In the third stage, it is reviewed by at least one member of the organizing committee for the suitability of references. In the fourth step, the language editor reviews the language for clarity.

Review Process

Abstracts and full-text reports uploaded to the conference system undergo a review procedure. Abstracts will be evaluated on the basis of abstracts/proposals. The conference system allows the full text to be sent if the abstract is accepted. Participants must wait for the evaluation results after uploading their article abstracts to the conference system. If their abstracts are accepted, they can upload their full texts to the conference system. The full texts are then sent to at least two reviewers for review. The conference has a double-blind peer-review process. Any paper submitted for the conference is reviewed by at least two international reviewers with expertise in the relevant subject area. Based on the reviewers' comments, papers are accepted, rejected or accepted with revision. If the comments are not addressed well in the improved paper, then the paper is sent back to the authors to make further revisions. The accepted papers are formatted by the conference for publication in the proceedings.

Aims & Scope

Engineering, technology and basic sciences are closely related fields. Developments and innovations in one of them affect the others. Therefore, the focus of the conference is on studies related to these three fields. Studies in the fields of engineering, technology and basic science are accepted to the conference even if they are not associated with other fields. The conference committee thinks that a study in only one field (for example, mathematics, physics, etc.) will contribute to other fields (for example, engineering, technology, etc.) in future studies, even if it is not associated with the presentation at the conference. In line with this perspective, studies in the following fields are accepted to the conference: Biology, Chemistry, Engineering, Mathematics, Physics and Technology.

The aim of the conference is to bring together researchers and administrators from different countries, and to discuss theoretical and practical issues in all fields of Engineering, Technology and
Basic Sciences.

The Eurasia Proceedings of Science, Technology, Engineering & Mathematics (EPSTEM)
ISSN: 2602-3199

Articles: 1- 35

CONTENTS

The Eurasia Proceedings of Science, Technology,
Engineering & Mathematics (EPSTEM)
ISSN: 2602-3199

The Eurasia Proceedings of Science, Technology, Engineering & Mathematics (EPSTEM)
ISSN: 2602-3199

The Eurasia Proceedings of Science, Technology, Engineering and Mathematics (EPSTEM), 2025

Volume 35, Pages 1-9

ICRETS 2025: International Conference on Research in Engineering, Technology and Science

An Examination of the Role of the Address Resolution Protocol in Computer Networks and the ARP Spoofing Threat

Ozge Tas
Cappadocia University

Abstract: Networks have become an integral part of today's world. In recent days, the ease of installation, low cost, and high data rates have contributed significantly to their popularity, whether they are directly connected to the Internet Provider (ISP) or through a local area network (LAN) along with other devices. There are many protocols designed to facilitate the process of setting up these networks. However, in some of them, preliminary measures have not been taken in terms of security. The address resolution protocol (ARP) is essential for communication between devices on the same network to function properly by facilitating the matching of IP addresses in MAC addresses. ARP works as a message-based protocol instead of an address-based protocol (Yavuz et al. 2018). The ability to resolve addresses is essential in the context of computer networks, as it enables efficient and accurate communication between devices. An Address Resolution Protocol (ARP) spoofing attack, also known as ARP poisoning, poses a significant threat to network security. This attack involves the transmission of fraudulent ARP requests or responses on the network, which leads to the poisoning of the ARP cache of the hosts. As a result, attackers can impersonate other hosts, perform man-in-the-middle attacks, and gain unauthorized access to sensitive information (Abad and Bonilla, 2007; Nasser and Hussain, 2022; Gouda and Huang, 2003; Lootah and others. , 2007) . Within the scope of this study, the role of address resolution protocol in computer networks and a sample application for ARP spoofing architecture and measures were simulated and anomaly analysis was performed with machine learning techniques.

Keywords: Machine learning, Un-supervised learning, ARP spoofing.

Introduction

Address Resolution Protocol (ARP) is used by computer networks to map network addresses (IPs) to physical addresses (MACs). This protocol is very important in LAN communications because each frame that leaves the host must contain a destination MAC address. ARP can be used with any network layer protocol, but IP is the most widely used network protocol. In this study, the performance of unsupervised machine learning techniques for the ARP spoofing threat will be compared by examining the address resolution protocol and its roles in computer networks.

Address resolution protocol (ARP) is a protocol used by computer networks to bind network addresses (IP) to physical addresses (MACs) (Abad and Bonilla, 2007). When a host wants to know the MAC address of another host, it broadcasts an ARP request asking for the MAC address of the host with IP (Internet Protocol) address X on the network. The host with the given IP responds with unicast ARP, which specifies the MAC address. The host that issued the request records the IP, MAC match in a local ARP cache so that it does not have to broadcast the same request in the near future. ARP has been proven to work well under normal conditions, but it is not designed to deal with malicious hosts. ARP is susceptible to various attacks, such as ARP cache poisoning, which can lead to serious vulnerabilities (Shah and Cosgrove, 2019). Today, machine learning techniques are used against network attacks. The potentials of hybrid models were compared by using KNN, logistic regression, and neural network model applications in developing IDS solutions (Rysbekov et al., 2025).

- Selection and peer-review under responsibility of the Organizing Committee of the Conference

Simultaneous detection of DNS and ARP fraud has been studied by using the random forest algorithm to identify spoofing attacks in internet of things (loT) environments, which is one of the environments where harp spoofing attacks are frequently encountered (Vajratiya et al., 2024). Similarly, Kumar and Dash (2024) compared ARP fraud detection from real-time data using random forest, LSTM, CNN, SVM, and isolation forest algorithms. In the study, Random forest outperformed other algorithms, achieving 94% accuracy. This requires the use of the random forest algorithm as a solution for real-time network security.

Application of Machine Learning to ARP Spoofing

ARP spoofing is a significant security threat that compromises the integrity of data packets in a network. To address this challenge, various machine learning techniques have been explored to enhance detection and mitigation strategies. Machine learning classifiers provide a dynamic approach to ARP spoofing detection by leveraging behavioral analysis of network packets, allowing for real-time identification of potential attacks (Alsaaidah, A. et. all. 2024)(Sahah, S., & Ali, A. 2025).

Machine learning techniques can be categorized into several distinct types, each applicable to specific tasks, including the detection and mitigation of ARP spoofing attacks. These techniques include supervised learning, unsupervised learning, semi-supervised learning, and reinforcement learning, each with its unique characteristics and applications.

Method

The dataset used in this study is a comprehensive cyber security dataset obtained from real-time ARP (Address Resolution Protocol) network traffic. The data collection process was carried out completely in its own isolated environment without risking third parties. During the 39-minute data collection process, a total of 33,932 ARP packets were captured.

There are two hosts in the scenario. Linux Kali 2023.4(Attacker) vs. Windows10(Victim) The two PCs are connected to the Linksys x35000 Modem/Router via ethernet cable. Windows10 ARP spoofing was performed on Kali Linux, and the Arp table was poisoned, allowing traffic on Windows10 to flow to Kali 2023.4. The experimental setup is given in Figure 1. The image of the network traffic when the ARP attack occurred is given above. These data are made suitable for analysis in the pcap file. Arp network traffic is given in Figure 2.

In the first place, 94% anomalous behaviors were detected in the data set, and the problem of imbalance of the data set was encountered. In other words, it has been observed that abnormal records are more than normal records. This situation causes the majority class to learn and the minority class to be ignored in machine learning models. In other words, it cannot correctly detect normal traffic as a real-life problem. In order to eliminate this imbalance, synthetic samples were produced for the low normal data by the SMOTE method. The change in the data as a result of the SMOTE application is given. This is shown in Figure 3.

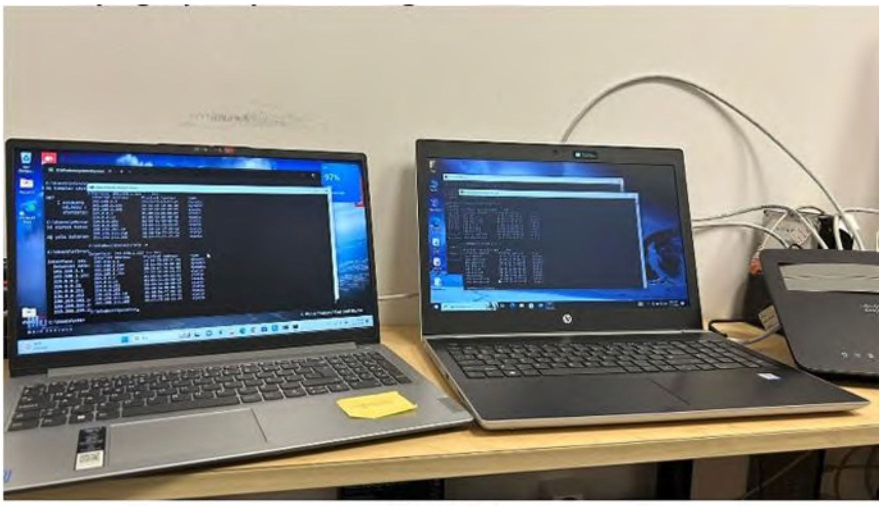

(Demo Setup)

Figure 1. First research model

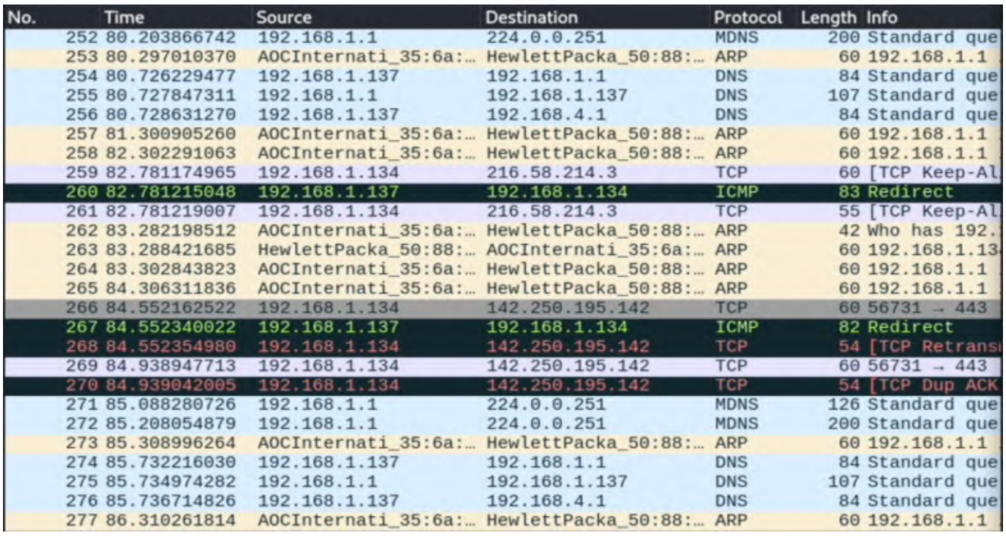

No.	Time	Source	Destination	Protocol	Length	Info
252	80.203866742	192.168.1.1	224.0.0.251	MDNS	200	Standard que
253	80.297010370	AOCInternati_35:6a:…	HewlettPacka_50:88:…	ARP	60	192.168.1.1
254	80.726229477	192.168.1.137	192.168.1.1	DNS	84	Standard que
255	80.727847311	192.168.1.1	192.168.1.137	DNS	107	Standard que
256	80.728631270	192.168.1.137	192.168.4.1	DNS	84	Standard que
257	81.300905260	AOCInternati_35:6a:…	HewlettPacka_50:88:…	ARP	60	192.168.1.1
258	82.302291063	AOCInternati_35:6a:…	HewlettPacka_50:88:…	ARP	60	192.168.1.1
259	82.781174965	192.168.1.134	216.58.214.3	TCP	60	[TCP Keep-Al
260	82.781215048	192.168.1.137	192.168.1.134	ICMP	83	Redirect
261	82.781219007	192.168.1.134	216.58.214.3	TCP	55	[TCP Keep-Al
262	83.282198512	AOCInternati_35:6a:…	HewlettPacka_50:88:…	ARP	42	Who has 192.
263	83.288421685	HewlettPacka_50:88:…	AOCInternati_35:6a:…	ARP	60	192.168.1.13
264	83.302843823	AOCInternati_35:6a:…	HewlettPacka_50:88:…	ARP	60	192.168.1.1
265	84.306311836	AOCInternati_35:6a:…	HewlettPacka_50:88:…	ARP	60	192.168.1.1
266	84.552162522	192.168.1.134	142.250.195.142	TCP	60	56731 → 443
267	84.552340022	192.168.1.137	192.168.1.134	ICMP	82	Redirect
268	84.552354980	192.168.1.134	142.250.195.142	TCP	54	[TCP Retrans
269	84.938947713	192.168.1.134	142.250.195.142	TCP	60	56731 → 443
270	84.939042005	192.168.1.134	142.250.195.142	TCP	54	[TCP Dup ACK
271	85.088280726	192.168.1.1	224.0.0.251	MDNS	126	Standard que
272	85.208054879	192.168.1.1	224.0.0.251	MDNS	200	Standard que
273	85.308996264	AOCInternati_35:6a:…	HewlettPacka_50:88:…	ARP	60	192.168.1.1
274	85.732216030	192.168.1.137	192.168.1.1	DNS	84	Standard que
275	85.734974282	192.168.1.1	192.168.1.137	DNS	107	Standard que
276	85.736714826	192.168.1.137	192.168.4.1	DNS	84	Standard que
277	86.310261814	AOCInternati_35:6a:…	HewlettPacka_50:88:…	ARP	60	192.168.1.1

Figure 2. Second research model

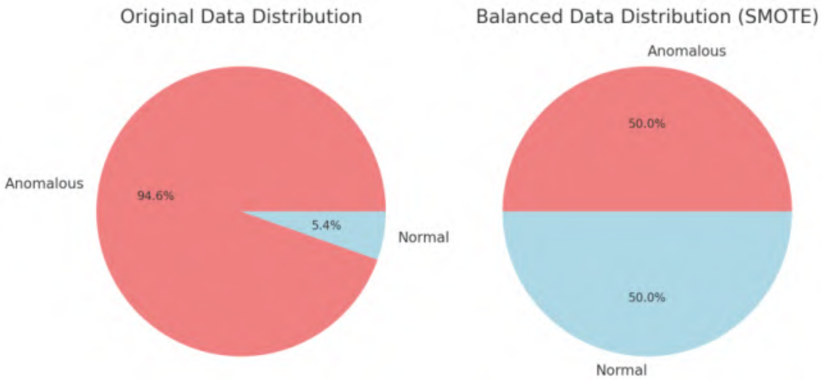

Figure 3. Data balance after SMOTE application

A total of 64,208 records and 6 variables were included in the analysis, including 32104 normal and 32104 anomalies. The variables and definitions of the data set are given below;

- **timestamp**: The time when the packet was captured
- **src_ip**: Source IP address
- **dst_ip**: Destination IP address
- **src_mac**: Source MAC address
- **dst_mac**: Destination MAC address
- **op_code**: ARF Application Code (1: Request, 2: Reply)
- **label**: Traffic classification (0: Normal, 1: Abnormal)

In the dataset, the number of unique IP addresses is 79, the number of destination IP addresses is 4,096, the number of unique source MAC addresses is 80, and the number of destination MAC addresses is 24. ARP request packets account for 98.6% of the data, while reply packets account for 1.4%. Unsupervised machine learning analyses of Isolation Forest, One-Class SVM and LSTM Autoencoder were used in the study. The aim of these models is to use them in ARP data and to compare their performances.

In the isolation forest analysis, 6 other variables were used apart from the labeled data. Normalization was performed on the dataset and the variables were converted numerically. It is important to separate the data set as 20% test and 80% training for comparison of performance. The contamination parameter was dynamically determined based on the proportion of samples labeled as anomalies in the data set. This ensures that the model is protected against overfitting. In the One-Class SVM analysis, 20% test and 80% training set were differentiated in the data. Optimal parameter selection was performed with the gird search method. The contamination rate was determined as 0.5 gamma parameter scale and Kernel (Kernel Parameter) as rbf (Radial Basis Function).

In LTSM Autoencoders analysis, the LTSM algorithm is an algorithm that works with time series architecture. Accordingly, time series conversion has been made. As autoencoders, 16 compressed space dimensions, 10 time series were calculated with window size and relu activation code parameters. The maximum epochs value is 50 and the number of samples processed in each step is 64. Mean squared error (mse) calculation was used to determine the reconstruction error. The optimal threshold value is calculated, which calculates the best F1 score with the Thresholds mote.

Results and Discussion

Arp spoofing attacks still pose a significant threat to networks. These attacks threaten to divert network traffic, laying the groundwork for eavesdropping, data manipulation, and even more sophisticated attacks. In this study, the performances of Isolation Forest, One-Class SVM and LSTM Autoencoder machine learning techniques were compared in the sample dataset. Traditional ARP Spoofing detection methods usually rely on static rules and predefined signatures. These methods become inadequate as the attackers' methods change. Machine learning-based approaches learn from anomalous behaviors and patterns in network traffic, allowing to develop detection mechanisms that can be developed more dynamically. This study is important in terms of demonstrating their ability to detect anomalous ARP packets by learning from normal network traffic data. In other words, it is advantageous in real-world scenarios where attacks can be detected without the need for information on infected attack data. Comparison of models with Isolation Forest, One-Class SVM and LSTM and Autoencoder methods used in the study is used to reveal the strengths and weaknesses of the model in this area. It provides best practice recommendations for future system developers and researchers, and reveals which model might work better with performance expectations in a given network environment.

In the confusion matrix graph given in Figure 4, incorrect and correct classifications are clearly visible. 3836 indicates the correct classification of values that show abnormal behavior, while the classification of normal network traffic is calculated as 3769.2652 indicates values that are actually normal but are estimated to be abnormal, and 2585 indicates values that are actually anomalies but classified as normal.

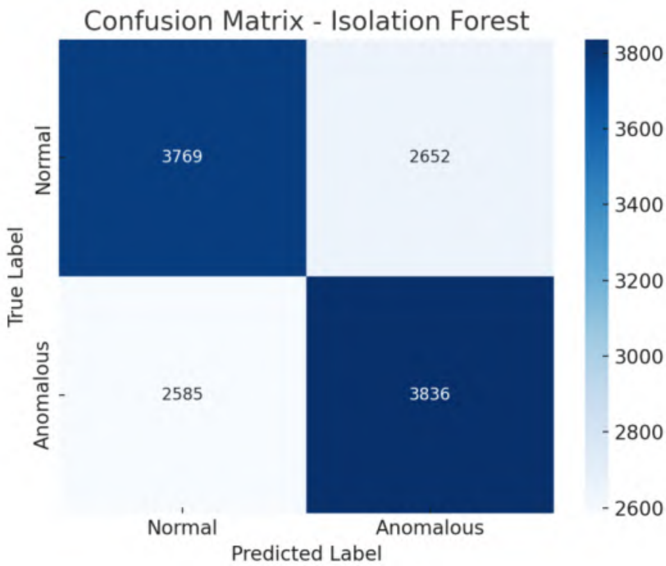

Figure 4. Isolation forest analysis confusion matrix results

According to the results of the isolation forest analysis, the accuracy value was calculated as 0.59 and it was concluded that the classification in the data set was not random. However, false positives and false negatives were found to be quite high, which poses a security risk and reduces the awareness of the attack. The recall value indicates that it successfully captures 0.59 of the anomalies. This is interpreted as intermediate for critical security areas such as ARP.

When Figure 5 is examined, it shows that the majority of the observations in this data set, which is concentrated in the range of 0 to +0.05, are perceived as normal by the model. The observation of a multi-peak structure indicates that the scores are concentrated at several points and not around a single nomal. This suggests that there may be more than one subgroup or different types of abnormalities in the data set.

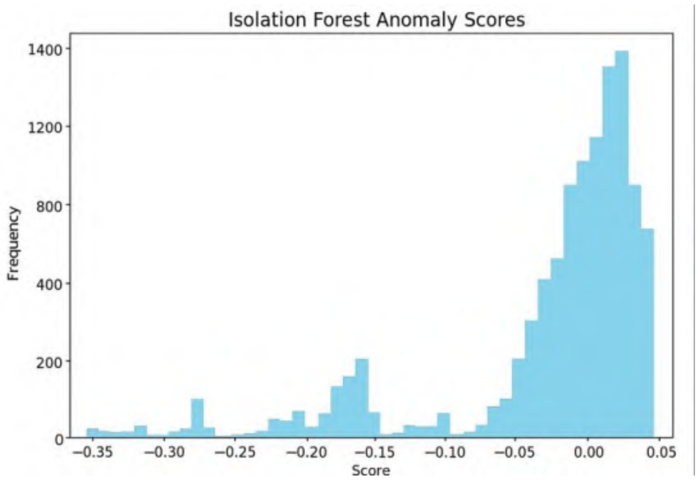

Figure 5. Isolation forest anomaly scores

In the One-Class SVM analysis, when Figure 3 is examined, 3,376 correctly identified normal observations and 3,332 correctly identified anomaly values were found according to the classification results. According to this table, it was observed that the model made a similar number of correct and incorrect predictions in both normal and anomaly classes.

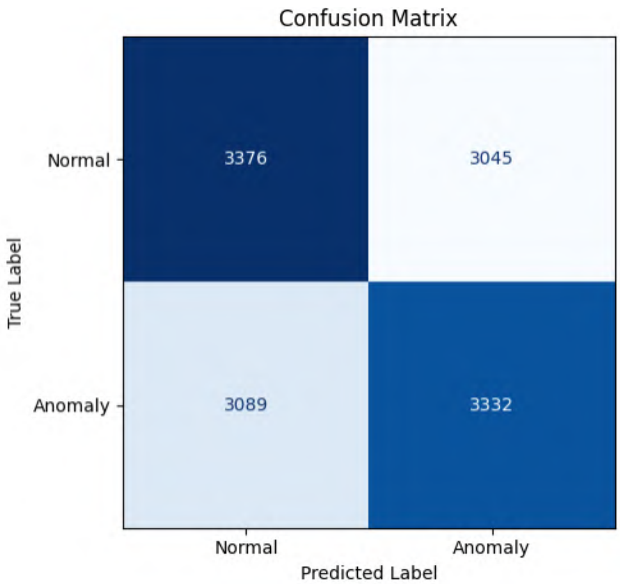

Figure 6. One-class SVM confusion matrix results

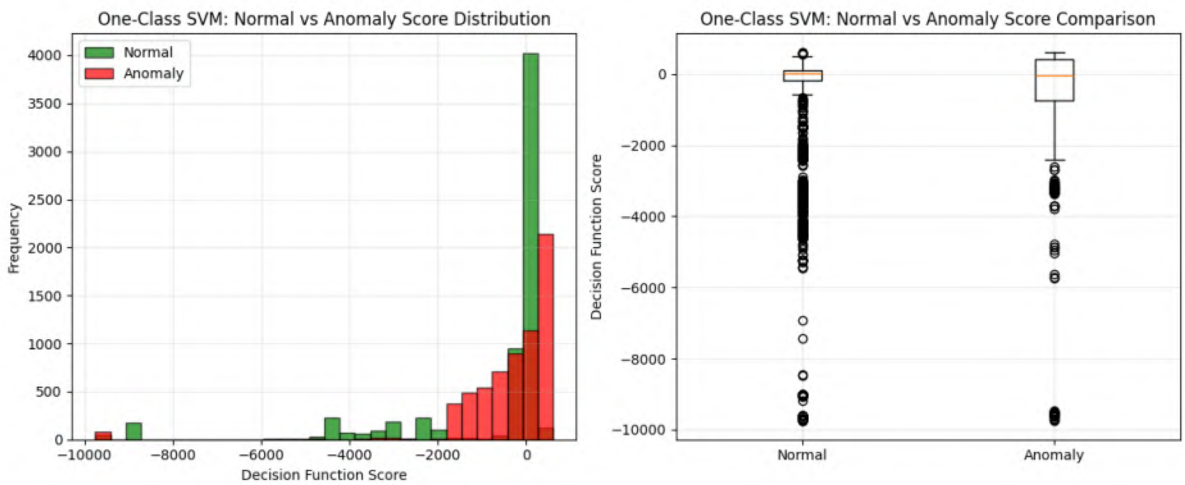

Figure 7. Score distributions and comparison of One-Class SVM normal, anomaly data

The accuracy rate of the model was calculated as 0.52. The ROC AUC value was found to be 0.4377. Since the model's success in distinguishing between anomaly and normal samples is below 0.5, its success is considered low. When examining Figure 7, we observe that the data of both classes are largely overlapping. Both groups are concentrated in similar score ranges. This indicates that the model cannot establish a discriminating decision boundary for anomaly detection. When examining the boxplot in Figure 4, it is observed that the statistical results of normal and anomalous cases are almost similar.It is assumed that the decision function of this model fails to distinguish between the two classes and that the scores are randomly distributed. The parameters selected are those that achieved the highest F1 score among the combinations tested in the model grid search parameter optimization. These are the kernel kernel function rbf, anomaly upper limit ratio 0.5, and gamma kernel parameter scale.

Data normalization was performed on the dataset prior to LSTM model training. Since the LSTM model operates in a time series structure, the data was divided into time windows of 10 time lengths. This approach is commonly used to capture short-term dependencies in time series data.Thus, the input data was reshaped. In the model design, an LSTM-based autoencoder architecture was created and designed to produce low-dimensional compressed input and output. The goal is to minimize the difference between the input and output. The reconstruction error (MSE) was calculated for each window in the test data. The threshold value was optimized to maximize the F1 score. Figure 8 shows that the model successfully classified normal data based on the confusion matrix results. 32,076 normal examples were correctly identified, while 19 normal examples were incorrectly classified as anomalies. 32,094 anomalies were correctly classified, while 10 anomaly observations were classified as normal.

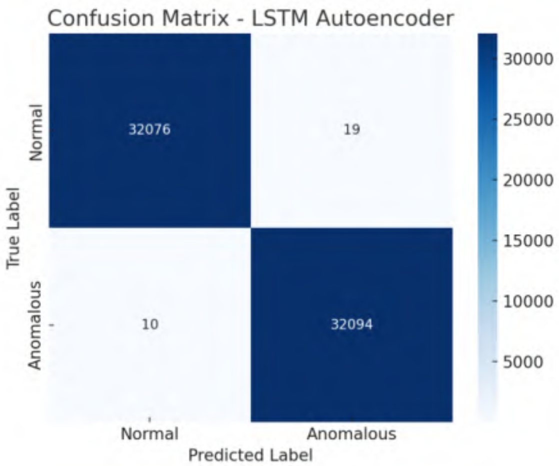

Figure 8. LSTM autoencoder confusion matrix results

Figure 9 shows the distribution of anomaly and normal observations. The distinction between normal and anomaly observations was clearly observed in the two dimensions specified as PCA1 and PCA2.

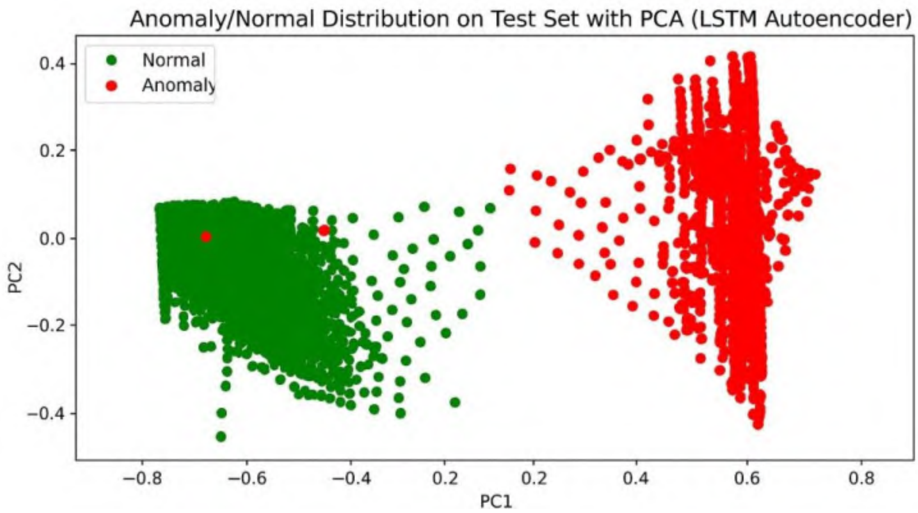

Figure 9.PCA results for test data in LTSM autoencoder analysis

The model was trained using only normal examples, and anomalies were detected using reconstruction errors (Mean Squared Error - MSE) on the test set. The histogram in Figure 10 below shows the distribution of error scores generated by the model, with the threshold value optimized using the F1 score (threshold = 0.0922) visualized as a red dashed line. This distribution is bimodal, clearly showing that normal data are clustered in the low error region, while anomalies are clustered above the threshold. The performance metrics obtained from the classification performed using this threshold value are noteworthy:

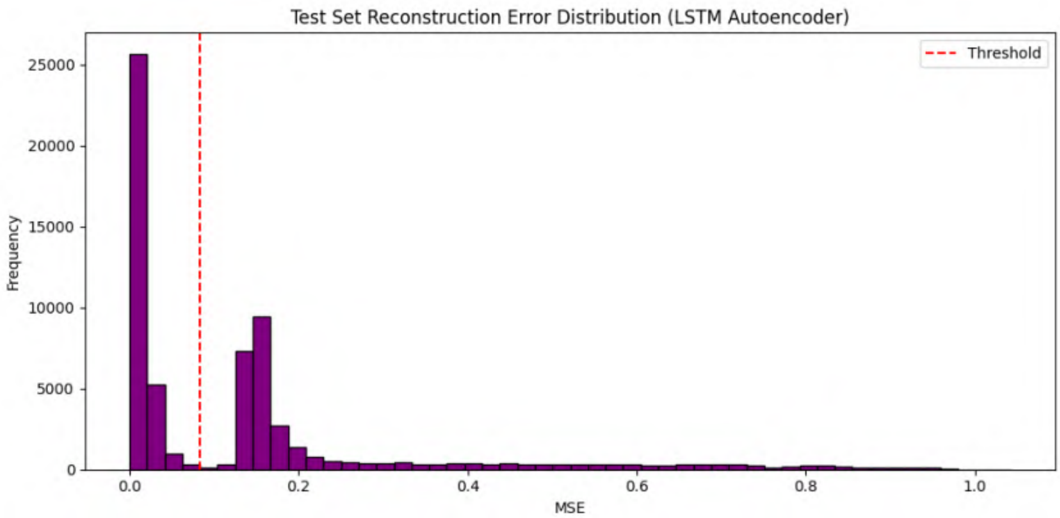

Figure 10. Optimized error rate threshold value

In this study, the LSTM Autoencoder-based anomaly detection model, trained based on reconstruction errors, demonstrates that the model has exceptional discrimination power: With an F1 score of 0.9995, precision of 0.9994, recall of 0.9997, and ROC AUC value of 1.0000, the model demonstrates both high sensitivity and high specificity.

Table 1. Air performance indicators to models

Model	Accuracy	Precision	Recall	F1 Score	ROC AUC
LSTM Autoencoder	0,9995	0,9994	0,9997	0,9995	1,0000
Isolation Forest	0,5922	0,5912	0,5974	0,5943	0,6023
One-Class SVM	0,5224	0,5226	0,5189	0,5207	0,4377

Table 1 shows that the LSTM Autoencoder model demonstrates superior performance compared to the other two models based on the results provided, containing metrics such as accuracy, precision, sensitivity, F1 Score, and ROC AUC. This model classifies data with very high success and shows that it is an excellent candidate for tasks such as anomaly detection. In particular, the ROC AUC score of 1.0000 indicates that the model can perfectly distinguish between positive and negative classes, which is a rare and impressive result.

Conclusion

The Isolation Forest model showed significantly lower performance compared to the LSTM Autoencoder: it performed only slightly better than random guessing, but is generally insufficient for real-world applications. In particular, the ROC AUC value (just above 0.5) indicates weak classification ability. The One-Class SVM model, on the other hand, has shown the lowest performance: the model's performance is very close to random predictions, and its ROC AUC value is even below 0.5 (0.4377), suggesting that the model performs worse than random predictions in distinguishing between positive and negative classes. These results clearly show that One-Class SVM is not suitable for this dataset and task. Overall, in light of the metrics provided, LSTM Autoencoder is the model that performs the best and should be the preferred option for this problem. Isolation Forest and One-Class SVM models are far from delivering acceptable performance in this scenario.

Recommendations

With these efforts, attacks can be identified and prevented before they damage the network or cause serious consequences such as data theft in an ARP Spoofing attack. In particular, future trends such as hardware acceleration and extended detection capabilities will increase the real-time application capacities of machine learning models and significantly strengthen the overall resilience of the IoT ecosystem by providing privacy-focused solutions. In this way, networks will become more resilient to ARP spoofing and other network vulnerabilities, while adaptive and constantly learning defense systems will be built against constantly evolving cyber threats.

Scientific Ethics Declaration

* In this study, no situation has been created that will put third parties at risk

* The author declares that the scientific ethical and legal responsibility of this article published in EPSTEM journal belongs to the author.

Conflict of Interest

* The author declares that there is no conflict of interest

Funding

* This research received no specific grant from any funding agency in the public, commercial, or not-for-profit sectors.

Acknowledgements or Notes

* This article was presented as an oral presentation at the International Conference on Research in Engineering, Technology and Science (www.icrets.net) held in Peja/Kosovo on July 10-13, 2025.

* I would also like to thank cyber security expert Mr. Irfan Cil for his mentor support.

* I would like to thank the ICRETS conference organizers and EPSTEM journal reviewers

References

Abad, C. L., & Bonilla, R. I. (2007). An analysis on the schemes fordetecting and preventing ARP cache poisoning attacks. *27th International Conference on Distributed Computing Systems Workshops (ICDCSW'07), IEEE,* pp. 60-60.

Alharbi, T., Durando, D., Pakzad, F., & Portmann, M. (2016). Securing arp in software defined networks. *2016 IEEE 41st Conference on Local Computer Networks (LCN)*, pp. 523-526.

Alsaaidah, A., Almomani, O., Abu-Shareha, A. A., Abualhaj, M. M., & Achuthan, A. (2024). ARP spoofing attack detection model in IoT network using machine learning: Complexity vs. accuracy. *Journal of Applied Data Sciences, 5*(4), 1850-1860.

Alsmadi, I. & Xu, D. (2015). Security of software defined networks: A survey. *Computers & Security*, 53, 79-108.

Girdler, T. (2021). Implementing an intrusion detection and prevention system using software-defined networking: defending against arp spoofing attacks and blacklisted mac addresses. *Computers & Electrical Engineering,* 90, 106990.

Gouda, M. & Huang, C. (2003). A secure address resolution protocol. *Computer Networks, 41*(1), 57-71.

Meghana, J. S., Subashri, T., & Vimal, K. R. (2017). A survey on ARP cache poisoning and techniques for detection and mitigation. *2017 Fourth International Conference on Signal Processing, Communication and Networking (ICSCN)*, 1–6.

Kang, J., Lee, Y., Kim, J., & Kim, E. (2014). Arp modification for prevention of ip spoofing. *Journal of Information and Communication Convergence Engineering, 12*(3), 154-160.

Kumar, M., & Dash, C. S. (2024). Detecting and preventing ARP spoofing attacks using real-time data analysis and machine learning. *International Journal of Innovative Research in Computer Science & Technology*, *12*(5), 47–55.

Lootah, W., Enck, W., & McDaniel, P. (2007). Tarp: ticket-based address resolution protocol. *Computer Networks, 51*(15), 4322-4337.

Nasser, H. & Hussain, M. (2022). Defending a wireless lan against arp spoofing attacks using a raspberry pi. *Basrah Researches Sciences, 48*(2), 123-135.

Taş, Ö. (2024). Comparison of the performances of clustering and dimensionality reduction approaches in collaborative filtering. *Advances in Artificial Intelligence Research*, *4*(2), 96–110.

Pansa, D., & Chomsiri, T. (2008). Architecture and protocols for secure LAN by using a software-level certificate and cancellation of ARP protocol. *Third International Conference on Convergence and Hybrid Information Technology*, 21–26.

Puangpronpitag, S., & Masusai, N. (2009). An efficient and feasible solution to ARP spoof problem. *6th International Conference on Electrical Engineering/Electronics, Computer, Telecommunications and Information Technology*, 910–913.

Rysbekov S, Aitbanov A, Abdiakhmetova Z, & Kartbayev A. (2025). Advancing network security: a comparative research of machine learning techniques for intrusion detection. *International Journal of Power Electronics and Drive Systems*, *15*(2), 2271.

Samvedi, A., Owlak, S., & Chaurasia, V. (2014). Improved secure address resolution protocol. *arXiv:1406.2930*

Shah, S. S., & Ali, A. (2025). Optimizing resource allocation and energy efficiency in federated fog computing for IoT. *arXiv:2504.00791*.

Shah, Z., & Cosgrove, S. (2019). Mitigating arp cache poisoning attack in software-defined networking (sdn): A survey. *Electronics, 8*(10), 1095.

Song, M., Lee, J., Jeong, Y., Jeong, H., & Park, J. (2014). Ds-arp: a new detection scheme for arp spoofing attacks based on routing trace for ubiquitous environments. *The Scientific World Journal,* 2014, 1-7.

Srinath, D., Panimalar, S., Simla, A., & Deepa, J. (2015). Detection and prevention of arp spoofing using centralized server. *International Journal of Computer Applications, 113*(19), 26-30.

Turna, C., & Guldenoglu, B. (2019). Investigation of the relationship between phonological decoding and word reading speed and accuracy in developmental perspective. *Education and Science*, *44*(198), 413-433.

Uysal, P. (2021). A method used to develop reading fluency, reading comprehension and vocabulary: Readers theater. *Ana Dili Eğitimi Dergisi, 9*(1), 76-93.

Vajrobol, V., Saxena, G. J., Pundir, A., Kannan, R. J., & Abouhawwash, M. (2024). Identify spoofing attacks in Internet of Things (IoT) environments using machine learning algorithms. *Journal of High Speed Networks, 31*(1), 61–70.

Wan, Y., Feng, X., Chen, Y., Zhou, L., Zhu, Y., & Wu, J. (2021). A dual detection method for siemens inverter motor modbus rtu attack. *Journal of Computer and Communications, 9*(07), 91-108.

Yavuz, A., & Tuna, G. (2019). Bilgi güvenliği tehditleri: Yazılım tanımlı ağlar geleneksel bilgisayar ağlarına karşı. *Kırklareli Üniversitesi Mühendislik ve Fen Bilimleri Dergisi, 5*(2), 200–209.

Yavuz, E., Sarica, S., & Artuç, E. (2018). Kontrol alan ağları için optimum statik mesaj zamanlaması. *Mühendislik Bilimleri ve Tasarım Dergisi, 6*(3), 532–540.

Younes, O. (2017). Modeling and performance analysis of a new secure address resolution protocol. *International Journal of Communication Systems, 31*(1), 1-22.

Author(s) Information

Ozge Tas
Cappadocia University
Mustafapaşa, 50420 Ürgüp / Nevşehir, Türkiye
Contact e-mail:*ozge.tas@kapadokya.edu.tr*

To cite this article:

Tas, O. (2025). An examination of the role of the address resolution protocol in computer networks and the ARP spoofing*, The Eurasia Proceedings of Science, Technology, Engineering and Mathematics (EPSTEM),* 1-9.

The Eurasia Proceedings of Science, Technology,
Engineering & Mathematics (EPSTEM)
ISSN: 2602-3199

The Eurasia Proceedings of Science, Technology, Engineering and Mathematics (EPSTEM), 2025

Volume 35, Pages 10-28

ICRETS 2025: International Conference on Research in Engineering, Technology and Science

Enhancing Visual and Cognitive Intelligence Memory with Fine-Tuning Modeling Based on Artificial Intelligence Large Language Models

Mesut Gun
Mersin University

Mustafa Baris Basturk
Mersin University

Abstract: This study investigates the potential of fine-tuning modeling based on Large Language Models (LLMs) to enhance visual and cognitive intelligence memory. A fine-tuning model was developed using the ChatGPT-4o framework to generate a narrative specifically tailored for a pedagogical audience. This process of guided text generation served as the core of our fine-tuning approach, which yielded the most effective results in creating a foundational narrative. The resulting text was subsequently visualized through detailed prompt engineering on three leading text-to-image AI platforms: DALL-E 3, Imagen 3, and Fooocus.ai. A comparative analysis revealed that the integrated method, initiated with the fine-tuned narrative from the ChatGPT-4o model and visualized with DALL-E 3, produced the most coherent and stylistically consistent outcomes. This synergy, which tightly integrates verbal and visual channels, supports cognitive frameworks like Dual Coding Theory and demonstrates a powerful method for strengthening memory and comprehension. The study highlights significant benefits, such as democratizing creativity and increasing student engagement. However, it also identifies critical risks, including cognitive offloading, the perpetuation of AI-driven biases, and complex copyright issues. In conclusion, this research confirms that fine-tuned AI models are powerful supplementary tools, not teacher replacements. Their effective integration requires a pedagogical shift where assessment focuses on the students' critical and creative process of guiding the model, rather than on the final AI-generated product.

Keywords: Artificial intelligence, Fine-tuning, Farge language models, Visual and cognitive memory

Introduction

The world order is undergoing constant transformation under the influence of technological innovations. This technological transformation is being taken to ever higher levels every day by engineers around the world who value development and innovation. Innovative approaches, new discoveries, and the further development of existing tools have affected most sectors around the world. One of these sectors is education (Al-Khatib, Al-Khatib, & Abo-Ajaj, 2025). In today's world, traditional teaching methods in education have been replaced by innovative approaches that focus on the student, encourage active participation, and aim to develop 21st century skills (critical thinking, creativity, collaboration, and communication) (Partnership for 21st Century Skills, 2019). One of these approaches, digital storytelling, has emerged as a powerful pedagogical tool that allows individuals to express their personal or fictional narratives by combining multimedia tools such as text, sound, images, and video (Robin, 2008). The role of storytelling in cognitive processes such as contextualizing information, enhancing retention, and concretizing complex concepts has long been recognized by educators (Haven, 2007).

In recent years, the revolution brought about by artificial intelligence in various fields has also opened new horizons in educational technologies (Uzun & Kayrici, 2025). In particular, the rise of generative AI models is

- Selection and peer-review under responsibility of the Organizing Committee of the Conference

fundamentally transforming visual and textual content production processes (Bandi et al., 2023). This technological leap is taking digital storytelling practice a step further by enabling AI-assisted visual storytelling. This new field enables students and educators to create high-quality visual narratives at a speed and with a level of ease that was previously unimaginable. This study aims to explore the potential of visual storytelling with AI tools in education, the engineering principles underlying this process, and its pedagogical outcomes.

The engineering aspect of the work forms the basis for next-generation storytelling tools. Text-to-image synthesis is one of the most notable components of this technology. Models such as DALL-E 2 and its later versions developed by OpenAI, Stability AI's Stable Diffusion, and Google's Imagen can generate original photorealistic or artistic images based on natural language descriptions (Basturk & Sen, 2025). These models are generally based on two main architectures: Generative Adversarial Networks (GANs) and Diffusion Models. Generative Adversarial Networks are a type of deep learning model used in machine learning, specifically designed to generate new and synthetic data examples such as realistic images, sounds, or text (Celard et al., 2023). The basic working principle is based on a game in which two neural networks compete against each other. As shown schematically in Figure 1, these two main components are: Generator and Discriminator. The generator network, represented by the green box in the figure, takes on the role of the artist or forger. Its task is to take a completely random noise vector (latent space) as input and transform this meaningless data into synthetic data that resembles real data (e.g., photographs). Initially, the output produced by the generator are quite meaningless and low-quality. However, during the training process, its goal is to learn to produce outputs that are realistic enough to fool the discriminator. The discriminator network, shown in the image as a red box, plays the role of the critic or detective. Its primary function is to determine whether the data presented to it is real or fake. During the training process, the discriminator is fed with both real data (e.g., real human faces) and fake examples created by the generator. The goal is to develop the ability to distinguish between real and fake data with the highest possible accuracy.

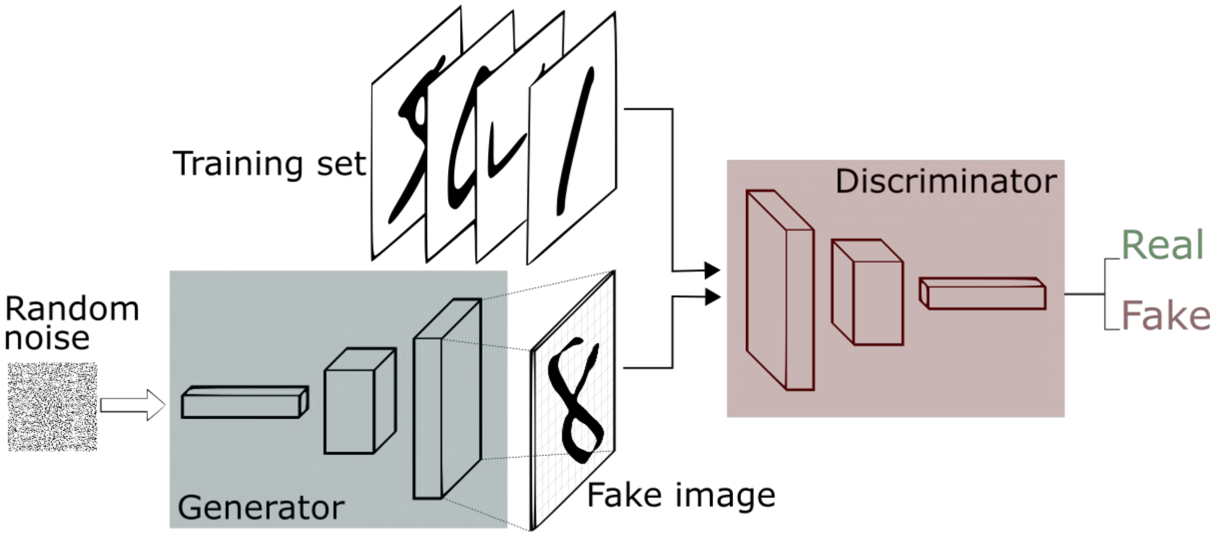

Figure 1. Generative adversarial networks - GANs working logic (Goodfellow et al., 2014).

Diffusion models, on the other hand, work by gradually adding noise to the data and then reversing this process to produce data from the noise (Croitoru et al., 2023). The engineering success of these models has been made possible by training massive neural networks with billions of parameters on large-scale visual-text datasets (e.g., LAION-5B) (Schuhmann et al., 2022). This process requires not only significant computational power (GPU/TPU clusters) but also advanced software engineering techniques such as distributed training algorithms and model parallelization (Bian et al., 2021).

Another critical element of storytelling is the process of creating a consistent narrative structure, which is where Natural Language Processing (NLP) technologies come into play. In particular, Large Language Models (LLMs) such as the GPT (Generative Pre-trained Transformer) series can generate story texts, scenarios, and character dialogues with logical flow based on a given concept or starting sentence (Xie et al., 2023). The transformer architecture underlying these models uses attention mechanisms to capture long-range semantic relationships within text, enabling the creation of consistent and contextually appropriate content (Huang et al., 2024). In an educational context, this means that students can collaborate with an AI assistant to design the plot, character development, and dialogue of their stories after selecting a theme.

The integration of these two core technologies (text-to-image and text generation) forms the engineering basis for fully-fledged visual storytelling platforms. The architecture of such a system typically has a modular structure: (1) The user interface (UI/UX) layer allows the student to enter the story concept. (2) The NLP module processes this input to generate a script or scene outline. (3) Keywords and descriptions are extracted from each scene in the script and sent as a prompt to the visual production module (text-to-image API). (4) The generated visuals are combined with text to form a story outline. (5) Optionally, text-to-speech modules can be used to add a narrator's voice or character voiceovers (Zakraoui et al., 2023). The development of these integrated systems presents significant engineering challenges, including API management, cloud computing infrastructure, and user data security.

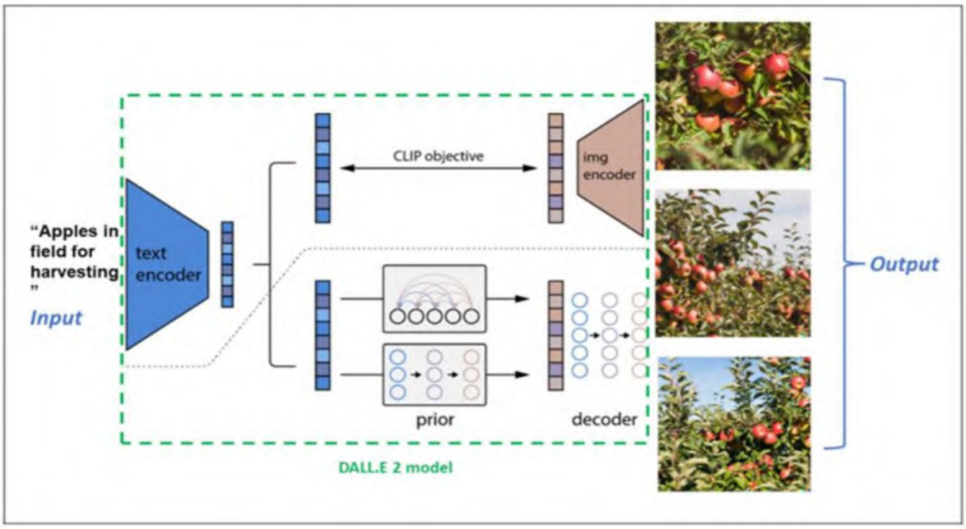

Figure.2 The functioning of artificial intelligence tools that generate images from text (Sapkota, 2023).

As shown in Figure 2, the operation of the *DALL·E 2* model involves a series of steps that convert text input into visual output. The process begins with a text input (e.g., "Apples in field for harvesting") being processed by a text encoder. This encoder converts the input into a meaningful representation, which is then passed to an image encoder via the CLIP target function. The image encoder creates an image representation that is consistent with the text representation. This representation is then processed by a prior model and a decoder. The *prior model* optimizes the relationship between text and images, while the *decoder* produces the final image. As a result, three different image outputs are obtained, showing a scene with apples ready for harvest in a field. This demonstrates the model's ability to generate realistic and contextually appropriate images from text-based inputs.

The field of natural language processing (NLP) has been fundamentally reshaped by the advent of large language models (LLMs), a class of deep learning models distinguished by their vast parameter counts and their training on extensive text corpora. These models, built upon the highly parallelizable transformer architecture, have demonstrated a remarkable ability to comprehend and generate human-like text, effectively creating a new paradigm for artificial intelligence research and application (Minaee et al., 2024). The foundation of modern LLMs is the transformer architecture, which, unlike its recurrent predecessors, processes entire sequences of text at once, using a mechanism known as self-attention to weigh the significance of different words in the input data (Vaswani et al., 2017). This architectural innovation has been a critical enabler for scaling models to sizes that were previously infeasible, allowing them to learn more nuanced and complex patterns of language from petabytes of data. Models such as the Generative Pre-trained Transformer (GPT) series and Bidirectional Encoder Representations from Transformers (BERT) exemplify this approach, where a model is first pre-trained on a massive, unlabeled dataset to acquire a general understanding of language, including grammar, facts, and reasoning abilities (Devlin et al., 2018; Radford et al., 2018). This pre-training phase results in a foundational model that, while powerful, is not inherently optimized for any single task. Its broad linguistic knowledge, however, serves as a potent starting point for more specialized applications. This is where the concept of fine-tuning becomes crucial. Fine-tuning is a form of transfer learning where the parameters of a pre-trained model are further trained on a smaller, task-specific dataset (Cai et al., 2024). This process adapts the general linguistic capabilities of the LLM to the specific nuances and requirements of the target domain or task, such as sentiment analysis, medical text summarization, or legal document review. By continuing the training process with labeled examples, fine-tuning adjusts the model's weights, steering its behavior to produce outputs that are more accurate and contextually appropriate for the specialized task (Houlsby et al., 2019). The remarkable efficacy of this approach has been demonstrated in models like GPT-4o, which showed that large-scale models could be adapted to a wide array of tasks with minimal task-specific data, a method often referred to as few-shot learning (Brown et al., 2020). Consequently, the combination of large-scale pre-training and subsequent fine-tuning has become a dominant methodology in NLP, enabling the development of highly capable and specialized language models without the prohibitive computational cost of training a new model from scratch for every unique application (Devlin et al., 2018).

From a pedagogical perspective, these AI-supported tools can serve as scaffolding to enable students to unleash their creativity (Umutlu & Gursoy, 2022). In particular, for students with limited drawing skills or who struggle to visualize their ideas, these technologies can remove the barrier between their imagination and concrete output (Gun et al., 2025). The Dual-Coding Theory, proposed by Paivio (1991), is one of the basic cognitive models that explains the processes of information processing, storage, and retrieval in human cognition. The theory posits that information is mentally represented through two fundamental and functionally independent yet interconnected systems: the verbal system and the non-verbal or imaginal system. This dual-channel structure provides an important framework for understanding complex cognitive processes such as learning, memory, language, and thought. Paivio's (1991) theory is based on the assumption that cognitive processes cannot be explained solely through linguistic representations, and that visual and other sensory-motor representations are at least as important as language. This provided an alternative to the dominant approaches of the time, which largely relied on linguistic and propositional models to explain cognition. Students can experience deeper and more lasting learning by transforming complex scientific processes (e.g., cell division) or historical events into visual stories (Sadoski & Paivio, 2013).

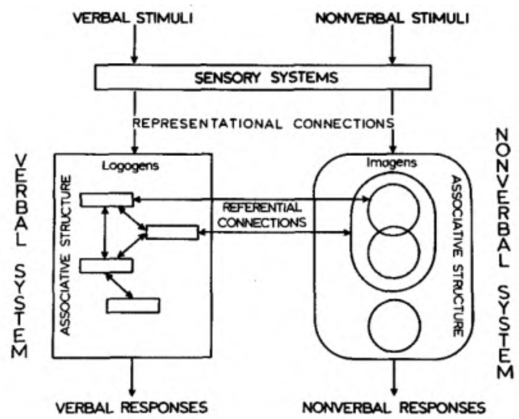

Figure 3. Schematized version of the dual coding theory (Paivio, 1990).

As shown in Figure 3, the basic structure and functioning of Paivio's *Dual Coding Theory* are presented schematically. The process begins with the reception of information from the outside world through the Sensory Systems at the top. These sensory inputs activate two different cognitive subsystems through representational connections. The verbal system, located on the left and consisting of linguistic units called logogens, processes linguistic information such as words and sentences, leading to Verbal Processes; the network-like structure between logogens represents the associative connections within this system. On the right side is the nonverbal system, which consists of holistic units called imagenes that represent visual-spatial images, and this system triggers Nonverbal Processes. The most critical point of the model is the thick referential connection that links these two independent systems. Through this connection, for example, a logogen (a word) can activate an imagen (a mental image), or the opposite can occur. The dual-channel encoding of information in both verbal and visual forms enables information to be processed more richly, leaving a stronger memory trace and thereby facilitating more lasting learning (Paivio, 1990). However, the use of these technologies also brings with it a new skill - prompt engineering. The ability to write clear, descriptive and creative prompts so that the learner can have the artificial intelligence produce the desired image or text in the most accurate way is a process that develops both linguistic and analytical thinking skills. Nevertheless, alongside this potential, there are important challenges and ethical concerns that need to be addressed. The originality of the content produced, copyright issues, potential biases in AI models, and the possible effects on students' critical thinking skills are all issues that need to be carefully evaluated (Hausken, 2024). If students passively accept the content produced by artificial intelligence without critically engaging in the process, this may result in them falling behind their learning objectives. Therefore, in order for these tools to be used effectively in education, it is critical to develop both a robust technical infrastructure and appropriate instructional designs that embed this technology within a pedagogical framework.

Storytelling is humanity's oldest, most instinctive, and most fundamental method of communication, information transfer, and the transmission of cultural values from one generation to the next. From the first drawings on cave walls to the fairy tales told around campfires, storytelling has been at the heart of human experience and learning. This innate predisposition in our language makes stories an indispensable tool for educational processes. Because stories do not merely convey dry information; they also enable us to empathize, make sense of complex ideas, and understand our place in the world (Baldwin, 2010). When combined with modern cognitive science findings, this ancient storytelling tradition becomes an even more powerful pedagogical tool: visual storytelling. At the heart of this approach lies a neurological fact known as the Visual Superiority Effect. Research shows that approximately 90% of the information transmitted to the human brain is visual and that the brain processes images 60,000 times faster than text (Eisenberg, 2014, as cited in Vanichvasin, 2021). The fact that vision precedes speech highlights that visualization is not merely an aesthetic preference in the learning process but a fundamental necessity that enhances cognitive efficiency (Rolandelli, 2009).

Most of the subjects taught in education are complex and abstract for students. Visual storytelling simplifies and concretizes these difficult ideas, making them easier to understand. For example, infographics break down complex data sets or processes into digestible pieces, helping students instantly grasp important concepts. Similarly, videos and animations bring abstract concepts to life by visualizing scientific processes (such as cell division) or historical events that are normally invisible to the naked eye, transforming them into vivid and memorable experiences. This method reduces cognitive load, allowing students to focus their mental resources on understanding and making connections rather than memorization. Visuals act as a universal translator of information, breaking down barriers for students with different learning styles, abilities, and linguistic backgrounds, thereby making learning more inclusive.

Learning is not only a cognitive process, but also an emotional experience. Stories are powerful emotional tools by nature; they can make people laugh, cry, think, and inspire them. Visual storytelling in education uses this emotional power to create a deep connection between students and learning materials. A well-crafted visual story can capture students' attention, spark their curiosity, and encourage active participation in the learning process. An empirical study conducted by Hava (2021) showed that digital storytelling activities have an excellent effect on increasing students' motivation. This emotional connection also supports the development of important social and emotional skills. Students try to understand the motivations and emotions of the characters in a story by putting themselves in their place. This process develops critical skills such as empathy, understanding different perspectives, and tolerance. Witnessing other lives and cultures increases students' social awareness and makes them more understanding individuals. In a study conducted by Kayahan (2010), it was found that students in the experimental group, where the storytelling method was applied in visual arts lessons, had a more expanded imagination, produced more original ideas, placed more importance on aesthetic arrangement in their work, and focused better on the subject without distractions compared to the control group, which used traditional methods. This method encourages students not only to listen to others' stories but also to write, design, and visualize their own stories. A student who creates their own digital story on a topic engages in higher-order cognitive activities such as analyzing, synthesizing, and evaluating information, which facilitates more lasting learning.

The success of visual storytelling does not depend on a single factor, but rather on a series of cognitive and emotional mechanisms that interact with each other. The process begins by capturing the student's attention due to the brain's natural predisposition to visual stimuli. This attention ensures that information is encoded more firmly in both verbal and visual channels, in accordance with the Dual Codings Theory, which dramatically increases recall rates. At the same time, the narrative structure of the story and the characters it contains facilitate the student's emotional connection with the content and the development of empathy. Increased motivation and this emotional connection encourage students to put more effort into challenging cognitive tasks such as understanding complex information and generating creative solutions. This creates a synergistic cycle where cognitive and affective benefits feed into each other, explaining why the method is so comprehensive and effective. Visual storytelling in education has entered a new and revolutionary era with the rise of generative AI. Text-to-image AI systems are fundamentally changing the process of creating visual content, offering innovative pedagogical opportunities. Unlike the limited and standardized visuals offered by static textbooks, these tools enable teachers and students to generate customized visuals for any subject in seconds, tailored to their specific needs and imagination. This means increased flexibility and personalization in learning materials. Perhaps one of the most significant benefits is that it makes visual production independent of artistic ability. Regardless of their drawing or design skills, every student can easily visualize complex scenes, fantastic characters, or abstract concepts in their minds. This opens new doors for students to express themselves, particularly in creative writing, art, and design courses. Detailed text prompts such as complex scientific processes (a DNA molecule replicating itself), abstract mathematical ideas (a visual representation of fractal geometry), or historical scenes (a marketplace during the Renaissance) can be instantly visualized through AI. This significantly deepens and makes abstract information more concrete and memorable. These AI systems can automatically generate alternative text (alt-text) descriptions for the visuals they produce. This feature makes materials more accessible to students with visual impairments. Additionally, it can facilitate the creation of personalized materials for students with different learning styles (e.g., visual learners).

Methodology

In this study, a qualitative research design was adopted to present a framework that integrates the engineering infrastructure and pedagogical potential of visual storytelling with artificial intelligence tools in education. Qualitative research focuses on understanding and interpreting phenomena within their natural context from a holistic perspective. In this context, case study analysis was used as the main research strategy, and document analysis was employed as the data collection technique.

Research Design

The design of this study is case study analysis, one of the qualitative research approaches. Case study analysis is an inductive research method that examines a current phenomenon within its real-life context, is used in situations where the boundaries between the phenomenon and its context are not clearly defined, and draws on multiple sources of evidence or data (Yin, 2009). This method focuses on the questions of how and why, enabling a comprehensive and in-depth understanding of complex social phenomena. In the context of this research, the case refers to text-to-image synthesis technology itself and the leading platforms that represent this technology. The study aims to examine in depth how AI-powered visual production tools (e.g., DALL-E 2, Stable Diffusion) function as a storytelling tool in educational settings and why they hold significant pedagogical potential, grounded in the underlying engineering principles and cognitive learning theories.

The data required to examine the case study were collected using the document analysis technique. Document analysis is a systematic process that involves analyzing written materials containing information about the phenomenon or phenomena being studied (Kutsyuruba, 2023). This method allows researchers to obtain rich and context-sensitive data without interfering with the existing situation. Within the scope of this study, various types of documents were examined to shed light on different dimensions of the case: (1) Scientific and Technical Articles: Peer-reviewed articles and conference papers explaining fundamental technologies such as Generative Adversarial Networks (GANs), Diffusion Models, Transformer architecture, and Large Language Models. (2) Theoretical and Conceptual Texts: Fundamental theoretical sources that form the pedagogical basis of the study, such as digital storytelling, dual coding theory, and scaffolding. (3) Technical Reports and White Papers: Official documents published by institutions developing artificial intelligence models (e.g., OpenAI, Google) detailing the architecture, training processes, and capabilities of their systems. (3) Ethical and Critical Evaluations: Academic publications addressing issues such as potential biases in artificial intelligence models, copyright issues, and the impact on critical thinking.

Validity and Reliability of the Study

To increase reliability, Miles and Huberman's (1994) reliability formula [Agreement / Agreement + Disagreement] was used. This formula aims to measure the percentage of consistency between two or more researchers when analyzing the same data set (e.g., interview transcripts, observation notes) in terms of the codes or themes they identify. The objective is to demonstrate that the findings of the research are not based on the personal interpretations or biases of a single researcher but are similarly interpreted by different researchers, thereby enhancing the reliability and credibility of the study. The reliability of the research was calculated as 0.90. A reliability score above 0.80 is considered acceptable for the reliability of the research (Miles & Huberman, 1994).

Research Problem and Sub-Problems

The framework of this study is based on the problem statement, “How can artificial intelligence tools be used in visual storytelling in education?” Two sub-problems have emerged within this framework:

- What are the differences between applications of artificial intelligence tools in visual storytelling?
- What are the positive and negative effects of artificial intelligence tools in visual storytelling on the educational process?

Limitations of the Study

The study is limited in terms of the applications used and language. Visual production was limited to DALL.E 3, Fooocus.ai, and Imagen 3. Only English was used in the prompts entered. The first story created was intended for 7th grade students, and the level was limited accordingly.

Data Analysis

The analysis of the collected data was conducted using a descriptive approach. The information obtained from the documents was synthesized to support the main argument of the study. During the analysis process, the technical functioning of artificial intelligence tools (e.g., how a text prompt is converted into an image) and the engineering principles behind this process were first revealed. This technical process was then interpreted in relation to pedagogical theories such as the Dual Coding Theory. This allowed us to demonstrate how technology's potential in education can be positioned not only as a technical innovation but also as a pedagogical tool that supports cognitive learning processes.

In analyzing the images produced by artificial intelligence tools, a multi-stage analysis process inspired by Collier and Collier's (1986) visual anthropology approach was followed. (1) Primary observation stage: Evaluating the images produced as a whole and recording general impressions. (2) Structured analysis stage: Systematic examination of the technical characteristics, composition, and content elements of the images. (3) Small-scale (micro) analysis stage: In-depth analysis of the details, symbolic elements, and cultural references in the images. (4) Comparative analysis phase: Comparison of images produced by different platforms and identification of differences. (5) Semantic matching phase: The extent to which the images reflect the story in accordance with the input prompt.

Results and Discussion

In the study, the prompt to create a story was first given to students who were taking English lessons at the 7th grade level and whose native language was English. The ChatGPT 4-o model was used in this process

Prompt 1: *Your primary goal is to generate a story specifically tailored for a 7th-grade, native English-speaking audience (typically 12-13 years old). With this target reader in mind, craft a timeless adventure story brimming with the spirit of friendship, courage, and the pure joy of discovery. Your story is titled "The Adventure of Jake and Max: The Lost Treasure." It should center on two 13-year-old best friends, Jake and Max, who live in a small, charming village by the sea. Establish their dynamic early on: Jake is the adventurous, brave leader, always ready to explore, while Max is his loyal friend, equally enthusiastic but slightly more cautious and thoughtful. The adventure ignites on a sunny afternoon near an old lighthouse, where Jake discovers a torn, ancient piece of a treasure map. The map must present them with their first clear instruction: "Follow the path of the red flowers and cross the river." Propelled by excitement, guide the boys as they pack a small bag containing snacks and, crucially, a flashlight for their journey into the deep forest bordering their village. Describe their trek as they follow the trail of red flowers and carefully navigate a river by stepping on large stones. Their path must lead them to a huge tree with a hollow in its middle. This is where a moment of tension should arise. Let Max express his hesitation about the darkness within the hollow, prompting Jake to provide reassurance by revealing his flashlight. Inside, they must discover a small, locked chest covered in dust. On top of the chest is a note containing a very specific riddle, which you must write exactly as: "I am always hungry, I must always be fed. The finger I touch, will soon turn red." It is the clever Max who must solve this riddle, correctly guessing the answer is "fire." In response, Jake must take a match from his bag, and the moment the flame touches the chest, it should click open. The treasure they find inside must consist of gold coins, sparkling jewels, and a golden compass. Capture their overwhelming joy and sense of accomplishment. Conclude the story as they head back home, filled with excitement, and leave the reader with a strong, optimistic feeling that this incredible discovery is not an ending, but the very beginning of many more adventures to come for Jake and Max. When creating the story, you should consider the students' levels and provide them with appropriate words, sentence structures, and contexts.*

After this, the story in Prompt 1 Result was created.

Prompt 1 Result: *The Adventure of Jake and Max: The Lost Treasure*
Once upon a time, in a small village by the sea, there were two best friends named Jake and Max. They were both 13 years old and loved to explore. Every day, they went on small adventures around their village, looking for interesting things and dreaming of finding hidden treasures.
One sunny afternoon, while playing near the old lighthouse, Jake found something strange. It was a piece of a map, old and torn. The map looked like it led to a hidden treasure somewhere deep in the forest. Excited, Jake ran to show Max.
"Look, Max!" Jake said, holding the map. "This could be the adventure we've been waiting for!"
Max's eyes widened. "A treasure map? This is amazing! But where do we start?"
Jake pointed to the first clue on the map. "It says, 'Follow the path of the red flowers and cross the river.' Let's go!"
The two friends packed a small bag with snacks and a flashlight, and they set off towards the forest. As they walked, they followed the path of red flowers that appeared along the way. They crossed the river by stepping on the big stones, being careful not to fall into the cold water.
After a long walk, they reached a huge tree with a hollow in the middle. Jake looked at the map again. "This is it! The map says the treasure is inside the tree!"
Max peered into the hollow. "But it's too dark inside. What if there's something dangerous in there?"
Jake smiled and pulled out his flashlight. "Don't worry, Max. We'll be fine!"
The two friends slowly crawled into the hollow. Inside, they found a small chest covered in dust. It was locked, but there was a note on top. The note said, "To open the chest, solve this riddle: 'I am always hungry, I must always be fed. The finger I touch, will soon turn red.'"
Max thought for a moment. "I know! It's fire!"
Jake quickly grabbed a match from his bag and lit it. As soon as the flame touched the chest, it opened with a soft click.
Inside, they found gold coins, sparkling jewels, and a golden compass. Jake and Max couldn't believe their eyes.
"We did it, Max!" Jake shouted, jumping up and down.
Max smiled. "This is the best adventure ever!"
The two friends carefully packed the treasure and made their way back home, ready to tell everyone about their incredible adventure. But as they walked back to the village, they knew one thing for sure: this was only the beginning of many more adventures to come.

Then, a prompt was entered requesting the generation of four cartoon-style images using the open-source Stable Diffusion-based Fooocus.ai application, ensuring that the images were consistent with the story and that the main points of the dialogue were written in speech bubbles. Figure 4 was created based on this prompt.

Figure 4. Image generated from Prompt 1 Result entered into the Fooocus.ai.

The images in Figure 5 were generated by Imagen-3 after a prompt was entered instructing Gemini to visualize the story from 'Prompt 1 Result' in four numbered images.

Figure 5. An image generated by Imagen 3 based on Prompt 1 Result.

Subsequently, the DALL-E 3 model, another application used in our study, was prompted based on 'Prompt 1 Result'. The prompt instructed the model to narrate the story in four visuals, specify an animation drawing style, and include a speech bubble in each image for narration, which resulted in the visuals shown in Figure 6.

Figure 6. Image generated by DALL.E 3 based on Prompt 1 Result.

Based on this information, it is necessary to start with the text that was first generated (Prompt 1 result). First, we specified in the prompt (Prompt 1) that the students are 7th graders. The text that was generated must be evaluated to determine the extent to which it is appropriate for the desired level of achievement based on the Common Core State Standards. Students can answer questions such as, “Where can you tell that Jake is excited? (Excited, Jake ran to show Max.)” or “Which sentence shows that Max is worried about danger?” They can answer questions such as (But it's too dark inside. What if there's something dangerous in there?) by finding direct evidence from the text. This is a basic level of evidence-based reasoning. The theme of the text (friendship, adventure, courage) is quite clear and can be easily identified by students. The plot of the text (finding the map, the journey, finding the treasure) is simple, so students can easily summarize it objectively. Students can analyze at a basic level how the characters (adventurous Jake and the more cautious Max) and the setting (the seaside village, the forest, the old trees) shape the plot. The linear and chronological structure of the story, with its introduction, development, and conclusion, is a good example for students to understand the basic narrative structure. Students can be asked to write a continuation of the story, retell the story from Max's point of view, or create their own adventure stories. This directly addresses narrative writing skills. The story is a suitable material for initiating classroom discussions with questions such as, “Was it right for Jake and Max to go into the forest alone?” or “If you were in their place, could you have solved the riddle?” Students can express their opinions and comment on others' ideas. This also supports the achievement of participation in discussions.

However, when looking at the text as a whole, its simplicity may limit the development of more complex and analytical skills expected of 7th grade students. The vocabulary used in the text (strange, hollow, sparkling) is quite basic. It does not allow for the analysis of literary devices such as figurative language (metaphor, simile), connotative meanings, or sound repetition (alliteration, etc.), which are targeted in 7th grade. The story is told by a simple third-person narrator. It is insufficient for more complex analysis, such as developing and comparing the perspectives of different characters. Since this is a fictional text, it does not provide opportunities for students to evaluate the validity of an author's argument or evidence. This also leaves a gap in the acquisition of argument and evidence evaluation (for informative texts). The text consists mostly of simple (Jake and Max couldn't believe their eyes.) and compound sentences (It was locked, but there was a note on top.). It does not provide examples of more complex and compound-complex sentence structures that students are expected to analyze and use. It does not contain academic words or field-specific terms at the 7th grade level. It does not advance students' vocabulary. It does not provide practice in deducing word meanings using strategies such as Latin/Greek roots. It does not provide examples of the use of more complex punctuation marks such as the semicolon (;) beyond basic punctuation marks (period, comma, question mark).

When the written prompt and the story product are compared, it is possible to state that they completely meet the target audience and theme, characters and dynamics, plot and special instructions (chest with riddles, first clue, etc.), solution and conclusion. Looking at the images created, it can be seen that the most important problem is consistency. In this regard, we can say that the most consistent image is the one in Figure 6. Looking at Figure 4, it can be said that the story is generally consistent, but there are differences in the details. The fact that the characters' faces change in each frame, their clothing is not consistent, and their hair styles and facial expressions vary has the potential to create confusion in the students' minds. However, the Fooocus.ai application has produced a successful product in terms of depicting fine details such as the red flowered road, the lighthouse, the map, and the gold.

Figure 5 adheres to the numbering details, and the images are numbered in the correct order. However, there are inconsistencies in the faces and clothing. In some photos, the haircuts, children's faces, and clothing have changed. This may cause confusion for students in visualizing the characters. In image 4 in Figure 5, it is not clear whether the product is gold or not. The modern style of the characters contradicts the “once upon a time” setting at the beginning of the story and does not fully reflect the desired effect. Additionally, although speech bubbles are absent, most of the fine details (the red flowered path, the lighthouse, the chest, the map) have been faithfully reproduced and incorporated into the visualization process.

Figure 6 provides the most consistent and understandable results according to the evaluation metrics. This consistency has been achieved in the physical characteristics, facial expressions, and clothing of the characters. Different clothing has not been used in different images. Or, as in Figures 4 and 5, the faces and hair of the characters have been kept unchanged. In addition, fine details (such as the red flowered road catching the eye or the gold shining) have been created to attract the reader's attention. When comparing the text with the image, images have been produced at a level that allows the student to concretize the text in their mind.

It may not be effective for the learning process if the instructor only uses these visuals to tell the story. In this case, the instructor can use AI tools as a complementary tool for training. This way, they can increase the efficiency of the process and save time. These tools can be utilized for pre-text preparation or post-text reading comprehension. However, if everything is done through these applications, this could potentially disrupt the educational process. The instructor should act as a guide, using artificial intelligence as a teaching tool.

Figure 7 presents the findings of a study conducted by Artificial Analysis in 2025 and compares the quality performance of the leading three AI tools that generate images from text. This comparison is based on ELO rating system scores, which are used to measure the quality of the images produced by the models. According to the graph, the highest quality score of 1165.99 ELO was achieved by the GPT-4o model developed by OpenAI. This model is closely followed by Stability AI's Stable Diffusion Large model with an ELO score of 1162.77. The small difference in scores between the two models indicates that, according to the current evaluation metrics, these two tools demonstrate highly comparable and competitive performance in terms of visual production quality. However, Google's Imagen 3 model ranks third with an ELO score of 1111.54. The significantly lower score of Imagen 3 compared to the other two models suggests that, according to this analysis, the model lags behind its competitors in terms of perceived visual quality.

Figure 7. ELO score of artificial intelligence tools that generate images from text (Artificial Analysis, 2025).

The ELO rating used in this evaluation is a statistical method that measures the performance of a player or system against their opponent. Originally developed to rank the relative strengths of chess players (Elo, 1986), this system has been adapted to evaluate the performance of competitive systems in various fields, such as artificial intelligence models, particularly through pairwise comparisons based on human preferences. In this context, users are presented with images generated by different models and asked which one they prefer. A model's ELO rating increases when it is preferred at a rate above expectations and decreases when it falls below expectations. Therefore, the scores in Figure 7 quantitatively represent the success level of the models' generated images in human evaluations. These results prove the visuals produced in this study and the ranking of the tools used. Looking at the metrics, the analysis shows that Figure 7 is the most desirable, followed by Figure 5, and finally Figure 6.

Another sub-problem examined was: “What are the positive and negative effects of visual storytelling with artificial intelligence tools on the education process?” Various findings were collected from experimental studies. The integration of AI-supported visual storytelling into educational processes offers numerous opportunities to enhance student creativity, participation, motivation, and higher-order cognitive skills. One of the most transformative effects is that it removes creativity from being a specific skill or set of abilities and makes it accessible to a wider audience. Traditional artistic production processes typically require technical skills, practice, and time. However, AI-supported visual creation tools significantly eliminate these barriers. AI tools enable even students without traditional drawing or design skills to create aesthetically rich, technically complex, and compelling visuals. A student can produce a painting in the style of a famous artist or a photorealistic scene with just a textual command. This encourages students who lack confidence in their artistic abilities or struggle to express themselves to participate in the creative process and boosts their self-confidence. Creativity is no longer the domain of those who can draw, but of those who can imagine and express themselves (Amini, 2025; Jasmer, 2024).

Artificial intelligence can function as an inspiration partner or brainstorming tool in the creative process. Students can explore by generating numerous different visual interpretations of an idea or concept in a matter of seconds. For example, for a history class, a student exploring the dark side of the Industrial Revolution could experiment with visualizing this theme in different styles, such as Victorian engravings, expressionist paintings, or cyberpunk aesthetics. This rapid prototyping process expands students' creative horizons, enables them to make unexpected connections, and encourages them to think outside the box.

The use of artificial intelligence tools not only equips students with content creation skills but also develops the fundamental innovation competencies required by the modern world. This process requires students to actively utilize 21st-century skills such as problem-solving, innovative thinking, digital literacy, and adaptability (Yusupova & Koyunlu Unlu, 2025).

AI-powered image generation tools have the potential to significantly increase student engagement and motivation by making the learning process more personalized, interactive, and engaging. One of the greatest promises of AI is the move away from the one-size-fits-all approach to education and toward personalized learning environments. AI-powered visual creation tools make this promise a reality. A teacher can create visual stories tailored to each student's individual interests, learning pace, and cultural background, or encourage students to create their own personal narratives. For example, in a literature class, a visual story explaining the theme of a novel using football metaphors can be created for a student interested in sports, while a story using musical notes and instruments can be created for another student interested in music. This level of personalization enables students to establish a deeper and more meaningful connection with the content, thereby increasing their participation and intrinsic motivation (Al Nabhani et al., 2025). Instead of static images, AI-generated entities (characters, backgrounds, objects), interactive simulations, game-based learning scenarios, and virtual reality (VR) applications can be used as basic material. Students can participate in a simulation that recreates a historical event, conduct a scientific experiment in a virtual laboratory, or progress through a game to solve a math problem (Nayiroglu & Tutak, 2024). Such dynamic, engaging, and enjoyable content transforms the learning process from a task into an adventure to be explored, thereby making students more motivated.

Visual storytelling tools, by their very nature, cater to different learning styles. They make complex textual information more accessible and understandable, especially for visual learners or students with reading and writing difficulties. Artificial intelligence can take this inclusivity even further. Teachers can quickly produce visual materials in different languages or cultural contexts, create visually-focused narratives for students with hearing impairments, or prepare simpler and clearer visual instructions for students on the autism spectrum. This creates a more equitable learning environment where every student can realize their full potential (Samuel, 2024). At this point, it is important to note that the impact of artificial intelligence on motivation is not merely due to its entertaining nature but is rooted in deeper psychological foundations.

The *Self-Determination Theory* pioneered by Ryan and Deci (2023) suggests that intrinsic motivation depends on the fulfillment of three basic psychological needs: competence, autonomy, and relatedness. AI-powered visual storytelling tools strongly fulfill the first two of these needs. When students are able to produce visual products of a quality and professionalism that they would not normally be able to achieve on their own, their feelings of competence increase. At the same time, when they are able to directly guide the creation process through textual commands and receive immediate results, their feelings of autonomy and control are strengthened. Meeting these two fundamental needs encourages students to take greater ownership of the process and become internally motivated. This is a far more lasting and meaningful source of motivation than superficial gamification effects (Jose et al., 2025).

Artificial intelligence has the potential to transform students from mere consumers of content into critical producers (prosumers) who question content. Teachers can teach students to view a visual produced by artificial intelligence as an object of analysis rather than accepting it as true or false. For example, students may be asked to analyze the potential biases of an image they have created, the perspective it represents, which stereotypes it reinforces, or which information it leaves out. This process helps students develop source evaluation, argument analysis, and critical media literacy skills, which are among the most fundamental competencies in the modern world (Kim, 2025).

The process of creating an effective visual requires much more than simply writing a sentence. This process, known as prompt engineering, requires the student to analyze the abstract idea they want to convey, break it down into its basic elements (objects, style, composition, lighting, atmosphere, etc.), and express these elements in a clear, logical, and detailed language that artificial intelligence can understand. This is a valuable exercise in analytical thinking and language skills in itself. As the student iteratively modifies and tests their commands to achieve the desired outcome, they also experience scientific thinking processes such as hypothesis formation, trial and error, and evaluation of results (Wen et al., 2025).

Empowering students with AI tools also comes with the responsibility of teaching them how these technologies work, their limitations, and potential pitfalls. When students learn that artificial intelligence can sometimes generate incorrect information (hallucinations), reflect biases in data sets, and is not always an impartial source of information, they learn to approach all information they encounter in the digital world with greater skepticism and critical thinking. This helps them become more informed and responsible digital citizens (Gouseti et al., 2025).

AI-powered visual storytelling tools have the potential to make learning and teaching processes more efficient by saving teachers and students a significant amount of time and effort. Teachers can produce high-quality, subject-specific visuals for lesson materials, presentations, worksheets, infographics, or assessment rubrics in minutes. Instead of spending hours searching the internet for suitable visuals or settling for simple drawings, they can create products that closely resemble the visuals they envision. This significantly reduces teachers' administrative and preparation workload, allowing them to devote their energy and time to one-on-one guidance, increasing in-class interaction and enabling more in-depth pedagogical planning (Chiu, 2024). Especially in student-centered approaches such as project-based learning (PBL), AI tools accelerate and enrich the process (Ramesh, 2024). Students can quickly visualize a project idea or story concept (prototyping), experiment with different approaches, and iteratively refine their work by receiving early feedback from teachers or peers. This encourages students to try bolder ideas and take more creative risks until they reach the final product (Kusmarni et al., 2025).

The efficiency and creativity potential provided by artificial intelligence inevitably requires an evolution in the understanding of assessment in education. If a student can produce a technically and aesthetically perfect visual or storyboard in seconds, the focus of assessment can no longer be on the final product itself. This renders traditional, product-focused assessment metrics and rubrics largely obsolete. Assessment must inevitably shift to the path leading to that product-that is, the process the student demonstrates. The teacher's role becomes one of evaluating the student's research process, the logic behind turning an idea into commands, the critical choices made from among the options offered by AI, how the output is analyzed, and how the process is improved based on that analysis. This represents a fundamental shift in the teacher's role, requiring them to be not just a grader but also a process guide, a thinking coach, and a facilitator of learning. This new assessment paradigm enables the visibility of learning and the measurement of true higher-order cognitive skills.

In addition to the exciting opportunities offered by AI-powered visual storytelling, it also presents serious challenges and potential negative impacts for educational processes. The uninformed or uncontrolled integration of this technology carries significant risks in terms of ethics, cognition, pedagogy, and security. The fundamental functioning of AI tools inevitably places them at the center of complex ethical dilemmas. These dilemmas require particular sensitivity in value-driven fields such as education. AI models are not intelligent or impartial entities; they are reflections of the vast datasets on which they are trained. These datasets, like the internet itself, are rife with existing social, cultural, and historical biases. These models tend to represent certain genders, races, professions, or cultures in a stereotypical manner or ignore them entirely (Zhang et al., 2024). For example, the overwhelming majority of images generated with the “CEO” command being white and male, or the “nurse” command predominantly producing female figures, are concrete examples of this bias. The use of such biased images in educational settings can unconsciously shape students' worldviews. It can reinforce harmful stereotypes and directly contradict the principles of equality and inclusivity that education aims to promote.

Most text-to-image AI models have been trained on billions of images collected from the internet, often without the permission or knowledge of the creators of these works. This has led to serious legal and ethical debates that challenge the fundamental principles of intellectual property law. Who owns the ownership of an image created by students using these tools? The student, the AI company, or the artist who inspired the image? This uncertainty could expose educational institutions to legal risks. Indeed, some university course syllabi have begun to include provisions stating that content generated by AI will be subject to plagiarism rules and citation limits (Akbaytogan, 2024).

The convenience and rapidity offered by artificial intelligence can pose a threat to students' cognitive development if not managed properly. People have become less reliant on mental arithmetic skills thanks to tools such as calculators. Similarly, students risk avoiding mental effort by delegating challenging cognitive tasks such as thinking, analyzing, synthesizing, and problem solving to artificial intelligence. An experimental study by Kosmyna et al. (2025) examined the neurocognitive and behavioral effects of large language models (LLMs) on academic writing processes. The 54 university students who participated in the study were randomly divided into three groups based on the tools they used for writing tasks: (A) Those using a Large Language Model (e.g., ChatGPT), (B) those using traditional search engines (e.g., Google), and (C) a control group that did not use any digital tools (based solely on brain activity). The most striking result of the study was observed in the group change during the fourth session. As expected, the group that had not previously used tools showed improved performance and cognitive adaptation when transitioning to LLM. However, the group that had become accustomed to using LLM in the first three sessions experienced significant difficulties in memory and text recall when switching to tool-free writing tasks, with declines in cognitive flexibility and overall performance. Reduced brain activity confirmed this finding at the neural level. These findings strengthen the hypothesis that continuous LLM use may create a form of cognitive debt. This concept refers to the idea that dependence on external cognitive tools like LLM may lead to a decline in an individual's core cognitive abilities (memory, critical thinking, synthesis) when these tools are not available. While LLM facilitate text production in the short term, they have been found to pose a risk of disrupting cognitive autonomy and deep learning in the long term.

Artificial intelligence, when used to generate an idea, structure an argument, or create a visual composition, can take away the student's opportunity to develop these skills on their own. This can lead to a weakening of critical thinking, problem-solving, and creative muscles in the long run (Vieriu & Petrea, 2025). AI models generate responses in a highly confident and persuasive manner. However, these responses are not always accurate, unbiased, or complete. Students' tendency to trust AI-generated visuals and texts uncritically and without question is a significant risk. This situation may lead students to accept information superficially and memorize it rather than deeply understanding and internalizing it (Goring et al., 2023). Indeed, an experimental study conducted by Gerlich (2025) using 666 participants examined the relationship between the use of artificial intelligence tools and critical thinking skills, as well as the role of cognitive offloading in this relationship. The study found that while AI-assisted individuals were more successful in procedural problem-solving, they scored lower on tests measuring their understanding of fundamental concepts. This demonstrates that while AI may make tasks easier, it does not always support understanding (Gerlich, 2025).

Artificial intelligence tools tend to learn and replicate popular aesthetic sensibilities, composition rules, and visual patterns. When millions of users employ the same tools with similar commands, there is a risk that the generated visuals will begin to resemble one another over time and cluster around a specific AI aesthetic. This situation can hinder students from discovering their own unique artistic voices and producing experimental and unconventional work, leading to the homogenization of creativity and a form of template creativity (Oh et al., 2020).

In the study by Hall and Schofield (2025), what was examined was the perception of creativity and value in artworks created by humans versus those generated by AI. To do this, the researchers conducted an online experiment where 27 participants were shown a mixed gallery of five images (five created by human artists, five by AI). The participants, who were unaware of the origin of each piece, were asked to rate them on metrics like creativity, monetary value, and the emotions they evoked. A finding that stands out from the research is that, despite the general preference for human-made works, images produced by artificial intelligence were selected by nearly 45% of participants. This result indicates an increasing acceptance of AI art and that the aesthetic quality of these works has reached a level that is nearly indistinguishable from human creativity (Hall & Schofield, 2025).

How to evaluate AI-generated work in a fair, reliable, and meaningful way is one of the biggest pedagogical challenges that needs to be addressed. Traditional, product-oriented rubrics and assessment criteria are inadequate when AI is involved in the process. The need to shift evaluation from product to process necessitates that teachers develop new evaluation tools and methods, which in turn requires additional expertise and workload.

High-quality and advanced artificial intelligence tools are generally fee-based. In addition, powerful computers and fast internet connections are required to run these tools efficiently. Socio-economic disparities between schools and students have the potential to create significant inequalities in access to these technologies. This situation risks deepening the digital divide, further advancing students who are already advantaged while leaving disadvantaged students behind.

At this point, it is evident that artificial intelligence's promise of reducing teachers' workload and increasing productivity has the potential to create a productivity paradox. While artificial intelligence reduces routine workloads such as material preparation, it places new and cognitively more demanding burdens on teachers. Teachers are no longer just lecturers; they must now also serve as technology curators, prompt engineering coaches, ethical guides, continuously learning technology experts, and curriculum designers developing entirely new assessment methodologies. This can create significant stress due to a fundamental shift in skills and roles, and it is not expected that all teachers will be prepared or willing to take on these new roles. Therefore, the promised increase in efficiency depends on how quickly and effectively teachers can adapt to these new and complex roles.

Conclusion

This study provides a comprehensive analysis of the integration of AI-powered visual storytelling into educational settings, examining both its engineering foundations and pedagogical implications. The research confirms that AI tools offer significant opportunities to enhance the learning process by bridging the gap between imagination and tangible creation, thereby fostering a more engaging and inclusive educational environment.

The investigation began by generating a narrative, "The Adventure of Jake and Max: The Lost Treasure," tailored for 7th-grade students using ChatGPT-4o. This text was then visualized using three distinct text-to-image platforms: Fooocus.ai (based on Stable Diffusion), Google's Imagen 3, and OpenAI's DALL-E 3. The analysis of the generated visuals revealed critical differences in performance, particularly concerning character and stylistic consistency. While Fooocus.ai and Imagen 3 produced images that captured specific details from the prompt, they struggled with maintaining consistent character appearances across different frames, which could lead to confusion for student viewers. In contrast, DALL-E 3 delivered the most coherent and stylistically consistent series of images, successfully translating the narrative's key moments into a visually cohesive comic-strip format that aligned well with the story's text. This finding is supported by external benchmarks, such as the ELO rating system, which positions OpenAI's models at the forefront of visual quality and human preference, corroborating this study's qualitative assessment.

From a pedagogical standpoint, the study highlights numerous positive impacts. AI tools act as a powerful scaffolding mechanism, removing technical barriers and enabling students with limited artistic skills to visualize and express complex ideas. This democratization of creativity has the potential to boost student motivation, engagement, and self-confidence. By allowing for rapid prototyping and the exploration of diverse visual styles, these tools can serve as a catalyst for brainstorming and innovative thinking. Furthermore, the process of prompt engineering-crafting precise and descriptive text commands-is in itself a valuable exercise that develops analytical thinking, language skills, and problem-solving abilities. The integration of these tools aligns with established learning theories, such as Paivio's Dual Coding Theory, which posits that processing information both verbally and visually leads to a richer cognitive encoding and more durable learning.

However, the research also identifies significant challenges and negative implications that must be addressed for a responsible implementation of this technology. A primary concern is the risk of cognitive offloading, where students may rely on AI to perform critical thinking tasks, potentially weakening their own analytical and problem-solving skills. The black box nature of these models, which can produce authoritative but factually incorrect hallucinations, poses a risk of students passively accepting information without critical evaluation.

Ethical issues are also paramount. AI models are trained on vast datasets that reflect existing societal biases, and they can perpetuate harmful stereotypes related to gender, race, and profession in the visuals they generate. This directly conflicts with the educational goals of fostering equity and inclusion. Moreover, the unresolved legal and ethical questions surrounding copyright and the ownership of AI-generated content create a precarious situation for educational institutions. Finally, the potential for these tools to create a homogenization of creativity, where aesthetic styles converge around a common AI aesthetic, could stifle true originality.

AI-powered visual storytelling stands as a transformative educational tool, not a replacement for the teacher. Its effective use hinges on a paradigm shift where the educator acts as a facilitator and guide. The focus of assessment must move from the final product to the creative and critical process: the quality of the prompts, the student's ability to critically analyze and iterate upon AI-generated outputs, and their understanding of the underlying ethical considerations. While the potential to enhance motivation, personalize learning, and develop 21st-century skills is immense, it must be carefully balanced against the risks of cognitive laziness, ethical missteps, and the erosion of authentic creativity. The successful integration of these powerful tools will ultimately depend on the development of new pedagogical frameworks that prioritize critical engagement and responsible use.

Recommendations

This study has revealed the potential of AI-supported visual storytelling in education through a qualitative case analysis and shed light on its fundamental dynamics. Future research in this field should test the findings in broader and more diverse contexts to contribute to the body of knowledge in this area.

Based on the limitations of the current study, it is recommended that future studies conduct similar investigations on student populations of different age groups (e.g., preschool or university), different disciplines (e.g., science, social studies, art education), and different socio-cultural contexts. Furthermore, beyond the specific artificial intelligence platforms used in this study (DALL-E 3, Imagen 3, Fooocus.ai), a comparative analysis of a wider range of alternatives, particularly open-source ones, would be valuable in understanding the accessibility of technology and its impact on the digital divide. To complement the qualitative case analysis, measuring the effects on student motivation, perception of creativity, and learning outcomes through quantitative or mixed-method experimental studies would provide more concrete evidence to support the pedagogical promises of this technology.

One of the most important risks revealed by the study, cognitive debt and the potential weakening of critical thinking skills, requires more in-depth and long-term examination. Future researchers are advised to follow the effects of artificial intelligence tools on students' higher-order cognitive skills through longitudinal studies. Monitoring changes in students' problem-solving, argumentation, and information synthesis abilities over several months or an academic year of regular use of these tools will provide more reliable data on the long-term cognitive outcomes of technology. In this process, considering the need to shift the focus of assessment from the product to the process, developing and testing new pedagogical frameworks and validated assessment rubrics that measure prompt engineering skills, the ability to critically analyze AI outputs, and the iterative development process is also emerging as a priority research area.

Ethical concerns regarding the use of artificial intelligence tools, particularly the reproduction of biases and intellectual property issues, are urgent issues awaiting resolution in the context of education. Future studies should focus on developing *critical digital literacy* interventions that enable students to identify and question stereotypical representations and potential biases in AI-generated content and measure the effectiveness of these interventions.

In addition, research is needed to develop ethical use frameworks and institutional policies to guide the practical application of artificial intelligence in education. Designing, implementing, and evaluating professional development programs that equip teachers with the necessary skills to use this new technology effectively and responsibly, as well as examining the impact of these programs on teacher competencies and student outcomes, will also address another critical research gap in this field.

Scientific Ethics Declaration

* The authors declares that the scientific ethical and legal responsibility of this article published in EPSTEM journal belongs to the authors.

Conflict of Interest

* The authors declare that they have no conflicts of interest

Funding

* This research received no specific grant from any funding agency in the public, commercial, or not-for-profit sectors.

Acknowledgements or Notes

* This article was presented as an oral presentation at the International Conference on Research in Engineering, Technology and Science (www.icrets.net) held in Peja/Kosovo on July 10-13, 2025.

References

Akbaytogan, K. (2024). *Arkin yaratıcı sanatlar ve tasarım üniversitesi iletişim fakültesi ders müfredatı*. Arkin Üniversitesi.

Al-Khatib, R., Al-Khatib, R., & Abo-Ajaj, J.(2025). Therole of artificial intelligence applications in enhancing understanding and data analysis using mind maps among primary school students within the green line. *The Eurasia Proceedings of Educational andSocial Sciences (EPESS), 40*, 17-32.

Al Nabhani, F., Hamzah, M. B., & Abuhassna, H. (2025). The role of artificial intelligence in personalizing educational content: Enhancing the learning experience and developing the teacher's role in an integrated educational environment. *Contemporary Educational Technology*, *17*(2), 573.

Amini, H. (2025). AI in art education: Innovation, ethics, and the future of creativity. *Art and Design Review*, *13*(02), 115-129.

Artificial Analysis. (2025, June). *Text to image API comparisons artificial analysis*. https://artificialanalysis.ai/leaderboards/providers

Baldwin, C. (2010). *Storycatcher: Making sense of our lives through the power and practice of story*. New World Library.

Bandi, A., Adapa, P. V. S. R., & Kuchi, Y. E. V. P. K. (2023). The power of generative AI: A review of requirements, models, input–output formats, evaluation metrics, and challenges. *Future Internet*, *15*(8), Article 8.

Basturk, B. M., & Sen, E. (2025). The level of comprehension of implicit meanings in English and Turkish proverbs by ai-based text-to-image generation tools. *The Journal of Limitless Education and Research, 10*(2), 523-572.

Bian, Z., Xu, Q., Wang, B., & You, Y. (2021). Maximizing parallelism in distributed training for huge neural networks. *ArXiv:2105.14450*.

Brown, T. B., Mann, B., Ryder, N., Subbiah, M., Kaplan, J., Dhariwal, P., ... & Amodei, D. (2020). Language models are few-shot learners. *arXiv:2005.14165*.

Celard, P., Iglesias, E. L., Sorribes-Fdez, J. M., Romero, R., Vieira, A. S., & Borrajo, L. (2023). A survey on deep learning applied to medical images: From simple artificial neural networks to generative models. *Neural Computing and Applications*, *35*(3), 2291-2323.

Chiu, T. K. F. (2024). *Empowering K-12 education with AI: Preparing for the future of education and work*. Routledge.

Collier, J., & Collier, M. (1986). *Visual anthropology: Photography as a research method*. University of New Mexico Press.

Croitoru, F.A., Hondru, V., Ionescu, R. T., & Shah, M. (2023). Diffusion models in vision: A survey. *IEEE Transactions on Pattern Analysis and Machine Intelligence*, *45*(9), 10850-10869.

Devlin, J., Chang, M. W., Lee, K., & Toutanova, K. (2018). Bert: Pre-training of deep bidirectional transformers for language understanding. *arXiv:1810.04805*.

Elo, A. E. (1986). *The rating of chessplayers, past and present* (2nd ed). Arco.

Gerlich, M. (2025). AI tools in society: Impacts on cognitive offloading and the future of critical thinking. *Societies*, *15*(1), 6.

Goodfellow, J. I., Pouget-Abadie, J., Mirza, M., Xu, B., Warde-Farley, D., Ozair, S., Courville, A., & Bengio, Y. (2014). Generative adversarial networks. *ArXiv:1406.2661*.

Goring, S., Ramachandra Rao, R. R., Merten, R., & Raake, A. (2023). Analysis of appeal for realistic AI-generated photos. *IEEE Access*, *11*, 38999-39012.

Gouseti, A., James, F., Fallin, L., & Burden, K. (2025). The ethics of using AI in K-12 education: A systematic literature review. *Technology, Pedagogy and Education*, *34*(2), 161-182.

Gun, M., Alkan, E., & Basturk, B. M. (2025). Yabancılara Türkçe öğretiminde yapay zekâ tarafından üretilen görsellerin kültür aktarımı bağlamında incelemesi. *International Journal of Language Academy, 13* (1), 293-308.

Hall, J., & Schofield, D. (2025). The value of creativity: Human produced art vs. AI-generated art. *Art and Design Review*, *13*(01), 65-88.

Hausken, L. (2024). Photorealism versus photography. AI-generated depiction in the age of visual disinformation. *Journal of Aesthetics & Culture*, *16*(1), 2340787.

Hava, K. (2021). Exploring the role of digital storytelling in student motivation and satisfaction in EFL education. *Computer Assisted Language Learning*, *34*(7), 958-978.

Haven, K. (2007). *Story proof: The science behind the startling power of story*. Bloomsbury.

Houlsby, N., Giurgiu, A., Jastrzebski, S., Morrone, B., De Laroussilhe, Q., Gesmundo, A., Attariyan, M. & Gelly, S. (2019). Parameter-Efficient transfer learning for NLP. *Proceedings of the 36th International Conference on Machine Learning, 97*, 2790-2799.

Huang, Y., Xu, J., Lai, J., Jiang, Z., Chen, T., Li, Z., Yao, Y., Ma, X., Yang, L., Chen, H., Li, S., & Zhao, P. (2024). Advancing transformer architecture in long-context large language models: A comprehensive survey. *ArXiv:2311.12351*.

Jasmer, B. W. (2024). *Balancing AI and human creativity: Adaptations in art education* (Master's thesis). Bethel University.

Jose, B., Cherian, J., Verghis, A. M., Varghise, M. S., Mumthas, S., & Joseph, S. (2025). The cognitive paradox of AI in education: Between enhancement and erosion. *Frontiers in Psychology*, *16*.

Kayahan, Z. (2010). İlköğretim 1. kademe 5. sınıf görsel sanatlar eğitimi dersinde hikâye anlatım yönteminin yaratıcılığa etkileri (Master's Thesis). Gazi Üniversitesi.

Kim, J. (2025). Perspectives on AI integration in K-12 schools: Opportunities, challenges, and strategic approaches. *Midwest Journal of Education*, *2*(1), 58-73.

Kosmyna, N., Hauptmann, E., Yuan, Y. T., Situ, J., Liao, X. H., Beresnitzky, A. V., Braunstein, I., & Maes, P. (2025). Your brain on chatGPT: Accumulation of cognitive debt when using an ai assistant for essay writing task. *arXiv:2506.08872.*

Kushwaha, R. K., Nzuza, D. Z. D., Yadav, P. K., & Yadav, S. (2024). *Collective intelligence: A resource for teachers,parents & policymakers*. Blue Rose.

Kusmarni, Y., Santosa, A., Winarti, M., Kurniawati Sumantri, Y., Yulianti, I., Gumelar, F., & Pangestu, D. (2025). Artificial intelligence in project-based learning as a resource for learning local history in bandung. *Diakronika*, *24*, 118-133.

Kutsyuruba, B. (2023). Document analysis. In J. M. Okoko, S. Tunison, & K. D. Walker (Eds.), *Varieties of qualitative research methods: Selected contextual perspectives* (ss. 139-146). Springer.

Miles, M. B., & Huberman, A. M. (1994). *Qualitative data analysis: An expanded sourcebook*. Sage.

Minaee, S., Kalchbrenner, N., Cambria, E., Nikzad, N., Chenaghlu, M., & Gao, J. (2024). Large language models: A survey. *arXiv:2401.02038*.

Nayiroglu, B., & Tutak, T. (2024). *Matematik öğretiminde yapay zekanın rolü: öğretimde kullanılan araçların incelenmesi*. *Turkish Journal of Educational Studies, 11*(1), 65-78.

Oh, C., Kim, S., Choi, J., Eun, J., Kim, S., Kim, J., Lee, J., & Suh, B. (2020). Understanding how people reason about aesthetic evaluations of artificial intelligence. *Proceedings of the 2020 ACM Designing Interactive Systems Conference*, 1169-1181.

Paivio, A. (1990). *Mental Representations: A dual coding approach*. Oxford University Press.

Paivio, A. (1991). Dual coding theory: Retrospect and current status. *Canadian Journal of Psychology / Revue Canadienne de Psychologie*, *45*(3), 255-287.

Partnership for 21st Century Skills (2019). *Framework for 21st century learning definitions.* Partnership for 21st Century Skills.

Radford, A., Narasimhan, K., Salimans, T., & Sutskever, I. (2018). *Improving language understanding by generative pre-training*. OpenAI.

Robin, B. R. (2008). Digital storytelling: A powerful technology tool for the 21st century classroom. *Theory Into Practice*, *47*(3), 220-228.

Ryan, R. M., & Deci, E. L. (2023). Self-determination theory. In A.C. Michalos (Ed.), *Encyclopedia of quality of life and well-being research* (ss. 6229-6235). Springer.

Sadoski, M., & Paivio, A. (2013). *Imagery and text: A dual coding theory of reading and writing*. Routledge.

Samuel, K. (2024). The role of digital storytelling in education: Enhancing literacy and communication skills. *Eurasian Experiment Journal of Scientific and Applied Research, 5*(2), 36–39.

Sapkota, R. (2023). Harnessing the power of ai based image generation model DALLE2 in agricultural settings. *ArXiv: 2307.08789.*

Schuhmann, C., Beaumont, R., Vencu, R., Gordon, C., Wightman, R., Cherti, M., Coombes, T., Katta, A., Mullis, C., Wortsman, M., Schramowski, P., Kundurthy, S., Crowson, K., Schmidt, L., Kaczmarczyk, R., & Jitsev, J. (2022). LAION-5B: An open large-scale dataset for training next generation image-text models. *36th Conference on Neural Information Processing Systems (NeurIPS 2022).*

Umutlu, D., & Gursoy, M. E. (2022). Leveraging artificial intelligence techniques for effective scaffolding of personalized learning in workplaces. In D. Ifenthaler & S. Seufert (Eds.), *Artificial intelligence education in the context of work* (ss. 59-76). Springer.

Uzun, Y.,& Kayrici, M. (2025). Use of artificial neural network in educational laboratory applications: Low-velocity impact test. *Journal of Education in Science, Environment and Health (JESEH), 11*(2), 82-92. https://doi.org/10.55549/jeseh.796

Vanichvasin, P. (2021). Effects of visual communication on memory enhancement of Thai undergraduate students, Kasetsart University. *Higher Education Studies*, *11*(1), 34-41.

Vaswani, A., Shazeer, N., Parmar, N., Uszkoreit, J., Jones, L., Gomez, A. N., ... & Polosukhin, I. (2017). Attention is all you need. *arXiv:1706.03762.*

Vieriu, A. M., & Petrea, G. (2025). The impact of artificial intelligence (AI) on students' academic development. *Education Sciences*, *15*(3), Article 3.

Wen, Z., Weng, L., Tang, Y., Zhang, R., Liu, Y., Pan, B., Zhu, M., & Chen, W. (2025). Exploring multimodal prompt for visualization authoring with large language models. *ArXiv:2504.13700*.

Wu, X.-K., Chen, M., Li, W., Wang, R., Lu, L., Liu, J., Hwang, K., Hao, Y., Pan, Y., Meng, Q., Huang, K., Hu, L., Guizani, M., Chao, N., Fortino, G., Lin, F., Tian, Y., Niyato, D., & Wang, F.-Y. (2025). LLM fine-tuning: Concepts, opportunities, and challenges. *Big Data and Cognitive Computing, 9*(4), 87.

Xie, Z., Cohn, T., & Lau, J. H. (2023). The next chapter: A study of large language models in storytelling. In C. M. Keet, H.Y. Lee, & S. Zarrieß (Eds.), *Proceedings of the 16th International Natural Language Generation Conference* (ss. 323-351). Association for Computational Linguistics.

Yin, R. K. (2009). *Case study research: Design and methods*. Sage.

Yusupova, A., & Koyunlu Unlu, Z. (2025). Sınıf öğretmen adaylarının hazırlamış oldukları dijital hikâyelerin 21. yüzyıl becerilerine etkisinin incelenmesi. *İnönü Üniversitesi Eğitim Fakültesi Dergisi*, *26*(1), 154-172.

Zakraoui, J., Saleh, M., Al-Maadeed, S., & Alja'am, J. M. (2023). A pipeline for story visualization from natural language. *Applied Sciences*, *13*(8), 5107.

Zhang, C., Zhang, C., Zhang, M., Kweon, I. S., & Kim, J. (2024). Text-to-image diffusion models in generative ai: A survey. *ArXiv:2303.07909*.

Author(s) Information

Mesut Gun	**Mustafa Baris Basturk**
Mersin University, Faculty of Education	Mersin University
Ciftlikkoy, Mersin Unv., 33110 Yenisehir	Institute of Educational Sciences, Mersin, Türkiye
Mersin, Türkiye	Contact e-mail: *barisbasturk8@gmail.com*

To cite this article:

Gun, M., & Basturk, B. M. (2025). Enhancing visual and cognitive intelligence memory with fine tuning modeling based on artificial intelligence large language models. *The Eurasia Proceedings of Science, Technology, Engineering and Mathematics (EPSTEM), 35,* 10-28.

The Eurasia Proceedings of Science, Technology, Engineering & Mathematics (EPSTEM)
ISSN: 2602-3199

The Eurasia Proceedings of Science, Technology, Engineering and Mathematics (EPSTEM), 2025

Volume 35, Pages 29-37

ICRETS 2025: International Conference on Research in Engineering, Technology and Science

A Comparative Analysis of Dataset Performance in Disease Prediction via Machine Learning Algorithm

Mustafa Cosar
Hitit University

Abstract: This study aims to investigate how dataset characteristics influence the predictive performance of machine learning (ML) algorithms in the context of disease diagnosis. While existing literature often focuses on evaluating the performance of various models on a single dataset, this study adopts a broader perspective. The UCI Heart Disease, Heart Failure, and Cleveland datasets were pre-processed using various techniques to ensure structural comparability and subsequently analyzed using models developed with the CatBoost algorithm. The study assesses the performance of these models on each dataset and explores the influence of different parameters. The model demonstrated strong predictive capability across all datasets, achieving high accuracy scores. For the UCI Heart Disease dataset, the model was able to effectively distinguish between classes, supported by an accuracy rate of 84.24% and other performance metrics. On the Heart Failure dataset, the model exhibited even higher performance, with an accuracy of 88.59%. The Cleveland dataset also yielded favorable results, achieving an accuracy of 85.25%. The results underscore the practical value of ML-based classifiers in the early prediction of heart-related medical conditions. By comparing model success across different datasets, the study highlights the applicability and effectiveness of these techniques and provides direction for future research involving larger datasets and alternative algorithms.

Keywords: Machine learning, Disease prediction, Importance of dataset, Performance analysis

Introduction

Diseases are an important factor that negatively affects human life. Cardiovascular diseases continue to be the foremost cause of global mortality, responsible for nearly 18 million deaths each year, predominantly resulting from ischemic heart disease and stroke. Recognizing the impact of timely diagnosis and intervention, the World Health Organization (WHO) has launched global initiatives to expand preventive care and treatment access for high-risk populations (WHO, 2025).

Machine learning (ML) has been favored in recent years as a successful approach that has reshaped data-driven methodologies in various fields, including healthcare. Its ability to automatically perform feature selection, model complex non-linear relationships, and enable risk stratification has made it particularly valuable in medical applications (Ahsan et al., 2022; Nagavelli et al., 2022). Among ML techniques, Gradient Boosting stands out for its strong predictive performance and has consistently demonstrated superiority over traditional models across various domains (Cosar, 2024).

CatBoost, a gradient boosting algorithm introduced by Yandex in 2017, excels in handling categorical features and reducing the need for extensive preprocessing. Gradient boosting models are used to minimize prediction drift. In this way, they attract attention with their successful performance on datasets from different fields. (Prokhorenkova et al, 2017). Its efficiency and accuracy have made it a strong candidate for clinical applications where speed and handling of heterogeneous data are vital.

Empirical studies support CatBoost's effectiveness in cardiovascular risk prediction. Kanagarathinam et al. 2022) achieved a mean accuracy of 94% with CatBoost using the hybrid "Sathvi" dataset combining multiple public sources. Mahalakshmi and Rout (2025) developed a hybrid MLP-CatBoost model optimized with Mayfly algorithm, reporting accuracies of up to 99.2%. Ensemble techniques such as stacking including CatBoost as meta-model reached 91% accuracy with explainable AI approaches (Sultan et al. 2025). Comprehensive reviews also highlight CatBoost's consistent AUC > 0.90 in large-scale clinical datasets (Kumar et al. 2025).

Given its superior treatment of categorical variables, robust performance, and minimal feature engineering requirements, CatBoost represents a compelling choice for predictive modeling in heart disease. This study therefore focuses on evaluating CatBoost's performance in heart disease prediction and comparing it to other ML approaches. In addition to evaluating model performance, this study examines how dataset characteristics influence predictive outcomes. Section 2 introduces the methods, providing comprehensive details on the datasets alongside the mathematical and algorithmic principles underpinning the model. Section 3 discusses the experimental outcomes, offering an in-depth analysis of the results. The final section, Section 4, draws conclusions and explores how dataset characteristics influence the model's predictive performance.

Method

This section provides a detailed explanation of the datasets used for heart disease prediction, the data preprocessing steps, and the mathematical and architectural structure of the employed ML model.

Dataset

This study utilizes three different datasets for predicting heart diseases: the UCI Heart Disease (UCI), Heart Failure (HF), and Cleveland datasets. Each of these datasets contains a rich data structure with various features and factors related to heart diseases.

- UCI Dataset: The dataset is one of the most well-known and widely used datasets for heart disease research (Janosi et al. 1989). This dataset includes various medical parameters and demographic characteristics of patients. It consists of 14 different features, such as sex, blood pressure, heart rate, age, cholesterol, and ECG results. Additionally, the disease status is divided into five categories (0, 1, 2, 3, and 4), where 0 represents no disease and 1 indicates the presence of disease.
- HF Dataset: The dataset is focused on heart failure conditions and includes various features related to heart diseases (Poolsawad et al. 2014). The dataset contains data on patients with heart failure, including age, blood pressure, heart rate, exercise tolerance, gender, ST-segment changes, and heart failure status. This dataset is a binary classification problem, where it distinguishes between patients who are experiencing heart failure (1) and those who are not (0).
- Cleveland Dataset: The dataset is another widely used dataset for heart disease diagnosis. It provides data aimed at predicting the presence or absence of heart disease based on individuals' physical and clinical characteristics (Zhou et al. 2024)..

Data Preprocessing

This pipeline step consisted of the following stages, which collectively enhance the dataset's interaction with the model, thereby improving the accuracy of the results.

1. **Missing Data Imputation:** Missing values were imputed using mean and median substitution to reduce their negative impact and maintain data consistency during model training.
2. **Categorical Encoding:** Categorical variables e.g., gender and chest pain type were converted into numerical format using One-Hot Encoding to enable algorithm compatibility (Géron, 2019).
3. **Feature Scaling:** Although not essential for tree-based models like CatBoost, feature standardization (using StandardScaler) was applied to improve training efficiency by normalizing features to zero mean and unit variance.
4. **Feature Selection:** Redundant and highly correlated variables were removed. In particular, certain features in the Cleveland dataset were excluded due to low informational value.
5. **Dataset split:** Each dataset was organized into test and training subsets with an 20/80 ratio to assess the model's capacity for generalization.

Model Architecture

This study employs the CatBoost algorithm to predict heart disease using structured clinical data. CatBoost, a gradient boosting method developed by Prokhorenkova et al. (2018), is specifically designed to handle categorical features with minimal preprocessing. Unlike traditional gradient boosting (GB) implementations, CatBoost employs Ordered Boosting, a strategy that mitigates prediction shift and reduces overfitting caused by target leakage.

In gradient boosting, a model is built in a stage-wise manner by iteratively combining weak learners, typically decision trees. At each iteration, the algorithm aims to correct the residuals (errors) from the previous stage. This process is mathematically represented in Formula 1.

$$F_t(x) = F_{t-1}(x) + \eta \cdot h_t(x) \tag{1}$$

where, $F_t(x)$ is the model's prediction at iteration t, $h_t(x)$ is the output of the weak learner at that step, η is the learning rate controlling the update magnitude. he objective is to minimize the discrepancy between predicted and actual values using a loss function, commonly defined in Formula 2.

$$L(\hat{y}, y) = \frac{1}{N} \sum_{i=1}^{N} \ell(\hat{y}_i, y_i) \tag{2}$$

where, $L(\hat{y}, y)$ is the predicted output, $\hat{y}_i$ is the predicted label, y_i is the true label, *N* is the number of samples in the dataset, and ℓ is a loss function like log-loss or cross-entropy (Bishop, 2006). CatBoost introduces innovations in handling categorical variables without explicit preprocessing such as one-hot encoding. It applies a form of target encoding that calculates statistics based on permutations of the training data to prevent data leakage. The encoding for each categorical variable is computed as shown in Formula 3.

$$C_k = \frac{1}{N} \sum_{i=1}^{N} y_i \tag{3}$$

where, C_k is the average target value for the *k*-th category, N_k is the number of samples in that category, and y_i represents the target value of each sample. To optimize the model, CatBoost building on the gradient descent approach described by Bottou (2010) updates to minimize the loss function, as illustrated in Formula 4.

$$\theta_{t+1} = \theta_t - \eta \cdot \nabla L(\theta_t) \tag{4}$$

where, θ_t represents the model parameters at the *t*-th iteration, while η is the learning rate and $\nabla L(\theta_t)$ is the gradient of the loss function. The final model output is the weighted sum of predictions from all weak learners, with weights determined by the learning rate, as shown in Formula 5.

$$\hat{y} = \sum_{i=1}^{T} \eta \cdot h_t(x) \tag{5}$$

here, *T* is the total number of iterations. CatBoost stands out for its effectiveness in class-weighted classification problems, particularly in domains like healthcare, where datasets often contain high-cardinality categorical variables.

The overall implementation process is summarized in Figure 1. Initially, the datasets were loaded, and categorical data was converted into numerical values using the LabelEncoder data transformation. In the UCI, HF, and Cleveland datasets, target variables were identified, and relevant features were selected for the model. In particular, unnecessary columns were removed in the UCI dataset. In the study on the UCI Heart Disease dataset, the classification problem was initially addressed with 5 different classes (0, 1, 2, 3, 4). However, in order to improve the model's performance, these classes were reduced to two classes (0 and 1), with classes 1, 2, 3, and 4 being merged. This enabled the distinction between patients with positive disease status (levels 1–4) and those with negative status (0).

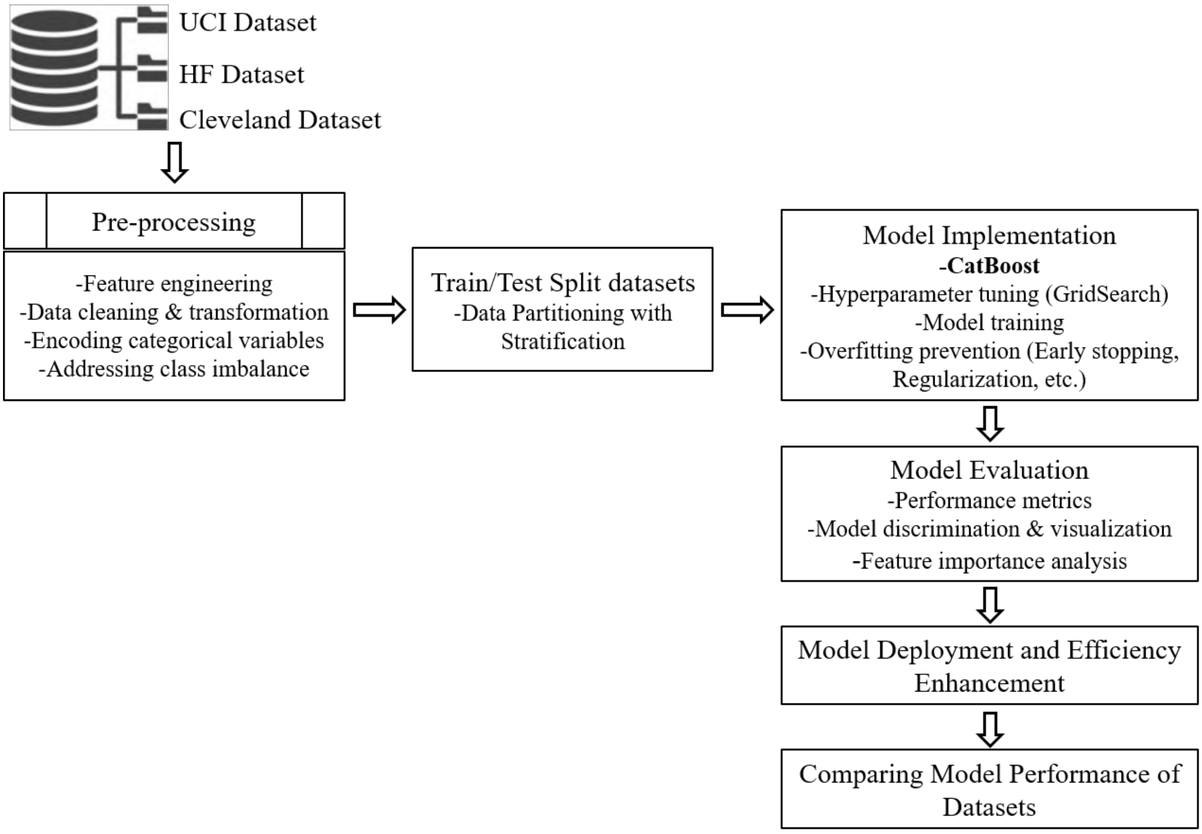

Figure 1. Research workflow and implementation steps

For model training, the CatBoostClassifier was employed with appropriate handling of categorical features via the cat_features parameter. To evaluate of the model, the training dataset was first processed. Then, the processes were repeated with the test dataset. For the model performance; metrics such as accuracy, precision, recall, F1 score and AUC-ROC were calculated.

Among the model's outputs, confusion matrices and ROC curves were visualized, allowing for a detailed examination of the model's prediction performance for each dataset. Additionally, feature importance analysis was conducted for each dataset to determine which features the model prioritized the most. This was useful in understanding which variables the model relied on to make decisions. The results indicate that the CatBoost algorithm performs effectively across different datasets and achieves high accuracy rates. This supports the use of CatBoost, particularly for its strengths and speed in processing categorical data, in applications such as heart disease prediction in the healthcare domain.

Results and Discussion

The performance results of the CatBoost algorithm applied to three separate heart disease datasets are reported in this section. The UCI dataset was evaluated as a multi-class classification problem, whereas the Heart Failure and Cleveland datasets were approached as binary classification tasks. CatBoost's performance was evaluated using standard classification metrics. The results highlight CatBoost's high predictive capability, particularly in handling categorical variables effectively and achieving consistent accuracy across different clinical datasets. Comparative analysis across datasets allows for a comprehensive assessment of the algorithm's adaptability and robustness in diverse healthcare data scenarios.

Model Performance

According to Table 1, the model has demonstrated successful performance with high accuracy rates across all three datasets. For the UCI dataset, the model is able to make strong distinctions between classes, which is supported by the accuracy and other metrics. For this dataset, the model's accuracy rate is 84.24%, precision is 89.22%, recall is 83.49%, F1 score is 86.26%, and the AUC-ROC value is 0.9211. For the Heart Failure dataset, the model shows even higher performance.

Table 1. Calculated values of model performance metrics

Dataset/Metric	Accuracy	Precision	Recall	F1 Score	AUC-ROC
UCI	0.8424	0.8922	0.8349	0.8626	0.9211
HF	0.8859	0.9135	0.8879	0.9005	0.9411
Cleveland	0.8525	0.8966	0.8125	0.8525	0.9386

For this dataset, the accuracy rate is 88.59%, precision is 91.35%, recall is 88.79%, F1 score is 90.05%, and the AUC-ROC value is 0.9411. The model also achieved successful results on the Cleveland dataset. For this dataset, the accuracy rate is 85.25%, precision is 89.66%, recall is 81.25%, F1 score is 85.25%, and the AUC-ROC value is 0.9386.

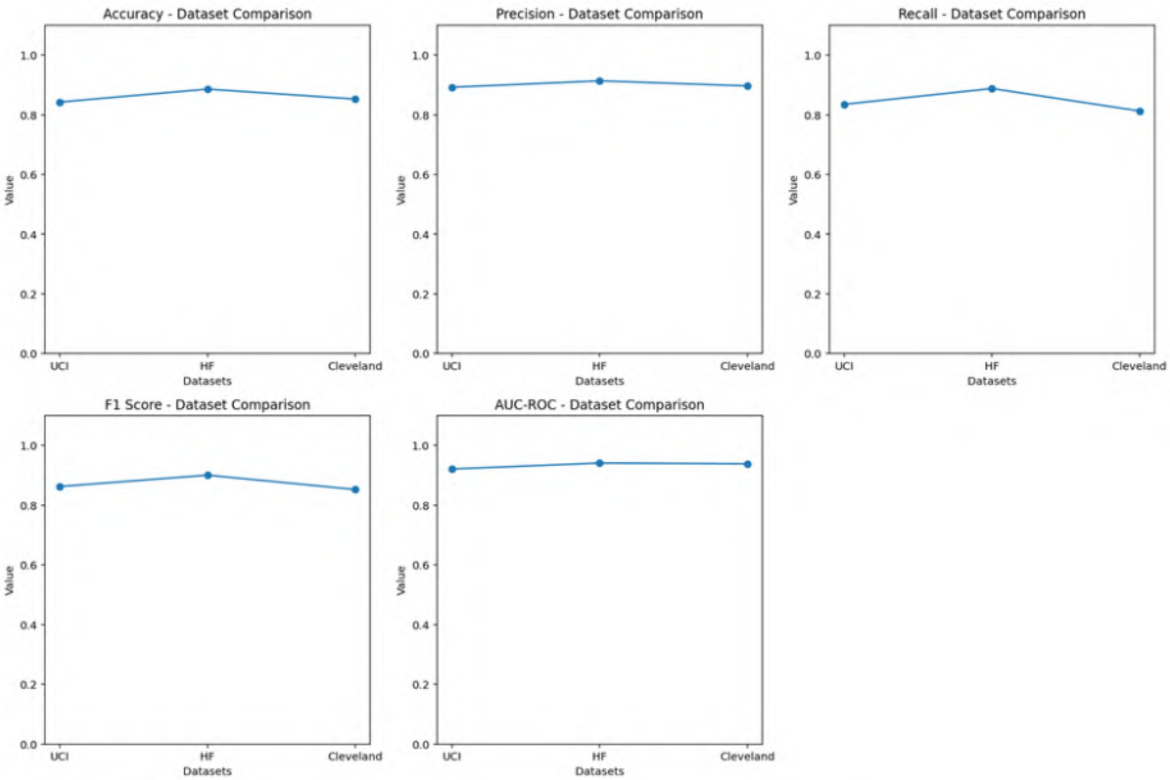

Figure 2. Performance metrics of datasets

Figure 2 shows the measured values of the metrics of the model calculated on three separate datasets (UCI, HF and Cleveland). The figure highlights essential evaluation metrics enabling a comprehensive assessment of the model’s effectiveness and variability across different data sources

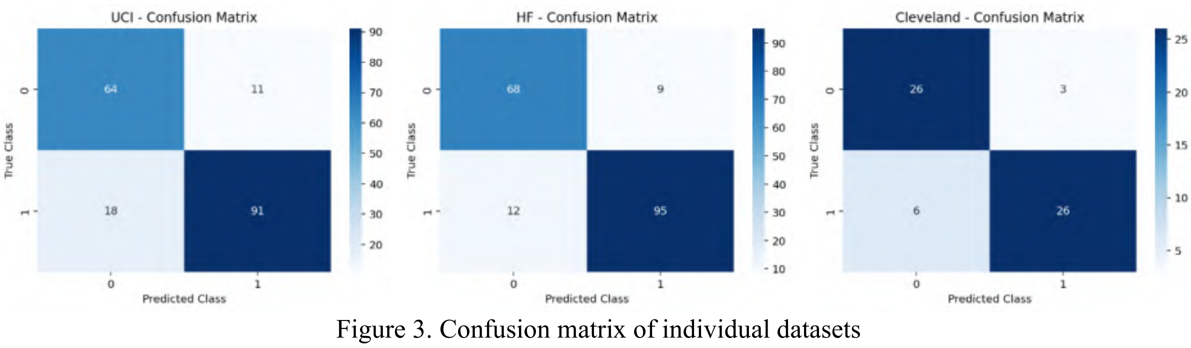

Figure 3. Confusion matrix of individual datasets

In Figure 3, the confusion matrices obtained for the three datasets (UCI, HF, Cleveland) are displayed. Each matrix shows values indicating the model's correct and incorrect classifications, presented as True Positive (TP), False Positive (FP), True Negative (TN), and False Negative (FN). These visuals allow for a more detailed analysis of the model's class imbalances and errors.

In Figure 4, the ROC curve graphs for each dataset are visualized. These graphs represent nonlinear curves used to evaluate the classification performance of the model on each dataset. ROC curves compare the model's TP Rate with the FP Rate, illustrating the overall success level of the model. The area AUC is an important metric for determining the model's prediction accuracy, and the AUC values for each dataset are visualized in this manner.

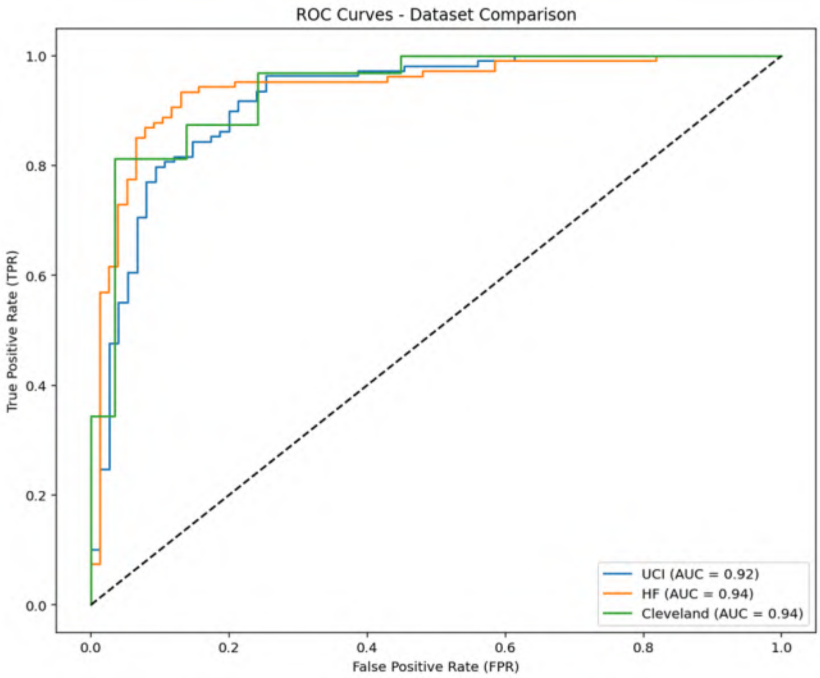

Figure 4. ROC curves of datasets

These findings show that the model exhibits high accuracy and strong classification performance on all three datasets. Although some class imbalances and false positive/negative rates are observed in certain datasets, the model’s predictive performance remains robust overall. Specifically, the ROC AUC score, as illustrated in Figure 4, indicates that the model offers strong discriminative ability across all three datasets.

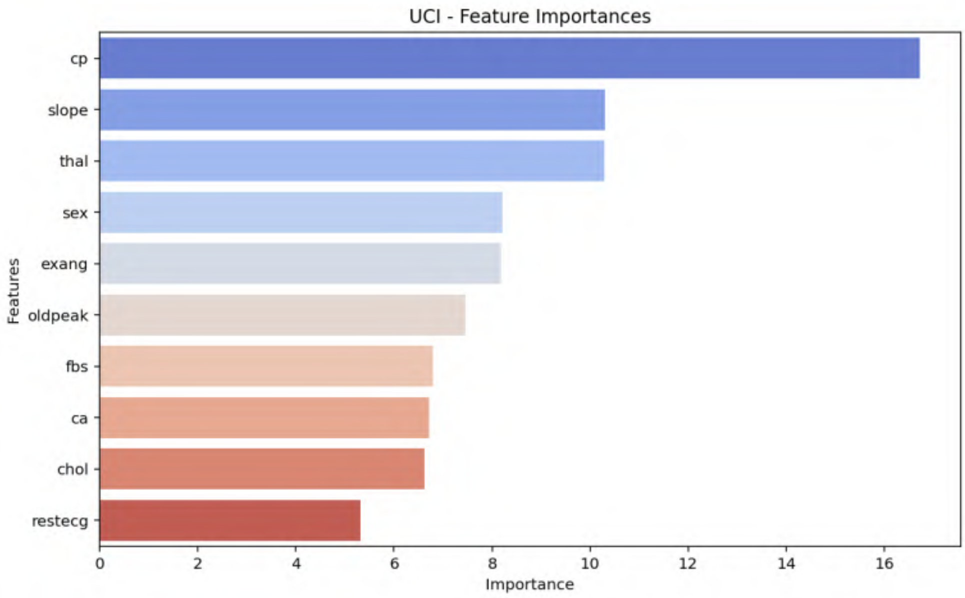

Figure 5. Feature importance levels of UCI dataset

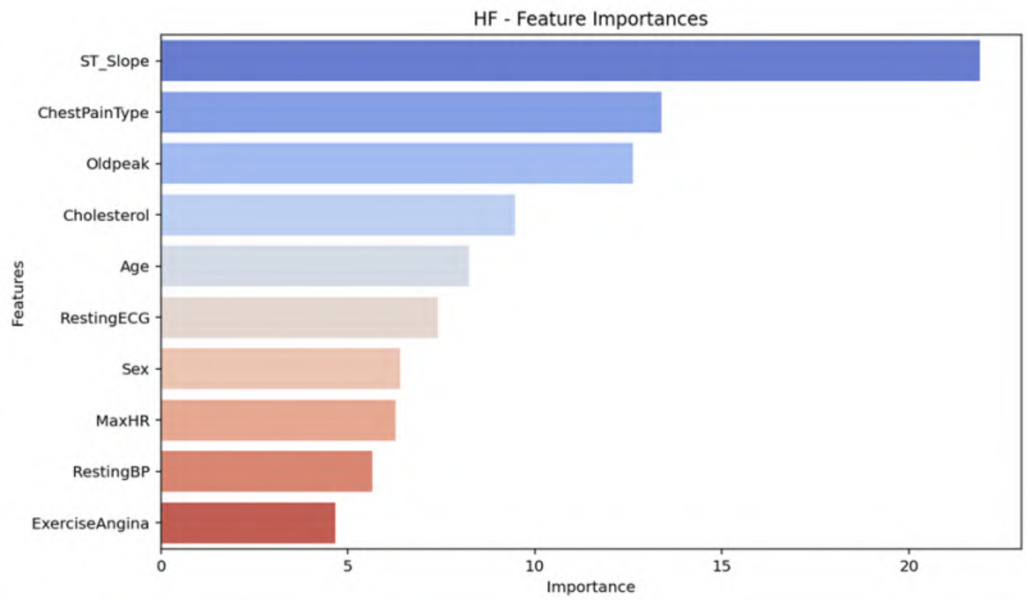

Figure 6. Feature importance levels of HF dataset

Figures 5, 6, and 7 visualize the feature importance rankings in the model for each dataset. For the UCI dataset, as shown in Figure 5, the "cp" (chest pain type) feature holds the highest importance at 16.72%. This is followed by "slope" (10.30%) and "thal" (10.29%). Other significant features include "sex" (gender) and "exang" (exercise-induced angina). These ranking reveals that, in predicting heart disease, both physical symptoms and factors related to physical activity play a crucial role.

In Figure 6, the feature importance ranking for the HF dataset assigns the highest importance to the "ST_Slope" feature (21.91%). This is followed by "ChestPainType" (13.39%) and "Oldpeak" (12.63%). In the HFR dataset, alongside traditional medical parameters such as age, gender, and resting ECG, exercise-related features also hold significant importance.

Finally, in Figure 7, when examining the feature importance ranking for the Cleveland dataset, the "ca" feature holds the highest importance at 14.64%, followed by "cp" (chest pain type) and "thal" (thalassemia) at 11.50% and 9.81%, respectively. In the Cleveland dataset, it is evident that features related to vascular health have a crucial role in the diagnosis of heart diseases, enhancing the predictive power of the model.

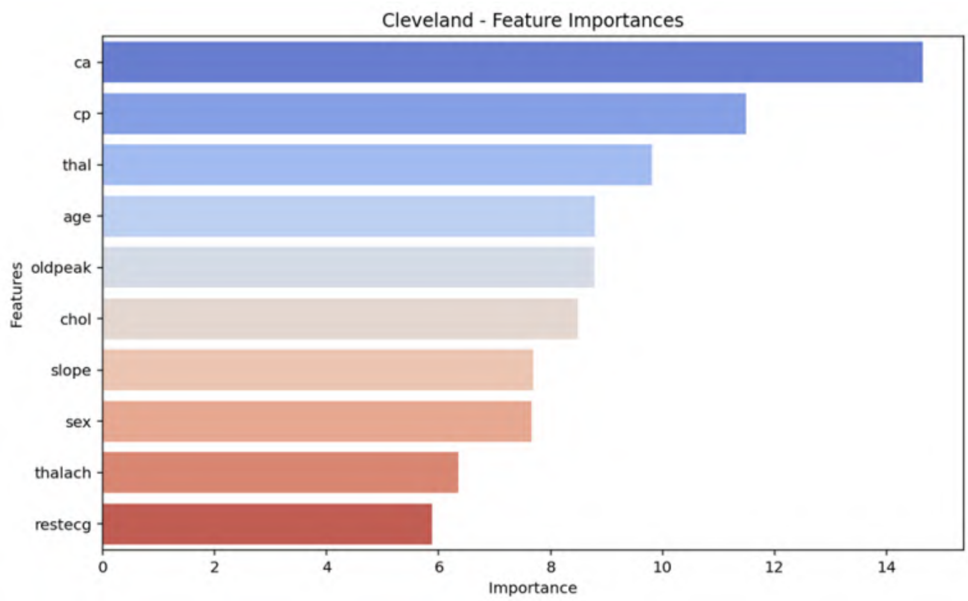

Figure 7. Feature importance levels of Cleveland dataset

These feature importance rankings help us understand that each dataset assigns different weights to the contribution of various features in the model, and they provide insight into which parameters play a critical role in predicting heart diseases.

Conclusion

This study was conducted to analysis the performance of the CatBoost ML algorithm on different datasets for predicting heart diseases and to compare the findings obtained in this regard. Based on the literature review and previous studies, the early diagnosis of critical health conditions such as heart diseases is of great importance for determining appropriate treatment processes and improving the quality of life of patients. This study calculated the predictive effectiveness of the CatBoost algorithm on the UCI, HF, and Cleveland datasets, and a comparative analysis was performed using various performance metrics.

The results obtained in this study demonstrate that the CatBoost algorithm performs successfully with high accuracy rates on all three datasets. The accuracy rate for the UCI dataset was found to be 84.24%, for the Heart Failure dataset 88.59%, and for the Cleveland dataset 85.25%. Furthermore, in all three datasets, the model's other performance metrics were found to be remarkably high, indicating that the model is a strong tool for predicting heart diseases. This further highlights the importance of factors such as dataset size, data type, quality, and preprocessing steps in determining model performance.

Performance differences across datasets illustrate how the features used and the nature of the datasets shape the model's success. Notably, features such as "ST_Slope," "ChestPainType," and "Oldpeak" were found to be of high importance in the HFP dataset, while features like "cp" in the UCI. dataset and "ca" in the Cleveland dataset were more dominant. These findings show that the model focuses on different features depending on the unique structure of each dataset, and the prediction power is shaped by these factors.

In conclusion, this study proves that the CatBoost algorithm is an effective model for predicting heart diseases. Moreover, the comparisons made across different datasets reveal the impact of dataset-specific features and preprocessing steps on model performance. These findings demonstrate how ML-based methods can be beneficial in the healthcare sector, especially in the early diagnosis of critical health conditions such as heart diseases. In future studies, comparing the performance of broader datasets and other ML algorithms can help build more comprehensive and reliable health prediction models.

Scientific Ethics Declaration

* The author declares that the scientific ethical and legal responsibility of this article published in EPSTEM journal belongs to the author.

Conflict of Interest

* The author declares that there is no conflict of interest.

Funding

* This research received no specific grant from any funding agency in the public, commercial, or not-for-profit sectors.

Acknowledgements or Notes

* This article is an updated and extended version of the abstract presented orally at the International Conference on Research in Engineering, Technology and Science (www.icrets.net) held in Peja/Kosovo on July 10-13, 2025.

References

Ahsan, M.M., Luna S.A., & Siddique Z. (2022). Machine-learning-based disease diagnosis: A comprehensive Review. *Healthcare (Basel)*, *10*(3), 541.

Bishop, C. M. (2006). *Pattern Recognition and Machine Learning*. New York NY: Springer.

Bottou, L. (2010). Large-scale machine learning with stochastic gradient descent**.** *Proceedings of COMPSTAT*, pp.177-186.

Cosar, M. (2024). Utilizing the eXtreme gradient boosting algorithm for artificial intelligence-supported learning analytics application. *The Eurasia Proceedings of Science, Technology, Engineering & Mathematics (EPSTEM)*, *28*, 277-285.

Géron, A. (2019). *Hands-on machine learning with scikit-learn, keras, and tensorflow* (2nd ed.). O'Reilly Media.

Janosi, A., Steinbrunn, W., Pfisterer, M., & Detrano, R. (1989). *Heart disease (Dataset)*. UCI Machine Learning Repository.

Kanagarathinam, K., Sankaran, D., & Manikandan, R. (2022). Machine learning-based risk prediction model for cardiovascular disease using a hybrid dataset. *Data & Knowledge Engineering, 140*, 102042.

Kumar, R., Garg, S., Kaur, R., Johar, MGM., Singh, S., Menon S.V., Kumar, P., Hadi A.M., Hasson S.A. & Lozanović J. (2025). A comprehensive review of machine learning for heart disease prediction: Challenges, trends, ethical considerations, and future directions. *Frontiers Artificial Intelligence*, *8*, 1583459.

Mahalakshmi, N.V., & Rout, R.K. (2025). Hyper tuning hybrid MLP-CatBoost classifier using Mayfly optimization for detection of heart disease. *Health Services and Outcomes Research Methodology,* 1-23.

Nagavelli, U., Samanta D., & Chakraborty, P. (2022). Machine learning technology-based heart disease detection models. *Journal of Healthcare Engineering*, 7351061.

Poolsawad, N., Moore, L., Kambhampati, C., Cleland, J. G. F., & et al. (2014). Issues in the mining of heart failure datasets. *International Journal of Automation and Computing, 11*(2), 162–17

Prokhorenkova, L.V., Gusev, G., Vorobev, A., Dorogush, A.V., & Gulin, A. (2018). CatBoost: Unbiased boosting with categorical features. *Proceedings of the 32nd International Conference on Neural Information Processing Systems*, 31.

Sultan, S. Q., Javaid, N., Alrajeh, N., & Aslam, M. (2025). Machine learning-based stacking ensemble model for prediction of heart disease with explainable ai and k-fold cross-validation: A symmetric approach. *Symmetry*, *17*(2), 185.

WHO. (2025). *Cardiovascular diseases (CVDs) fact sheet*. World Health Organization.

Zhou, C., Dai, P., Hou, A, Zhang, Z. Liu, L. Li, A. & Wang, F. (2024). A comprehensive review of deep learning-based models for heart disease prediction. *Artificial Intelligence Review*, *57*(10), 263.

Author(s) Information

Mustafa Coşar
Hitit University, Department of Computer Engineering,
19030, Corum/Turkiye
Contact e-mail: *mustafacosar@gmail.com*

To cite this article:

Cosar, M. (2025). A comparative analysis of dataset performance in disease prediction via machine learning algorithm. *The Eurasia Proceedings of Science, Technology, Engineering and Mathematics (EPSTEM), 35,* 29-37.

The Eurasia Proceedings of Science, Technology, Engineering and Mathematics (EPSTEM), 2025

Volume 35, Pages 38-45

ICRETS 2025: International Conference on Research in Engineering, Technology and Science

Improving Preventive Maintenance of Machinery Using Count Lifetime

Raphipat Chuaitakhu
Suranaree University of Technology

Pornsiri Jongkol
Suranaree University of Technology

Abstract: This project developed an integrated system that enabled equipment to autonomously count and monitor the service lifetime of internal machine components, thereby assessing their condition in real time and determining optimal maintenance intervals. By embedding this functionality into the equipment, the system facilitated proactive decision-making for maintenance activities before component failure occurs. Furthermore, a preventive maintenance system was designed, installed, and calibrated to automatically inspect, detect, and issue alerts when any component approached or exceeded its designated service lifespan. This predictive capability significantly reduced the likelihood of unexpected breakdowns, minimizes potential damage, and ultimately shortens machine downtime. The system was implemented and tested in a case study factory specializing in the production of electronic parts. Quantitative data were collected during both the pre-implementation period and after the system was fully operational. The comparison of these datasets allowed for an evaluation of the system's impact on production continuity and maintenance efficiency. This research, adopting a quantitative methodology, enhanced preventive maintenance practices and improved overall manufacturing performance through more accurate and timely maintenance scheduling.

Keywords: Preventive maintenance, Count lifetime, Mechanical engineering

Introduction

At present, machinery plays a crucial role in the production process by enhancing efficiency and speed. Without proper maintenance, malfunctions may occur, affecting both product quality and delivery timelines. Therefore, maintaining machines in optimal working condition is essential to ensure continuous and efficient production operations. (Rungruang, 2009). It has been found that systematic maintenance planning can significantly reduce operational costs, lower labor expenses, and minimize machine downtime for repairs. However, key challenges commonly encountered in the maintenance process include the uncertainty in predicting the lifespan and deterioration rate of machinery or its components, the use of ineffective maintenance plans, and the high costs associated with repair processes.

This study focused on applying preventive maintenance to Integrated Measurement System (IMS) machines, which play a critical role in the production process of the case study factory, a manufacturer of electronic components. The IMS machines were utilized in the final stage of production before products were delivered to customers. These machines required extended periods of downtime for preventive maintenance, which adversely affected production efficiency and may cause delays in product delivery.

There were three IMS machines in operation, each of which required periodic preventive maintenance to ensure continuous and efficient performance. Data on machine downtime for preventive maintenance was collected over a five-month period, from July to December 2024. The findings revealed that the three IMS machines experienced an average downtime of 186.33 minutes per machine for preventive maintenance, which was considered relatively

- Selection and peer-review under responsibility of the Organizing Committee of the Conference

lengthy. This prolonged downtime had a direct impact on the overall production process, particularly in terms of operational efficiency and production costs.

Therefore, the objective of this study was to improve the efficiency of maintenance operations by enhancing the preventive maintenance process for three Integrated Measurement System (IMS) machines, which were critical components in the production line. The research focused on improving the most time-consuming inspection items, which served as a model for developing a more efficient maintenance system. This improvement aimed to reduce machine downtime and increase the availability rate of the machines.

Related Theories and Research

Maintenance

Maintenance is a critical process in the industrial sector that ensures machines operate efficiently, prevents equipment failure, reduces production downtime, and extends the service life of machinery. It contributes to improved product quality, reduced operational costs, and enhanced organizational competitiveness. Effective maintenance emphasizes systematic inspection, repair, and upkeep to ensure safety, reliability, and long-term efficiency in production processes (Limprasert, 2008).

The Role of Maintenance in Industry

Maintenance plays a vital role in enhancing production efficiency, minimizing losses, errors, and costs. To achieve this, appropriate maintenance planning is essential, including the use of data management systems to analyze failure causes and the effective allocation of resources. Preventive maintenance should be carried out according to relevant standards, considering aspects such as system management, team responsibilities, and equipment complexity. Additionally, clear planning regarding tasks, resources, and budgets must be established (Inseemeesak, Jatunitanon & Kunghun, 2021).

Planned Maintenance

Preventive maintenance refers to the proactive and regular care of machinery to reduce the risk of breakdowns or unscheduled stoppages. It focuses on inspections, adjustments, and the replacement of worn components before issues arise. Maintenance schedules are typically derived from manufacturer manuals, maintenance histories, and actual usage patterns, ensuring maximum maintenance effectiveness. In general, preventive maintenance can be categorized into three main types (Phonphoem, 2019).

1. Time-Based Maintenance (TBM): Maintenance or part replacement is carried out at predetermined intervals, suitable for components that degrade over time.
2. Condition-Based Maintenance (CBM): Equipment is monitored during operation using sensor data, and maintenance is performed only when abnormalities are detected.
3. Predictive Maintenance (PdM): Detailed inspections are conducted at scheduled intervals, often involving disassembly to detect wear and replace parts before failure occurs.

Remaining Useful Life (RUL) prediction of bearings-critical components in the drive systems of pharmaceutical manufacturing machinery. The approach leverages high-frequency vibration signals obtained from sensors, combined with data processing using AutoEncoders, a type of deep learning model designed for dimensionality reduction and anomaly detection.

The methodology begins with the installation of vibration sensors to continuously collect signals during various stages of machine operation. An AutoEncoder model is then trained to learn the normal operational patterns of the equipment. When deviations from these patterns (anomalies) are detected, the system flags them in real-time. These anomaly indicators are further analyzed using trend analysis techniques to predict when degradation or failure of the bearing is likely to occur. This predictive capability is particularly valuable in planning preventive maintenance, as it helps minimize unexpected downtime and reduces the risk of severe machine failure.

The conceptual foundation presented in this research is directly relevant to the current study, which aims to enhance preventive maintenance by tracking the operational life of internal machine components. While the current study employs a simpler method-such as tracking the number of cycles or operational hours-the underlying principle is similar: to estimate the usable lifespan of machine parts and perform maintenance before failure occurs. This aligns with the broader strategy of Predictive Maintenance (PdM).

The methodology introduced by Juodelyte et al. can serve as a foundation for future enhancement of the current system, particularly through the integration of real-time sensor data to assess actual wear conditions instead of relying on fixed thresholds. Furthermore, incorporating artificial intelligence (AI) and machine learning (ML) techniques into the analysis of long-term operational data could significantly improve accuracy and facilitate the transition toward a more intelligent and autonomous maintenance management system (Juodelyte, Cheplygina, Graversen & Bonnet, 2022).

Method

Proposed Methodology and System Model

To establish a standardized approach for preventive maintenance of machinery, this study developed a component life-cycle monitoring system that utilizes machine-based tracking and management. The system enabled accurate monitoring of component usage and facilitated the scheduling of part replacements in a timely and effective manner. The system began by setting the expected lifespan of each component, along with a pre-defined threshold for early warning notifications. As the machine operates, the system continuously tracked the usage duration of each component. When a component reaches 80% of its designated lifespan, the system issued a warning message, allowing maintenance personnel to prepare for part replacement in advance. Once the component reached its full lifespan, the machine automatically stopped operating to allow for replacement. After the part was replaced, the system reset the usage counter to zero. This process ensured more effective maintenance practices and reduced the risk of machine failure due to worn components. The system's operational flowchart is shown in Figure 1.

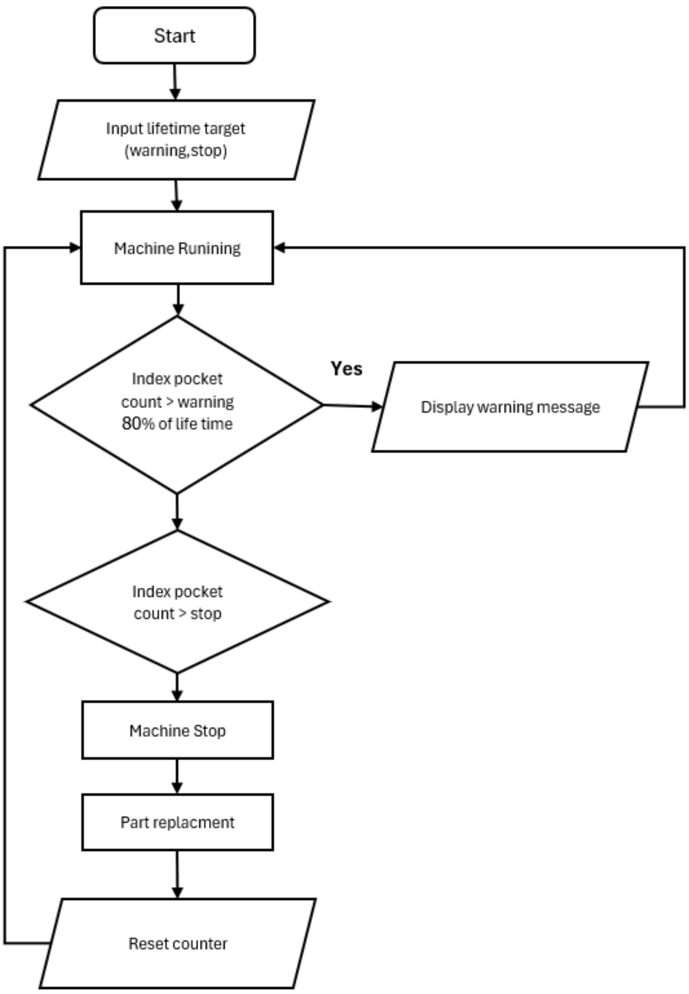

Figure 1. Working diagram of the life cycle system

Implementation

In this study, the developed preventive maintenance system was installed and tested on IMS machines. The system included a component life tracking mechanism that enabled monitoring and early warning notifications before a component reached its end-of-life threshold. The responsible maintenance technicians were trained on how to use the system, including operating procedures, inspection protocols upon reaching the defined threshold, and the advantages of the system in supporting proactive and systematic maintenance planning. This system helped reducing the risk of unexpected machine failures and minimizes unnecessary downtime for repairs. When the system alerted that a component was nearing the end of its lifespan, maintenance staff prepared and scheduled replacement at an appropriate time. Usage data was continuously recorded to monitor system performance, analyze potential failure trends, and provide valuable input for future maintenance planning. The system interface for tracking component lifespan is shown in Figure 2. The warning screen indicating that the lifespan is nearing its limit is presented in Figure 3, and the final warning screen upon reaching the end of the component lifespan is shown in Figure 4.

Figure 2. Part life count display screen

Figure 3. Notification when the specified expiration date is approaching

Figure 4. Warning on screen when expiration date

Effectiveness Evaluation

Assessment of Preventive Maintenance System Improvement

After implementing the improved preventive maintenance system and completing data collection, the system's effectiveness is evaluated using the following key performance indicators (Arkararungraingkul and Chandrangsi, 2009)

1. Machine Downtime – The amount of time lost due to machine stoppages, measured in minutes, as recorded in the system.
2. Mean Time to Repair (MTTR) – Refers to the average time required to repair a machine after a failure occurs. This is calculated by averaging the total repair time across all incidents. The MTTR can be computed using Equation (1).

$$\text{Mean Time To Repair} = \frac{Tme\ machine\ stops}{Number\ of\ times\ the\ machine\ stops} \qquad (1)$$

$$Availability\ Rate = \frac{Loading\ Time}{Operation\ Time} \qquad (2)$$

Where:

Operation Time	=	Loading Time − Machine Downtime	(3)
Loading Time	=	Shift Working Time − Planned Downtime	(4)
Planned Downtime	=	Scheduled Machine Downtime + Scheduled Break Time	(5)

These equations define the key components for calculating the Availability Rate, where operation time accounts for the actual productive period by subtracting unplanned stoppages, and loading time is derived from total shift hours excluding planned non-operating periods such as scheduled maintenance or operator breaks.

Results and Discussion

The results of data collection for comparing performance before and after the implementation of the component life-tracking system within the machinery revealed the following:

Table 1 presents a comparison of the average machine downtime before and after the implementation of the component life-tracking system in IMS machines. The results indicated a significant reduction in downtime across all three machines. Specifically, the average downtime of IMS No.1 decreased from 190 to 120 minutes, representing a 36.84% reduction. IMS No.2 saw a reduction from 186 to 119 minutes (36.02%), and IMS No.3 from 183 to 119 minutes (34.97%). These findings demonstrated the effectiveness of the implemented system in minimizing unplanned stoppages and improving operational continuity.

Table 1. Down time

Machine	Average Time Before Action	Average Time After Operation	Percentage Decreased
IMS No.1	190	120	36.84%
IMS No.2	186	119	36.02%
IMS No.3	183	119	34.97%

Table 2 presents a comparison of the Mean Time to Repair (MTTR) for each IMS machine before and after the implementation of the component life-tracking system. The results showed a notable decrease in the average repair time. For IMS No.1, the MTTR was reduced from 93.4 to 60 minutes, reflecting a 35.76% reduction. IMS No.2 showed a decrease from 92.9 to 59.5 minutes (35.95%), and IMS No.3 from 92.2 to 59.5 minutes (35.47%). These reductions clearly demonstrated the effectiveness of the system in streamlining maintenance activities and minimizing machine downtime.

Table 2. Mean time to repair (MTTR)

Machine	MTTR Before Operation (Minutes)	MTTR After operation (minutes)	Percentage Decreased
IMS No.1	93.4	60	35.76%
IMS No.2	92.9	59.5	35.95%
IMS No.3	92.2	59.5	35.47%

Table 3 shows a comparison of the Availability Rate for each IMS machine before and after implementing the component life-tracking system. The results indicated an improvement in machine availability across all three units. IMS No.1 saw an increase from 89.2% to 91.5%, equivalent to a 2.58% improvement. IMS No.2 increased from 90.1% to 91.3% (1.33%), while IMS No.3 improved from 90.3% to 91.2% (1.00%). These results demonstrated that the system contributed to higher machine readiness, supporting more continuous and reliable production operations.

Table 3. Availability rate

Machine	Available (%) Before Operation	Available (%) After processing	Percentage Increase
IMS No.1	89.2	91.5	2.58%
IMS No.2	90.1	91.3	1.33%
IMS No.3	90.3	91.2	1.00%

Conclusion

This research was conducted with the primary objective of enhancing the operational efficiency of the maintenance department by improving the preventive maintenance approach for Integrated Measurement System (IMS) machines. These machines, which played a critical role in the final stage of the production process at the case study factory, were frequently subject to extended downtime due to reactive or unsystematic maintenance procedures.

To address this issue, a component life-tracking system was developed and implemented as a key part of the preventive maintenance strategy. The system was designed to monitor the operational lifespan of internal machine components, providing early notifications for scheduled part replacements. This allowed maintenance teams to proactively plan and carry out maintenance activities, rather than relying on reactive methods after failures occurred.

After implementation, the effectiveness of the new system was evaluated based on three key performance indicators: average downtime, mean time to repair (MTTR), and machine availability rate. The results demonstrated a clear improvement in all measured areas. Specifically, the average downtime was reduced from 186.33 minutes to 119.33 minutes, marking a 35.95% decrease. The mean time to repair (MTTR) also dropped from 92.83 minutes to 59.67 minutes, a reduction of 35.73%. Additionally, the availability rate improved from 89.87% to 91.33%, indicating a 1.64% increase in machine readiness for production.

These outcomes confirm that the application of a component life-tracking system in preventive maintenance planning is both practical and effective. Not only did it reduce unplanned downtime and repair durations, but it also alleviated the burden on maintenance personnel by minimizing the need for repeated manual inspections. Furthermore, it helped reduce indirect costs related to production delays and unnecessary part replacements.

In conclusion, this study demonstrates that incorporating automated tracking and data-driven maintenance strategies can significantly improve the reliability, efficiency, and cost-effectiveness of preventive maintenance processes in industrial environments. The developed system serves as a replicable model for similar applications in other manufacturing contexts and offers a foundation for future enhancements, including predictive maintenance and IoT integration.

Recommendations

A major strength of this research lies in the application of a component life-tracking system to improve the efficiency of preventive maintenance. The system clearly contributed to the reduction of machine downtime and repair time (MTTR), while enhancing machine availability. To further develop and expand upon the results of this study, the following recommendations are proposed for future research and practical implementation:

- Integration with IoT and cloud-based systems: If the component life-tracking system is integrated with Internet of Things (IoT) technology or real-time cloud-based monitoring, it will allow the maintenance department to plan and respond more rapidly. This would facilitate a transition toward smart maintenance and ultimately enable predictive maintenance.
- Development of visualization and dashboard interfaces: To enhance user-friendliness and operational clarity, it is recommended to develop a visual monitoring interface or dashboard that displays component usage data through intuitive graphics, color-coded alerts, or visual cues. This can minimize interpretation errors and support faster decision-making.
- Predictive modeling using artificial intelligence and machine learning: With sufficient long-term operational data, machine learning techniques could be employed to analyze wear patterns of specific components. This would enable accurate prediction of failure trends and support the development of a more precise, data-driven preventive maintenance strategy-further advancing toward predictive maintenance practices.

These recommendations positively elevate the current system into a more intelligent and autonomous solution, ultimately supporting greater reliability, cost-efficiency, and productivity in industrial maintenance operations.

Scientific Ethics Declaration

* The authors declare that the scientific ethical and legal responsibility of this article published in EPSTEM journal belongs to the authors.

Conflict of Interest

* The authors declare that they have no conflicts of interest

Funding

* This research received no specific grant from any funding agency in the public, commercial, or not-for-profit sectors.

Acknowledgements or Notes

* This article was presented as an oral presentation at the International Conference on Research in Engineering, Technology and Science (www.icrets.net) held in Peja/Kosovo on July 10-13, 2025.

References

Akkararungruangkul, R., & Chantararungsee, S. (2009). Setting of preventive maintenance system for improving machine efficiency. In Kasetsart University (Ed.), *Proceedings of the 47th Kasetsart University Annual Conference: Architecture and Engineering*, 152–159. The Thailand Research Fund.

Inseemeesak, B., Jarunitanon, P., & Kunghun, W. (2021). Preventive maintenance for machinery: A case study of automotive seat manufacturing company. *SAU Journal of Science & Technology, 7*(1), 1–14.

Juodelyte, D., Cheplygina, V., Graversen, T., & Bonnet, P. (2022). Predicting bearings degradation stages for predictive maintenance in the pharmaceutical industry. *Proceedings of the 28th ACM conference on knowledge discovery and data mining*, 3107-3115 .

Limprasert, S. (2008). *Improvement of preventive maintenance process: A case study of fiber optic fusion splicing machine* (Master's thesis). Thammasat University.

Phonphoem, P. (2019). *Improvement of preventive maintenance system in animal food packaging process using failure mode and effects analysis (FMEA)* (Master's thesis). Burapha University

Rungreong, K. (2009). *Preventive maintenance planning for machinery in the relay industry* (Master's thesis). Dhurakij Pundit University.

Author(s) Information

Raphipat Chuaitakhu
Institute of Engineering, Suranaree University of Technology, 111, University Avenue, Suranaree Sub-district, Muang, Nakhon Ratchasima 30000 Thailand.
Contact e-mail: *m6602734@g.sut.ac.th*

Pornsiri Jongkol
Institute of Engineering, Suranaree University of Technology, 111, University Avenue, Suranaree Sub-district, Muang, Nakhon Ratchasima 30000 Thailand.

To cite this article:

Chuaitakhu, R. & Jongkol, P. (2025). Improving preventive maintenance of machinery using count lifetime. *The Eurasia Proceedings of Science, Technology, Engineering and Mathematics (EPSTEM), 35,* 38-45.

The Eurasia Proceedings of Science, Technology, Engineering & Mathematics (EPSTEM)
ISSN: 2602-3199

The Eurasia Proceedings of Science, Technology, Engineering and Mathematics (EPSTEM), 2025

Volume 35, Pages 46-54

ICRETS 2025: International Conference on Research in Engineering, Technology and Science

ELIF: An End-to-End Architecture for an Observable and Continuously Learning AI Assistant

Eren Caglar
Aktif Investment Bank Inc.

Mustafa Keles
Aktif Investment Bank Inc.

Mehmet Kutanoglu
Aktif Investment Bank Inc.

Muhammet Demir
Aktif Investment Bank Inc.

Abstract: This paper details the end-to-end design and implementation of "ELIF," an enterprise-ready AI assistant for corporate knowledge management. The system is engineered to provide verifiable and accurate information to bank representatives by utilizing a Retrieval-Augmented Generation (RAG) framework. The knowledge base is built upon both static corporate documents (PDF, web content, JSON, Excel, PPTX) and dynamic user feedback. Its modular architecture, built on Python/Flask and orchestrated by LangGraph, ensures scalability and maintainability. A key engineering achievement is the closed-loop continuous learning pipeline. User feedback is not merely logged but is actively processed by a Large Language Model (LLM) to generate structured Q&A data. This data autonomously enriches a FAISS vector database, allowing the system to learn from interactions without manual intervention. The solution includes comprehensive user and admin interfaces built with React, offering features like performance analytics, chat history monitoring, and manual training triggers. Deployed via a REST API and integrated into Microsoft Teams, ELIF serves as a practical blueprint for building, deploying, and maintaining observable, self-improving AI systems in a corporate environment.

Keywords: Artificial intelligence, Retrieval-augmented generation, Large language models, Continuous learning, Knowledge management

Introduction

The digital transformation of the financial sector has led to an exponential increase in the volume and complexity of internal corporate knowledge. For institutions like banks, providing employees with rapid and accurate access to information regarding products, services, and compliance procedures is paramount for operational efficiency and service quality. However, this knowledge is often trapped in disparate silos and unstructured formats, leading to significant productivity losses. While enterprise chatbots were introduced as a potential solution, first-generation systems have largely failed to meet expectations (Adamopoulou & Moussiades, 2020). Their primary limitations include: (i) an inability to provide verifiable, source-grounded answers, often leading to factual inaccuracies or "hallucinations"; (ii) a lack of domain-specific understanding, rendering them ineffective in specialized fields like banking; and (iii) a critical "empathy deficit," where rigid, impersonal responses result in poor user experience and adoption rates. Furthermore, concerns regarding data privacy and security in the handling of sensitive corporate information pose a significant barrier to their widespread implementation.

- Selection and peer-review under responsibility of the Organizing Committee of the Conference

This paper introduces ELIF (End-to-end Learning and Inference Framework), a comprehensive software architecture and applied AI system designed to overcome these challenges. As the R&D team responsible for its creation, we have engineered ELIF not merely as a question-answering tool, but as a continuously learning, sentiment-aware knowledge partner for enterprise users. Our work presents a multi-faceted approach that integrates state-of-the-art software engineering practices with advanced AI methodologies.

The primary contributions of our research and engineering efforts are threefold: A Hybrid AI Core: We fuse a Retrieval-Augmented Generation (RAG) pipeline, which grounds responses in verified corporate documents (Lewis et al., 2020), with a sophisticated sentiment analysis model. This dual-core design ensures that responses are not only factually accurate but also empathetically appropriate to the user's emotional state. Domain-Specific Model Specialization: We detail the R&D process of fine-tuning open-source Large Language Models (LLaMA 3.1) on a proprietary Turkish banking dataset (Zhang et al., 2022). This specialization allows the model to comprehend and generate nuanced, industry-specific language, a critical step for achieving high fidelity in a corporate context. A Scalable, Modular, and Self-Improving Architecture: We present a robust system built on a microservices architecture, orchestrated with Docker and Kubernetes. This engineering choice ensures scalability and maintainability. More importantly, we introduce an innovative closed-loop continuous learning mechanism that leverages user feedback to autonomously enrich the system's knowledge base, thus creating a truly self-improving system.

Literature Review

The limitations of traditional question-answering (QA) systems have been extensively documented. Chen et al. (2023) and Yu et al. (2024) highlight that LLM-only QA pipelines suffer from hallucination, lack of contextual grounding, and limited interpretability in enterprise applications. Similarly, Saad-Falcon et al. (2023) and Es et al. (2023) introduce robust evaluation frameworks—ARES and RAGAS, respectively—that expose current RAG systems' inability to consistently retrieve semantically relevant and source-grounded answers.

In the financial sector, recent research has explored domain-specific applications of Retrieval-Augmented Generation (RAG). Iaroshev et al. (2024) evaluate RAG-based architectures on financial documents, establishing benchmarks for financial QA performance. Landolsi et al. (2025) introduce CAPRAG, a hybrid graph-vector pipeline tailored to banking operations, showcasing its advantage over vanilla RAG systems. Choi et al. (2025) contribute the FinDER dataset, enriching the resources available for domain-specific fine-tuning and benchmarking. New research has also emphasized long-context reasoning in QA workflows. Qi et al. (2024) and Gan et al. (2025) propose updated metrics and architecture modifications that enable RAG models to better handle complex and lengthy queries. Guinet et al. (2024) employ Item Response Theory (IRT) to evaluate the robustness and generalizability of RAG under examination-style conditions.

These works collectively form the foundation for our own research in ELIF. In contrast to the above systems, ELIF introduces a Turkish-language, banking-specific fine-tuned LLM integrated with real-time sentiment analysis and autonomous feedback learning. This positions ELIF as a novel contribution to both the practical and academic development of intelligent, adaptive QA systems for enterprise use.

Motivation and Strategic Impact

The development of ELIF was driven by a strategic need to transcend the limitations of existing enterprise tools and create tangible value across multiple domains. The anticipated outcomes of this R&D project are not confined to internal efficiency gains but extend to national and international contributions.

Corporate Benefits

From a corporate perspective, ELIF is engineered to deliver a distinct competitive advantage. By providing a platform that not only delivers information but also analyzes user sentiment and experience, our organization will accumulate invaluable knowledge in applied AI for customer and employee interactions. This capability directly translates into higher user satisfaction and a more responsive internal support ecosystem. The system's ability to reduce information retrieval times and streamline workflows will lead to measurable productivity increases across various departments.

National Contributions

On a national scale, this project addresses a notable gap in the domestic technology market, where sentiment-aware, enterprise-grade AI assistants are scarce (Ribeiro et al., 2016). By developing this technology locally, we are contributing to the national innovation ecosystem. We anticipate that the novel architectural patterns and machine learning methodologies developed during this project will be eligible for patent applications, thereby protecting and valorizing domestically produced intellectual property. Furthermore, the successful deployment of ELIF in critical sectors like call centers will serve as a benchmark, potentially increasing employee performance and overall corporate success on a national level.

International Academic Contributions

Our commitment extends to contributing to the global scientific community. The findings from our research, particularly in the areas of domain-specific LLM fine-tuning and the practical application of sentiment analysis in RAG pipelines, are of significant interest. We plan to disseminate our results, including methodologies and performance benchmarks, through publications in peer-reviewed international conferences and journals, fostering further research and development in the field of applied AI.

Novelty and Competitive Landscape

The innovative nature of ELIF lies in its unique synthesis of multiple advanced features, which are not collectively present in current market offerings. Key Innovations Sentiment-Aware RAG Pipeline: Unlike traditional RAG systems that are truthfulness-focused, ELIF integrates a real-time sentiment analysis module directly into its response generation loop, allowing it to modulate its tone and provide empathetic responses. User-Driven Knowledge Enrichment: The system empowers non-technical users to directly contribute to the knowledge base by uploading documents through a secure 'drive' interface, a feature that democratizes and accelerates the training process. Department-Specific Modularity: The architecture is designed for multi-tenancy, allowing different business units within the organization to maintain and train their own discrete knowledge bases and chatbot personas, ensuring data segregation and contextual relevance. Autonomous Learning from Feedback: The closed-loop feedback mechanism, which uses an LLM to interpret and structure user corrections, enables the system to learn and improve autonomously, reducing the manual MLOps overhead (Wu et al., 2022).

Methodology and Success Criteria

The ELIF project was executed with a rigorous R&D methodology centered on three core pillars. Each pillar had a defined objective, a clear experimental procedure, and a set of quantifiable success criteria to measure its outcome. This approach ensures that each component of the system is not only conceptually sound but also empirically validated.

R&D Focus 1: Domain-Specific LLM Fine-Tuning

Objective: To overcome the limitations of general-purpose Large Language Models (LLMs) in understanding and generating the specific terminology, context, and nuances of the Turkish banking sector.

Methodology: Our methodology involved the fine-tuning of a powerful open-source foundation model, LLaMA 3.1. We curated a proprietary dataset comprising a wide range of internal documents, including product manuals, policy documents, and anonymized customer-representative dialogues. The model was integrated into a Retrieval-Augmented Generation (RAG) pipeline to ensure all generated text was grounded in verified source documents.

Success Criteria: The performance of the fine-tuned model was benchmarked using the BLEU score (Papineni et al., 2002). Target: BLEU > 0.6

R&D Focus 2: Transformer-based Sentiment Analysis

Dataset Specifications: The proprietary dataset used to fine-tune ELIF's LLaMA 3.1 model consists of approximately 1.2 million entries, encompassing both structured and unstructured content from the Turkish banking sector. This includes anonymized customer-representative chat transcripts, internal policy documents, product manuals, regulatory documents, and FAQ-style data. The dataset is multilingual but primarily in Turkish and was cleaned, standardized, and converted into formats such as plain text (.txt), JSON, and CSV for training purposes.

Annotation & Labeling: Each entry was manually or semi-automatically annotated to extract question–answer (QA) pairs and sentiment labels. In total, the dataset includes over 400,000 labeled QA pairs and 50,000 sentiment-tagged utterances categorized into positive, neutral, or negative classes. Annotation guidelines were designed by domain experts to ensure fidelity in capturing banking-specific terminology and context.

Anonymization: To preserve data privacy, all customer identifiers, financial account details, and institution-specific sensitive metadata were fully anonymized using named entity recognition (NER) pipelines and manual audits.

Diversity & Distribution: Data was collected from more than 8 different departments (e.g., retail banking, corporate finance, compliance) to ensure semantic diversity and role-specific linguistic variance, which contributes to ELIF's high contextual adaptability in production.

Objective: To develop a highly accurate sentiment classification model capable of discerning the emotional tone from user queries in Turkish.

Methodology: We explored transformer-based models such as DistilBERT and RoBERTa (Liu et al., 2019), training them on a custom labeled dataset of user interactions.

Success Criteria: Sentiment Classification Accuracy > 85%

R&D Focus 3: Distributed and Scalable Microservice Architecture

Objective: To engineer a backend system that is robust, scalable, and maintainable in enterprise environments.

Methodology: We implemented a microservice architecture using Docker and Kubernetes (Leite et al., 2020). Each service-API gateway, RAG, sentiment analysis, feedback processing-was containerized and orchestrated independently.

Success Criteria: - Response Time ≤ 5 seconds - Uptime ≥ 99.9%

System Architecture and Technology Stack

The ELIF system is engineered based on modern software design principles, prioritizing modularity, scalability, and maintainability. The architecture is composed of distinct layers, each responsible for a specific set of tasks, which communicate through well-defined interfaces.

High-Level Architectural Overview

Our system is designed as a set of distributed microservices, providing resilience and independent scaling. It includes a Web Service Layer for communication, an Orchestration Layer for logic, and a Data Persistence Layer for storage. This separation enables clean design and complexity management in AI-driven systems.

Core System Layers

- Orchestration Layer (LangGraph): Manages execution flows via a stateful graph (LangGraph, 2024). Handles task sequencing (e.g., sentiment analysis → retrieval → generation).

- Web Service Layer (Flask): Provides RESTful API endpoints, handling auth, routing, and validation.
- Data Persistence Layer (MongoDB & Azure Blob Storage): MongoDB stores structured data; Azure handles large unstructured documents and FAISS indexes. End-to-End Workflow: A user query goes through sentiment analysis, document retrieval from FAISS, and LLM-based response generation. The result is returned via the Flask API, all within a 5-second latency target.

End-to-End Workflow: A user query goes through sentiment analysis, document retrieval from FAISS, and LLM-based response generation. The result is returned via the Flask API, all within a 5-second latency target.

Technology Stack Summary

- Programming & Core Libraries: Python 3.x, Pandas, NumPy
- AI / ML Frameworks: LangChain, TensorFlow, Keras, Scikit-learn
- NLP & LLM: Hugging Face, NLTK, spaCy, FAISS • LLM: LLaMA 3.1 (fine-tuned)
- Web Framework: Flask
- Databases & Storage: MongoDB, Azure Blob Storage
- Deployment: Docker, Kubernetes
- Cloud Services: Microsoft Azure, Azure OpenAI Service

Risk Analysis and Mitigation Strategies

A proactive approach to risk management is integral to our software engineering methodology. During the development of ELIF, we identified several potential technical challenges and established clear mitigation and contingency plans to ensure project integrity and success.

- Data Integrity: Risk of insufficient data quality. Mitigation: rigorous preprocessing and version control. Contingency: data augmentation and synthetic generation.
- Design Integrity: Risk of logical flaws in architecture. Mitigation: iterative feedback with analysts. Contingency: intermediate result approval checkpoints.
- AI Model Performance: Risk of models underperforming. Mitigation: hyperparameter tuning and dataset enrichment. Contingency: try alternate models or transfer learning.
- System Integration: Risk of integration issues. Mitigation: pre-alignment on formats. Contingency: middleware for translation.
- User Adoption: Risk of low feedback participation. Mitigation: intuitive UI and analytics. Contingency: conduct interviews and surveys.

Conclusion

This paper has presented ELIF, a comprehensive AI system that addresses enterprise knowledge management challenges. We detailed its RAG-based architecture combined with real-time sentiment analysis, domain-specific fine-tuning of LLaMA 3.1, and a scalable microservices infrastructure. The system is self-improving via autonomous feedback processing. Our primary contribution is a holistic architecture that merges cutting-edge AI and engineering practices to form a continuously learning system. Defined success metrics and robust risk management validate the feasibility and reliability of ELIF in production environments.

Future Work: We plan to enhance contextual relevance with improved re-ranking in RAG, evolve ELIF into a proactive task-oriented agent, and explore multi-modal capabilities for document parsing. ELIF represents the beginning of a new paradigm in enterprise AI collaboration.

Scientific Ethics Declaration

* The authors declare that the scientific ethical and legal responsibility of this article published in EPSTEM journal belongs to the authors.

Conflict of Interest

* The authors declare that they have no conflicts of interest.

Funding

* This research received no specific grant from any funding agency in the public, commercial, or not-for-profit sectors.

Acknowledgements or Notes

* This article was presented as an oral presentation at the International Conference on Research in Engineering, Technology and Science (www.icrets.net) held in Peja/Kosovo on July 10–13, 2025.

* We gratefully acknowledge the support and contribution of the Aktif Bank R&D Center throughout the development, implementation, and evaluation of the ELIF system.

References

Adamopoulou, E., & Moussiades, L. (2020). Chatbots: History, technology, and applications. *Machine Learning with Applications, 2,* 100006.

Chen, W., Zhang, Y., Liu, X., & Zhu, J. (2023). Evaluating retrieval-augmented generation models. arXiv preprint *arXiv:2309.01431*.

Choi, K., Lee, J., & Kim, D. (2025). FinDER: A financial dataset for rag evaluation. arXiv preprint *arXiv:2504.15800.*

Es, K., Salazar, J., & Min, S. (2023). RAGAS: Retrieval-augmented generation assessment. arXiv preprint *arXiv:2309.15217*.

Gan, Z., Chen, Y., & Wang, M. (2025). Retrieval-augmented generation evaluation in the era of large language models. arXiv preprint *arXiv:2504.14891*.

Guinet, A., Pillai, R., & Li, X. (2024). IRT-RAG: An item response theory-inspired evaluation of rag systems. arXiv preprint *arXiv:2405.13622*.

Iaroshev, A., Piskorski, J., & Ulan, D. (2024). Evaluating retrieval-augmented generation for financial reports. *Applied Sciences, 14*(20), 9318.

Landolsi, H., Shih, C., & Chan, A. (2025). CAPRAG: Hybrid vector + graph rag for banking qa. arXiv preprint *arXiv:2501.13993.*

LangGraph. (2024). *LangGraph documentation*. Retrieved from https://docs.langchain.com/langgraph/

Leite, L., Rocha, T., & Santos, M. (2020). Microservices architecture in software systems. *IEEE Software, 37*(1), 70–77.

Lewis, M., Liu, Y., Goyal, N., Ghazvininejad, M., Mohamed, A., Levy, O., ... & Zettlemoyer, L. (2020). Retrieval-augmented generation for knowledge-intensive nlp tasks. *Advances in Neural Information Processing Systems, 33*, 9459–9474.

Liu, Y., Ott, M., Goyal, N., Du, J., Joshi, M., Chen, D., ... & Stoyanov, V. (2019). RoBERTa: A robustly optimized bert pretraining approach. arXiv preprint *arXiv:1907.11692*.

Papineni, K., Roukos, S., Ward, T., & Zhu, W. J. (2002). BLEU: A method for automatic evaluation of machine translation. *Proceedings of the 40th Annual Meeting of the Association for Computational Linguistics*, 311–318.

Ribeiro, M. T., Singh, S., & Guestrin, C. (2016). 'Why should i trust you?': Explaining the predictions of any classifier. *Proceedings of the 22nd ACM SIGKDD International Conference on Knowledge Discovery and Data Mining*, 1135–1144.

Saad-Falcon, D., Mukherjee, S., & Ladhak, F. (2023). ARES: An automated evaluation framework for rag systems. arXiv preprint *arXiv:2311.09476*.

Wu, Y., et al. (2022). AutoTrain: Towards automated mlops for continuous learning. *Proceedings of the 28th ACM SIGKDD Conference on Knowledge Discovery and Data Mining*, 1859–1869.

Qi, J., Liu, X., & Wang, Y. (2024). Evaluating long-context and long-form retrieval-augmented generation. arXiv preprint *arXiv:2410.23000.*

Yu, C., Ma, X., Liu, H., & Zhang, Y. (2024). Evaluation of retrieval-augmented generation: A survey. arXiv preprint *arXiv:2405.07437.*

Zhang, Y., Sun, S., Galley, M., Chen, Y. C., Brockett, C., Gao, X., & Dolan, B. (2022). DialoGPT: Large-scale generative pre-training for conversational response generation. arXiv preprint *arXiv:2001.09977.*

Author(s) Information

Eren Caglar
Aktif Investment Bank Inc.
Esentepe District, Kore Şehitleri Street No: 8/1 Şişli
İstanbul, Türkiye

Mustafa Keles
Aktif Investment Bank Inc.
Esentepe District, Kore Şehitleri Street No: 8/1 Şişli
İstanbul, Türkiye
Contact e-mail: *mehmet.Kutanoglu@aktifbank.com.tr*

Mehmet Kutanoglu
Aktif Investment Bank Inc.
Esentepe District, Kore Şehitleri Street No: 8/1 Şişli
İstanbul, Türkiye

Muhammet Demir
Aktif Investment Bank Inc.
Esentepe District, Kore Şehitleri Street No: 8/1 Şişli
İstanbul, Türkiye

To cite this article:

Caglar, E., Keles, M., Kutanoglu, M., & Demir, M. (2025). ELIF: An end-to-end architecture for an observable and continuously learning AI assistant. *The Eurasia Proceedings of Science, Technology, Engineering and Mathematics (EPSTEM), 35,* 46-54.

Appendix

Below are the visual materials for the ELIF system detailed in this paper.

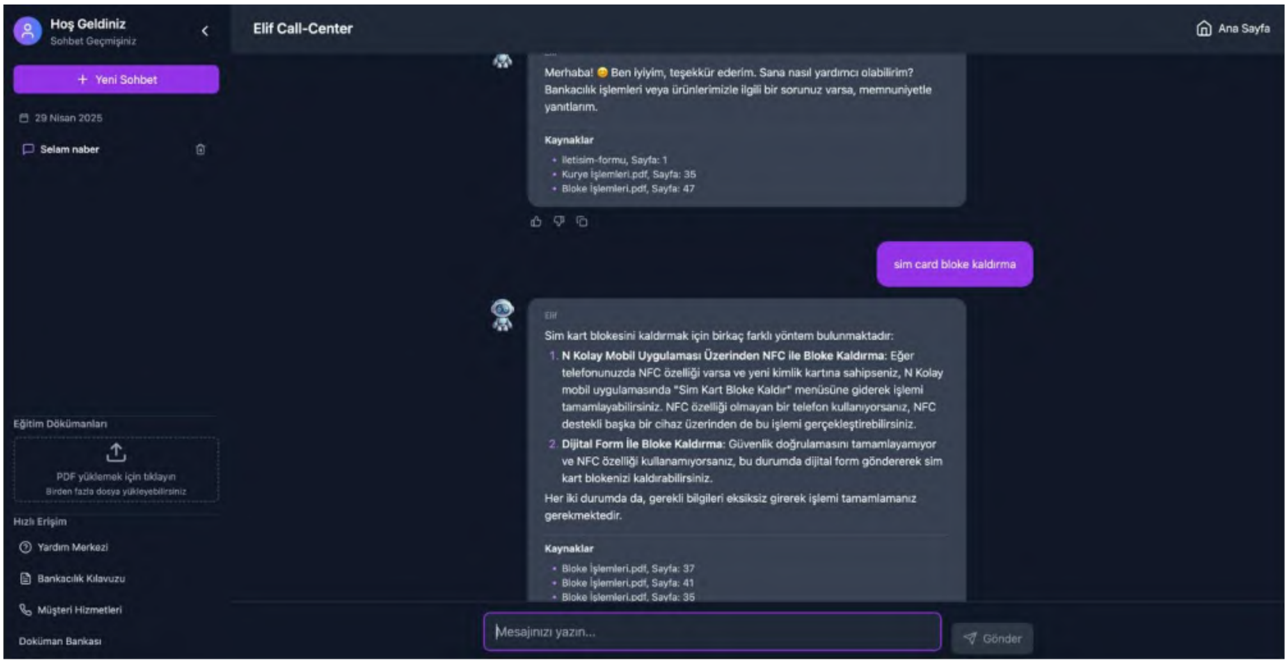

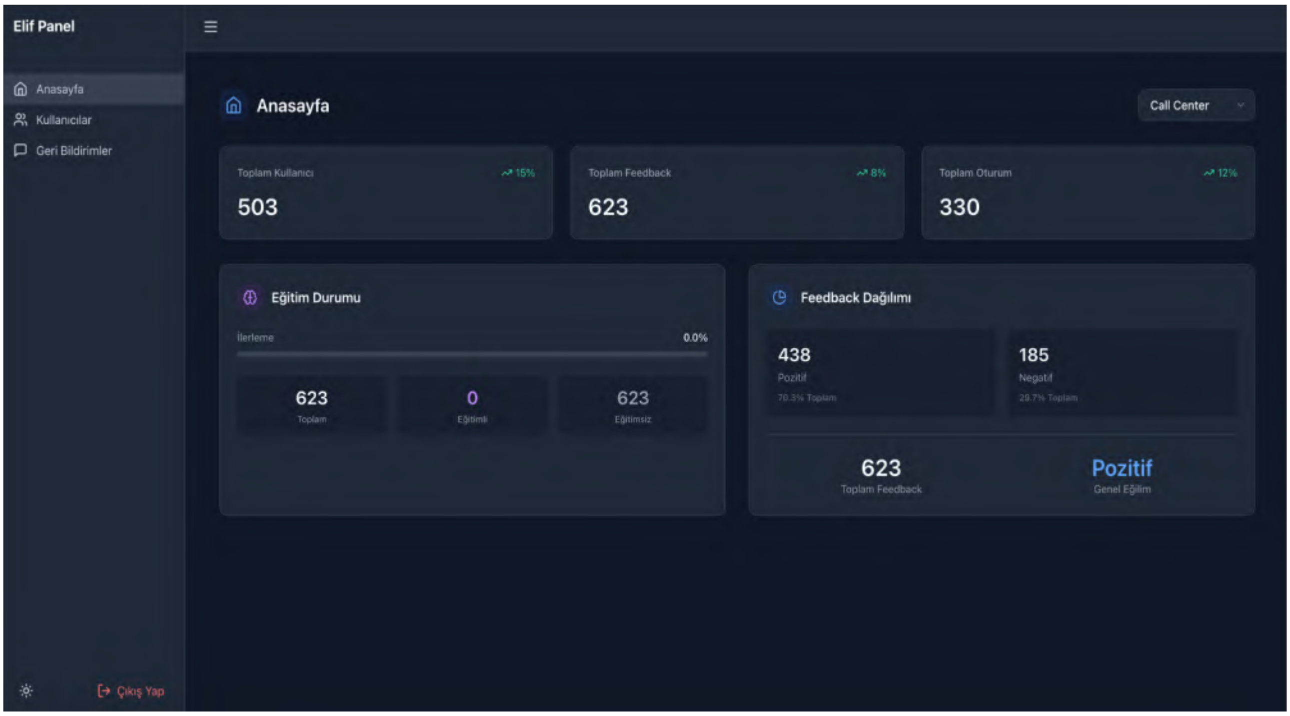

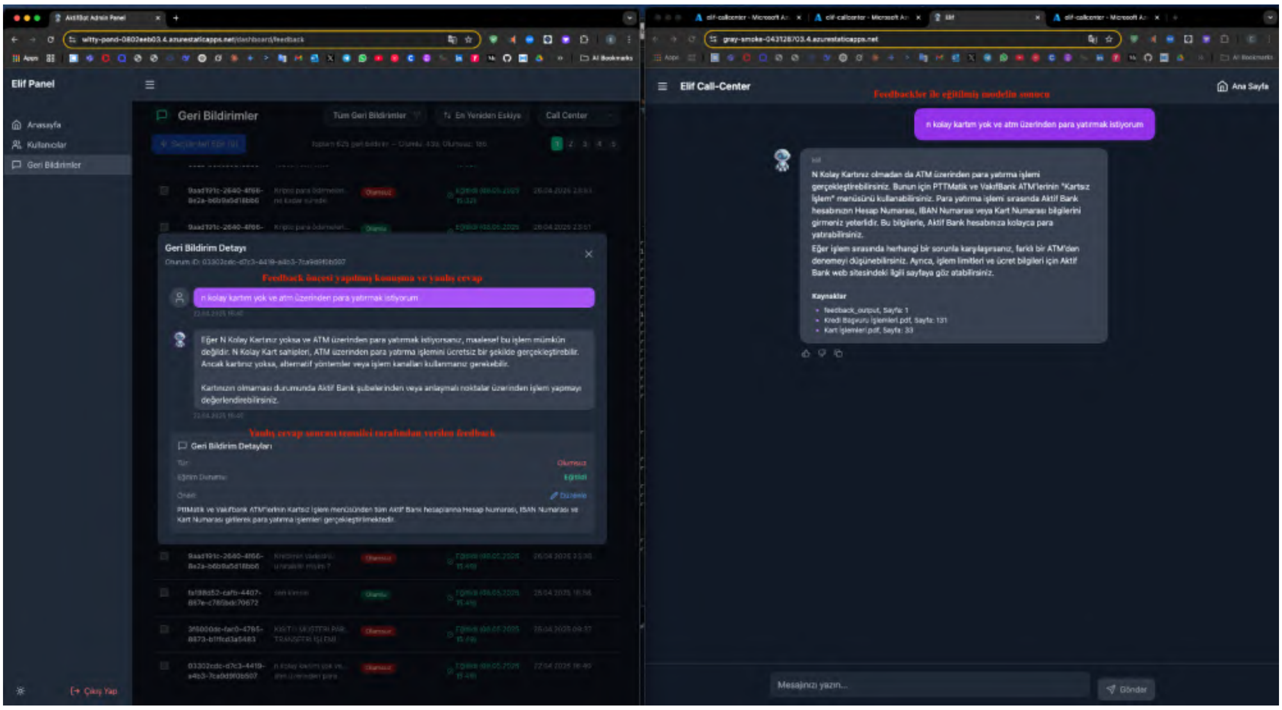
Elif Panel
Anasayfa
Kullanıcılar
Geri Bildirimler
Geri Bildirimler
Tüm Geri Bildirimler
En Yeniden Eskiye
Call Center
Geri Bildirim Detayı
Feedback öncesi yapılmış konuşma ve yanlış cevap
n kolay kartım yok ve atm üzerinden para yatırmak istiyorum
Eğer N Kolay Kartınız yoksa ve ATM üzerinden para yatırmak istiyorsanız, maalesef bu işlem mümkün değildir. N Kolay Kart sahipleri, ATM üzerinden para yatırma işlemini ücretsiz bir şekilde gerçekleştirebilir. Ancak kartınız yoksa, alternatif yöntemler veya işlem kanalları kullanmanız gerekebilir.
Kartınızın olmaması durumunda Aktif Bank şubelerinden veya anlaşmalı noktalar üzerinden işlem yapmayı değerlendirebilirsiniz.
Yanlış cevap sonrası temsilci tarafından verilen feedback
Geri Bildirim Detayları
Eğitildi
Düzenle
PTTMatik ve Vakıfbank ATM'lerinin Kartsız İşlem menüsünden tüm Aktif Bank hesaplarına Hesap Numarası, IBAN Numarası ve Kart Numarası girilerek para yatırma işlemleri gerçekleştirilmektedir.
Çıkış Yap
Elif Call-Center
Feedbackler ile eğitilmiş modelin sonucu
Ana Sayfa
n kolay kartım yok ve atm üzerinden para yatırmak istiyorum
N Kolay Kartınız olmadan da ATM üzerinden para yatırma işlemi gerçekleştirebilirsiniz. Bunun için PTTMatik ve VakıfBank ATM'lerinin "Kartsız İşlem" menüsünü kullanabilirsiniz. Para yatırma işlemi sırasında Aktif Bank hesabınızın Hesap Numarası, IBAN Numarası veya Kart Numarası bilgilerini girmeniz yeterlidir. Bu bilgilerle, Aktif Bank hesabınıza kolayca para yatırabilirsiniz.
Eğer işlem sırasında herhangi bir sorunla karşılaşırsanız, farklı bir ATM'den denemeyi düşünebilirsiniz. Ayrıca, işlem limitleri ve ücret bilgileri için Aktif Bank web sitesindeki ilgili sayfaya göz atabilirsiniz.
Kaynaklar
feedback_output, Sayfa: 1
Kredi Başvuru İşlemleri.pdf, Sayfa: 131
Kart İşlemleri.pdf, Sayfa: 33
Mesajınızı yazın...
Gönder

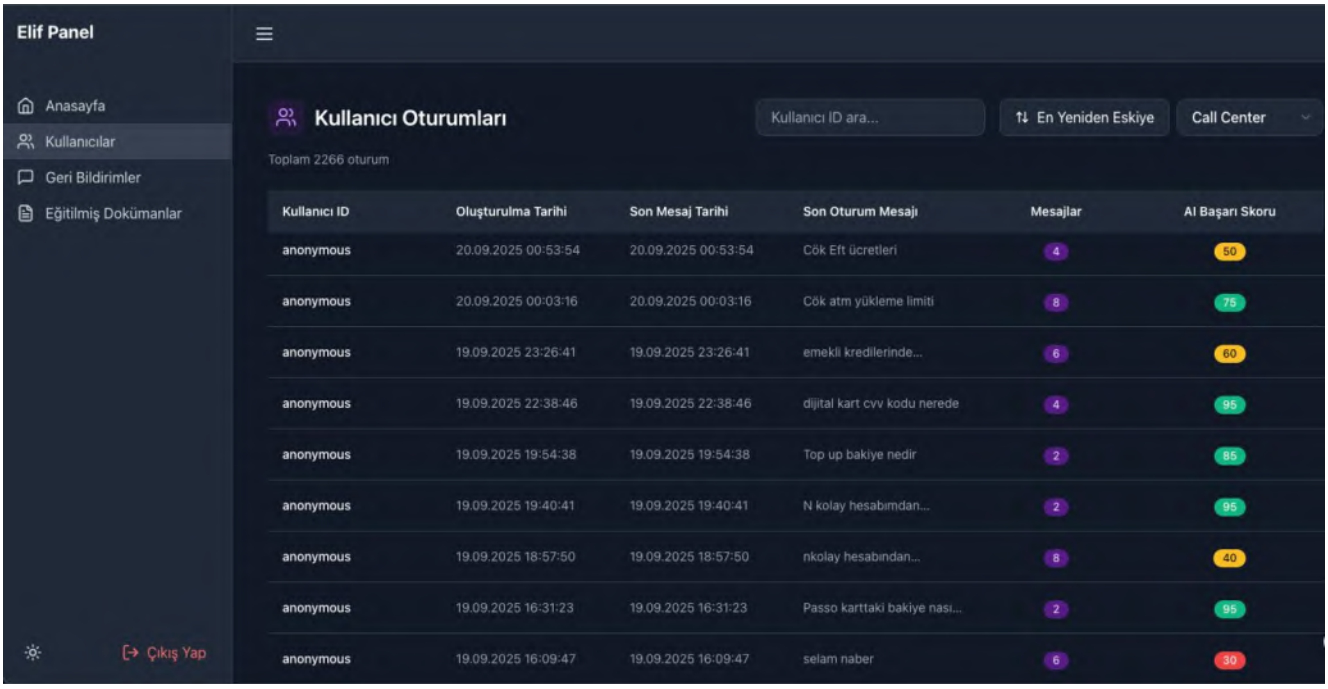
Elif Panel
Anasayfa
Kullanıcılar
Geri Bildirimler
Eğitilmiş Dokümanlar
Çıkış Yap
Kullanıcı Oturumları
Kullanıcı ID ara...
En Yeniden Eskiye
Call Center
Toplam 2266 oturum
Kullanıcı ID | Oluşturulma Tarihi | Son Mesaj Tarihi | Son Oturum Mesajı | Mesajlar | AI Başarı Skoru
anonymous | 20.09.2025 00:53:54 | 20.09.2025 00:53:54 | Cök Eft ücretleri | 4 | 50
anonymous | 20.09.2025 00:03:16 | 20.09.2025 00:03:16 | Cök atm yükleme limiti | 8 | 75
anonymous | 19.09.2025 23:26:41 | 19.09.2025 23:26:41 | emekli kredilerinde... | 6 | 60
anonymous | 19.09.2025 22:38:46 | 19.09.2025 22:38:46 | dijital kart cvv kodu nerede | 4 | 95
anonymous | 19.09.2025 19:54:38 | 19.09.2025 19:54:38 | Top up bakiye nedir | 2 | 85
anonymous | 19.09.2025 19:40:41 | 19.09.2025 19:40:41 | N kolay hesabımdan... | 2 | 95
anonymous | 19.09.2025 18:57:50 | 19.09.2025 18:57:50 | nkolay hesabından... | 8 | 40
anonymous | 19.09.2025 16:31:23 | 19.09.2025 16:31:23 | Passo karttaki bakiye nası... | 2 | 95
anonymous | 19.09.2025 16:09:47 | 19.09.2025 16:09:47 | selam naber | 6 | 30

The Eurasia Proceedings of Science, Technology, Engineering & Mathematics (EPSTEM)
ISSN: 2602-3199

The Eurasia Proceedings of Science, Technology, Engineering & Mathematics (EPSTEM), 2025

Volume 35, Pages 55-62

ICRETS 2025: International Conference on Research in Engineering, Technology and Science

Lead-Zinc Concentrates Quality Improve by Enhancing Slurry Agitation Process

Mihail Petrov
University of Mining and Geology "St. Ivan Rilski"

Teodora Yankova
University of Mining and Geology "St. Ivan Rilski"

Irena Grigorova
University of Mining and Geology "St. Ivan Rilski"

Rozalia Kirilova
University of Mining and Geology "St. Ivan Rilski"

Abstract: Lead-zinc sulphide ore mined from the Toranica deposit and is processed in the concentrator. The deposit is located in the Osogovo mountain, the northeastern part of the Republic of North Macedonia, near the Bulgarian Macedonian border. The main ore minerals in the lead-zinc ore are represented by galena, sphalerite, chalcopyrite, pyrite, and the non-ore minerals by quartz, carbonates, barite. After crushing and grinding, the ore is beneficiated using a direct selective flotation. It is common knowledge that slurry agitation is important for the flotation efficiency and makes the mineral particles fully mix with the flotation reagent. It was established that with the available conditioning tank agitator in the Toranica lead-zinc concentrator, the necessary slurry agitation is not achieved. This leads to inefficient flotation process and low-quality Pb and Zn concentrates production. During certain periods of the concentrator's operation, a zinc concentrate with an average monthly content of lead impurities is produced, reaching up to 6.08%, while at the same time a lead loss was registered in the final flotation tails. To eliminate the causes leading to deteriorate technological indicators, the lead-zinc ore mineral composition was investigated. Moreover, slurry agitation has been improved by implementing an advanced conditioning tank. High-quality final concentrates production was achieved, and the recovery degree was also increased. This paper is organized divided into four sections. Section 1 gives a brief overview of sulphide lead-zinc ores, their flotation beneficiation, reagents and flowsheets. The second section examines our research and development program to establish the technological possibilities for replacement of an available conditioning tank agitator. In the third section the case study is analyzed, and we propose a new procedure for conditioning tank agitator improvement. Our conclusions are drawn in the final section.

Keywords: Mining engineering, Conditioning tank agitator, Concentrates quality

Introduction

As many authors stated mining industry is witnessing an epochal revolution due to the metals growing demand (copper, iron, aluminum, nickel, gold, lead and zinc), industrial minerals and energy resources (oil, uranium) all over the world and especially in the currently developing economies (Tomova, 2023; Yankova, et. al, 2023). The lead and zinc growing consumption and the global tendency to exhaust deposits containing high-quality lead-zinc ores place increasingly high demands on the efficient lead-zinc ores processing and the full metals recovery. The main lead and zinc source is sulphide lead-zinc ores, which beneficiation by flotation.

- Selection and peer-review under responsibility of the Organizing Committee of the Conference

Lead-zinc ores characteristic feature is presence of aggregates associated with sulfides, located among a mass of non-ore minerals or host rocks, which necessitates the fine ore grinding below 74 µm (Barnov et al., 2018; Nayak et al., 2020). Appropriate technological flowsheet selection is of great importance for flotation efficiency, as well as highly selective flotation reagents, which are dependent on several factors such as: mineral and chemical ore composition, physical properties, mineral aggregates size, oxide phases presence, etc. (Nayak et al., 2021; Wei et al., 2021; Zhang et al., 2022; Yang et al., 2022).

In addition to conventional flotation reagents used so far in the concentrators practice, new reagents with improved performance are constantly being developed and synthesized, including biodegradable ones, which are essential for technological circuits (Zhang et al., 2022; Neisiani, Chelgani, 2024). In selective flotation for the separation of galena from sphalerite, xanthates are widely used. However, these reagents are toxic and exhibit some instability in acidic media. The effectiveness of new reagents which, compared to xanthates, have a stronger collection ability and maximum selectivity have been studied (Dong et al., 2021; Wang et al., 2021; Kong et al., 2024).

Lead-zinc sulphide ore mined from the Toranica deposit is processed in the Toranica concentrator nearby Kriva Palanka city. The deposit is in the Osogovo mountain, in the northeastern part of the Republic of North Macedonia, about 24 km from the Kriva Palanka town, near the Bulgarian-Macedonian border. Industrial operation began in 1987 with the production of 41 232 tonnes ore per year, currently reaching around and over 300 000 t (Despodov et al., 2021). According to Serafimovski et al. (2022) the deposit has lead-zinc ore reserves of 4 959101 t and ore resources of 7 640899 t, with Pb+Zn content from 6.33 to 7.40%, Ag 20 g/t. Ore bodies have elongated banded, layered, lens-like shape or irregular morphology. The main ore minerals are represented by sulphides galena, sphalerite, chalcopyrite, pyrite, and non-ore minerals by quartz, carbonates, barite (Serafimovski et al., 2022).

In certain periods of the Toranica concentrator activity, the concentrates produced show deteriorated technological indicators and do not meet the metallurgical processing requirements. This paper describes the results of the research conducted to identify and eliminate the factors, having a negative impact on the flotation efficiency and metals recovery. It was found that the use of current outdated model conditioning tank agitator for reagent addition at the beginning of flotation circuits, contact between reagents and the slurry was not obtained.

Slurry agitation is insufficient, and as a result the subsequent flotation processes efficiency is also reduced. As is well known, proper agitation provides optimal blending due to ensuring a large area of influence. Conditioning tanks prepare the slurry for flotation by ensuring that reagents are effectively mixed. With conditioning tank agitator implementation in the Toranica concentrator the sustainable production of quality concentrates and an increase in metals recovery rate have been achieved.

Materials and Methods

In lead-zinc ore treatment, the main ore minerals were represented by galena and sphalerite, as subordinate by distribution is pyrite and chalcopyrite are observed, and pyrrhotite, pyrite-marcasite pseudomorphs after pyrrhotite, magnetite, hematite, etc. are found in a relatively minor amount. Gangue minerals are represented by quartz, carbonates, barite, micas, skarn minerals from the pyroxene group, garnets, clay minerals, etc.

As illustrated in Figure 1a, the main ore minerals galena and sphalerite usually occur together in common aggregates and are much less often observed in individual form. Corroded grains of pyrite and chalcopyrite are present in the galena in places, and in places of pyrrhotite and pseudomorphoses from pyrite-marcasite after pyrrhotite (Figures 1b, 1c, 1d), as well as quartz and other gangue minerals. Two different varieties of sphalerite are distinguished. The early sphalerite contains emulsion and fine chalcopyrite inclusions, and the later sphalerite is chalcopyrite emulsion-free, homogeneous (Figure 1a, 1c). Pyrite is more abundant than chalcopyrite and is in most cases closely associated with galena. Inclusions of pyrrhotite and pyrite-marcasite pseudomorphs after pyrrhotite are found in places in galena, more rarely in sphalerite (Figures 1c, 1d). The presence of pyrrhotite in the investigated ore due to is magnetic properties will adversely affect the sphalerite flotation properties.

In Toranica concentrator, sulphide lead-zinc ore is being processed by crushing, milling, flotation and concentrate dewatering. Figure 2 presents a detailed mineral processing flowsheet of the concentrator.

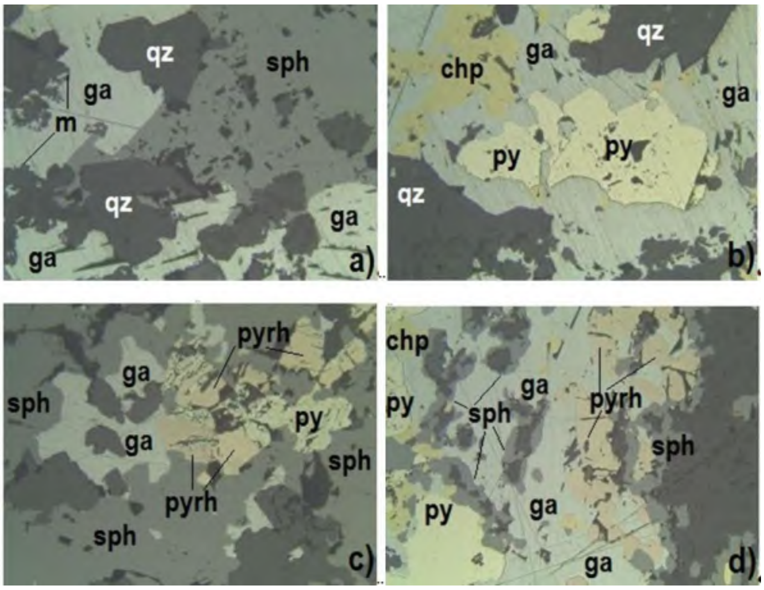

Figure 1. Photomicrographs of lead-zinc ore from the Toranica deposit. a) Sphalerite (sph) and galena (ga), with inclusions of quartz (qz) and flaky aggregates of mica (m); c) Pyrite (py) and chalcopyrite (chp) in galena (ga), corroded by quartz (qz); c) Sphalerite (sph) and galena (ga), with inclusions of pyrrhotite (pyrh) and pyrite (py) pseudomorphosis after pyrrhotite (pyrrh); d) Galena (ga), with inclusions of elongated aggregates of pyrrhotite (pyrh), sphalerite (sph), grains of pyrite (py) and chalcopyrite (chp). Reflected light, N II, length of the observation field 820 µm.

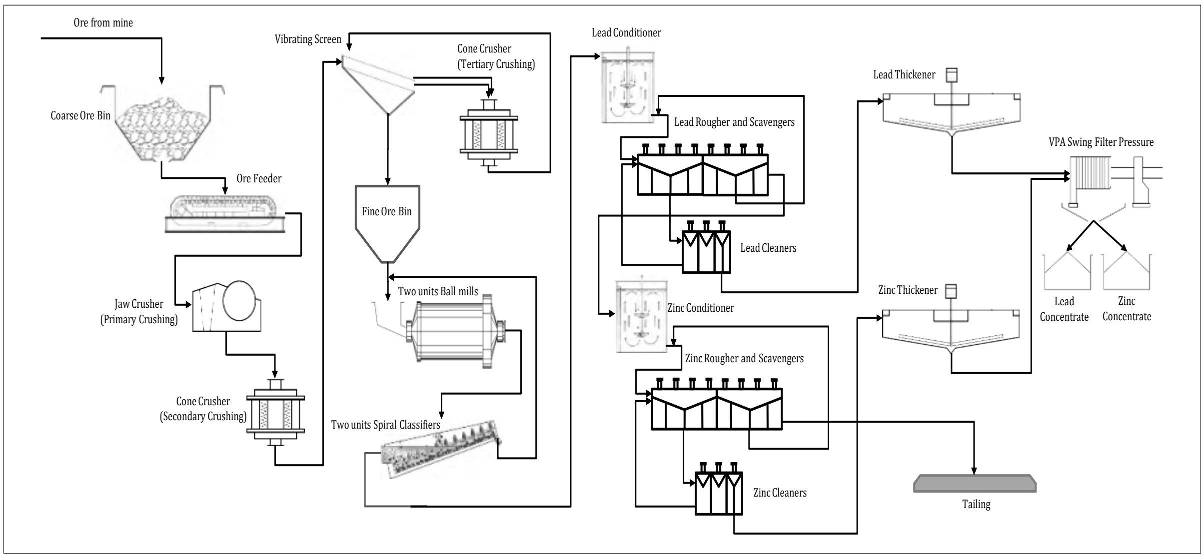

Figure 2. Toranica concentrator mineral processing flowsheet

At the Toranica concentrator, the lead-zinc ore after size reduction, including crushing and grinding are beneficiated using a direct selective flotation flowsheet (Petrov et al., 2024). In this technological flowsheet, galena flotation is initially carried out upon sphalerite depression and after activation of the depressed sphalerite zinc flotation is performed. In the processing industry, direct selective flotation is widely used for lead-zinc sulfide ores beneficiation (Bulatovic, 2007).

Lead and zinc flotation is carried out with mechanical flotation machines which are widely used in non-ferrous, ferrous and precious metals and coal processing. These machines are universal, reliable, have a simple design, facilitating their operation and maintenance. Mechanical flotation machines are highly productive and provide high selectivity and concentrates purity, being considered to be most effective at solid phase content in the slurry up to 30-35%. Slurry agitation, before flotation is important for achieving effective flotation and more complete ore processing metal recovery. With conditioning tank agitator intensive slurry stirring is carried out, in order to evenly distribute the mineral particles and prevent them from settling at the tank bottom. Moreover, uniform distribution of the flotation reagents added is achieved and their reactivity is improved. Slurry agitation contributes to better results in subsequent flotation process, improved metal recovery and reduced production costs.

Research and development program has started to establish the technological possibilities for replacement of an available conditioning tank agitator. The observations we conducted showed that as a result of impossibility of carrying out appropriate agitation, deteriorated technological indicators of the concentrates produced and metals loss in the final waste are established (Table 1 and Figure 3). Table 1 demonstrates that the average monthly lead content in the zinc concentrate during the period July - September 2023 varies from 4.89 to 6.08%, the lead recovery varies from 78.8 to 80.95%, and the lead loss in final tail reaches 0.51%.

Table 1. Average monthly Pb and Zn contents in the ore, concentrates and waste in 2023, before new conditioning tank agitator implementation

2023	Ore		Pb concentrate		Zn concentrate		Tails		Yield (%)		Recovery (%)	
	Grade (%)											
	Pb	Zn	Pb	Zn	Zn	Pb	Pb	Zn	Pb	Zn	Pb	Zn
April	2.25	1.50	69.49	2.42	48.94	3.67	0.39	0.19	2.57	2.57	79.30	83.99
May	2.45	1.43	71.34	2.15	48.75	4.14	0.41	0.16	2.75	2.49	80.01	85.22
June	2.82	1.91	73.46	2.32	49.46	3.42	0.45	0.21	3.11	3.34	80.95	86.19
July	2.83	1.57	71.02	2.03	48.17	5.11	0.49	0.17	3.14	2.79	78.78	85.60
August	3,07	1.46	68.43	2.69	47.54	6.08	0.51	0.18	3.55	2.51	79.28	81.92
September	2.77	1.38	69.61	2.11	48.05	4.89	0.44	0.16	3.22	2.42	80.90	83.98

Figure 3 reports the lead and zinc contents in flotation products, before new conditioning tank agitator implementation in Toranica technological cycle.

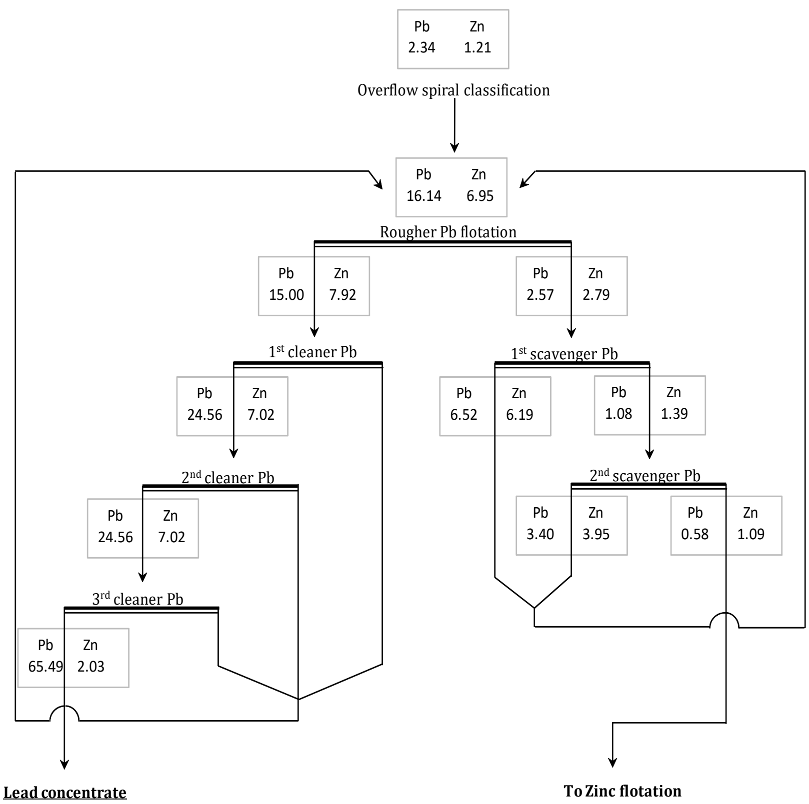

Figure 3. Pb and Zn contents of flotation products in the lead flotation cycle, before new conditioning tank agitator implementation

In order to eliminate the factors adversely affecting the flotation efficiency, quality concentrates production and metals recovery higher degree, studies in depth were carried out to determine the lead-zinc ore mineral composition.

Results and Discussion

Implementation an Advanced Conditioning Tank Agitator

In the literature there are few examples of conditioning tank agitator improvements carried out. In their paper of 2021, Wu et al. noted that regular maintenance shutdowns are required for conditioning tanks to clean sedimentation and scale. The labour cost and production loss during maintenance negatively impact on the economics of the operation (Wu et al., 2021). In (Wu et al., 2021) the authors proposes Swirl Flow technology, developed to improve the reliability of agitation and to maximise conditioning tank agitator online time between maintenance intervals.

In order to improve slurry agitation, an advanced conditioning tank has been put into operation. An air installation from the blower to conditioning tank impeller was affixed. Thus, preventing slurry being precipitation upon impeller. The blades diameter has increased by 100 mm, thus their final diameter reaches 540 mm. The blades angle has been changed by 40, which reaches a value of 370. As a result of the centrifugal force effect from the impeller rotation, the slurry is pushed upwards and does not sedimentation the bottom of the agitator. The power of the electric motor has increased from 15 kW/750 rpm to 18 kW/950 rpm.

As mentioned by Arfken et al. (1984), the Reynolds number is a useful parameter, dimensionless, used to determine if a fluid flow will be steady or turbulent based on the fluid density, flow speed, dynamic viscosity, and a characteristic length associated with the flow. Based on the modified impeller data, comparative Reynolds number values were calculated to determine the fluid flow using the formula:

$$R_e = \frac{\varrho N d^2}{\mu},$$

where: Re – Reynolds number, ϱ – fluid density, g/cm^3, N – rotational speed, rpm, d – impeller diameter, mm, μ - fluid viscosity = 10^{-4}

Before changing the impeller diameter, blades tilt and shaft rotation speed, the Reynolds number is: R_e = 2.17.10^4, and after changing is: R_e = 3.97.10^4.
Based on the calculations obtained, it can be assumed that before and after changing the impeller diameter, blades tilt and shaft rotation speed, the fluid flow is highly turbulent, but at the Reynolds number higher value there is a better stirring media that is more suitable for the operation of the conditioning tank agitator.

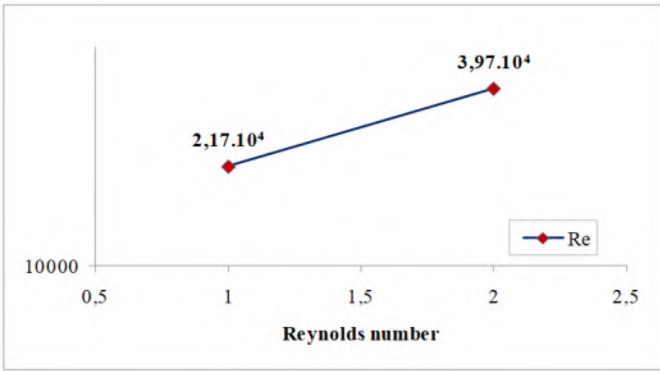

Figure 4. Reynolds number before and after changing the impeller diameter, blades tilt and shaft rotation speed

Table 2. Average monthly Pb and Zn contents in the concentrates and tails after implementation of advanced conditioning tank in the concentrator technological cycle

2023	Ore		Pb concentrate		Zn concentrate		Tails		Yield (%)		Recovery (%)	
	Grade (%)											
	Pb	Zn	Pb	Zn	Zn	Pb	Pb	Zn	Pb	Zn	Pb	Zn
October	2.65	1.41	69.37	2.22	46.42	3.37	0.41	0.17	3.13	2.54	82.14	83.92
November	3.04	1.17	69.95	2.70	49.85	2.96	0.44	0.13	3.68	1.91	84.50	81.22
December	2.92	1.43	69.76	2.73	49.08	2.98	0.39	0.17	3.56	2.40	85.09	82.27

After the changes in the parameters of the conditioning tank agitator, operation in continuous mode was achieved. Better agitation of the flotation reagents added in the slurry is ensured.
The monthly average lead and zinc contents in the concentrates and tails during October - December 2023 are presented in Table 2.

Table 2 demonstrates lead recovery higher degree, which reaches 82.14 – 85.09%. No significant reduction in lead loss was recorded in the final flotation tail. The results of the flotation product sampling show that better selectivity is achieved. Zinc concentrate does not contain lead impurities and fully meets the metallurgical processing requirements (Table 2, Figure 5).

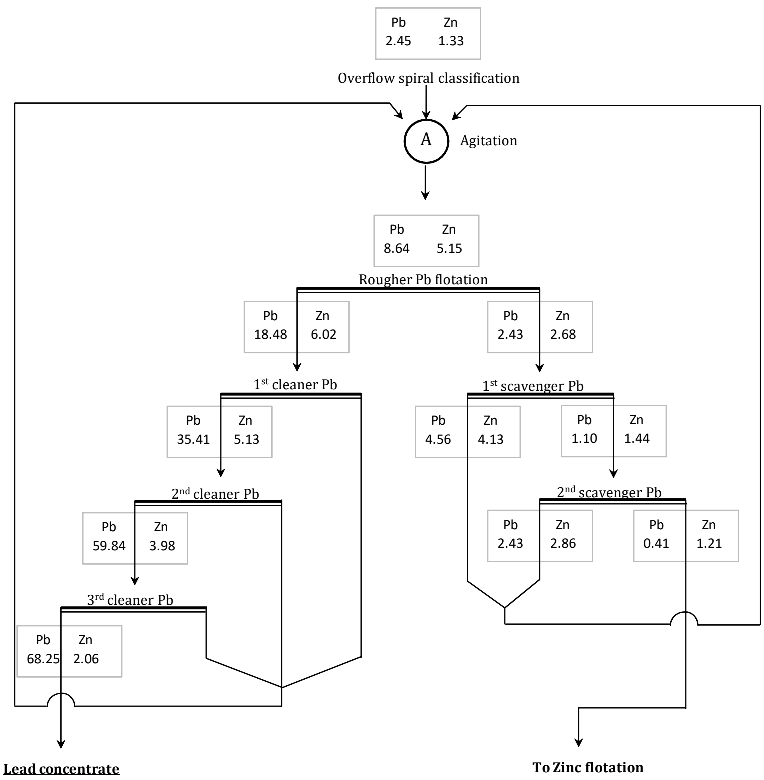

Figure 5. Pb and Zn contents (%) in the flotation products in lead flotation cycle, after advanced conditioning tank implementation

Conditioning tank agitators are crucial components in mineral processing, particularly in the preparation and treatment of slurry before it undergoes flotation (Wu et al., 2015). Wu and co-workers (2015) highlights design improvements for agitated tanks as developed in CSIRO's laboratories, which have solved practical problems in minerals processing operations involving viscous slurries, and this seems to be a reliable approach, because solving problems of rapid tank scaling, sediment build-up and poor mixing of reagent is of great importance. Regular maintenance is essential to ensure optimal performance, prevent wear and tear, and avoid issues like buildup of materials that can affect mixing efficiency. In summary, conditioning tank agitators play a vital role in mineral processing by facilitating the mixing of reagents with mineral slurry, which is key to improving recovery rates and overall process efficiency.

Conclusion

As stated in the Introduction, our main purpose was to identify and eliminate the factors, having a negative impact on the Pb-Zn flotation efficiency and metals recovery. Although more research is needed to identify the lead-zinc sulphide ores beneficiation underlying mechanisms, findings suggest that insufficient slurry agitation leads to the subsequent flotation processes inefficiency. For the efficient flotation it is necessary to strictly observe the optimal regent mode, ensuring a certain contact between the reagents and the mineral particles in the slurry.

The contributions made here have wide applicability. In general, the main achievements, including contributions to the field can be summarised as follows: with implementation an advanced conditioning tank agitator in the concentrator technological circuit has achieved: better slurry agitation with the supplied reagents and produced concentrates selectivity. In our view these results represent an excellent step toward better metals recovery and sustainable quality concentrates production for meeting the metallurgical processing requirements.

Scientific Ethics Declaration

* The authors declare that the scientific ethical and legal responsibility of this article published in EPSTEM journal belongs to the authors.

Conflict of Interest

* The authors declare that they have no conflicts of interest

Funding

* This research received no specific grant from any funding agency in the public, commercial, or not-for-profit sectors.

Acknowledgements or Notes

* This article was presented as a poster presentation at the International Conference on Research in Engineering, Technology and Science (www.icrets.net) held in Peja/Kosovo on July 10-13, 2025.

References

Arfken, G.B., Griffing, D.F., Kelly, D.C., & Priest, J. (1984). *University physics*. New York, NY: Academic Press.

Barnov, N.G., Lavrinenko, A.A., Lusinyan, O.G., & Chikhladze V.V. (2018). Effect of a crushing technique on lead-zinc ore processing performance. *Journal of Mining Science*, *53*, 7711-777.

Bulatovic, S. M., & Bulatovic, S. M. (2007). Flotation of copper sulfide ores. In *Handbook of flotation reagents chemistry, theory and practice* (pp. 235–293). Elsevier.

Concha, F. A., & Bascur O.A. (2024). *The engineering science of mineral processing: A fundamental and practical approach.* CRC Press.

Despodov, Z., Doneva, N., Mijalkovski, S., & Hadži-Nikolova, M. (2021). Methodology for selection of the variant for opening the deeper parts of the Toranica mine. *Podzemni Radovi*, 38, 1-13.

Dong, Z., Jiang, T., Xu, B., Li, Q., Zhong, H., & Yang, Y. (2021). Selective flotation of galena using a novel collector S-benzyl-N-ethoxycarbonyl thiocarbamate: An experimental and theoretical investigation. *Journal of Molecular Liquids*, 330, 115643.

Kong, L., Fu, X., Lu, L., Wang, R., Wang, H., Meng, Y., & Zhang, X. (2024). A novel selective galena collector based on modified dithiophosphate in Pb-Zn flotation separation and its adsorption mechanism. *Advanced Powder Technology*, *35*(6), 104489.

Nayak, A., Ashrit, S., Jena, M.S., & Venugopal, R. (2020). Mineralogical characterization for selection of possible benefication route for low-grade lead-zinc ore of Rampura Agucha, India. *Transactions of the Indian Institute of Metals*, 73, 775-784.

Nayak, A., Jena, M. S., & Mandre, N. R. (2021). Benefication of lead-zinc ores – a review. *Mineral Processing and Extractive Metallurgy Review*, *43*(5), 564-583.

Neisiani, A.A., & Chelgani S.C., (2024). Biodegradable acids for pyrite depression and green flotation separation – an overview. *Critical Review in Biotechnology*, *44*(6), 1226-1240.

Petrov, M., Yankova, T., & Grigorova, I. (2024). *Lead-zinc ores mineral processing in the Republic of Bulgaria and the Republic of North Macedonia*. Geology and Mineral Resources, 2-9. Springer.

Serafimovski, T., Tasev, G., Stafilov, T. (2022). General features of some polymetallic ore deposits in the Republic of North Macedonia. *Geologica Croatica, 75*(3), 349-364.

Tomova, M. (2023). Geophysical techniques for monitoring of ıntegrated mine waste storage facility: Case study of Southeastern Bulgaria. *The Eurasia Proceedings of Science Technology Engineering and Mathematics,* 26, 341-347.

Wu, J., Nguyen, B., Graham, L., Hurley, M., Harris, D., Short, G., Kieruj, J., Connor, T. (2021). Increased agitation reliability for slurry suspension in mineral processing, *Minerals Engineering*, *170*(2021), 107008.

Wang, J., Ji, Y., Cheng, S., Liu S., Cao, J., & Chen, P. (2021). Selective flotation separation of galena from sphalerite via chelation collectors with different nitrogen functional groups. *Applied Surface Science*, 568, 150956.

Wei, Q., Dong, L., Qin, W., Jiao, F., Qi, Z., Feng, Ch., Sun, D., Wang, L., & Xiao, S. (2021). Efficient flotation recovery of lead and zinc from refractory lead-zinc ores under low alkaline conditions. *Geochemistry*, *81*(4), 125769.

Wu, J., Wang, S., Nguyen, B., Lane, G., Graham, L., Short, G., & Ruster, J. (2015). Improved viscous slurry agitation for minerals processing, *Minerals Engineering*, *78*(2015), 21-31.

Yang, L., Xiong, T., Jinfang, L. V., Xian X., Qiang, S., & Peiqiang, F. (2022). Research progress on flotation separation of lead-zinc sulfide minerals. *Conservation and Utilization of Mineral Resources*, *42*(3), 106-114.

Yankova, T., & Grigorova, I. (2023). Physıco-mechanıcal propertıes of a mıxed-type sulphıde-oxıde ore from a porphyry-copper deposıt. *Annual of the University of Mining and Geology “St. Ivan Rilski”*, *66*(66), 87-90.

Zhang, Z., Liu, S., Liu, F., Ahmed M. M., Qu, X., & Liu, G. (2022). The flotation separation of sphalrite from pyrite through a novel flotation reagent system of $FeCl_3$ – $CuSO_4$ -aminotriazolethione. *Journal of Molecular Liquids*, 345, 116997.

Author(s) Information

Mihail Petrov
University of Mining and Geology “St. Ivan Rilski”
Prof. Boyan Kamenov Str., 1700 Sofia, Bulgaria
Contact e-mail: *m.petrov@mgu.bg*

Teodora Yankova
University of Mining and Geology “St. Ivan Rilski”
Prof. Boyan Kamenov Str., 1700 Sofia, Bulgaria

Irena Grigorova
University of Mining and Geology “St. Ivan Rilski”
Prof. Boyan Kamenov Str., 1700 Sofia, Bulgaria

Rozalia Kirilova
University of Mining and Geology “St. Ivan Rilski”
Prof. Boyan Kamenov Str., 1700 Sofia, Bulgaria

To cite this article:

Petrov, M., Yankova, T., Grigorova, I. & Kirilova, R. (2025). Lead-zinc concentrates quality improve by enhancing slurry agitation process. *The Eurasia Proceedings of Science, Technology, Engineering & Mathematics (EPSTEM), 35,* 55-62.

The Eurasia Proceedings of Science, Technology, Engineering & Mathematics (EPSTEM)
ISSN: 2602-3199

The Eurasia Proceedings of Science, Technology, Engineering and Mathematics (EPSTEM), 2025

Volume 35, Pages 63-71

ICRETS 2025: International Conference on Research in Engineering, Technology and Science

Key Assessment Indicators for Safety in Mineral Processing Plant

Nadezhda Kostadinova
University or Mining and Geology “St. Ivan Rilski”

Blagovesta Vladkova
University or Mining and Geology “St. Ivan Rilski”

Abstract: Mineral processing plants are an important element of the overall process of extraction and processing of mineral raw materials. They combine different technologies, various types of production equipment, operate with high capacities and generally observe a rather complex technological process. Working in such an enterprise requires good knowledge of technologies, and coordination between engineering staff and management, which should correspond to the management of processes and personnel in order to achieve optimal results. This complex nature creates safety risks and is a prerequisite for the occurrence of accidents at work as well as material damage. The regular performance of safety audits aims to monitor the level of safety assurance at the mineral processing plant and the organisation of the work process. The aim of the report is to state the key indicators for safety of this system, to analyse incident prevention measures and to recommend health and safety procedures in similar types of industrial facilities. The article is based on engineering experience and good practices from the mining industry.

Keywords: Mineral processing plant, Key indicators, Mining engineering

Introduction

Ensuring health and safety at work in an processing plant is not an easy task and requires a comprehensive approach. Skillful process management and good docking between units plays a key role in the success of the enterprise. One of the indicators of the status of the processing plant is the level of safety assurance along the entire chain, and this level is monitored through the regular performance of safety audits. Based on the information received from the audit, the weaknesses and opportunities for improving the level of safety, as well as the application of good engineering practices, are identified. Of course, many of the safety factors stem from the type of equipment and specific machinery used in the beneficiation process (Gao, 2025). For this purpose, safety instructions are applied, work procedures, rules are drawn up, monitoring and control are carried out.

The aim of this paper is to provide a better understanding of complexity of safety procedures in mineral processing plats trough a) understandig of causes of accidents and incidents and b) following a step by step safety odit for monitoring and controll. Safety as a key assessment indicator provides minimisation of posible accidents and to mitigates the risk level of damages for personel and material loses.

Safety Key performance Indicators. Why Key Assessment Indicator?

When considering the overall concept of safety the goal to take all the precousious measures, to investigate and identificate hazards and posssible risk from equipment, and processes, so no incidents and accidents occure. A useful tool for that are safety key performance indicators (SKPI). They are definied as measaruble indicators tracable over the time focused on progress toward an intended result. A good example for the process of

- Selection and peer-review under responsibility of the Organizing Committee of the Conference

developing KPIS for process safety and how critical is the management involvment and a garentieed transparent reporting of the KPIs progress for the succes of the safety procedures are given by Brown case study (Brown, 2009). However there are some consideration about the reability, validation, cost-effectivness etc. of the KPIs to be made before implmentation (Hale, 2009). In the presented paper as useful safetyKPIs are considered metric parameters, such as:

- KPI related to accidents and usafe behaivioor - incident rate; recordable injury frequency; lost time incident ratio; near misses rate; fatal accidents and medical cost expenditure
- KPI related to personal training and work organisation - employment training; average employee overtime hours; shift work; corrective actions; employee attendance rate
- KPI related to technical equipment – equipment breakdowns rate; mashine inspections; hazard and appropried PPEs

Developing safety procedures in complex environment such as mineral processing plant requires implementation of not only measurable indicators but also an evaluative and quality based approach. Safety schould be considered as assesment tool for the perfomance of the entire enterprise. The safety audit consist also measures and recomendations for improving the safety culture on every hierarchic management and employee levels, open and direct comunication.; in this aspect it corresponds to the definition for key assessment indicator.

Overview of Ore Processing as part of the Extraction of Mineral Raw Materials

Ore processing is a stage of the overall process of mining and processing of mineral raw materials and this is the stage of obtaining concentrate before the metallurgical plant (Alabi, 2018). This process can be generally represented with the following scheme Figure 1.

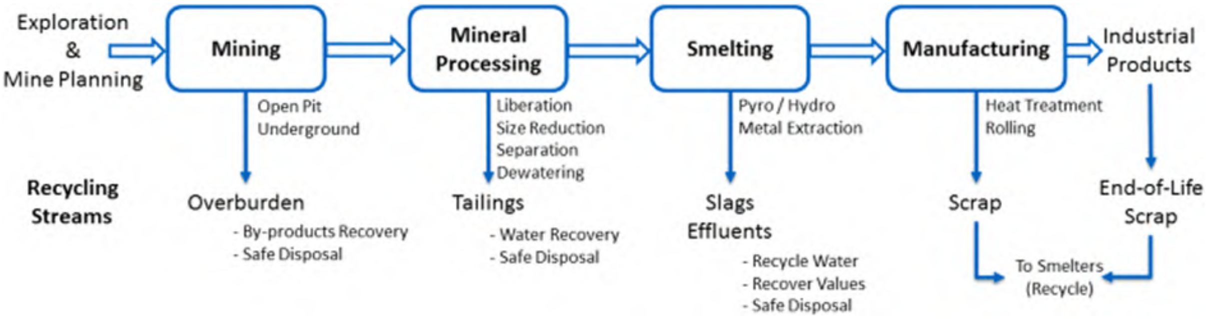

Figure 1. Mineral processing and metal extraction ındustry, overview, (Pradip Gautham et al. 2019).

In general, an ore processing plant includes the following technological processes: size distribution control of the raw material (coarse, medium and fine crushing), screening, grinding, flotation, thickening and concentrate production (IHSA, Canada 2019) . These processes are schematically presented in Figure 2.

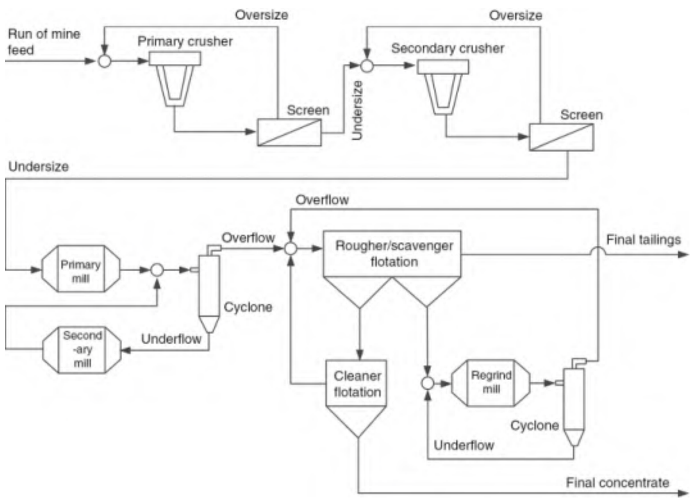

Figure 2. Common technological proces in mineral processing plant (Forbes, et al. 2017)

In practice, various types of research are conducted that are related to improving the efficiency of equipment and machines used in the mineral processing (Minin & Hristova, 2024,). Some of the efficiency indicators are energy consumption, grinding medium consumption, reagent consumption, cladding, etc (Trinh, et al, 2025). Mining equipment and mining mechanisation are a specific type of machinery, which are characterised by large dimensions, high energy consumption and specialized maintenance. Due to the high loads and wear of individual components of the processing machines, regular scheduled repairs and maintenance are carried out (Gorbounov, & Chen, 2019). This requires ensuring a high level of safety, as it is necessary to coordinate several work teams simultaneously. In mineral processing in general, various types of reagents and additional chemicals (fuels, lubricants etc.) are used, which are subject to special storage and waste treatment regimes (Yankova & Grigorova, 2020, Mollova, 2024).

Statistics

According to Eurostat data, for 2022 there are 17,033 mining enterprises employing 371,000 people (Figure 3).

Key indicators: Mining and quarrying statistics (NACE Section B), EU, 2022

	Value
Main indicators	
Number of enterprises (number)	17 033
Number of persons employed (number)	371 000
Net turnover (€ million)	173 566
Value added (€ million)	64 082
Share in business economy total (%)	
Number of enterprises	0.1
Number of persons employed	0.2
Value added	0.6
Derived indicators	
Apparent labour productivity (thousand € per head)	172.7
Employee benefits expense (thousand € per head)	43.7
Wage-adjusted labour productivity (%)	395.0
Gross operative rate (%)	27.7

Source: Eurostat (online data code: sbs_ovw_act)

eurostat

Figure 3. Mining and quarrying statistics, 2022

Table 1 presents statistical data for Bulgaria for the period 2019-2024, which examines the number of accidents and fatalities compared to the number of people employed in the mining industry. The data are obtained from the National Statistical Institute of Bulgaria and processed by the authors.

Table 1. Bulgarian mineral extraction (MEI) and mineral processing (MPI) industry statistics

Indicators / Year		2019	2020	2021	2022	2023	2024*
Persons employed [Number]	Bulgaria	2525933	2392082	2456366	2495772	2302922	2231677
	MEI	19728	19159	18857	18973	18433	18055
	MPI	14165	13714	13986	14376	n. a.	n. a.
Work accidents [Number]	BG	2763	2345	2427	2615	2709	2823
	MEI	130	113	94	101	97	76
	MPI	72	66	57	49	59	40
Fatalities [N]	BG	102	109	84	98	87	64
	MEI	3	3	0	5	2	2
	MPI	0	3	1	1	0	1
Labor day lost [N]	BG	229801	201478	211870	203759	168597	164478
	MEI	9938	7111	5860	7540	6318	4409
	MPI	6789	4235	5671	5128	4772	2005

*Tha data obtained for 2024 from Bulgarian National statistical institute is not fully processed and published

Figure 4 shows a downward trend in occupational accidents in the mining and processing industry for the period 2019-2024 with an average of 31.000 workers in the sector.

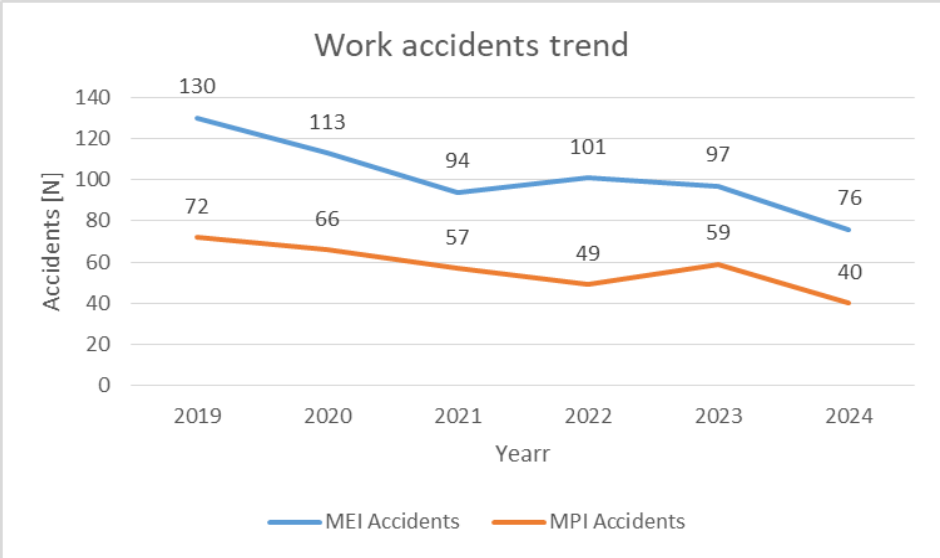

Figure 4. Work accidents in mineral extraction and processing industries from 2019 to 2024.

Scope of the Safety Audit

The scope of the safety audit for a processing plant includes all technological units, machinery, equipment, operating mode, etc. Objects subject to audit in the processing plant are: coarse crushing, storage, disintegration, medium and fine crushing, intermediate hoppers, mill compartment, flotation, reagent compartment, thickening and filtration, concentrate warehouse. The characteristics of the main and auxiliary labor activities, implemented technologies, raw materials and products used, working premises and workplaces, work equipment, high-risk facilities are described. The audit also covers the management of basic and support work activities; personnel management - composition, qualification structure, health status, risk groups, remuneration, social partnership, motivation.

Method

For the purpose of the analysis, those elements of the organization of labor activity that are of key importance for ensuring health and safety at work have been considered. The subject of the analysis does not include factors affecting only labor productivity, company costs, return on investment and other similar indicators that are primarily of a financial and economic nature. The following basic methods were used to conduct the research and analysis:

- Critical evaluation method;
- Random observation and in situ inspections method;
- Comparison method;
- Sociological research method (surveys, interviews and discussions);
- Statistical research method;
- Expert method;
- Fieldwork, which includes extensive photographic material with comments and links to the regulatory framework
- Evaluation by indicators in each production part
- Checklists

A graphical representation of the condition of each technological unit is prepared through a comprehensive assessment of compliance with 14 selected criteria (Table 2). The maximum compliance is 100% corresponding to an ideal condition, a comparison to those gives the extent to which the criterion is met is assessed. A 70% compliance is accepted for satisfactory coverage of the requirements under the individual criteria. The analysis is prepared based on a comprehensive processing of available documentation, photographs, planned and unannounced field inspections by the auditing team. Figure 5 is an example for assessment of one technological unit. The graph allows visualisation of the strong and the weak areas in the unit. Figure 6 combines the evaluation of technological units in mineral processing plant.

Table 2. Example of evaluation criteria score for one unit

Criteria	Result
House keeping	52.73%
Electrical Fuses	67.14%
Stop buttons	72.00%
Fire safety	76.92%
Overhead cranes and hoists	80.00%
Electro equipment	66.00%
Safety signs	71.11%
Confined spaces	46.00%
Workplaces	46.00%
Safety behavior	48.00%
Procedures	61.67%
Ergonomics	65.45%
Sanitary and household complexes	72.50%
Warehouses	52.50%

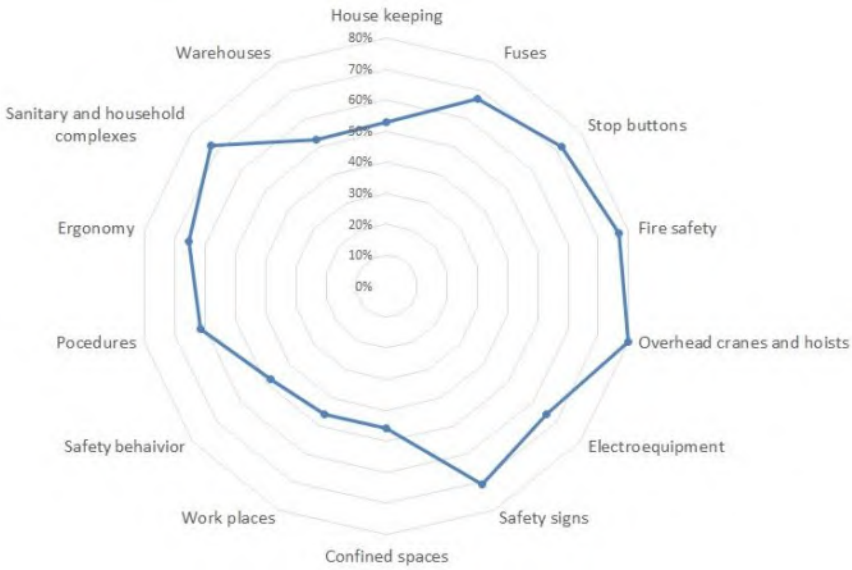

Figure 5. Example graph of the score for each unit

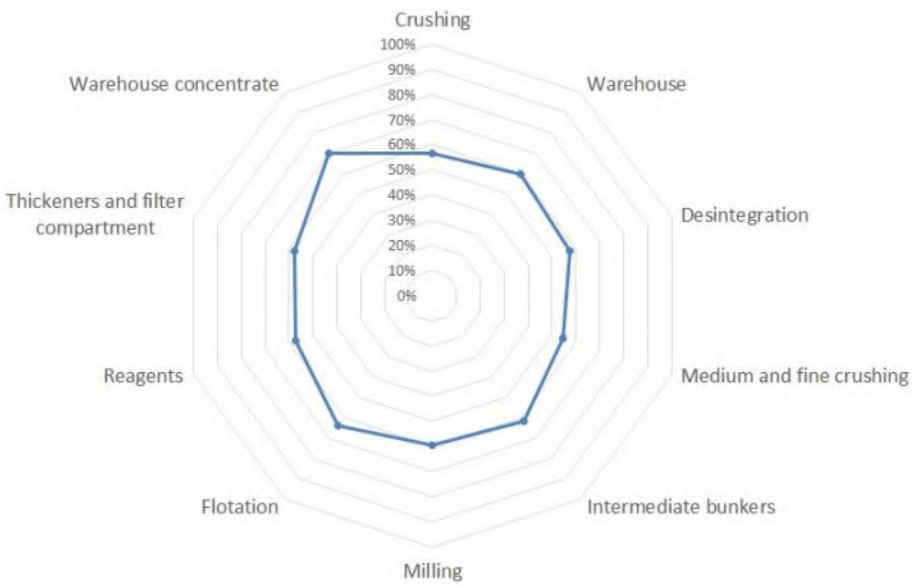

Figure 6. Graphical comparison of the overall safety level assessment for the entire processing plant

Key Factors for Occupational Health and Safety

Working conditions are classified into several groups:

1. Organizational and technical elements – production equipment / machines, facilities, technological processes and work sites, buildings in two aspects: safety and ergonomics.
2. Elements of safety and health at work – working environment (factors of the working environment and the work process), sanitary services and medical and prophylactic elements.
3. Psychophysiological and psychosocial elements.
4. Ergonomic elements – ergonomics of equipment, workwear, interior.
5. Socio-economic elements – qualifications, discipline, incentives, communications.

It turns out that there are factors that are usually not evaluated in detail or remain on the sidelines in terms of importance, but in reality they have a very big role in ensuring safety, i.e. they are key. The assessment of these factors reveals in detail the new safety in an enterprise and can serve as guidelines for its improvement (Basdew, 2023).

- *Working at height;*
- *Poor Housekeeping;*
- *Hand hazards* - Cuts. Scrapes. Broken fingers. Amputations;
- *Electricity* - five common electrical safety errors may occur: treating electrical work casually, not accounting for all scenarios, improper use of PPE, underestimating arc flash boundary and relying on institutional knowledge;
- *Confined spaces;*
- *Fire safety* – a mineral processing plant is at high risk of fire accidents. For this reason, it is necessary to provide reliable equipment for rapid detection and extinguishing of fires (Makedonska D., & Michaylov M., 2019).
- *Transportation incidents* - According to Bureau of Labor Statistics data, nearly 40% of worker deaths each year are related to transportation;
- *Accidents at work, incidents / Morbidity* **-** The annual analysis of the incidence of temporary disability for each calendar year is considered. Based on the results of the examinations, as well as on the basis of sick leaves, an analysis is prepared.
- *Shift work* - In practice, there are different ways of organizing work with a 24-hour shift mode (for example, shifts 2 X 12 hours or 3 X 7 hours). 12-hour shifts can lead to the accumulation of regular fatigue and subsequent illnesses. Combining a 12-hour shift work schedule and an insufficient number of staff negatively affects working capacity and concentration and is a prerequisite for accidents. The disadvantage of 7-hour shifts is the repetition of one type of shift (first; second; night) in 5 consecutive days, and it is not recommended to accumulate 5 consecutive night shifts.

Factors of the working environment: Working conditions in the performance of the main and auxiliary labor activities, which affect the quality and efficiency of the work activity, are directly related to the factors of the working environment. They affect the functional state of a person - working capacity, health, attitude to work and production efficiency. Health and safety at work is an essential element of the quality of work (Caffrey S., et al. 2017). Quality and low-risk working conditions are not only a legal requirement, but can be a powerful catalyst for innovation and higher productivity. With regard to the factors of the working environment on the territory of each processing plant, there are all potential hazards that could lead to accidents or the occurrence of an occupational disease - dust, noise, vibrations, harmful substances, microclimate, etc.

Safety of the work process, wearing PPE by the staff: Despite the legal minimum requirements for safety and protection of the health of workers when using personal protective equipment at the workplace and the control by the management staff, it is found that there are cases when workers do not wear PPE. This practice can be improved by conducting trainings and briefings, sanctions or other appropriate motivation.

Neuropsychic tension, neurosensory and neuro-emotional tension related to the nature of work activity: The work of the staff in the ore processing plant is associated with a high neuropsychic load. The work of the management and engineering staff - production director, shift supervisor, etc., is associated with a high degree of responsibility and the implementation of tasks in a short time (Bruce, P.J., et al. (2024). Neuropsychic tension is manifested by easy fatigue, rapid depletion of concentration, irritability, short-temperedness and nervousness. Neuropsychic tension is determined by:

- the degree of complexity of the tasks;
- perception and evaluation of information;
- from neurosensory /visual/ load related to the duration of observation and density of useful signals.

The work of the employees in the processing plant is also associated with a high neuropsychic load related to the perception of information, responsibility in relation to the position held, work with documents, work with people, relationships in the team, motivation and satisfaction with the work performed, etc.

Occupational Safety and Health Signs and Alerts: Safety signs and instructions must correspond to the risk assessment and be clearly visible. The size of the signage and indication signs must be appropriate, the evacuation exits must be marked.

Conducting Briefing and Training of Workers and Employees

Organization and manner of work of the OSH Department: The OSH department must have a high degree of autonomy, which will make its work flexible and more efficient. To have freedom in making quick operational decisions, to have a budget for current expenses. Having your own budget will allow the department to plan and implement measures to eliminate and reduce the likelihood of accident and accident conditions. The budget should be adopted on an annual basis in the enterprise.

Cause Analysis

Efficiency is expressed in the performance of daily work, meaning "fastest with least cost". When determining the effectiveness of management, the results obtained are mainly used. Establishing the efficiency of the company's activities can also be considered as management efficiency. Economic efficiency is related to financial results, but they are directly related to the level of safety of the work process.

Results and Discussion

After a safety audit, some basic recommendations for improving the level of safety can be noted, especially with regard to some less typical factors.

- *Introduction of flexible work shifts* with a different schedule and duration than the existing ones. In addition, a regular day shift should be introduced, which will provide the necessary personnel for technological processes, so that there are no isolated workplaces. This will allow compliance with the physiological regime of work and rest for all employees from of the processing plant.
- *Increasing staff motivation through more trainings*. In order to ensure that all employees understand the importance of their actions and their contribution to the fulfillment of the quality objectives, appropriate training should be provided. The training of the staff covers all levels: workers, specialists, heads of departments, departments and production units, management of the company. within the company, workers and specialists. The training of the staff is part of the practical implementation of the regulations of the policy on quality, health and safety at work and environmental protection. It is recommended to organize trainings and courses with highly qualified specialists from external organizations, companies and higher education institutions or to send the staff to specialized courses and seminars outside the territory of the enterprise. All trainings must end with a test or other form of control. When conducting on-site trainings, practical demonstrations are recommended.
- *Improvement of workplace lighting* **-** A particular problem for manufacturing enterprises is workplace lighting**.** The level of lighting in the working premises is often underestimated, not in accordance with the nature of the work and may be insufficient. Due to the heavy contamination of the windows with dust, a large part of the natural lighting sometimes does not reach the premises. It is a good practice to carry out periodic inspections to establish the presence of non-working lighting fixtures and burnt out bulbs, as well as periodic cleaning of lighting fixtures from dust and other dirt. This reduces the risk of accidents and accidents due to poor lighting.
- *Wearing PPE* **-** The type and technical characteristics of PPE should be coordinated depending on the risk and specific hazards at each workplace. Mandatory use of PPE according to the findings of the workplace risk assessment. Continuous monitoring of compliance with the requirement for the use of PPE. Conducting staff trainings on the proper use of PPE.
- *Incident investigation* **-** Registration, recording, analysis of incidents and accidents at work, as well as publicity of data would lead to awareness of workers and the sociate about what happened and when

and what the causes are. Lessons learned from each incident and sharing experiences are key to increasing safety.

- *Control and monitoring* **-** In hard-to-reach workplaces that are at high risk of accidents at work, innovative methods of control and monitoring can be applied. (Gospodinova V et al., 2017). Such methods as three-dimensional surveying, the use of drones, IoT, find application not only in the main technological processes, but also in various secondary activities in the extraction of raw materials, such as transportation, storage, transfer of materials (Gospodinova V, & Todorov T, 2023).

Conclusion

Maintaining healthy and safe working conditions, reducing injuries and morbidity, improving the psycho-climate and managing all other elements related to human resources, directly or indirectly brings direct or long-term benefits to the existence of the company, its competitiveness, efficiency, ability to bring profit and return on investments. Ensuring a high level of safety in the processing plant will lead to:

- Reduction of losses - man-hours due to worker absences due to (sick leave, trauma, accidents).
- Increased worker motivation
- Improving labor productivity and economic performance
- Increasing the image and social rating of the company
- Increased trust from business partners
- Financial gain

Scientific Ethics Declaration

* The authors declare that the scientific ethical and legal responsibility of this article published in EPSTEM journal belongs to the authors.

Conflict of Interest

* The authors declare that they have no conflicts of interest

Funding

* This research received no specific grant from any funding agency in the public, commercial, or not-for-profit sectors.

Acknowledgements or Notes

* This article was presented as an oral presentation at the International Conference on Research in Engineering, Technology and Science (www.icrets.net) held in Peja/Kosovo on July 10-13, 2025.

References

Alabi, O. O. (2018). Mineral processing route and safety in plant operations. *Journal of Advanced Research in Manufacturing, Material Science & Metallurgical Engineering*, *5*(3), 29-32.

Brown, M. (2009). Developing KPIs that drive process safety improvement. *SPE Offshore Europe Oil and Gas Conference and Exhibition,* Aberdeen, UK.

Bruce, P. J., Hrymak, V., Bruce, C., & Byrne, J. (2025). The role of interpersonal conflict as a cause of work-related stress in construction managers in Ireland. *Construction Innovation: Information Process Management*, *25*(1), 61–77.

Caffrey, S., Lara, L. V., Murtagh, C., Leva, M. C., & Hrymak, V. (2019). Task based risk assessment for human factors impact on aviation maintenance deviations: A case study on three specific tasks and their operational implications. In *Proceedings of the 29th European Safety and Reliability Conference (ESREL)*.

Forbes, E., Ma, M., & Bruckard, W. (2017). Clay minerals in flotation and comminution operations. In M. Gräfe, C. Klauber, A. J. McFarlane, & D. J. Robinson (Eds.), *Clays in the minerals processing value chain* (pp. 302–326). Cambridge: Cambridge University Press.

Gao, X. (2025). Study on the mineral processing technology of copper-nickel sulfide ore. *Journal of Engineering and Applied Science*, *72*, 29.

Gorbounov, Y., & Chen, H. (2019). Technological aspects and applications of large power switched reluctance motors in mining. *Journal of Mining and Geological Sciences*, *62*(3), 82–91.

Gospodinova, V., & Todorov, T. (2023). Three-dimensional modeling of a bridge by integrating terrestrial and aerial photogrammetry applying an adapted capture method. *Aerospace Research in Bulgaria*, *35*, 87–97.

Gospodinova, V., Begnovska, M., & Petkov, R. (2017). Research the possibilities of unmanned aerial vehicles to solve surveying tasks. *Geodesija, Kartografija, Zemeustrojstvo* 1-26.

Hale, A. (2009). Why safety performance indicators? *Safety Science*, *47*(4), 479–480.

Basdew (2023, March 21). *Hazards associated with an ore processing Plant*. Retrieved from https://www.mineralprocessing.co.za/358/hazards-associated-with-an-ore-processing-plant/tsf/basdew/

Infrastructure Health & Safety Association. (2019). *Construction health and safety manual: Mineral processing*. Toronto, Canada. IHSA.

Makedonska, D., & Michaylov, M. (2019). Need for fixed firefighting systems in road tunnels. *Journal of Mining and Geological Sciences*, *62*, 60–65.

Minin, I., & Hristova, T. (2024). Possibilities to reduce consumption of steel balls in drum mills while saving energy consumption. In *Proceedings of the 2024 5th International Conference on Communications, Information, Electronic and Energy Systems (CIEES)* (pp. 1–6).

Mollova, Z. (2024). Advancements in civil explosives: Novel formulations and sustainable fuel solutions. *Sustainable Extraction and Processing of Raw Materials*, *5*(5), 45–49.

Pradip, Gautham, B. P., Reddy, S. S., Prasad, P. S. R., Kumar, S. R. T., Kumar, K. R., ... Singh, D. D. N. (2019). Future of mining, mineral processing and metal extraction industry. *Transactions of the Indian Institute of Metals*, *72*(8), 2159–2177.

Trinh, H. B., Kim, S., Son, T., Song, J., & Lee, J. (2025). Evaluation of energy consumption for mineral processing of tungsten ore in Mongolia: Khovd Aimag and Erdene-Soum as case studies. *Minerals*, *15*(6), 660.

Yankova, T., & Grigorova, I. (2020). Automated waste collection systems: Possibilities, trends and application. *International Multidisciplinary Scientific GeoConference SGEM*, *20*(4.1), 221–228.

Author(s) Information

Nadezhda Kostadinova	Blagovesta Vladkova
University or Mining and Geology "St. Ivan Rilski"	University or Mining and Geology "St. Ivan Rilski"
Sofia, Bulgaria	Sofia, Bulgaria
Contact e-mail: *Nadezhda.kostadinova@mgu.bg*	

To cite this article:

Kostadinova, N. & Vladkova, B. (2025). Key assessment indicators for safety in mineral processing plant. *The Eurasia Proceedings of Science, Technology, Engineering and Mathematics (EPSTEM), 35,* 63-71.

The Eurasia Proceedings of Science, Technology, Engineering & Mathematics (EPSTEM)
ISSN: 2602-3199

The Eurasia Proceedings of Science, Technology, Engineering and Mathematics (EPSTEM), 2025

Volume 35, Pages 72-83

ICRETS 2025: International Conference on Research in Engineering, Technology and Science

Overcoming Communication Challenges in the Construction Industry: A Comparative Study of Kuwait and Saudi Arabia

Akram Suleiman
University of Jordan

Abstract: Lack of communication is a major barrier in the construction zone, particularly in Kuwait and Saudi Arabia, and can critically influence the gaining or drub of a project. This survey engaged consultants, clients, and contractors in the Kuwaiti and Saudi construction industry through a comprehensive survey, which listed 32 potential sources and 21 possible consequences of bad communication. The survey revealed that the important reasons of ineffective communication in both countries include the complexity of the industry, poor planning and coordination, reduction of communication techniques and preparation, differences in skill levels among teams, and poor detailed drawing. The greatest notable impact of poor communication includes mistakes, misunderstanding, low satisfaction, poor teamwork, poor planning, time overruns, low productivity, and adverse impacts on the design process. Interestingly, the survey results indicated a substantial agreement between Saudi and Kuwaiti respondents on the roots and influences of bad communication. To improve communication in these industries, it is crucial to treat the identified reasons and implement effective communication procedures and training. This study's findings provide valuable insights for the construction sectors in Kuwait and Saudi Arabia and may also be relevant to other developing countries. Upcoming study should highlight the development and implementation of effective communication strategies based on these findings.

Keywords: Communication, Construction industry, Comparative study

Introduction

The industry of construction of any country is vital to its economic evolution and progress. The construction industry counts on the execution and success of many participants in delivering the necessary construction projects (consultants, contractors, clients, suppliers, and subcontractors). To succeed, these sides needed to communicate and collaborate. The execution of a project relies on active communication. (Anantatmula, 2015). Effective connection is essential to achieving a constructing project (Dainty et al., 2007; Emmitt & Gorse, 2006). To accomplish its objectives, a construction project requires good collaboration and information exchange among its partners (Akinradewo et al., 2017). Communication proficiency are vital for project stakeholders; they were rated as having the greatest critical adequacy between Palestinian construction project administrators (Omran & Suleiman, 2017). Effective communication improves project performance by saving time, increasing productivity, and increasing customer satisfaction. Inefficient communication leads to time overruns, lost production, and client dissatisfaction.

In the construction industry, poor communication can own a major leverage on the prosperity of a project, leading to delays, confusion, cost overruns, disputes, and even injuries (Hwang et al., 2019). To understand the extent to which poor communication negatively impacts construction projects, it is important to examine literature from scientific journals. An earlier study found that lack of communication between stakeholders is a major contributor to poor project performance (Atkinson, 2002; Ng et al., 2004). Similarly, improved communication amongst stakeholders is essential to achieving project goals, according to (Meng, 2012) findings. In the construction sector, lack of connection can be referred to as unproductive, ineffectual, and bad communication of project data (Berntzen, 1988). Lack of connection in the construction area can establish cost

- Selection and peer-review under responsibility of the Organizing Committee of the Conference

overruns, schedule delays, conflicts, and even project collapse, among other consequences. One of the primary reasons of increased project costs is a shortage of effective communication among members of the project team (Mahamid, 2016). As stated by Hyväri (2007), project managers that have the capability to connect effectively are critical to the attainment of any project. The vast majority of construction-related issues stem from a lack of clear and timely communication. (Kazi, 2005). Communication breakdowns are one of the furthermost major impedances which Palestinian project managers face when supervising construction projects in Palestine (Omran, Hardan & Suleiman, 2016).

The construction industry in Kuwait and Saudi Arabia suffers from a lack of effective communication, which is examined in this paper. To improve project performance, it gives workable ways to treat with the underlying reasons and effects of these issues. Preliminary studies have concentrated on the sources and special effects of reduced communication in industrialized countries including the United States and Europe This means that findings from research undertaken in developed countries may not be applicable to countries in the world's developing. Furthermore, no research has been done on the construction industry in Kuwait or Saudi Arabia. For this reason, this research targets to plug this knowledge hiatus and join to the form of awareness about the reasons and impacts of bad communication in the construction zone in Kuwait and Saudi Arabia. The investigation has two objectives: the first is to classify and prioritize the cause and impact of lack communication; the second is to define whether there is a statistically major variance between Kuwaiti and Saudi respondents when it comes to assessing the cause and impacts of bad communication.

Literature Review

In the area of building management, there has been a growing concentration on the issue of lack of communication in recent years. This is due to the understanding that successful construction projects hinge on effective communication. It's often cited as a primary cause of project letdown (Abdul Rahman et al., 2013), rework increases costs and program (Emuze & James, 2013), and misunderstandings between construction parties (Lee & Bernold, 2008). In a comparative study by Oshodi and Rimaka (2013), poor communication was rated as the 11th and 12th most major reasons of construction project delays in Iran and Nigeria, respectively.

Large construction projects often grapple with poor communication, which is frequently identified as a primary cause of project failure. A comprehensive literature review by Hussain et al. (2018) recognized 30 reasons and 20 effects of bad communication in the construction industry. Darvik & Larsson (2010) discovered that quality defects and material distribution discrepancies were due to a shortage of communication and communication disappointment between main stakeholders. Gamil & Rahman (2017) showed a notional analysis of the reasons and impacts of poor communication, identifying several common factors including ineffective communication among construction personnel, poor communication abilities, language obstacles, and a shortage of uphold for developed communication.

Poor communication can increase project execution time variances midst construction associates, cost overruns, rework and redesign events, high accident rates, project weakness, and dejected manpower. Vdovin (2020) and Brookins (2020) also identified several popular aspects of poor place of work communication, including unclear aims, poor guidance, cultural assortment in the workplace, dispirited workers, individual matters, and employee obstacles. Helpless communication midst construction associates can lead to important construction project disputes, tardiness, and cost override. Studies have shown that construction time and cost overruns are greatest frequently produced by bad communication. Time overrun is a common issue in the construction industry, having a harmful impact on project achievement (Faridi & El-Sayegh, 2006). Abdul Rahman et al. (2013) identified a shortage of communication as one of the highest reasons of construction delays. Cost overruns have their greatest influence on the Egyptian construction industry during the design phase. They are produced due to lack of proper communication and collaboration between design participants from different experiences (Bassioni et al., 2013). Lack of connection midst construction associates was similarly one of the roots of cost overruns in Saudi Arabia (Alhomidan, 2013).

In conclusion, poor communication in the building industry can significantly influence the success of a project, leading to delays, confusion, cost overruns, disputes, and even injuries. To ensure effective communication, it is crucial to make sure that all communication is clear, concise, and tailored to the recipient's knowledge level. By prioritizing effective communication, construction companies can improve project outcomes, reduce costs, and enhance team morale, ultimately leading to a safer and more productive work environment.

Despite the wealth of research on the impact of lack of connection in the industry of construction, there is a noticeable gap in the literature when it comes to the construction industry in Kuwait and Saudi Arabia. This research goals to seal this hiatus by inspecting the roots and effects of shortage communication in the construction region of these two countries.

Method

The current research is established on a questionnaire survey that aimed to gather data from several contributors in the construction industry in Kuwait and Saudi Arabia. The survey includes 53 criteria associated to reasons and impacts of bad communication on building projects. The investigation was split into two portions: the first portion assessed the roots and effects of poor communication on a five-point Likert scale, and the second portion gathered data on the participant's organization and private data. The questionnare was sent to owners, contracting and consulting construction companies. Project managers with more than five years' experience were asked to complete it. The survey was sent in person and electronically via email.

The current research attentions on civil engineers working in the industry of construction in Kuwait and Saudi Arabia. As of 2020, there were 18,046 Saudi engineers recorded with the Saudi Council of Engineers and nearly 14,500 Kuwaiti engineers listed with the Society of Engineers. A mathematical equation (Equation 1) was used to define the sample size desired for the study.

$$N_o = (t^2 * S^2)/(d^2) \qquad (1)$$

Where t = value of the selected α level of 0.025 in each tail=1.96; s =estimate of standard deviation in the population=1.25; d = acceptable margin of error for mean being estimated=0.15;
Equation 2 shall be used to make the correction:

$$N = No/[1 + \left(\frac{No}{pop}\right)] \qquad (2)$$

In over-all, 243 surveys were spread, and 112 replies were answered, response rate 46%.

Reliability

An experimental study was conducted to define the reliability of the survey applied in the current research. Reliability was determined using Cronbach's coefficient alpha, which is a generally used measure of reliability. A value of 0.7 or higher is considered reliable, according to (Cronbach & Shavelson, 2004). The Cronbach's coefficient alpha for the reasons and influence of bad communication were 0.948 and 0.922 respectively, as displayed in Table 1. These values are overhead 0.7, showing that the questionnaire is reliable and the study results can be replicated in additional experiments under identical conditions.

Table 1. The survey instrument's reliability

Subscale	No. of Items	Reliability (Cronbach's Alpha)
Causes	32	0.948
Effects	21	0.922
Total Scale	53	0.961

The information gathered from the survey was investigated applying several analytical techniques. The data was transformed to a usable format by using SPSS Version 17.0 for data analysis and evaluated for results. To test the whole profile and experience of the participants'' companies, descriptive statistics such as means and frequencies were applied. This provided an understanding of the general characteristics of the sample population.

Results and Discussion

Demographic Description

Participants were asked about their years of practice, company kind, company specialty, and company years of experience. Percentages are used to describe the respondents' demographic characteristics. Table 2 offers an indication of the setting of the participants and their construction firms. The plurality of the participants (50%) were clients, followed by consulting firms (33%) and contracting firms (17%). In terms of the specialization of the organizations, most respondents (68%) worked in building construction, followed by highway construction (18%), water and sanitation (7%), and other types of construction (7%). In terms of experience, most respondents (33%) had 6-10 years of experience, followed by 11-15 years (35%), 16-20 years (14%), and more than 20 years (18%). Similarly, most organizations (36%) had more than 20 years of experience, followed by 16-20 years (21%), 11-15 years (16%), 6-10 years (14%), and 0-5 years (13%).

Table 2. Background of respondents and construction firms

Item	Percent
Type of the organization	
Contracting	17
Client	50
Consulting	33
Specialization of the organization	
Buildings	68
Water & sanitation	7
Highway	18
Other	7
Respondents` experience in years	
6 – 10	33
11-15	35
16 – 20	14
More than 20	18
Organization experience in years	
0-5	13
6 – 10	14
11-15	16
16 – 20	21
> 20	36

Ranking of Causes and Effects in KSA

An ordinal measuring scale was utilized in this study, which ranks rating data based on numbers in descending or ascending order. On an ordinal scale, data were analyzed applying a relative importance index (RII). The RII is a straightforward yet efficient technique for evaluating point of view regarding commonly surveyed variables in construction research. Participants were requested to list the reasons and effects factors in order of significance using a five-point Likert scale (1 = strongly disagree; 2 = disagree; 3 = neutral; 4 = agree; 5 = highly agree). The RII was assessed using the RII equation relied on the survey response (Omran & Suleiman, 2017; Salem & Suleiman, 2020) as presented in the subsequent formula (3):

$$\mathrm{RII}=\frac{\sum W}{(A*N)} \qquad (3)$$

Relative importance index (RII), the weight of each item by participants, which ranges from 1 to 5, is represented by W. It indicates the maximum weight, which is 5 in this situation. N signifies the whole amount of participants. The RII value lies between 0 and 1 (inclusive), and a higher RII number indicates a more important cause or effect. Next, the RIIs were categorized, with the outcomes offered in Tables 3 and 4. RII values ranged from 0.88 to 0.44, indicating that participants considered each of these factors important.

Table 3 offerings a summary of the reasons for poor communication in Saudi Arabia (KSA) as indicated by survey participants. The causes are categorized relied on their values of relative importance index (RII), with a higher RII indicating a higher level of importance. The top reason of poor communication in KSA is possessing different skills levels among construction teams (RII=0.88), followed by lack of communication procedure and training (RII=0.77), incorrect instructions or technical information (RII=0.76), lack of effective communication system and platform (RII=0.75), and lack of effective communication between construction parties (RII=0.73). Other causes in the top 10 include poor communication skills, inaccurate delivery of project information, contractual barriers, lack of support for advanced communication technologies, and poor planning and coordination. Other causes listed in the table include language barrier, complexity of the construction industry, improper communication channels, and gender differences. Overall, the table shows that poor communication in the KSA construction industry is caused by a combination of factors, including technical and organizational issues, personal and cultural barriers, and a lack of appropriate communication procedures and training.

The results in Table 3 suggest that the top causes of poor communication in the KSA construction industry are related to the skills and expertise of the construction teams, as well as the communication procedures and training in place. Possessing different skills levels among construction teams is likely to lead to misunderstandings and misinterpretations, which can have a harmful impact on the prosperity of the project. Similarly, a lack of communication procedure and training can result in confusion and inefficiency among team members, leading to poor communication and coordination.

Incorrect instructions or technical information and lack of effective communication systems and platforms are also likely to cause poor communication, because it can lead to misinterpretation and faults in the construction process. Lack of effective communication between construction parties can also create barriers to communication and hinder the flow of information. The results also indicate that poor planning and coordination, poor communication skills, and inaccurate delivery of project information are among the top causes of poor communication in the KSA construction industry. These issues can result in delays, cost overruns, and poor-quality construction. Language barriers, complexity of the construction industry, and poor detailed drawing can also contribute to lack of communication in the KSA construction industry. These factors can create challenges for communication and understanding among team members with different languages or from different cultural backgrounds.

Table 3. Descriptive analysis and ranking of poor communication causes in KSA

Cause	RII	Overall ranking
Possessing differed skills levels among construction teams	0.88	1
Lack of communication procedures and training	0.77	2
Incorrect instructions or technical information	0.76	3
Lack of effective communication system and platform	0.75	4
Lack of effective communication between construction parties	0.73	5
Poor communication skills	0.73	6
Inaccurate delivery of project information	0.72	7
Contractual barrier	0.72	8
Lack of support for advanced communication technologies	0.71	9
Poor planning and coordination	0.71	10
Poor communication management	0.71	11
Unavailability of information in the time of need	0.71	12
Lack of communication plan	0.69	13
Slow information flow between	0.69	14
Lack of adequate representation for project stakeholders	0.69	15
Lack of understanding among parties	0.68	16
Possessing different level of education among construction teams	0.67	17
Personal barrier	0.65	18
Diversity of culture and ethics among construction teams	0.64	19
Inaccessibility of information	0.61	20
Improper communication time management	0.61	21
Lack of mutual respect and trust among construction teams	0.61	22
Weak organizational structure	0.61	23
Lack of appropriate communications medium	0.60	24
Lack of clear objectives	0.60	25
Technology malfunction	0.57	26
Frequent changes of project contract	0.57	27
Poor detailed drawing	0.57	28
Language barrier	0.55	29
Complexity of the construction industry	0.53	30
Improper communication channels	0.49	31
Gender differences	0.48	32

Gender differences also can be a cause of poor communication as well. Generally, the outcomes propose that shortage of communication in the KSA construction industry is produced by a combination of factors, including technical and organizational issues, personal and cultural barriers, and a shortage of appropriate communication processes and preparation. Improving communication in the industry will require addressing these causes and implementing effective communication procedures and training.

Table 4. Descriptive analysis and ranking of poor communication effects in KSA

Effect	RII	Overall ranking
Misinterpretation	0.79	1
Misunderstanding	0.76	2
Low Level of satisfaction among construction parties	0.76	3
Poor team work	0.75	4
Poor planning	0.75	5
Demotivated workforces	0.73	6
Conflict among construction parties	0.71	7
Cost overrun	0.69	8
Design errors	0.69	9
Frequent remedies in design and planning schedule	0.67	10
Poor project documentation	0.67	11
Low productivity	0.65	12
Poor risk management	0.65	13
Affects design process	0.65	14
Rework and redesign occurrence	0.64	15
Unclear channels	0.63	16
Waste generation	0.61	17
Time overrun	0.60	18
Failure of the project	0.60	19
Late response to disaster	0.56	20
High accident rate	0.44	21

Table 4 displays an outline of the impacts of lack communication in the Kingdom of Saudi Arabia (KSA) as documented by the survey respondents. The effects are classified rely on their relative importance index (RII) values, with a higher RII indicating a higher level of importance. The top effect of poor communication in KSA is misinterpretation (RII=0.79), followed by misunderstanding (RII=0.76), low level of satisfaction among construction parties (RII=0.76), poor teamwork (RII=0.75), and poor planning (RII=0.75). Other effects in the top 10 include demotivated workforces, conflict among construction parties, cost overrun, design errors and frequent remedies in design and planning schedule.

The results also indicate that poor project documentation, low productivity, poor risk management, affects design process and rework and redesign occurrence are among the top effects of poor communication in the KSA construction industry. These issues can result in delays, cost overruns, and poor-quality construction. Late response to disaster and high accident rate are also among the top effects of poor communication. Overall, the results suggest that lack of communication in the KSA construction industry can produce a variety of undesirable impacts, including misinterpretation, misunderstanding, low satisfaction, poor team work, poor planning, demotivated workforces, conflict, cost overrun, design errors, poor project documentation, low productivity, poor risk management, affects design process, rework and redesign occurrence, unclear channels, waste generation, time overrun, failure of the project, delayed reply to calamity and high accident rate. Treating the reasons of poor communication in the industry can help to mitigate or eliminate these negative effects and improve the overall success of construction projects.

The outcomes shown in Table 4 suggest that poor communication in the KSA construction industry can create a variety of undesirable impacts on the project's success. Misinterpretation and misunderstanding are likely to occur when communication is poor, leading to confusion and errors among team members. This make a detrimental influence on the project's result, including on the design process, and lead to rework, redesign and errors (Salem & Suleiman, 2020). Small scale of contentment through construction parties and poor teamwork are also likely to be effects of poor communication. Construction projects are complex and need the collaboration of multiple parties, and poor communication can create barriers to collaboration and cooperation, leading to low satisfaction and poor teamwork. Poor planning is also an effect of poor communication as it can lead to delays, cost overruns, and poor-quality construction. The results also indicate that poor communication can lead to demotivated workforces, conflict among construction parties, design errors, poor project documentation, low productivity and poor risk management.

The results suggest that poor communication can create a time exceed in addition to cost overrun and failure of the project. This can also lead to a high accident rate, late response to disaster, waste generation and unclear channels. Overall, the results suggest that the lack of communication can have an extensive skope of negative effects on construction projects in the KSA, including misinterpretation, misunderstanding, low satisfaction, poor team work, poor planning, demotivated workforces, conflict, cost overrun, design errors, poor project documentation, low productivity, poor risk management, affects design process, rework and redesign occurrence, unclear channels, waste generation, time overrun, failure of the project, late response to disaster and high accident rate. Addressing the causes of poor communication can help to mitigate or eliminate these negative effects and improve the overall success of construction projects. It's worth noting that several studies, including (Gamil & Rahman, 2017; Hussain et al., 2018; Rahman & Gamil, 2019), categorized the same reasons and impacts in the top 10, but in slightly various order.

Ranking of Causes and Effects in Kuwait

Table 5 summarizes the reasons of shortage communication in the Kuwaiti construction industry as identified by the survey respondents. The causes are ordered depended on their relative importance index (RII) values, with a higher RII indicating a higher level of importance. The top cause of poor communication in Kuwait is Poor detailed drawing (RII=0.69), followed by Complexity of the construction industry (RII=0.65), Poor planning and coordination (RII=0.65), Lack of communication procedure and training (RII=0.65) and Possessing differed skills levels among construction teams (RII=0.64). Other causes in the top 10 include Lack of clear objectives, Inaccessibility of information, frequent changes of project contract, inaccurate delivery of project information and unsuitable communication time administration.

The outcomes propose that the lack of communication in the Kuwaiti construction industry can be established by a assortment of impacts such as poor detailed drawing, complexity of the construction industry, poor planning and coordination, shortage of communication procedure and training, owning varied expertise levels between construction stakeholders, lack of clear objectives, inaccessibility of information, frequent changes of project contract, inaccurate delivery of project information, and improper communication time management. Addressing these causes can help to improve communication and the overall achievement of construction projects in Kuwait.

The overhead outcomes recommend that bad communication in the Kuwaiti construction industry can be caused by a variety of factors, including poor detailed drawing, complexity of the construction industry, poor planning and coordination, lack of communication procedure and training, having changed knowledge levels amongst construction teams, lack of clear objectives, inaccessibility of information, frequent changes of project contract, inaccurate delivery of project information, and improper communication time management.

Poor detailed drawing can make it hard for parties to realize the project requirements and can lead to misunderstandings and misinterpretations. Complexity of the construction industry can make it difficult for stakeholders to understand the project requirements and can lead to misunderstandings and misinterpretations. Poor planning and coordination can make it difficult for stakeholders to understand the project requirements and can lead to misunderstandings and misinterpretations. Lack of communication procedure and training can make it problematic for parties to recognize the project requirements and can lead to misunderstandings and misinterpretations. Keeping varied abilities levels between construction sides can create it hard for stakeholders to realize the project requirements and can lead to misunderstandings and misinterpretations.

Lack of clear aims establishes some problems for stakeholders to know the project requirements and can lead to misunderstandings and misinterpretations. Inaccessibility of information can produce hard issues for stakeholders to comprehend the project necessities and can lead to misunderstandings and misinterpretations. Frequent changes of project contract can make it problematic for parties to understand the project requirements and can lead to misunderstandings and misinterpretations. Inaccurate delivery of project information can make it tough for stakeholders to appreciate the project requirements and can lead to misunderstandings and misinterpretations. Improper communication time management can make it problematic for participants to recognize the project desires and can lead to misunderstandings and misinterpretations.

Addressing these causes of poor communication can help to improve communication and the overall success of construction projects in Kuwait. By taking steps to ensure that stakeholders have access to accurate and complete information, that communication procedures are in place and training is provided, that skills levels are appropriate, that objectives are clear, and that communication is managed properly, construction projects in Kuwait will be more likely to be successful.

Table 5. Descriptive analysis and ranking of poor communication causes in Kuwait

Cause	RII	Overall ranking
Poor detailed drawing	0.69	1
Complexity of the construction industry	0.65	2
Poor planning and coordination	0.65	3
Lack of communication procedures and training	0.65	4
Possessing differed skills levels among construction teams	0.64	5
Lack of clear objectives	0.64	6
Inaccessibility of information	0.63	7
Frequent changes of project contract	0.63	8
Inaccurate delivery of project information	0.63	9
Improper communication time management	0.61	10
Possessing different levels of education among construction teams	0.60	11
Incorrect instructions or technical information	0.60	12
Poor communication skills	0.59	13
Technology malfunction	0.59	14
Poor communication management	0.59	15
Weak organizational structure	0.59	16
Unavailability of information in the time of need	0.59	17
Contractual barrier	0.59	18
Language barrier	0.57	19
Lack of communication plan	0.57	20
Slow information flow between	0.57	21
Lack of effective communication system and platform	0.56	22
Lack of support for advanced communication technologies	0.56	23
Personal barrier	0.56	24
Lack of adequate representation for project stakeholders	0.56	25
Lack of mutual respect and trust among construction teams	0.55	26
Diversity of culture and ethics among construction teams	0.53	27
Lack of appropriate communications medium	0.53	28
Lack of understanding among parties	0.53	29
Lack of effective communication between construction parties	0.52	30
Improper communication channels	0.51	31
Gender differences	0.49	32

Table 6 shows the results of a survey conducted on construction stakeholders in Kuwait, specifically civil engineers working in the construction industry. The survey aimed to identify the reasons and effects of lack of communication in the construction sector in Kuwait. Table 5 shows the highest roots of bad communication as identified by the survey respondents, with "Poor detailed drawing" being the most significant cause with an RII value of 0.69. Other notable causes include "Complexity of the construction industry", "Poor planning and coordination", "Lack of communication procedure and training" and "Possessing differed skills levels among construction teams".

Table 6 shows the top effects of poor communication, with "Time overrun" being the most significant effect with an RII value of 0.73. Other notable effects include "Poor planning", "Conflict among construction parties", "Low productivity" and "Affects design process". These results suggest that poor communication in the construction sector in Kuwait can lead to significant issues such as project delays, increased costs, and reduced productivity. To mitigate these issues, it is important for the stakeholders in the construction industry to improve their communication practices and invest in effective communication tools and training.

It is generally understandable that poor communication can lead to a wide range of negative effects in the construction industry. Time overruns and poor planning can produce delays at the end of the project, which can cause additional costs and inconvenience to all parties involved. Disputes between construction sides can also lead to delays and additional costs. Low productivity, design errors, and cost overruns can be a consequence of poor planning and lack of coordination among the parties.

Misunderstandings and unclear channels can lead to misinterpretation and misinterpretation of design, leading to errors and rework, which can increase the project cost and time. Bad danger administration, lack of project records and poor teamwork can lead to a high accident rate and project failure. Overall, all the effects listed in the table can have a undesirable influence on the project and the satisfaction of the sides involved.

Table 6. Descriptive analysis and ranking of poor communication effects in Kuwait

Effect	RII	Overall ranking
Time overrun	0.73	1
Poor planning	0.72	2
Conflict among construction parties	0.71	3
Low productivity	0.71	4
Affects design process	0.71	5
Design errors	0.69	6
Cost overrun	0.68	7
Misunderstanding	0.68	8
Demotivated workforces	0.67	9
Late response to disaster	0.67	10
Poor risk management	0.67	11
Poor project documentation	0.67	12
Low Level of satisfaction among construction parties	0.65	13
Unclear channels	0.65	14
Frequent remedies in design and planning schedule	0.64	15
Misinterpretation	0.63	16
Failure of the project	0.61	17
Waste generation	0.61	18
Rework and redesign occurrence	0.60	19
Poor teamwork	0.59	20
High accident rate	0.51	21

Hypothesis Testing

Formulating the primary hypothesis was crucial for accomplishing the study's second objective. The Mann-Whitney test, a non-parametric method, was utilized to explore this. The Mann-Whitney test was conducted to ascertain if there was a statistically significant discrepancy in the ranking of poor communication causes at the 0.05 level. The initial hypothesis, H1, posits that there is no substantial difference in the perceptions of respondents from KSA and Kuwait regarding the ranking of poor communication causes. This group comprises 32 variables. Respondents from Saudi Arabia perceived these factors to have a Relative Importance Index (RII) ranging from 0.88 to 0.48, while respondents from Kuwait perceived them to have a RII ranging from 0.69 to 0.49. The high RII values from Saudi respondents and moderately high values from Kuwaiti respondents suggest that these variables significantly influence the causes of poor communication.

Table 7. The results for the hypothesis

	KSA		Kuwait	
	Causes	Effects	Causes	Effects
N	57	57	55	55
Mean Rank	17.73	15.90	13.27	15.1
Sum of Ranks	266.0	238.5	199.0	226.5
Mann-Whitney U for causes	79.0			
Mann-Whitney U for effects	106.5			
Sig for causes	0.163			
Sig for effects	0.802			

The mean rank for the causes in KSA was 17.73 and for Kuwait it was 13.27, and for effects in KSA it was 15.9 and for Kuwait it was 15.1. The Mann-Whitney U test was used to compare the causes and effects between the two countries and the significance level for the causes is 0.163, and for the effects is 0.802. These results suggest that the roots and impacts of poor communication in the construction industry in Saudi Arabia and

Kuwait are not significantly different, and that both countries face similar challenges in this area. It can be inferred that the study found that poor communication in the construction industry is an issue in both countries, and that the causes and effects of poor communication are similar in both countries.

The second hypothesis, H2, posits that there is no important variance in the insights of participants from Saudi Arabia and Kuwait regarding the ranking of the negative effects of poor communication. This category includes 21 variables. Respondents from Saudi Arabia assigned Relative Importance Index (RII) values between 0.79 and 0.44 to these factors, while respondents from Kuwait assigned RII values between 0.73 and 0.51. Both Saudi and Kuwaiti respondents have relatively high RII values, suggesting that these variables significantly influence the negative effects of poor communication. As shown in Table 7, both the Mann-Whitney value of 106.5 and the p-value of 0.802 exceed the 0.05 level of significance. Therefore, the null hypothesis is accepted. This means that there is no statistically significant difference between the perceptions of Saudi and Kuwaiti respondents regarding the undesirable impacts of poor communication.

Conclusions

This investigation pointed to inspect the reasons and influences of lack of communication in the construction industry in Saudi Arabia (KSA) and Kuwait. Results indicated that there were 53 roots and influences of bad communication identified, which were categorized applying the relative importance index (RII) technique. All reasons and special effects were found to be highly important, with an RII above 0.5. Additionally, there was a great level of arrangement between participants in KSA and Kuwait in terms of the classification of bad communication sources and impacts.

The top causes of poor communication in KSA were found to be lack of communication procedures and training, lack of effective communication systems and platforms, lack of effective communication between construction parties, and poor planning and coordination. The top effects of poor communication in KSA were misinterpretation, misunderstanding, low satisfaction among construction parties, poor teamwork and poor planning. Similarly, in Kuwait, the highest roots of poor communication were poor detailed drawing, complexity of the construction industry, poor planning and coordination, lack of communication procedures and training and lack of clear objectives. The upper impacts of bad communication in Kuwait were time overrun, poor planning, conflict among construction parties, low productivity and design errors. Generally, the outcomes of this research highlight the importance of effective communication in the construction industry and the necessity for urgent solutions to address the communication crisis in the construction sector in KSA and Kuwait.

Recommendations

Depending on the outcomes of this survey, the next commendations can be created to recovery the communication crisis in the construction industry in Saudi Arabia (KSA) and Kuwait:

- Implement effective communication procedures and provide training to all construction parties to ensure clear and accurate communication.
- Invest in modern communication systems and platforms to facilitate better communication between construction parties.
- Improve planning and coordination efforts to prevent misunderstandings and misinterpretations.
- Address the complexity of the construction industry by providing clear and specific objectives for all construction projects.
- Improve the detailed drawings provided to construction parties to reduce design errors and improve productivity.
- Address the issues of poor team work, low satisfaction, and conflict among construction parties.
- Work to reduce time overruns and improve overall project planning.
- Encourage continuous improvement in communication practices through regular evaluations and feedback.

Scientific Ethics Declaration

* The author declares that the scientific ethical and legal responsibility of this article published in EPSTEM journal belongs to the author.

Conflict of Interest

* The author declares that there is no conflict of interest

Funding

* There is no fund available at this time.

Acknowledgements or Notes

* This article was presented as an oral presentation at the International Conference on Research in Engineering, Technology and Science (www.icrets.net) held in Peja/Kosovo on July 10-13, 2025.

References

Akinradewo, O. F., Ojo, L. D., & Oyefusi, O. N. (2017). Effects of communication among professionals on building projects delivery in Nigeria. *Journal of Contemporary Research in the Built Environment*, *1*(2), 50–66.

Anantatmula, V. S. (2015). Strategies for enhancing project performance. *Journal of Management in Engineering*, *31*(6), 4015013.

Atkinson, A. R. (2002). The pathology of building defects; a human error approach. *Engineering, Construction and Architectural Management*, *9*(1), 53-61.

Berntzen, P. (1988). *Communication and related work problems in the construction industry*. University of Texas at Austin.

Cronbach, L. J., & Shavelson, R. J. (2004). My current thoughts on coefficient alpha and successor procedures. *Educational and Psychological Measurement*, *64*(3), 391–418.

Dainty, A., Moore, D., & Murray, M. (2007). *Communication in construction: Theory and practice*. Routledge.

Emmitt, S., & Gorse, C. (2006). *Communication in construction teams*. Routledge.

Enshassi, A., Mohamed, S., Mustafa, Z. A., & Mayer, P. E. (2007). Factors affecting labour productivity in building projects in the Gaza Strip. *Journal of Civil Engineering and Management*, *13*(4), 245–254.

Gamil, Y., & Rahman, I. A. (2017). Identification of causes and effects of poor communication in construction industry: A theoretical review. *Emerging Science Journal*, *1*(4), 239–247.

Hussain, A. M. A., Othman, A. A., Gabr, H. S., & Aziz, T. A. (2018). Causes and impacts of poor communication in the construction industry. *2nd International Conference on Sustainable Construction and Project Management–Sustainable Infrastructure and Transportation for future Cities* (pp. 16-18).

Hyväri, I. (2007). *Project management effectiveness in different organizational conditions*. Helsinki School of Economics.

Kazi, A. S. (2005). *Knowledge management in the construction industry: A socio-technical perspective*. IGI Global.

Mahamid, I. (2016). Micro and macro level of dispute causes in residential building projects: Studies of Saudi Arabia. *Journal of King Saud University-Engineering Sciences*, *28*(1), 12–20.

Meng, X. (2012). The effect of relationship management on project performance in construction. *International Journal of Project Management*, *30*(2), 188–198.

Ng, S. T., Skitmore, R. M., Lam, K. C., & Poon, A. W. (2004). Demotivating factors influencing the productivity of civil engineering projects. *International Journal of Project Management*, *22*(2), 139–146.

Omran, A., & Hardan Suleiman, A. S. (2016). Problems facing project managers in the Palestinians 'construction projects. *Annals of the Faculty of Engineering Hunedoara-International Journal of Engineering*, *14*(4), 39-46.

Omran, A., & Suleiman, A. (2017). Identifying the competence components of the construction project managers in the Palestinian construction industry. *The Engineering Project Organization Journal*, *7*(2), 2–27.

Rahman, I. A., & Gamil, Y. (2019). *Assessment of cause and effect factors of poor communication in construction industry*. IGI Global.

Salem, Z. T. A., & Suleiman, A. (2020). Risk factors causing time delay in the Jordanian construction sector. *International Journal of Engineering Research and Technology*, *13*(2), 307–315.

Author(s) Information

Akram Suleiman
Civil and Infrastructure Engineering Department
Al-Zaytoonah University of Jordan, Amman, Jordan
Contact e-mail: *a.suleiman@zuj.edu.jo*

To cite this article:

Suleiman, A. (2025). Overcoming communication challenges in the construction industry: A comparative study of Kuwait and Saudi Arabia. *The Eurasia Proceedings of Science, Technology, Engineering and Mathematics (EPSTEM), 35,* 72-83.

ISRES Publishing

The Eurasia Proceedings of Science, Technology, Engineering & Mathematics (EPSTEM)
ISSN: 2602-3199

The Eurasia Proceedings of Science, Technology, Engineering and Mathematics (EPSTEM), 2025

Volume 35, Pages 84-93

ICRETS 2025: International Conference on Research in Engineering, Technology and Science

Treatment of Industrial Wastewater Using a Mechanical Vapour Recompression Heat Pump System as a Source of Biomass

Slav Valchev
University of Food Technology

Nenko Nenov
InnoSolv Ltd

Abstract: A prospective method for treatment of wastewater from food and flavor industry with mechanical vapour recompression heat pump system, which achieves both recycling of purified water for repeated use and separation of waste with a high concentration of organic matters and use for production of biogas, is considered. Experimental results of wastewater treatment according to specified method are presented. A number of parameters of source wastewater and resulting concentrated sludge were compared: total microbial count, dissolved dry matter, undissolved dry matter, total dry matter, chemical oxygen demand, active reaction, electrical conductivity. It has been established that using the mechanical vapour recompression method for treatment of industrial wastewater two outflows are generated - of clean condensate with characteristics of pure distilled water and sludge rich in concentrated organic substances. Through use of the method, a waste-free technology for the treatment of industrial wastewater is realized.

Keywords: Wastewater treatment, Biomass, Mechanical vapour recompression.

Introduction

In various branches of food industry, technological processes are carried out, which generate significant amounts of wastewater. Wastewater has a high content of organic impurities, which is a problem for their discharge and disposal into the environment. On the other hand, the valuable organic substances contained in them, which can be used to produce biofuels, are lost after their treatment in centralized or local treatment plants. Increasingly high European environmental protection requirements, combined with impending shortage of conventional fuels, necessitate search for effective technologies for waste-free treatment of industrial wastewater (Ordinance No.6 of 09.11.2000; Ordinance No.7 of 14.11.2000). In this sense, methods for wastewater treatment that achieve both recycling of purified water for repeated use and separation of waste with a high concentration of organic substances and its use for biogas production are particularly promising. From a thermodynamic point of view, wastewater can be considered as a binary mixture of pure water and impurities. The latter are a combination of organic substances (residues of fruits, vegetables, leaves, particles of food products), pure and saponified fats, acids, bases, organic solvents, detergents, solid inorganic dissolved and undissolved substances (soil particles, salts), etc. The majority of these impurities are non-volatile substances or those with boiling points higher than those of water. The exception is some organic acids found in wastewater from processing dairy products, vegetables, etc. with boiling points lower than those of water. This allows a given wastewater as a mixture of water and non-volatile impurities to be thermally separated by evaporation method (Weimar et al., 1983). In this method, the wastewater is separated by applying heat and boiling into a volatile part - pure or almost pure water (condensate) and a non-volatile part - concentrated waste (sludge). The resulting condensate (purified water) can be recycled for reuse in relevant production when clean water standards are reached or discharged to sewage system or a natural water source. Due to the fact that specified method is extremely energy-intensive, mechanical compression of the secondary vapours obtained in

- Selection and peer-review under responsibility of the Organizing Committee of the Conference

evaporation process is applied. In recent years, there has been an increased implementation of systems using the described method for industrial wastewater treatment. Various indicators of wastewater such as composition, concentration of impurities, temperature, etc. determine the economic feasibility of applying this method in practice (Gallerani et al. 2002; Liang et al. 2013; Tuan et al., 2013). This method of water treatment is favorably affected by low values of dry matter concentration in source wastewater. This allows achieving a high degree of wastewater regeneration with efficient operation of the mechanical compressor. For example, with a 20-fold compression of wastewater, the sludge will have a relatively low total dry matter concentration (from 2 to 10%). In this case, 95% of wastewater flow will be purified to condensate, and 5% of wastewater will be discarded as sludge. The potential for using industrial wastewater sludge can be assessed based on analyses of its physical and chemical parameters (Pascual et al., 2018). Parameters such as acidity, electrical conductivity, chemical oxygen demand, bacterial composition, etc. provide guidance on how concentrated sludge can be used subsequently – for biogas, organic fertilizers, compost, etc. (Vatachi, 2019; Onet et al., 2014; Cudjoe et al., 2022; Abdel – Shafi & Mansour, 2014; Bacos et al., 2024). In addition to their use as a stand-alone raw material, a number of studies have shown that mixing them with biofuels produced from plant matter improves the ignition properties of the pellets, resulting in highly efficient fuel combustion in boiler. Through anaerobic digestion processes, biogas can be obtained from resulting sludge (Yurten & Ozdemir, 2024). The values of parameters such as total dry matter matter in sludge, carbohydrates and proteins determine the amount of biogas produced from sludge (Deena et al, 2022; Kazimierowicz et al., 2021; Vo´ca et al., 2021; Makisha & Semenova, 2018; Rulkens, 2008).

Method

For practical application of described wastewater treatment method, a pilot mechanical vapour recompression (MVR) heat pump system has been created for its implementation. A pilot MVR heat pump system performance is between 5.0 and 16.0 kg/h evaporated water from intake wastewater flow. On Figure 1 are shown schematic diagram of MVR heat pump system for wastewater treatment.

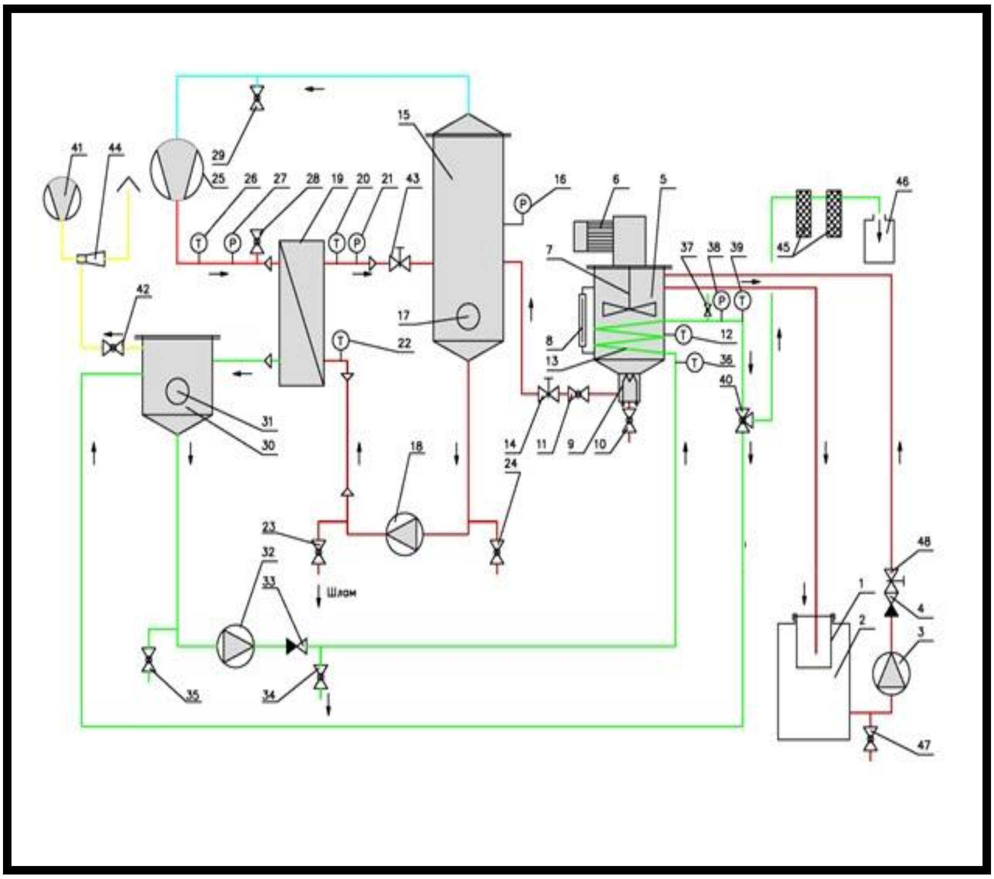

Figure 1. Schematic diagram of MVR heat pump system

On Figure 2 are shown general appearance of MVR heat pump system for wastewater treatment.

Figure 2. General appearance of MVR heat pump system

The first parameter for evaluating performance of MVR heat pump system is degree of wastewater regeneration ε. It is defined as ratio between mass flow of resulting condensate and mass flow of source wastewater:

$$\varepsilon = \frac{\dot{m}_C}{\dot{m}_W}$$

The degree of wastewater regeneration shows how much of it has been transformed into clean water (condensate) with the potential to be discharged to a sewage system in an environmentally effective manner or reused as clean water. The second important indicator of performance of MVR heat pump system, considered as an evaporation plant, is degree of concentration of wastewater φ. It is defined as ratio of concentration of dry matter in sludge ξ_S and concentration of dry matter in source wastewater ξ_W:

$$\varphi = \frac{\xi_S}{\xi_W}$$

Experimental treatment of five samples of industrial wastewater of different origin were carried out on created MVR heat pump system. The initial information for samples studied includes:

Sample 1 - wastewater from purge of a water condenser of an industrial refrigeration plant. This type of water is characterized by a temperature of 35-40°C and an increased content of inorganic substances - dissolved calcium salts, increasing its hardness. In general, this type of water is free of organic contaminants. The samples were taken from a dairy processing plant.

Sample 2 - wastewater from steam boiler blowdown. This type of water is discharged at a high temperature in range of 93-95°C. It is characterized by an increased content of various non-volatile inhibitors added to boiler water of inorganic origin - anti-corrosion and anti-scale additives, chemical deaeration. There are no organic impurities. The samples were taken from a dairy processing plant.

Sample 3 - wastewater from cleaning in place (CIP) system for washing technological equipment in milk processing. The separation of this type of water is characterized by a different composition depending on operating cycle of CIP system. The sample collected in this case is a composite of all operating cycles of washing system - rinsing, washing with sodium hydroxide and neutralization with citric acid. The main impurities in water are dissolved and undissolved organic and inorganic substances – fats, proteins, saponified fat residues, inorganic substances, etc. The samples were taken from a dairy processing plant.

Sample 4 - wastewater from washing vehicles for transporting packaged food products. This type of water is discharged at ambient temperature and contains mainly inorganic dissolved and undissolved substances - dust, soil particles, detergents (phosphates). The samples were taken from a canning plant.

Sample 5 – wastewater from washing dishes for public catering. The water is generated from process of washing dishes in a dishwasher. It is discharged as warm water in range of 40 – 45°C, containing dissolved and undissolved organic substances – fats, proteins, carbohydrates, as well as inorganic ones – saponified fats, detergents. The samples were taken from a public catering establishment.

To assess the efficiency of purification using studied method, certain physicochemical indicators of two groups of water for each type were measured - source wastewater and concentrated wastewater - sludge. For each of described groups, the content of dissolved, undissolved and total dry matter, active reaction (pH), chemically required oxygen (COD) and electrical conductivity were measured. The presence of temperature influence during evaporation method implies pasteurization of effluent sludge water streams. For several examples of industrial wastewater microbiological analysis are made - results for values of colony forming unit and pathogens are received. A microbiological analysis of part of the studied wastewater samples was carried out in terms of total microbial count at temperatures of 37 and 20 ºC and content of pathogenic microorganisms. When evaluating results of microbiological analysis, temperature impact on samples during the process and its duration are taken into account. The source water is heated for a relatively short time before entering MVR heat pump system in order to quickly reach the boiling temperature. The condensate is maintained at a condensation temperature in MVR heat pump system for a time equal to its residence in condensate tank. The sludge is maintained at a boiling temperature in MVR heat pump system for a time equal to its residence time in separator and heat exchanger. In Table 1 environment temperature and holding time of wastewater and sludge are shown.

Table 1. Environment temperature and holding time of wastewater and sludge

Designation	Environment temperature wastewater, °C	Environment temperature sludge, °C	Holding time wastewater, min	Holding time sludge, min
Sample 1	78-80	70-75	5-6	30-40
Sample 2	78-80	70-75	5-6	30-40
Sample 3	78-80	70-75	5-6	30-40

Process of taking samples from sewage is made according to procedures of ISO 5667-3:2024 standard. For processes of taking samples of industrial wastewater procedures of BDS ISO 5667-10:2020 standard were observed. The samples of industrial wastewater were collected from industrial enterprises. This was done immediately after the technological process that generated them. The sampling frequency included three times within one working day. A method was used with taking a composite sample proportional to time (described three times), with single quantities of spot sample of 0.50 dm^3 and their subsequent mixing. The measurement of wastewater parameters was carried out within 24 hours after sampling. The storage of samples between collection and analysis is in refrigerated conditions. The rules of BDS EN ISO 5667-3:2024 standard are followed during preservation, transportation and storage of samples.

Microbiological analyses were performed in terms of determining total microbial count at 20°C and 37°C and content of pathogenic microorganisms in them (Pseudomonas auruginosa, sulfite-reducing anaerobes, intestinal enterococci, Escherichia coli and coliform bacteria). These indicators were determined for three characteristic flows in studied system - incoming wastewater and outgoing sludge. Methodologically, the procedures of the following standards were used:

- For total microbial count at 20°C and 37°C - BDS EN ISO 6222:2002;
- For Pseudomonas auruginosa - BDS EN ISO 16266:2008;
- For sulfite-reducing anaerobes - BDS EN ISO 26461-2:2004;
- For intestinal enterococci - BDS EN ISO 7899-2:2003;
- For Escherichia coli and coliform bacteria – BDS EN ISO 9308-1:2004.

The content of undissolved dry matter in wastewater is determined according to BDS 17.1.4.04-80 standard. The method consists of retaining the undissolved particles on a filter, drying them at 105° C and determining their mass.

Chemical oxygen demand (COD) was determined by using the spectrophotometric method described in BDS ISO 6060:2020 standard. A test set of the necessary reagents in round cuvettes Spectroquant 1.14541.0001 from Merck, Germany, was used. The analysis was performed using a Nova 60 microprocessor photometer and a 750 mg/dm^3 COD Spectroquant Combi Check 20 standard solution.

Electrical conductivity of industrial wastewater are measured using a WTW Inolab COND7110 conductometer with a range of the device from 0 to 1000 mS/cm, with an error of ± 0.5%. The device is equipped with a Tetracon 325 measuring sensor. Acid disinfectant Septacid is used to clean the sensor before the experiments. Active reaction is measured using a pH meter WTW INOLAB pH7110 with three-point calibration - at active reaction values of 4.01, 7.01 and 10.01, device range from -2.00 to 20.00 pH +0.01 equipped with a pH electrode WTW SenTix 6L with a pH range of 0-14 (0-100ºC) 3 kmol/l KCl.

All parameters were measured three times, and the obtained results are presented as an arithmetic mean value. In addition, the obtained values were evaluated statistically by determining variance and root mean square deviation of average result, as well as confidence error and dependence interval (Raichkov, 2001):
For mean score variance $S^2(\overline{x})$:

$$S^2(\overline{x}) = \frac{1}{m.(m-1)} \sum_{i=1}^{m} (x_i - \overline{x})^2$$

For root mean square deviation of the mean score S $(\overline{x})$:

$$S(\overline{x}) = \sqrt{S^2}\,\overline{(x)}$$

For confidence error ε $(\overline{x})$:

$$\varepsilon(\overline{x}) = t(p, m-1).\overline{S(x)}$$

where t (p, m-1) is Student's criterion for accepted confidence probability p=0.95 and number of repeated measurements m - 1 = 2. A value of t (0.95, 2) = 4.303 is reported.
For confidence interval:

$$x = \overline{x} \pm \overline{\varepsilon(x)}$$

The graphical representation of results shows the average values of studied parameters - dissolved, undissolved and total dry matter, active reaction (pH), chemically required oxygen (COD) and electrical conductivity.

Results and Discussion

Studied Indicators of MVR Heat Pump System

Dependence between the Degree of Regeneration and Degree of Concentration

The joint consideration of these two dependencies together with material balance of MVR heat pump system shows that degree of regeneration of wastewater depends on degree of concentration in following expression:

$$\varepsilon = 1 - \frac{1}{\varphi}$$

It is evident that dependence between degree of regeneration and degree of concentration is directly proportional. A higher degree of regeneration is achieved at higher degrees of concentration of wastewater. This dependence is graphically shown in Figure 3 for practically important intervals of φ = 1-50.

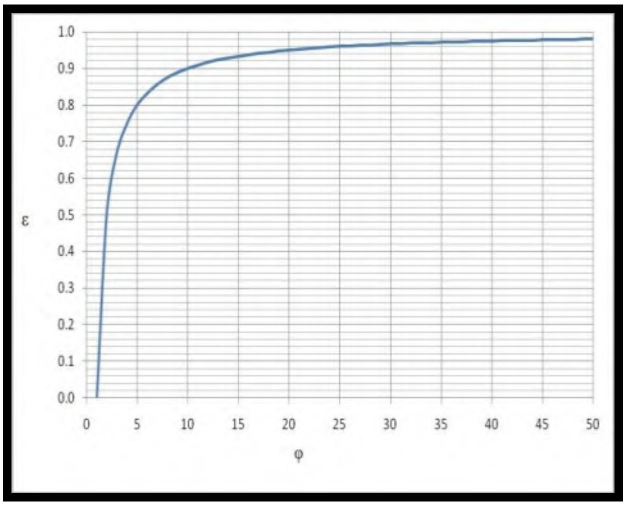

Figure 3. Dependence between degree of regeneration and degree of MVR system

Studied Indicators of Source Wastewater and Sludge

Total Microbial Count

On Figure 4 values of total microbial count for wastewater and sludge at 37 °C are shown.

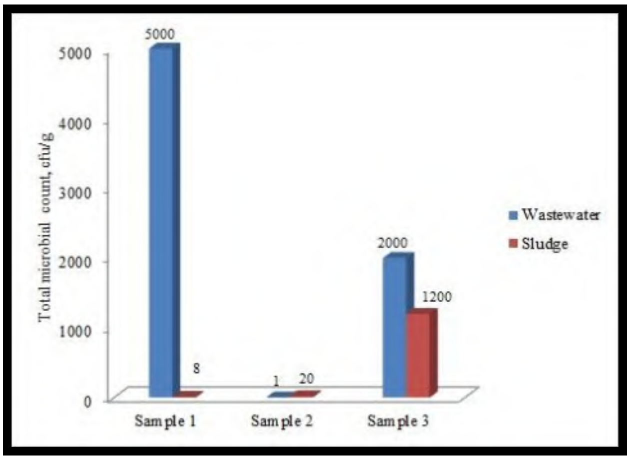

Figure 4. Values of total microbial count at 37 ºC on wastewater and sludge

On Figure 5 values of total microbial count for wastewater and sludge at 20 °C are shown.

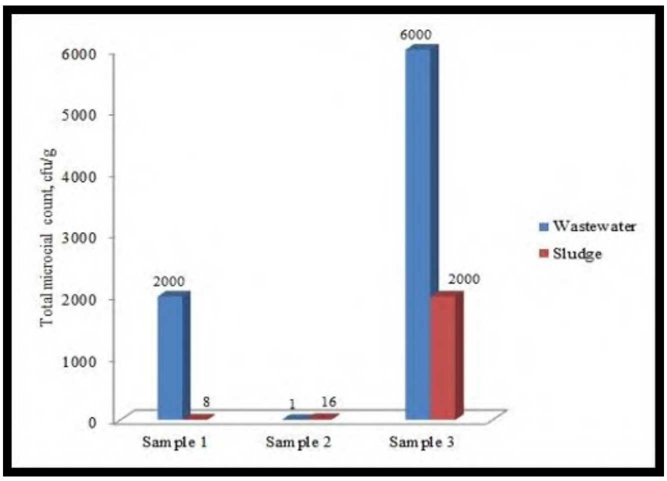

Figure 5. Values of total microbial count at 20 ºC on wastewater and sludge

Dry Matter Content

On Figure 6 values of dissolved dry matter on wastewater and sludge are shown.

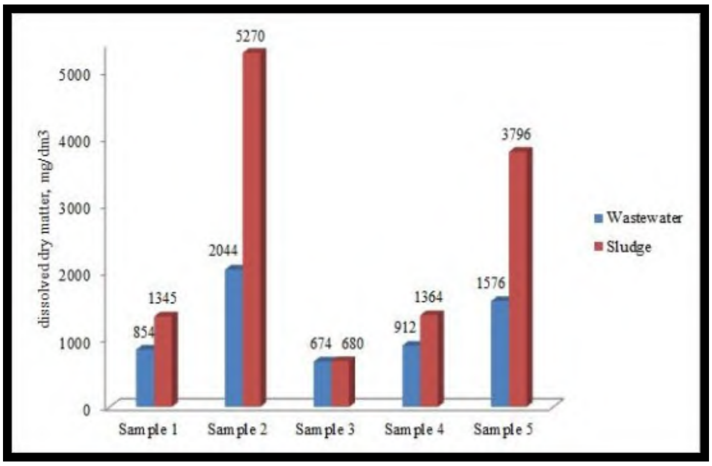

Figure 6. Values of dissolved dry matter on wastewater and sludge

On Figure 7 values of undissolved dry matter on wastewater and sludge are shown.

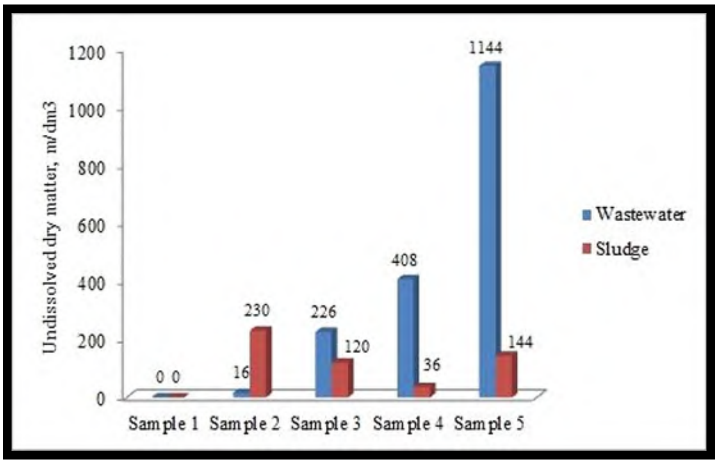

Figure 7. Values of undissolved dry matter on wastewater and sludge

On Figure 8 values of total dry matter on wastewater and sludge are shown.

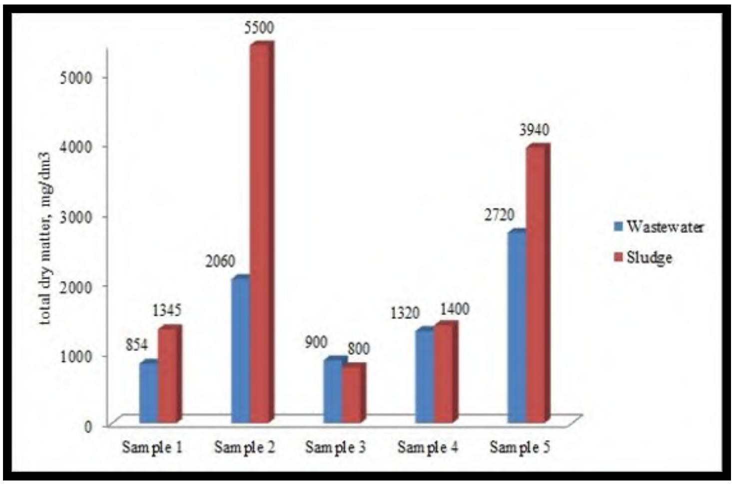

Figure 8. Values of total dry matter on wastewater and sludge

Chemical Oxygen Demand, Active reaction (pH), Electrical conductivity

On Figure 9 values of chemical oxygen demand (COD) on wastewater and sludge are shown.

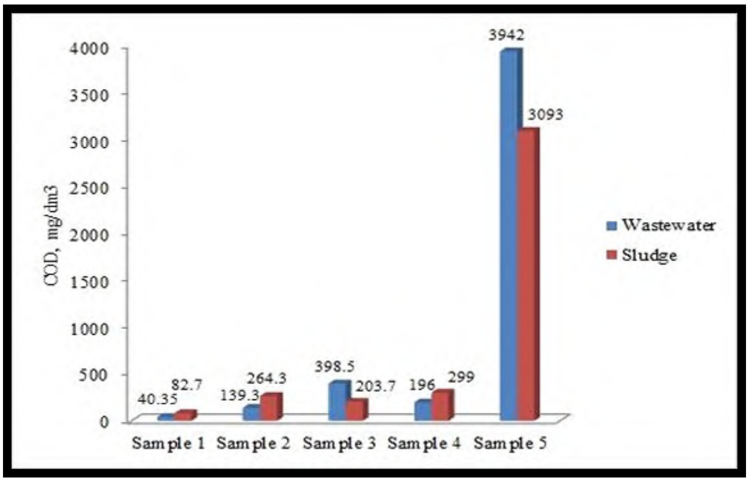

Figure 9. Values of chemical oxygen demand (COD) on wastewater and sludge

On Figure 10 active reaction (pH) values on wastewater and sludge are shown.

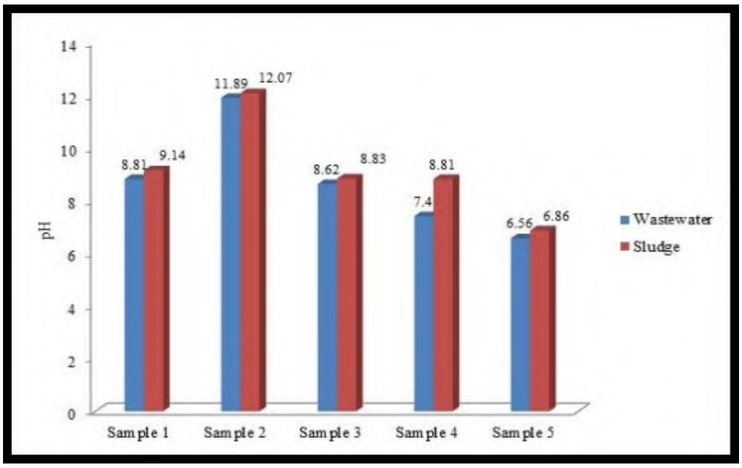

Figure 10. pH values on wastewater and sludge

On Figure 11 values of electrical conductivity on wastewater and sludge are shown.

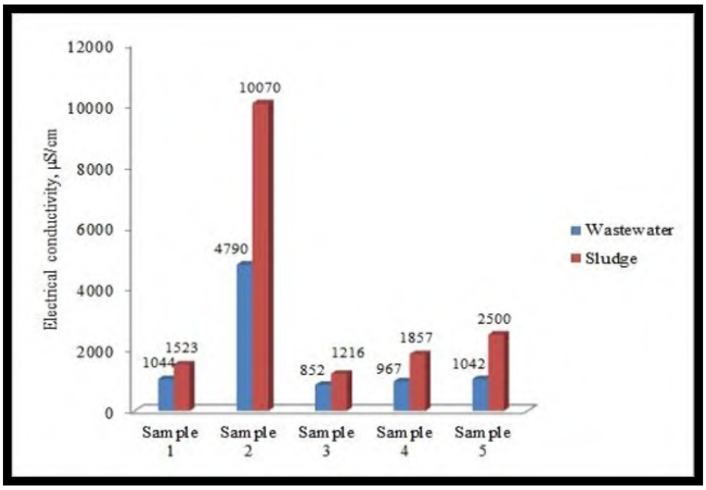

Figure 11. Values of electrical conductivity on wastewater and sludge

Conclusion

When carrying out water purification using MVR method, the passage of microorganisms from source wastewater into sludge is observed. The presence of temperature effects when carrying out MVR method implies pasteurization of outgoing water flows - condensate and sludge. For resulting sludge, a pasteurization effect was observed in terms of boiling temperatures and retention times. The results obtained show that it is sufficient to destroy thermolabile non-spore-forming microorganisms in sludge of studied samples. Boiling wastewater under vacuum conditions below 100°C does not allow destruction of resistant spore-forming microorganisms, requiring higher temperatures for sterilization. This effect is observed in treatment of Sample 3, where the non-spore-forming (fecal enterococci) microorganisms present in source wastewater are destroyed and the spore-forming (sulfite-reducing) microorganisms survive. In the absence of spore-forming microorganisms, significant sterility of both condensate and resulting sludge is observed (for Samples 1 and 2). In presence of criteria for microbiological purity of the resulting sludges (for example, when reusing them), it is possible to define appropriate boiling temperatures of wastewater in order to ensure their sufficient pasteurization. For the majority of those obtained sludges, an increase in values of total dry matter content, active reaction, electrical conductivity, chemically oxygen demand compared to same values of source wastewater was found. The values of indicators of obtained sludges: total dry matter content (800 – 5500 mg/dm^3), active reaction pH (6,86 – 12,07), electrical conductivity (1216 – 10070 μS/cm), chemically oxygen demand COD (82,7 – 3093 mg/dm^3) show that they can be used as a raw material for biofuels or to improve energy characteristics of already produced biomass fuels.

Scientific Ethics Declaration

* The authors declare that the scientific ethical and legal responsibility of this article published in EPSTEM journal belongs to the authors.

Conflict of Interest

* The authors declare that they have no conflicts of interest

Funding

* This research received no specific grant from any funding agency in the public, commercial, or not-for-profit sectors.

Acknowledgements or Notes

* This article was presented as an oral presentation at the International Conference on Research in Engineering, Technology and Science (www.icrets.net) held in Peja/Kosovo on July 10-13, 2025.

References

Abdel-Shafi, H.I., & Mansour, M.S.M. (2014). Biogas production as affected by heavy metals in the anaerobic digestion of sludge. *Egyptian Journal of Petroleum, 23,* 409–417.

Bacos, T.B., Cioabla, A.E., Popescu, F., Vintilă, T., & Borborean, A.T. (2024). Biogas from wastewater's sludge as potential resource for transportation. Experimental approach. *IOP Conf. Series: Materials Science and Engineering, 1303,* 012030.

Cudjoe, D., Zhu, B., & Wang, H. (2022). Towards the realization of sustainable development goals: Benefits of hydrogen from biogas using food waste in China. *Journal of Cleaner Production, 360,* 132161.

Deena, S.R., Vickram, A.S., Manikandan, S., Subbaiya, R, Karmegam, N., Ravindran, B., Chang, S.W., & Awasthi, M.K. (2022). Enhanced biogas production from food waste and activated sludge using advanced techniques - A review. *Bioresource Technology, 355,* 127234.

Gallerani, P. et al. (2002). Evaluation of hadwaco MVR evaporator. *U.S. Environmental Protection Agency*, 1-19.

Kazimierowicz, J. Zielinski, M., & Debowski, M. (2021). Influence of the heating method on the efficiency of biomethane production from expired food products. *Fermentation, 7,* 12.

Liang, L., Han, D., Ma, R., & Peng, T. (2013). Treatment of high-concentration wastewater using double-effect mechanical vapor recompression. *Desalination, 314*, 139-146.

Makisha, N., & Semenova, D. (2018). Production of biogas at wastewater treatment plants and its further application. *MATEC Web of Conferences, 144,* 04016.

Oneț C., Romocea T., Pantea E., & Oneț A. (2014). The physical and chemical characteristics of the wastewaters from food processing industry. *Annals of the University of Oradea, Fascicle: Environmental Protection, 23,* 895-902.

Pascual, J.A., Morales, A.B., Ayuso, L.M., Segura, P., & Ros, M. (2018). Characterisation of sludge produced by the agri-food industry and recycling options for its agricultural uses in a typical Mediterranean area, the Segura River basin (Spain), *Waste Management, 82*, 118–128.

Raichkov, G. (2001). *Measurements and appliances in heat engineering. (in Bulgarian)*. Plovdiv, PL: Academic Publishing of University of Food Technology.

Rulkens, W. (2008). Sewage sludge as a biomass resource for the production of energy: Overview and assessment of the various options. *Energy & Fuels, 22,* 9–15.

Tuan,C.I., Cheng, Y.T., Yeh, Y.L., Hsu, L.F., Chen, T.C. (2013). Performance assessment of a combined vacuum evaporator -Mechanical vapor re-compression technology to recover boilerblow-down wastewater and heat. *Sustainable Environmental Research, 23(2),* 129-139.

Vatachi, N. (2019). Wastewater sludge to energy production. A review. *IOP Conf. Series: Materials Science and Engineering, 595,* 012053.

Vo´ca, N., Leto,J., Karažija, T., Bilandžija, N., Peter, A.,Kutnjak, H., Šuri´c, J., & Poljak, M. (2021). Energy properties and biomass yield of miscanthus x giganteus fertilized by municipal sewage sludge. *Molecules, 26,* 4371.

Weimer, L.M., Fosberg, T.M., & Musil, L.A. (1983). Maximizing water recovery/reuse via mechanical vapor-recompression (MVR) evaporation. *Environmental Progress, 2(4),* 246–250.

Yurten, M., & Ozdemir, S. (2024). Enhancing biomass fuel properties of municipal sewage sludge with carbon-rich and low ash energy crops common reed and miscanthus. *Industrial Crops & Products, 222,* 120128.

Author(s) Information

Slav Valchev
University of Food Technology
Plovdiv, 26 Maritza Boulevard, Bulgaria,
Contact e-mail: *slavvalchev@uft-plovdiv.bg*

Nenko Nenov
InnoSolv Ltd, Bulgaria

To cite this article:

Valchev, S. & Nenov, N. (2025). Treatment of industrial wastewater using a mechanical vapour recompression heat pump system as a source of biomass. *The Eurasia Proceedings of Science, Technology, Engineering and Mathematics (EPSTEM), 35,* 84-93.

ISRES Publishing

The Eurasia Proceedings of Science, Technology, Engineering & Mathematics (EPSTEM)
ISSN: 2602-3199

The Eurasia Proceedings of Science, Technology, Engineering and Mathematics (EPSTEM), 2025

Volume 35, Pages 94-106

ICRETS 2025: International Conference on Research in Engineering, Technology and Science

The Importance of Disaster Management and Planning in Chemical, Biological, Radiological and Nuclear Events: Thematic Trends in Postgraduate Theses in Türkiye

Ali Sert
Burdur Mehmet Akif Ersoy University

Abstract: Chemical, biological, radiological, and nuclear (CBRN) incidents pose significant threats to public health and safety due to their potential for large-scale harm and rapid dissemination. This study aims to systematically analyze postgraduate theses conducted in Türkiye between 2009 and July 2025, identify thematic trends, and highlight critical gaps in current research. Key factors for effective CBRN disaster management identified in the theses include early warning systems, communication and coordination, education and preparedness, efficient use of resources, environmental impact mitigation, and comprehensive risk assessment. Additionally, the importance of interdisciplinary collaboration, regular practical training and realistic drills, periodic revision of disaster management plans, psychosocial support integration, and continuous environmental monitoring is emphasized. Findings underscore that systematic pre-disaster risk assessments significantly enhance preparedness and reduce damage. Results indicate increased academic attention, predominantly focusing on education, training, and preparedness, while operational, field-based studies remain limited. To address existing gaps, recommendations include strengthening practical training modules, increasing the frequency and realism of drills, enhancing inter-agency coordination, promoting standardization and integration of domestically developed technologies, and expanding qualitative, mixed-methods, and internationally comparative research. Ultimately, this study aims to contribute to improving Türkiye's overall resilience and preparedness capacity against CBRN threats.

Keywords: CBRN disasters, Disaster management, Risk assessment

Introduction

Chemical, Biological, Radiological, and Nuclear (CBRN) incidents are complex events that increasingly threaten public health and safety, arising not only from natural disasters but also from human-made threats (Coleman, 2019; Arıcı & Polat, 2024). Their ability to spread rapidly, impact large populations, and require multidisciplinary responses makes CBRN incidents a strategic priority for both healthcare systems and disaster management (Sert et al., 2022). Effective management of such incidents relies heavily on well-designed planning, training, and exercise processes. Enhancing the knowledge, attitudes, and skills of healthcare professionals, first responder teams, and hospital administrators on CBRN-related issues is critical to strengthening preparedness (Mohammadi et al., 2022). Planned intervention scenarios, regular training programs, and realistic drills contribute directly to building both individual and institutional capacity. In recent years, academic interest in CBRN has grown significantly in Türkiye, with postgraduate theses constituting a substantial part of this body of work. As fundamental components of scientific knowledge production, theses reflect current academic trends, field needs, and national awareness levels. Moreover, since they are prepared through systematic data collection and undergo advisory and ethical review processes, theses are considered reliable sources of information. Analyzing the content and methodology of postgraduate theses in a multidisciplinary field like CBRN which intersects public safety, health, and disaster management offers valuable insights. Such analysis can inform institutional awareness, educational policies, planning approaches,

- Selection and peer-review under responsibility of the Organizing Committee of the Conference

and the implementation of drills. However, to date, no comprehensive, systematic, and thematic analysis of postgraduate theses on CBRN in Türkiye has been conducted. This study aims to fill this gap by examining academic trends in the field. To this end, the study analyzes postgraduate theses, which have shown notable growth particularly since 2019. Theses employing quantitative, qualitative, and mixed methods, published between 2009 and July 2025, are included in the analysis. The study seeks to identify academic trends, key themes, and structural deficiencies revealed through these theses. Additionally, it aims to highlight contributions and gaps in planning, training, and exercise dimensions, thereby enriching the scientific knowledge base and offering actionable recommendations for institutions and decision-makers. Ultimately, the study intends to support institutional and academic efforts to strengthen disaster management and planning processes.

Method

This study was conducted using a descriptive survey model in order to examine postgraduate theses on Chemical, Biological, Radiological, and Nuclear (CBRN) issues in Türkiye. A comprehensive search was carried out in the Council of Higher Education (YÖK) National Thesis Center database, and postgraduate theses addressing CBRN topics and employing quantitative, qualitative, or mixed-method approaches were identified. The scope of the study covers theses published since 2009. As emphasized by Baltacı (2018) in the study titled *“A Conceptual Analysis of Sampling Strategies and the Issue of Sample Size in Qualitative Research”*, providing detailed explanations of sampling and data collection processes is of critical importance for ensuring the reliability and validity of qualitative research. Accordingly, essential information regarding the theses examined in this study including the YÖK thesis number, research design, type of thesis, key findings, and conclusions-is summarized in Table 1.

Dataset Construction Process

The postgraduate theses analyzed in this study were selected from among those completed at higher education institutions in Türkiye and uploaded to the National Thesis Center of the Council of Higher Education (YÖK Thesis). The YÖK Thesis database is the official digital platform that archives all master’s and doctoral theses prepared in Türkiye. The keywords “CBRN” and “Chemical, Biological, Radiological, Nuclear” were used to query the database. Theses related to the CBRN department were selected. This search identified a total of 67 postgraduate theses. However, one thesis (YÖK Thesis ID: 870813) could not be accessed due to restricted access permission.

Data Analysis and Ethical Considerations

This study did not involve the collection of new field data, the processing of personal data, or any intervention with participants. Since the analysis was conducted solely on publicly accessible academic documents, obtaining separate ethical approval was not required. The content of the theses was evaluated through thematic analysis and classified under the following headings: YÖK Thesis ID, Research Type, Thesis Type, Key Findings and Conclusions

Results and Discussion

A total of 66 postgraduate theses on CBRN, prepared between 2009 and July 2025, were examined in this study. The vast majority of the theses were master’s theses (n=59, 89.4%), while doctoral dissertations (n=4, 6.1%) and medical specialization theses (n=3, 4.5%) constituted a more limited proportion. An analysis of the distribution of theses by year revealed that the highest number was prepared in 2022 (n=16, 24.2%). This was followed by 2021 (n=11, 16.7%), 2019 (n=10, 15.2%), 2023 (n=10, 15.2%), 2020 (n=8, 12.1%), and 2024 (n=8, 12.1%). The number of theses prepared in july 2025 was relatively limited, accounting for 4.5% of the total (n=3). Regarding data collection methods, questionnaires emerged as the most frequently used tool. The majority of the studies (n=53, 80.3%) employed questionnaires, while knowledge tests (n=5, 7.6%), observation forms (n=5, 7.6%), and scale development studies (n=3, 4.5%) were used to a lesser extent.These findings indicate a marked increase in postgraduate research on CBRN, particularly in 2022, and show that questionnaires have been predominantly preferred as the primary data collection method in these theses.

Table 1. Systematic analysis of postgraduate theses on CBRN in Türkiye (2009–July 2025)

Thesis ID	Research Type	Thesis Type	Key Findings and Conclusions
311640	A Descriptive Case Study and Model Proposal	PhD Thesis	A behavioral model was developed for responding to CBRN-related mass casualties in military hospitals. It was emphasized that, for an effective response, all processes including organizational structure, training, logistics, security, and public relations should be planned in advance (Sezigen, 2009).
421639	Survey Study	Master's Thesis	The participants' level of knowledge and awareness regarding CBRN was found to be insufficient, and it was concluded that it should be improved through regular training and drills (Ayvazoğlu, 2015).
545391	Survey Study	Master's Thesis	It was determined that the response processes of AFAD CBRN teams were carried out in accordance with the plan and that the teams were knowledgeable; however, deficiencies in equipment and shortcomings in interagency coordination were observed. To enhance response capacity, improvements in training, inventory, and interagency collaboration were recommended (Yıldırım, 2019).
545788	Survey Study	Master's Thesis	The level of preparedness for CBRN incidents in public institutions was found to be low. A weak but significant positive correlation was identified between participants' knowledge, training, and exercise needs and their level of preparedness. The need to improve training and exercise programs was clearly highlighted (Doğan, 2019).
546799	Survey Study	Master's Thesis	The risk perception and preparedness attitudes of first response teams involved in CBRN incidents were assessed. Participants were found to have high levels of risk perception and preparedness, with a significant positive relationship identified between the two variables. Those with prior training and drill experience demonstrated higher levels of risk perception and preparedness. It was recommended that training and practical drills be continued (Yücel, 2019).
575400	Descriptive and Cross-Sectional Study	PhD Thesis	A mortality rate of 7.69% was observed in sulfur mustard exposure and 4.34% in chlorine gas exposure. Both groups exhibited severe respiratory and skin symptoms, and hospital stays were prolonged. The study emphasizes the importance of preparing healthcare personnel through training and drills, as well as the need for standardized intervention algorithms (Öztürk, 2019).
578145	Prospective Observational Study	PhD Thesis	The preparedness level of emergency medicine personnel for CBRN incidents was found to be low. Most participants had not received CBRN training and had not participated in drills. Knowledge of personal protective equipment was inadequate (33.7%), and the availability of diagnostic devices was low (13.5%). The study emphasized the need to strengthen training, drills, equipment, and interagency coordination (Dönmez, 2019).
617329	Experimental Study	Master's Thesis	The study found that activated carbon produced from silkworm cocoons had a high surface area, an amorphous structure, and a mesoporous form. The fabric coated with activated carbon demonstrated effective retention against both *Escherichia coli* and *Enterococcus faecalis* bacteria. These findings were considered promising for the development of biologically protective materials against CBRN threats (Dilbilmez, 2019).
623982	Survey Study	Master's Thesis	The study found that students' perceived preparedness for CBRN incidents was high, while their knowledge level was moderate. Students with higher perceptions of response and post-disaster preparedness also demonstrated higher knowledge levels. However, no significant relationship was found between perceived preparedness and knowledge level (Kızılkaya, 2020).
626580	Survey Study	Master's Thesis	The study revealed that participants' basic knowledge of CBRN, as well as their training and drill experience, were inadequate, and the content of existing training programs was ineffective. However, it was concluded that personnel were receptive to training due to their awareness of the risks, and that CBRN-specific planning should be incorporated into disaster plans (Kaynak, 2020).
626709	Descriptive and Comparative Literature Review	Master's Thesis	It was observed that collective protection systems for CBRN in Türkiye are insufficient, whereas successful practices have been implemented in the EU and the US through effective planning, legislation, training, and infrastructure. The study concluded that priority in Türkiye should be given to improving legislation, strengthening technical infrastructure, and raising public awareness (Buluş, 2020).
633480	In-Depth Interview Study	Master's Thesis	The study evaluated the knowledge, skills, experience, and attitudes of personnel from institutions involved in CBRN response through qualitative interviews. The findings revealed significant deficiencies in the areas of training, planning, drills, PPE, and equipment. It was emphasized that the CBRN preparedness and response capacities of institutions need to be improved (Şahin, 2020).
634557	Descriptive and Comparative Literature Review	Master's Thesis	It was observed that forensic duties in CBRN incidents in Türkiye are inadequate in terms of both legislation and practice, whereas the U.S. example demonstrates a more systematic and comprehensive approach. The study concluded that Türkiye needs to improve its legislation, training, interagency collaboration, and technical capacity (Oğur, 2020).
639519	Survey Study	Medical Specialty Thesis	The study found that a significant portion of participants had received CBRN training; however, the training was outdated, and their drill experience was very limited. The majority of participants considered their knowledge level inadequate and stated that CBRN training should be increased. Consequently, the study highlighted the need to address deficiencies in knowledge, training, and drills (Öner, 2020).
640069	Retrospective Descriptive Study	Master's Thesis	The impact of medical CBRN awareness training provided to 112 emergency healthcare personnel was evaluated, and a significant improvement in knowledge and skills was observed when pre- and post-training test results were compared. It was recommended that the training be continued, further developed, and supported with practical methods (Altınarık, 2020).
643456	Descriptive and Method Study	Master's Thesis	This study was conducted as a descriptive research to assess the knowledge levels and training needs of healthcare professionals and students in the health field regarding CBRN. Based on the findings, a competency-based modular training program was developed (Sezigen, 2009).
675336	A Descriptive SWOT Analysis Study.	Master's Thesis	The study determined that the preparedness level of pre-hospital emergency health services for CBRN threats was insufficient. However, personnel's willingness to respond and their field experience emerged as notable strengths. To enhance preparedness, it was recommended to develop training programs, ensure the provision of equipment, and strengthen interagency collaboration (Titiz, 2021).
694182	Experimental Study	Master's Thesis	The developed drone-based radiation detector successfully operated in the field due to its lightweight and portability, accurately measuring low dose rates and transmitting data wirelessly without issues. The study demonstrated that the system is feasible and effective for remote radiation detection in CBRN incidents (Düzen, 2021).
698289	Survey Study	Master's Thesis	Perceived CBRN preparedness, PPE usage, and willingness to respond were found to be high; however, knowledge levels were low. The proportion of participants who had received formal training was low, with most knowledge acquired through in-house training. Significant differences were observed based on age, professional title, and educational background. It was recommended to integrate CBRN training into curricula and to support it with regular drills (Demir, 2021).
702511	Survey Study	Master's Thesis	The study found that AFAD search and rescue personnel demonstrated moderate levels of CBRN knowledge, attitudes, and behaviors, with insufficient participation in training and drills. Notable deficiencies were observed in awareness of local CBRN plans and in the availability of equipment. Improvements in training, drills, and equipment were recommended (Özcan, 2021).

709073	Survey Study	Master's Thesis	The study revealed that hospital staff had insufficient levels of CBRN knowledge and awareness, which was identified as a risk to the safety of staff, patients, and the environment. It was recommended to enhance awareness through regular training programs (Cirit, 2022).
714071	Survey Study	Master's Thesis	The study found that hospital personnel generally had insufficient levels of CBRN knowledge, while those who had received training and those who had witnessed an incident demonstrated higher knowledge levels. Nurses were found to have lower knowledge levels compared to other professional groups (Günenç, 2021).
716127	Experimental Study	Master's Thesis	The study demonstrated that the developed CBRN decontamination material exhibited antibacterial activity against *E. coli*, *B. subtilis*, and its spores, and did not induce coagulation in human blood. These findings suggest that the material could be a safe and effective option for biological decontamination (Tosun, 2022).
716716	Qualitative Descriptive Study	Master's Thesis	The study developed sample animation scenarios aimed at increasing the awareness and protective consciousness of children aged 9–12 against CBRN threats. The scenarios were designed with educational and comprehensible content appropriate to the age characteristics of the children, and it was emphasized that such materials could be effective in enhancing disaster awareness (Ekici, 2021).
717043	An Analytical Cross-Sectional Study	Master's Thesis	The study found that family medicine residents had insufficient levels of disaster preparedness and low knowledge and awareness regarding disaster management. It was recommended to incorporate training programs into the curriculum and support them with drills to enhance disaster preparedness (Kurt, 2022).
718780	Survey Study	Master'sThesis	Knowledge and skills regarding personal protective equipment (PPE) were found to be insufficient. Participants who had received PPE training demonstrated significantly higher levels of knowledge and skills, which increased with higher educational attainment. It was observed that regular training made a significant contribution to improving PPE knowledge and skills (Yıldırım, 2022).
719327	Scale Development Study	PhD Thesis	The study developed a valid and reliable scale to measure hospitals' awareness and preparedness levels for CBRN threats. The scale comprised four factors (equipment, collaboration, consciousness, awareness) and demonstrated high internal consistency. It was concluded that the scale would contribute to assessing current preparedness levels and improving efforts in hospitals (Ergin, 2022).
729483	Literature Review Study	Master's Thesis	The study found that institutional structures and legislation related to CBRN-toxicological disasters in Türkiye are inadequate and fragmented compared to international examples. It was recommended to update the legislation, enhance interagency cooperation, and develop a national strategy for effective response (Türkeri, 2022)
731835	Literature Review Study	Master's Thesis	The study identified the strengths of Türkiye's health system in preparing for CBRN threats as awareness and legislative support, while weaknesses included deficiencies in training, equipment, and coordination. International collaboration opportunities emerged as a key opportunity, whereas lack of interagency communication was identified as the greatest threat. It was recommended to improve training, drills, and strategic planning (Gün, 2022).
742288	Survey Study	Medical Specialty Thesis	Healthcare workers were found to have insufficient knowledge and preparedness levels regarding CBRN incidents. Deficiencies in training, drills, equipment, and planning were particularly pronounced in district hospitals. As education level and length of service increased, the accuracy of knowledge improved; however, overall self-confidence and perceived preparedness among workers remained low (Gülkaya, 2022).
744139	Survey Study	Master's Thesis	The study found that healthcare workers' knowledge and preparedness levels regarding CBRN were insufficient, with notable deficiencies in training and drills. A positive correlation was observed between knowledge level and both training and length of service. The importance of regular training and planning to enhance preparedness was emphasized (Parlak, 2022).
751605	Methodology Study Based on Literature Review	Master's Thesis	The study demonstrated that thermal cameras could be an effective method for contactless and rapid assessment of patients and casualties in CBRN incidents. It was concluded that integration with UAVs and artificial intelligence could provide safe and accurate data collection over large areas, thereby contributing to incident management (Kadirsoy, 2022).
766835	Survey Study	Master's Thesis	Although most of the 112 personnel were knowledgeable about CBRN and had received training, their response competence and preparedness levels were low. Notably, gaps in knowledge regarding legal responsibilities were identified. The study emphasizes the importance of training and drills to increase awareness (Gül, 2022).
788006	A Quasi-Experimental Study	Medical Specialty Thesis	The study found that the CBRN training program developed for students was effective in increasing their knowledge and self-efficacy levels. Significant improvements were observed in both knowledge and self-efficacy scores among students who received the training, indicating that the program contributed to enhancing their preparedness (Oktar, 2023).
803611	Descriptive Cross-Sectional Study	Master's Thesis	Most law enforcement personnel had prior awareness of CBRN and possessed basic knowledge; however, their response competence and preparedness levels were low. Deficiencies were particularly noted in practical skills, highlighting the need to increase training and drills (Yakut, 2023).
803749	Survey Study	Master's Thesis	The study found that the majority of pre-hospital emergency medical personnel possessed basic knowledge of CBRN; however, deficiencies in practice and high levels of response-related stress were identified. Those who had received CBRN training demonstrated significantly higher knowledge levels. The findings highlight the importance of increasing regular training and drills to improve knowledge and skills (Kaynar, 2023).
807945	Survey Study	Master's Thesis	The knowledge levels of nurses regarding CBRN were found to be moderate, their attitudes positive, and their self-efficacy at a moderate level. Nurses who had received training and had experience with CBRN cases demonstrated significantly higher levels of knowledge, attitude, and self-efficacy. Consequently, it is recommended that educational activities be expanded to enhance nurses' preparedness for CBRN incidents (Eren, 2023).
808342	Experimental Study	Master's Thesis	In the study, the levels of heavy metals in the peppers used for pepper spray production were found to be below the WHO-FAO limits, and no significant accumulation was detected. However, it was emphasized that regular monitoring and control are necessary during the production processes to mitigate the risk of environmental contamination (Arıcı, 2023).
813493	Literature Review Study	Master's Thesis	The study comprehensively examined the detection, decontamination, and protection methods related to radiological and nuclear agents in CBRN incidents. It emphasized the effectiveness of detectors and dosimeters, the necessity of selecting decontamination methods based on the nature of the incident, and the importance of preparedness. The study concluded that the selection of appropriate methods and effective decontamination in CBRN threats plays a critical role in reducing casualties and environmental damage (Kaya, 2021).
820453	Survey Study	Master's Thesis	A positive relationship has been found between CBRN risk perception and preparedness among healthcare workers. Those who have received training and have prior incident experience show higher levels of preparedness. Training programs aimed at increasing risk perception are recommended (Tazearslan, 2021).
829576	Survey Study	Master's Thesis	The CBRN awareness, knowledge, and attitude levels of 112 Emergency Medical Services personnel were found to be at a moderate level. Although the majority of participants had heard of the term CBRN,

			deficiencies were identified in their practical competencies. Personnel who had received training demonstrated significantly higher levels of knowledge and preparedness attitudes. As a result, it was recommended that regular training and drills be increased (Savaş, 2023).
844562	Survey Study	Master's Thesis	Although emergency medical personnel had received CBRN training, their levels of preparedness and practical application were found to be insufficient. Those who had participated in a CBRN incident demonstrated higher levels of risk perception and knowledge. A significant relationship was identified between risk perception and preparedness, and it was recommended that training and drills be increased (Artcı, 2023).
848808	An Applied Descriptive Study	Master's Thesis	The most suitable locations for the placement of CBRN sensors were determined using Geographic Information Systems (GIS) and multi-criteria decision analysis. The analysis, which considered factors such as population density, critical infrastructure, educational institutions, and industrial zones, revealed that sensors should primarily be concentrated around city centers and industrial areas. As a result, it was demonstrated that this GIS-supported method can provide decision-makers with an effective roadmap for CBRN risk management (Kütükoğlu, 2024).
850153	Experimental Study	Master's Thesis	The study found that the synthesized nanomaterials achieved over 97% efficiency in arsenic removal, maintained cell viability without exhibiting toxicity, and demonstrated antibacterial activity against gram-positive bacteria. Consequently, these nanomaterials were proposed as an effective and environmentally friendly option for the removal of CBRN agents (Çiğdem, 2024).
850617	Bibliometric Analysis Study	Master's Thesis	The study revealed that due to their mass destruction potential, CBRN weapons attract the interest of terrorist groups. CBRN terrorist attacks were found to occur most frequently in South Asia and least frequently in Central America and the Caribbean. The study was conducted using a mixed-method approach, combining literature review and data analysis (Sarpkaya, 2023).
853596	Survey Study	Master's Thesis	The rate of receiving education on CBRN-E (Chemical, Biological, Radiological, Nuclear – Explosives) among healthcare students is low; however, their desire for such education is high. Those who have received training demonstrate higher levels of knowledge, attitude, and self-efficacy. As knowledge increases, professional attitudes improve accordingly. Therefore, it is recommended that CBRN-E education be incorporated into the curriculum (Karakoç, 2024).
854136	Survey Study	Master's Thesis	Although most healthcare personnel have heard of CBRN-E and received related training, their intervention competency remains low. As the level of education and years of professional experience increase, knowledge and attitude levels improve; however, practical skills are still insufficient. It is therefore recommended that training programs be enhanced with hands-on practice (Polat, 2024).
856750	Literature Review Study	Master's Thesis	The study demonstrated that information technologies provide significant advantages in nursing interventions during CBRN incidents. It emphasized that technology plays a critical role in rapid diagnosis, coordination, and effective response, and highlighted the need to enhance nurses' competencies in this area (Yalçın, 2023).
857292	Qualitative Study	Master's Thesis	Using the General Morphological Analysis (GMA) method, the relationships between different incident types, response capacities, and vulnerable factors were revealed, demonstrating that potential scenarios can be planned in a more consistent and practical manner. It was emphasized that GMA can serve as an effective scenario development tool in CBRN risk management and enhance crisis management preparedness (Çavlan, 2024).
857702	Survey Study	Master's Thesis	The attitudes and self-efficacy of pre-hospital emergency healthcare personnel in CBRN incidents were examined. In the study conducted with 402 participants, it was found that age, professional title, education, and incident experience positively influenced attitude and self-efficacy. Male personnel, those who had received CBRN training, and those who had responded to actual incidents scored higher. The study emphasized the importance of training and drills to enhance the knowledge and skills of healthcare personnel (Kurt, 2024).
867548	Experimental Study	Master's Thesis	An activated carbon and PVC-supported nanofibrous filter material was developed from biomass, with the best performance achieved using 30% $ZnCl_2$ activation. The developed material was shown to possess properties suitable for use as a protective filter against CBRN attacks (Küçük, 2024).
872053	Qualitative Study	Master's Thesis	The study found that advanced CBRN decontamination systems in the EU and the USA are more diverse and effective compared to those in Türkiye. It emphasized the need to improve Türkiye's existing infrastructure, adopt new technologies, and enhance national capacity (Kurtuluş, 2024).
881980	Quasi-Experimental Study	Master's Thesis	Pre and post training assessments revealed significant increases in students' knowledge levels. Students reported that the training was beneficial and stated that animated materials facilitated learning. As a result, animation-supported educational methods were found to be effective in enhancing CBRN awareness (Karakuş, 2024).
882112	Survey Study	Master's Thesis	Twenty-five percent of healthcare workers had received CBRN-E training, and 8% had participated in CBRN-E incidents. Nurses exhibited a higher perception of preparedness compared to other professional groups. Those who had received training showed significantly better levels of preparedness and crisis management. The study highlights that institutional training and drills are effective in enhancing preparedness and management processes for CBRN-E incidents (Demircan, 2024).
882270	Survey Study	Master's Thesis	The study found that students with knowledge of CBRN exhibited higher levels of environmental awareness, and that CBRN education integrated into the curriculum strengthened their environmental attitudes. This result indicates that CBRN training provided within the field of disaster management is effective not only in delivering technical knowledge but also in enhancing environmental consciousness (Akan, 2024).
892367	Survey Study	Master's Thesis	Although most emergency medical personnel had received CBRN training, it was found that the training was insufficient and that there was no significant relationship between training and practical skills. Participants demonstrated knowledge gaps particularly regarding CBRN zones and warning and alarm signals. The study emphasizes that CBRN training should be extended in duration, supported with scenario-based exercises and drills, and repeated periodically (Yıldız, 2024).
898921	Survey Study	Master's Thesis	It was determined that both healthcare and support personnel have insufficient knowledge and awareness regarding CBRN management. Effective training in line with national standards is needed, and existing knowledge gaps must be addressed promptly. The study provides a valuable tool for enhancing CBRN awareness within hospital disaster management (Ulusoy, 2024).
899746	Survey Study	Master's Thesis	Among emergency healthcare workers, CBRN knowledge levels were found to be significantly associated with age, job role, and length of service, while knowledge of personal protective equipment (PPE) was significantly related to unit, profession, education, and work experience. These findings indicate that training and awareness programs should be planned by taking demographic differences into account (İncedağ, 2024).
908602	Literature Review Study	Master's Thesis	The study provided comprehensive support recommendations aimed at developmental, immediate-response, and post-incident guidance for both the community and personnel to mitigate psychosocial impacts during CBRN incidents. To reduce psychosocial risks, school-based preventive programs, casualty needs assessment forms, and clearly defined task distributions were developed (Çetin, 2023).
909798	Quasi-Experimental	Master's Thesis	CBRN training modules tailored to different professional groups led to significant improvements in participants' knowledge and skill levels. Notably, auxiliary search and rescue personnel, who had shown

	Study		low performance prior to the training, demonstrated the greatest improvement afterward. Customizing training based on profession enhances effectiveness, and it is recommended that programs be further developed with the integration of advanced technologies and psychological resilience training (Çebi, 2024).
909994	Experimental Study	Master's Thesis	The study addresses the development of wireless sensor networks for the early detection and monitoring of CBRN threats. This technology, which offers low power consumption and wide coverage, enables reliable monitoring of CBRN parameters in both rural and urban areas and facilitates early warning in case of changes. Experimental results demonstrated that the system's monitoring range is sufficient and provides effective response capabilities against CBRN threats (Akan, 2024).
920012	Scale Development Study	Master's Thesis	In the study, a valid and reliable scale was developed to measure university students' levels of perception, knowledge, awareness, and response regarding CBRN. The 40-item scale demonstrated high reliability and validity in the conducted analyses, effectively addressing the need for a scientific measurement tool in this field (Budak, 2025).
929949	Quasi-Experimental Study	Master's Thesis	The first aid and CBRN training provided led to a significant increase in students' knowledge levels. The rate of correct responses rose markedly after the training; however, a decline in knowledge was observed two months later. It is therefore recommended that such training programs be expanded and made more widespread (Kaleli, 2025).
930950	Literature Review Study	Master's Thesis	The study analyzed the risks posed by these chemicals to human health and the environment, and developed new criteria and innovative response methods for their integration into CBRN defense strategies. Additionally, it provided policy and training recommendations aimed at enhancing the effectiveness of disaster management plans against such chemical threats and strengthening the resilience of industrial facilities (Alboga, 2024).
936471	Experimental Study	PhD Thesis	The study examined the production, morphology, mechanical and filtration properties, as well as the toxicological and antibacterial effects of nanofiber-based CBRN mask filters, which were domestically produced using the electrospinning method. The developed filters demonstrated high filtration efficiency (93.19% for PM0.3), good air permeability, and formaldehyde adsorption capacity. Additionally, they exhibited low toxicity on healthy cells and showed antibacterial properties. As a result, these filters have the potential to be used both in ambient air filtration and in personal protective mask applications (Bilgiseven, 2025).
940340	Experimental Study	PhD Thesis	The study investigated the production and effectiveness of three different hydrogel-based wound care materials designed for the treatment of wounds and burns caused by CBRN agents. The antibacterial properties, cellular compatibility, and wound-healing effects of the prepared hydrogels were evaluated through both in vitro and in vivo experiments. The results indicated that hydrogel applications accelerated wound healing and offered potential for biocompatibility and controlled drug release. However, more extensive research is required for their widespread use in clinical settings (Baş, 2025).

CBRN: Chemical, Biological, Radiological, Nuclear
CBRN-E: Chemical, Biological, Radiological, Nuclear, Explosive
PPE: Personal Protective Equipment
Master's Thesis: Master of Science Thesis
PhD thesis: Doctoral Thesis
Med. Spec.: Medical Specialization
WHO–FAO: World Health Organization – Food and Agriculture Organization
GIS: Geographic Information Systems
UAV: Unmanned Aerial Vehicle
GMA: General Morphological Analysis

This section evaluates the findings based on a total of 66 postgraduate theses published between 2009 and July 2025.

The Increase in Postgraduate Theses on CBRN in Türkiye and Their Alignment with the Literature

In recent years, there has been a marked increase in academic interest in Chemical, Biological, Radiological, and Nuclear (CBRN) issues in Türkiye. The year 2022 emerged as the peak in thesis production, followed by a noticeable decline beginning in 2023. This trend can be interpreted as a reflection of the global COVID-19 pandemic, industrial accidents within the country, and growing public awareness, all of which have significantly influenced the direction of academic research. Notably, the studies of Yıldırım (2019) and Özcan (2021), which examined the preparedness and knowledge levels of AFAD personnel, together with Artcı's (2023) research on CBRN risk perception, exemplify this rising scholarly attention. More recently, the theses of Budak (2025), Çebi (2024), Kaleli (2025), Akan (2024), Küçük (2024), Baş (2025), and Bilgiseven (2025) have expanded the scope of CBRN-related research, addressing a wide spectrum ranging from healthcare workers to first response teams and administrators, and even incorporating experimental studies. Similarly, Coleman et al. (2019) emphasized that interest in CBRN preparedness tends to rise in the aftermath of large-scale incidents. They further noted that preparedness planning still relies predominantly on measurable and model-based approaches, whereas contextual analyses and insights derived from practical experience remain relatively underrepresented in literature.

Strengths and Weaknesses of CBRN Disaster Management and Planning Processes in Türkiye

Theses reviewed indicate that disaster management and planning processes related to CBRN incidents in Türkiye are developing, yet still exhibit significant structural deficiencies. In particular, shortcomings such as lack of interagency coordination, low levels of preparedness, and the absence of CBRN-specific provisions in disaster plans are frequently reported. For example, Yıldırım (2019), who examined the preparedness of AFAD personnel and identified several deficiencies, emphasized that existing plans remain limited to general disaster frameworks and highlighted operational shortcomings specific to CBRN. Similarly, Artcı (2023) noted the inadequacy of risk perception and preparedness processes regarding CBRN, advocating for increased training and awareness-raising activities. Budak (2025) pointed to the absence of certain scale development studies in the CBRN field. Akan (2024) stressed that CBRN education should not only provide technical knowledge but also foster environmental awareness. Kaleli (2025) drew attention to the lack of student preparedness for roles in CBRN-related disasters and recommended the expansion of educational programs. Özcan (2021), meanwhile, reported weaknesses in the knowledge levels of search and rescue personnel regarding the content of disaster plans. At the global level, Beik Mohammadi et al. (2022) emphasized that hospitals exhibit shortcomings in terms of planning, coordination, and staff training for CBRN disaster management, and argued that preparedness levels must be strengthened through a multidisciplinary approach. Similarly, the systematic review by Qzih and Ahmad (2024) supported these findings, revealing that hospital-based CBRN preparedness still largely reflects general disaster planning. The review underscored the absence of CBRN-specific scenarios, practical drills, and coordination mechanisms, and called for these dimensions to be reinforced through interdisciplinary collaboration. All these findings strongly demonstrate the necessity of implementing disaster management strategies that are multidisciplinary, based on interagency cooperation, and tested through scenario-oriented planning processes.

Deficiencies in Training, Drills, Standardization, and Institutional Capacity

Findings indicate that the weakest component of disaster management and planning processes lies in the domains of training and practice. It has been revealed that preparedness training often fails to reach their target audience, lacks standardized content, and are rarely supported with practical exercises. For instance, Öner (2020) found that CBRN preparedness training did not sufficiently include practical modules and that opportunities for drill experience were limited. Doğan (2019) emphasized low participation rates in drills and inconsistencies in evaluation processes. Ulusoy (2024) reported that the content of CBRN trainings aligned inadequately with national standards. Şahin (2020) identified significant deficiencies in training, planning, drills, and equipment. Kurt (2022) recommended the inclusion of CBRN training programs in curricula and their reinforcement through drills to enhance disaster preparedness. Oğur (2020) underscored the necessity for Türkiye to strengthen its legislation, training, interagency cooperation, and technical capacity. Consequently, it is of critical importance for institutions to develop a unified CBRN training curriculum and standardized drill protocols.

Similarly, Farhat et al. (2024) highlighted at the global level that CBRN preparedness strategies lacked clear definitions, continuously updated training programs, and adequate hands-on exercises. They stressed that preparedness can only be enhanced through multidisciplinary collaboration and robust hospital-based coordination mechanisms. Likewise, Razak et al. (2018) identified major shortcomings in four core dimensions of CBRN preparedness within emergency departments preparedness, response, decontamination, and personal protective equipment—and argued that effective response cannot be achieved without coordination at organizational, technological, and individual levels.

The Potential and Implementation Gaps of Innovative Technological Studies

Experimental studies provide encouraging evidence for the development of domestic and innovative technologies in response to CBRN threats in Türkiye. In particular, advances in nanomaterial-based filters, hydrogel-based wound care products, sensor systems, and UAV-supported radiation detection technologies have emerged as the primary areas of focus. For instance, Akan (2024) conducted research on CBRN sensor systems. Bilgiseven (2025) carried out studies on nanomaterial-based CBRN mask filters. Kadirsoy (2022) investigated the integration of UAVs with artificial intelligence to enable safe and accurate data collection across wide areas. Baş (2025), meanwhile, developed three different hydrogel-based materials for the treatment of CBRN-induced wounds and burns, testing their effectiveness through both in vitro and in vivo experimental procedures. At the international level, Duan et al. (2024) emphasized the biomedical advantages of nanomaterial-based hydrogels, such as flexibility, conductivity, and biocompatibility, while noting the need for improvements in standardization and long-term stability for large-scale applications. Similarly, Cooper et al. (2023) developed an innovative city-scale multi-sensor network platform designed to detect and track radiological/nuclear sources by leveraging contextual data. Their findings demonstrated that data aggregated at the network level from multiple detectors significantly enhanced the identification of low-level radiation sources.

Academic Contribution and Practice-Oriented Recommendations

This study constitutes one of the pioneering efforts in the literature to systematically and thematically examine postgraduate theses on CBRN in Türkiye, offering a significant academic contribution. By revealing the trends and thematic focus areas of the increasing academic output in recent years, the study provides a guiding framework for both the academic community and policymakers. In light of the findings, the following recommendations are highlighted for enhancing CBRN preparedness processes: enriching educational content in accordance with established standards and integrating practical modules; increasing the frequency and scope of exercises and simulations; developing mechanisms to strengthen inter-institutional coordination; and supporting the development and field testing of indigenous and innovative technologies to facilitate their widespread adoption.

Limitations of the Study and Future Research Directions

The primary limitation of this study is its reliance solely on postgraduate theses registered in the National Thesis Center of the Council of Higher Education (YÖK). Studies from other databases or those published as journal articles were not included. Furthermore, the extent to which the findings and recommendations reported in these theses have been implemented and their actual impact in the field were not evaluated.
Future research is recommended to focus on the following areas:

- Quantitative and qualitative verification of the implementation levels of strategies proposed in the theses within institutions and in the field,
- Case studies and field tests to monitor the effectiveness and sustainability of CBRN preparedness plans,
- Increased contextual analyses based particularly on qualitative and mixed-methods approaches,
- Broader international comparative studies examining Türkiye's CBRN preparedness level,
- Promotion of applied research focusing on the field integration of innovative technologies and user experience.

Such studies will contribute to filling existing gaps in literature and developing more concrete and actionable recommendations for policymakers.

Ethical Approval and Data Availability Statement

This study did not involve human participants or the collection of personal or sensitive data. All data analyzed in this research were obtained from the publicly accessible academic thesis repository of the Turkish Council of Higher Education (YÖK). Therefore, no ethical approval or informed consent was required.

Conclusion and Recommendations

This study systematically and thematically examined postgraduate theses on Chemical, Biological, Radiological, and Nuclear (CBRN) topics prepared in Türkiye between 2009 and July 2025, revealing trends, strengths, and weaknesses in the field while providing a guiding framework for policymakers and academic communities. The findings indicate that CBRN preparedness in Türkiye has garnered increasing academic interest in recent years; however, significant deficiencies remain in training, drills, planning, standardization, and inter-agency coordination. One of the most notable findings is that academic production largely relies on quantitative methods, with limited contextual and in-depth analyses. Training programs are often theoretical, short in duration, and lack practical modules, while drills are conducted infrequently and with limited scope. Furthermore, the absence of CBRN-specific details in disaster plans, insufficient inter-agency coordination, and the limited effectiveness of planning processes stand out as critical factors weakening preparedness. On the other hand, indigenous technologies developed within experimental studies point to a promising potential for Türkiye CBRN preparedness. Nanomaterial-based filters, hydrogel-based wound care products, UAV-supported detection systems, and sensor technologies represent significant innovative advances in this field. However, further research is needed to conduct field testing, standardization, and operational integration of these products into disaster management systems.

In conclusion, enhancing CBRN preparedness in Türkiye necessitates the standardization and modularization of training programs with practical components; increasing the frequency and scope of drills; strengthening national mechanisms that facilitate inter-agency collaboration; and supporting the development and field integration of indigenous innovative technologies. Additionally, expanding contextual, qualitative, and mixed-methods research and situating Türkiye situation within a broader international comparative framework will contribute to the literature and support policymaking processes. It should be emphasized that CBRN is not only an academic research area but also a strategic priority for public health and national security. Therefore, holistic, interdisciplinary, and practice-oriented strategies must be developed to address these challenges effectively.

Scientific Ethics Declaration

* The author declares that the scientific ethical and legal responsibility of this article published in EPSTEM journal belongs to the author.

* This study does not involve human participants, animal experiments, interventions, surveys/scales, or the processing of personal data. All data/materials were obtained from openly accessible public sources, and the terms of use and citation requirements of these sources were followed. Therefore, no ethics committee (IRB) approval was required for this study. Since no participant data were used, informed consent was not applicable.

Conflict of Interest

* The authors declare that they have no conflicts of interest

Funding

* The author's participation in this international scientific event was supported by the Scientific and Technological Research Council of Türkiye (TÜBİTAK) under the 2224-A Program for Supporting Participation in International Scientific Events.

Acknowledgements or Notes

* This article was presented as a oral presentation at the International Conference on Research in Engineering, Technology and Science (www.icrets.net) held in Peja/Kosovo on July 10-13, 2025.

* The author gratefully acknowledges the support provided by the Scientific and Technological Research Council of Türkiye (TÜBİTAK) under the 2224-A Program for Supporting Participation in International Scientific Events, which enabled participation in this international scientific event. The author also wishes to thank all colleagues and institutions who contributed to the successful completion of this work.

References

Akan, A. (2024). *The effect of AYAY students' CBRN knowledge levels on their attitudes towards the environment: the case of Canakkale Onsekiz Mart Unıversity* (Master's thesis). Çanakkale On Sekiz Mart University. Çanakkale/ Türkiye

Akan, C. M. (2024) *Lorawan based wireless CBRN threat detection and tracking system* (Master's thesis). Sivas Cumhuriyet University. Sivas/Türkiye.

Alboga, M. (2024).*Evaluation of toxic industrial chemical substances emerging as a result of natural disasters as CBRN agent* (Master's thesis). İskenderun Technical University. Hatay/Türkiye

Altinarik, S. (2020). *Evaluation of medical CBRN awareness trainings for 112 Emergency Health Care workers in Istanbul European Side* (Master's thesis). Bezm-i Alem Vakıf University.

Arici, E. (2023). *Determination of major HEAVY metal levels in pepper gases used as chemical agents in the field of CBRN* (Master's thesis). Burdur Mehmet Akif Ersoy University. Burdur/Türkiye.

Arici, E., & Polat, M. (2024). Determination of major heavy metal levels in pepper gas used as chemical agents in CBRN field. *Süleyman Demirel University Journal of Health Sciences, 15*(2), 226-235.

Artci, F. (2023). *Determination of CBRN risk perceptions, preparedness levels, and related factors of Emergency Health Services personnel: The case of Tekirdağ province* (Master's thesis). Çanakkale On Sekiz Mart University. Çanakkale/ Türkiye

Ayvazoglu, G. (2015). *CBRN preparedness and volunteer for determining the level of study: The case of Gümüşhane* (Master's thesis). Gümüşhane University. Gümüşhane/Türkiye.

Baltaci, A. (2018). A conceptual examination of sampling methods and the problematic of sample size in qualitative research. *Bitlis Eren University Journal of Social Sciences, 7*(1), 231–274.

Bas, K. (2025). *Production and application of hydrogel based wound care materials for the treatment of wounds and burns caused by CBRN agents* (Doctoral dissertation). Selçuk University. Konya/Türkiye.

Bilgiseven, I. M. (2025). *Domestic production and application of protective mask filters against CBRN threats* (Doctoral dissertation*)* Selçuk University. Konya/Türkiye.

Budak, E. (2025). *A scale development study to measure cbrn perception, awareness, knowledge and intervention levels of higher education students* (Master's thesis). Niğde Ömer Halisdemir University. Niğde/Türkiye

Bulus, A. (2019). *Research for the collective protection systems in EU and USA and analyse for implementing in Turkey* (Master's thesis). National Defense University. İstanbul/ Türkiye

Cirit, G. (2022). *The knowledge level assesment of workers in Çiğli Training and Research Hospital with in the scope of the quality of hospital standard version 6 chemical, biological radiological and nuclear (cbrn) hazards management standard* (Master's thesis). Dokuz Eylül University. İzmir/Türkiye.

Coleman, C. N., Bader, J. L., Koerner, J. F., Hrdina, C., Cliffer, K. D., Hick, J. L., ... & Hatchett, R. (2019). Chemical, biological, radiological, nuclear, and explosive (CBRNE) science and the CBRNE science medical operations science support expert (CMOSSE). *Disaster Medicine and Public Health Preparedness*, *13*(5-6), 995-1010.

Cooper, R. J., Abgrall, N., Aversano, G., Bandstra, M. S., Hellfeld, D., Joshi, T. H., ... & Volkova, S. (2023). Networked sensing for radiation detection, localization, and tracking. *Journal of Physics: Conference Series*. IOP Publishing.

Cavlan, B. (2024). *Scenario development for possible CBRNE incidents with the method of general morphological analysis: Sample chemical incidents scenarios* (Master's thesis). Tekirdağ Namık Kemal University. Tekirdağ/Türkiye

Cebi, B. (2024).*Evaluating the effectiveness of CBRN training modules across various profession groups* (Master's thesis). University of Health Sciences. İstanbul/Türkiye

Cetin, N. (2023). *Psychosocial effects of CBRN events and psychosocial support intervention proposal* (Master's thesis). İskenderun Technical University. Hatay/Türkiye.

Cigdem, Y. (2024). *Synthesis of manganese oxide nanomaterials and their use in the removal of arsenic, a CBRN polluting agent* (Master's thesis). Selçuk University. Konya/Türkiye.

Demir, A. (2021). *Determination of the preparation perception of the airport personnel against CBRN events and the level of knowledge; Example of Erzurum* (Master's thesis). Gümüşhane University. Gümüşhane/Türkiye.

Demircan, E. (2024). *Examining the perception of preparedness and crisis management level for chemical, biological, radiological, nuclear and explosive (CBRN-P) incidents in the field of health* (Master's thesis). Tekirdağ Namık Kemal University. Tekirdağ/Türkiye.

Dilbilmez, S. G. (2019). *Protective against cbrn (Chemical, biological, radiation, nuclear) threats* (Master's thesis). Muğla Sıtkı Koçman University. Muğla/Türkiye.

Dogan, G. (2019). *The study of determining information, training and exercise needs of institutions against KBRN events: The case of Gümüşhane and Trabzon provinces* (Master's thesis). Gümüşhane University. Gümüşhane/Türkiye

Donmez, M. A. (2019). *Survey on emergency medicine workers' attention, notion and attitude against (CBRN) chemical, biologic, radiologic and nuclear accidents* (Master's thesis). Bezmialem Vakıf University. İstanbul/Türkiye.

Duan, H., Zhang, Y., Zhang, Y., Zhu, P., & Mao, Y. (2024). Recent advances of stretchable nanomaterial-based hydrogels for wearable sensors and electrophysiological signals monitoring. *Nanomaterials*, *14*(1 7), 1398.

Duzen, B. (2021). *Radiation detection and measurement with drone for emergency situations within CBRN* (Master's thesis). İstanbul University. İstanbul/Türkiye

Ekici, M. (2021). *Preparing sample animation scenarios on awareness and prevention measures of CBRN threats for 9-12 age group children* (Master's thesis). İskenderun Technical University. Hatay/Türkiye.

Eren, T. (2023). *Determining the knowledge, attitude and self- efficiencies of the nurses working at a university hospital on chemical, biological, radiological, and nuclear hazards* (Master's thesis). İstanbul Medipol University. İstanbul/Türkiye

Ergin, S. (2022). *Scale development study for hospitals' awareness and preparedness towards chemical, biological, radiological, nuclear threats and dangers* (Doctoral dissertation). İstanbul Okan University. İstanbul/Türkiye.

Farhat, H., Alinier, G., Chaabna, K., El Aifa, K., Abougalala, W., Laughton, J., & Ben Dhiab, M. (2024). Preparedness and emergency response strategies for chemical, biological, radiological and nuclear emergencies in disaster management: a qualitative systematic review. *Journal of Contingencies and Crisis Management*, *32*(3), e12592.

Gul, S. (2022). *Study on CBRN awareness, knowledge, attitudes and behaviors on Adana 112 provincial ambulance service employees* (Master's thesis). İskenderun Technical University. Hatay/Türkiye.

Gulkaya, S. (2022). *Measuring the preparedness and knowledge levels of the emergency service units in Sivas and the physicians and other HEALTH professionals working here for chemical biological radiological nuclear (CBRN) cases* (Specialization in Medicine). Sivas Cumhuriyet University. Sivas/Türkiye.

Gun, S. B. (2022). *Determining a road map on vaccine development against biological warfare agents within the scope of national CBRN defence by reviewing global efforts on developing COVID-19 vaccines* (Master's thesis). National Defense University. İstanbul/ Türkiye

Gunenc, N. D. (2021). *Investigation of personal protection knowledge level of personnel working in risky units of the hospital against CBRN hazard* (Master's thesis). Bezmialem Vakıf University. İstanbul/Türkiye.

Incedag, B. (2024). *Emergency healthcare workers' knowledge levels of CBRN and personal protective equipment: A case study of Kayseri 112* (Master's thesis). Niğde Ömer Halis Demir University. Niğde/Türkiye.

Kadirsoy, C. (2022). *Thermal camera use for evaluation of patients and injured in CBRN events* (Master's thesis). İskenderun Technical University. Hatay/Türkiye.

Kaleli, G. (2025). *The effect of first aid and CBRN training given to high school 9th grade students on students' knowledge levels* (Master's thesis). Niğde Ömer Halisdemir University. Niğde/Türkiye

Karakoc, N. (2024). *Determination of chemical, biological, radiological, nuclear and explosive (CBRN-E) event knowledge, attitudes and self-efficacy of future health professionals* (Master's thesis). Tekirdağ Namık Kemal University. Tekirdağ/Türkiye.

Karakus, E. (2024). *The role of animation supported education in raising children's awareness for the protection of children from chemical, biological, radiological and nuclear (CBRN) threats and hazards* (Master's thesis). Tekirdağ Namık Kemal University. Tekirdağ/Türkiye.

Kaya, M. (2021). *Methods used in the detection and decontamination of protection agents from CBRN agents specific to radioactive and nuclear agents* (Master's thesis). Muğla Sıtkı Koçman University. Muğla/Türkiye.

Kaynak, C. (2020). *To make a survey of a sample of hospital disaster team's knowledge level about possible cbrn (Chemical, biological, radioactive, nuclear) hazards after natural disasters* (Master's thesis). Çanakkale On Sekiz Mart University. Çanakkale/ Türkiye.

Kaynar, E. (2023). *Evalution of the general approach knowledge level of healthcare personnel providing prehospital healthcare services to cbrn (Chemical, biological, radiological and nuclear) cases* (Master's thesis). Çanakkale On Sekiz Mart University. Çanakkale/ Türkiye.

Kızılkaya, M. (2020). *Determination of preparatory perceptions and knowledge levels of Çanakkale Onsekiz Mart University Department of Emergency and Disaster Management Students against CBRN events* (Master's thesis). Çanakkale On Sekiz Mart University. Çanakkale/ Türkiye.

Kurt, E. (2022). *The place and approaches of family medicine doctors in the health management of CBRN events* (Specialization in Medicine) University of Health Sciences. İstanbul/Türkiye.

Kurt, İ. (2024). *Attitudes and self-efficacy of pre-hospital emergency health services employees in chemical, biological, radiological, nuclear hazards* (Master's thesis). Ege University. İzmir/Türkiye.

Kurtulus, U. S. (2024). *Evaluating the comparison of CBRN decontamination methods and systems used in EU countries and the USA with the example of Turkey* (Master's thesis). National Defense University. İstanbul/ Türkiye

Kucuk, F. (2024). *Production and characterization of activated carbon-based polyvinylchloride polymers for CBRN filters by electrospinning method* (Master's thesis). Selçuk University. Konya/Türkiye.

Kutukoglu, O. (2024). *GIS-based most suitable location analysis for electronic sensor systems to be applied in the field for detection of CBRN threats: Eskişehir example* (Master's thesis). Eskişehir Technical University. Eskişehir/Türkiye.

Mohammadi, S. B., Amirheidari, B., Danesh, T., Moghadam, M. N., Yazdi-Feyzabadi, V., Hassani, E., & Habibzadeh, H. (2022). Identification and analysis of parameters and global experiences of hospital preparedness against chemical, biological, radiological and nuclear disasters: a scoping review. *J Clin Res Paramed Sci*, *11*(1), e123626.

Ogur, E. (2020). *Evaluation of forensic mission efficiency in CBRN threat environment: A comparison between Turkey and the USA* (Master's thesis). Ankara University. Ankara/Türkiye.

Oktar, D. (2023). *Developing a training program to increase the level of knowledge and self-efficacy about chemical, biological, radiological and nuclear events in medical faculty students and evaluating the efficiency: A quasi-experimental study* (Specialization in Medicine). Eskişehir Osmangazi University. Eskişehir/Türkiye.

Oner, U. (2020). *Cbrn knowledge levels of family physicians providing primary health care and 112 emergency and first aid medical personnel* (Specialization in Medicine). University of Health Sciences. İstanbul/Türkiye

Ozcan, Z. (2021). *Measurement and evaluation of the behavior, attitude and knowledge level of the disaster and emergency management presidency (AFAD) staff based on the Turkey disaster response plan under the chemical, biological, radiological and nuclear (CBRN) cases* (Master's thesis). Bayburt University. Bayburt/Türkiye.

Ozturk, A. (2020). *Development of CBRN training program for higher education students in health sciences* (Master's thesis). University of Health Sciences. İstanbul/Türkiye.

Ozturk, I. (2019). *CBRN intervention system in terms of disaster medicine: An example of the management of chemical weapons in Syria* (Doctoral dissertation). Bezmialem Vakıf University. İstanbul/Türkiye.

Parlak, D. (2022). *CBRN threats in İskenderun shipping* (Master's thesis). İskenderun Technical University. Hatay/Türkiye.

Polat, Y. (2024). *Pre-hospital healthcare personnel's preparedness, awareness, attitudes, and behaviors towards chemical, biological, radiological, nuclear, and explosive (CBRNE) threats: A case study of Sakarya province* (Master's thesis). Tekirdağ Namık Kemal University. Tekirdağ/Türkiye

Qzih, E. S., & Ahmad, M. M. (2024). Hospital-based preparedness measures for CBRNE disasters: A systematic review. *Environmental Health Insights*, *18*, 1-12.

Razak, S., Hignett, S., & Barnes, J. (2018). Emergency department response to chemical, biological, radiological, nuclear, and explosive events: A systematic review. *Prehospital and Disaster Medicine*, *33*(5), 543-549.

Sarpkaya, U. (2023). *Examining the relation of weapons of mass destruction and terrorism with CBRN* (Master's thesis). İskenderun Technical University. Hatay/Türkiye.

Savas, T. (2023). *Examining the relationship between secondary effects of natural disasters and vulnerability to cbrn disasters* (Master's thesis). İskenderun Technical University. Hatay/Türkiye.

Sert, A., Polat, M., & Erdemir, S. (2022). The importance of blood toxic gases (hcn, co, as) from chemical biological radiological nuclear (cbrn) agents. *International Journal of Interdisciplinary Interaction in Health Sciences, 1*(1), 42–51.

Sezigen, S. (2009). *Developing a behavioral model that is intending for cbrn mass casualties in health facilities* (Doctoral dissertation). University of Health Sciences(GATA). İstanbul/Türkiye

Sahin, F. (2020). *Measurement of knowledge, skills, experience and opinions about the subject of employees of some institutions that take place in CBRN events, with in-depth interview technique: The case of Gümüşhane and Erzurum provinces* (Master's thesis). Gümüşhane University. Gümüşhane/Türkiye.

Tazearslan, Z. (2021). *Evaluation of the relationship between risk perception and prepadness of emergency health care workers towards CBRN threats* (Master's thesis). İskenderun Technical University. Hatay/Türkiye.

Titiz, G. (2021). *An evaluation of CBRN threats management in terms of pre-hospital emergency health services: SWOT analysis* (Master's thesis). İskenderun Technical University. Hatay/Türkiye.

Tosun, Ç. B. (2022). *Assessment of antimicrobial and coagulant activities of CBRN decontamination materials* (Master's thesis). Middle East Technical University. Ankara/Türkiye.

Turkeri, B. N. (2022). *Comparison of institutional structures created against chemical, biological, radiological, nuclear (CBRN)-toxicological disasters in the world and Turkey in the context of legislation and practices* (Master's thesis). Tekirdağ Namık Kemal University. Tekirdağ/Türkiye

Ulusoy, S. (2024). *Evaluation of institution employees awareness to the management standard of chemical biological radiological nuclear (cbrn) hazards in Antalya Training and Research Hospital* (Master's thesis). Dokuz Eylül University. İzmir/Türkiye

Yakut, S. (2023). *Effect of CBRN threats on safety staff and possible measures (OC pepper gas example* (Master's thesis). İskenderun Technical University. Hatay/Türkiye.

Yalcın, H. (2023). *Association of information technologies used in nursing practices and CBRN* (Master's thesis). İskenderun Technical University. Hatay/Türkiye.

Yıldırım, S. (2022). *Ppe usage, knowledge and skills status of pre-hospital emergency medical services employees against cbrn incidents: The case of Adana province* (Master's thesis). İskenderun Technical University. Hatay/Türkiye.

Yıldırım, T. (2019). *Investigation of the event intervention methods of CBRN teams: Adana AFAD case study* (Master's thesis). Bitlis Eren University. Bitlis/Türkiye.

Yıldız, G. (2024). *Evalution of practices, knowledge and attitude of emergency health services personnel in cbrn events* (Master's thesis). Çanakkale On Sekiz Mart University. Çanakkale/ Türkiye

Yucel, H. (2019). *Assessment of the relationship between the risk perception and preparedness attitudes of some teams involved in the first response in cbrn events to hazards at the event site: The sample of Adana city* (Master's thesis). Gümüşhane University. Gümüşhane/Türkiye.

Author(s) Information

Ali Sert
Burdur Mehmet Akif Ersoy University
Burdur Vocational School of Health Services, Türkiye
Contact e-mail: *alisert@mehmetakif.edu.tr*

To cite this article:

Sert, A. (2025). The importance of disaster management and planning in chemical, biological, radiological and nuclear events: thematic trends in postgraduate theses in Türkiye. *The Eurasia Proceedings of Science, Technology, Engineering and Mathematics (EPSTEM), 35,* 94-106.

The Eurasia Proceedings of Science, Technology, Engineering & Mathematics (EPSTEM)
ISSN: 2602-3199

The Eurasia Proceedings of Science, Technology, Engineering and Mathematics (EPSTEM), 2025

Volume 35, Pages 107-114

ICRETS 2025: International Conference on Research in Engineering, Technology and Science

A Non-Calculus Approach to Solving the Cost Minimization Problem with the Modified Spillman Production Function

Vedran Kojic
University of Zagreb

Abstract: Cost minimization is a fundamental problem for all firms. In this study, we consider the cost minimization problem in the context of a farm business, where output is described by the modified Spillman production function. This problem holds significant importance in agricultural economics. Mathematically, it represents an application of unconstrained optimization to economic and business problems. The conventional approach to solving this problem involves the use of calculus, specifically the Lagrange multiplier method. However, the application of differential calculus requires nontrivial steps that may not be easily understood without a solid background in mathematical analysis. The aim of this paper is to introduce a novel non-calculus approach to solving the given problem. Our approach is new and relies solely on the weighted arithmetic mean–geometric mean inequality and basic algebra, making it more accessible and intuitive compared to calculus-based techniques. Furthermore, we provide an elementary derivation of the interpretation of the Lagrange multiplier as a tool for sensitivity analysis.

Keywords: Cost minimization, Modified Spillman production function, Non-calculus approach

Introduction

The cost of a firm's output is the expenditure it must make to get the inputs required for the production of that output. Generally, technology allows each output level to be produced using different combinations of inputs, all of which can be represented by the level sets of the production function. Consequently, the firm must determine which production plan to adopt. If the firm's goal is to maximize profits, it will always select the least expensive, or cost-minimizing, production plan for each output level. This principle applies to all firms, whether they operate as monopolists, perfect competitors, or anything in between (Jehle & Reny, 2011). In agricultural economics, various functional forms of production functions are commonly used, such as Cobb-Douglas, CES, and translog-like functions (Debertin, 2012). However, one of the earliest attempts to estimate a production function in agriculture was made by Spillman (1923,1924), whose classical production function follows an exponential form.

This study examines the cost minimization problem using a modified version of the Spillman production function, as introduced by Jaworski (1977). The conventional approach to solving this problem is the Lagrange multiplier method. However, as Jaworski noted, applying differential calculus often involves "some toilsome calculations". Moreover, many scholars agree that alternative methods for finding extrema can provide valuable insights, particularly for managers, students, and others who may lack a strong background in mathematical analysis (Oxman et al., 2018). Numerous studies on non-calculus-based approaches to extrema problems exist, particularly in inventory theory (Caliskan, 2023). Additionally, many classical and generalized problems in economic theory, including utility, cost, and profit optimization, can be solved without the use of differential calculus (Kojić, 2017; Kojić & Lukač, 2018a, 2018b, 2019; Kojić et al., 2021, 2023; Kojić & Krpan, 2021; Kojić, 2024). In light of this, to determine the firm's minimal cost under the modified Spillman production function, our approach uses the weighted arithmetic mean – geometric mean (AM-GM) inequality, basic algebra, and solely the definition of global extrema.

- Selection and peer-review under responsibility of the Organizing Committee of the Conference

The paper is structured as follows. Following the introduction, the second section presents the preliminaries and problem formulation. The third section provides solutions to the cost minimization problem using both the Lagrange multiplier method and the weighted AM-GM inequality, along with a remark on how the interpretation of the Lagrange multiplier can be derived elementarily. Finally, the fourth section concludes the paper.

Preliminaries and Problem Formulation

We assume that firm operates in perfectly competitive input markets, meaning it cannot influence prices and must accept the given market prices. Let $w_1 > 0,\ w_2 > 0$ be the prices of inputs, and $x_1 > 0,\ x_2 > 0$ be the inputs the firm can buy. Since the firm wants to maximize profit, it will choose to produce output using the least expensive combination of inputs. Therefore, the cost of producing a given output $y_0 > 0$ is the lowest possible cost of inputs needed at given prices. One of the first production functions in agricultural economics is classical Spillman production function $y = m - a v_1^{x_1} v_2^{x_2}$, where $y \geq 0$ is the amount of the output, and $m > 0,\ a > 0,\ 0 < v_1 < 1,\ 0 < v_2 < 1,$ are given parameters such that $m - a \geq 0$. In this paper, we assume that the firm's production technology follows the modified Spillman production function proposed by Jaworski (1977):

$$y = y(x_1, x_2) = m - a(x_1 + 1)^{-v_1} (x_2 + 1)^{-v_2}, \tag{1}$$

whit assumption $m > y_0 > 0$. The cost minimization problem can now be written as the following constrained optimization problem:

$$\begin{cases} \min\limits_{x_1, x_2 > 0} \ f(x_1, x_2) = w_1 x_1 + w_2 x_2 \\ \text{s.t.} \ \ g(x_1, x_2) = m - a(x_1 + 1)^{-v_1} (x_2 + 1)^{-v_2} = y_0 . \end{cases} \tag{2}$$

We will solve problem (2) in the usual way, using the Lagrange multiplier method and differential calculus. After that, we will show how the same problem can be tackled without calculus, as well as the advantages and disadvantages of such an approach. To do so, we will need the following lemma.

Lemma 1 (Weighted AM – GM Inequality) Let $z_1 > 0, z_2 > 0, \lambda_1 > 0, \lambda_2 > 0$ such that $\lambda_1 + \lambda_2 = 1$. Then

$$z_1 + z_2 \geq \left(\frac{z_1}{\lambda_1}\right)^{\lambda_1} \left(\frac{z_2}{\lambda_2}\right)^{\lambda_2}. \tag{3}$$

Equality in (3) holds if and only if $\dfrac{z_1}{\lambda_1} = \dfrac{z_2}{\lambda_2}$.

The proof of the weighted AM-GM inequality can be found, for example, in Bullen (2003), Cvetkovski (2012), or Mitrinović (1970).

Results

In the literature, the cost minimization problem is tipically solved using differential calculus, specifically the Lagrange multiplier method (Jehle & Reny, 2011; Mas-Colell et al., 1995; Simon & Blume, 1994; Sydsaeter et al., 2005; Varian, 2010). Jaworski, (1977) examined problem (2) in the same way but omitted detailed calculations and steps. For this reason, we will first present a step-by-step solution to problem (2) using the Lagrange multiplier method. After that, we will introduce an alternative approach to solving the same problem.

Differential Calculus Approach

The Lagrangian function for the problem (2) is

$$L(x_1, x_2, \lambda) = f(x_1, x_2) + \lambda\big(g(x_1, x_2) - y_0\big) = w_1 x_1 + w_2 x_2 + \lambda\Big(m - a(x_1 + 1)^{-v_1} (x_2 + 1)^{-v_2} - y_0\Big). \tag{4}$$

Taking the partial derivatives of the first and the second order, we get:

$$L_{x_1} = w_1 + \lambda a v_1 \left(x_1+1\right)^{-v_1-1}\left(x_2+1\right)^{-v_2}, \tag{5}$$

$$L_{x_2} = w_2 + \lambda a v_2 \left(x_1+1\right)^{-v_1}\left(x_2+1\right)^{-v_2-1}, \tag{6}$$

$$L_{\lambda} = m - a\left(x_1+1\right)^{-v_1}\left(x_2+1\right)^{-v_2} - y_0, \tag{7}$$

$$g_{x_1} = a v_1 \left(x_1+1\right)^{-v_1-1}\left(x_2+1\right)^{-v_2}, \tag{8}$$

$$g_{x_2} = a v_2 \left(x_2+1\right)^{-v_1}\left(x_2+1\right)^{-v_2-1}, \tag{9}$$

$$L_{x_1x_1} = -\lambda a v_1\left(v_1+1\right)\left(x_1+1\right)^{-v_1-2}\left(x_2+1\right)^{-v_2}, \tag{10}$$

$$L_{x_2x_2} = -\lambda a v_2\left(v_2+1\right)\left(x_1+1\right)^{-v_1}\left(x_2+1\right)^{-v_2-2}, \tag{11}$$

$$L_{x_1x_2} = L_{x_2x_1} = -\lambda a v_1 v_2\left(x_1+1\right)^{-v_1-1}\left(x_2+1\right)^{-v_2-1}. \tag{12}$$

From the first order conditions

$$L_{x_1}=0,\ L_{x_2}=0,\ L_{\lambda}=0, \tag{13}$$

we get a unique stationary point

$$\left(\tilde{x}_1,\tilde{x}_2,\tilde{\lambda}\right), \tag{14}$$

where

$$\tilde{x}_1 = \left(\frac{v_1 w_2}{v_2 w_1}\right)^{\frac{v_2}{v_1+v_2}}\left(\frac{a}{m-y_0}\right)^{\frac{1}{v_1+v_2}} - 1, \tag{15}$$

$$\tilde{x}_2 = \left(\frac{v_2 w_1}{v_1 w_2}\right)^{\frac{v_1}{v_1+v_2}}\left(\frac{a}{m-y_0}\right)^{\frac{1}{v_1+v_2}} - 1, \tag{16}$$

$$\tilde{\lambda} = -\frac{1}{m-y_0}\left(\frac{a}{m-y_0}\right)^{\frac{1}{v_1+v_2}}\left(\frac{w_1}{v_1}\right)^{\frac{v_1}{v_1+v_2}}\left(\frac{w_2}{v_2}\right)^{\frac{v_2}{v_1+v_2}}. \tag{17}$$

Note that input prices w_1, w_2 and parameters a, m, y_0, v_1, v_2 must be given in such a way that (15) and (16) are positive. Additionally, since $m-y_0>0$, expression in (17) is negative, i.e.

$$\tilde{\lambda} < 0. \tag{18}$$

To prove that (14) is the point of minimum, we need to check the sign of the bordered Hessian at the point (14):

$$\begin{aligned}
\det H\left(\tilde{x}_1,\tilde{x}_2,\tilde{\lambda}\right) &= \begin{vmatrix} 0 & g_{x_1}\left(\tilde{x}_1,\tilde{x}_2,\tilde{\lambda}\right) & g_{x_2}\left(\tilde{x}_1,\tilde{x}_2,\tilde{\lambda}\right) \\ g_{x_1}\left(\tilde{x}_1,\tilde{x}_2,\tilde{\lambda}\right) & L_{x_1x_1}\left(\tilde{x}_1,\tilde{x}_2,\tilde{\lambda}\right) & L_{x_1x_2}\left(\tilde{x}_1,\tilde{x}_2,\tilde{\lambda}\right) \\ g_{x_2}\left(\tilde{x}_1,\tilde{x}_2,\tilde{\lambda}\right) & L_{x_2x_1}\left(\tilde{x}_1,\tilde{x}_2,\tilde{\lambda}\right) & L_{x_2x_2}\left(\tilde{x}_1,\tilde{x}_2,\tilde{\lambda}\right) \end{vmatrix} = \\
&= \left(\left(\tilde{x}_1+1\right)^{-v_1-1}\left(\tilde{x}_2+1\right)^{-v_2-1}\right)\cdot\left(\left(\tilde{x}_1+1\right)^{-v_1-2}\left(\tilde{x}_2+1\right)^{-v_2-1}\right)\cdot\left(\left(\tilde{x}_1+1\right)^{-v_1-1}\left(\tilde{x}_2+1\right)^{-v_2-2}\right)\cdot \\
&\cdot\begin{vmatrix} 0 & a v_1\left(\tilde{x}_2+1\right) & a v_2\left(\tilde{x}_1+1\right) \\ a v_1\left(\tilde{x}_1+1\right)\left(\tilde{x}_2+1\right) & -\tilde{\lambda} a v_1\left(v_1+1\right)\left(\tilde{x}_2+1\right) & -\tilde{\lambda} a v_1 v_2\left(\tilde{x}_1+1\right) \\ a v_2\left(\tilde{x}_1+1\right)\left(\tilde{x}_2+1\right) & -\tilde{\lambda} a v_1 v_2\left(\tilde{x}_2+1\right) & -\tilde{\lambda} a v_2\left(v_2+1\right)\left(\tilde{x}_1+1\right) \end{vmatrix} = \\
&= \tilde{\lambda}\underbrace{\left(v_1+v_2\right)v_1 v_2\left(\tilde{x}_1+1\right)^{-3v_1-2}\left(\tilde{x}_2+1\right)^{-3v_2-2}}_{>0}.
\end{aligned} \tag{19}$$

Thus, the sign in (19) depends on the Lagrange multiplier $\tilde{\lambda}$ from (17). Since it is negative (see (18)), the sign of the bordered Hessian in (19) is also negative, which implies that the minimum cost of problem (2) is achieved at the input levels (15) and (16), and is equal to

$$f\left(\tilde{x}_1,\tilde{x}_2\right) = w_1\tilde{x}_1 + w_2\tilde{x}_2 \overset{(15)-(16)}{=} \left(\frac{w_1}{v_1}\right)^{\frac{v_1}{v_1+v_2}}\left(\frac{w_2}{v_2}\right)^{\frac{v_2}{v_1+v_2}}\left(v_1+v_2\right)\left(\frac{a}{m-y_0}\right)^{\frac{1}{v_1+v_2}} - w_1 - w_2. \tag{20}$$

Finally, in the context of economic theory (see, for example, Jehle & Reny (2011), p. 136) let us point out that solving the cost minimization problem with the modified Spillman production function (2), we obtain the cost function $c:\mathbb{R}_{+}^{3}\to\mathbb{R}$ from (20), where

$$c(w_1, w_2, y_0) = \left(\frac{w_1}{v_1}\right)^{\frac{v_1}{v_1+v_2}} \left(\frac{w_2}{v_2}\right)^{\frac{v_2}{v_1+v_2}} (v_1 + v_2)\left(\frac{a}{m - y_0}\right)^{\frac{1}{v_1+v_2}} - w_1 - w_2 . \tag{21}$$

Similarly, relations (15) and (16) give conditional input demands as functions $x_1, x_2 : \mathbb{R}^3_+ \to \mathbb{R}$ where

$$x_1(w_1, w_2, y_0) = \left(\frac{v_1 w_2}{v_2 w_1}\right)^{\frac{v_2}{v_1+v_2}} \left(\frac{a}{m - y_0}\right)^{\frac{1}{v_1+v_2}} - 1 , \tag{22}$$

$$x_2(w_1, w_2, y_0) = \left(\frac{v_2 w_1}{v_1 w_2}\right)^{\frac{v_1}{v_1+v_2}} \left(\frac{a}{m - y_0}\right)^{\frac{1}{v_1+v_2}} - 1 . \tag{23}$$

Let us emphasize once again that input prices w_1, w_2 and parameters a, m, y_0, v_1, v_2 must be given in such a way that (21) – (23) are positive for economic reasons.

Non-calculus Approach

From the constraint $g(x_1, x_2) = y_0$ in (2), the variable x_2 can be expressed as

$$x_2 = \left(\frac{a}{m - y_0}\right)^{\frac{1}{v_2}} (x_1 + 1)^{-\frac{v_1}{v_2}} - 1 . \tag{24}$$

Consequently, inserting (24) into the objective function in (2), the cost minimization problem (2) equivalently transforms into the following unconstrained problem:

$$\min_{x_1 > 0} \varphi(x_1) = w_1(x_1 + 1) + w_2 \left(\frac{a}{m - y_0}\right)^{\frac{1}{v_2}} (x_1 + 1)^{-\frac{v_1}{v_2}} - w_1 - w_2 . \tag{25}$$

Let

$$z_1 = w_1(x_1 + 1),\ z_2 = w_2 \left(\frac{a}{m - y_0}\right)^{\frac{1}{v_2}} (x_1 + 1)^{-\frac{v_1}{v_2}} . \tag{26}$$

Then, by applying the weighted AM-GM inequality (see Lemma 1) to the terms in (26), we obtain from (25) the following inequality:

$$\varphi(x_1) \geq \left(\frac{w_1}{\lambda_1}\right)^{\lambda_1} \left(\frac{w_2}{\lambda_2}\left(\frac{a}{m - y_0}\right)^{\frac{1}{v_2}}\right)^{\lambda_2} (x_1 + 1)^{\lambda_1 - \frac{v_1}{v_2}\lambda_2} - w_1 - w_2 , \tag{27}$$

where $\lambda_1 > 0,\ \lambda_2 > 0,\ \lambda_1 + \lambda_2 = 1$. By setting the exponent $\lambda_1 - \dfrac{v_1}{v_2}\lambda_2$ from (27) equal to 0, we can easily calculate weights λ_1 and λ_2:

$$\left.\begin{aligned} \lambda_1 + \lambda_2 &= 1 \\ \lambda_1 - \frac{v_1}{v_2}\lambda_2 &= 0 \end{aligned}\right\} \Rightarrow \lambda_1 = \frac{v_1}{v_1 + v_2},\ \lambda_2 = \frac{v_2}{v_1 + v_2} . \tag{28}$$

Note that for the weights λ_1 and λ_2 from (28), the-right-hand side of (27) becomes a constant. That is, from (27) and (28) we obtain the following inequality:

$$\varphi(x_1) \geq (v_1 + v_2)\left(\frac{w_1}{v_1}\right)^{\frac{v_1}{v_1+v_2}} \left(\frac{w_2}{v_2}\right)^{\frac{v_2}{v_1+v_2}} \left(\frac{a}{m - y_0}\right)^{\frac{1}{v_1+v_2}} - w_1 - w_2 . \tag{29}$$

Inequality (29) holds for all $x_1 > 0$, where, by Lemma 1, equality holds if and only if

$$\frac{z_1}{\lambda_1} = \frac{z_2}{\lambda_2} . \tag{30}$$

From (30), (28), and (26), equality in (29) is possible if and only if

$$x_1 = \left(\frac{v_1 w_2}{v_2 w_1}\right)^{\frac{v_2}{v_1+v_2}} \left(\frac{a}{m - y_0}\right)^{\frac{1}{v_1+v_2}} - 1 . \tag{31}$$

Since the inequality (29) holds for all $x_1 > 0$, with equality if and only if (31) holds, the definition of global extrema implies that the function $\varphi(x_1)$ from (25) has a global minimum

$$\varphi_{\min} = (v_1 + v_2)\left(\frac{w_1}{v_1}\right)^{\frac{v_1}{v_1+v_2}}\left(\frac{w_2}{v_2}\right)^{\frac{v_2}{v_1+v_2}}\left(\frac{a}{m-y_0}\right)^{\frac{1}{v_1+v_2}} - w_1 - w_2 , \tag{32}$$

with a unique minimizer at level (31). Consequently, (32), (31) and (24) imply that the solution of the cost minimization problem with the modified Spillman production function (2) is the same as the solution (21) – (23) obtained using Lagrange multiplier method.

In comparison to differential calculus, we can see that the presented approach uses the weighted AM–GM inequality, which requires only simple algebraic steps. The solution follows directly from the definition of global extrema. Although differential calculus is a more powerful tool that can solve a larger set of optimization problems, in the case of the cost minimization problem with the modified Spillman production function, our approach avoids the nontrivial task of checking the first and second-order conditions, which, as Jaworski (1977) mentioned, lead to “some toilsome calculations”.

On a Non-Calculus Approach to the Interpretation of the Lagrange Multiplier

In the cost minimization problem with the modified Spillman production function (2), the interpretation of the Lagrange multiplier in equation (17) follows from the formula

$$\frac{\partial f(\tilde{x}_1, \tilde{x}_2)}{\partial y_0} = -\tilde{\lambda} > 0 , \tag{33}$$

which means that if production y at level y_0 increases by 1 unit, the minimal cost in (21) will increase approximately by

$$-\tilde{\lambda} = \frac{1}{m-y_0}\left(\frac{a}{m-y_0}\right)^{\frac{1}{v_1+v_2}}\left(\frac{w_1}{v_1}\right)^{\frac{v_1}{v_1+v_2}}\left(\frac{w_2}{v_2}\right)^{\frac{v_2}{v_1+v_2}} \tag{34}$$

units. This interpretation follows directly from the definition of the first derivative, i.e.

$$\text{at level } y = y_0, \text{ if } y \uparrow \text{ 1 unit } \Rightarrow c(w_1, w_2, y_0) \uparrow \approx \frac{1}{m-y_0}\left(\frac{a}{m-y_0}\right)^{\frac{1}{v_1+v_2}}\left(\frac{w_1}{v_1}\right)^{\frac{v_1}{v_1+v_2}}\left(\frac{w_2}{v_2}\right)^{\frac{v_2}{v_1+v_2}} \text{ units.} \tag{35}$$

Let us now derive the same interpretation in a more elementary way. First, we will use a well-known approximation formula for all real numbers $\alpha > 0$ and $x > 0,\ x \approx 0$:

$$(1+x)^{\alpha} \approx 1 + \alpha x . \tag{36}$$

Secondly, for “small” $\delta > 0$, let us calculate the exact change Δc in the minimal cost (21) when production level y_0 increases to $y_0 + \delta$. Using some elementary algebraic steps, we obtain

$$\begin{aligned}
\Delta c &= c(w_1, w_2, y_0 + \delta) - c(w_1, w_2, y_0) \\
&= \left(\left(\frac{a}{m-y_0-\delta}\right)^{\frac{1}{v_1+v_2}} - \left(\frac{a}{m-y_0}\right)^{\frac{1}{v_1+v_2}}\right)(v_1+v_2)\left(\frac{w_1}{v_1}\right)^{\frac{v_1}{v_1+v_2}}\left(\frac{w_2}{v_2}\right)^{\frac{v_2}{v_1+v_2}} \\
&= \left(\left(\frac{m-y_0}{m-y_0-\delta}\right)^{\frac{1}{v_1+v_2}}\left(\frac{a}{m-y_0}\right)^{\frac{1}{v_1+v_2}} - \left(\frac{a}{m-y_0}\right)^{\frac{1}{v_1+v_2}}\right)(v_1+v_2)\left(\frac{w_1}{v_1}\right)^{\frac{v_1}{v_1+v_2}}\left(\frac{w_2}{v_2}\right)^{\frac{v_2}{v_1+v_2}} \\
&= \left(\left(1 + \frac{\delta}{m-y_0-\delta}\right)^{\frac{1}{v_1+v_2}} - 1\right)\left(\frac{a}{m-y_0}\right)^{\frac{1}{v_1+v_2}}(v_1+v_2)\left(\frac{w_1}{v_1}\right)^{\frac{v_1}{v_1+v_2}}\left(\frac{w_2}{v_2}\right)^{\frac{v_2}{v_1+v_2}} .
\end{aligned} \tag{37}$$

Substituting $x = \dfrac{\delta}{m-y_0-\delta} \approx 0$ and $\alpha = \dfrac{1}{v_1+v_2} > 0$ into (36), from (37) we get the approximation of the exact change Δc:

$$\Delta c \approx \left(1+\frac{1}{(v_1+v_2)(m-y_0-\delta)}-1\right)\left(\frac{a}{m-y_0}\right)^{\frac{1}{v_1+v_2}}(v_1+v_2)\left(\frac{w_1}{v_1}\right)^{\frac{v_1}{v_1+v_2}}\left(\frac{w_2}{v_2}\right)^{\frac{v_2}{v_1+v_2}} = \\ = \frac{1}{m-y_0-\delta}\left(\frac{a}{m-y_0}\right)^{\frac{1}{v_1+v_2}}\left(\frac{w_1}{v_1}\right)^{\frac{v_1}{v_1+v_2}}\left(\frac{w_2}{v_2}\right)^{\frac{v_2}{v_1+v_2}}. \tag{38}$$

Note that for "small" $\delta > 0$ the following approximation holds

$$\frac{1}{m-y_0-\delta} \approx \frac{1}{m-y_0}. \tag{39}$$

By inserting (39) in (38) we get

$$\Delta c = c(w_1,w_2,y_0+\delta)-c(w_1,w_2,y_0) \approx \frac{1}{m-y_0}\left(\frac{a}{m-y_0}\right)^{\frac{1}{v_1+v_2}}\left(\frac{w_1}{v_1}\right)^{\frac{v_1}{v_1+v_2}}\left(\frac{w_2}{v_2}\right)^{\frac{v_2}{v_1+v_2}}. \tag{40}$$

Specially for "small" $\delta = 1$, from (34) and (40) we obtain

$$c(w_1,w_2,y_0+1) \approx c(w_1,w_2,y_0)+\frac{1}{m-y_0}\left(\frac{a}{m-y_0}\right)^{\frac{1}{v_1+v_2}}\left(\frac{w_1}{v_1}\right)^{\frac{v_1}{v_1+v_2}}\left(\frac{w_2}{v_2}\right)^{\frac{v_2}{v_1+v_2}}. \tag{41}$$

By comparing (33)–(35) with (41), we can see that we have derived the interpretation of the Lagrange multiplier in an elementary way, without using calculus.

Conclusion

Minimizing costs is a crucial challenge for all firms. In this paper, we examine the cost minimization problem within the framework of farm businesses, where output is modeled using the modified Spillman production function. The standard method for solving this problem typically relies on differential calculus, which often requires nontrivial steps that may be difficult to grasp without a strong foundation in mathematical analysis. The objective of this paper is to present an alternative approach that does not involve calculus. Our method is novel and is based solely on the weighted arithmetic mean–geometric mean inequality and fundamental algebra, making it more accessible and intuitive than traditional calculus-based solutions. The solution for the minimal cost follows directly from the definition of global extrema. Although differential calculus is a more powerful tool that can solve a larger set of optimization problems, in the case of the cost minimization problem with the modified Spillman production function our approach avoids toilsome task of checking the first and second-order conditions, which makes it more accessible and intuitive. Finally, we show how the Lagrange multiplier's interpretation as a tool for sensitivity analysis can be derived in a simple algebraic way, without calculus.

Recommendations

Despite the fact that differential calculus is a standard tool in mathematical analysis for solving the vast majority of optimization problems, we believe that, whenever possible, alternative non-calculus methods can provide a deeper and better understanding of certain problems. In this regard, our approach can offer new insights to managers, high school students, first-year college students, and other audiences who may be unfamiliar with the application of calculus in solving the cost minimization problem with the modified Spillman production function. Additionally, our approach should not be seen as superior to calculus, but rather as a complementary validation method for the results obtained using derivatives.

Scientific Ethics Declaration

* The authors declare that the scientific ethical and legal responsibility of this article published in EPSTEM journal belongs to the authors.

Conflict of Interest

* The authors declare that they have no conflicts of interest

Funding

* This research received no specific grant from any funding agency in the public, commercial, or not-for-profit sectors.

Acknowledgements or Notes

* This article was presented as an oral presentation at the International Conference on Research in Engineering, Technology and Science (www.icrets.net) held in Peja/Kosovo on July 10-13, 2025.

References

Bullen, P. S. (2003). *Handbook of means and their inequalities*. Springer Dordrecht.
Caliskan, C. (2023). A general approach for the derivation of optimal solutions without derivatives. *International Journal of Systems Science: Operations & Logistics*, *10*:1, 2005845.
Cvetkovski, Z. (2012). *Inequalities*. Berlin: Springer-Verlag.
Debertin, D. L. (2012). *Agricultural production economics*. Agricultural Economics Textbook Gallery.
Jaworski, J. (1977). Decision aspects of the Spillman production function. *Canadian Journal of Agricultural Economics, 25*(3), 48–53.
Jehle, G. A., & Reny, P. J. (2011). *Advanced microeconomic theory*. New Jersey: FT Prentice.
Kojić, V. (2025). An elementary approach to solving the optimal taxation of a perfectly competitive firm with CES production function as a bilevel programming problem. *Central European Journal of Operations Research*, *33*(2), 679–696.
Kojić, V., Krpan, M., & Lukač, Z. (2023). A simple approach to solving monopolist's long-run profit maximization problem: the case of the hyperbolic inverse demand and Cobb-Douglas production functions with two factors of production. *Proceedings of the 17th International Symposium on Operational Research in Slovenia SOR'23.* Ljubljana: University of Maribor, 405-410.
Kojić, V., & Krpan, M. (2021). On the application of Weighted AM-GM inequality to profit maximization problem in the case of the Cobb-Douglas production function with input factors (in Croatian). *Economic Thought and Practice*, *30* (1), 205-223.
Kojić, V., Krpan, M. & Lukač, Z. (2021). Teaching cost minimization-can a non-calculus approach help? *International Journal of Mathematical Education in Science & Technology*, *52* (8), 1281-1294.
Kojić, V., & Lukač, Z. (2019). On the cost minimization problem with CES technology: reverse Hölder's inequality approach. *Proceedings of the 15th International Symposium on Operational Research in Slovenia SOR'19.* Ljubljana: University of Maribor, 593-598.
Kojić, V., & Lukač, Z. (2018a). An alternative approach to solving cost minimization problem with Cobb-Douglas technology. *Central European Journal of Operations Research*, *26*(3), 629-643.
Kojić, V., & Lukač, Z. (2018b). Solving profit maximization problem in case of the Cobb-Douglas production function via weighted AG inequality and geometric programming. Proceedings from: *2018 IEEE International Conference on Industrial Engineering and Engineering Management (IEEM)*, Bangkok, Thailand, 1900-1903.
Kojić, V. (2017). Solving the consumer's utility-maximization problem with CES and Cobb-Douglas utility function via mathematical inequalities. *Optimization letters, 11* (4), 875-884.
Mas-Colell, A., Whinston, M. D., & Green, J. R. (1995). *Microeconomic theory.* London: Oxford University Press.
Mitrinović, D. S. (1970). *Analytic inequalities*. Berlin: Springer-Verlag.
Oxman, V., Stupel, M., & Jahangiri, J. M. (2018). Finding extrema without resorting to calculus. *Cogent Education*, *5*(1), 1551299.
Simon, C. P., & Blume L. (1994). *Mathematics for economists.* New York, NY: W. W. Northon & Company.
Spillman, W. J. (1923). Application of the law of diminishing returns to some fertilizer and feed data. *Journal of Farm Economics*, *5*(1), 36-52.
Spillman, W. J. (1924). Law of the diminishing increment in the fattening of steers and hogs. *Journal of Farm Economics*, *6*(2), 166-178.
Sydsaeter, K., Hammond, P., Seierstad, A. & Storm, A. (2005). *Further mathematics for economic analysis*. London: Prentice Hall.

Varian, H. L. (2010). *Intermediate microeconomics: A modern approach.* New York, NY: W. W. Norton & Company.

Author(s) Information

Vedran Kojic
Faculty of Economics and Business, University of Zagreb
Trg J. F. Kennedyja 6, 10000 Zagreb, Croatia
Contact e-mail: *vkojic@efzg.hr*

To cite this article:

Kojic, V. (2025). A non-calculus approach to solving the cost minimization problem with the modified Spillman production function. *The Eurasia Proceedings of Science, Technology, Engineering and Mathematics (EPSTEM), 35,* 107-114.

The Eurasia Proceedings of Science, Technology, Engineering & Mathematics (EPSTEM)
ISSN: 2602-3199

The Eurasia Proceedings of Science, Technology, Engineering and Mathematics (EPSTEM), 2025

Volume 35, Pages 115-123

ICRETS 2025: International Conference on Research in Engineering, Technology and Science

Performance Assessment of Determinant Kernels in Content-Based Video Retrieval: A Non-Square Determinant Approach

Besnik Duriqi
South East European University

Halil Snopce
South East European University

Armend Salihu
South East European University

Artan Luma
South East European University

Azir Aliu
South East European University

Abstract: Content-Based Video Retrieval (CBVR) relies on efficient similarity metrics to enhance the accuracy of the retrieval and reduce the computational overhead. This work explores the efficiency of determinant kernels by computing non-square determinants for similarity score calculation in high-dimensional feature spaces. Based on determinant-based computations, we propose a new method that increases the efficiency as well as the retrieval quality. The work focuses on the creation of a rigorous mathematical framework that integrates determinant kernels in the similarity measurement process, which forms a crucial building block in CBVR systems. Based on rigorous experiments on standard video datasets, we analyze the degree to which non-square determinant computations capture variations in the video content that other approaches might not capture. Our analysis demonstrates that the new method significantly increases the processing efficiency, leading to more accurate retrieval results. Additionally, the method proves to be computationally efficient, making it suitable for real-time applications as well as for large-scale video databases. The findings of this work make substantial contributions to the area of CBVR techniques and pave the way for future work in efficient video content analysis.

Keywords: Content-based video retrieval, Determinant kernels, Non-square determinants, Similarity score

Introduction

Nowadays, there is a huge amount of video data available to individuals on the internet. It is not feasible for a human to categorize or arrange video sequences in a large video data set, or to locate the desired scene or the necessary parts of the movie. In order to create video search engines that act as a source of data filter and arrange a database of initially relevant videos, video retrieval is a necessary technique. Finding an interesting video scene in video retrieval needs an efficient method of measuring shot similarities. A shot is a collection of images taken by one camera in a single, continuous camera motion in space and time (Zhu, 2023). Finding useful shots requires a lot of processing power and time and is very sensitive to visual features and similarity measures. For end-users of multimedia systems and applications, such as digital libraries, publications, education, broadcasting, and entertainment, video data contains a great amount of information. Only until video retrieval algorithms are capable enough to retrieve videos and other significant data from enormous databases

- Selection and peer-review under responsibility of the Organizing Committee of the Conference

within a short period of time can such applications be useful (Accattoli, 2020). However, it is very difficult for the current online search engines to find videos on the internet, thus new approaches that have the ability to change the video data with respect to the content are necessary (Nixon, 2024). A fusion of multimedia data are stored and organized for multimedia mining by using techniques such as video classification and annotation (Yuan, 2024).

Since video retrieval is not effective with the traditional query-by-text retrieval approach, Content Based Video Retrieval (CBVR) is regarded as one of the most feasible approaches to achieve quality video retrieval (Patel, 2023). With the use of rich video content, there is tremendous potential for the field of video retrieval to advance the performance of traditional search engines (Khan, 2024), which has made the research field of CBVR promising for the development of more effective video search engines in the future (Nandini, 2022). The majority of web-based video retrieval systems operate by indexing and retrieving videos based on texts associated with them (Dong, 2022).

The foundation of video retrieval is feature extraction. There are various kinds of features, including color-based features, texture-based features, and shape-based features (Ge, 2022), which can be extracted from images and video data. The most effective feature of video retrieval is color-based. Specifically, the color histogram is a simple yet effective approach (Shamoi, 2022). We employed the RGB color space's color histogram with 255 blocks in this paper.

Kernel Based Approach for Similarity Measurements

Kernel-based multimedia retrieval techniques have been successful in various applications including shape recognition (Kumar, 2023), image retrieval (Kumar, 2023), and event detection (Xiao, 2023). Most techniques begin by formulating a kernel function from supervised data (Yang, 2024), upon which a classifier like support vector machines (SVM) is learned. There have been several recent attempts (Wu, 2022) that have developed kernel techniques for semi-supervised metric learning as well. Two kernel-based metric learning algorithms based on pairwise similarity constraints (Kernel-A and Kernel-b) are introduced in (Hoi, 2007). (Yeung, 2007) developed an extension of the Kernel-b approach introduced in (Hoi, 2007).

In addition, there are also variety of query types that include example-based queries (Qiu, 2023), sketch-based queries (Woo, 2024), object-based queries (Jagtap, 2024), keyword-based queries, natural language-based queries (Kim, 2024), and combination-based queries (Mishra, 2024). In this paper, we have considered query by example. If a query arrives, then based on a similarity technique, the most similar shots can be retrieved. For retrieving a video captured, similarity measures are necessary. There are several types of similarity techniques as well such as: combination-based matching (Adly, 2022), ontology-based matching (Sathiyaprasad, 2023), text matching (Ali, 2022), and feature matching (Gao, 2023). In this paper, we have presented a new determinant kernel-based similarity approach for similarity calculation based on extracted features.

Kernel functions define the inner product. between the shot-feature matrices and yield a real number. Numerous kernel functions exist, including KPCA (Ma, 2024), KLDA (Vinodha, 2024), RBF, and Fisher kernel (Zhang, 2022). Essentially, kernel functions operate on vectors and square matrices; however, the representation matrices of actual data like shot-feature matrices are not square one. Nearly all existing methods condense input non-square matrices to render them suitable for kernel functions, resulting in some data being lost. In this research, we have extended the concept of the determinant of non-square feature matrices processing. We'll continue with kernel introduced in (Perronnin, 2007) for non-square matrices following non square determinant definition (Zhou, 2004) and applied with Chio's like methods adapted by the authors (Salihu, 2021) and (Salihu, 2023) , and assess the effectiveness of the resulting kernels by retrieving video clips of movies videos where the videos are segmented into shots manually.

Determinant Kernels between Non-Square Matrices

Kernels and determinants are two fundamental notions in linear algebra, particularly in matrices. A matrix is a array of numbers or symbols organized in rows and columns. The kernel of a matrix is the collection of vectors that, when multiplied by the matrix, produce a zero vector. A matrix's determinant is a scalar value calculated from its members that represents certain matrix features. Kernels and determinants are used in a variety of domains, including physics, engineering, economics and computer science. In computer science, image processing employs both kernels and determinants (Lafferty, 2002).

Kernels are mathematical functions that take two inputs and compute a similarity measure between them. Determinant kernels, in particular, are a class of kernels that utilize the determinant of matrices (often derived from feature matrices or covariance matrices) to quantify the similarity between two data points or feature sets. The application of determinant kernels in CBVR involves integrating these kernels into various stages of the retrieval pipeline: feature extraction, similarity computation using determinant kernels, and ranking of results based on the similarity scores.

Non-Square Determinant Definition and Processing Methods

Related to rectangular determinant, initially it was introduced by Cullis/Radic in equation (1):

$$det(A_{m\times n}) = |A_{m\times n}| = \begin{vmatrix} a_{11} & a_{12} & \cdots & a_{1n} \\ a_{21} & a_{22} & \cdots & a_{2n} \\ \vdots & \vdots & \ddots & \vdots \\ a_{m1} & a_{m2} & \cdots & a_{mn} \end{vmatrix} =$$

$$= \sum_{1<j_1<\cdots<j_m<n} (-1)^{r+s} \begin{vmatrix} a_{1j_1} & a_{1j_2} & \cdots & a_{1j_m} \\ a_{2j_1} & a_{2j_2} & \cdots & a_{2j_m} \\ \vdots & \vdots & \ddots & \vdots \\ a_{mj_1} & a_{mj_2} & \cdots & a_{mj_m} \end{vmatrix} \quad (1)$$

where $r = 1 + \cdots + m, s = j_1 + \cdots + m$,
and further generalized by Bayat as in the equation (2):
Determinant of $A \in \mathbb{C}^{m\times n}$ is a function $\det_{(\vec{\varepsilon},p)}: \mathbb{C}^{m\times n} \longrightarrow \mathbb{C}$ defined by:

$$\underset{(\vec{\varepsilon},p)}{det}(A) = \begin{cases} \sum_{\substack{I\in Q_{p,m} \\ J\in Q_{p,n}}} \vec{\varepsilon}_{I,J} \det(A[I,J]), & if\ 1 \le p \le \min\{m,n\} \\ 1 & if\ p = 0, \\ 0 & otherwise, \end{cases}$$

(2)

scalars $\vec{\varepsilon}_{I,J}$ are elements of vector $\vec{\varepsilon} \in \mathbb{C}^k$ for $k = \binom{m}{p}\binom{n}{p}$.

Further on, authors of papers (Salihu, 2021) and (Salihu A. S., 2023) have provided with Chio's like methods for rectangular determinant calculation, modified with one and two order reduction respectively:

$$\begin{vmatrix} a_{11} & a_{12} & \cdots & a_{1n} \\ a_{21} & a_{22} & \cdots & a_{2n} \\ \vdots & \vdots & \ddots & \vdots \\ a_{m1} & a_{m2} & \cdots & a_{mn} \end{vmatrix}_{m\times n} = \frac{|A_c|}{a_{11}^{m-2}} + (-1)^m \begin{vmatrix} a_{12} & a_{13} & \cdots & a_{1n} \\ a_{22} & a_{23} & \cdots & a_{2n} \\ \vdots & \vdots & \ddots & \vdots \\ a_{m2} & a_{m3} & \cdots & a_{mn} \end{vmatrix}_{m\times(n-1)}, \quad (3)$$

where:

$$|A_c| = \begin{vmatrix} \begin{vmatrix} a_{11} & a_{12} \\ a_{21} & a_{22} \end{vmatrix} & \cdots & \begin{vmatrix} a_{11} & a_{1n} \\ a_{21} & a_{2n} \end{vmatrix} \\ \vdots & \ddots & \vdots \\ \begin{vmatrix} a_{11} & a_{12} \\ a_{m1} & a_{m2} \end{vmatrix} & \cdots & \begin{vmatrix} a_{11} & a_{1n} \\ a_{m1} & a_{mn} \end{vmatrix} \end{vmatrix}_{(m-1)\times(n-1)} \quad (4)$$

and $a_{11} \neq 0$.

and

$$\begin{vmatrix} a_{11} & a_{12} & \cdots & a_{1n} \\ a_{21} & a_{22} & \cdots & a_{2n} \\ \vdots & \vdots & \ddots & \vdots \\ a_{m1} & a_{m2} & \cdots & a_{mn} \end{vmatrix}_{m\times n} = \frac{|A_c|}{\begin{vmatrix} a_{11} & a_{12} \\ a_{21} & a_{22} \end{vmatrix}^{m-2}} + (-1)^m \begin{vmatrix} a_{12}-a_{11} & a_{13} & \cdots & a_{1n} \\ a_{22}-a_{21} & a_{23} & \cdots & a_{2n} \\ \vdots & \vdots & \ddots & \vdots \\ a_{m2}-a_{m2} & a_{m3} & \cdots & a_{mn} \end{vmatrix}_{m\times(n-1)} \qquad (5)$$

where:

$$|A_c| = \begin{vmatrix} \begin{vmatrix} a_{11} & a_{12} & a_{13} \\ a_{21} & a_{22} & a_{23} \\ a_{31} & a_{32} & a_{33} \end{vmatrix} & \cdots & \begin{vmatrix} a_{11} & a_{12} & a_{1n} \\ a_{21} & a_{22} & a_{2n} \\ a_{31} & a_{32} & a_{3n} \end{vmatrix} \\ \vdots & \ddots & \vdots \\ \begin{vmatrix} a_{11} & a_{12} & a_{13} \\ a_{21} & a_{22} & a_{23} \\ a_{m1} & a_{m2} & a_{m3} \end{vmatrix} & \cdots & \begin{vmatrix} a_{11} & a_{12} & a_{1n} \\ a_{21} & a_{22} & a_{2n} \\ a_{m1} & a_{m2} & a_{mn} \end{vmatrix} \end{vmatrix}_{(m-2)\times(n-2)} \qquad (6)$$

and $\begin{vmatrix} a_{11} & a_{12} \\ a_{21} & a_{22} \end{vmatrix} \neq 0$.

Which will be applied for calculation of determinant kernels.

System Overview

During the video transformation process for video retrieval purposes, initially the features of the query video as well as the features of the videos in the database are transformed and represented with the relevant matrices. Features can be colors, textures, shapes, etc. Further, the features of the videos, in order to compare their similarity, are transformed into the matrix known as the Gram matrix, which represents the scalar product of dots (further dot product) between two matrices. After creating the Gram matrix, the kernel-determinant (hereafter kernel determinant) is calculated for image/video retrieval purposes. The input to the kernel determinant function is a scalar product from the feature matrix. The Kernel function takes the input points (features) and returns a real number that represents the level of their similarity, while the kernel itself in this case is calculated by means of the determinant. Since non-square videos generate non-square matrices and their kernel is very complex to calculate depending on the size of the feature matrix, this case presents situations of more efficient determinant-kernel processing.

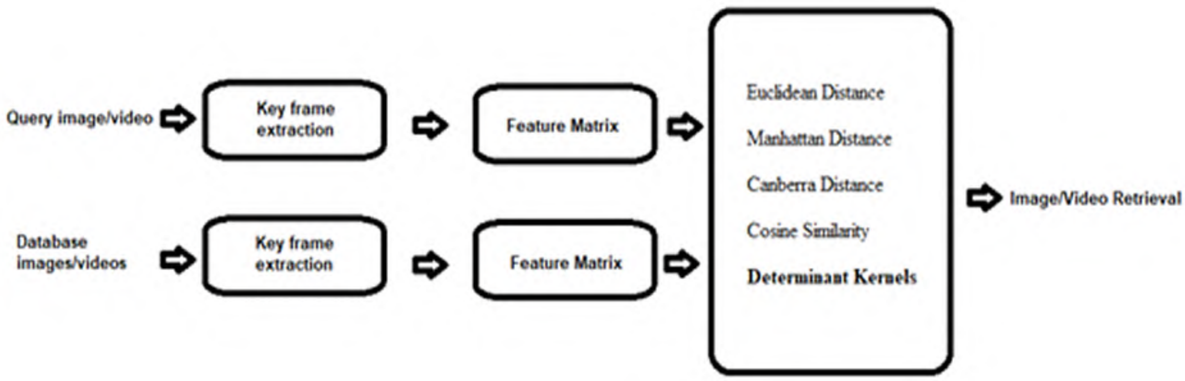

Figure 1. Video retrieval system model

In the above example, two feature matrices were compared using the determinant kernel for non-square matrices where the output is a real number; and the absolute value of this number is close to zero, and the two shots are more similar to each other.

If A is feature-matrix of a shot with n key frames and B is feature-matrix of a shot with m key frames, then for $C_{mxn}(m \leq n)$ we have:

$$C_{mxn} = A^T * B$$

(7)

$$C_{m\times n} = \begin{bmatrix} a_{1,1} & a_{2,1} & \cdots & a_{m,1} \\ a_{1,2} & a_{2,2} & \cdots & a_{m,2} \\ \vdots & \vdots & \ddots & \vdots \\ a_{1,125} & a_{2,125} & \cdots & a_{m,125} \end{bmatrix}_{mx125} * \begin{bmatrix} b'_{1,1} & b'_{1,2} & \cdots & b'_{1,125} \\ b'_{2,1} & b'_{2,2} & \cdots & b'_{2,125} \\ \vdots & \vdots & \ddots & \vdots \\ b'_{n,125} & b'_{n,125} & \cdots & b'_{n,125} \end{bmatrix}_{125xn}$$

(8)

Gram matrix representing the dot product between feature matrices is:

$$C_{m\times n} = \begin{bmatrix} c_{1,1} & c_{1,2} & \cdots & c_{1,n} \\ c_{2,1} & c_{2,2} & \cdots & c_{2,n} \\ \vdots & \vdots & \ddots & \vdots \\ c_{m,1} & c_{m,2} & \cdots & c_{m,n} \end{bmatrix}_{mxn} \quad (9)$$

Where $c_{i,j} = \sum_{k=1}^{125} a_{i,k} b'_{k,j} = for\ i = 1, 2, \ldots, m\ and\ j = 1, 2, \ldots, n, m > n$

Further the determinant kernel is calculated as following:

$$K_x(A,B) = \det(A^T * B) = \det\,(C_{m\times n}) \quad (10)$$

and the higher the dependency between vectors, then determinant of $C_{m\times n}$ is closer to zero.
Based on mathematical context, Modified Chio's method has been shown more efficient in processing the rectangual determinant compared to Radic (Salihu A. S., 2023). We well proceed with comparative evaluation in content-based video retrieval context.

In the following table are shown the similarity scores as well as their processing times based on those methods: Radić's method provides a theoretical foundation and methodology for non-square determinant calculation and has numerous significant properties and advantages to compare with other definitions. Specially, it has almost all the properties of determinant of square matrices. According to its definition (Radic, 1966) , it is evident that the determinant of a non-square matrix can be computed as sum of specially signed square sub matrices. These sub matrices is obtained by calculating specific permutation of columns of non-square matrix. Although this definition is easy to compute and understand, it has exponential time complexity. Chio's like methods as proposed by authors (Salihu, 2021) and (Salihu A. S., 2023) provide with a faster and more efficient methods for non-square determinant processing that is crucial for determinant kernel calculation for similarity evaluation in CBVR. In the following we will show the algorithmic approach of above mentioned methods based on which we will perform comparative evaluation in processing determinant kernels. In the following is shown the algorithm for non-square determinant calculation based on Radic method applied in equation (10). The result of it is a scalar value or score that represents the level of similarity between two video shots:

A 1.1: Algorithm1 - based on Cullis-Radic definition for rectangular determinant calculations

```
Step 1: Identify combinations for creating the square blocks:
        if m=n
            It is a square determinant.
        else
            Identify all combinations of number of columns over number of
            rows B=Combinations(1:n,m);
Step 2: Based on the combinations found on step 1, create an object matric
        of all square determinants created:
        Create loop from 1 to length of vector B, which represents the
        number of combinations
            D{i}= A(1:m,B(i,1:m)));
Step 3: Calculate determinants of each block inside the object matrix D
```

In the following is shown the algorithm for non-square determinant calculation based on Chios like method with one order reduction (Salihu, 2021) applied in equation (10).

The result of it is a scalar value or score that represents the level of similarity between two video shots:

A 1.2: Algorithm2 - Recursive algorithm det_Chio for Theorem 2.2 (Chio's-like) method to calculate rectangular determinants of order $m \times n$

```
Step 1: Insert the rectangular determinant A
Step 2: Determine the order of rectangular determinant m×n
        [m,n] = size(A);
Step 3: Checking if A(1,1) is equal to 0
        if A(1,1) = 0
            Exchange rows to find nonzero element
Step 4: Calculating sub matrices
      Initialize B=0;
      Create Loop for i from 1 to m-1
            Create Loop for j from 1 to n-1
                  B(i,j) = A(1,1) * A(i + 1, j + 1) - A(1, j + 1) * A(i +
1, 1)
            end
      end
Step 5: Calculate the final result of rectangular determinant
      d = 1/A(1,1)^(m - 2) * det_Chio(B) + (-1)^m * det_Chio(A(1:m, 2:n));
Step 5: Display the result of the determinant
```

While here is presented the algorithm for non-square determinant calculation based on Chios like method with two order reduction (Salihu A. S., 2023) applied in equation (10). The result of it is a scalar value or score that represents the level of similarity between two video shots:

A 1.3: Algorithm3 - Pseudocode of det_Chio2 algorithm for Theorem 4 (Modified Chio's-like) method to calculate rectangular determinants of order $m \times n$

```
Step 1: Checking for conditions:
      if m>n
            d=0;
            return
      end
      if m==n
            Calculate determinant with Radic Definition
            return
      end
      if m<3
            Calculate determinant with Radic Definition
            return
      end
Step 2: Calculate pivot block:
      Pivot = det(A(1:2,1:2));
      if Pivot == 0
            Interchange rows to have another nonzero pivot block
      end
Step 3: Calculating sub matrices
      Initialize B=zeros(m-2,n-2);
      Create Loop for i from 3 to m
      Create Loop for j from 3 to n
            B(i-2, j-2) = det(A([1 2 i], [1 2 j]));
            end
      end
Step 4: Calculate the result of rectangular determinant
        d=det_Chio2(B)/Pivot^(m-3)+(-1)^m*det_Chio2([bsxfun(@minus,
        A(1:m,2),A(1:m,1)) A(1:m,3:n)]);
```

Results and Discussion

In the following we have tested the execution time of similarity score generation based on the algorithms presented above as applied in equation (8) and compared with the execution time of algorithms based on A1.1: Algorithm1 (based on Cullis-Radic definition), Theorem 1 (see: Algorithm 1.1) and Theorem 2 (see: Algorithm 1.2. We simulated the execution time for different order of determinant kernels in equation (8) by which are calculated the similarity scores between two input video shots, query and database video, representing feature matrices of query and database videos and we have presented a simulation of a sample dataset of about hundred video shots; the results of these calculations are scalar numbers that represent the level of similarity between compared video shots. This simulation is performed in MATLAB 2021b version environment, in Asus ROG Flow Z13, with 12th Gen Intel(R) Core(TM) i7-12700H, 16.0 GB of RAM, NVIDIA GeForce RTX 3050 GPU. Sample of results of the simulation are presented in the following table 1.

Table 1. Comparison of algorithms for video shots similarity score calculation execution time based on simulation

Score	Execution time			A 1.1 vs A 1.2	A 1.1 vs A 1.3	A 1.2 vs A 1.3	A 1.1 vs A 1.2 %	A 1.1 vs A 1.3 %	A 1.2 vs A 1.3 %
	T_A 1.1	T_A 1.2	T_A 1.3						
3.824E-25	0.0083	0.0072	0.0059	0.0011	0.0023	0.0012	15.28%	39.21%	20.76%
9.399E-33	6.2491	5.1343	4.3413	1.1148	1.9079	0.7931	21.71%	43.95%	18.27%
4.786E-28	0.0489	0.0409	0.0345	0.0080	0.0144	0.0064	19.46%	41.70%	18.61%
5.692E-32	0.0064	0.0053	0.0045	0.0011	0.0020	0.0009	20.86%	44.49%	19.55%
3.704E-29	1.6318	1.3533	1.1767	0.2784	0.4551	0.1766	20.57%	38.67%	15.01%
9.910E-27	2.8256	2.3250	2.0045	0.5005	0.8211	0.3206	21.53%	40.96%	15.99%
6.228E-28	28.6784	23.3548	20.1122	5.3236	8.5662	3.2426	22.79%	42.59%	16.12%
6.680E-33	0.0141	0.0115	0.0101	0.0026	0.0040	0.0014	22.40%	39.60%	14.06%
8.700E-31	28.6815	23.3351	19.2786	5.3464	9.4029	4.0565	22.91%	48.77%	21.04%
6.933E-30	0.0106	0.0090	0.0074	0.0016	0.0031	0.0015	17.76%	42.14%	20.71%
5.073E-29	0.0014	0.0012	0.0010	0.0002	0.0004	0.0002	16.75%	36.08%	16.56%
1.927E-32	0.0981	0.0829	0.0705	0.0151	0.0276	0.0124	18.25%	39.07%	17.61%
1.406E-27	0.0074	0.0061	0.0052	0.0013	0.0022	0.0009	22.08%	43.05%	17.18%
6.091E-31	0.0047	0.0041	0.0035	0.0006	0.0012	0.0006	15.97%	34.61%	16.07%
8.374E-28	0.5873	0.4827	0.4148	0.1046	0.1725	0.0679	21.67%	41.59%	16.37%

Conclusion

This paper analyses and perform comparative assessment of the modified Chio-like method versus Radic method for calculation of similarity scores between video shots based on a sample video dataset for the efficiency of similarity score generation in content-based video retrieval. Modified Chio's like methods presented in algorithms A1.2 and A1.3) shows increase speed in processing of non-square feature matrices for similarity score generation of query and database videos compared to standard Radic's method as following: A1.2 execution time is about 22.34% and A1.2 39.28% faster compared to Radic's method respectively, and Chio's like methods A1.3 execution time is about 16.44% faster to A1.2. This advancement can further find application in multimedia retrieval for more efficient calculation of similarity scores that are essential in multimedia comparison in the retrieval process.

Scientific Ethics Declaration

* The authors declares that the scientific ethical and legal responsibility of this article published in EPSTEM journal belongs to the authors.

Conflict of Interest

* The authors declare that they have no conflicts of interest

Funding

* This research received no specific grant from any funding agency in the public, commercial, or not-for-profit sectors.

Acknowledgements or Notes

* This article was presented as a poster presentation at the International Conference on Research in Engineering, Technology and Science (www.icrets.net) held in Peja/Kosovo on July 10-13, 2025.

References

Accattoli, S., Sernani, P., Falcionelli, N., Mekuria, D. N., & Dragoni, A. F. (2020). Violence detection in videos by combining 3d convolutional neural networks and support vector machines. *Applied Artificial Intelligence, 34*(4), 329–344.

Adly, A. S., Hegazy, I., ELARIF, T., & Abdelwahab, M. S. (2022). Development of an effective bootleg videos retrieval system as a part of content-based video search engine. *Int. J. Comput, 21*(2), 214-227.

Ali, A., Schwartz, I., Hazan, T., & Wolf, L. (2022). Video and text matching with conditioned embeddings. *Proceedings of the IEEE/CVF Winter Conference on Applications of Computer Vision* (pp. 1565-1574).

Dong, J., Wang, Y., Chen, X., Qu, X., Li, X., He, Y., & Wang, X. (2022). Reading-strategy inspired visual representation learning for text-to-video retrieval. *IEEE Transactions on Circuits and Systems for Video Technology, 32*(8), 5680-5694.

Gao, M., Han, J., Zheng, F., Yu, J. J., & Montana, G. (2023). Video object segmentation using point-based memory network. *Pattern Recognition, 134*, 109073.

Hoi, S. C., Jin, R., & Lyu, M. R. (2007). Learning nonparametric kernel matrices from pairwise constraints. *Proceedings of the 24th International Conference on Machine Learning* (pp. 361-368).

Jagtap, S., & Chopade, N. B. (2024). Object-based image retrieval and detection for surveillance video. *International Journal of Electrical and Computer Engineering (IJECE), 14*(4), 4343-4351.

Khan, A. A., Muhammed, Shaji, A. M., Sujith, D., Nath, A. G., & Udmale, S. S. (2024). InVideo search: Scene description clustering and integrating image and audio captioning for enhanced video search. *International Conference on Distributed Computing and Intelligent Technology* (pp. 195-208). Cham: Springer Nature Switzerland.

Kim, D., Lee, K., Jang, I. S., Kim, K. J., Kim, P. K., & Yoo, J. (2024, July). MOVES: Motion-oriented video sampling for natural language-based vehicle retrieval. *2024 IEEE International Conference on Advanced Video and Signal Based Surveillance (AVSS)* (pp. 1-7). IEEE.

Kumar, N. R., & Kumar, R. (2023). Efficient medical image retrieval system using geometric invariant point bilateral transformation (GIPBT). *Measurement: Sensors, 27*, 100705.

Kumar, S., Singh, M. K., & Mishra, M. (2023). Efficient deep feature based semantic image retrieval. *Neural Processing Letters, 55*(3), 2225-2248.

Ma, W. W., Gao, Y., & Huang, D. (2024). Video target tracking based on KPCA and structured support vector machines. *Journal of Network Intelligence, 9*(4), 2424-2437.

Mishra, P. K., Mihailidis, A., & Khan, S. S. (2024). Skeletal video anomaly detection using deep learning: Survey, challenges, and future directions. *IEEE Transactions on Emerging Topics in Computational Intelligence, 8*(2), 1073-1085.

Nandini, H. M., Chethan, H. K., & Rashmi, B. S. (2022). Video shot retrieval using multi-feature approach. *IOT with Smart Systems: Proceedings of ICTIS 2021* (pp. 297-305). Springer Singapore.

Nixon, L., Galanopoulos, D., & Mezaris, V. (2024). Finding video shots for immersive journalism through text-to-video search. *2024 International Conference on Content-Based Multimedia Indexing (CBMI)* (pp. 1-6). IEEE.

Patel, B., & Singh, B. (2023). Content-based video retrieval systems: A review. *2023 3rd International Conference on Innovative Mechanisms for Industry Applications (ICIMIA)* (pp. 441-449). IEEE.

Qiu, Y., Misu, T., & Busso, C. (2023). Example-based query to identify causes of driving anomaly with few labeled samples. *2023 IEEE Intelligent Vehicles Symposium (IV)* (pp. 1-7). IEEE.

Salihu, A., & Marevci, F. (2021). Chio's-like method for calculating the rectangular (non-square) determinants: Computer algorithm interpretation and comparison. *European Journal of Pure and Applied Mathematics, 14*(2), 431-450.

Salihu, A., Snopce, H., Luma, A., & Ajdari, J. (2023). Modified chios-like method for rectangular determinant calculations. *Advanced Mathematical Models & Applications, 8*(3).

Salihu, A., Snopce, H., Luma, A., & Ajdari, J. (2023). Comparison of time complexity growth for different methods/algorithms for rectangular determinant calculations. *2023 International Conference on Recent Trends in Electronics and Communication (ICRTEC)* (pp. 1-6). IEEE.

Sathiyaprasad, B. (2023). Ontology-based video retrieval using modified classification technique by learning in smart surveillance applications. *International Journal of Cognitive Computing in Engineering, 4*, 55-64.

Shamoi, P., Sansyzbayev, D., & Abiley, N. (2022). Comparative overview of color models for content-based image retrieval. *2022 International Conference on Smart Information Systems and Technologies (SIST)* (pp. 1-6). IEEE.

Vinodha, K., Gopi, E.S. (2024). High-Resolution remote sensing image classification with kernel linear discriminant analysis. In A. J. Kulkarni, A. H. Gandomi (eds.), *Handbook of Formal Optimization*. Springer, Singapore.

Woo, S., Jeon, S. Y., Park, J., Son, M., Lee, S., & Kim, C. (2024). Sketch-based video object localization. *Proceedings of the IEEE/CVF Winter Conference on Applications of Computer Vision* (pp. 8480-8489).

Wu, H., Liu, J., Xiao, F., Wen, Z., Cheng, L., & Qin, J. (2022). Semi-supervised segmentation of echocardiography videos via noise-resilient spatiotemporal semantic calibration and fusion. *Medical Image Analysis, 78*, 102397.

Xiao, S., Zhang, X., & Zhang, P. (2023, June). Multi-dimensional frequency dynamic convolution with confident mean teacher for sound event detection. *ICASSP 2023-2023 IEEE International Conference on Acoustics, Speech and Signal Processing (ICASSP)* (pp. 1-5). IEEE.

Yang, R., He, F., He, M., Wang, K., & Huang, X. (2024). Data imputation by pursuing better classification: A supervised kernel-based method. *arXiv preprint arXiv:2405.07800*.

Yeung, D. Y., & Chang, H. (2007). A kernel approach for semisupervised metric learning. *IEEE Transactions on Neural Networks, 18*(1), 141-149.

Yuan, Z., Zhang, K., & Huang, T. (2024). Positive label is all you need for multi-label classification. *2024 IEEE International Conference on Multimedia and Expo (ICME)* (pp. 1-6). IEEE.

Zhang, G., Zuo, Q., & Dang, H. (2022). Probability loop closure detection with fisher kernel framework for visual SLAM. *International Conference of Pioneering Computer Scientists, Engineers and Educators* (pp. 219-239). Singapore: Springer Nature Singapore.

Zhu, W., Huang, Y., Xie, X., Liu, W., Deng, J., Zhang, D., ... & Liu, J. (2023). Autoshot: A short video dataset and state-of-the-art shot boundary detection. *Proceedings of the IEEE/CVF Conference on Computer Vision and Pattern Recognition* (pp. 2238-2247).

Author(s) Information

Besnik Duriqi
Faculty of Computer Science
South East European University - SEEU
Republic of North Macedonia
Contact e-mail: *bd30521@seeu.edu.mk*

Halil Snopçe
Faculty of Computer Science
South East European University - SEEU
Republic of North Macedonia

Armend Salihu
Department of Computer Science
UNI Universum International College
Prishtina, Republic of Kosovo

Artan Luma
Faculty of Computer Science
South East European University - SEEU
Republic of North Macedonia

Azir Aliu
Faculty of Computer Science
South East European University - SEEU
Republic of North Macedonia

To cite this article:

Duriqi, B., Snopce, H., Salihu, A., Luma, A., & Aliu, A. (2025). Performance assessment of determinant kernels in content-based video retrieval: A non-square determinant approach. *The Eurasia Proceedings of Science, Technology, Engineering and Mathematics (EPSTEM), 35,* 115-123.

The Eurasia Proceedings of Science, Technology, Engineering & Mathematics (EPSTEM)
ISSN: 2602-3199

The Eurasia Proceedings of Science, Technology, Engineering and Mathematics (EPSTEM), 2025

Volume 35, Pages 124-132

ICRETS 2025: International Conference on Research in Engineering, Technology and Science

Exploring the Interplay between Big Data Maturity Position Awareness and Strategic Performance: The Moderating Role of Big Data Investments

Fatmir Desku
South East European University

Adrian Besimı
South East European University

Abstract: This study explores the relationship between big data maturity position awareness and strategic performance, as well as the moderating role of big data investments in organizations. The research explores how an organization's awareness of its big data maturity, influences its strategic performance, and how investments in resources such as human capital, infrastructure, and policy initiatives can enhance this relationship. Data were collected from 106 respondents acting in leading positions across various units and industries in Kosovo. Three surveys wew developed to measure 1) big data maturity awareness, 2) strategic performance, and 3) big data investments. Statistical analyses, including reliability and validity assessments, regression analysis, and moderated regression analysis, were used. The findings indicate that big data maturity awareness significantly impacts strategic performance, with a strong positive relationship. Additionally, big data investments were found to moderate this relationship, amplifying the effect of big data maturity awareness on strategic performance. The findings also show that big data investments alone do not directly drive significant improvements in strategic performance. However, when investments on big data are paired with high big data maturity position awareness a significant positive interaction is observed. This means that the relationship between big data maturity position awareness and strategic performance is enhanced when big data investments are high, indicating that the two factors work together to improve performance. The study highlights the importance of increasing big data maturity awareness and investing in big data resources to enhance organizational strategic performance.

Keywords: Big data maturity, Strategic performance, Business engineering

Introduction

This paper explores the relationship between an organization's big data maturity position awareness and its strategic performance, while examining how this relationship is moderated by investments in big data. Specifically, the study seeks to understand how the positive impact of investments in big data (human resources, infrastructure or policy level initiatives) is enhanced when an organization makes those investments based on a proper knowledge for their big data maturity level.

The relationship between organizational strategic performance and big data capabilities is increasingly significant in today's data-driven business environment (Bresciani, et al., 2021). Organizations that understand their capabilities in big data can better align their strategic objectives with their needs, enhancing their performance, as an end result (Elgendy, Elragal & Päivärinta, 2022). In this relationship, it is particularly crucial to undersant wether big data investments can serve as a moderating factor in this relationship, influencing how effectively organizations can increase their big data capabilities to achieve their strategic goals.

For organizations to understand their level of capabilities regarding big data, several Big Data Maturity Models have been developed (Mouhib et al., 2020). These models provide a framework for organizations to assess their current capabilities and identify areas for improvement. For instance, organizations at higher maturity levels are often better equipped to integrate big data into their decision-making processes, leading to improved strategic outcomes (Rialti et al., 2020). As noted by Caputo et al. (2019) organizations that invest in big data capabilities are likely to experience increased revenues, demonstrating a direct link between big datamaturity and financial performance.

The moderating role of big data investments cannot be understated. Investments in big data can significantly enhance an organization's ability to leverage data for strategic decision-making. For instance, Akter et al. (2016) highlight that the alignment of big data analytics capabilities with business strategies can positively influence organizational performance. This suggests that organizations that actively invest in big data capabilities are more likely to achieve superior performance outcomes. However, it is important to note that investments in big data should be made based on an prior analysis of the level of big data maturity of an organizations. By understanding their maturity positioning, organizations can make informed decisions about where to allocate resources and how to adapt their strategies to enhance big data effectively.

Literature Review

This literature review provides an exploration of three essential variables that influence organizational success in the context of big data: Big Data Maturity Position Awareness Strategic Performance, and Big Data Investments. These variables are interconnected and crucial for understanding how organizations use big data to improve their strategic outcomes.

Big Data Maturity Models

Big Data Maturity Models are frameworks designed to evaluate an organization's ability to effectively utilize big data across various dimensions, such as technology, processes, culture, and organizational capabilities. These models assist organizations in understanding their current level of big data adoption and guide them in achieving higher maturity levels by addressing gaps. Research by Al-Sai et al. (2022) has identified multiple maturity models, each with unique dimensions and limitations, emphasizing the importance of selecting the model best suited to an organization's specific context. Each model offers distinct perspectives, targeting differenbt dimensions like infrastructure, allowing organizations to choose a framework tailored to their unique needs.

Understanding an organization's positioning within big data maturity models is crucial for effectively using big data to enhance performance and achieve strategic objectives. Moreover, awareness of an organization's maturity level in big data is linked to its ability to implement effective strategies that drive performance improvements (Dubey et al., 2019). Therefore, organizations that accurately assess their maturity level can identify gaps in their capabilities and prioritize investments in areas that will result in the highest returns. Additionally, the dynamic nature of big data needs organizations continuously evaluates their maturity to remain agile and responsive to market changes. Okuyucu & Yavuz (2020) highlight that many organizations, especially in the public sector, have yet to fully explore big data maturity models, which can hinder their ability to adapt to the constantly changing and evolving world. By assessing their maturity, organizations can identify strengths and weaknesses, prioritize investments, and develop strategies that enhance their capabilities and competitive positioning. Therefore, maintaining a clear understanding of maturity level in which an organization position will be essential for those aiming to succeed in a data-driven environment.

Organizational Strategic Performance

Organizational strategic performance refers to the extent to which an organization achieves its long-term objectives through the alignment of resources, strategies, and actions Wolf and Floyd (2017). It is a multidimensional construct, including financial outcomes, operational efficiency, and competitive positioning, guided by a clear strategic vision. Strategic performance serves as a critical indicator of an organization’s ability to adapt in a dynamic environment.

Digital transformation has redefined organizational strategic performance. Big data analytics, artificial intelligence, and digital platforms enable organizations to enhance strategic decision-making and operational efficiency. Companies that use these technologies effectively can develop personalized customer experiences, optimize supply chains, and innovate at scale, all of which contribute to improved strategic outcomes (Elezaj et al., 2018). The integration of big data into organizational strategies enables firms to utilize vast amounts of information to inform decision-making processes, ultimately leading to improved performance. For instance, data-driven decision-making, supported by big data technologies, can significantly enhance business performance by facilitating automatic decision-making at scale (Nazari et al., 2020). However, the relationship between big data utilization and organizational performance is not straightforward. While there is a correlation between effective big data use and organizational performance, the evidence of its value can vary, suggesting that organizations may face challenges in measuring the impact of big data initiatives (Wang et al., 2018). While the potential for enhanced performance through data-driven decision-making is substantial, organizations must navigate the complexities of effectively measuring and implementing big data initiatives.

Big Data Investment

The investment in big data analytics has emerged as a critical factor for organizations seeking to enhance their performance and competitive advantage (Lambrecht and Tucker 2015). As businesses increasingly recognize the potential of big data, the need for substantial investment in capabilities becomes evident. However, as highlighted by Bean and Davenport (2019), managers hold differing perspectives on the extent to which big data influences a firm's performance. This variation suggests that managers may have encountered diverse experience with big data investments and their returns in terms of performance. Furthermore, this underscores the concept that investments in big data alone do not inherently deliver valuable competitive advantages. Instead, their true value lies in understanding the specific conditions that enhance their effectiveness and contribute meaningfully to an organization's strategic performance (Marketing Science Institute, 2018).

While the potential benefits of big data are substantial, the financial burden of these investments is equally an issue. Advanced systems, employee training, and policy frameworks often come with high costs, making these initiatives a substantial commitment for organizations. Despite this, the potential return on investment is significant. Research highlights profit increases of 6% to 9% over several years for companies using big data analytics (Olabode et al., 2022), and stock market investors tend to view such investments positively, anticipating enhanced future returns (Zhang et al., 2017). However, to fully capitalize on these investments, firms must ensure their strategies align with supportive conditions that maximize big data's strategic value.

Strategic investments in big data analytics should be carefully tailored to the assessed needs of organizations and based in a analysis of their specific challenges and objectives. Organizations that base their investments in big data strategies on comprehensive assessments and implement them effectively are more like experience enhanced strategic performance.

Research Methodology

Research Problem

Recently organizations are increasingly recognizing the importance of big data as a strategic asset that can drive competitive advantage and enhance overall performance. However, there exists a significant gap in understanding how an organization's awareness of its positioning within big data maturity models influences its strategic performance. Furthermore, the role of big data investments as a moderating factor in this relationship remains underexplored. By investigating this research problem, this study aims to provide insights into how organizations can better align their big data maturity awareness with strategic performance goals, while also understanding the critical role that big data investments play in facilitating this alignment. The findings will contribute to the existing literature on big data analytics and provide practical implications for managers aiming to enhance their organizations' performance through informed big data strategies.

Research Questions

This section examines the connection between strategic performance and big data maturity position awareness, as well as how big data investments influence this relationship. The analysis is guided by the following research questions:

1. How does an organization's big data maturity position awareness influence its strategic performance?
2. How do investments in big data resources, such as human resources, infrastructure, and policy-level initiatives, moderate the relationship between big data maturity position awareness and strategic performance?

Hypotheses

Based on the research questions, the following hypotheses are proposed to examine the relationship of big data maturity position awareness and strategic performance and the moderating role of big data investments:

1. Big data maturity position awareness has a positive effect on an organization's strategic performance.
2. The positive relationship between big data maturity position awareness and strategic performance is moderated by big data investments in big data resources, including human resources, infrastructure, and policy-level initiatives.

Methodology

This section outlines the methodological framework of the study, which employs a quantitative research approach to investigate the relationships between key constructs. The structured design ensures objectivity, reliability, and generalizability of the findings. The methodology includes a comprehensive overview of the study's variables, data collection methods, procedures, instruments, and data analysis techniques, providing a clear roadmap for replicability.

Data

The following section covers details about the data and variables used in the study.

Variables

The three variables in this study are Big Data Maturity Position Awareness (BDMPA), Strategic Performance (SP), and Big Data Investments (BDI). BDMPA serves as an independent variable in both Hypothesis 1 and Hypothesis 2, representing an organization's awareness of its position in relation to big data maturity. It is a continuous variable that reflects how well an organization recognizes its capabilities in leveraging big data for strategic advantage. SP, also a continuous variable, acts as the dependent variable in both hypotheses, reflecting the organization's success in achieving its strategic goals. In Hypothesis 2, BDI is introduced as a moderator, influencing the relationship between BDMPA and SP. BDI, which refers to an organization's financial and resource investments in big data technologies, is also continuous, and its role is to moderate how BDMPA impacts strategic performance, potentially enhancing or diminishing the effect depending on the level of investment.

Data Collection

This study includes a sample of 106 representatives from high-level positions across various industries. These participants will be senior executives, managers, and directors with significant influence and decision-making authority within their organizations. This diverse group is expected to offer a broad perspective on big data maturity position awareness, strategic performance, and the role of big data investments within different industry contexts.

Process

The survey instrument was developed to measure key variables such as big data maturity position awareness, strategic performance, and big data investments, ensuring that all dimensions were accurately captured. It was then distributed online as a Google Form to 470 email addresses, targeting mainly leading positions across various industries in Kosovo. A total of 106 responses were received, over a period of two weeks, providing a diverse sample of industry professionals with decision-making roles. The data collected were analyzed using Stata Software, where statistical analysis like reliability testing, confirmatory factor analysis (CFA), regression analysis, and moderated regression analysis were applied to explore the relationships between big data maturity awareness, strategic performance, and the moderating role of big data investments.

Instruments

The three instruments used in this study are designed to measure the key variables: Big Data Maturity Position Awareness (BDMPA), Strategic Performance (SP), and Big Data Investments (BDI). Survey 1 focuses on BDMPA and assesses awareness of existing big data capabilities and the use of frameworks to evaluate big data maturity. Survey 2 measures Strategic Performance by examining four dimensions: market responsiveness, operational efficiency, competitive advantage, and customer satisfaction and retention. Finally, Survey 3 Big Data Investments focuses on investment related to big data initiatives including capacity building on human resource development for big data initiatives, infrastructure investment and the policies and governance structures related to big data utilization. These instruments are designed to capture the dimensions of each variable comprehensively, contributing to a better understanding of their relationships in the context of big data adoption and its impact on organizational performance.

Data Analysis

The data analysis process involved several statistical techniques to ensure the robustness and validity of the findings. Reliability was assessed using Cronbach's alpha to confirm the internal consistency of constructs related to big data maturity, strategic performance, and investment impact. Construct validity was established through confirmatory factor analysis (CFA), ensuring that the measured variables represented the theoretical constructs accurately. To address potential multicollinearity, Variance Inflation Factor (VIF) analysis was conducted, confirming that the independent variables were not excessively correlated.

For hypothesis testing, a linear regression analysis was performed to examine the direct effect of big data maturity position awareness (independent variable) on strategic performance (dependent variable), determining the strength and significance of this relationship for Hypothesis 1. For Hypothesis 2, a moderated regression analysis was applied to explore the moderating role of big data investments, such as human resources, infrastructure, and policy-level initiatives. This included adding an interaction term (big data maturity position awareness × big data investments) to the regression model and evaluating its significance to assess how big data investments strengthened the relationship between big data maturity position awareness and strategic performance. This rigorous approach ensured the reliability, validity, and depth of the analysis in testing the proposed hypotheses.

Results and Discussion

This section outlines the key findings of the study, beginning with an evaluation of the reliability and validity of the instruments used for data collection. It then delves into the results of the hypothesis testing, addressing the relationships between big data maturity position awareness, strategic performance, and the moderating role of big data investments. These findings provide critical insights into the study’s research questions and contribute to a deeper understanding of how big data strategies influence organizational outcomes.

Reliability and Validity

The reliability analysis indicates that the scale used in the study has a high level of internal consistency. The scale reliability coefficient (Cronbach's alpha) is 0.9156, which exceeds the commonly accepted threshold of 0.7, indicating excellent reliability. This suggests that the 28 items included in the scale consistently measure the same underlying construction, with minimal random errors. The results confirm that the scale is suitable for measuring the constructs of interest in this study.

The validity assessment conducted through structural equation modeling (SEM) confirms that the constructs in the study are well-measured and reliable. For Big Data Maturity Awareness Position (BDMAP), the indicator loadings ranged from 0.86 to 1.08, with all p-values < 0.001, and the construct explained 95% of the variance, indicating a strong and robust measurement. Strategic Performance (SP) showed indicator loadings between 0.84 and 1.15, all highly significant ($p < 0.001$), with 84% of the variance explained, confirming a reliable and meaningful representation. Big Data Investment (BDI) indicators ranked between 0.80 and 1.20, with all p-values < 0.001, accounting for 76% of the variance, demonstrating a solid measurement, albeit slightly less robust than the other constructs. Overall, the high and significant factor loadings across all constructs confirm strong convergent validity.

Findings for the Hypothesis

In order to understand whether the independent variables correlate to each other, causing a multicollinearity the Variance Inflation Factor analysis was performed. This analysis indicates that multicollinearity is not a concern in the model. Both Big Data Investments (BDI) and Big Data Maturity Awareness Position (BDMAP) have VIF values of 1.05, which are well below the commonly accepted threshold of 5 for multicollinearity. This suggests almost no correlation between the independent variables, meaning each contributes uniquely to explaining the variance in the dependent variable.

Table 1. Linear regression analysis for hypothesis 1

Strategic_performa ~e	Coef.	St.Err.	t-value	p-value	[95% Conf	Interval]	Sig
BDMPA	1.139	.042	26.97	0	1.055	1.222	***
Constant	2.132	1.125	1.89	.061	-.1	4.363	*
Mean dependent var		31.028	SD dependent var			9.931	
R-squared		0.875	Number of obs			106	
F-test		727.138	Prob > F			0.000	
Akaike crit. (AIC)		570.172	Bayesian crit. (BIC)			575.499	

*** *p<.01,* ** *p<.05,* * *p<.1*

The regression analysis for Hypothesis 1 demonstrates that Big Data Maturity Awareness Position (BDMPA) significantly influences Strategic Performance. The model explains 87.49% of the variance in strategic performance, with a high F-statistic (727.14) and a p-value of < 0.001, confirming the model's significance. The coefficient for BDMPA is 1.1387, meaning a 1-unit increase in BDMPA leads to a predicted increase of approximately 1.14 units in strategic performance, with a confidence interval between 1.0549 and 1.2224. Overall, BDMPA is a strong predictor of strategic performance, highlighting the importance of enhancing big data maturity awareness to improve organizational performance.

Table 2. Moderated regression analysis for hypothesis 2

Strategic_performa ~e	Coef.	St.Err.	t-value	p-value	[95% Conf	Interval]	Sig
BDMPA	.467	.308	1.52	.132	-.144	1.078	
Interaction_Term	.022	.01	2.18	.032	.002	.043	**
Constant	16.295	7.938	2.05	.043	.549	32.04	**
Mean dependent var		31.028	SD dependent var			9.931	
R-squared		0.881	Number of obs			106	
F-test		252.585	Prob > F			0.000	
Akaike crit. (AIC)		568.526	Bayesian crit. (BIC)			579.180	

*** *p<.01,* ** *p<.05,* * *p<.1*

In Hypothesis 2, the analysis investigates how Big Data Investments (BDI) as a moderated variable impacts the effect of Big Data Maturity Position Awareness (BDMPA) on Strategic Performance. The model is highly significant, explaining 88.14% of the variance in strategic performance, with a significant interaction term ($p = 0.032$), showing that the effect of BDMPA on strategic performance depends on the level of BDI. The coefficient for BDMPA is positive (0.4669, $p = 0.132$), indicating a potential positive relationship with strategic performance, though not statistically significant. The interaction term is significant (0.0224, $p = 0.032$), showing that BDI enhances the effect of BDMPA on strategic performance. Thus, higher investments, when paired with greater big data maturity awarness, lead to significantly better strategic performance.

Table 3. Matrix of correlations

Variables	(1)	(2)	(3)	(4)
(1) Strategic_Perf~e	1.000			
(2) BDMPA	0.935	1.000		
(3) BDI	0.951	0.932	1.000	
(4) Interaction_Term	0.959	0.982	0.980	1.000

$p < .01$. Values closer to 1.000 indicate a stronger positive linear relationship between the variables.

To further support these findings, the analysis of matrix of correlations has been performed. Findings indicate that all of the variables have strong positive connections, according to the correlation matrix. There is a substantial association between the Interaction Term (0.9592), Big Data Investments (0.9515), and Big Data Maturity Positioning Awareness (0.9353) and Strategic Performance. Likewise, there is a strong correlation between Big Data Investments and Big Data Maturity Positioning Awareness (0.9318). The strongest correlations are seen between the Interaction Term and Big Data Investments (0.9798) and Big Data Maturity Positioning Awareness (0.9818). According to these findings, strategic performance is strongly correlated with big data maturity, big data investments, and their interplay, underscoring the significance of these factors taken together in promoting strategic.

Discussion

The regression analysis for Hypothesis 1 highlights the critical role of Big Data Maturity Awareness Position (BDMPA) in enhancing organizational strategic performance. These findings align with prior research emphasizing the significance of big data maturity in organizational outcomes. Big data maturity encompasses an organization's ability to utilize advanced analytics, integrate data-driven insights, and optimize decision-making processes. As noted by Müller et al. (2018), organizations with higher big data maturity can better adapt to market dynamics, drive innovation, and deliver personalized customer experiences—key factors contributing to strategic performance.

Hypothesis 2 reveals that Big Data Investments (BDI) alone do not directly translate into significant improvements in strategic performance. However, synergistic interaction is observed when BDI is paired with high BDMPA. This suggests that the impact of BDMPA on strategic performance is amplified by substantial big data investments. Simply increasing investments without aligning them with an organization's data maturity is insufficient to maximize strategic outcomes. These results underscore the necessity for organizations to align their investments with their data maturity level to achieve optimal results. The interaction effect illustrates that while investments in big data are critical, their effectiveness is contingent on a high level of data maturity. Combined, BDI and BDMPA significantly enhance strategic performance, highlighting the strategic importance of aligning investments with big data maturity to achieve impactful outcomes.

In summary, the findings addressing the first research question demonstrate that organizations with higher BDMPA are better positioned to leverage data for strategic decision-making, operational efficiency, and competitive advantage. Awareness of big data capabilities enables organizations to align their strategies and operations, resulting in improved market responsiveness, customer satisfaction, and overall performance. Regarding the second research question, while investments in big data are crucial, their full potential is realized only when organizations are aware of and actively align their big data maturity with their strategic goals. This awareness allows organizations to allocate resources effectively—whether in human capital, infrastructure, or policy initiatives—ensuring that investments complement their data capabilities and organizational needs.

Conclusion

This study provides a comprehensive analysis of the relationships between Big Data Maturity Position Awareness (BDMPA), Big Data Investments (BDI), and Strategic Performance (SP), highlighting critical insights into how these elements interact to influence organizational outcomes. The findings underscore the importance of not only investing in big data capabilities but also ensuring that these investments are strategically aligned with the organization's maturity in data practices. The strong reliability and validity of the study's tools confirm the credibility of the results. The findings show that Big Data Maturity in Practices and Awareness (BDMPA) is a key factor in improving strategic performance. This means that organizations with higher big data maturity tend to achieve better strategic outcomes.

The study also found that when big data maturity (BDMPA) combines with significant Big Data Investments (BDI), their combined effect enhances strategic performance even further. This highlights the importance of both improving big data practices and making strategic investments to achieve the best results. From a strategic viewpoint, organizations should focus on two key areas: understanding their level of maturity regarding their big data capabilities, and making well-planned investments in big data technologies., based on that understanding. Simply increasing investments without considering data maturity can lead to wasted resources and poor outcomes. On the other hand, aligning investments with the organization's data maturity helps use resources effectively and achieve better returns.

This study offers both theoretical and practical insights. Theoretically, it adds to existing knowledge about the importance of aligning big data practices with strategic goals. Practically, it provides a guide for organizations to improve performance by investing, based on the information for their big data maturity level, leading to better decisions, increased efficiency, and competitive advantage.

In summary, the study emphasizes that aligning big data maturity awarness postion and investments is essential for achieving meaningful outcomes. Organizations need to advance through maturity stages and align investments accordingly to fully benefit from big data. This alignment helps turn big data capabilities into real strategic gains, ensuring long-term success.

Scientific Ethics Declaration

* The authors declares that the scientific ethical and legal responsibility of this article published in EPSTEM journal belongs to the authors.

Conflict of Interest

* The authors declare that they have no conflicts of interest

Funding

* This research received no specific grant from any funding agency in the public, commercial, or not-for-profit sectors.

Acknowledgements or Notes

* This article was presented as a oral presentation at the International Conference on Research in Engineering, Technology and Science (www.icrets.net) held in Peja/Kosovo on July 10-13, 2025.

References

Akter, S., Wamba, S. F., Gunasekaran, A., Dubey, R., & Childe, S. J. (2016). How to improve firm performance using big data analytics capability and business strategy alignment? *International Journal of Production Economics, 182,* 113–131.

Bean, R., & Davenport, T. H. (2019). *Companies are failing in their efforts to become data-driven*. Harvard Business Review. Retrieved from: https://hbr.org/2019/02/companies-are-failing-in-their-efforts-to-become-data-driven

Bresciani, S., Ciampi, F., Meli, F., & Ferraris, A. (2021). Using big data for co-innovation processes: Mapping the field of data-driven innovation, proposing theoretical developments, and providing a research agenda. *International Journal of Information Management, 60*, 102347.

Caputo, F., Mazzoleni, A., Pillicelli, A., & Müller, J. (2019). Over the mask of innovation management in the world of big data. *Journal of Business Research, 119*, 330-338.

Elezaj, O., Tole, D., & Baci, N. (2018). Big Data in e-government environments: Albania as a case study. *Academic Journal of Interdisciplinary Studies, 7*(2), 117.

Elgendy, N., Elragal, A., & Päivärinta, T. (2022). DECAS: A modern data-driven decision theory for big data and analytics. *Journal of Decision Systems, 31*(4), 337–373.

Kara, A. (2024). Simulations of public debt. *The Eurasia Proceedings of Educational and Social Sciences, 37*, 33-38.

Lambrecht, A., & Tucker, C. (2015). Can big data protect a firm from competition? *SSRN Electronic Journal*. Retrieved from https://ssrn.com/abstract=2705530

Marketing Science Institute. (2018). *Research priorities 2018–2020.* Cambridge, Mass: Marketing Science Institute.

Mouhib, S., Anoun, A., Ridouani, M., & Hassouni, L. (2020). Towards a global big data maturity model. In *2020 Fourth International Conference on Intelligent Computing in Data Sciences (ICDS).*

Müller, O., Fay, M., & vom Brocke, J. (2018). The effect of big data and analytics on firm performance: An econometric analysis considering industry characteristics. *Journal of Management Information Systems, 35*(2), 488–509.

Olabode, O. E., Boso, N., Hultman, M., & Leonidou, C. N. (2022). Big data analytics capability and market performance: The roles of disruptive business models and competitive intensity. *Journal of Business Research, 139,* 1218–1230.

Tan, C., & Zhan, Y. (2016). Improving new product development using big data: A case study of an electronics company. *R&D Management, 46*(5), 847–863.

Tan, Y., Li, S., & Zhang, C. (2015). Harvesting big data to enhance supply chain innovation capabilities: An analytic infrastructure based on deduction graph. *International Journal of Production Economics, 165*, 223–233.

Wang, Y., Kung, L., & Byrd, T. A. (2018). Big data analytics: Understanding its capabilities and potential benefits for healthcare organizations. *Technological Forecasting and Social Change, 126*, 3–13.

Wolf, C., & Floyd, S. W. (2017). Strategic planning research: Toward a theory-driven agenda. *Journal of Management, 43*(6), 1754–1788.

Z. A. Al-Sai, R. Abdullah, & M. H. Husin. (2019). A review on big data maturity models. In *2019 IEEE Jordan International Joint Conference on Electrical Engineering and Information Technology (JEEIT)* (pp. 860–865). Amman, Jordan.

Zhang, C., Tian, Q., & Chen, L. (2017). A big data analytics architecture for cleaner manufacturing and maintenance processes of complex products. *Journal of Cleaner Production, 142*, 626–641.

Zhang, J., Wang, Y., & He, Q. (2022). Big data capability and sustainable competitive advantage: The mediating role of ambidextrous innovation strategy. *Sustainability, 14*(14), 8249.

Author(s) Information

Fatmir Desku
South East European University
Tetovo, Republic of North Macedonia
Contact e-mail: *fd31392@seeu.edu.mk*

Adrian Besimi
South East European University
Tetovo, Republic of North Macedonia

To cite this article:

Desku, F., & Besimi, A. (2025). Exploring the interplay between big data maturity position awareness and strategic performance: The moderating role of big data investments. *The Eurasia Proceedings of Science, Technology, Engineering and Mathematics (EPSTEM), 35,* 124-132.

The Eurasia Proceedings of Science, Technology, Engineering & Mathematics (EPSTEM)
ISSN: 2602-3199

The Eurasia Proceedings of Science, Technology, Engineering and Mathematics (EPSTEM), 2025

Volume 35, Pages 133-139

ICRETS 2025: International Conference on Research in Engineering, Technology and Science

Minimising the Cycle Time with Assembly Line Balancing and Worker Assignment: A Case Study in a Medical Device Manufacturer Company

Aysenur Kayser
Abdullah Gul University

Gulse Sipahi
Abdullah Gul University

Ozlem Sevimli
Abdullah Gul University

Nurullah Toplu
Abdullah Gul University

Serhat Turan
Abdullah Gul University

Ugur Satic
Abdullah Gul University

Abstract: In this research, we considered the mixed-model assembly line balancing and worker assignment problems of a medical device manufacturer in Türkiye. We combined these problems into a single integer programming model where multiple types of products can be assembled simultaneously on a single assembly line, and workers are assigned to workstations based on their abilities while ensuring the balance and efficiency of the assembly line. Our proposed approach seeks to minimise the cycle time and ability-based assignment costs on the assembly line. We used the Gurobi solver to find the optimal solution for the proposed problem. Our approach provides higher efficiency and results in a 76% increase in productivity without requiring additional work hours or workers.

Keywords: Assembly line balancing, Mixed-model, Cycle time minimisation

Introduction

Production systems, where production stations are oriented as a serial flow, are called assembly lines. In an assembly line, workpieces usually move sequentially through the stations. (Boysen et al., 2008). Assembly lines play a vital role in large-scale production due to cost and time efficiency without compromising quality. Assembly line balancing involves distributing workloads to workstations in a balanced manner to use resources effectively (Shtub & Dar-El, 1989). Therefore, assembly line balancing techniques promise significant decreases in product costs while increasing production capacity and efficiency (Teshome et al., 2024).

Due to the great importance of assembly line balancing in modern production systems, various studies have been conducted on this subject from the 1950s to the present. In the literature, the main objectives of the assembly line balancing problem are minimising cycle time and minimising the number of workstations. For example, Klein & Scholl (1996) proposed a branch-and-bound algorithm, while Uğurdağ et al. (1997) suggested a two-stage

- Selection and peer-review under responsibility of the Organizing Committee of the Conference

heuristic procedure based on integer programming, and Akpınar (2017) employed a large neighbourhood search algorithm to minimise cycle time. On the other hand, Wu et al. (2008) employed a branch-and-bound algorithm, Mura and Dini (2016) adopted a genetic algorithm, Delice et al. (2018) applied an ant colony optimisation algorithm, Sahin et al. (2018) offered a hybrid simulated annealing algorithm combined with integer programming, while Shadkam and Ghavidel (2021) presented a global criteria method to minimise the number of workstations.

In the literature, assembly line problems are classified according to various criteria, such as product variety, resource usage, and optimisation techniques. The mixed-model assembly line balancing problem is one of the generalisations of the assembly line problem, where different product models and their tasks are assigned to the same assembly line (Gökçen & Erel, 1998). Similar to the assembly line balancing problem, the popular objectives of the mixed-model assembly line balancing problem are minimising cycle time and minimising the number of workstations. For instance, Karabatı and Sayın (2003) designed a heuristic approach, Simaria and Vilarinho (2004) suggested a genetic algorithm, Çavdur and Kaymaz (2020) presented an integer programming model for minimising the cycle time. However, Bukchin (2002) offered a branch-and-bound approach to minimising the number of workstations. Additionally, some researchers have considered both minimising cycle time and minimising the number of workstation goals together. For example, Elia and Nagaraj (2014) applied a branch-and-bound-based solution approach that aims to minimise both the number of stations and cycle time in mixed-model assembly line balancing problems.

According to our literature review, the most common goal of mixed-model assembly line balancing is minimising cycle time and, in doing so, increasing the efficiency of production processes. To achieve this goal, the resource utilisation problem, which considers the task distribution, and the worker assignment problem, which considers assigning workers to stations according to their skills, must be considered together (Zhang & Gen, 2011). Yılmaz (2022) emphasises that considering worker skills and abilities while performing assembly line balancing activities maximises resource utilisation.

Workers' skills, expertise levels, and areas critically affect the assembly line balancing process and effective work performance (Katiraee et al., 2023). Considering the competence levels of employees with different task abilities is a critical factor that reduces the cycle time in assembly line balancing (Katiraee et al., 2023). For this reason, many researchers have considered the assembly line balancing and worker assignment problems together. For example, Ramezanian and Ezzatpanah (2015) suggested an Imperialist Competitive Algorithm to minimise total cycle time and operating costs related to worker assignment based on skill levels, and Yilmaz (2022) proposed a mixed integer mathematical model that that reduces cycle time and minimises labour costs.

In this study, we aim to reduce the cycle time on the assembly line by developing a mixed mathematical model and addressing the dual challenges of assembly line balancing and worker assignment. We present a multi-objective mixed-integer linear programming (MILP) model to solve a mixed-model assembly line balancing problem with integrated task, worker, and station assignments while ensuring optimal worker-task assignments based on competency levels. The mixed-integer model minimises the total cycle time of the two different models while minimizing ability-based worker assigment.

Material and Method

Assembly Line Balancing and Worker Assignment Problem

We developed a mixed-integer linear programming (MILP) model that handles the assembly line balancing and worker assignment problems. Our model seeks to minimise the cycle time by adjusting the workload distribution among workstations while ensuring optimal worker-task assignments based on the competency levels of the workers and the requirements of the tasks.

Objective Function

Since our model seeks to minimise the cycle time and minimise the skill-based worker-task assignments, we use two objection functions. Our first and primary objection function is minimising the cycle time of the assembly line, which is shown in Equation (1):

$$\text{Min } Z_1 = \sum_{m=1}^{2} c_m \tag{1}$$

Here, c_m represents the cycle time of the product model m. The cycle time calculation is shown in Equation (2).

$$Cycle\ time = \frac{Production\ time\ available\ per\ day}{Units\ required\ per\ day} \tag{2}$$

Our second and secondary objective is to minimise ability-based assignment costs. The secondary objective function is shown in Equation (3). After solving the mixed-integer model with the primary objective and obtaining the optimal cycle time, the model is resolved with the secondary objective function, while the previously obtained cycle time (Z_1^*) is imposed as a constraint.

$$\text{Min } Z_2 = \sum_i \sum_w a_{iw} * y_{iw}, \quad subject\ to\text{:}\ Z_1 = Z_1^* \tag{3}$$

Here, a_{iw} represents the ability score of worker w to do the job i for model m. Table 1 explains ability scores (a_{iw}). y_{iw} is a binary decision variable that takes the value 1 if worker w is assigned to the job i, and takes the value 0, otherwise. ($Z_1 = Z_1^*$) represents that we search secondary objective within the set of solutions that yield the optimal value of Z_1.

Table 1. Competency scores and explanations

Score	Explanation
1	No experience
2	Basic skills
3	The worker can work with a master/service representative.
4	Workers can work alone.
5	Trainer/master

Using multiple objectives in this manner is known as we used the ε-constraint method. The ε-constraint method transforms a multi-objective problem into a single-objective problem by selecting a primary objective to be optimised while treating the other objectives as constraints bounded by a parameter ε (Miettinen, 2019). Since we limited the solution space only to the optimal solution of the primary objective, running the MILP model for the second time for the secondary objective takes significantly less computational time. The primary advantages of this approach include the ability to prioritise and optimise two independent objectives separately, the reduction of model complexity and solution time, and the achievement of the main objective by giving precedence to cycle time minimisation.

Constraints

$$\textstyle\sum_{j=1}^{J} x_{ij} = 1, \forall i \tag{4}$$
$$\textstyle\sum_{j=1}^{J} j * x_{ij} - \sum_{j=1}^{J} j * x_{kj} \leq 0, \forall (i,k) \in P_r \tag{5}$$
$$\textstyle\sum_{i=1}^{I} t_{im} * x_{ij} \leq c_m, \forall j, m \tag{6}$$
$$\textstyle\sum_{w=1}^{W} y_{iw} = 1, \forall i \tag{7}$$
$$a_{iw} \geq h_{im} * y_{iw}, \forall i, w, m \tag{8}$$
$$\textstyle\sum_{w=1}^{W} z_{wj} = 1, \forall j \tag{9}$$
$$x_{ij} \geq y_{iw} + z_{wj} - 1, \forall i, j, w \tag{10}$$
$$y_{iw} \geq x_{ij} + z_{wj} - 1, \forall i, j, w \tag{11}$$
$$z_{wj} \geq x_{ij} + y_{iw} - 1, \forall i, j, w \tag{12}$$
$$x_{ij}, y_{iw}, z_{wj} \in \{0,1\}, \forall i, j, w \tag{13}$$
$$c_m \geq 0 \tag{14}$$

Equation (4) ensures that each task is assigned to exactly one workstation. Equation (5) is the precedence relations of tasks. This constraint ensures that a task k can be assigned to a workstation only if all of its predecessors $\forall(i,k)$ are currently assigned to the current or previous workstations. Equation (6) ensures that the processing time (t_{im}) of each station does not exceed the cycle time. Equation (7) ensures that each job is assigned to exactly one worker.

Equation (8) states that the skill score of a worker must be greater than or equal to the difficulty score of the job assigned to the worker. The difficulty score of the job depends on the size, quantity of the workpiece and the required equipment. Table 2 explains hardness scores (h_{im}). Equation (9) ensures that each worker is assigned to exactly one workstation. Equation (10) ensures that each workstation is assigned to at most one worker. Equations (11), (12), and (13) ensure consistency among job, worker, and station assignments. If a job is assigned to a worker and a station, then that worker must also be assigned to that station, and vice versa. Equation (14) indicates that the decision variables are binary. Equation (15) ensures that the cycle time is non-negative. Table 3 shows the nomenclature of the variables used in our model.

Table 2. Hardness scores and explanations

Score	Explanation
1	Very easy
2	Easy
3	Moderate
4	Hard
5	Very hard

Table 3. Nomenclature of the model

Nomenclature	Description
I	Set of jobs
J	Set of workstations
M	Set of product models to be assembled
W	Set of workers
t_{im}	Operation time of job i for model m
$(i, k) \in Pr$	Precedence relationships, job i must be completed before job k
a_{iw}	Ability score of worker w to do job i for model m
h_{im}	Hardness score of job i for model m
x_{ij}	1, if job i is assigned to the workstation j; 0, otherwise
y_{iw}	1, if worker w is assigned to the job i; 0, otherwise
z_{wj}	1, if worker w is assigned to the workstation j; 0, otherwise
c_m	Cycle time of model m

Results and Discussion

In this study, we first discuss how the necessary data were obtained, including task durations, precedence diagrams between tasks, processing times, and the employee competency matrix. Then, we present the results of our mathematical model, implemented using Gurobi, a mathematical model solver, within Python environment.

Data Collection

In this research, task durations and priority relationships of tasks are collected via observation and time study from a medical device manufacturer in Türkiye. According to our observations, we spotted two types of product models and 74 tasks for each product model. The task order for both models is almost the same, and the precedence relationship of tasks in the production of a medical device is shown in Figure 1. The tasks that a particular model does not require are assigned with zero processing time for that model.

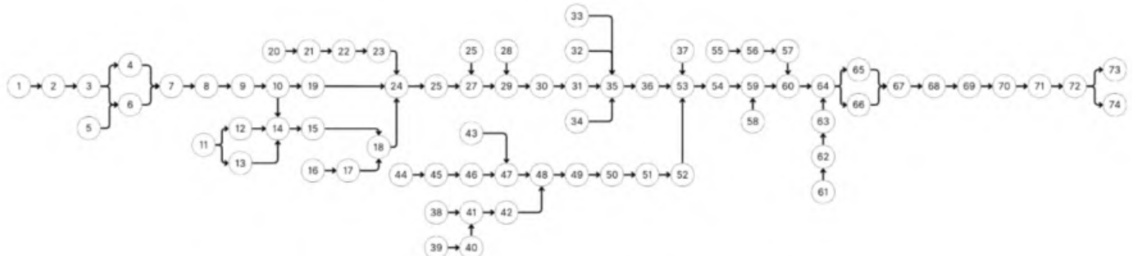

Figure 1. Precedence relationship of a medical device

In our observations, we noted that there is a base number of workers on the assembly line that focused on this research. However, there are also other workers on other assembly lines. Other workers sometimes work partially on the focused assembly line to increase productivity when needed. All workers' ability scores on all tasks are recorded in a Competency Matrix, and worker assignments to stations are done based on their scores on the Competency Matrix. A simplified and reduced version of the Competency Matrix is given in Table 4. An explanation of the scores on the Competency Matrix is given in Table 1.

Table 4. Competency matrix

Worker No	Task 1	Task 2	Task 3	…	Task I
1	2	3	3	…	1
2	5	5	3	…	1
3	3	3	2	…	1
…	…	…	…	…	…
Worker W	5	5	5	…	3

Results of the Assembly Line Balancing and Worker Assignment Problem

We used the Gurobi solver to find the optimal solution to the problem considered, including determining task assignments for workstations, worker-task allocations, and the minimum achievable cycle time. The cycle time obtained from the initial run was incorporated into the model as a constraint in the second run, and the second objective function was used in the second run. The first run took 266 seconds, and the second run took 33 seconds on a laptop computer with an AMD Ryzen5 4600H CPU with 3.00 GHz clock speed and 16 GB of RAM.

Table 5. Comparison of current and proposed models

Metric	Current	Proposed
Cycle Time (sec.)	100%	57%
Capacity (unit)	100%	176%
Productivity	100%	176%
Efficiency	53%	98%

According to the analysis, our proposed model reduced the cycle time to 57%, increased the capacity and productivity by 76% and boosted the efficiency to 98% with the same number of workers and working hours. These findings demonstrate our optimised model's effectiveness in enhancing operational performance through improved line balancing and worker assignment strategies.

Conclusion

In this research, a real-world assembly line balancing and worker assignment problem was investigated. Our problem is a complex optimisation problem since it includes the simultaneous assembly of different product models with varying task durations combined with the variability in worker skills. We developed a mixed integer linear programming (MILP) model that aims to minimise cycle time and ability-based assignment costs. The proposed solution offers a 76% increase in productivity and improves efficiency from 53% to 98% without additional workers or extra working hours.

Future research should focus on extending the proposed optimisation model to all types of products produced in the factory, and standard line balancing should be implemented across the factory. Integrating real-time data sources (worker availability, machine status, and order priorities) can improve the model's responsiveness and decision accuracy. Additionally, future work might incorporate multi-period planning elements and dynamic resource allocation, which can provide better medium-term production planning.

Recommendations

There are several opportunities for future improvements and broader application of the optimisation model and interface we are working on. By extending the methodology to all products manufactured in the plant, line balancing practices can be standardised. Furthermore, while the current model optimises based on static input provided each morning, integrating real-time data sources such as worker availability, machine status, or order priority can further increase the responsiveness and accuracy of daily planning.

Incorporating multi-period planning can also improve medium-term planning decisions, especially during periods of demand volatility or labour variability. Further developments could include user feedback mechanisms and automated performance reporting to monitor the long-term impact of optimisation decisions.

Scientific Ethics Declaration

* The authors declare that the scientific ethical and legal responsibility of this article published in EPSTEM journal belongs to the authors.

Conflict of Interest

* No conflicts of interest

Funding

* This research received no specific grant from any funding agency in the public, commercial, or not-for-profit sectors.

Acknowledgements or Notes

* This article was presented as a oral presentation at the International Conference on Research in Engineering, Technology and Science (www.icrets.net) held in Peja/Kosovo on July 10-13, 2025.

* This paper is based on the undergraduate thesis work of the authors conducted at Abdullah Gül University.

References

Akpınar, Ş. (2017). Large neighbourhood search algorithm for Type-II assembly line balancing problem. *Pamukkale University Journal of Engineering Sciences*, *23*(4), 444–450.

Boysen, N., Fliedner, M., & Scholl, A. (2008). Assembly line balancing: Which model to use when? *International Journal of Production Economics*, *111*(2), 509–528.

Bukchin, J., Dar-El, E. M., & Rubinovitz, J. (2002). Mixed model assembly line design in a make-to-order environment. *Computers & Industrial Engineering*, *41*(4), 405–421.

Çavdur, F., & Kaymaz, E. (2020). A mixed-integer programming model for cycle time minimization in assembly line balancing: Using rework stations for performing parallel tasks. *International Journal of Production Management and Engineering, 8*(2), 109–121.

Delice, Y., Aydoğan, E. K., Söylemez, İ., & Özcan, U. (2018). An ant colony optimisation algorithm for balancing two-sided U-type assembly lines with sequence-dependent set-up times. *Sādhanā*, *43*, 1-15.

Elia, A. K., & Nagaraj. (2014). Minimizing number of stations and cycle time for mixed model assembly line. *International Journal of Engineering Research & Technology (IJERT), 3*(8), 1039–1044.

Gökçen, H., & Erel, E. (1998). Binary integer formulation for mixed-model assembly line balancing problem. *Computers & Industrial Engineering, 34*(2), 451–461.

Katiraee, N., Calzavara, M., Finco, S., & Battini, D. (2021). Consideration of workforce differences in assembly line balancing and worker assignment problem. *IFAC PapersOnLine*, *54*(1), 13-18.

Karabatı, S., & Sayın, S. (2003). Assembly line balancing in a mixed-model sequencing environment with synchronous transfers. *Computers and Industrial Engineering, 149*(2), 417-429.

Klein, R., & Scholl, A. (1996). Maximizing the production rate in simple assembly line balancing — A branch and bound procedure. *European Journal of Operational Research, 91*, 367-385.

Miettinen, K. (1999). *Nonlinear multiobjective optimization*. Springer Science & Business Media.

Mura, M. D., & Dini, G. (2016). Worker skills and equipment optimization in assembly line balancing by a genetic approach. *Procedia CIRP*, *44*, 102–107.

Ramezanian, R., & Ezzatpanah, A. (2015). Modelling and solving multi-objective mixed-model assembly line balancing and worker assignment problem. *Computers & Industrial Engineering, 87*, 74–80.

Sahin, M., Kellegoz, T., & Soylemez, I. (2018). Çok işçili montaj hatlarında istasyon ve kaynak yatırımı maliyetinin enküçüklenmesine yönelik tavlama benzetimi ve tam sayılı doğrusal programlamaya dayalı yeni bir algoritma. *Dicle Üniversitesi Mühendislik Fakültesi Mühendislik Dergisi*, *9*(2), 727-739.

Shadkam, E., & Ghavidel, F. (2021). Presentation and implementation multi-objective mathematical models to balance the assembly line. *International Journal of Research in Industrial Engineering, 10*(1), 56-66.

Shtub, A., & Dar-El, E. M. (1989). A methodology for the selection of Assembly Systems. *International Journal of Production Research*, *27*(1), 175–186.

Simaria, A. S., & Vilarinho, P. M. (2004). A genetic algorithm-based approach to the mixed-model assembly line balancing problem of type II. *Computers and Industrial Engineering, 47*(4), 391-407.

Teshome, M. M., Meles, T. Y., & Yang, C.-L. (2024). Productivity improvement through assembly line balancing by using simulation modeling in case of Abay Garment Industry gondar. *Heliyon*, *10*(1).

Ugurdag, H. F., Rachamadugu, R., & Papachristou, C. A. (1997). Designing paced assembly lines with fixed number of stations. *European Journal of Operational Research*, *102*(3), 488–501.

Wu, E.-F., Jin, Y., Bao, J.-S., & Hu, X. (2008). A branch-and-bound algorithm for twosided assembly line balancing. *International Journal of Advanced Manufacturing Technology*, *39*, 1009-1015.

Yılmaz, H. (2022). Assembly line worker assignment and balancing problem by considering labor cost. *Journal of Innovative Science and Engineering (JISE)*, 6(1), 22-31.

Zhang, W., & Gen, M. (2011). An efficient multiobjective genetic algorithm for mixed-model assembly line balancing problem considering demand ratio-based cycle time. *Journal of Intelligent Manufacturing, 22*(2), 173–181.

Author(s) Information

Aysenur Kayser
Abdullah Gul University
Sümer Kampüsü, Barbaros, Erkilet Blv., 38080
Kocasinan/Kayseri, Türkiye

Gulse Sipahi
Abdullah Gul University
Sümer Kampüsü, Barbaros, Erkilet Blv., 38080
Kocasinan/Kayseri, Türkiye

Ozlem Sevimli
Abdullah Gul University
Sümer Kampüsü, Barbaros, Erkilet Blv., 38080
Kocasinan/Kayseri, Türkiye

Nurullah Toplu
Abdullah Gul University
Sümer Kampüsü, Barbaros, Erkilet Blv., 38080
Kocasinan/Kayseri, Türkiye

Serhat Turan
Abdullah Gul University
Sümer Kampüsü, Barbaros, Erkilet Blv., 38080
Kocasinan/Kayseri, Türkiye

Ugur Satic
Abdullah Gul University
Sümer Kampüsü, Barbaros, Erkilet Blv., 38080
Kocasinan/Kayseri, Türkiye
Contact e-mail: *ugur.satic@agu.edu.tr*

To cite this article:

Kayser, A., Sipahi, G., Sevimli, O., Toplu, N., Turan, S., & Satic, U. (2025). Minimising the cycle time with assembly line balancing and worker assignment: a case study in a medical device manufacturer company. *The Eurasia Proceedings of Science, Technology, Engineering and Mathematics (EPSTEM), 35,* 133-139.

The Eurasia Proceedings of Science, Technology, Engineering & Mathematics (EPSTEM)
ISSN: 2602-3199

The Eurasia Proceedings of Science, Technology, Engineering and Mathematics (EPSTEM), 2025

Volume 35, Pages 140-152

ICRETS 2025: International Conference on Research in Engineering, Technology and Science

Comparative Analysis of the Effects of Natural Disasters on Volatility in Money and Capital Markets: The Cases of Türkiye and Myanmar

Beste Alpaslan
OSTIM Technical University

Abstract: This study presents a comparative analysis of the effects of natural disasters on volatility in money and capital markets, focusing on the cases of Türkiye and Myanmar (Burma). The primary objective is to assess the fluctuations observed in financial markets following major earthquakes in both countries and to estimate the economic impacts of these natural disasters. For Türkiye, the analysis covers the period from February 6, 2019, to February 6, 2024, focusing on the market dynamics following the Kahramanmaraş-centered earthquake. In the case of Myanmar, the period from March 28, 2020, to May 28, 2025, is examined to identify market volatility triggered by the earthquake in the Sagaing Region. In the methodology section, ARCH (Autoregressive Conditional Heteroskedasticity) and GARCH (Generalized Autoregressive Conditional Heteroskedasticity) models are employed to analyze the volatility in financial markets that emerged after the earthquakes in both countries, as well as the economic consequences of these natural disasters. These models are selected as appropriate tools for measuring the temporal dynamics of volatility in the financial markets of each country. Additionally, the study provides a detailed examination of the impact of these two major earthquakes on exchange rates. The market responses in Türkiye after the aforementioned earthquake are benchmarked against the market reactions in Myanmar following its seismic event, in order to identify both similarities and differences. By analyzing the market fluctuations observed in the aftermath of each disaster, the study explores the economic implications of such events and discusses the differences in market dynamics based on the economic structures and international market integration of the two countries. The overall analysis aims to provide a comprehensive framework for understanding the uncertainty and volatility in financial markets caused by natural disasters.

Keywords: Natural disaster, Volatility, Money and capital markets, Heteroskedasticity, GARCH models

Introduction

Natural disasters are defined in the literature as events of natural origin that occur beyond human control and cause sudden and destructive effects on infrastructure, social life, and economic systems (TDK, 2025). Disasters are events that occur as a result of natural or human-induced causes and cause people to experience physical, economic and social losses (Akcay, et al., 2023). The impact of such disasters on macroeconomic indicators becomes particularly evident through increased fluctuations observed in financial markets. Recent studies indicate a growing academic interest in the economic consequences of natural disasters, especially in developing countries where financial infrastructure is relatively weaker, in parallel with the rising frequency and severity of such events. In this context, financial market volatility is considered one of the primary indicators through which the economic implications of disasters can be clearly observed. However, empirical studies that comparatively analyze market responses following disasters in developing economies remain limited.

This study aims to contribute to the literature by conducting a comparative analysis of the volatility effects observed in the financial markets of Türkiye and Myanmar, both of which have experienced large-scale earthquakes in recent years. In this regard, the earthquakes that occurred on February 6, 2023, in Kahramanmaraş, Türkiye (Cabuk et al, 2025), and on March 28, 2023, in the Sagaing Region of Myanmar

- Selection and peer-review under responsibility of the Organizing Committee of the Conference

constitute the core events of this research. The selected sample period covers February 6, 2019, to February 6, 2024, for Türkiye, and March 28, 2020, to May 28, 2025, for Myanmar, with daily closing exchange rate data being used as the primary financial variable. The analysis aims to identify common patterns and divergences in market responses across the two countries.

The methodology of this research draws on an extensive body of literature that examines the financial repercussions of natural disasters and the spread of volatility following such events. Although several studies have investigated these dynamics, there is a growing consensus that traditional approaches often fall short in capturing volatility behavior, and that GARCH-type models offer more consistent and reliable results. Accordingly, the present analysis adopts GARCH-family models to measure market reactions and contributes to the understanding of volatility patterns in the aftermath of natural disasters. Through this comparative approach, the study seeks to offer insights into the impact of natural disasters on financial stability in developing economies. The selection of Türkiye and Myanmar is based on the significant earthquakes they experienced in the recent past, and the analysis relies on daily closing exchange rate data. Ultimately, the study aims to enrich the existing literature by providing a robust framework to assess the financial volatility caused by natural disasters in emerging markets.

Literature

Natural disasters often result in large-scale destruction, severely disrupting infrastructure and economic activities. Consequently, such damage can significantly affect market stability, reduce investor confidence, and cause long-term interruptions in production, trade, and employment. Moreover, the cascading impacts of these disasters may extend to environmental degradation, weakening the resilience of both local and global economies. In this regard, the existence of a comprehensive body of literature on the subject is inevitable (Panwar & Sen, 2019).

According to relevant studies, Ferreira and Karali (2015) examined the effects of major earthquakes that occurred over the past two decades on stock markets in 35 different countries using GARCH-type models. They concluded that, with the exception of Japan, global financial markets generally exhibit resilience to shocks caused by earthquakes. However, they also discussed that in some cases, macroeconomic indicators and the characteristics of the earthquakes could influence stock returns. Similarly, Worthington (2008) analyzed the effects of natural disasters on stock market returns in Australia. In this study, the GARCH-M model was applied using daily price and cumulative return data. Likewise, Fakhry et al. (2018) analyzed the volatility surge in financial markets following the 2011 Tohoku earthquake in Japan using GARCH models, concluding that such models are effective in modeling the impacts of disasters. They reached a consensus that the models accurately capture short-term shocks and volatility clustering, thereby enhancing our understanding of market responses in the post-disaster period.

Another study used data from the United States between 1919 and 2017 to investigate the relationship between economic growth and volatility through the GARCH-M model. This study focused on how major shocks such as World War II, economic crises, strikes, and natural disasters influence output fluctuations, providing a framework to measure the potential impact of uncertainty on growth (Charles & Darné, 2021). Tao et al. (2022) examined the economic effects of natural disasters through two major earthquakes in California and analyzed stock market responses. Using the GARCH model, which is among the prominent time-series methods, they demonstrated the effects of earthquakes on market volatility. Another study explored the wealth and risk effects of disasters on the insurance sector and stock markets using GARCH models, aiming to identify fluctuations during periods of heightened risk (Wang & Kutan, 2013).

Worthington and Valadkhani (2004) focused on the short-term effects of natural disasters on stock returns and market volatility in Australia. Similarly, Yang et al. (2008) used the event study method to analyze the short-term impacts of disasters on price movements and volatility in stock markets. In a related study, using daily data from the Nairobi Stock Exchange (NSE) for the period 2000–2018, the impact of structural breaks on the volatility dynamics of stock returns was examined. GARCH models revealed that accounting for structural breaks increased forecasting accuracy and improved risk assessment outcomes (Ndei et al., 2019).

In a related context, Ewing and Malik (2016) investigated volatility spillovers between oil prices and U.S. stock markets. Using daily data, they applied univariate and bivariate GARCH-type models that incorporated structural breaks and identified strong volatility transmission between the two markets. Another study examined the effects of the 2011 Tōhoku earthquake not only on Japanese stock markets but also on the stock markets of its trade partners. The study found significant fluctuations in the returns of 19 different sectors in Japan and in markets of countries collaborating with these sectors (Yamori & Kobayashi, 2002). Similarly, Odell and Weidenmier (2004) observed the international financial market impacts of the 1906 San Francisco earthquake. Following the disaster, a large influx of gold into the U.S. and subsequent policy responses eventually led the country into recession, setting the stage for the 1907 Panic. Another study investigated the effects of major natural disasters on stock returns and volatility of U.S.-based firms using GARCH models. The findings revealed that severe natural disasters caused abnormal changes in stock returns and volatility, especially for firms located in affected areas (Bourdeau-Brien & Kryzanowski, 2017).

Additionally, an empirical study examined how natural disasters impacted the stock price volatility of U.S. property-liability insurance companies. GARCH models demonstrated that these disasters increased financial risk, with effects not limited to the directly affected regions (Montero et al., 2024). In another study, the impact of the 10 most costly disasters in the U.S. insurance sector on volatility and correlation was analyzed using GARCH models. The results indicated that natural disasters significantly increased the volatility of insurance stocks and their correlation with the overall market (Thomann, 2013). Similarly, Galido and Marites (2013) investigated the impact of natural disasters on the Philippine stock market using the GARCH-M model, showing that disasters increase market volatility and influence investor risk perception. Finally, using daily data from September 10, 2007, to February 26, 2015, Al Rahahleh and Kao (2018) examined the volatility forecasting performance of GARCH-family models for the Saudi Arabian Stock Exchange and the petrochemical industry index.

Unit Root Tests

In time series analysis, the stationarity of return series is among the basic assumptions for the validity of many models. In testing this assumption, unit root tests are generally utilized. Accordingly, the first method used in this study is the Extended Dickey-Fuller (ADF) test developed by Dickey and Fuller (1981). The ADF test is modeled as equation (1) for the model with only constant term and equation (2) for the model with constant and trend term in order to test stationarity under different structures.

$$\Delta y_{ti} = \alpha_0 + \alpha_2 y_{t-1} + \sum_{i=1}^{k} \beta \, \Delta y_{t-i} + \varepsilon_i \tag{1}$$

$$\Delta y_{ti} = \alpha_0 + \alpha_1 trend + \alpha_2 y_{t-1} + \sum_{i=1}^{k} \beta \, \Delta y_{t-i} + \varepsilon_i \tag{2}$$

The test statistics presented in Equation (1) and Equation (2) are compared with the critical values in the relevant statistical tables. If the null hypothesis — which tests whether the return series is non-stationary — is rejected, it can be concluded that the series satisfies the condition of stationarity. Furthermore, the Phillips-Perron (PP) test, which is an improved version of the ADF test and eliminates the problem of autocorrelation, is employed to analyze the stationarity condition. The rejection of the null hypothesis in the PP test indicates that the examined return series meet the stationarity condition (Phillips & Perron, 1988).

ARCH-LM Test

Following the evaluation of the stationarity condition of the return series, the presence of an ARCH (Autoregressive Conditional Heteroskedasticity) effect in the series is investigated. The existence of this effect is a necessary condition for the applicability of ARCH-type models (Engle, 1979). The presence of the relevant effect is analyzed using the ARCH-LM test, which is constructed based on the auxiliary regressions presented in Equation (3).

$$e_t^2 = \beta_0 + \left(\sum_{s=1}^{q} \beta_s e_{t-s}^2 \right) + v_t \tag{3}$$

Following the ARCH-LM test, the calculated F-statistic is compared with the critical value from the table. If the F-statistic exceeds the critical value, the null hypothesis is rejected, indicating the presence of an ARCH effect in the analyzed return series. In this case, it is concluded that there is a heteroskedasticity problem. Accordingly, the existence of such a problem suggests that the return series is suitable for modeling with a GARCH (Generalized Autoregressive Conditional Heteroskedasticity) type model.

GARCH Model

Bollerslev (1986) extended the ARCH model by incorporating lagged values of the conditional variance into the model, introducing the GARCH model to the literature. Compared to the ARCH model, the GARCH model provides a more flexible framework, allowing for a more effective modeling of volatility by considering past variance information. The variance equation used in the GARCH model for volatility modeling is presented in Equation (4).

$$h_t = \omega + \alpha\varepsilon_{t-1}^2 + \beta h_{t-1}, \omega > 0, \alpha \geq 0, \beta \geq 0, \alpha + \beta < 1 \tag{4}$$

As shown in Equation (4), the parameter ω represents the constant component in the variance equation, while the parameter α reflects the impact of shocks on the series, and β captures the effect of previous period volatility on the current period.

Exponential Generalized Autoregressive Conditional Heteroskedasticity (EGARCH)

Developed by Nelson (1991), the EGARCH model was introduced as an alternative to the traditional GARCH model, allowing for the analysis of the asymmetric effects of positive and negative shocks on volatility. In this context, the existence of the leverage effect is also examined through this model. The EGARCH(1,1) model used in the analysis is presented in Equation (5).

$$log(h_t^2) = \omega + \alpha\left[\left|\frac{u_{t-1}}{h_{t-1}}\right| - \sqrt{2/\pi}\right] + \beta\, log(h_{t-1}^2) + \delta\frac{u_{t-1}}{h_{t-1}} \tag{5}$$

Threshold Generalized Autoregressive Conditional Heteroskedasticity (TGARCH)

The TGARCH model, proposed by Zakoian (1994), has made significant contributions to the relevant literature. In this model, predictions are made based on the conditional standard deviation rather than the conditional variance. While the leverage effect is defined through a logarithmic structure in the EGARCH model, it is modeled in an asymmetric form using a quadratic specification in the TGARCH model, as expressed in Equation (6).

$$h_t^2 = \omega + \alpha u_{t-1}^2 + \beta h_{t-1}^2 + \gamma u_{t-1}^2 l_{t-1} \tag{6}$$

Asymmetric Power ARCH (APARCH)

Ding, Granger, and Engle (1993) developed the APARCH model based on the conditional standard deviation approach, which relies on the lagged absolute values of error terms. This model offers the advantage of simultaneously capturing both the leverage effect and the Taylor effect within a single framework. In this context, the APARCH model is represented by Equation (7).

$$h_t^\delta = \omega + \alpha(|u_{t-1}| - \gamma u_{t-1})^\delta + \beta h_{t-1}^\delta \tag{7}$$

Data

In this study, the volatility dynamics of exchange rates (denominated in US dollars) representing the monetary and capital markets of Türkiye and Myanmar are comparatively analyzed. The aim is to determine the best-fitting model using GARCH-type models for the period between 06/02/2019 and 06/02/2024 for Türkiye, and between 28/03/2020 and 28/05/2025 for Myanmar. The exchange rate data used in the analysis were obtained from the Thomson Reuters database. The selection of these countries is based on their recent experiences with natural disasters and the intention to examine the impact of such events on the volatility of their monetary and capital markets.

The daily closing prices of exchange rates and stock market indices were used. The return series employed in the models are represented in Equation (8) below. In Equation (8), R_t denotes the return of the index on day t, while P_t indicates the closing price on day t.

$$R_t = \ln(P_t / P_{t-1}) \tag{8}$$

Analysis of Türkiye

In this study, the USD/TRY exchange rate is taken as the basis for analyzing exchange rate volatility in Türkiye, focusing on the two-year period between 06/02/2019 and 06/02/2024. Although the USD/TRY exchange rate generally exhibited an upward trend during the analysis period, fluctuations were observed in certain intervals. The earthquakes centered in Kahramanmaraş on February 6, 2023, which had severe economic and social consequences across the country, created significant uncertainty in financial markets. As a result of this disaster, sudden and sharp fluctuations occurred in the foreign exchange markets.

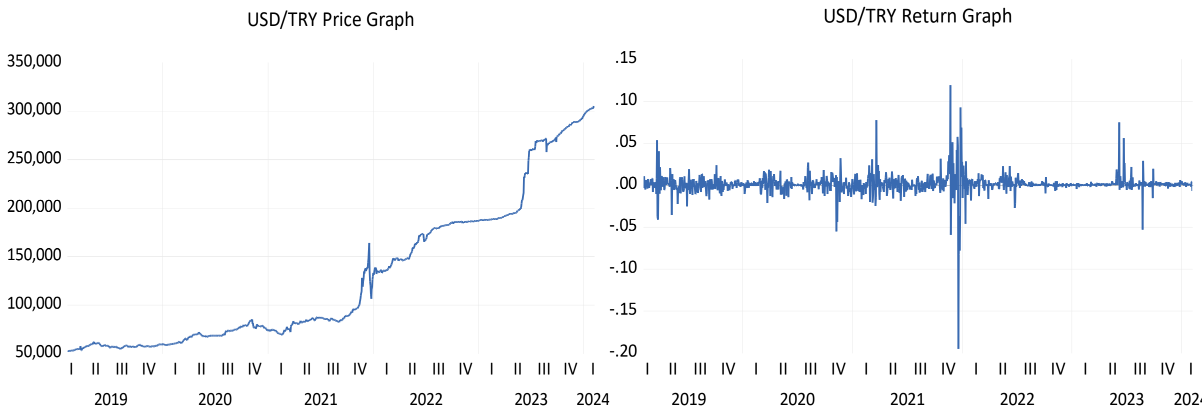

Figure 1. Price and return series of the USD/TRY ındex for the period 06/02/2019 – 06/02/2024

An examination of the USD/TRY exchange rate and return series presented in Figure 1 reveals that, although the series displayed occasional fluctuations throughout the analysis period, it generally followed an upward trend. One of the major developments that increased volatility and caused significant fluctuations in Türkiye's foreign exchange markets during the analysis period was the devastating earthquake centered in Kahramanmaraş on February 6, 2023. This natural disaster intensified economic uncertainties, leading to sharp and short-term movements in the exchange rate and resulting in a marked increase in the volatility of the USD/TRY exchange rate. Descriptive statistics for the return series of the USD/TRY exchange rate are presented in Table 1.

Table 1. Descriptive statistics (USD/TRY)

	Return	Price
Mean	0.001351	128838.6
Median	0.000870	85806.50
Maximum	0.119174	305341.0
Minimum	-0.195044	52464.00
Std. Dev.	0.012120	75332.00
Skewness	-2.181351	0.854415
Kurtosis	72.62886	2.480058
Jarque-Bera	264451.8	173.3472
Probability	0.000000	0.000000
Sum	1.761881	1.68E+08
Sum Sq. Dev.	0.191396	7.39E+12
Observations	1304	1304

The descriptive statistics presented in Table 1 indicate that the price series exhibited a volatile pattern during the relevant period, while the return series displayed a high level of volatility. In this context, the relatively high standard deviations of the series suggest a fluctuating structure in exchange rate movements. The results of the Jarque-Bera test reveal that both the price and return series deviate from the assumption of normal distribution. The skewness value of the return series indicates asymmetry in the distribution, while the notably high kurtosis value suggests that the series has fat tails and that extreme values occur frequently. To evaluate the stationarity properties of the return series, the ADF and PP tests were conducted, and the results are presented in Table 2.

Table 2. Stationarity tests (USD/TRY)

Tests		USD/TRY
ADF	With intercept	-31.89383***
	With intercept and Trend	-31.90901***
PP	With intercept	-31.71513***
	With intercept and Trend	-31.71894***

***⟶Significance at the 1% level.
Source: Author's Calculations

In Table 2, the presence of unit roots in the return series was examined, and the null hypothesis of a unit root was rejected. It was determined that the return series satisfy the stationarity condition at the 1% significance level. With this condition met, the ARCH-LM test was subsequently applied to assess the suitability of the return series for GARCH-type modeling, and the test results are presented in Table 3.

Table 3. ARCH-LM test results (USD/TRY)

Tests	USD/TRY
ARCH-LM-F Statistic	3.696513***

***⟶Significance at the 1% level.
Source: Author's Calculations

According to the ARCH-LM test results presented in Table 3, the presence of heteroskedasticity in the return series was analyzed, and the null hypothesis of no heteroskedasticity was rejected, indicating the existence of this issue at the 1% significance level. Based on these findings, it was concluded that GARCH-type models can be applied for volatility modeling. Following this assessment, considering the Akaike Information Criterion and the significance levels of the coefficients, the TGARCH model was selected as the most appropriate, and its results are presented in Table 4.

Table 4. Volatility model results

Parameters	GARCH (1,1)	EGARCH (1,1)	TGARCH (1,1)	APARCH (1,1)
c	0.000332	0.000887	0.000688	0.000702
AR (1)	0.000216	-0.029524	-0.019793	-0.017513
ω	1.30E-06	-0.331314	1.09E-07	3.15E-07
α	0.336351	0.236311	0.235644	0.118376
β	0.768626	0.119783	-0.195273	-0.439005
EGARCH (γ)	-	0.981896	-	-
TGARCH (γ)	-	-	0.896466	-
APARCH (γ)	-	-	-	0.902092
APARCH (σ)	-	-	-	1.824578
Akaike	-7.034742	-7.112256	-7.113021	-7.112094
ARCH	0.000358	4.579659	3.191931	4.182313
Q^2	2.8684	3.3206	2.4380	2.1369

In Table 4, the dynamics of USD/TRY exchange rate volatility were examined using GARCH(1,1), EGARCH(1,1), TGARCH(1,1), and APARCH(1,1) models. The findings were determined by considering the significance levels and signs of the model parameters, while model comparisons were based on the Akaike Information Criterion, ARCH effect tests, and Ljung-Box Q^2 statistics. According to the analysis, the most explanatory model was identified as TGARCH(1,1). It was observed that negative shocks have a volatility-increasing effect in the market within this model. In this context, it can be concluded that natural disasters generate high volatility effects on financial markets in emerging countries like Türkiye.

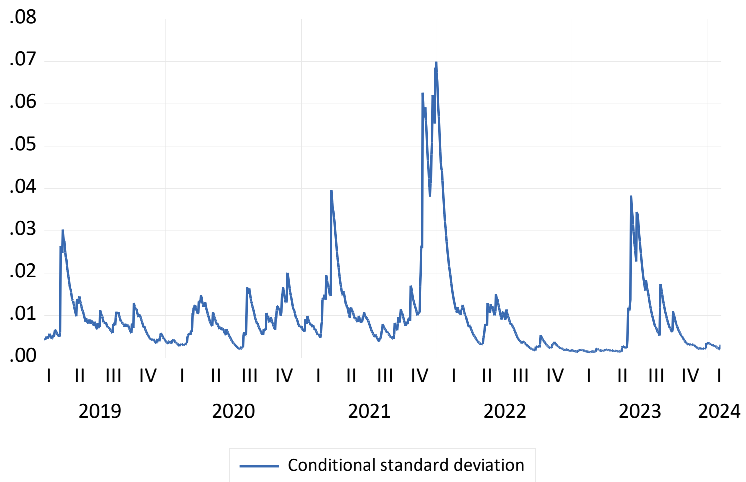

Figure 2. Conditional standard deviation of the USD/TRY exchange rate

Figure 2 illustrates the time series variation of the conditional standard deviations of the USD/TRY exchange rate obtained using the GARCH model. The findings for the analysis period indicate that the conditional volatility of the exchange rate significantly increased during certain intervals.

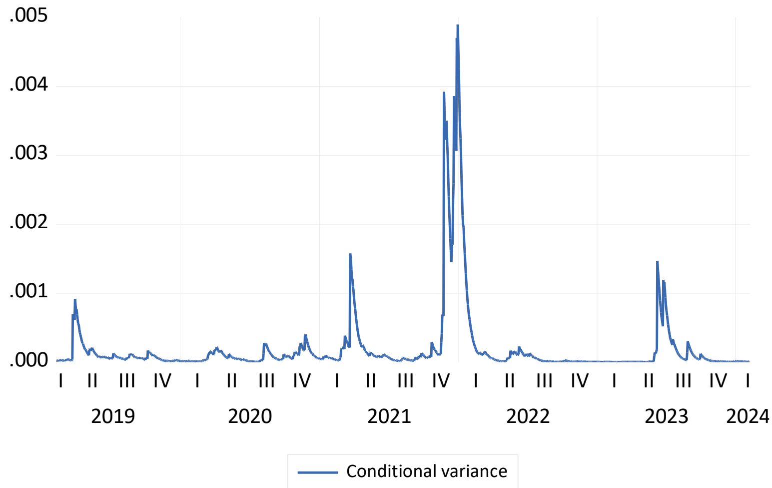

Figure 3. Conditional variance of the USD/TRY exchange rate

Figure 3 presents the conditional variances of the mentioned index. It is observed that the volatilities of the index, which represents stock prices, remained high following the February 6, 2023 earthquake.

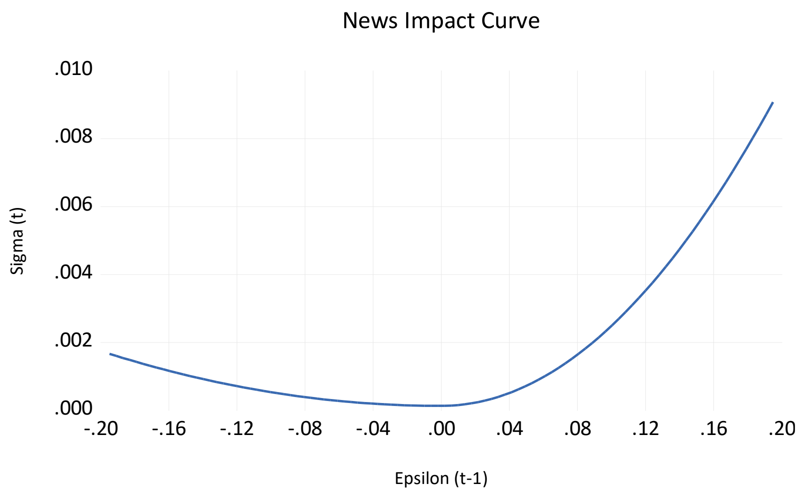

Figure 4. News impact curve of the USD/TRY exchange rate

The news impact curve of the relevant exchange rate, presented in Figure 4, measures how volatility responds when new information arrives in the market. It shows that negative shocks have a stronger effect than positive shocks, creating a leverage effect in the market.

Analysis of Myanmar

In this study, the USD/MMK exchange rate was examined to analyze exchange rate volatility in Myanmar, focusing on the period from 28/03/2020 to 28/05/2025. While the volatility of the USD/MMK exchange rate generally exhibited a stable trend during the analysis period, fluctuations were observed at certain intervals.

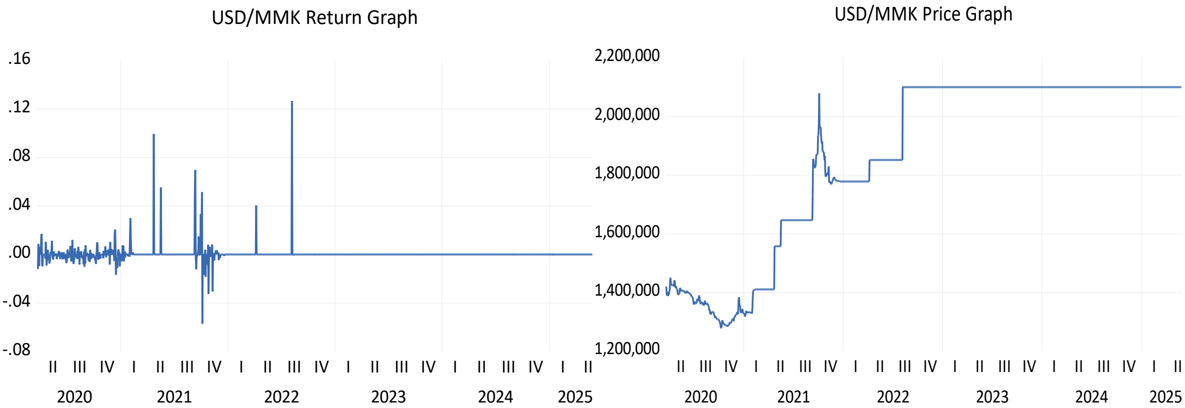

Figure 5. Price and return charts of the USD/MMK exchange rate for the period 23/03/2020 – 28/05/2025

Figure 5 illustrates the time series variation of the daily return and price series of the USD/MMK exchange rate. Upon examining the graphs, it is observed that returns exhibited relatively low and stable levels starting from the second quarter of 2020, whereas significant fluctuations occurred during 2021 and 2022. The sharp rises and falls during this period can be attributed to the political instability in Myanmar, particularly the increased market uncertainty following the military coup in 2021. Finally, from 2023 to the present, no significant volatility has been observed in the returns. Descriptive statistics for the return series of the USD/MMK exchange rate are presented in Table 5.

Table 5. Descriptive statistics (USD/MMK)

	Return	Price
Mean	0.000290	1862727.
Median	0.000000	2100000.
Maximum	0.126655	2101500.
Minimum	-0.057144	1278000.
Std. Dev.	0.006410	296063.4
Skewness	10.22353	-0.781129
Kurtosis	182.6939	2.015210
Jarque-Bera	1841187.	191.9807
Probability	0.000000	0.000000
Sum	0.391280	2.52E+09
Sum Sq. Dev.	0.055461	1.18E+14
Observations	1351	1351

The descriptive statistics presented in Table 5 reflect the basic statistical properties of the USD/MMK exchange rate and its return series during the analysis period. The mean return being very close to zero indicates that the exchange rate generally follows a stationary path over the long term. However, the wide range between the maximum and minimum values, along with the relatively high standard deviation, suggests that the series occasionally experiences significant fluctuations.

Additionally, the high kurtosis value of the return series and the statistically significant Jarque-Bera test result reveal the presence of numerous extreme values and that the return distribution deviates substantially from the normal distribution. In light of these findings, it is feasible to analyze the return series using models such as GARCH, which account for time-varying volatility. To assess the stationarity properties of the USD/MMK return series, ADF and PP tests were conducted, and the results are presented in Table 6.

Table 6. Stationarity tests (USD/MMK)

Tests		USD/MMK
ADF	With intercept	-34.94845***
	With intercept and trend	-34.96013***
PP	With intercept	-34.92305***
	With intercept and trend	-34.92999***

***⟶Significance at the 1% level.
Source: Author's Calculations

Table 7. ARCH-LM test results (USD/MMK)

Tests	USD/MMK
ARCH-LM-F Statistic	1.380006***

***⟶Significance at the 1% level.
Source: Author's Calculations

In Table 7, the presence of unit roots in the return series was examined, and the null hypothesis of a unit root was rejected. It was determined that the return series satisfy the stationarity condition at the 1% significance level. With this condition met, the ARCH-LM test was conducted to assess the suitability of the return series for GARCH-type modeling, and the test results are presented in Table 8.

Table 8. Volatility model results

Parameters	GARCH (1,1)	EGARCH (1,1)	TGARCH (1,1)	APARCH (1,1)
c	0.000185	0.000239	0.000326	0.000290
AR (1)	0.096785	0.024094	-0.000395	0.042853
ω	3.09E-05	-9.270056	2.98E-05	0.000293
α	0.408850	0.146629	0.701530	0.312668
β	-0.014338	0.452038	-0.719931	-0.999827
EGARCH (γ)	-	0.104433	-	0.022363
TGARCH (γ)	-	-	0.016490	-
APARCH (γ)	-	-	-	1.558115
APARCH (σ)	-	-	-	-
Akaike	-7.466962	-7.467414	-7.486394	-7.483704
ARCH	0.003224	0.004723	0.005116	0.007038
Q^2	0.1745	0.5301	1.4906	0.6488

According to the data presented in Table 8, it was concluded that the Myanmar foreign exchange market is highly sensitive to shocks; however, the findings indicate that the effects of these shocks mostly persist for a short period. The analyses identified the TGARCH model as the best-fitting model based on the lowest Akaike Information Criterion value in terms of statistical adequacy. The results suggest that natural disasters or external shocks in Myanmar may lead to high but short-lived volatility fluctuations in the exchange rate.

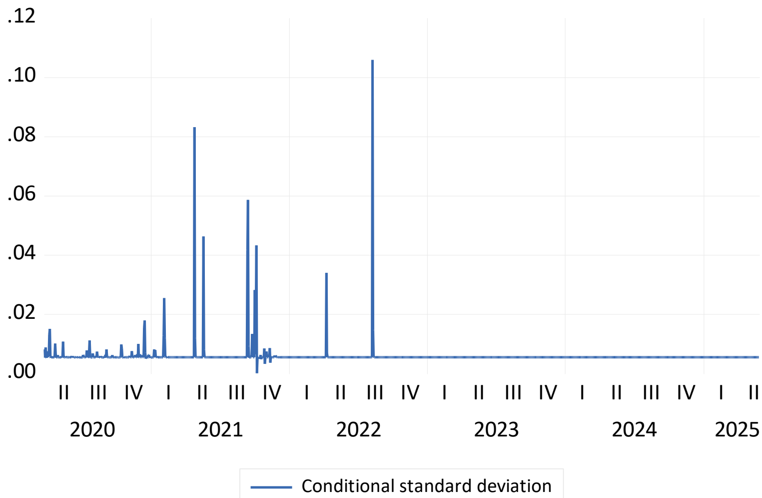

Figure 6. Conditional standard deviation of the USD/MMK exchange rate

Figure 6 illustrates the time variation of the estimated conditional standard deviation values for the USD/MMK exchange rate. This graph was obtained using the GARCH model to reveal the volatility dynamics of the exchange rate. A noticeable upward trend can be observed starting from mid-2020. Throughout 2021, sharp spikes in volatility occurred, reflecting increased uncertainty and fluctuations in the markets, followed by a period of relative stability.

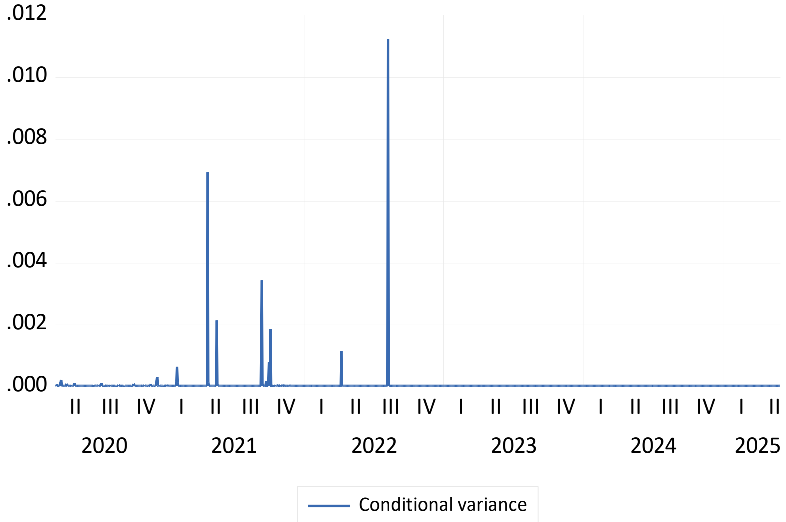

Figure 7. Conditional variance of the USD/MMK exchange rate

The graph presented in Figure 7 depicts the conditional variance values obtained for the USD/MMK exchange rate. Notably, significant increases in volatility were observed during 2021 and 2022. The consecutive spikes in 2021 indicate substantial uncertainty in the market. Thus, the heightened volatility of the exchange rate during this period is interpreted as a reflection of its high sensitivity to economic, political, or external shocks. However, starting from 2023, the variance values have declined to near zero, maintaining very low levels.

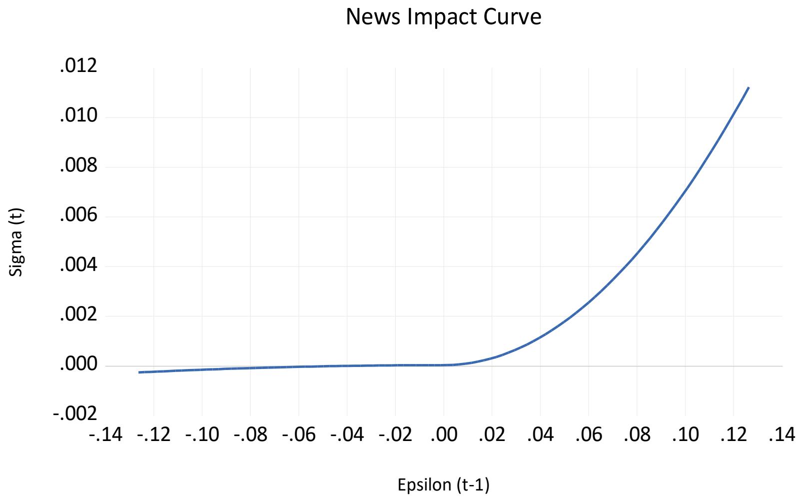

Figure 8. News ımpact curve of the USD/MMK exchange rate

As shown in Figure 8, positive shocks have a clearly increasing effect on the conditional variance along the curve. However, the impact of negative shocks on the conditional variance of the USD/MMK exchange rate appears to be limited or almost negligible. In this context, it is assessed that positive news or upward movements in the exchange rate lead to higher levels of volatility in the USD/MMK market, whereas adverse shocks exert a weaker effect.

Conclusion

This study aims to comparatively analyze the volatility effects of recent natural disasters in developing countries on international currency markets, using the cases of Türkiye and Myanmar. Volatility fluctuations observed in financial markets following large-scale earthquakes in both countries were examined through GARCH-type models. The findings reveal that natural disasters generate asymmetric effects on financial markets, and that the magnitude and duration of these effects vary depending on the countries' economic and financial structures.

In the methodological part of the study, a significant increase in volatility was observed in the USD/TRY exchange rate following the earthquakes centered in Kahramanmaraş on February 6, 2023. Within the framework of the TGARCH model, it was found that negative shocks had a significant impact on volatility. In this context, it was determined that negative news increases uncertainty and risk in the market, consequently amplifying exchange rate fluctuations. Based on data from the 2020–2025 period, the analysis for Myanmar identified periodic fluctuations and rising volatility trends in the USD/MMK exchange rate following the Sagaing earthquake.

When comparing the volatility patterns of the two countries, it was observed that fluctuations in the USD/TRY exchange rate were more persistent and of greater magnitude in the case of Türkiye, whereas the increase in volatility in Myanmar was more short-lived and limited. The TGARCH model was found to be the most appropriate for both countries, although the response to shocks appeared to be relatively milder in Myanmar. These differences are considered to stem from the divergence in financial market depth, macroeconomic fundamentals, and structural factors influencing investor behavior in the two countries.

The results obtained are largely consistent with the post-disaster market reactions reported in prior studies such as Ferreira and Karali (2015), Worthington (2008), and Fakhry et al. (2018). In this context, by comparatively examining two distinct developing countries, the study aims to make an original contribution to the existing literature by focusing on asymmetric volatility responses and news impact curves in financial markets. In conclusion, this research concretely demonstrates the volatility-increasing effects of natural disasters on the currency markets of developing countries and provides an empirical basis for understanding financial market dynamics.

Recommendations

For future studies, the effects of various types of natural disasters on financial markets can be examined in different countries by employing models other than the GARCH-type models used in this research. Additionally, economic impacts can be analyzed in greater detail by considering short- and long-term volatility changes, machine learning techniques, and multivariate models. Furthermore, sectoral analyses can be conducted to investigate the effects of natural disasters on sector-specific market dynamics.

Scientific Ethics Declaration

* The author declares that the scientific ethical and legal responsibility of this article published in EPSTEM journal belongs to the author.

Conflict of Interest

* No conflicts of interest

Funding

* This study received no external funding.

Acknowledgements or Notes

* This article was presented as an oral presentation at the International Conference on Research in Engineering, Technology and Science (www.icrets.net) held in Peja/Kosovo on July 10-13, 2025.

References

Akcay, A.O., Karahan, E., Bozan, M.A., Ardic, F., & Garan, O. (2023). Design-based natural disaster education practices for primary school teachers. *Journal of Education in Science, Environment and Health (JESEH), 9*(2), 146-161. https://doi.org/10.55549/jeseh.1279773

Al Rahahleh, N., & Kao, R. (2018). Forecasting volatility: Evidence from the Saudi stock market. *Journal of Risk and Financial Management, 11*(4), 84.

Bollerslev, T. (1986). Generalized autoregressive conditional heteroskedasticity. *Journal of Econometrics, 32,* 307-327.

Bourdeau-Brien, M., & Kryzanowski, L. (2017). The impact of natural disasters on the stock returns and volatilities of local firms. *The Quarterly Review of Economics and Finance, 63*, 259-270.

Cabuk, A., Cabuk, S. N., Ozenen-Kavlak, M., & Caki, A. (2025). Learning from Nature: Recommendations for the Process of Rebuilding Antakya After the 6th February Earthquakes. *The Eurasia Proceedings of Educational and Social Sciences*, *43*, 96-101.

Charles, A., & Darné, O. (2021). Econometric history of the growth–volatility relationship in the USA: 1919–2017. *Cliometrica, 15*(2), 419-442.

Dickey, D.A., & Fuller, W.A. (1981). Likelihood ratio statistics for autoregressive time series with a unit root. *Econometrica, 49*(4), 1057-1072.

Ding, Z., Granger, C. W. J., & Engle, R. F. (1993). A long memory property of stock market returns and a new model. *Journal of Empirical Finance*, *1*(1), 83–106

Engle, R.F. (1979). *A general approach to the construction of model diagnostics based upon the lagrange multiplier principle*. The Warwick Economics Research Paper Series, University of Warwick.

Ewing, B. T., & Malik, F. (2016). Volatility spillovers between oil prices and the stock market under structural breaks. *Global Finance Journal*, *29*, 12–23.

Fakhry, B., Aktan, B., Masood, O., Tvaronavičienė, M., & Celik, S. (2018). The impact of a recent natural disaster on the Japanese financial markets: Empirical evidence. *Journal of Competitiveness, 10*(2), 56.

Ferreira, S., & Karali, B. (2015). Do earthquakes shake stock markets?. *PloS one, 10*(7), e0133319.

Galido, A. P., & Marites, A. (2013). Natural disasters and the Philippine stock exchange index: A garch-m analysis. *DLSU Business & Economics Review, 22*(2), 54-63.

Montero, J. M., Naimy, V., Abi Farraj, N., & El Khoury, R. (2024). Natural disasters, stock price volatility in the property-liability insurance market and sustainability: An unexplored link. *Socio-Economic Planning Sciences, 91*, 101791.

Ndei, C. M., Muchina, S., & Waweru, K. (2019). Modeling stock market return volatility in the presence of structural breaks: Evidence from Nairobi securities exchange, Kenya. *International Journal of Research in Business and Social Science, 8*(5), 156-171.

Nelson, D. B. (1991). Conditional heteroskedasticity in asset returns: A new approach. *Econometrica*, *59*(2), 347–370.

Odell, K. A., & Weidenmier, M. D. (2004). Real shock, monetary aftershock: The 1906 San Francisco earthquake and the panic of 1907. *The Journal of Economic History, 64*(4), 1002-1027.

Panwar, V., & Sen, S. (2019). Economic impact of natural disasters: An empirical re-examination. *Margin: The Journal of Applied Economic Research, 13*(1), 109-139.

Phillips, P.C., & Perron, P. (1988). Testing for a unit root in time series regression. *Biometrika,75*(2), 335-346.

Tao, Z., Zheng, X., Wang, X., Han, L., Huang, Y., Li, J., & Tao, Z. (2022). Economic resilience in California against two earthquakes. *International Journal of Disaster Risk Reduction, 76*, 102993.

Thomann, C. (2013). The impact of catastrophes on insurer stock volatility. *Journal of Risk and Insurance, 80*(1), 65-94.

Türk Dil Kurumu. (2025). *Doğal afet*. Türk Dil Kurumu Güncel Türkçe Sözlük. Retrieved from: https://sozluk.gov.tr/

Wang, L., & Kutan, A. M. (2013). The impact of natural disasters on stock markets: Evidence from Japan and the US. *Comparative Economic Studies, 55*(4), 672-686.

Worthington, A. C. (2008). The impact of natural events and disasters on the Australian stock market: A GARCH-M analysis of storms, floods, cyclones, earthquakes and bushfires. *Global Business and Economics Review, 10*(1), 1-10.

Worthington, A., & Valadkhani, A. (2004). Measuring the impact of natural disasters on capital markets: An empirical application using intervention analysis. *Applied Economics, 36*(19), 2177-2186.

Yamori, N., & Kobayashi, T. (2002). Do Japanese insurers benefit from a catastrophic event?: Market reactions to the 1995 Hanshin–Awaji earthquake. *Journal of the Japanese and international economies, 16*(1), 92-108.

Yang, C. C., Wang, M., & Chen, X. (2008). Catastrophe effects on stock markets and catastrophe risk securitization. *The Journal of Risk Finance, 9*(3), 232-243.

Zakoian, J.-M. (1994). Threshold heteroskedastic models. *Journal of Economic Dynamics and Control*, *18*(5), 931–955.

Author(s) Information

Beste Alpaslan
OSTIM Technical University
Ankara, Türkiye
Contact e-mail: *beste.alpaslan@ostimteknik.edu.tr*

To cite this article:

Alpaslan, B. (2025). Comparative analysis of the effects of natural disasters on volatility in money and capital markets: The cases of Türkiye and Myanmar. *The Eurasia Proceedings of Science, Technology, Engineering and Mathematics (EPSTEM), 35,* 140-152.

The Eurasia Proceedings of Science, Technology, Engineering & Mathematics (EPSTEM)
ISSN: 2602-3199

The Eurasia Proceedings of Science, Technology, Engineering and Mathematics (EPSTEM), 2025

Volume 35, Pages 153-171

ICRETS 2025: International Conference on Research in Engineering, Technology and Science

Development of Experimental Equipment for Testing Fire Extinguishing Nozzles in Underground Mining Sites

Diana Makedonska
University of Mining and Geology St. Ivan Rilski

Vasil Tsanov
Academy of Ministry of Interior

Abstract: The paper reviews the dispersion characteristics of sprinkler nozzles and the possibility for introducing them in underground facilities. For this purpose, a stand has been designed and constructed for simultaneous testing of two nozzles, intended for areas where it is impossible to build larger installations (Shopov & Bonev, 2019) (due to restrictions in the mass of the facility and its reinforcement in the rock massifs in underground conditions). The possibilities and scope of application of water fire extinguishing systems have been established through experimental research of the spraying intensity of the water jet on a protected area. At the same time, based on a study of the dispersion characteristics of sprinkler and spiral nozzles and screw sprinklers, the optimal choice of a fire extinguishing system has been analyzed. The presented comparative analysis of the data from the measurements focuses on the applicability in existing underground facilities.

Keywords: Mining sites, Sprinkler nozzles, Fire safety, Test bench

Introduction

Fire safety is extremely important for the protection of life and property. Fires can occur anywhere, at any time, and can spread quickly, causing significant damage in a short time. (Ivanov & Tsankov, 2018). The development of highly effective fire prevention and control systems is of paramount importance, taking into account the dynamics of the occurrence and development of fires in underground facilities. In this regard, it is necessary to have equipment with automatic fire protection systems, designed both for early detection and extinguishing of emerging fires, and for fire extinguishing with water or other extinguishing agents (Tsankov, 2024) in the conditions under consideration.

To ensure the reliability and effectiveness of fire protection systems in underground mining sites (Borghetti, & Derudi, 2016; Beard & Carvel, 2012) and in connection with the increasing requirements of fire safety, the issue of designing and building a test stand for sprinkler nozzles for extinguishing fires is particularly relevant. Sprinkler installations (Yordanov, Klisarski & Nenov, 2018) can completely extinguish a fire or localize it, i.e. restrain the spread of fire until the arrival of emergency and rescue teams. (Koychev, Chochev & Nenov, 1998) Their ability to automatically trigger water jets upon detection of fire or high temperature (Nenov, Lepniyski & Popova, 2001) makes them particularly suitable for use in underground sites.

Relevance of the Problem

Fires in the mining industry have an adverse impact on the processes of extraction and processing of mineral raw materials, including on the complex mechanization in underground workings and in open pit mines and quarries (Aleksandrova & Koprev, 2015; Aleksandrova & Asenovski, 2019). The negative consequences of fires

- Selection and peer-review under responsibility of the Organizing Committee of the Conference

or explosions in the above-mentioned sites are often manifested in major material damage, encompassing production equipment, buildings and facilities, which can lead to a long-term suspension or forced closure of production activities due to financial insolvency (Aleksandrova, 2007). Underground and surface self-propelled and mobile mining equipment, underground fuel storage areas, buildings and equipment for enrichment and processing of ore at the surface and auxiliary facilities are associated with these activities.

Fire and ore processing facilities associated with them include combustible and flammable reagents, dielectric and hydraulic oils, electrical cables (Ivanov & Tsankov, 2018), and combustible structures. Due to these hazards, significant fires and explosions can occur in enrichment plants (Tsankov, 2021). Fig. 1 presents a graph of the distribution of fires according to the heat source, and Fig. 2 shows the distribution of fires according to the extinguishing agents used.

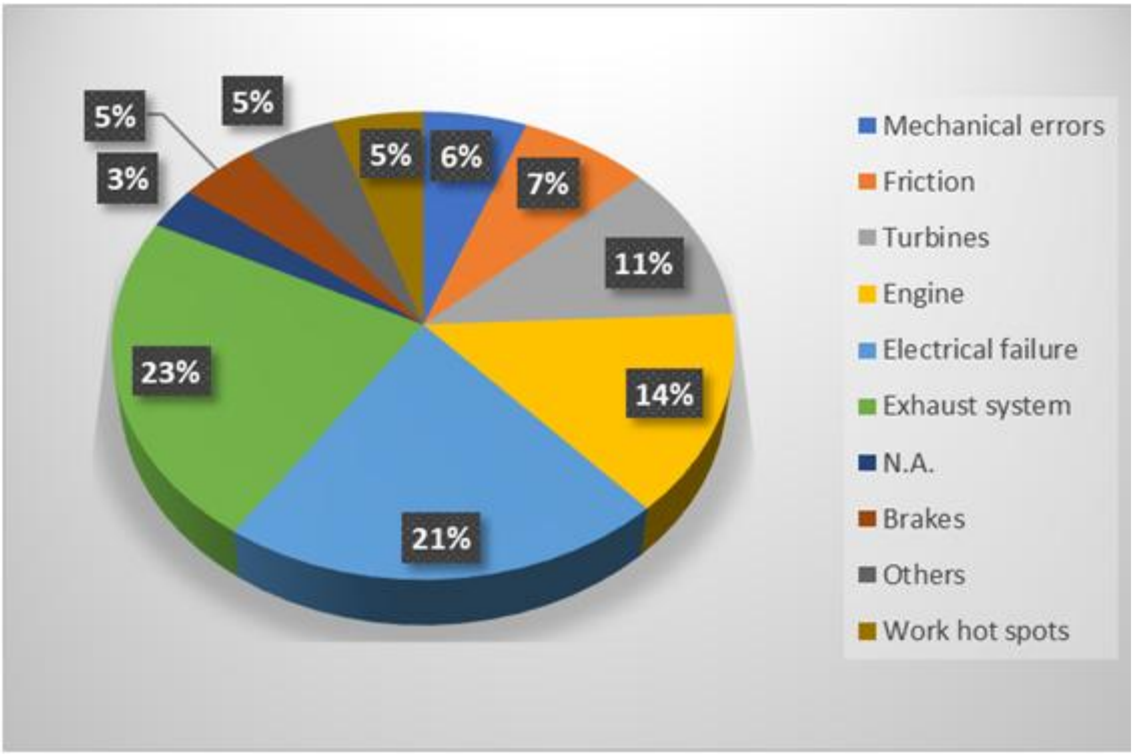

Figure 1. Fire distribution according to the heat source used

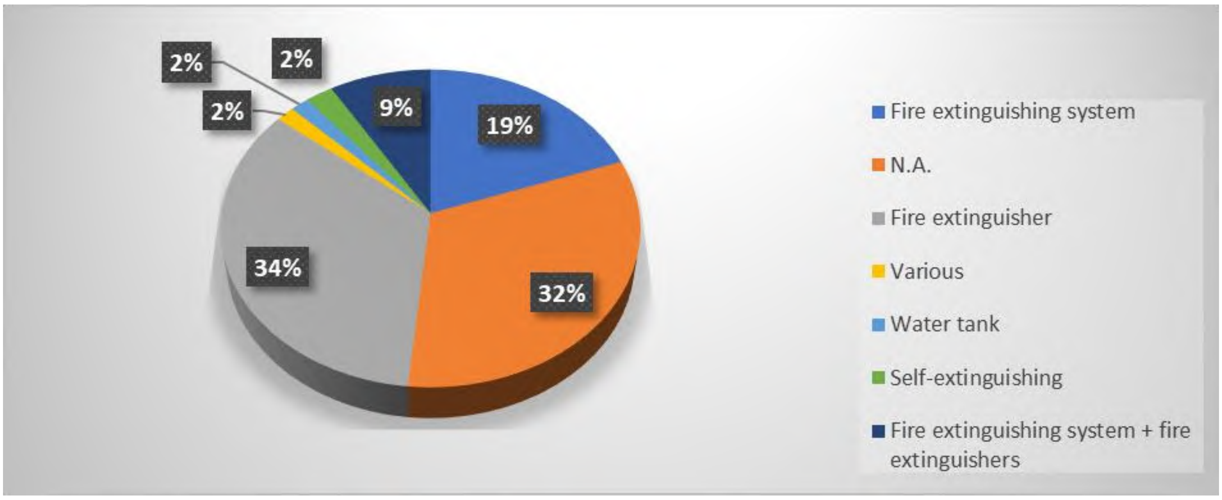

Figure 2. Distribution of fires according to the type of extinguishing agents used

Most fires involving mobile or self-propelled mining equipment (Fig. 3 and Fig. 4) - whether underground or surface - occur on or near engine exhaust systems, high-speed drive lines, malfunctioning high-pressure, high-temperature hydraulic systems, or faulty electrical components.

Figure 3. Fire in mobile equipment in an underground metal ore mine in Bulgaria (author's personal archive)

Figure 4 Explosives fire in an underground metal ore mine in Bulgaria (author's personal archive)

Completely eliminating the fire hazards of equipment is impossible because ignition sources and fuel for fires are inherent in the basic design of the equipment. The problem of fires is further complicated by the accumulation of environmental waste. Therefore, efforts to reduce fire losses from mobile equipment should be directed towards preventing and extinguishing fires. The situation of fires in underground mobile equipment (Hansen, 2009) can be seen in Figure 5 and the type of mobile equipment involved in the fires is shown in Figure 6.

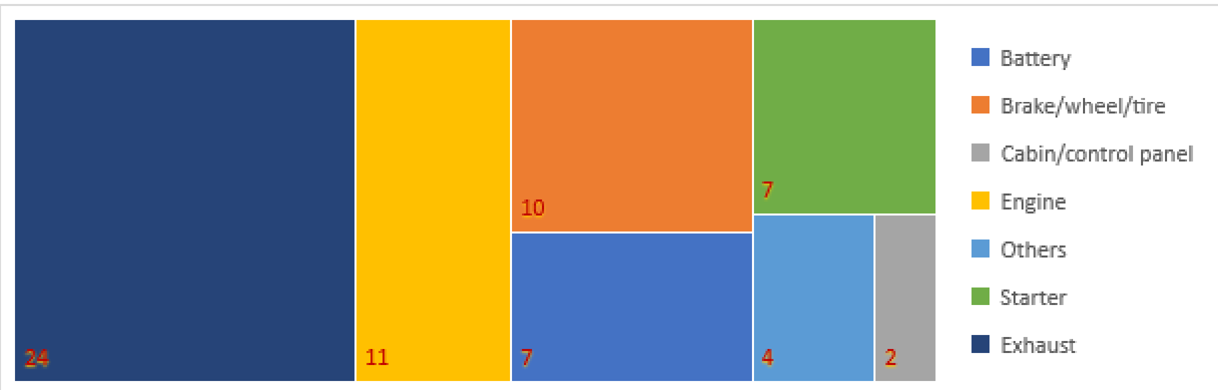

Figure 5. Distribution of fires in underground mobile equipment according to the structural location of occurrence

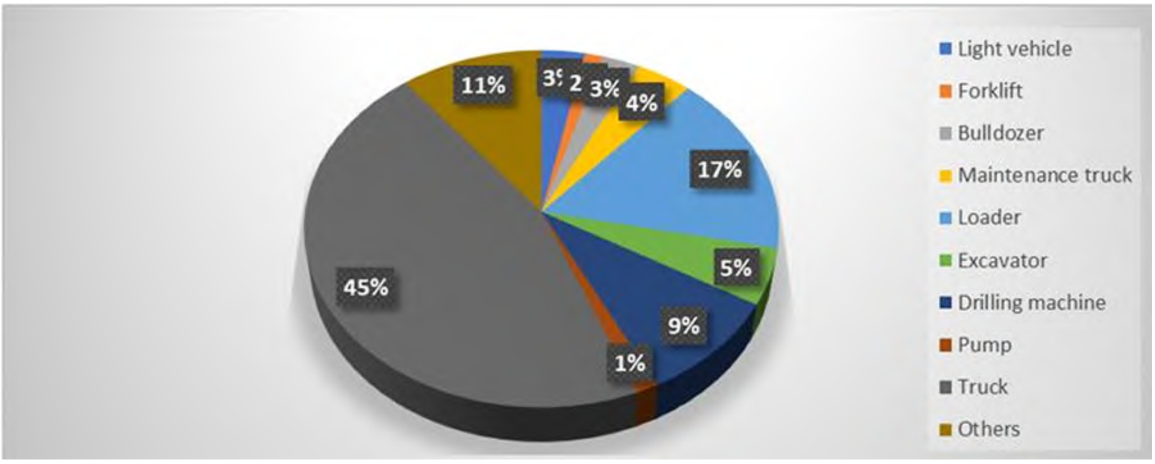

Figure 6. Distribution of fires in mobile equipment by vehicle type

The analysis of the data shows that of the mobile equipment involved in the fires, heavy trucks account for the largest share, followed by loaders and drilling machines. Fires in vehicles/mobile equipment in underground mines are more common than fires in open pit mines. Most fires are extinguished using fire extinguishers. In about one third of fires where a fire suppression system was applied, one or more fire extinguishers were also used.

In order to improve the fire protection and prevention of mining equipment, some mining equipment manufacturers have emphasized the reduction of the fire potential of specific elements in the original design of their equipment. Such elements include turbochargers, exhaust manifolds and exhaust pipe screens and insulation, the location of flammable and combustible liquid tanks, and the routing of hydraulic and fuel lines. This inevitably affects mining technology, the geometric parameters of underground mine workings, mining equipment and the overall planning of production costs. (Aleksandrova & Zlatanov, 2008). The risk of fires in underground mines is greatest in workings with belt conveyors. According to statistics, underground fires in Russia, Ukraine and Kazakhstan (Gavrilova, 2019) most often occur in the following places (Fig. 7):

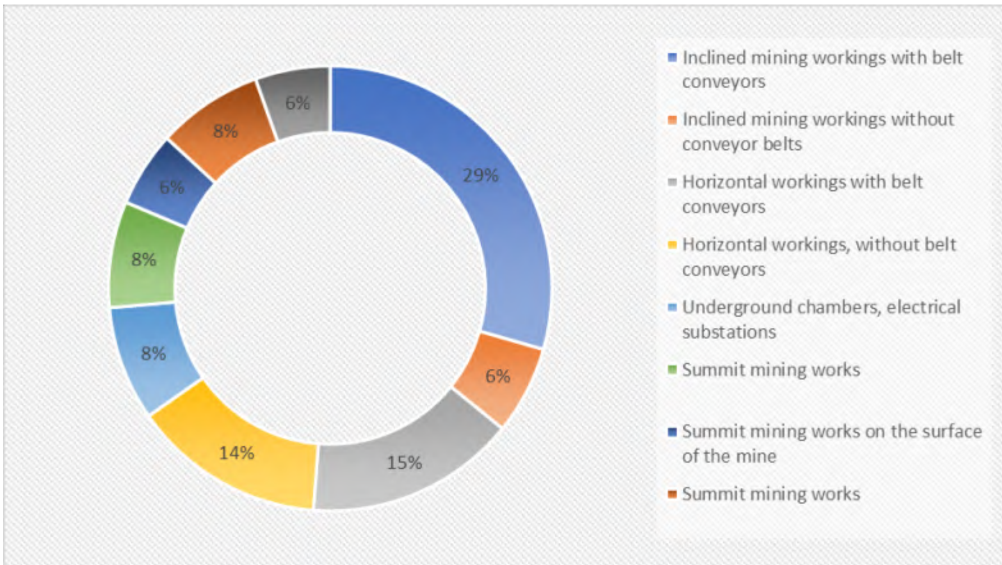

Figure 7. Location of fires starting in underground mines in Russia, Ukraine and Kazakhstan

Material losses from fires on belt conveyors in underground mines in different countries range from 18% to 27% of all unforeseen emergency losses in them. Investigations of fires that occurred on belt conveyors (Fig. 8) led to the formulation of the following conclusions. Fires in mining workings with belt transportation occur under the following circumstances:

- friction during slipping (emergency sliding) of the belt on the driving drum;
- friction of the belt in non-driving end (reversing) or tensioning drums;
- friction of the belt in non-rotating rollers;

- friction of the belt in the metal structure of the conveyor;
- friction of the belt in metal elements of the fastening or in the walls of the working;
- short circuit of electrical equipment of the conveyor and in the electrical network
- ignition from external sources.

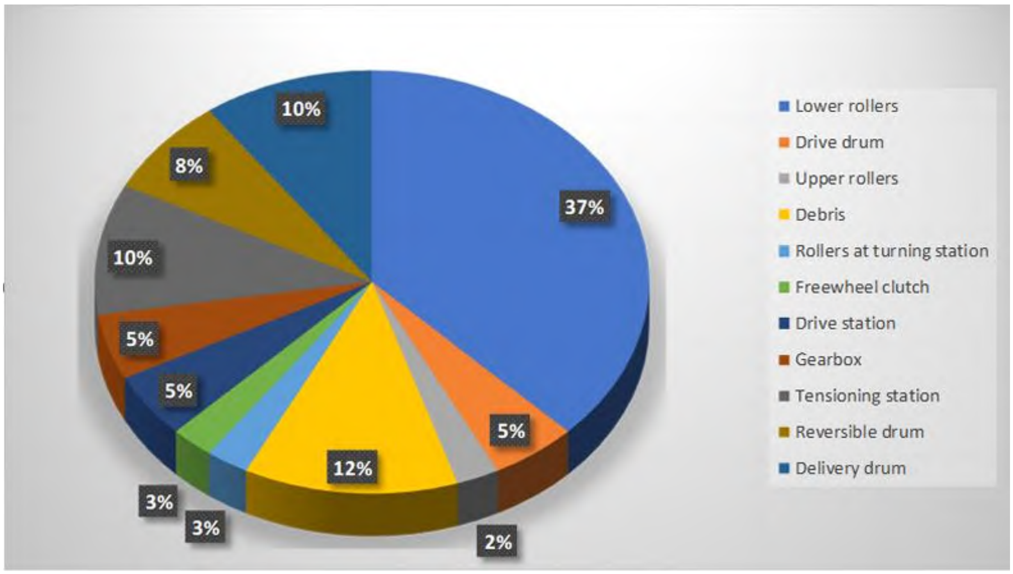

Figure 8. Average data for reported underground fires on rubber conveyor belts

Conveyor belts pose a serious risk as they have the ability to spread fire over long distances. Most mining facilities should have at least one portable fire extinguisher installed in an easily accessible location. Fire extinguishers are most effective when used by trained operators. However, given the size and configuration of the machinery found in underground mines, fires can be difficult or impossible to extinguish with a portable fire extinguisher. For this reason, fire suppression systems have been developed to help extinguish those fires that are difficult to reach, thereby reducing damage and loss (Michaylov, Krilchev & Vladkova 2011). Automatic fire suppression systems, combined with adequate emergency response, are effective in limiting fire damage. Fire suppression systems, including portable fire extinguishers, offer the mining industry a cost-effective tool for protecting personnel and investments in mining equipment.

Causes of Fires in Underground Mining Sites

The causes of fires in the underground mining industry are shown in Fig. 9.

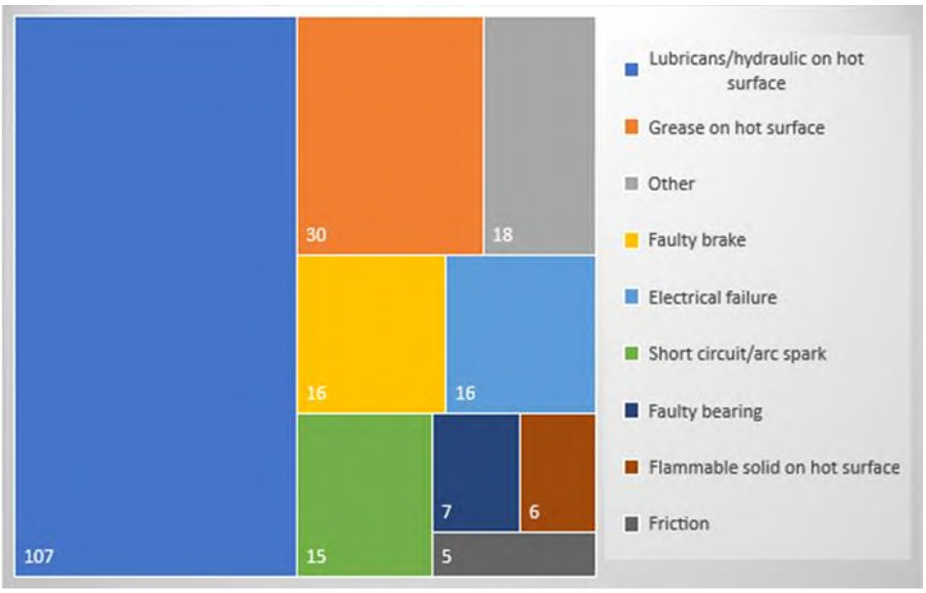

Figure 9. Fractional distribution of fire causes in underground mines

The most common cause of fire is engine, transmission, gear, hydraulic and/or similar technical oils on a hot surface. Followed by diesel in contact with a hot surface and damaged brakes. The engine area is the section of the vehicle where most fires occur, and the specific component of the vehicle where most fires occur is exhaust. Fires can also be caused by forgotten rags on hot surfaces, improperly installed components, etc.

Fire Safety in Underground Mines

Fire safety in underground mines is critically important due to the particular conditions and risks associated with working in an underground environment. For mining companies, the issues of evacuation and rescue operations in the event of a fire are closely linked to the policies, the protection of the working environment and their systematic work on fire safety. The main problem with mines today is that they are becoming increasingly complex, with an endless number of galleries, shafts, ramps and crossings, and it is difficult to control the way smoke and heat spread in the event of a fire. The design of fire protection systems should be based on a fire study carried out in accordance with standards. Automatic fire alarm systems installed in areas where there is a significant risk of fire can provide early warning. Such areas include:

• explosives fillers
• storage of ammonium nitrate emulsion and solid ammonium nitrate
• fuel stores, fuel loading bays and transfer equipment
• combustible material stores
• conveyor transport
• substations and oil transformers.

Smoke detection systems installed at the top of galleries can provide general warning of fire. Continuous thermal monitoring and maintenance of a fixed installation should be installed where the operation of such equipment presents a significant risk of fire underground. Stationary fire extinguishing systems must be installed in emulsion storage areas (Fig. 10).

Figure 10. Fire extinguishing system in an emulsion warehouse in an underground metal mine in Bulgaria (personal archive)

The activation of the fire extinguishing system should be triggered by an alarm on the surface for stationary equipment or in the operator's cabin for mobile equipment. In the mining industry, as in all industries, the main emphasis is placed on safety and adequate training, health and safety risks at work and improving its achievements in this area. Conveyor belts (Fig. 11) are part of the machines that are the source of many accidents, deaths and fires every year. The continuous-action transport machine is known in practice as a rubber-belt conveyor. In the mining industry, mining transport systems with very high productivity can be obtained by means of working together with mining machines such as rotary excavators. For these reasons, the use of rubber-belt conveyors in underground mining is widespread, and the installed driving power of each machine can reach 8-10 MW.

Figure 11. Stationary fire extinguishing installation mounted on a rubber conveyor belt in an underground mine from the mining industry (personal archive)

In many countries and regions, the installation of fire protection systems in underground mines is mandatory according to local and international safety standards. In Bulgaria, stationary fire extinguishing installations on belt conveyors have also been built (Fig. 25). Measuring and visualizing the velocity field in confined and semi-confined spaces will help to pre-assess the velocity field before activating the nozzles and thus predict what the impact on the “flooding” of the areas with water will be and how far the drops will be carried before reaching the floor or the protected surface (Dinchev, Gorbounov & Kostadinova 2018).

Their timely activation can quickly extinguish a fire, reducing the risk of fire spreading in the mine. This is especially important in confined and difficult-to-access spaces such as underground mines. Rapid fire suppression can prevent serious damage to equipment and infrastructure, while preserving the integrity of the conveyor. Ensuring a safe working environment by reducing the risk of fires is key to the health and safety of workers.

Standards and Regulations When Testing Nozzles

The design of fire protection systems is carried out in accordance with the requirements set out in the laws and regulations of each country. For the conditions of the Republic of Bulgaria, the European Union and the USA, the following major standards and regulatory documents apply:

Standards and Regulations

BS EN 12259-1:1999 Fixed firefighting systems-Components for sprinkler and water spray systems —Part 1:

Sprinklers

This European Standard specifies requirements for construction and performance of sprinklers which are operated by a change of state of an element or bursting of a glass bulb under the influence of heat, for use in automatic sprinkler systems conforming to EN 12845, Automatic sprinkler systems — Design and installation. Test methods and a recommended test schedule for type approval testing are also given.

BS EN 12845:2004+A2:2009 Fixed firefighting systems. Automatic sprinkler systems. Design, installation and maintenance

BS EN 12845 sets out the minimum requirements for the design, installation and maintenance of fixed fire sprinklers in buildings and industrial plants. These best-practice recommendations also apply to any addition, extension, repair or modification to built-in fire extinguishers. BS EN 12845 looks at the classification systems of hazards, the provision of water supply, and the components that are used in the installation, performance testing, maintenance and the extension of existing systems. It also identifies the construction details of buildings.

The EN 54 Fire detection and fire alarm systems is a series of European standards that includes product standards and application guidelines for fire detection and fire alarm systems as well as voice alarm systems.

DS CEN/TS 14816:2008 Fixed firefighting systems - Water spray systems - Design, installation and maintenance.

This standard specifies requirements and gives recommendations for the design, installation and maintenance of fixed deluge water spray systems internal and external to buildings and industrial plant and other premises on land. This standard covers only the use of the types of sprinklers and sprayers specified in EN 12259-1. The requirements and recommendations of this standard are also applicable to any addition, extension, repair or other modification to a water spray system.

NFPA 502:2023 Standard for Road Tunnels, Bridges, and Other Limited Access Highways

This standard provides fire protection and fire-life safety requirements for limited access highways, road tunnels, bridges, elevated highways, depressed highways, and roadways that are located beneath air-right structures.

NFPA 122, Standard for Fire Prevention and Control in Metal/Nonmetal Mining and Metal Mineral Processing Facilities 2020 ed.

Mining and mineral processing facilities represent significant fire and explosion exposures to both personnel and production equipment and buildings. Critical to safety, the 2015 NFPA 122 Standard for Fire Prevention and Control in Metal/Nonmetal Mining and Metal Mineral Processing Facilities addresses the protection of diesel-powered equipment and storage and handling of flammable and combustible liquids at these specialized sites.

NFPA 120 Standard for Fire Prevention and Control in Coal Mines

This standard covers minimum requirements for reducing loss of life and property from fire and explosion in underground bituminous coal mines, coal preparation plants designed to prepare coal for shipment, surface building and facilities associated with coal mining and preparation, and surface coal and lignite mines.

Theoretical Background

Automatic Stationary Fire Extinguishing Installations

A stationary fire extinguishing installation is understood to be a stationary system consisting of a certain supply of fire extinguishing agent, connected to one or more stationary nozzles, through which the agent is supplied manually or automatically, for extinguishing a fire. Fire extinguishing installations, as one of the technical means of fire protection, are used in those cases when fires in their initial stage can develop intensively and cause an explosion, destruction of structures, disrupt the normal operation of responsible systems of the protected site, and cause large material losses.

Automatic Sprinkler Systems

Automatic sprinkler systems are designed to detect a fire and extinguish it with water in its initial stages or to keep the fire under control so that its extinguishing can be completed by other means. A sprinkler system (Chochev, 2013) consists of a water supply (water pipe or tank and pump group) and one or more sprinkler installations. Each sprinkler installation consists of a control and signal valve and a row of pipes equipped with sprinkler heads. Sprinklers are installed in certain places depending on the protected site. The water supply can be activated, i.e. the system is put into operation to extinguish a fire, either after the opening of a sprinkler located above the fire source, or after a signal from the control unit, as a result of an automatic or manual fire detector being triggered. It is important to take into account the type of pipeline network (Shopov & Bonev, 2019), its regular maintenance (Shopov, Bonev & Brayanov, 2018) and the types of sprinklers (including their geometric and topographical characteristics).

Research Methodology

The methodological program we propose is based on one of the fundamental accepted approximations that the use of water in mining sites should be minimized in terms of its volume. The number of sprinklers needs to be minimized. That is why installations with two nozzles are being studied. This makes the structure lighter and facilitates its maintenance. As we have mentioned, corrosion, vibrations and difficult reinforcement always greatly complicate the engineering activities of fire extinguishing installations and, above all, reduce their reliability. Hence, we propose the following methodology:

1. To examine in detail the international and national standards and regulatory documents regarding stationary fire extinguishing installations, including components of sprinklers and water spraying systems.
2. To create a methodology for determining the intensity of water coverage on the protected area, using a symmetry model relative to the center of the sprayed area.
3. Based on the previous conclusions, to develop a methodology for determining the distribution of drops by size.
4. To construct a stand for testing sprinkler nozzles.
5. To statistically process the results and graphically present them in a diagrammatic form.

In conclusion, draw the appropriate conclusions and redefine the users of this information.

Design and Construction of a Sprinkler Nozzle Test Bench

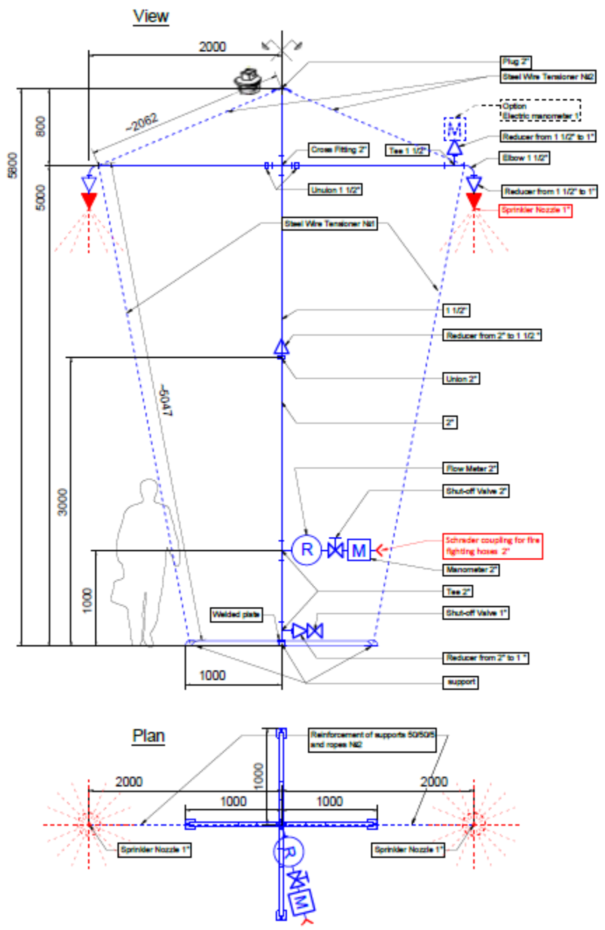

Figure 12. Stand for researching the distribution of the intensity of water jet coverage from sprinkler nozzles

One of the tasks set in the development is to study the dispersion characteristics of fire extinguishing nozzles, with simultaneous operation of two nozzles (Nikolov & Georgiev & Nenov, 2015) in order to optimize the selection of suitable nozzles for the respective system. This study went through experimental measurement of the characteristics of sprinkler nozzles with a specially constructed stand, after which the measurements were processed according to the presented methodology. The design of a fire sprinkler test stand includes several key stages and components that must be taken into account:

- Detailed study of the standards and regulatory requirements in the Republic of Bulgaria, the EU and the USA.
- Determination of the geometric dimensions, depending on the specific application.
- Determination of the parameters to be tested, such as flow rate, pressure and intensity.

After the study, the design of the stand, shown in Fig. 12, was started. The experimental stand was built in the yard of the Laboratory Block of the University of Mining and Geology in Sofia, Bulgaria, and is a tubular structure on a stand, reinforced with metal ropes. The height of the stand is 5.00 m in order to strengthen the handrails on which the tested nozzles will be installed. This height is intended to study the characteristics of fire extinguishing nozzles for use in underground mining sites. The design of the stand is modular with the possibility of reducing the height to 3.00 m and testing nozzles for other applications, such as underground garages, subways, etc.

The distance between the two nozzles is 3 m, which is selected in accordance with the requirements of the standard EN 12845:2015+A1:2020. Stationary fire extinguishing installations. Automatic sprinkler installations. Design, installation and maintenance, taking into account the hazard class in underground sites.

Galvanized pipes - 2", 1.5" and 1" - were used to make the stand, as well as fittings - tees, couplings, elbows, union nuts, etc.

The construction of the stand in real dimensions began with the selection of profiles for making a stand that would ensure the mobility of the stand. Square profiles with a thickness of 5 mm were selected. 4 profiles with a length of 1 m were cut, which were connected by a cross-shaped weld using a welding machine.

Stages in the Design and Construction of the Stand

The main body of the stand is a galvanized pipe with a diameter of 2" and a height of 3 m. Threads are made on both sides of the pipe. Through one thread, the pipe is connected to the stand. A collar is screwed onto the second thread and a transition to a pipe with a diameter of 11/2 "is made. A cross is screwed onto the upper side of the pipe, to which two pipes with a length of 1.5 m and a diameter of 1 ½" are connected, on which the tested nozzles can be mounted using elbows and adapters. Using a pipe with a length of 0.80 cm, mounted on the cross and steel ropes, the resistance of the experimental stand is created.

A hole is drilled into the main pipe of the test stand, to which a "Storz" type connector is welded. A flow meter, a stopcock and a pressure gauge are mounted to the connector, Fig. 13. The devices shown are necessary for controlled water supply and shutdown, as well as measuring the flow rate and monitoring the operating pressure in the system.

Figure 13. Control devices – flow meter and pressure gauge

The working pressure is intended to be provided by a fire hydrant.

Selection of Sprinkler Nozzles for Research

Sprinklers, as well as any other equipment on which the safety of people is dependent, are subject to special requirements. These requirements are regulated in the relevant national and international standards concerning sprinklers and installations constructed with them.

One of the main characteristics of sprinklers is the uniform distribution of water over the protected area. It must be ensured even in the most unfavorable places for irrigation, including under the "dictating", i.e. the most unfavorable located sprinkler, where the water pressure is minimal due to hydraulic losses. In such a task setting, it will be crucial whether the respective sprinkler, under certain operating conditions, will provide the required coverage intensity over the entire protected area, both when operating independently and when two adjacent sprinklers work together.

EN 12259-1 specifies the requirements for the design and performance of sprinklers that operate by changing the state of an element or by breaking a glass ampoule under the influence of heat and are intended for use in automatic sprinkler systems, in accordance with EN 12845.

The company TYCO FIRE & BUILDING PRODUCTS, USA, also presents its own test methods for some characteristics of sprinklers, such as:

- “jet profile” method;
- “cross-section” method;
- “wet wall” method.

The “jet profile” method tests provide information primarily on the type of jet and the spray radius and is most appropriate for use with sprinklers with a standard water spray. However, the data from the jet profile studies do not provide an idea of whether this spray radius is the same in all directions and how it is affected by the spatial orientation and design of the sprinkler. The “cross-section” method shows the actual contour and upper limit of water jet coverage and is primarily used for wall-mounted horizontal sprinklers. In the “wet wall” method, the sprinkler under study is placed within chambers (rooms) of various sizes and areas. It is believed that this method is the best for depicting the type of water jet from wall-mounted sprinklers with extended coverage and residential pendant sprinklers.

In real conditions, due to insufficient extinguishing intensity, the combustion process can develop in an undesirable scenario, when the fire source begins to develop significantly, increasing its area. In this case, there is a risk that more powerful combustion sources will not be extinguished. Unfortunately, among the characteristics of sprinklers offered today by various companies, there are no indicators for the distribution of extinguishing intensity over the protected area. After conducting research in leading companies for the design and construction of sprinkler installations, it was found that over 85% of the sites are equipped with sprinklers with medium water dispersion. Therefore, a TYCO Series sprinkler with a K-factor of 8 and a trigger temperature of 68˚C was chosen as the object of the study (Fig. 14).

Figure 14. Sprinkler nozzle series TY4151

The TYKO series of sprinkler nozzles are designed for both standard and hazardous sites, such as underground sites. Their coating is corrosion resistant. The sprinkler construction is made of copper/brass and the ampoule is made of glass. The glass bulb contains a liquid that expands when exposed to heat. When the rated temperature is reached, the liquid expands enough to break the glass bulb, allowing the sprinkler to activate and water to flow.

Experimental Methodology

Two nozzles are installed on the constructed stand (Fig. 15).

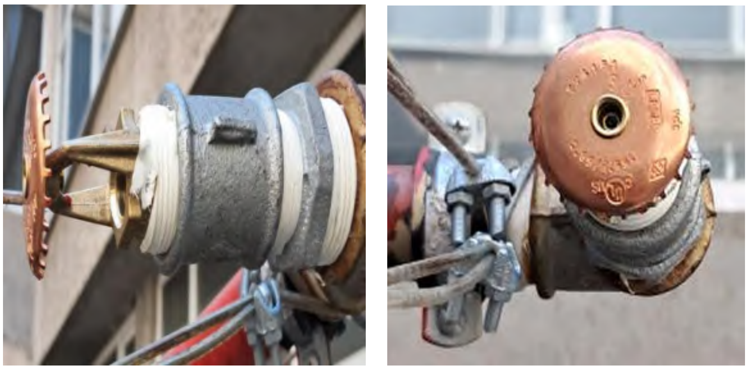

Figure 15. Sprinkler nozzles mounted on the stand

The aim of the experiment is to determine the zone and intensity of irrigation in the investigated irrigation area. In order to determine these characteristics, it is necessary to place identical measuring/collection vessels in the irrigation area, arranged in a checkerboard pattern (Fig. 16).

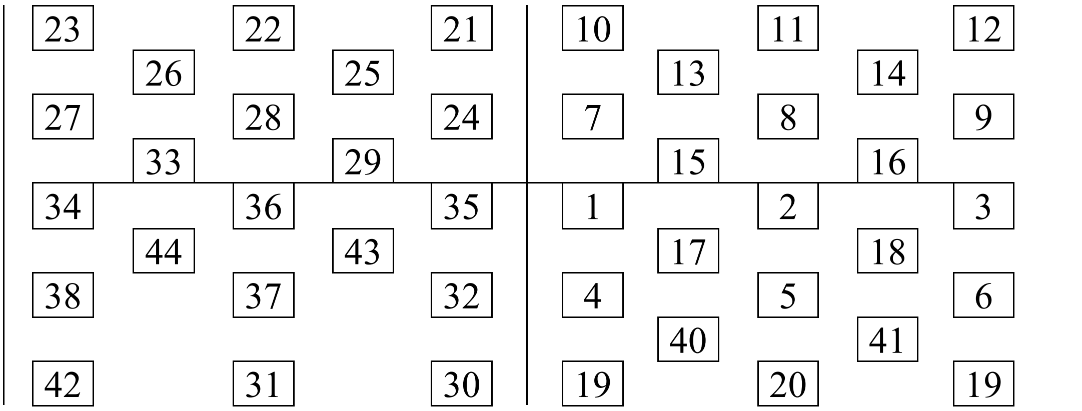

Figure 16. Layout and numbering scheme of water collection vessels

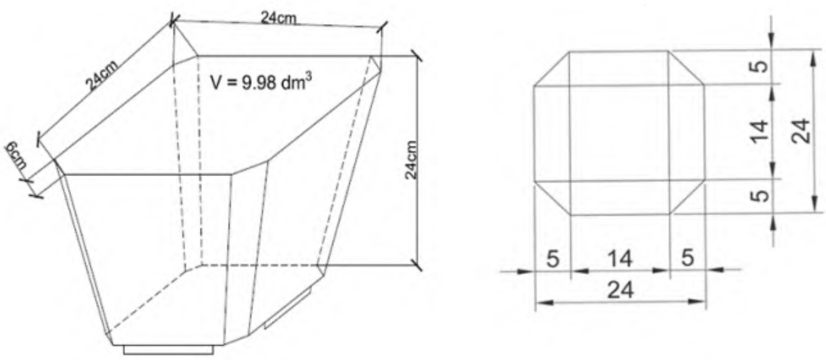

Figure 17. Dimensions of collection container.

The amount of water distributed over the area under the sprinkler is collected using octagonal collection vessels with dimensions: 0.25 x 0.25 x 0.30 m and an area of 1 collection vessel of 0.0526 m2 (Fig. 17). The water content is measured using laboratory measuring cups with capacities of 100 ml, 250 ml, 500 ml and 1000 ml with a reading of ±1 ml, ±2 ml and ±50 ml, respectively, which, when compared to the average content in the measuring vessels, ensures an accuracy of ±1%. The duration of the experiments is between 4 and 10 min. The time is measured with an electronic stopwatch. Two experiments are carried out at different pressures. The working pressure is created by a fire hydrant. After the experiments are completed, the volume of water in each collection vessel is measured. The volume, the time for its receipt and the area of the vessel are the main values for determining the intensity of dew (I), namely:

$$I = \frac{V}{S\tau}\left[\frac{dm^3}{dm^2 min \frac{mm}{min}}\right] \tag{1}$$

where:
V – is the volume of water in the vessel, dm^3; S – is the area of the vessel, dm^2;
τ- is the duration of the experiment, min.
The experimental setup for the experiments is presented in Fig.18.

Figure 18. 3D image of the stand.

Experimental Part and Results

Conducting Experiment 1

Experiment parameters:

Date	18.06.2024
Number of nozzles	2
Type of nozzles	Sprinkler TY4151 – Upright 8.0K, 3/4″ NPT
Pressure	0.8 bar
Duration/time	4 min

An experiment was conducted with two sprinkler nozzles to study the distribution of extinguishing intensity. The location of the collection vessels and the amount of water that has entered them are shown in Fig. 19.

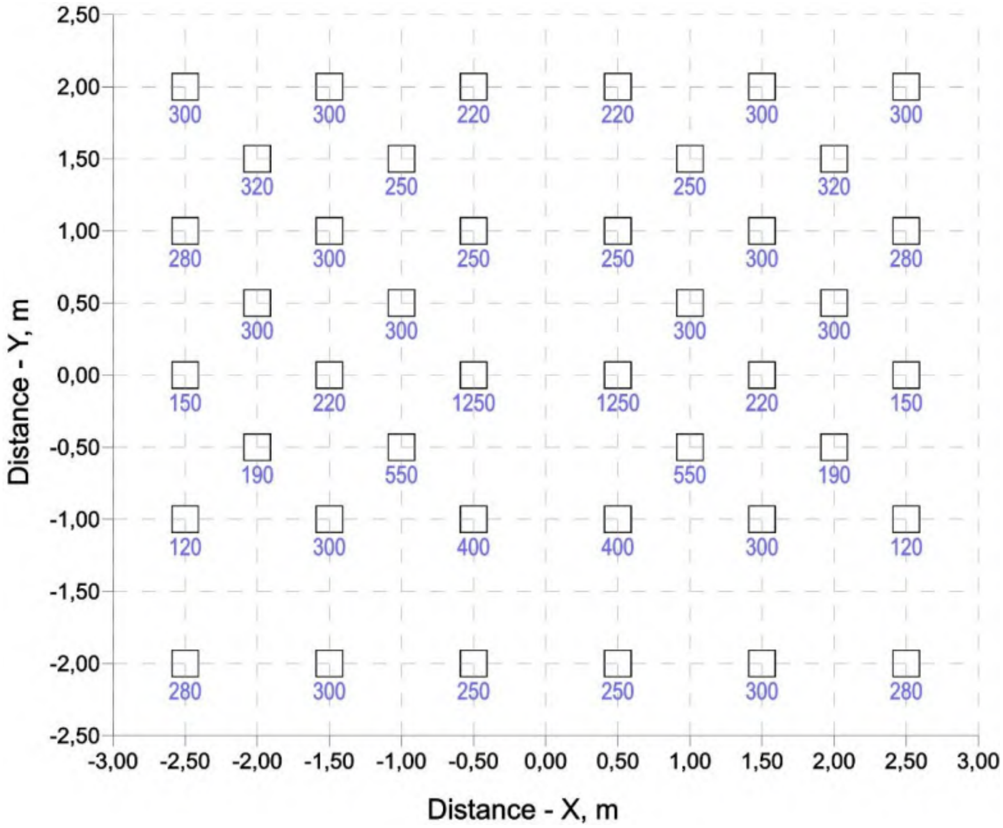

Figure 19. Diagram of the collection of vessels and the amount of water that has fallen

After the experiment was completed, the amount of water in the collection vessels was recorded and the intensity of precipitation was calculated.

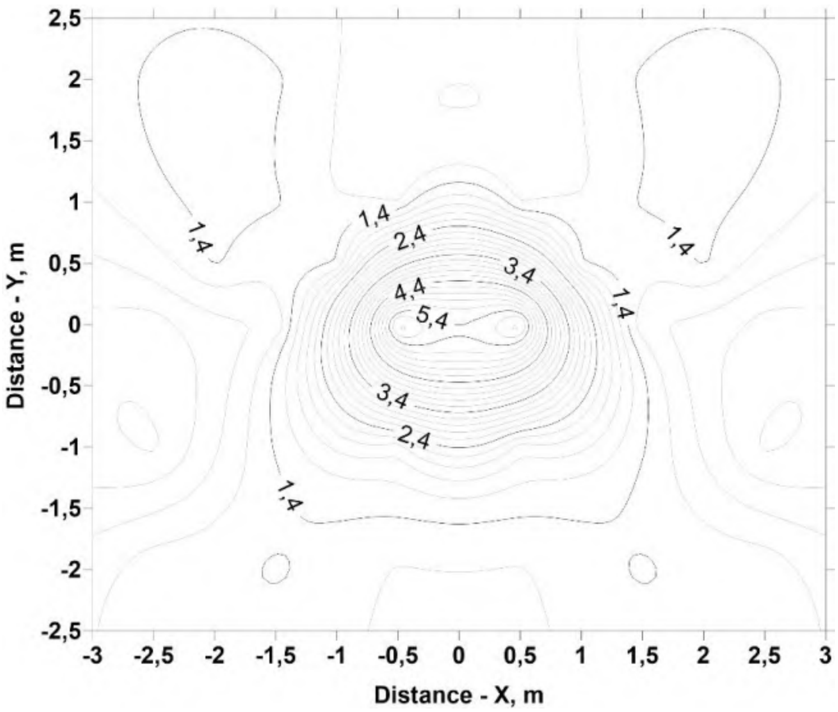

Figure 20a. Isolines of dew intensity [mm/min], P=0.8 bar

Area diagrams of dew intensity were drawn using the Surfer program and are illustrated as contours in Fig. 20a and Fig. 20b, and as volume diagrams in Fig. 21.

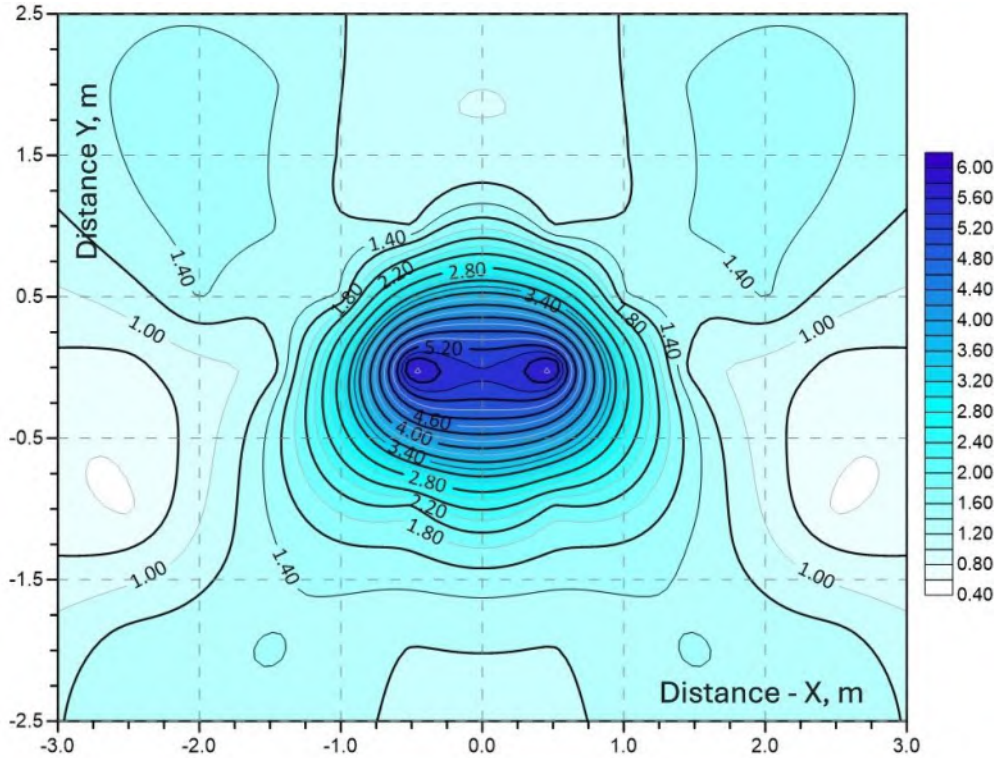

Figure 20b. Isolines of dew intensity [mm/min], P=0.8 bar

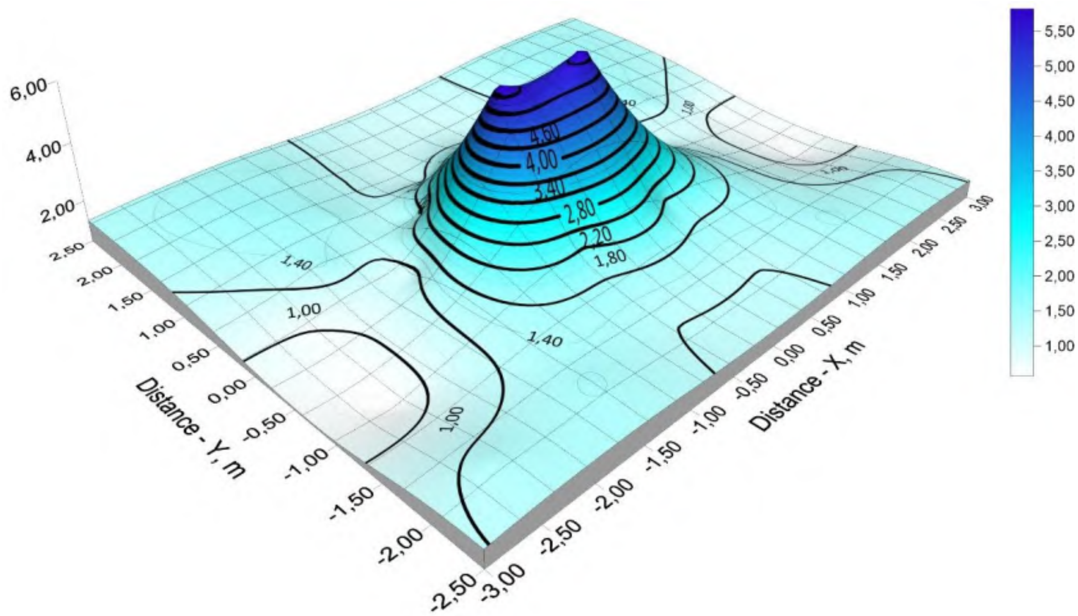

Figure 21. Distribution of water coverage intensity from sprinkler nozzles

Conducting Experiment 2

Experiment Parameters:

Date	04.10.2024
Number of nozzles	2
Type of nozzles	Sprinkler
Pressure	TY4151 – Upright 8.0K, 3/4″ NPT
Duration/time	2 min

A second experiment was conducted with two sprinkler nozzles to study the distribution of gas intensity and pressure of 2 bar. The results of the experiment conducted at a pressure of 2 bar are shown in Fig. 22 and Fig. 23.

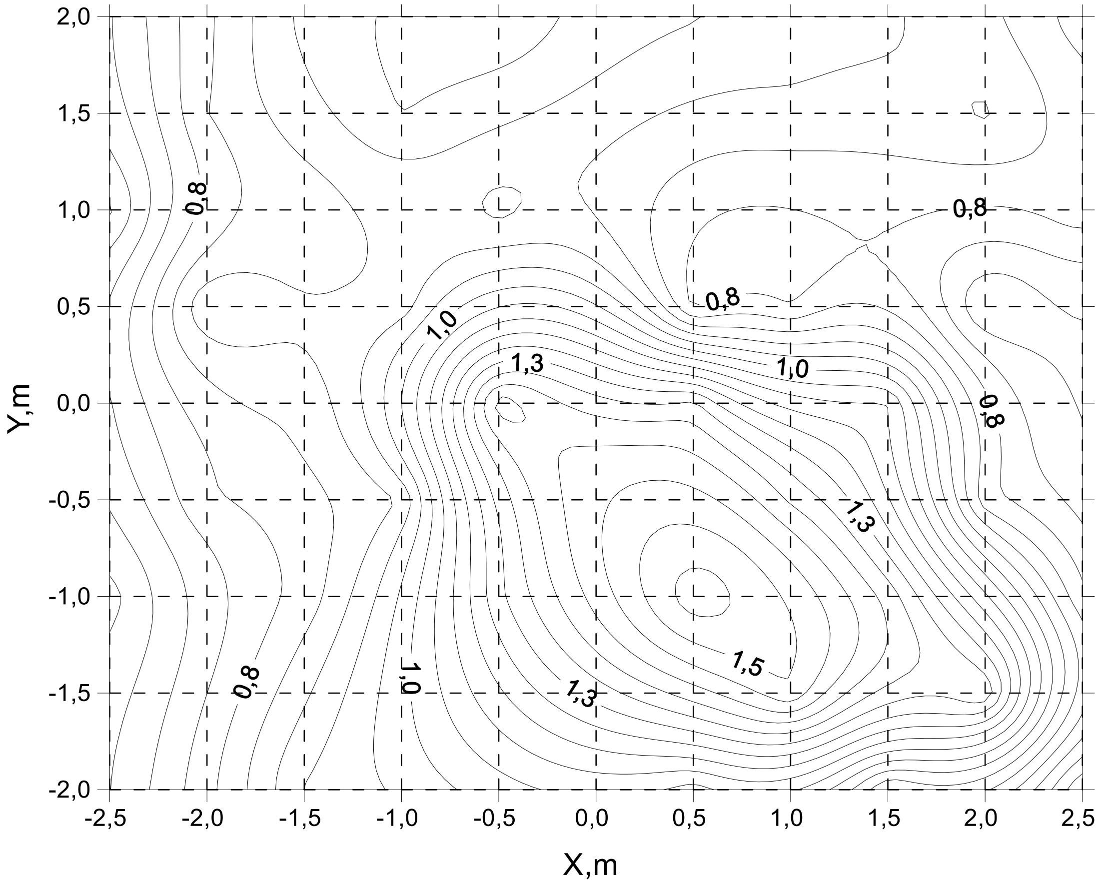

Figure 22. Dew intensity contours [mm/min], P=2.0 bar

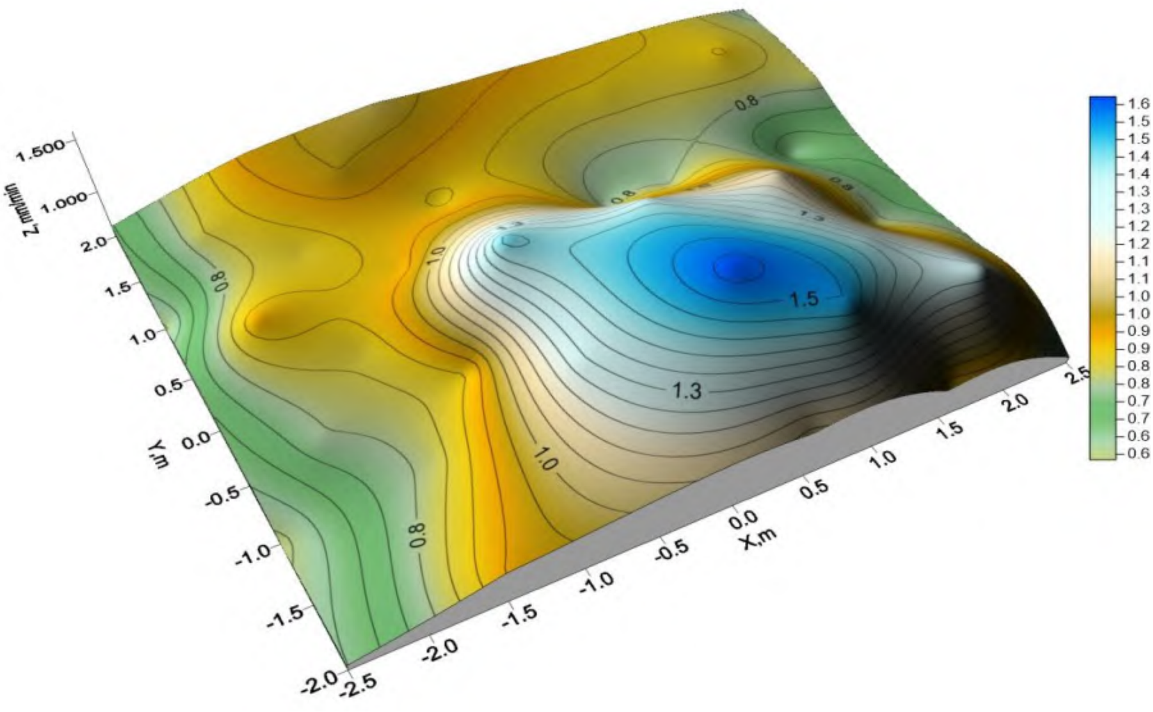

Figure 23. Distribution of water coverage intensity from sprinkler nozzles

Analysis of the Results Obtained

The results obtained allow:

- Testing different types of water nozzles on the built stand and studying their characteristics;
- Determining the intensity of water coverage from simultaneous operation of two nozzles;
- Comparative analysis between sprinkler, screw and spiral nozzles;
- Analyzing the influence of pressure on the size of the drops;
- Optimal selection of a system for application in underground facilities.

The distribution of the intensity of spraying over the area is the main characteristic of each fire extinguishing nozzle. The measurements were carried out at the minimum height of the nozzle H=5.00 m above the protected area adopted by us. During the operation time of the nozzles of 5 min, the volume of water received in each of the 40 collection vessels was measured and the intensity of spraying I [mm/min] was determined by dividing the receiving area and the spraying time. This measurement scheme also aims to assess the radial variation of the intensity.

Conclusion

Complex fires can develop in underground facilities, resulting in serious accidents and incidents, as well as significant material damage. Stationary fire extinguishing systems can control fires in the initial period of ignition and prevent the linear spread of the fire in the facility. This would support the actions of the rescue teams and would shorten the time of access to the fire. The time until the arrival of firefighters and the moment of starting extinguishing actions depends on the location of the fire in the facility, the access of the fire truck and the situation. Knowledge of the real situation implies the choice of the right tactics. The time for starting extinguishing actions by the mine rescue and fire services or other specialized units significantly exceeds the time for the ignition of the design and real fires, which makes extinguishing prolonged and, in some cases, ineffective. That is why the application of stationary fire extinguishing systems has a positive effect on the overall fire extinguishing process.

The construction of a fire sprinkler test stand is a key step towards increasing the safety and efficiency of fire protection systems. These systems play a crucial role in protecting buildings and infrastructure from the destructive effects of fire by automatically triggering water jets upon detection of fire or high temperature. Through detailed and precise testing, sprinkler systems will function properly and provide maximum protection in the event of a fire.

Recommendations

The results/findings of the study are of interest both for mining and industrial enterprises, as well as for underground spaces in residential buildings and commercial complexes, where the fire load is heterogeneous and its protection with an appropriate fire extinguishing installation will keep the fire at a low energy level.

Scientific Ethics Declaration

* The authors declare that the scientific ethical and legal responsibility of this article published in EPSTEM journal belongs to the authors.

Conflict of Interest

* The authors declare that they have no conflicts of interest

Funding

* This research is supported by the Bulgarian Ministry of Education and Science under the National Programme "Young Scientists and Postdoctoral Students – 2" (Stage II 2024-2025).

Acknowledgements or Notes

* This article was presented as an oral presentation at the International Conference on Research in Engineering, Technology and Science (www.icrets.net) held in Peja/Kosovo on July 10-13, 2025.

References

Aleksandrova, E. (2008). Economic method at projection of mines. *Challenges for Science in Relation to Bulgaria's EU Membership: International Scientific Conference: Vol. 3. Technical sciences, chemistry and physics* (pp. 72–77). Stara Zagora, Bulgaria.

Aleksandrova, E., & Zlatanov, P. (2008). Planning the expansion of mining production using the dynamic optimization method. *Scientific Conference with International Participation "Science in the Conditions of Globalization"*, October 1-2, pp. 332 – 336.

Aleksandrova, E., Asenovski, S., Georgiev, D., Kaykov, D., & Koprev, I. (2019). Methods for determining an optimal technological solution for underwater mining. *Journal of Mining and Geological Sciences*, *62*(2), 5–8.

Aleksandrova, E., Koprev, I., Dzhobov, I., & Petkov, T. (2015). New technologies and trends in open-pit mining for the development of thin, low-productivity coal seams. *National Scientific and Technical Conference Mineral Resources and Sustainable Development,* November 25, Sofia, pp. 124–129.

Beard, A., & Carvel, R. (2012). *Handbook of tunnel fire safety*, Default Book Series.

Borghetti, F., Derudi, M., Gandini, P., Frassoldati, A., & Tavelli, S. (2016). *Tunnel fire testing and modeling*. Springer Cham.

Chochev, V. (2013). *Research on the extinguishing intensity of sprinklers* (Doctoral dissertation). AoMoI, Sofia

Dinchev, Z., Gorbounov, Y., & Kostadinova, N. (2018). Velocity field visualization, measured with 3D ultrasonic anemometer. *Journal of Mining and Geological Sciences*, *61*(2), 39–44.

Gavrilova M. (2019). *Fire protection of products equipped with belt conveyors* (Master's thesis). Donetsk National Technical University

Hansen, R. (2009). *Literature survey – fire and smoke spread in underground mines.* Technical Report.

Ivanov I., Tsankov, T. (2018). State of the Art safety and human health risk analysis of accidents with gas installations and appliances, in particular related with electrical origin, in buildings at Bulgaria. *10th Scientific Conference BulEF'2018*, September 11-14.

Ivanov I., Tsankov, T. (2018). Safety culture in disasters and accidents and human health risk management. *6th Regional European Safe Community Conference ESCON'2018*, October 3-5, Skopje, Nord Macedonia.

Koychev, K., Chochev, V., & Nenov, M. (1998). Research into the problems of development and extinguishing in the event of a fire in the faculty of chemistry at the Sofia University, *Collection of Reports from the Scientific Session VVISU 98*, November 18-19 Sofia, Bulgaria, pp. 467-473

Michaylov M., Krilchev, A., Vladkova, & B., Dimova, B. (2011). Forschung eines neues mittels zur profilaktik und loschen von endogenous branden. *Zeitschrift Bergbau 3*, Germany.

Nenov, M., Lepniyski, D., & Popova, N. (2001). Analysis of the possibilities for extinguishing fires caused by ignition of non-traditional materials. *Collection of Reports from the Scientific Session VSU 2001* -, May 29 - June 1, Sofia, Bulgaria.

Nikolov, I., Georgiev, B., Nenov, M., & Stefanov, G. (2015). Portable stand and methodology for hydrostatic testing of pressure resistance of fire hoses. *AoMoI, 22*, 275-283.

Shopov, A., & Bonev, B. (2019). Ascertainment of the change of the ductility in corroded steel specimens by experiment. *International Journal of Civil Engineering and Technology, 10*(1), 1551-1560.

Shopov, A., & Bonev, B. (2019). Experimental determination on the change of geometrical characteristics and the theoretical ultimate-load capacity of corroded steel samples. *International Journal of Civil Engineering and Technology 10*(2), 320-329.

Shopov, A., Bonev, B., & Brayanov, N. (2018). Change of spring constant for springs with corrosion. *Proceedings of the 5th International Conference on Road and Rail Infrastructure CETRA 2018*, Zadar, Croatia, pp. 291-297

Tsankov T. (2021). Scenario and modelling of fire due reason from electrical character in a gasified building. *BulEF, IEEE*.

Tsankov T. (2024) Analysis and risk assessment of an electric car fire in an underground garage. *Energy Forum 2024*, June 25–28, Proceedings Collection.

Yordanov, Sv., Klisarski, P., & Nenov, M. (2018). Trends in the development of sprinkler fire extinguishing installations, *Collection of Reports from the Scientific Session Sofia*, Bulgaria, pp. 585-588

Author(s) Information

Diana Makedonska
University of Mining and Geology St. Ivan Rilski
Sofia, 1700 Prof. Boyan Kamenov St., Bulgaria,
Contact e-mail: *diana.makedonska@mgu.bg*

Vasil Tsanov
Academy of Ministry of Interior
Sofia, 1 Alexander Malinov Blvd., Bulgaria,

To cite this article:

Makedonska, D., & Tsanov, V. (2025). Development of experimental equipment for testing fire extinguishing nozzles in underground mining sites. *The Eurasia Proceedings of Science, Technology, Engineering and Mathematics (EPSTEM), 35,* 153-171.

ISRES Publishing

The Eurasia Proceedings of Science, Technology, Engineering & Mathematics (EPSTEM)
ISSN: 2602-3199

The Eurasia Proceedings of Science, Technology, Engineering and Mathematics (EPSTEM), 2025

Volume 35, Pages 172-177

ICRETS 2025: International Conference on Research in Engineering, Technology and Science

Comprehensive Analysis of Abnormal Assembly Situations in Automated Screwing Processes

Kaan Pehlivan
Samsung Electronics

Abstract: Comprehensive Analysis of Abnormal Assembly Situations Encountered in Automatic Screwing Processes This article examines in detail an abnormal assembly situation that can be encountered in automatic screwing processes commonly used in electronic device manufacturing. It analyzes whether a screw with a higher hardness than the case can leave deformation on a phone case made of Aluminum alloy (ALS36) as material and whether a significant angular deviation occurs during screw assembly. During this article, the ductility of ALS36 is determined and the material undergoes plastic deformation. The possible causes of this abnormal situation, related engineering principles, material properties and possible deviations in manufacturing processes are discussed in detail. The study also presents preventive measures to be taken to prevent similar manufacturing defects and possible directions for future research.

Keywords: Automatic screwing, Assembly, Alignment, Deviation, Aluminum alloy, Electronic device

Introduction

In phone production lines, precise positioning during screwing, equipment vibration that causes screws to deviate from their axis, instability of equipment footing, and guide hole misalignments are critical contributors to fastening defects. The quality of screw joints is one of the most fundamental factors ensuring mechanical integrity, tightness, and durability in mobile devices. Screws not only hold components together but also contribute to the product's overall structural performance and aesthetic durability. However, challenges such as hardness mismatches, torque deviations, and angular misalignments can severely compromise the connection strength. ALS36 aluminum alloy is widely used for mobile device housings due to its lightweight structure, good machinability, and surface finish potential.

This study aims to evaluate the impact of angular deviations during torque screwing (up to 20°), material deformation, and equipment vibration on the mechanical performance of ALS36-based housings. Past research has shown that the fatigue performance of aluminum alloys is highly sensitive to surface notching and geometric discontinuities, especially under cyclic loading conditions (Oskouei et al., 2016). Moreover, torque-angle tightening techniques have proven superior to traditional torque-only methods in terms of preload reliability, reducing the risk of joint failure due to torque scatter (Junker, 1969).

More recently, a NASA study demonstrated that vibration-induced loosening causes significant preload loss in fasteners over time — even in aerospace applications where advanced locking mechanisms are used. The study revealed that vibrations cause gradual unwinding of threaded joints, weakening the structural connection (DellaCorte et al., 2018).

To better understand these effects within a smartphone assembly context, seven torque screwing trials were conducted on ALS36 aluminum samples with controlled angular deviations between 0° and 20°. These tests were used to examine resulting stress distributions, force misalignments, and surface deformations. The results

- Selection and peer-review under responsibility of the Organizing Committee of the Conference

aim to inform design improvements, assembly process optimization, and material usage guidelines in consumer electronics manufacturing.

Material and Screw Specification

ALS36 Aluminum Alloy (Phone Case Material)

ALS36 is a structural aluminum alloy known for its light weight, thermal conductivity and machinability, especially used in mobile device cases (Machining-Custom, 2023). It is also preferred in phone cases due to its electromagnetic protection and environmental resistance. The reason why this material is preferred is because it is low in terms of flexibility, ductility and hardness. We need to know Vickers hardness, Tensile strength, Yield strength and Elongation coefficient from material properties.

- *Vickers Hardness*: The Vickers hardness test measures the material's resistance to plastic deformation and is particularly preferred for thin materials (World of Test, n.d.). This test is important for predicting surface deformations during screwing.
- *Yield Strength*: Yield strength is the stress at the point where a material exceeds its elastic limit and initiates permanent deformation (SendCutSend, 2024).
- *Tensile Strength*: This value indicates the maximum amount of stress the material can withstand before rupture and determines the performance under critical loading (SendCutSend, 2024).
- *Elongation:* It refers to the plastic deformation ability of the material. Elongation determines the energy absorption capacity of the material against impact or local stresses (Cambridge Materials Database, 2023).

Screw Properties and Mounting Parameters

Steel-based screws are used in mobile device assemblies and are known for their high hardness properties. When applied with softer materials such as ALS36, they may pose a risk of deformation due to the hardness difference, but in the same case, they can guide a screw hole that is not guided correctly with the correct positioning. For this situation, the surface hardness of the screw, the tightening torque of the screw and the tightening time are important.

- *Surface Hardness* : Screw hardness affects the local pressure applied to the body surface during assembly. A hard screw creates a risk of crushing when installed in a soft body (Pinchback, 2021).
- *Torque* : Torque determines the screw tightening force. High torque values can lead to cracking of the body material or failure of the threads (Mudge Fasteners, 2023).
- *Assembly Process* : Fast assembly is advantageous for automation, but angular deviations can occur if alignment accuracy is insufficient. Therefore, the assembly process and application dimensions need to be precisely controlled (Lee et al., 2011).
- *ALS36 Phone Case:*
  - Vickers Hardness: 130-170 HV
  - Yield Strength (σ_y): 220-300 MPa
  - Tensile Strength (σ_t): 320-400 MPa
  - Elongation: > %2
- *Screw*
  - Surface Hardness: 350-550 HV
  - Applied Torque: 1.3 kgf-cm ≈ 0.1275 Nm
  - Assembly Time: 2.5 seconds

Deflection After Screw Assembly and Its Effect on the Body

The axial deflection that occurs after screw installation impairs installation accuracy and causes disproportionate load distribution on the body material. Steel-based screws with high hardness compared to ALS36 may cause plastic deformation on the material surface. This manifests itself as localized crushing and surface deterioration.
When deflection occurs during assembly, the contact area decreases due to the screw not being in full contact with the body, which leads to the accumulation of tensile loads at certain points. Studies have shown that such

stress concentrations create crack initiation points on the material surface. On the surface of ALS36, which has insufficient hardness, this can cause micro cracks and irreversible crushing that can damage the structural integrity of the body. Moreover, assembly failures are not limited to structural deformation; they are often manifested by aesthetic degradation, loose screws and functional problems. In scenarios where assembly precision is low, such deformations should be considered as factors that directly affect production quality.

Yield and Tensile Strength and Surface Stress Analysis

Basic mechanical stress calculations are used to understand the stress effects of the mechanical forces applied during assembly on the ALS36 body material. In these analyses, nominal and local (actual) stress values are calculated to determine whether the yield limit of the material is exceeded.

- *Contact Area (A):* The effective circular contact area under the screw head is assumed to be 7.07 mm^2.
- *Applied Force (F):* A tightening force of approximately 130 N is applied in response to the torque value.
- *Nominal Stress (σ_nom):* σ_nom=F/A = 130N/7.07mm2 =18.4MPa
- This formula specifies the unit stress induced by the applied force on the contact area. In mechanical design, this stress is used to predict the general behavior of the material.
- *Actual Stress (σ_local):* σ_local= σ_nom x Kt =18.4MPa x 3 =55.2 MPa

Here Kt is the stress concentration coefficient and usually refers to the effect of holes, indentations or geometry defects. The nominal stress multiplied by this coefficient expresses the local stress concentration to which the material is subjected. The actual stress represents the risk of local deformations such as microscopic crack formation. In this case, the calculated localized stress of 55.2 MPa is below the yield strength of ALS36 (220-300 MPa). However, according to the literature, localized stresses at this level can cause the onset of plastic deformation and structural micro damages, especially in cases such as screwing errors and angular deflections.

Method and Cases

In this study, the effect of axial positioning errors on seven mobile devices with ALS36 aluminum alloy housings was investigated. After assembly, the screw assemblies in each device were analyzed by X-ray imaging, and the positional deviations were recorded in detail. Samples 1, 3, 4, 5, and 6: X-ray analysis of this group of samples showed that the screws had axial deviations of 1-20° after assembly. Plastic deformation, localized crushing, and geometric distortion were also observed in the screw holes. After the screws were removed and reassembled with the same torque value, proper alignment was achieved by re-centering thanks to the elongation capacity of the holes. After repeated reassembly, it was observed that the screws remained in place, did not loosen, and did not create new defects on the housing surface. These results support the reshapeability ability of ALS36, which has an elongation ratio of over 2%.

- Sample 1 has a deviation of approximately 7-8 degrees and plastic deformation was observed in the screw hole Sample 3 has a deviation of approximately 13-15 degrees and plastic deformation in the screw hole and damage occurred to the phone case protector
- Sample 4 has a deviation of more than 20 degrees, plastic deformation in the screw hole and damage to the phone case protector that cannot be reused.
- Sample 5 has a deviation of 3-4 degrees and caused a small plastic deformation
- Sample 6 has a deviation of less than 2 degrees and did not cause any plastic deformation in the screw hole.

Samples 2 and 7;

These two samples were analyzed as reference control samples. X-ray imaging showed no angular deviation or deformation of the assembly. The screws were found to be assembled with correct axial centering due to the accuracy of CNC machining or tapping. This demonstrates that, in a process balancing speed and precision, CNC-induced hole drift can have a minimal impact.

Technical Assessment

The fact that deformations caused by angular deviations during initial assembly can be eliminated by reassembling other samples (including Sample 4) with similar deformation behavior is explained by the elastic-plastic behavior of the material. The elongation value of the ALS36 alloy above 2% increases the deformation capacity after plastic deformation. This allows for compensation of geometry errors during tightening. Initial X-ray analysis of Sample 4 revealed a deviation of approximately 20°, as well as lack of contact and local deformation due to the difference between the screw and hole axes. However, when the screw was removed and correctly reassembled, surface deformation was minimized, the screw head was fully seated on the case surface, and the screw axis was correctly positioned. This is because ALS36 provides sufficient plasticity and the assembly torque (1.3 kgf-cm) does not exceed the yield limit of the material, allowing the deformation to be reversed. In addition, with the correct alignment of the assembly axis, even if the material had been deformed before, it was able to adapt to the new position and restore its structural integrity. In conclusion, these results show that in the material-assembly interaction, not only the initial application but also the rework ability of the material should be taken into account. This means that soft aluminum alloys can absorb assembly defects within their structural tolerances.

Table 1. Sample based screw assembly observations

No	X-ray result	Deformation	Re-mounting result	Notice	Images
1	Deviation 7°-8° between	Screw hole	Without a hitch	It caused a defect due to contact with the phone cover and the problem was solved by reassembly	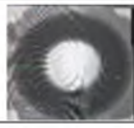
2	No defect	No	Without a hitch	Reference mounting high guide accuracy	
3	Deviation 13°-15° between	Screw hole & Phone rear	Without a hitch	It caused a defect due to contact with the phone cover and the problem was solved by reassembly	
4	Deviation 20°+	Screw hole Phone rear	Without a hitch	The axis was deviated by 20°, this deviation damaged the back cover and the hole was visibly deformed, but the error was corrected by reassembly	
5	Deviation 3°-4° between	Screw hole	Without a hitch	Problem was solved by reassembly	
6	Deviation <2°	Screw hole	Without a hitch	Nearly OK hole	
7	No Defect	No	Without a hitch	Reference mounting, high guide accuracy	

Results and Discussion

Equipment-related positioning errors on the assembly line are one of the most common causes of screw deflection. The following conditions can lead to these deviations:

- *Loose mounting table:* Unstable mounting surfaces cannot absorb the torque force applied by the screw machine and can cause the instantaneous position of the device to change.
- *Worn or incorrect installation of the guide parts*: Guiding plays a critical role for the correct orientation of the screw axis. Worn, loose or misaligned guides lead to misalignment.
- *Vibration and reaction forces during assembly*: Counter moment forces generated during the screw tightening process or vibrations from surrounding equipment can cause micron-level machine misalignment.
- *Operator-induced positioning errors:* In manually assisted systems, the directional force exerted by the operator on the screw machine or the mounting angle can cause skewed entry.
- *Inadequate fixturing or slippery surfaces:* If the part is not secured or the mounting surface is slippery, both the screw hole and the stability of the equipment at the time of installation are adversely affected.

Recommendations

- *Periodic control and calibration of guides:* Guiding systems should be replaced and measured for accuracy on a regular basis.
- *Vibration isolation:* The vibration effect of the equipment around the assembly line should be reduced, if necessary, the screw machine should be fixed to vibration absorbing platforms.
- *Operator training:* Especially in semi-automatic systems, operators should be trained not to apply directional pressure.

These measures prevent systematic assembly errors caused by equipment slippage and improve overall assembly quality.

Conclusion

In this study, the axial deflection, deformation and structural defects experienced during the screw assembly process on the ALS36 aluminium body were investigated in detail. Analyses of seven specimens revealed that all deflections were eliminated when the off-axis and deformed screws from the initial assembly were re-installed in the correct position through the same holes, and equipment calibration and routine checks are important. These results demonstrate that the ALS36 material can tolerate screw hole deformations due to its elongation rate exceeding 2% and its medium-low hardness value. Furthermore, the analyses showed that the screw heads were properly seated and that all defects were eliminated by reassembly.

Scientific Ethics Declaration

* The author declares that the scientific ethical and legal responsibility of this article published in EPSTEM journal belongs to the author.

Conflict of Interest

* No conflicts of interest

Funding

* This study received no external funding.

Acknowledgements or Notes

* This article was presented as an oral presentation at the International Conference on Research in Engineering, Technology and Science (www.icrets.net) held in Peja/Kosovo on July 10-13, 2025.

References

Cambridge Materials Database (2023). *Material properties: Elongation.* Retrieved from https://www-materials.eng.cam.ac.uk

Lee, N., An, Y. & Tsung, F. (2005). Studying effects of screw-fastening process on assembly accuracy. *Int J Adv Manuf Technol, 25*, 493–499.

Scruton, R. (1996). The eclipse of listening. *The New Criterion, 15*(30), 5-13.

Oskouei, R. H., Ibrahim, R. N., & Barati, M. (2016). A review on the fatigue performance of notched aluminium alloys: Influencing factors and practical implications. *Materials, 9*(3), 141.

Junker, G. H. (1969). New criteria for self-loosening of fasteners under vibration. *Sae Transactions*, 314-335.

DellaCorte, C., Howard, S. A., & Hess, D. P. (2018). Preload loss in a spacecraft fastener via vibration-ınduced unwinding. *NASA Technical Publication, 2018*‑219787.

Pinchback, T. (April 10, 2021). *Core hardness and surface hardness in fasteners.* Wilson-Garner. Retrieved from https://wilsongarner.com/core-hardness-and-surface-hardness-in-fasteners/

Machining-Custom (October 10, 2023). *Custom CNC machining aluminum mobile phone case.* https://www.machining-custom.com/

Mudge Fasteners (October 12, 2023). *Torque in fastener ınstallation.* Retrieved from https://www.mudgefasteners.com/news/torque-in-fastener-installation

SendCutSend (October 10, 2024). *Materials properties: Yield strength vs. tensile strength.* Retrieved from https://sendcutsend.com

World of Test (n.d.). *Ultimate guide to vickers hardness tester.* Retrieved from https://www.worldoftest.com

Author(s) Information

Kaan Pehlivan
Samsung Electronics
Mimar Sinan Neighbourhood, 103. Street No:72, 59500
Kapaklı/Tekirdağ, Türkiye
Contact e-mail: *k.pehlivan@samsung.com*

To cite this article:

Pehlivan, K. (2025). Comprehensive analysis of abnormal assembly situations in automated screwing processes. *The Eurasia Proceedings of Science, Technology, Engineering and Mathematics (EPSTEM), 35,* 172-177.

The Eurasia Proceedings of Science, Technology, Engineering & Mathematics (EPSTEM)
ISSN: 2602-3199

The Eurasia Proceedings of Science, Technology, Engineering and Mathematics (EPSTEM), 2025

Volume 35, Pages 178-183

ICRETS 2025: International Conference on Research in Engineering, Technology and Science

The Synthesis of Hetrocyclic Schiff Bases and Investigation of [(Fe(Salen)Cl] Metal Complexes

Ziya Erdem Koc
Selcuk University

Abstract: In this study, 2,4,6-triamino-s-triazine (melamine) as the starting material. Schiff base reaction took place with the condensation reaction of melamine and 3-hydroxybenzaldehyde. Then, tripodal s-triazine-core asymmetric Schiff base ligand complexes were obtained by obtaining a single oxygen-bridged compound of [(Fe(Salen)Cl] ligand complexes, which we synthesized tripodal Schiff base s-triazine tripodal by literature. The obtained multidirectional s-triazine-core Schiff base ligand complexes were under reflux with 3-hydroxybenzaldehyde compounds. Consequently, the structures of the obtained ligand and complexes were characterized using elemental analysis, FT-IR spectroscopy, ^{1}H-NMR spectroscopy and magnetic susceptibility measurement techniques.

Keywords: Melamine, Schiff base, s-Triazine, Salen, Heteronuclear complexes.

Introduction

s-Triazine Melamine, which is one of its compounds, is rapidly increasing in polymer chemistry, coordination chemistry, environmental chemistry, biochemistry, dyestuff chemistry, pharmaceutical chemistry and electronics industry (Uysal et al., 2012). In addition, s-triazine Schiff base compounds are used in medicine, especially as molecular magnetic material, and such heterocyclic compounds are used as active ingredients of antitumor and anticancer drugs (Arslaner et al., 2017; Koc & Uysal, 2016). Melamine compounds have gained importance in environmental chemistry in the storage of gases with metal-organic lattice structures (Yu et al., 2008).

Schiff bases (imines) are very important structures condensation products of primary amines with aldehydes for synthetic organic chemistry (Schiff, 1869). Schiff-base is considered a dynamic compound with a reversible imine bond derived from the dehydration reaction between amine and carbonyl groups (Zhang et al., 2021). Over the years, Schiff bases and metal complexes have played an important role in the development of coordination chemistry, chelating ligands and complex biochemical reactions as they readily form stable complexes with most of the transition metals (Jayabalakrishnan et al., 2002; Kocyigit et al., 2010). In recent years, the widespread use of Schiff bases and metal complexes, especially in various qualitative and quantitative analyses, enrichment of radioactive materials, pharmacological properties, the paint industry, and plastics industry has further increased, and it has attracted much attention due to their biochemical activities (Koc, 2011; Koc & Ucan, 2007; Koc & Uysal, 2010, 2011; Li et al., 2021; Uysal & Koc, 2010). Nitrogen-containing heterocycles are highly important due to their classification as a significant group of synthetic and natural compounds(Thamer Abd Rehan, 2024). Then, the obtained s-triazine monomer was coordinated with the salen ligand complex with a single oxygen and monopodal melamine centered monomer complexes were obtained (Celikbilek & Koc, 2014).

Experimental

- Selection and peer-review under responsibility of the Organizing Committee of the Conference

Materials and Methods

The chemicals were purchased from Aldrich and Merck was used as received. Melting points were measured using an Optimelt Automated Melting Point System (Digital Image Processing Technology) SRS apparatus (Nyköping-Sweden). Elemental analyses (C, H, N) were performed using a Leco, CHNS-932 model analyzer (Massachusetts, USA). ^{1}H NMR spectra were recorded by the Varian, 400 M spectrometer at room temperature. (California, USA). FT-IR spectra were recorded using a Perkin-Elmer Spectrum 100 with Universal ATR Polarization Accessory (Shelton, USA). Magnetic susceptibilities of the metal samples were measured at 296 K using a Sherwood Scientific MX Gouy magnetic susceptibility apparatus (Gouy method) with Hg[Co(SCN)4] as a calibration by the constant magnetic field. The effective magnetic moments, μeff, per metal atom were calculated from the expression, B.M., where χM is the molar susceptibility (Cambridge, UK). TGA analyses of the compounds were performed on the Mettler Toled*Third Level Headings*

3-((4,6-Diamino-1,3,5-triazine-2-imino)methyl)phenol (DTMP)

2,4,6-Triamino-1,3,5-triazine (Melamine) was suspended in 60 mL of benzene (1 mmol, 1.26 g). The mixture was stirred for 1 s under the back cooler. Then 4-hydroxybenzaldehyde (1 mmol, 1.22 g) was added to the mixture piece by piece. The resulting mixture was mixed for 24 h at 100 °C under the back cooler. To separate the precipitated monomer, the mixture was cooled and the solid was filtered apart. The resulting white precipitate was dried. **$C_{10}H_{10}N_6O$:** ^{1}H NMR (DMSO-d_6, ppm): 10.64 (s, H, OH), 9.71 (s, H, CH=N), 8.55 (s, H, Ar-H), 7.83-6.88 (m, 3H, Ar-H). FT-IR (cm^{-1}) 3467-3414 (NH_2), 3167 (OH), 1649 (C=N), 1526 (C=$N_{triazine}$).

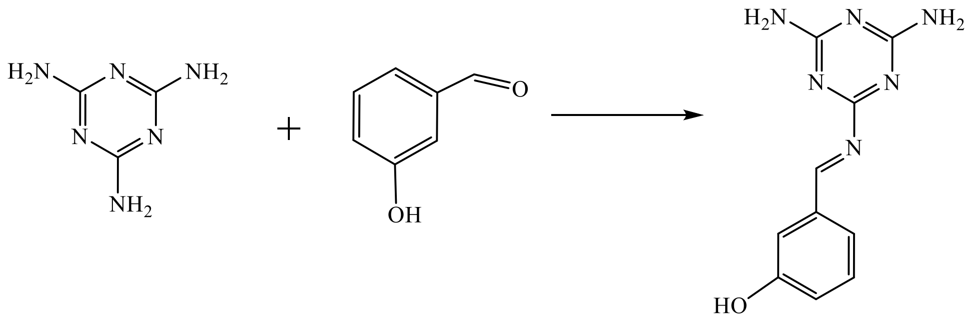

3-((4,6-diamino-1,3,5-triazin-2-imino)methyl)phenol

Figure 1. Synthesis of (DTMP) ligand

Synthesis of Salen ligand and Salen complexes

The synthesis of Salen Ligand and Salen Complexes has been synthesized according to the mentioned literature. (Gembicky et al., 2000; Kopel et al., 1998).

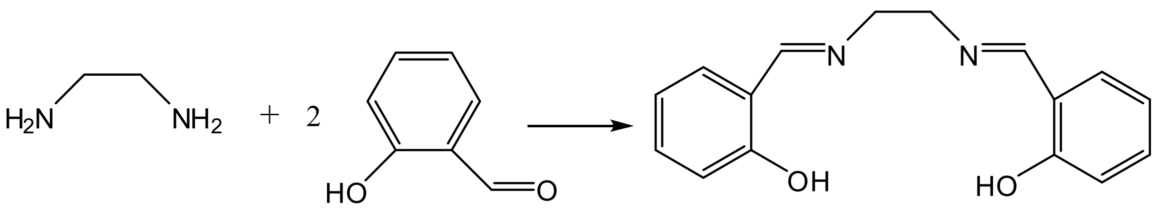

Figure 2. Salen was ligand.

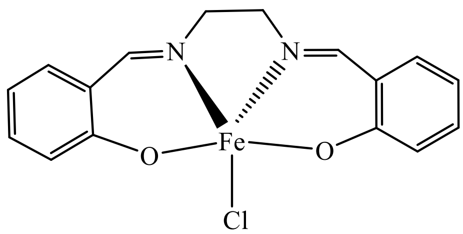

Figure 3. [Fe(salen)Cl] complex

3-((4,6-diamino-1,3,5-triazine-2-imino) methyl)phenol [Fe(salen)Cl] complex

Suspension solution was prepared in the resulting monomer (1 mmol, 0.23 g) ethanol. [Fe(salen)Cl] (1 mmol, 0.37 g) dissolved in ethanol was added to the complex compound monomer. The reaction mixture was stirred for four hours at 100 °C under a back cooler. The reaction solution was filtered and dried in a sedimentary oven. **$FeC_{27}H_{26}N_8O_3$:** FT-IR(cm^{-1}) 3317-3354 (NH_2), 1635 (C=N), 1546 (C=Ntriazin).

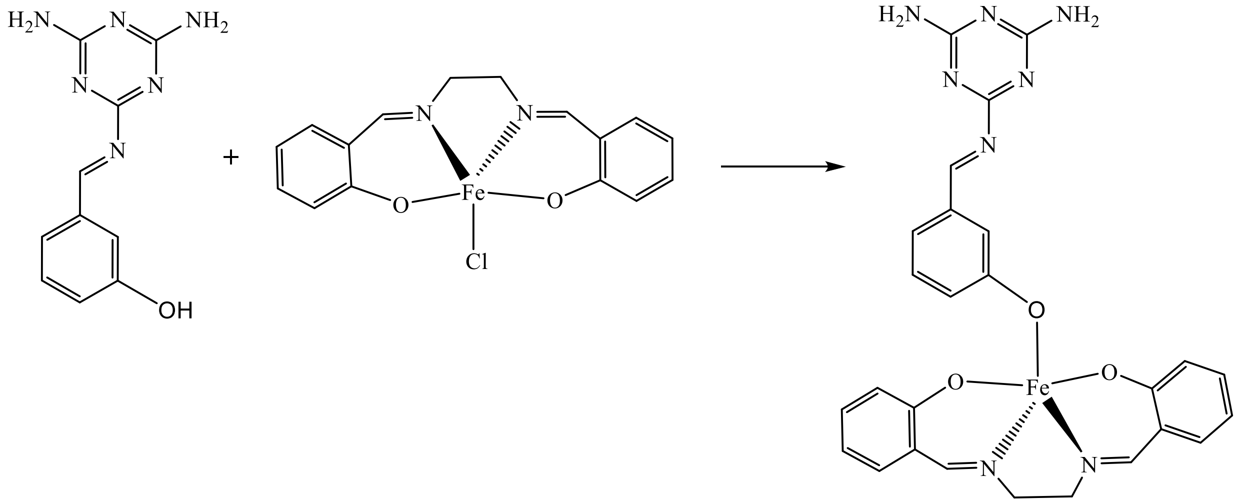

Figure 4. (DTMP)-[Fe(salen)Cl] complex

Results and Discussion

In this study, heterocyclic Schiff base monomer 3-((4,6-diamino-1,3,5-triazine-2-imino)methyl)phenol (DTMP) was synthesized by the reaction of 2,4,6-triamino-1,3,5-triazine (Melamine) and 3-hydroxybenzaldehyde [HB], which was used as the output material. A single oxygen-coordinated bridged monomer complex obtained with the synthesized (DTMP) and [Fe(salen)Cl] complex was obtained

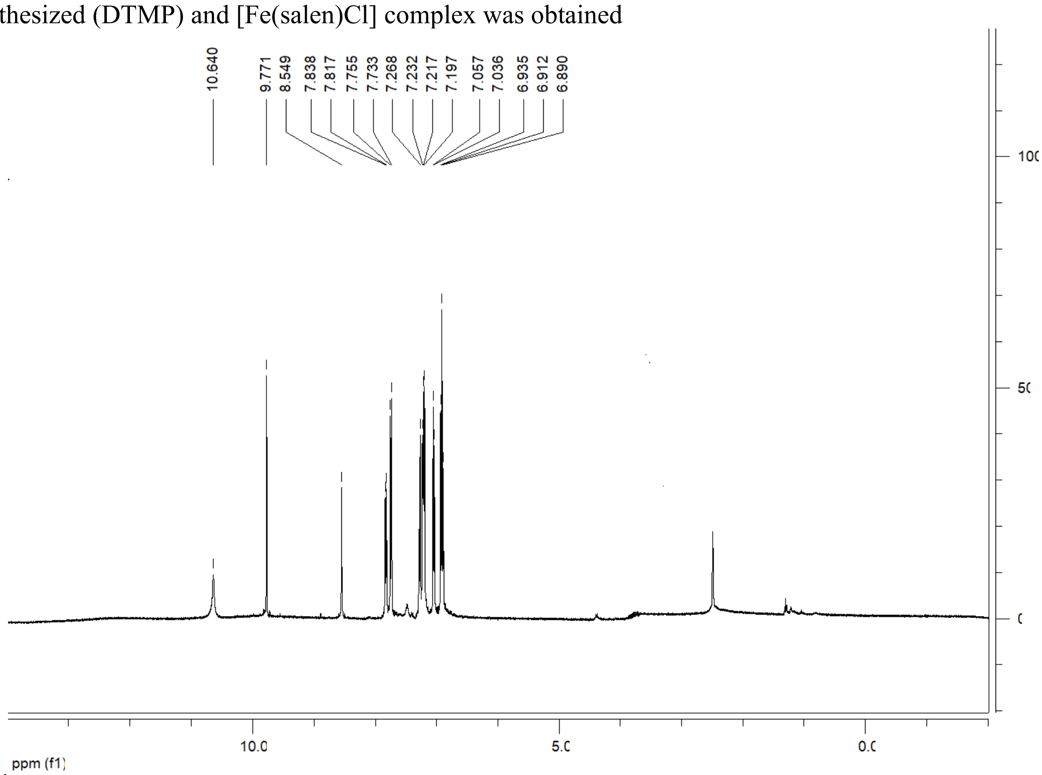

Scheme 1. ^1H NMR spectrum of the monomer ligand (DTMP)

OH protons in the ^1H NMR spectrum of the monomer ligand (DTMP) observed a corresponding singlet chemical shift value of 10.64 ppm. In addition, aromatic CH was observed to be 8.55/7.83-6.88 ppm and 9.71 ppm respectively at CH=N singlet chemical shift (Tahmassebi & Sasaki, 1998). FT-IR spectra of the compounds were obtained. The obtained monomer ligand and their FT-IR spectral data of the Fe(III) complex are given in the experimental section. When we examine these values; OH peaks, which were not found in the input materials of the monomer ligand, were observed as OH 3167 cm^{-1} as a result of the condensation reaction with 3-hydroxybenzaldehyde, as well as a new peak of OH 3167 cm^{-1} in the C = N group 1649 cm^{-1}. In addition, amine vibrations seen in the complexes of the monomer ligand at 3467 and 3414 cm^{-1} were synthesized using the literature and it was observed that the OH peaks of the bridged compounds coordinated with a single oxygen were lost. In Salen complexes, M-O and M-N bonds were also observed at 760-830 cm^{-1} and 753-685cm^{-1}, respectively (Koc & Ucan, 2007).

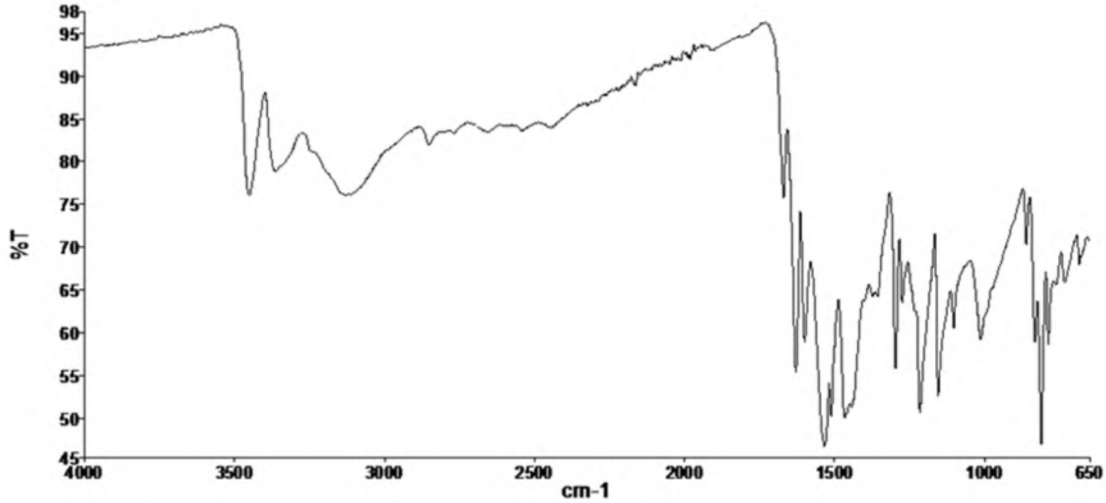

Scheme 1. FTIR spectrum of the monomer ligand (DTMP)

The synthesized **(DTMP)** and Fe(III) complex **[(DTMP)Fe]** obtained compounds were observed in $t_{2g}^3e_g^2$, with weak field effects for BM values of 5.27, respectively. As a result, it was estimated that it had a triangular pyramidal (dsp3) geometric structure because it showed a weak field complex feature. As a result, since the complex structure has a theoretically calculated d^5 electron configuration and shows weak ligand properties, it is estimated that it has a triangular bipyramid geometry in sp3d hybridization (Table 1.) (Koc & Ucan, 2008).

Table 1. Physical properties of monomer and salene complex

Compound	**Color**	**Yield (%)**	**M.P. (°C)**	**μ_{eff}**	**Found (Calculated) (%)**		
					C	**H**	**N**
$C_{10}H_{10}N_6O$ (DTMP)	White	80	183	-	53.17 (52.17)	4.75 (4.38)	36.48 (36.50)
$C_{27}H_{26}N_8O_3Fe(III)$ [(DTMP) Fe(III)(salen)]	Black	75	160	5.27	57.09 (57.26)	4.98 (4.63)	19.83 (19.72)

Conclusion

In this study, 2,4,6-triamino-1,3,5-triazine (Melamine) was used as the starting material. 2,4,6-triamino-1,3,5-triazine (Melamine) reacted with the addition of NaOH and 3-hydroxybenzaldehyde in the presence of 1,4-dioxane to obtain 3-((4,6-Diamino-1,3,5-triazine-2-imino)methyl)phenol (DTMP) complexation was carried out with the obtained 3-((4,6-Diamino-1,3,5-triazine-2-imino)methyl)phenol (DTMP) , anhydrous $FeCl_3$. In addition, 2,4,6-triamino-1,3,5-triazine (Melamine) reacts with 3-hidroxybenzaldehyde was 3-((4,6-Diamino-1,3,5-triazine-2-imino)methyl)phenol (DTMP) obtained. Schiff base compounds with different donor groups were synthesized by the condensation of these aldehyde and amine group molecules. Its bidirectional Fe(III) complexes by hydroxyl groups.

Recommendations

The introductory substances used in this study are ligands and complexes that are newly studied and not encountered in literature. We think that the obtained ligands and complexes will gain importance especially in terms of environmental chemistry. In addition, in our studies that progress as molecular magnetic materials due to their magnetic properties, new and more usable properties will be examined by focusing more on this issue.

Scientific Ethics Declaration

* The author declares that the scientific ethical and legal responsibility of this article published in EPSTEM journal belongs to the author.

Conflict of Interest

* The authors declare that there is no conflict of interest related to this work.

Funding

* This study received no external funding.

Acknowledgements or Notes

* This article was presented as an oral presentation at the International Conference on Research in Engineering, Technology and Science (www.icrets.net) held in Peja/Kosovo on July 10-13, 2025.

References

Arslaner, C., Karakurt, S., & Koc, Z. E. (2017). Synthesis of benzimidazole Schiff base derivatives and cytotoxic effects on colon and cervix cancer cell lines. *Biointerface Research in Applied Chemistry*, *7*(4), 2103-2107.

Celikbilek, S., & Koc, Z. E. (2014). Investigation of Ddipodal oxy-Schiff base and its salen and salophen Fe(III)/Cr(III)/Mn(III) schiff bases (N2O2) caped complexes and their magnetic and thermal behaviors. *Journal of Molecular Structure*, *1065*, 205-209.

Gembicky, M., Boca, R., & Renz, F. (2000). A heptanuclear Fe(II)-Fe(III)(6) system with twelve unpaired electrons. *Inorganic Chemistry Communications*, *3*(11), 662-665.

Jayabalakrishnan, C., Karvembu, R., & Natarajan, K. (2002). Catalytic and antimicrobial activities of new ruthenium(II) unsymmetrical Schiff base complexes. *Transition Metal Chemistry*, *27*(7), 790-794.

Koc, Z. E. (2011). Complexes of Iron(III) and Chromium(III) salen and salophen schiff bases with bridging 1,3,5-triazine derived multidirectional ligands. *Journal of Heterocyclic Chemistry*, *48*(4), 769-775.

Koc, Z. E., & Ucan, H. I. (2007). Complexes of iron(III) salen and saloph Schiff bases with bridging 2,4,6-tris(2,5dicarboxyphenylimino-4-formylphenoxy)-1,3,5-triazine and 2,4,6-tris(4-carboxyphenylimino-4'-formylphenoxy)-1,3,5-triazine. *Transition Metal Chemistry*, *32*(5), 597-602.

Koc, Z. E., & Ucan, H. I. (2008). Complexes of Iron(III) and Chrom(III) salen and saloph schiff bases with bridging 2,4,6-tris(4-nitrophenylimino-4'-formylphenoxy)-1,3,5-triazine. *Journal of Macromolecular Science Part a-Pure and Applied Chemistry*, *45*(12), 1074-1079.

Koc, Z. E., & Uysal, A. (2016). Investigation of novel monopodal and dipodal oxy-schiff base triazine from cyanuric chloride: Structural and antimicrobial studies. *Journal of Macromolecular Science Part A-Pure and Applied Chemistry*, *53*(2), 111-115.

Koc, Z. E., & Uysal, S. (2010). Synthesis and characterization of dendrimeric bridged salen/saloph complexes and ınvestigation of their magnetic and thermal behaviors. *Helvetica Chimica Acta*, *93*(5), 910-919.

Koc, Z. E., & Uysal, S. (2011). Synthesis and characterization of tripodal oxy-schiff base (2,4,6-Tris(4-carboxymethylenephenylimino-4 '-formylphenoxy)-1,3,5-triazine) and the thermal and magnetic properties of its Fe(III)/Cr(III) complexes. *Journal of Inorganic and Organometallic Polymers and Materials*, *21*(3), 400-406.

Kocyigit, O., Kursunlu, A. N., & Guler, E. (2010). Complexation properties and synthesis of a novel Schiff base with triphenylene nucleus. *Journal of Hazardous Materials*, *183*(1-3), 334-340.

Kopel, P., Sindelar, Z., & Klicka, R. (1998). Complexes of iron(III) salen and saloph schiff bases with bridging dicarboxylic and tricarboxylic acids. *Transition Metal Chemistry*, *23*(2), 139-142.

Li, J., Karjule, N., Qin, J., Wang, Y., Barrio, J., & Shalom, M. (2021). Low-temperature synthesis of solution processable carbon nitride polymers. *Molecules*, *26*(6), 1646.

Schiff, H. (1869). Untersuchungen über salicinderivate. *Justus Liebigs Annalen der Chemie*, *150*(2), 193-200.

Tahmassebi, D. C., & Sasaki, T. (1998). Synthesis of a three-helix bundle protein by reductive amination. *Journal of Organic Chemistry*, *63*(3), 728-731.

Thamer Abd Rehan, A. s., Ahmad Rahman Salih. (2024). Synthesis and characterization of triazine derivatives as ımportant heterocyclic compounds and study their biological activities. *International Journal of Innovative Science and Research Technology*, *9*(8), 2273-2277.

Uysal, S., & Koc, Z. E. (2010). Synthesis and characterization of dendrimeric melamine cored [salen/salophFe(III)] and [sale n/salophCr(III)] capped complexes and their magnetic behaviors. *Journal of Hazardous Materials*, *175*(1-3), 532-539.

Uysal, S., Koc, Z. E., Celikbilek, S., & Ucan, H. I. (2012). Synthesis of star-shaped macromolecular schiff base complexes having melamine cores and their magnetic and thermal behaviors. *Synthetic Communications*, *42*(7), 1033-1044.

Yu, Q., Schwidom, D., Exner, A., & Carlsen, P. (2008). Synthesis of novel homo-n-nucleoside analogs composed of a homo-1,4-dioxane sugar analog and substituted 1,3,5-triazine base equivalents. *Molecules*, *13*(12), 3092-3106.

Zhang, K., Huang, Y., Shen, Y. J., Zhang, L. F., Ma, S., Chen, T. T., Zheng, Z. Q., Zhang, S. S., & Li, B. X. (2021). Imine bond transformation of a dynamic Sm(III) macrocycle-based chemosensor: The indirect approach for detecting cyanuric chloride. *Analytica Chimica Acta*, *1144*, 34-42.

Author(s) Information

Ziya Erdem Koc
Faculty of Science, Department of Chemistry
Selcuk University, 42130-Konya, Türkiye
Contact e-mail: *zkoc@selcuk.edu.tr*

To cite this article:

Koc, Z. E. (2025). The synthesis of hetrocyclic schiff bases and investigation of [(Fe(salen)Cl] metal complexes. *The Eurasia Proceedings of Science, Technology, Engineering and Mathematics (EPSTEM), 35,* 178-183.

The Eurasia Proceedings of Science, Technology, Engineering & Mathematics (EPSTEM)
ISSN: 2602-3199

The Eurasia Proceedings of Science, Technology, Engineering and Mathematics (EPSTEM), 2025

Volume 35, Pages 184-192

ICRETS 2025: International Conference on Research in Engineering, Technology and Science

Effect of Elastic Supports on Lengthwise Fracture in Functionally Graded Beams under Changing Twist Angle

Victor Rizov
University of Architecture, Civil Engineering and Geodesy

Abstract: There are many engineering applications in which various structures are supported by different elastic supports. On the other hand, usage of functionally graded materials for making of load-carrying structures in various sectors of current engineering is growing constantly. The safety and reliability of these structures relay in high extent on their fracture behavior. In view of this, the present paper is focused on analyzing of lengthwise fracture in beam structures that are functionally graded along the radius of the cross-section. The right-hand end of the beam is rigidly fixed, while the left-hand end is supported by a circular elastic spring. The beam is under changing twist angle. The circular spring support acts on the beam by a twist moment. The beam hosts a lengthwise crack representing a circular surface. The functionally graded material has viscoelastic behavior under changing shear strains due to the twist. One of the primary motives for developing of this analysis is to evaluate the effect of the elastic spring support on the lengthwise fracture. In this relation, the strain energy release rate is determined. The solutions accounts for the circular spring support. The solution is verified upon methods known from the scientific literature. It is clarified how the circular elastic spring support influences the strain energy release rate under changing twist angle.

Keywords: Twist angle, Functionally graded beam, Spring, Lengthwise fracture.

Introduction

Functionally graded structural materials have found a variety of applications in numerous areas of current engineering (Mahamood & Akinlabi, 2017). The strong interest towards these relatively new continuously inhomogeneous composite materials is due to their undisputed advantages compared to the homogeneous structural materials (Gandra et al., 2011; Miyamoto et al., 1999). The advantages may include high strength and stiffness, stability at elevated temperature, good fatigue properties, improved performance at harsh environment, efficient work under dynamic loadings, etc. These advantages are conditioned mainly by the fact that the microstructure of the functionally graded materials change continuously in the solid (Radhika et al., 2020; Riov, 2018). Besides, this change may be tailored in the manufacturing process in order to achieve various predefined goals concerning the strength, hardness, stiffness, stability, and other properties of the material (Fanani et al., 2021; Wu et al., 2014). For example, the microstructure of the functionally graded material can be tailored so as to improve the strength in more heavily loaded parts of a structural member under given loading conditions.

However, these efficient materials have some drawbacks related to lengthwise fracture performance. This is due to the layered structure of some functionally graded materials (for instance, these materials that are manufactured layer-by-layer (Mahamood & Akinlabi, 2017). Lengthwise cracks propagating between layers cause significant reduction of stiffness and load-bearing ability of functionally graded structural components and may threaten their normal functioning (Dowling, 2007; Rizov, 2005; Rizov & Altenbach, 2020).

This paper deals with lengthwise fracture in functionally graded beams under changing twist angle. In particular, the paper is focused on the effect of elastic circular spring support on the lengthwise fracture. In relation to this, the strain energy release rate (SEER) in the beam hosting a lengthwise circular cylindrical crack is derived. The beam has viscoelastic behavior. The circular spring support acts on the beam with a torsion moment that is proportional to the twist at the free end of the beam. The SERR solution obtained is applied for clarifying the effect of the elastic circular spring support when the beam is under changing twist angle.

Theoretical Analysis

The beam structure in Figure 1 has circular cross-section of radius, R_δ.

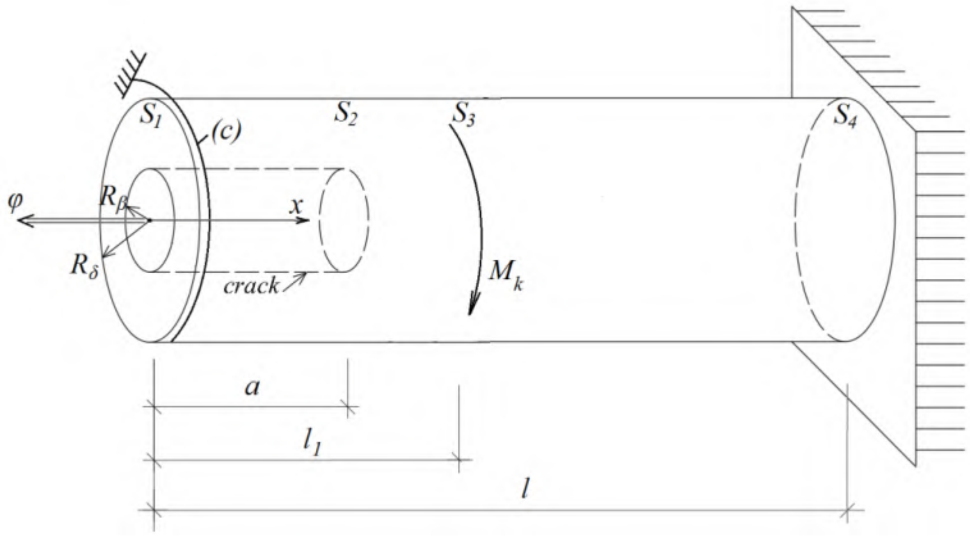

Figure 1. Static diagram of the beam

The right-hand end of the beam is rigidly fixed. The left-hand end of the beam is supported by an elastic circular spring support located in the plane perpendicular to *x*-axis. The constant of this spring is denoted by c. The beam hosts a lengthwise crack representing a circular surface of radius, R_β, and length, a. This crack is located in portion, S_1S_2, of the beam. The free end of the internal arm of the lengthwise crack is under twist angle, φ, as illustrated in Figure 1. The twist angle changes with time, t, as written in Eq. (1).

$$\varphi = \lambda t, \tag{1}$$

where λ is the twist angle velocity.

The torsion moment, M_c, that appears in the circular spring support is obtained by Eq. (2).

$$M_c = c\varphi_{S1}, \tag{2}$$

where φ_{S1} is the twist angle of end section, S_1, of the external arm of the crack.

A moment, M_k, acts in section, S_3, of the beam. This moment resists to the twist of section, S_3. The moment is found by Eq. (3).

$$M_k = k\dot{\varphi}_{S3}, \tag{3}$$

where k is a parameter, $\dot{\varphi}_{S3}$ is the velocity of the twist angle of section, S_3.

The beam has viscoelastic behavior treated by the model consisting of two springs with shear modules, G_1 and G_2, and a dashpot with coefficient of viscosity, μ, as shown in Figure 2. The viscoelastic model is under shear strain, γ. The change of γ with time is described by Eq. (4).

$$\gamma = \alpha t, \tag{4}$$

where α is a parameter.

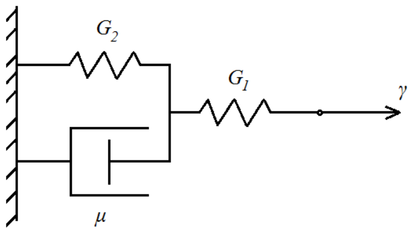

Figure 2. Viscoelastic model diagram

The stress-strain-time relation of the viscoelastic model is written in Eq. (5) (Zubchaninov, 1990).

$$\tau = G_* \alpha t + n(G_1 - G_*)\left(1 - e^{-\frac{t}{n}}\right)\alpha, \tag{5}$$

where

$$n = \frac{\mu}{G_1 - G_2}, \tag{6}$$

$$G_* = \frac{G_1 G_2}{G_1 + G_2}. \tag{7}$$

In Eq. (5), τ is the shear stress. Equation (5) is applied for modeling the mechanical behavior of the beam in Figure 1. Since the beam is functionally graded along the radius of the cross-section, the shear modules and the coefficient of viscosity change continuously in radial direction according to the laws in Eqs. (8), (9) and (10), respectively.

$$G_1 = G_{1cnt} + \frac{G_{1srf} - G_{1cnt}}{R_\delta^{n_1}} R^{n_1}, \tag{8}$$

$$G_2 = G_{2cnt} + \frac{G_{2srf} - G_{2cnt}}{R_\delta^{n_2}} R^{n_2}, \tag{9}$$

$$\mu = \mu_{cnt} + \frac{\mu_{srf} - \mu_{cnt}}{R_\delta^{n_3}} R^{n_3}, \tag{10}$$

where

$$0 \leq R \leq R_\delta. \tag{11}$$

In Eqs. (8), (9) and (10), R is a running radius, n_1, n_2 and n_3 are parameters, the subscripts, cnt and srf, refer to the centre and the surface of the beam, respectively.

The SERR, G, is determined by Eq. (12).

$$G = \frac{dU}{dA}, \tag{12}$$

where U is the strain energy in the beam, A is the crack area.

$$A = 2\pi R_\beta a \, . \tag{13}$$

Therefore, Eq. (13) is re-written as

$$G = \frac{dU}{2\pi R_\beta da} \, . \tag{14}$$

Equation (15) is applied for determining of U.

$$U = U_1 + U_2 + U_3 + U_4 \, , \tag{15}$$

where

$$U_1 = \iiint\limits_{(V_1)} u_{01} dV \, , \tag{16}$$

$$U_2 = \iiint\limits_{(V_2)} u_{02} dV \, , \tag{17}$$

$$U_3 = \iiint\limits_{(V_3)} u_{03} dV \, , \tag{18}$$

$$U_4 = \iiint\limits_{(V_4)} u_{04} dV \, . \tag{19}$$

In Eqs. (15) – (19), V_1, V_2, V_3 and V_4 are the volumes of the internal and external arms of the crack, and portions, S_2S_3 and S_3S_4, of the beam, u_{01}, u_{02}, u_{03} and u_{04} are the specific strain energies in the internal and external arms of the crack, and portions, S_2S_3 and S_3S_4, of the beam, respectively.

Equation (20) is applied for calculating of u_{01}.

$$u_{01} = \int \tau_1 d\gamma_1 \, , \tag{20}$$

where τ_1 and γ_1, are the shear stress and strain in the internal arm of the crack, respectively.

The change of γ_1 in the cross-section of the internal arm of the crack is presented by Eq. (21).

$$\gamma_1 = \frac{\gamma_{1s}}{R_\beta} R \, , \tag{21}$$

where

$$0 \le R \le R_\beta \, . \tag{22}$$

In Eq. (21), γ_{1s} is the shear strain at the surface of the internal arm of the crack.

Having in mind Eq. (21), the twist angle of the free end of the internal arm is obtained by Eq. (23).

$$\varphi = \frac{\gamma_{1s}}{R_\beta} a + \frac{\gamma_{3s}}{R_\delta}\left(l_1 - a\right) + \frac{\gamma_{4s}}{R_\delta}\left(l - l_1\right), \tag{23}$$

where γ_{3s} and γ_{4s} are the shear strains at the surface of portions, S_2S_3 and S_3S_4, of the beam, l is the beam length, l_1 is the abscissa of section, S_3.

The twist angle of end section, S_1, of the beam is determined by Eq. (24).

$$\varphi_{s1} = \frac{\gamma_{2s}}{R_\delta} a + \frac{\gamma_{3s}}{R_\delta}(l_1 - a) + \frac{\gamma_{4s}}{R_\delta}(l - l_1), \tag{24}$$

where γ_{2s} is the shear strain at the surface of portion, S_1S_2, of the beam.

The twist angle of section, S_3, is derived by using Eq. (25).

$$\varphi_{s3} = \frac{\gamma_{4s}}{R_\delta}(l - l_1). \tag{25}$$

The equilibrium of the end section, S_1, of the external arm of the crack is analyzed by Eq. (26).

$$M_2 + M_c = 0, \tag{26}$$

where M_2 is the torsion moment in the external arm. This torsion moment is related to the shear stress, τ_2, in the external arm by Eq. (27).

$$M_2 = \iint_{(A_2)} \tau_2 R dA, \tag{27}$$

where A_2 is the area of the external arm section. By using Eqs. (2), (26) and (27), we obtain

$$\iint_{(A_2)} \tau_2 R dA + c\varphi_{S1} = 0. \tag{28}$$

The equilibrium of the torsion moments in section, S_2, of the beam is written in Eq. (29).

$$M_1 + M_2 + M_3 = 0, \tag{29}$$

where M_1, M_2, and M_3 are the bending moments in the internal and external arms of the crack, and in portion, S_2S_3, of the beam. The bending moments, M_1 and M_3, are expressed by Eqs. (30) and (31).

$$M_1 = \iint_{(A_1)} \tau_1 R dA, \tag{30}$$

$$M_3 = \iint_{(A_3)} \tau_3 R dA, \tag{31}$$

where τ_3 is the shear stress in portion, S_2S_3, of the beam, A_3 is area of the section.

Equations (27), (29), (30) and (31) lead to

$$\iint_{(A_1)} \tau_1 R dA + \iint_{(A_2)} \tau_2 R dA + \iint_{(A_3)} \tau_3 R dA = 0. \tag{32}$$

Equation (33) is used for analyzing the equilibrium of the torsion moments in section, S_3, of the beam.

$$M_3 + M_4 + M_k = 0, \tag{33}$$

where M_4 is the torsion moment in portion, S_3S_4, of the beam. M_4 is expressed by the shear stress, τ_4, in portion, S_3S_4, via Eq. (34).

$$M_4 = \iint_{(A_4)} \tau_4 R dA , \tag{34}$$

where A_4 is area of the section.

Equations (23), (28), (32) and (33) are used for determining the shear strains by the MatLab. The strain energy is derived by Eqs. (15) – (19) (the MatLab is applied for the integration). The SERR is found by Eq. (14). The compliance method is applied for verifying the SERR through Eq. (35) (Zubchaninov, 1990).

$$G = \frac{1}{2b} M_1^2 \frac{dC_{M1}}{da} , \tag{35}$$

where

$$C_{M1} = \frac{\varphi}{M_1} . \tag{36}$$

Results and Discussion

The results reported here clarify how the SERR in the functionally graded beam structure under changing twist angle is influenced by the elastic circular spring support (Figure 1). The influence of other parameters like λ and κ, and the ratios, a/l, l_1/l, G_{1srf}/G_{1cnt}, G_{2srf}/G_{2cnt} and μ_{srf}/μ_{cnt}, on the SERR is clarified too. The influences are illustrated by the graphs plotted in Figures 3, 4, 5 and 6. The case of a beam with $l = 0.800$ m, $R_\beta = 0.030$ m, $R_\delta = 0.050$ m, $n_1 = 0.5$, $n_2 = 0.6$ and $n_3 = 0.7$ is considered.

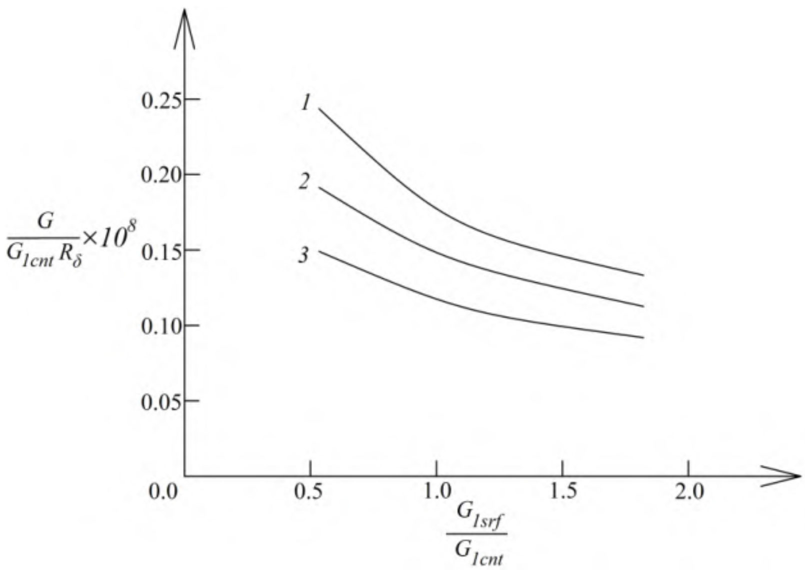

Figure 3. Change of the SERR with increase of G_{1srf}/G_{1cnt} ratio

Graphs illustrating the influence of G_{1srf}/G_{1cnt} ratio on the SERR at $c = 100$ kNm/rad (curve 1), $c = 200$ kNm/rad (curve 2), and $c = 300$ kNm/rad (curve 3) are given in Figure 3. It can be observed that increase of the value of c induces reduction of the SERR. Increase of G_{1srf}/G_{1cnt} ratio has a similar influence, i.e. the SERR reduces (Figure 3).

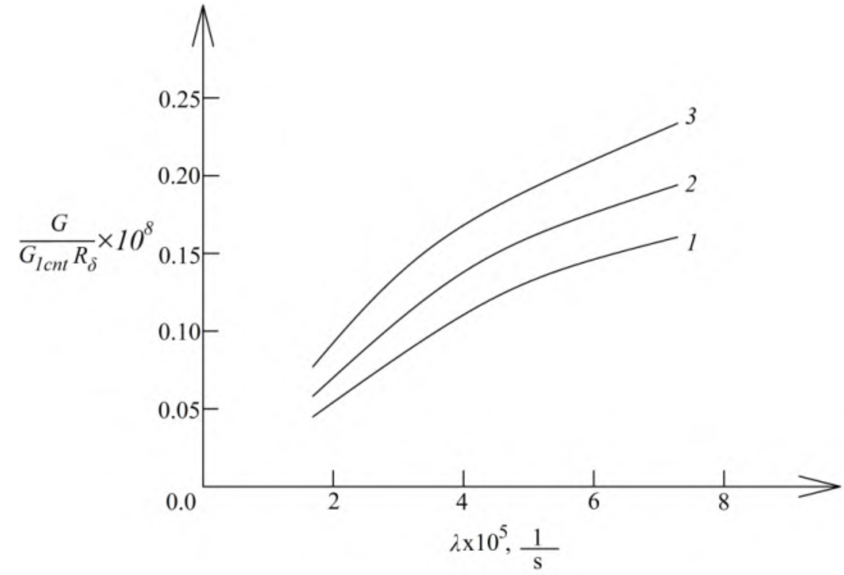

Figure 4. Change of the SERR with increase of λ

The influence of the twist angle velocity, λ, on the SERR at $a/l = 0.15$ (curve 1), $a/l = 0.30$ (curve 2), and $a/l = 0.45$ (curve 3) is illustrated by the graphs given in Figure 4. It is evident that increase of the value of λ leads to a quick growth of the SERR at each of the considered a/l ratios (Figure 4). Increase of a/l ratio also generates growth of the SERR as one can see in Figure 4.

Figure 5 illustrates the influence of l_1/l ratio on the SERR at $k = 50$ kNms (curve 1), $k = 100$ kNms (curve 2), and $k = 150$ kNms (curve 3). The inspection of the graphs shown in Figure 5 reveals a growth of the SERR with increase of l_1/l ratio. The increase of the value of the parameter, k , leads to reduction of the SERR (Figure 5).

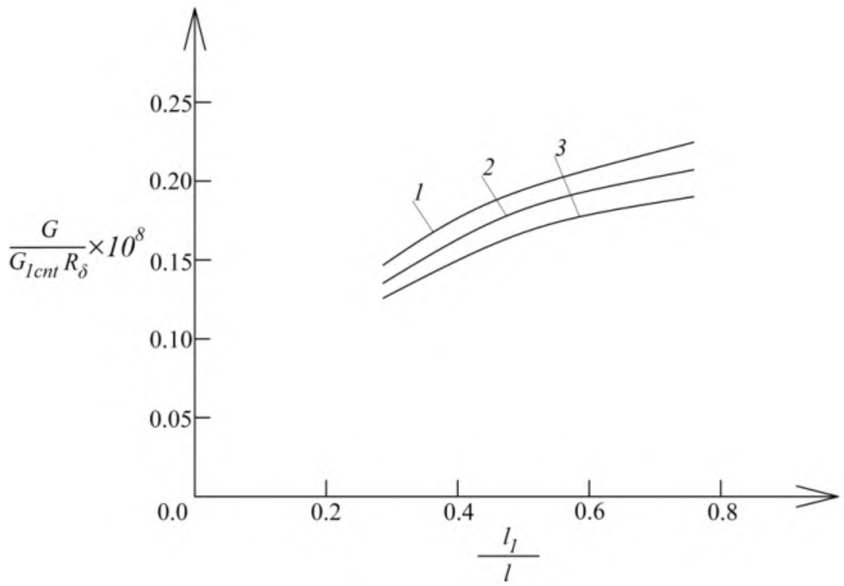

Figure 5. Change of the SERR with increase of l_1/l ratio

The influence of G_{2srf} / G_{2cnt} ratio on the SERR at $\mu_{srf} / \mu_{cnt} = 0.5$ (cure 1), $\mu_{srf} / \mu_{cnt} = 1.0$ (curve 2), and $\mu_{srf} / \mu_{cnt} = 2.0$ (curve 3) is illustrated by the graphs shown in Figure 6. The growth of G_{2srf} / G_{2cnt} and μ_{srf} / μ_{cnt} ratios cause reduction of the SERR (Figure 6).

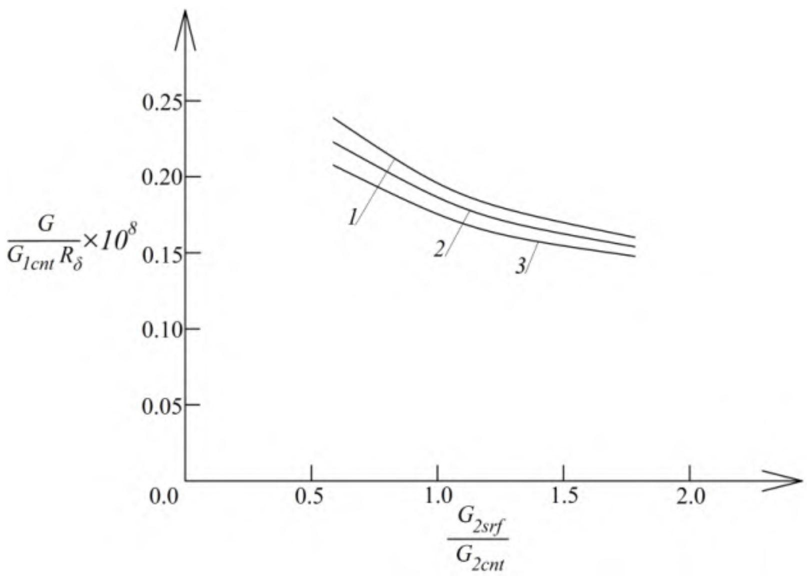

Figure 6. Change of the SERR with increase of G_{2srf} / G_{2cnt} ratio

Conclusion

Lengthwise fracture in functionally graded beam structures under changing twist angle is analyzed. For this purpose, the SERR is derived. The main aim of the analysis is to evaluate the influence of the elastic circular spring support on the lengthwise fracture. The spring support is located at the beam free end in the plane perpendicular to the longitudinal axis of the beam. The beam has viscoelastic behavior. The analysis performed indicates that the elastic circular spring support has a positive effect on the lengthwise fracture in the beam under changing twist angle since this support leads to reduction of the SERR. This positive effect is stronger at higher rigidity of the spring. The influence of G_{1srf} / G_{1cnt}, G_{2srf} / G_{2cnt} and μ_{srf} / μ_{cnt} ratios on the SERR is evaluated too. It is found that increase of these ratios also has a positive effect on the lengthwise fracture since the SERR reduces.

Recommendations

Using of elastic circular spring support of higher rigidity can be recommended for improving lengthwise fracture behavior of beams under changing twist angle.

Scientific Ethics Declaration

* The author declares that the scientific ethical and legal responsibility of this article published in EPSTEM journal belongs to the author.

Conflict of Interest

* The author declares that he has no conflicts of interest.

Funding

* This study was funded by the Research and Design Centre (contract BN-297/24).

Acknowledgements or Notes

* This article was presented as an oral presentation at the International Conference on Research in Engineering, Technology and Science (www.icrets.net) held in Peja/Kosovo on July 10-13, 2025.

References

Dowling, N. (2007). *Mechanical behavior of materials*. New York, NY: Pearson.

Fanani, E. W. A., Surojo, E., Prabowo, A. R., & Akbar, H. I. (2021). Recent progress in hybrid aluminum composite: manufacturing and application. *Metals, 11,* 1919-1929.

Gandra, J., Miranda, R., Vilaca, P., Velhinho, A., & Teixeira, J.P. (2011). Functionally graded materials produced by friction stir processing. *Journal of Materials Processing Technology, 211,* 1659-1668.

Mahamood, R. C., & Akinlabi, E. T. (2017). *Functionally graded materials*. New York, NY: Springer.

Miyamoto, Y., Kaysser, W.A., Rabin, B.H., Kawasaki, A., & Ford, R.G. (1999). *Functionally graded materials: Design, processing and applications*. London: Kluwer Academic Publishers.

Radhika, N., Sasikumar, J., Sylesh, J. L., & Kishore, R. (2020). Dry reciprocating wear and frictional behaviour of B4C reinforced functionally graded and homogenous aluminium matrix composites. *Journal of Materials Research and Technology*, *9,* 1578-1592.

Rizov, V. I. (2005). *Mechanics of composite materials*. BIAP.

Rizov, V. I. (2018). Non-linear delamination in two-dimensional functionally graded multilayered beam. *International Journal of Structural Integrity, 9,* 646-663.

Rizov, V. I., & Altenbach, H. (2020). Longitudinal fracture analysis of inhomogeneous beams with continuously varying sizes of the cross-section along the beam length. *Frattura ed Integrità Strutturale*, *53,* 38-50.

Wu, X.L., Jiang, P., Chen, L., Zhang, J.F., Yuan, F.P., & Zhu, Y.T. (2014). Synergetic strengthening by gradient structure. *Mater. Res. Lett.*, *2*, 185–191.

Zubchaninov, V.G. (1990). *Fundamentals of theory of elasticity and plasticity*. Vishaia Shkola.

Author(s) Information

Victor Rizov
University of Architecture, Civil Engineering and Geodesy
1 Chr. Smirnensky blvd. 1046-Sofia / Bulgaria
Contact e-mail: *v_rizov_fhe@uacg.bg*

To cite this article:

Rizov, V. (2025). Effect of elastic supports on lengthwise fracture in functionally graded beams under changing twist angle. *The Eurasia Proceedings of Science, Technology, Engineering and Mathematics (EPSTEM), 35,* 184-192.

The Eurasia Proceedings of Science, Technology,
Engineering & Mathematics (EPSTEM)
ISSN: 2602-3199

The Eurasia Proceedings of Science, Technology, Engineering and Mathematics (EPSTEM), 2025

Volume 35, Pages 193-200

ICRETS 2025: International Conference on Research in Engineering, Technology and Science

Optimization of an Experimental Stand with Four Nozzles for Assessing the Intensity of Irrigation in Underground Mining Sites

Diana Makedonska
University of Mining and Geology St. Ivan Rilski

Vasil Tsanov
Academy of Ministry of Interior

Abstract: This study presents an upgraded experimental methodology for analyzing the dispersion and hydrodynamic characteristics of sprinkler nozzles applicable in underground mining sites. This article is a scientific upgrade of the topic "Development of experimental equipment for testing fire extinguishing nozzles in underground mining sites". An improved stand equipped with four nozzles has been developed, which allows for a more precise assessment of the intensity of the water coverage on a protected area. The study includes measuring the spatial distribution of water through a network of measuring vessels and determining key parameters such as flow rate, pressure and uniformity of spraying. The achieved results demonstrate the possibility of effective calibration of fire extinguishing systems in order to minimize the risk of fire in an underground environment. A comparative analysis is presented with a previous stand with two nozzles, taking into account the advantages of the expanded configuration.

Keywords: Underground mining sites, Fire extinguishing system, Misting intensity, Sprinkler nozzles

Introduction

Fire safety in underground mines is a critical challenge due to the specific architecture, limited ventilation and high density of combustible materials and fluids used. The development of automated fire suppression systems based on water spray is a crucial factor in limiting the damage from incidents that occur. Sprinkler installations are a proven technical tool for early detection and suppression of fires. The growing demand for flexible, yet reliable solutions in underground environments requires precise adaptation of the nozzles used to the hydraulic and geometric features of the sites. The current development builds on a previous experimental study that used a two-nozzle setup. The new four-nozzle configuration allows for an expanded analysis scope and higher accuracy in estimating the intensity and distribution of the water jet.

Aim and Relevance of the Research

The purpose of this study is to design and build an experimental four-nozzle test rig to analyze key water coverage parameters corresponding to real-world conditions in underground mining facilities. The study aims to:

- optimize the selection of nozzles for specific underground applications;
- improve the methodology for measuring and analyzing the spray intensity;
- provide a basis for subsequent validation of mathematical models and CFD simulations of water systems.

The relevance of the topic is emphasized by the frequent incidents in the mining industry, which have an adverse impact on the processes of seizing and processing mineral raw materials, including on the complex mechanization in underground workings and in open-pit mines and quarries (Aleksandrova & Koprev, 2015), (Aleksandrova & Asenovski, 2019), where significant losses are observed due to fires, often caused by delayed reaction or ineffective initial extinguishing. Approaches related to sustainable resource management and the application of circular economy principles in the mineral industry (Grigorova, 2020) emphasize the need for effective and optimized engineering solutions, such as water spraying systems through nozzles in underground sites.

Theoretical Basis

Stationary automatic fire extinguishing systems are engineering solutions designed to detect and extinguish fires in their initial phase. They consist of fixed networks of pipelines and nozzles, to which a certain volume of fire extinguishing agent is connected. The supply of this agent can be either manual or automatic, depending on the configuration of the system and the method of activation.

These systems play a crucial role as a part of comprehensive fire safety measures, especially in environments with an increased risk of rapid-fire development and the possibility of explosions (Tsankov, 2024), structural destruction, interruption of critical production processes or significant material damage. Their effectiveness is based on the ability to quickly localize and/or suppress flames in their infancy, which reduces the need for additional intervention and minimizes the consequences of the incident (Tsankov, 2021).

Automatic Sprinkler Systems

Automatic sprinkler systems are among the most common types of fixed water fire extinguishing installations. They are designed to detect the occurrence of a fire and respond by spraying water into the area of the fire. Their main function is either to extinguish the fire in its initial stage, or to keep it under control until additional forces arrive or additional extinguishing agents are activated.

A typical sprinkler system configuration includes a water source (e.g., a water main or a reservoir with a pumping station) and one or more distribution networks with sprinkler heads installed. Each installation contains a control valve and branch pipes located in the protected space. The system is activated automatically when one or more sprinkler heads open due to thermal deformation (melting of a heating element) or by a signal from a fire alarm system. The effectiveness of a sprinkler system depends not only on its proper design and hydraulic sizing, but also on the type of sprinklers used, their geometry, location, and the condition and maintenance of the piping network. These parameters are critically important in the design and testing of new types of sprinkler devices, as investigated through bench experiments.

Methodology

The study is focused on determining the intensity of water coverage during simultaneous operation of four sprinkler nozzles mounted on a specially constructed stand. For this purpose, a network of measuring vessels located on a protected horizontal area is used to quantitatively assess water dispersion under different hydraulic conditions.

The calculation of water distribution is carried out using the following formula:

$$I = \frac{V}{S\tau}\left[\frac{dm^3}{dm^2 \min} * 100 = \frac{mm}{\min}\right] \quad (1)$$

where:

$\boldsymbol{I}$ – dew intensity, [mm/min];
$\boldsymbol{V}$ – volume of water in the container, [dm^3]; $\boldsymbol{S}$ - court area, [dm];
$\boldsymbol{S}$ - area of the measuring vessel [dm^2]; $\boldsymbol{\tau}$ - duration of the experiment, [min].

Specialized SURFER software is used to visualize the intensity and its distribution, through which isolines and three-dimensional profiles are prepared.

Experimental Stand Construction

The constructed experimental stand is designed for testing up to four nozzles, at different heights and distances between them, in accordance with the standards EN 12845 and EN 12259-1. The stand is constructed of galvanized pipes and a steel support frame with height adjustment between 3.00 m and 5.00 m. The mounting platform allows the fixing of four nozzles in different configurations - linear, rectangular or square grid. Main technical characteristics:

- Working height: 5.00 m (adjustable to 3.00 m);
- Mounting module for 4 nozzles with a center distance of 3.00 m;
- Control devices: pressure gauge, flow meter, stopcock;
- Connection to a "Storz" type fire hydrant to ensure water supply;

Structural stability through steel cables and reinforcing elements. After the study, the design of the stand, shown in Figure. 1, was started.

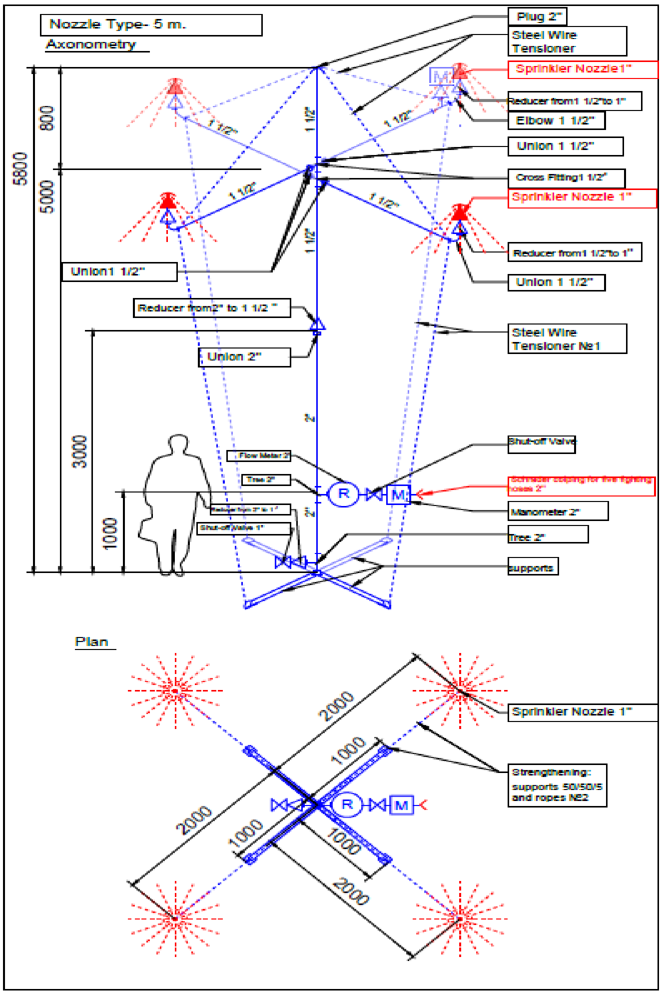

Figure 1. Stand for researching the distribution of the intensity of water jet coverage from sprinkler nozzles

The experimental stand was implemented in the open area of the Laboratory Block at the University of Mining and Geology "St. Ivan Rilski" - Sofia. It is a modular tubular structure mounted on a metal support stand and stabilized by steel cables. The structural height of the stand is 5.00 m, which allows the installation of test nozzles on specially constructed railings, in order to analyze their behavior during simulation of fires in underground mining sites.

Given the modularity of the structure, the height can be reduced to 3.00 m, which expands the applicability of the stand for testing nozzles intended for other infrastructure environments - underground garages, transport tunnels, metro stations, etc. The distance between the installed nozzles is 3.00 m, in accordance with the requirements of standard EN 12845:2015+A1:2020 "Fixed fire extinguishing systems - Automatic sprinkler systems: design, installation and maintenance", taking into account the relevant fire hazard class for underground facilities. The structure is made of galvanized pipes with diameters of 2", 1.5" and 1", connected by standard fittings - tees, sleeves, elbows, collars, etc. The supporting frame is made of steel square profiles with a thickness of 5 mm, with four profiles with a length of 1.00 m welded in a cross-shaped configuration, ensuring the necessary stability and mobility of the facility.

Selection of Sprinkler Nozzles for Research

For the needs of the experiment, TYCO sprinkler nozzles series TY4151 (Upright 8.0K, 3/4" NPT) were selected, characterized by corrosion resistance, activation temperature 68˚C and standardized parameters according to EN 12259-1 (Figure 2).

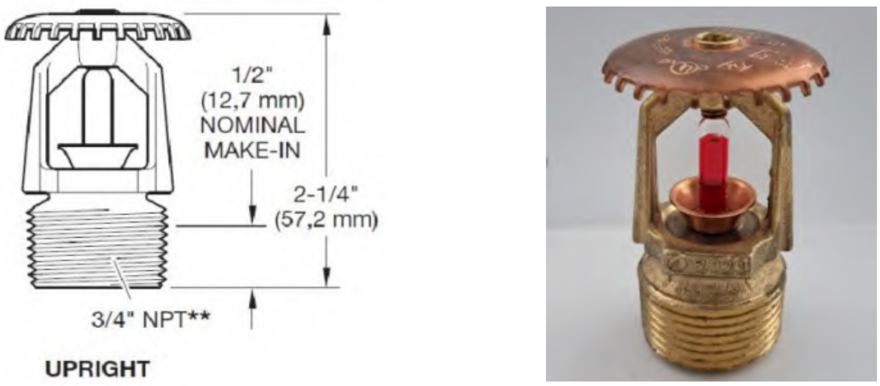

Figure 2. Sprinkler nozzle series TY4151

The choice is based on their frequent application in real underground sites, which allows extrapolation of the results to practical operation. The system is designed to be able to test other types of nozzles (spiral, screw), allowing comparative analysis.

Methodology of the Experiment

Four nozzles are installed on the already built stand (Figure. 3).

Figure 3. Sprinkler nozzles mounted on the stand

The tests are conducted on a built experimental stand equipped with four TY4151 sprinkler nozzles. The aim is to determine the intensity and distribution of the water jet on a horizontal plane by analyzing the measured air flows before the nozzles are activated. This creates conditions for predicting the spatial distribution of the water phase, including the expected coverage of the protected surfaces and the distance the droplets travel before reaching the floor or other critical areas (Dinchev, Gorbounov & Kostadinova 2018).

A network of measuring vessels is constructed in the irrigation zone, arranged in a checkerboard configuration. Each vessel has an area of 0.0526 m², and the volume of collected water is measured with laboratory measuring cylinders with an accuracy of ±1%. The experimental setup for experiments is presented in Figure 4.

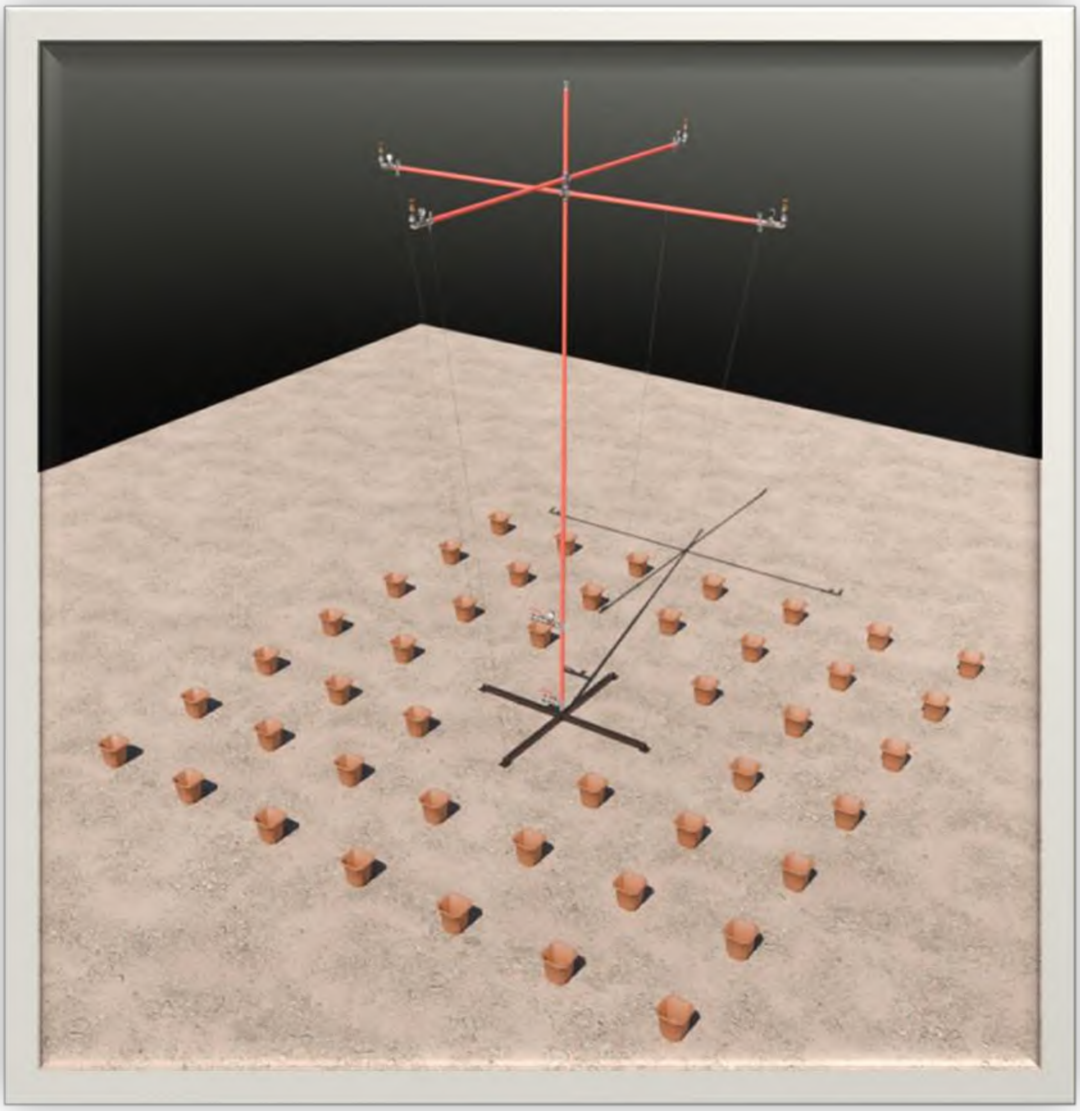

Figure 4. 3D experimental setup

Experimental Part and Results

Carrying Out an Experiment

Experiment parameters	
Date	30.10.2024
Number of nozzles	4
Type of nozzles	Sprinkler TY4151 – Upright 8.0K, 3/4″ NPT
Pressure	8 bar
Duration/time	10 min

On October 30, 2024, an experiment was conducted with four sprinkler nozzles to study the distribution of extinguishing intensity. The location of the collection vessels and the amount of water that has entered them are shown in Figure 5.

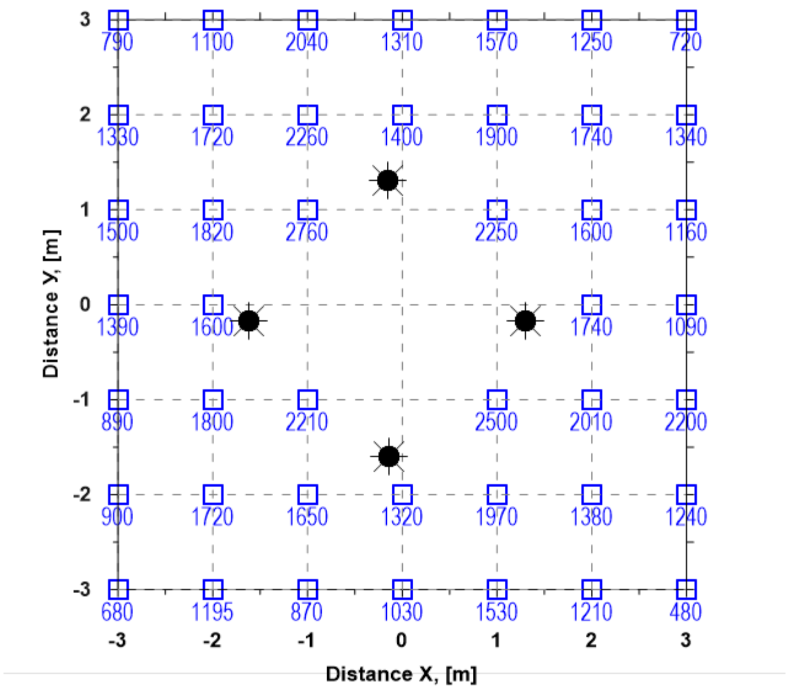

Figure 5. Diagram of the collection vessels and the amount of water that has fallen

After the experiment was completed, the amount of water in the collection vessels was recorded and the dew intensity was calculated. The results are presented by dew intensity isolines Figure 6 and a 3D surface diagram Figure 7, generated with Surfer software. They show the spatial distribution of the water jet and the areas of maximum and minimum intensity.

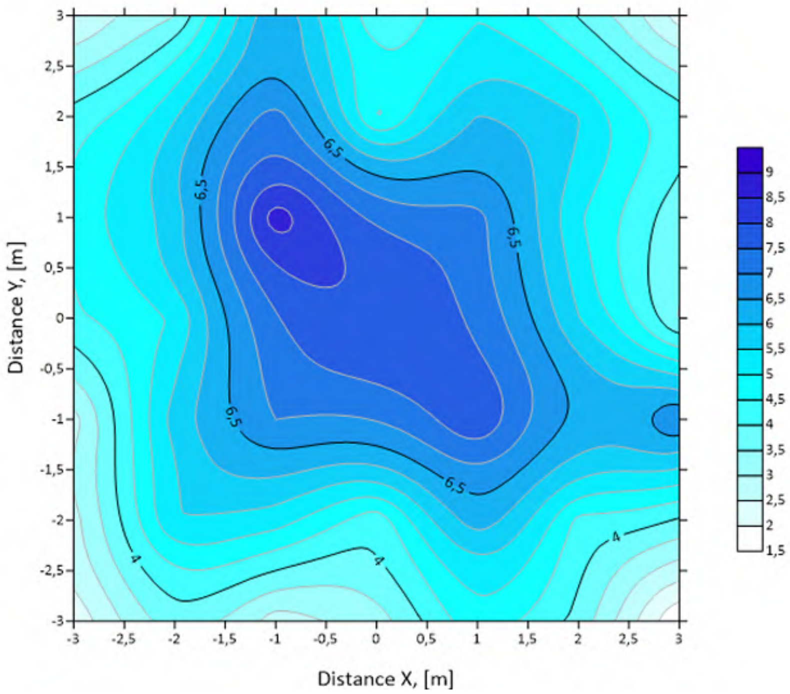

Figure 6. Dew intensity contours [mm/min], P=8 bar

Analysis of the Results Obtained

The analysis of the experimental data reveals a clearly pronounced symmetry in the distribution of the water jet in the central zone, with significant variations in the peripheral areas. When the pressure is increased to 8.0 bar, the following trends are observed:

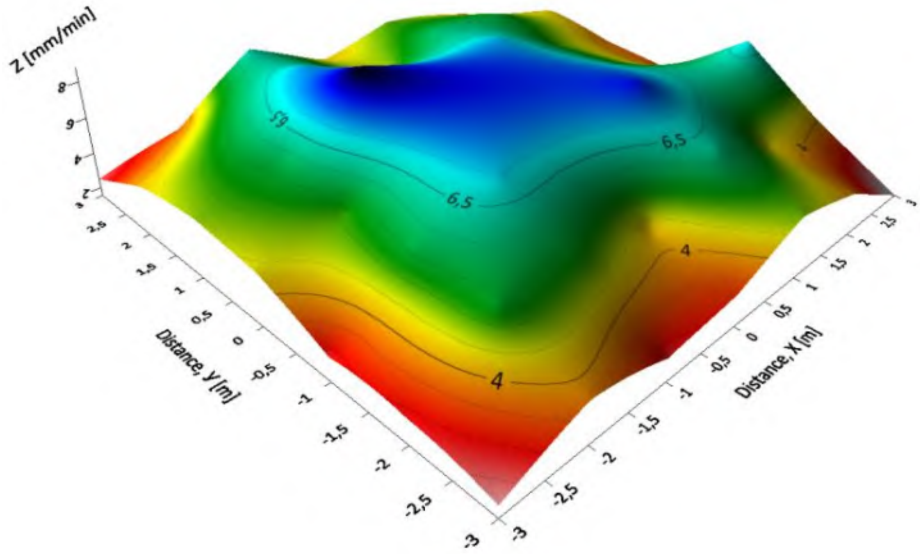

Figure 7. Distribution of water coverage intensity from sprinkler nozzles

- increased spray intensity;
- improved overlap between the zones of action of the individual nozzles;
- reduction of areas with insufficient coverage ("dry" areas);
- increase in droplet size, determined by observing rebound and accumulation.

The four-nozzle configuration demonstrates significantly higher spray efficiency compared to the two-nozzle setup, providing more uniform hydrodynamic coverage and an expanded controlled area. This increases the reliability of the system in real-world conditions where the direction of fire development does not always coincide with the preset nozzle placement.

Conclusion

Underground mining sites represent an environment with a high potential for the occurrence of complex and rapidly developing fires (Michaylov et al., 2011), which can lead to serious incidents, human casualties and significant material losses. Stationary fire extinguishing systems are a key component in the strategy for early fire control, limiting its linear spread and creating conditions for safe and faster access of emergency and rescue teams to the source. Due to the specifics of the mining environment, the time for mobilization and access to the fire often exceeds the time for the fire to fully ignite. This necessitates the use of automated systems that can be activated immediately and localized, even at the initial stage of fire occurrence. In this context, precise testing and evaluation of the characteristics of the nozzles in laboratory conditions is essential for the reliability and effectiveness of the overall fire protection system. The obtained results confirm that increasing the number of nozzles leads to higher coverage efficiency and creates conditions for stable and reliable system operation even under variable conditions and fire orientation. Such a configuration can play a crucial role in the future design of stationary fire extinguishing systems for underground sites with a high-risk profile.

Recommendations for Future Research

In view of the achieved results and the potential for practical application, future research should focus on additional parameters affecting the effectiveness of fire extinguishing systems – such as nozzle type, spray angle, viscosity and temperature of the fluid used, as well as the impact of air flows characteristic of a mining environment. Conducting experiments in scaled tunnel models or real underground sections will allow validation of laboratory results and will contribute to the development of standardized methodologies for evaluating fire extinguishing systems in specific industrial conditions.

Scientific Ethics Declaration

* The authors declare that the scientific ethical and legal responsibility of this article published in EPSTEM journal belongs to the authors.

Conflict of Interest

* The authors declare that they have no conflicts of interest

Funding

* This research is supported by the Bulgarian Ministry of Education and Science under the National Programme "Young Scientists and Postdoctoral Students – 2" (Stage II 2024-2025).

Acknowledgements or Notes

* This article was presented as an oral presentation at the International Conference on Research in Engineering, Technology and Science (www.icrets.net) held in Peja/Kosovo on July 10-13, 2025.

References

Aleksandrova, E., Asenovski, S., Georgiev, D., Kaykov, D., & Koprev, I. (2019). Methods for determining an optimal technological solution for underwater mining. *Journal of Mining and Geological Sciences*, *62*(2), 5–8.

Aleksandrova, E., Koprev, I., Dzhobov, I., & Petkov, T. (2015). New technologies and trends in open-pit mining for the development of thin, low-productivity coal seams. *Proceedings of the National Scientific and Technical Conference: Mineral resources and sustainable development* (pp. 124–129). Sofia, Bulgaria: Scientific and Technical Union of Mining, Geology and Metallurgy.

Dinchev, Z., Gorbounov, Y., & Kostadinova, N. (2018). Velocity field visualization, measured with 3D ultrasonic anemometer. *Journal of Mining and Geological Sciences*, *61*(2), 39–44.

Grigorova, I. (2020). Circular economy in the Bulgarian mineral raw materials industry. *Geology and Mineral Resources*, *27*(4–5), 2–7.

Michaylov, M., Krilchev, A., Vladkova, B., & Dimova, B. (2011). Forschung eines neues Mittels zur Profilaktik und Loschen von endogenous Branden. *Bergbau*, *62*(3), 114–118.

Tsankov, T. (2021). Scenario and modelling of fire due reason from electrical character in a gasified building. *13th Electrical Engineering Faculty Conference (BulEF)* (pp. 1–6).

Tsankov, T. (2024). Analysis and risk assessment of an electric car fire in an underground garage. In *Proceedings of the Energy Forum 2024* (pp. 513-528). Retrieved from: https://www.ntse-bg.org/UPLOADS/conf/EF2024/Articles/Energien_forum_2024.pdf

Author(s) Information

Diana Makedonska University of Mining and Geology St. Ivan Rilski 1700 Prof. Boyan Kamenov St. Sofia, Bulgaria, Contact e-mail: *diana.makedonska@mgu.bg*	**Vasil Tsanov** Academy of Ministry of Interior 1 Alexander Malinov Blvd. Sofia, Bulgaria,

To cite this article:

Makedonska, D., & Tsanov, V. (2025). Optimization of an experimental stand with four nozzles for assessing the intensity of irrigation in underground mining sites. *The Eurasia Proceedings of Science, Technology, Engineering and Mathematics (EPSTEM), 35,* 193-200.

The Eurasia Proceedings of Science, Technology, Engineering & Mathematics (EPSTEM)
ISSN: 2602-3199

The Eurasia Proceedings of Science, Technology, Engineering and Mathematics (EPSTEM), 2025

Volume 35, Pages 201-207

ICRETS 2025: International Conference on Research in Engineering, Technology and Science

Polysulfone-Based Nanocomposite Membranes with Multi-Walled Carbon Nanotubes for Efficient Perfluorooctanoic Acid (PFOA) Removal from Water

Abderrazek El-Kordy
University of Sharjah

Tahar Laoui
University of Sharjah

Ismail Walid Khalil Almanassra
University of Sharjah

Lubna Jaber
University of Sharjah

Khalil Abdelrazek Khalil
University of Sharjah

Muataz Ali
University of Sharjah

Abstract: Perfluorooctanoic acid (PFOA) is a persistent environmental pollutant of increasing concern due to its chemical stability and associated health risks. This study reports on the development and evaluation of polysulfone (PSF)-based nanocomposite membranes containing multi-walled carbon nanotubes (MWCNTs) for effective PFOA removal from water. The bare PSF membrane and the modified membrane with 5 wt% MWCNT loading were fabricated by the non-solvent induced phase separation and tested under continuous flow conditions at different PFOA concentrations. The modified membrane achieved approximately 98% PFOA removal at a concentration of 100 parts per billion (ppb), demonstrating sustained and robust performance. Although the inclusion of MWCNTs reduced water permeance, this was offset by the significant enhancement in contaminant retention. Structural and morphological analyses confirmed the uniform dispersion and integration of MWCNTs within the membrane matrix. These results highlight the potential of PSF-MWCNT nanocomposite membrane for advanced water treatment applications targeting per-fluorinated compounds.

Keywords: PFOA, MWCNT, Polysulfone, PSF-MWCNT nanocomposite membrane, Water purification

Introduction

In its natural state, water is pure and serves as a vital medium for the extraction, purification and dissolution of various substances. This has earned it the title of 'universal solvent' due to its high polarity and essential role in sustaining life. However, natural sources of water, such as seas, rivers, clouds (in the form of rain, ice and snow) and underground reservoirs, can be altered by non-polluting elements, such as minerals, sediments and biological growth, as well as by pollutants introduced through human activity. These contaminants compromise water

- Selection and peer-review under responsibility of the Organizing Committee of the Conference

quality, making clean water increasingly scarce. Consequently, safeguarding water sources and developing effective purification technologies has become a global priority (Kumar et al., 2022; Liu et al., 2017).

Contamination by perfluorooctanoic acid (PFOA) is a global issue, particularly in natural waterways and industrial waste. PFOA is a frequently used per-fluorinated chemical in several industries such as textiles, non-stick coatings, and firefighting foams (Glüge et al., 2020). Due to its chemical inertness and resistance to degradation, PFOA has become a common contaminant in the environment, particularly in surface and groundwater systems. The persistence of PFOA and its potential to bioaccumulate pose serious health concerns, including carcinogenic and endocrine-disrupting effects. Consequently, regulatory bodies around the world are advocating for the development of more efficient water treatment solutions.

In this regard, the U.S. Environmental Protection Agency (USEPA) has established a stringent advisory limit of 4 parts per trillion (ppt) for PFOA in drinking water (Sahu, 2023). To address this concern, various treatment strategies have been explored, including activated carbon adsorption, reverse osmosis, advanced oxidation processes, electrochemical oxidation, and photochemical degradation. However, these conventional methods often encounter limitations in terms of cost-effectiveness, operational complexity, and scalability. Among the available technologies, membrane filtration has emerged as a particularly promising approach due to its high removal efficiency at the micro-scale and relatively low energy requirements, highlighting its potential as a sustainable and efficient solution for PFOA remediation in water treatment systems. (Sayed et al., 2024; Turdean, 2011).

In recent years, nanotechnology has emerged as a promising frontier in water purification. Nanocomposite membranes, which integrate nanomaterials into polymer matrices, offer enhanced permeability, selectivity, and fouling resistance. Among these, carbon nanotubes (CNTs) have drawn significant attention due to their high surface area, strong adsorption capacity, and unique physicochemical properties (Stobinski et al., 2014; Zhou et al., 2015).

Polysulfone (PSF), a mechanically robust and chemically stable thermoplastic, is frequently used in membrane fabrication. The incorporation of multi-walled carbon nanotubes (MWCNTs) into PSF matrix creates a composite membrane with improved adsorption characteristics and transport properties (Aruchamy et al., 2023; Benkhaya et al., 2019; Akale & Shaikh, 2024; Kumar & Bellare, 2025).

The aim of this work is to develop new PSF-MWCNT composite membranes with two different loadings of: 0% and 5%. The objective is to evaluate the effectiveness of these membranes in removing PFOA from water. The MWCNTs were characterized using XRD and FTIR analysis. The morphology of the fabricated membranes was investigated and tested for PFOA removal in continuous filtration mode.

Materials and Methods

Chemicals

Multi-walled carbon nanotubes (MWCNTs) were obtained from a certified supplier in China. Polysulfone (PSF) and dimethylacetamide (DMA) were purchased from Merck (Germany). Polyvinylpyrrolidone (PVP), acquired from Sigma-Aldrich (USA), was used as a pore-forming agent. PFOA, 95% was obtained from Sigma-Aldrich (China). Deionized water with a resistivity of 15.0 MΩ•cm was used throughout the experiments. All chemicals were of analytical grade and used without further purification.

Membrane Fabrication

A polymer stock solution was formulated with a composition of 16 wt% polysulfone (PSF), 82 wt% dimethylacetamide (DMA), and 2 wt% additional PSF used as an additive. Initially, PSF pellets were dissolved in a predetermined volume of DMA by stirring overnight. Subsequently, 2 wt% polyvinylpyrrolidone (PVP) was added while maintaining the solution at a constant temperature (45–50 °C) using an oil bath. This prolonged stirring ensured complete dissolution and homogeneity. PVP was added as a pore-forming agent, improving the membrane’s structural properties and enhancing the rheological behavior of the casting solution by reinforcing polymer-solvent interactions. For PSF-MWCNTs nanocomposite membrane, 5 wt% MWCNTs were added to the solution, followed by 60 minutes of mechanical stirring and 60 minutes of ultrasonication using a probe sonicator (UP400St, Hielscher Ultrasonics) in an ice bath.

Before casting, the mixture was degassed for 60 minutes to eliminate entrapped air bubbles. Both the PSF membrane and PSF-MWCNTs nanocomposite membrane were fabricated via the nonsolvent-induced phase separation (NIPS) method. The casting was carried out at room temperature using an automatic thick film applicator (MSK-AFA-II, MTI Corporation, China) with a casting thickness of 200 µm and a knife speed of 4.5 cm/s on a clean glass plate. The cast films were immediately immersed in a coagulation bath containing deionized water to induce phase separation. After precipitation, the membranes were repeatedly washed and stored in deionized water for characterization and testing. The membrane labels are indicated in Table 1.

Table 1. Prepared unmodified and modified membranes

Membrane		Label
Unmodified membrane	Polysulfone	M0
	Polysulfone/ 5wt% MWCNTs	M5

Characterization Techniques

Characterization was conducted to examine the physicochemical properties of the synthesized unmodified and modified membranes. The chemical characteristics of MWCNTs was identified using Fourier Transform Infrared Spectroscopy (FTIR) (Model 6300, Jasco, Japan), recording spectra in the range of 4000 to 400 cm^{-1}. X-ray diffraction (XRD) analysis of MWCNTs was conducted using a Bruker D8 Advance diffractometer equipped with a Cu Kα radiation source (λ = 1.54056 Å), operated at 40 kV and 40 mA. The microstructure and surface morphology of the membranes were analyzed using a Field Emission Scanning Electron Microscope (FE-SEM) (Apreo C, Thermo Scientific), operated at an accelerating voltage of 15 kV. The permeance performance (flux and rejection) of the fabricated membranes was tested using DI water and PFOA-contaminated solutions utilizing a stirred dead-end filtration cell (Sterlitech HP4750) connected to a pressurized air cylinder.

Results and Discussion

XRD Analysis

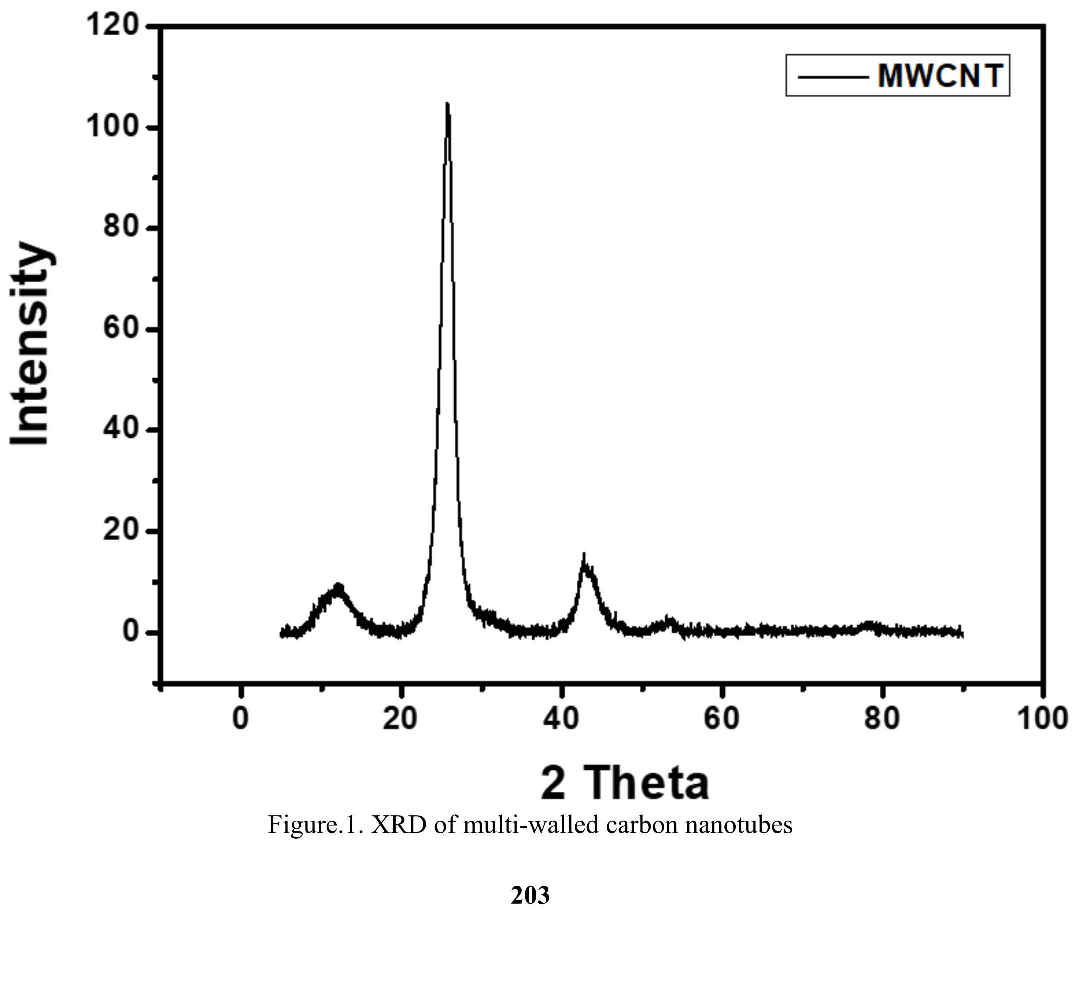

Figure.1. XRD of multi-walled carbon nanotubes

The X-ray diffraction (XRD) pattern of the multi-walled carbon nanotubes (MWCNTs) exhibits a prominent peak at approximately 2θ ≈ 26°, corresponding to the (002) plane of graphitic carbon. This reflection is characteristic of the hexagonal graphite structure and confirms the presence of well-ordered graphitic layers stacked along the walls of the nanotubes. The sharpness and intensity of this peak indicate a high degree of crystallinity and structural order within the MWCNTs, with minimal impurities. Additionally, a weaker and broader peak observed near 2θ ≈ 43° is typically attributed to the (100) or (101) reflections of less-ordered graphitic planes. This feature suggests the presence of turbostratic or disordered carbon regions, commonly found in multi-walled nanotube structures due to interlayer misalignment or structural defects.

FTIR Analysis

The FTIR spectrum of MWCNTs, used as a nanoadditive in the PSF membrane, revealed several characteristic absorption bands indicative of surface functional groups, as shown in Figure 2. A broad peak observed at 3474 cm^{-1} corresponds to the stretching vibration of hydroxyl (-OH) groups. The peaks at 2925 cm^{-1} and 2833 cm^{-1} are attributed to asymmetric and symmetric stretching vibrations of aliphatic C-H bonds, respectively. A distinct peak at 1638 cm^{-1} is assigned to the C=C stretching vibration of aromatic structures characteristic to the graphitic backbone of MWCNTs, as well as possible contributions from C=O (carbonyl) stretching. Additional peaks at 1320 cm^{-1} and 1017 cm^{-1} are associated with C-OH stretching vibrations, further confirming the presence of oxygen-containing carboxylic functional groups on the nanotubes surface.

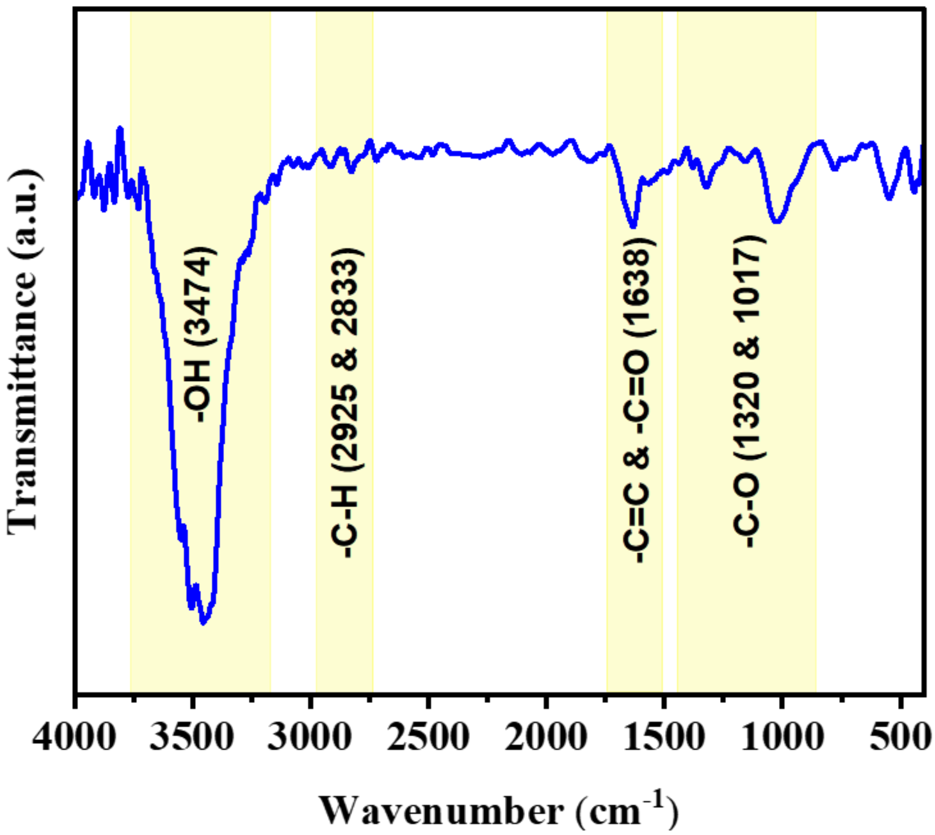

Figure 2. FTIR spectra of MWCNT

FESEM Analysis

Figure 3 shows the surface morphology and cross-sectional structure of bare and MWCNTs-modified PSF membranes. SEM images revealed that the bare PSF membrane had a smooth and homogeneous surface without defects. However, incorporating 5 wt% MWCNT into the PSF matrix noticeably altered the surface texture, causing a reduction in smoothness. White particles were visibly dispersed across the membrane surface, due to static and chemical interactions between the MWCNT and the polymer chains resulting in the migration of particulates towards the membrane surface. Despite these morphological variations, SEM images of the modified membrane showed no evidence of cracks or voids on the surface. This suggests that the membrane's structural integrity was preserved and that the MWCNT were successfully and uniformly dispersed within the polymer matrix. Similarly, the effect of incorporating MWCNT on the cross-sectional morphology of the PSF membrane was examined. The unmodified PSF membrane had a thin, dense skin layer on top of an asymmetric structure characterized by short, irregular, finger-like pores. Adding 5% MWCNTs to the PSF membrane remarkably thickened the membrane's top surface and partially blocked the membrane channels. This effect is primarily due to the carbon nanomaterial altering the polymer matrix's rheological properties and thermodynamic behavior. At high concentrations, the increased viscosity of the casting solution limits the mobility and interaction of the polymer chains, thus reducing the effective surface area available for proper phase separation. Consequently, the membrane exhibits smaller pore sizes and reduced pore volume, leading to obstruction of the pores. However, these characteristics are beneficial for PFOA adsorptive membranes, as it is the top surface rather than the cross-sectional membrane channels that plays a critical role in the removal and filtration of PFOA contaminants.

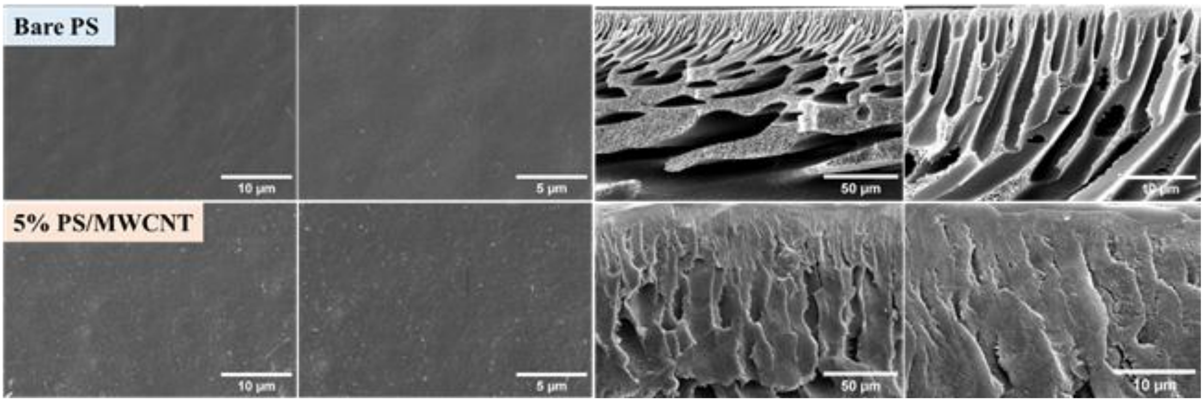

Figure 3. Surface morphology and cross-sectional views of bare PSF and PSF modified with 5% MWCNTs membranes.

Membrane Flux and Rejection

The permeance performance of both bare PSF membrane and MWCNTs-modified PSF nanocomposite membrane is presented in Figure 4a, which shows the time-dependent permeance under pure water (DI water) and PFOA-containing feed solutions. The bare PSF membrane (M0) demonstrated consistently high water permeance, averaging approximately 426.4 LMH (liters per square meter per hour) during the initial 30 minutes of DI water filtration. Upon switching to a feed solution containing 100 ppb PFOA at the 31st minute, the permeance remained nearly unchanged, with only a slight decrease to around 424.4 LMH by the 90th minute. This minimal variation indicates that the presence of PFOA had no significant effect on the flux, and even at an increased concentration of 300 ppb, the permeance remained similarly stable, confirming negligible interaction between PFOA and the bare PSF membrane. In contrast, the MWCNTs-modified PSF membrane exhibited a markedly lower initial water permeance of approximately 250 LMH, which gradually declined to about 238 LMH over the same time period. This reduction is attributed to the incorporation of 5 wt% MWCNTs into the membrane matrix, which likely reduced pore accessibility and water mobility due to enhanced surface interactions, while being specifically tailored to promote PFOA adsorption. The observed trade-off between permeability and adsorption capacity is consistent with the intended functional modification.

The PFOA rejection performance of the membranes is summarized in Figure 4b, comparing the bare PSF membrane (M0) with the MWCNTs-modified PSF membrane (M5) at initial feed solution concentrations of 100 ppb and 300 ppb. The M0 membrane exhibited a poor rejection efficiency, with values of 14.3% and 11.7% for 100 ppb and 300 ppb, respectively, indicating that PSF lacks significant affinity for PFOA removal. In contrast, the M5 membrane achieved a substantial enhancement in rejection, reaching 98.2% at 100 ppb and 94.6% at 300 ppb. This remarkable performance is attributed to the adsorptive properties of the incorporated MWCNTs, which provide active sites for PFOA interaction and retention, demonstrating sustained and robust performance. Although the inclusion of MWCNTs reduced water permeance, this was offset by the significant enhancement in contaminant retention. It is important to note that typical environmental concentrations of PFOA in real water matrices are significantly lower than the concentrations tested in this study. This suggests that the MWCNTs-functionalized PSF membrane is not only effective but also highly promising for practical applications, particularly as a pretreatment step in water and wastewater treatment systems targeting trace-level PFOA contamination.

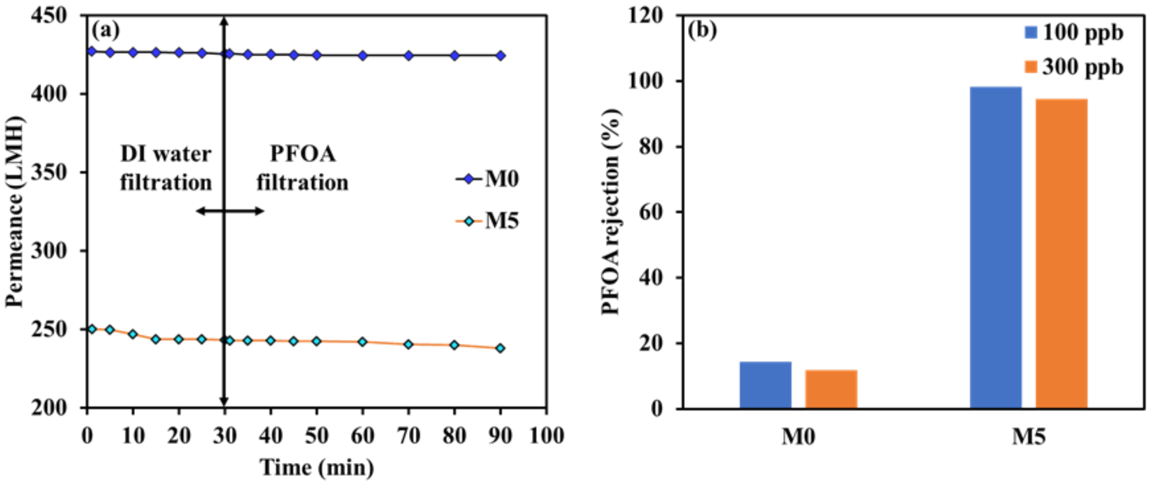

Figure. 4. (a) Permeance measurements of DI water and PFOA contaminated water, (b) Average rejection of PFOA over 1 h of filtration at different initial PFOA concentrations.

Conclusion

Polysulfone (PSF) and PSF-based nanocomposite membranes containing multi-walled carbon nanotubes (MWCNTs) were successfully fabricated and proved being effective in removing perfluorooctanoic acid (PFOA) from water. The characterization techniques indicated the crystallinity and structural order of the MWCNTs with the presence of oxygen-containing carboxylic functional groups on the nanotubes surface. The bare PSF membrane presented a smooth, homogeneous, and defect-free surface, while the incorporation of 5 wt% MWCNTs into the PSF matrix resulted in an alteration of the surface texture, with a reduction in smoothness and pore size, but no evidence of surface cracks or voids. Although a decrease in water permeance was observed upon adding MWCNTs, the modified PSF membrane containing 5% MWCNTs loading demonstrated an excellent PFOA rejection efficiency. These results confirm that MWCNTs serve as both structural enhancers and active adsorption sites, thereby transforming conventional PSF membrane into highly efficient separation platforms. These findings highlight the potential of PSF-MWCNTs nanocomposite membrane as a practical, scalable and sustainable solution for addressing persistent organic pollutants such as PFOA in water treatment applications.

Scientific Ethics Declaration

* The authors declares that the scientific ethical and legal responsibility of this article published in EPSTEM Journal belongs to the authors.

Conflict of Interest

* The authors declare that they have no conflicts of interest.

Funding

* This research was funded by the University of Sharjah, via the Research Institute of Sciences and Engineering.

Acknowledgements

* This article was presented as an oral presentation at the International Conference on Research in Engineering, Technology and Science (www.icrets.net) held in Peja/Kosovo on July 10-13, 2025.

References

Akale, S., & Shaikh, I. N. (2024). Mixed-matrix membrane designed with water channels and sieving effect for effective removal of heavy metals. *Environmental Nanotechnology, Monitoring and Management*, *22*, 100985.

Aruchamy, K., Jegathambal, P., & Praveen, A. (2023). Performance evaluation of Polysulfone/MWCNT nanocomposite membrane for the efficient removal of blue CA dye. *Emergent Materials*, *6*(5), 1519–1526.

Benkhaya, S., Achiou, B., Ouammou, M., Bennazha, J., Alami Younssi, S., M'rabet, S., & El Harfi, A. (2019). Preparation of low-cost composite membrane made of polysulfone/polyetherimide ultrafiltration layer and ceramic pozzolan support for dyes removal. *Materials Today Communications*, *19*, 212–219.

Glüge, J., Scheringer, M., Cousins, I. T., Dewitt, J. C., Goldenman, G., Herzke, D., Lohmann, R., Ng, C. A., Trier, X., & Wang, Z. (2020). An overview of the uses of per- and polyfluoroalkyl substances (PFAS). *Environmental Science: Processes and Impacts*, *22*(12), 2345–2373.

Kumar, R., Singh, S., Kumar, R., & Sharma, P. (2022). Groundwater quality characterization for safe drinking water supply in Sheikhpura district of Bihar, India: A geospatial approach. *Frontiers in Water*, *4*, 1–13.

Kumar, V., & Bellare, J. (2025). Heavy metals removal from contaminated water with Psf hollow fiber membrane blended with Fe_3O_4/MWCNTs –COOH nanohybrid. *Journal of Water Process Engineering*, *69*, 106880.

Liu, G., Zhang, Y., Knibbe, W. J., Feng, C., Liu, W., Medema, G., & van der Meer, W. (2017). Potential impacts of changing supply-water quality on drinking water distribution: A review. *Water Research*, *116*, 135–148.

Sahu, O. (2023). Remediation of perfluorooctanoic acid (PFOA) with nano ceramic clay: Synthesis, characterization, scale-up and regenerations. *Environmental Pollution*, 121241.

Sayed, N. S. M., Ahmed, A. S. A., Abdallah, M. H., & Gouda, G. A. (2024). ZnO@ activated carbon derived from wood sawdust as adsorbent for removal of methyl red and methyl orange from aqueous solutions. *Scientific Reports*, *14*(1), 1–18.

Stobinski, L., Lesiak, B., Malolepszy, A., Mazurkiewicz, M., Mierzwa, B., Zemek, J., Jiricek, P., & Bieloshapka, I. (2014). Graphene oxide and reduced graphene oxide studied by the XRD, TEM and electron spectroscopy methods. *Journal of Electron Spectroscopy and Related Phenomena*, *195*, 145–154.

Turdean, G. L. (2011). Design and development of biosensors for the detection of heavy metal toxicity. *International Journal of Electrochemistry*, *2011*, 1–15.

Zhou, F., Qiu, K., Peng, G., & Xia, L. (2015). Silver/carbon nanotube hybrids: A novel conductive network for high-rate lithium ion batteries. *Electrochimica Acta*, *151*, 16–20.

Author(s) Information

Abderrazek El-Kordy
University of Sharjah, Sharjah 27272, United Arab Emirates
Research Institute of Sciences and Engineering, University of Sharjah, Sharjah P.O. Box 27272, United Arab Emirates
Contact e-mail: *abderrazekelkordy@gmail.com*

Tahar Laoui
Department of Mechanical and Nuclear Engineering, College of Engineering, University of Sharjah, Sharjah P.O. Box 27272, United Arab Emirates

Ismail Walid Khalil Almanassra
Research Institute of Sciences and Engineering, University of Sharjah, Sharjah P.O. Box 27272, United Arab Emirates

Lubna Jaber
Center for Advanced Materials Research, Research Institute of Sciences and Engineering, University of Sharjah, Sharjah 27272, United Arab Emirates

Khalil Abdelrazek Khalil
Department of Mechanical and Nuclear Engineering, College of Engineering, University of Sharjah, Sharjah P.O. Box 27272, United Arab Emirates

Muataz Ali
Chemical and Water Desalination Engineering Program, College of Engineering, University of Sharjah, Sharjah 27272, United Arab Emirates

To cite this article:

El-Kordy, A., Laoui, T., Almanassra, K. W. I., Jaber, L., Khalil, A. K., & Ali, M. (2025). Polysulfone-based nanocomposite membranes with multi-walled carbon nanotubes for efficient perfluorooctanoic acid (PFOA) removal from water. *The Eurasia Proceedings of Science, Technology, Engineering and Mathematics (EPSTEM), 35,* 201-207.

The Eurasia Proceedings of Science, Technology, Engineering & Mathematics (EPSTEM)
ISSN: 2602-3199

The Eurasia Proceedings of Science, Technology, Engineering and Mathematics (EPSTEM), 2025

Volume 35, Pages 208-215

ICRETS 2025: International Conference on Research in Engineering, Technology and Science

Standardizing Competencies in Management Information Systems

Ali Ucucu
OSTIM Technical University

Basak Gok
Gazi University

Hadi Gokcen
Gazi University

Abstract: The discipline of Management Information Systems (MIS) is inherently multidisciplinary. While this characteristic enables graduates to be employed across diverse sectors and domains, it also leads to ambiguity in the academic positioning of the field. This ambiguity presents significant challenges in defining and standardizing the core competencies expected of MIS graduates. The primary aim of this study is to identify the fundamental competencies expected from MIS graduates in Türkiye and to categorize these competencies within a systematic framework. The research draws upon three primary data sources: university program learning outcomes, expert opinions, and global competency trends identified by the World Economic Forum. A qualitative content analysis was conducted using QDA Miner software on the publicly available program outcomes of 64 MIS programs in Türkiye and the 22 expert opinions in the field. During the analysis, a thematic framework was developed based on six foundational disciplines that inform the MIS field: Computer Science, Operations Research, Management Science, Sociology, Psychology, and Economics. The 29 identified competencies were synthesized based on their frequency and significance within the data sources. Finally, these competencies were classified into two overarching categories: "personal skills" and "professional skills." This classification contributes to aligning MIS curricula with industry expectations and global trends and serves as a valuable reference for accreditation and quality assurance processes.

Keywords: Business engineering, Management information systems, Core competencies

Introduction

Management Information Systems (MIS) programs are inherently sociotechnical disciplines that aim to provide students with technical and managerial competencies (Laudon & Laudon, 2020). This unique structure enables MIS graduates to take on active roles in IT-driven decision-making processes within organizations. However, in Türkiye, the fact that MIS programs are housed under various faculties has led to significant differences in curricula affecting graduates' competency levels (Council of Higher Education / YOK, 2023). Program content and academic approaches vary considerably across institutions (Aktas et al., 2022). The absence of common academic standards and the diversity of courses offered may lead to the emergence of graduate profiles that differ significantly in terms of knowledge, skills, and competencies (Henkoglu & Serefoglu, 2019).

Literature frequently highlights both the similarities and gaps between the educational outcomes provided by MIS programs and the competencies expected by the private sector (Baser & Bakirtas, 2023; Vural, 2019). As a result, the importance of quality assurance and accreditation systems in higher education has increased, emphasizing the need to standardize program outcomes (Dogan, 1999; Kılıcaslan, 2020). International accreditation bodies such as AACSB and ABET play a vital role in evaluating the alignment between curriculum content and industry expectations (Turel & Altintas, 2018; AACSB, 2020). Türkiye's participation in the Bologna Process has established a framework through the Turkish Qualifications Framework (TQF) to ensure this alignment (Sezgin et al., 2011; Ayvaz et al., 2016).

This study aims to identify the core competencies that MIS programs should cultivate by analyzing the learning outcomes of Turkish MIS programs and the expectations of industry professionals through qualitative methods. In this context, university-level program outcomes and sectoral expectations for MIS graduates have been examined. Based on the findings, the essential competencies for MIS graduates have been identified. This research seeks to contribute to the positioning of MIS programs from both academic and industrial perspectives and to highlight the competencies that will enhance graduates' employability.

Theoretical Framework

Management Information Systems (MIS) is a multidisciplinary academic field that integrates technical and managerial dimensions, focusing on strategically using information technologies to solve organizational problems. The origins of MIS can be traced back to the 1960s, when information systems were first developed to generate managerial reports for businesses. Over time, these systems evolved into academic programs, with the first graduate-level MIS program launched at the University of Minnesota in 1968 (Davis, 1983; Dickson, 1981, as cited in George & Hadidi, 2023). In Türkiye, the first MIS undergraduate program was established in 1995 at Boğaziçi University. Today, MIS undergraduate programs are offered at 83 universities nationwide (Council of Higher Education / YOK, 2023).

The positioning of MIS programs under different faculties—such as Faculties of Economics and Administrative Sciences, Engineering, and Applied Sciences—has led to significant variations in curricula (Aktas et al., 2022). These structural differences contribute to a wide range of competency levels among graduates. While this diversity, stemming from interdisciplinary interactions, adds richness to the field, it also results in noticeable imbalances in graduate profiles due to the lack of standardization.

At this point, the concepts of quality assurance and accreditation in higher education gain significance. Accreditation is a system that evaluates the quality and adequacy of academic programs offered by higher education institutions (Dogan, 1999). At the national level, organizations such as YÖKAK, FEDEK, and MÜDEK, and at the international level, bodies such as AACSB, ABET, and FIBAA aim to ensure standardization in education by assessing the academic qualifications of programs. AACSB, in particular-holding a prominent position in the field of social sciences-evaluates criteria such as curriculum, strategic planning, faculty qualifications, and learning outcomes to measure the overall quality of academic programs (AACSB, 2020; Turel & Altintas, 2018).

With the launch of the Bologna Process, the European Union aimed to establish a common framework in higher education, and Türkiye joined this process in 2001. In line with Bologna principles, the Turkish Qualifications Framework (TQF), published in 2011, defines the knowledge, skills, and competency levels that higher education programs are expected to provide (Sezgin et al., 2011; Ayvaz et al., 2016). This framework seeks to define learning outcomes at the national level and enhance comparability among different programs.

Academic studies in the field of MIS highlight significant diversity in both curricula and graduate competencies. For instance, Vural (2019) classified the competencies expected from MIS graduates into four main categories: social, managerial, technical, and core technical skills. Similarly, Ugur et al. (2016), through an analysis of course content from 16 universities, found that 26.78% of MIS courses focused on technical topics, 26.17% on managerial issues, 21.35% on analytical skills, and 15.13% on communication. In another comparative study, Aktas et al. (2022) examined MIS job postings in both the United States and Türkiye, revealing that social and managerial competencies are emphasized in both contexts, while skills such as data analytics and leadership are more prominently demanded in the U.S.

In light of these findings, aligning and standardizing MIS programs with industry expectations is crucial—not only to improve graduate employability but also to strengthen the academic identity of the discipline. Accordingly, this study aims to comprehensively analyze both program learning outcomes and industry expectations, ultimately leading to the development of a Competency List for the MIS field.

Methods

This research was conducted within a qualitative research design with the aim of analyzing the competencies that undergraduate Management Information Systems (MIS) programs in Türkiye seek to instill in their graduates and evaluating these competencies in comparison with industry expectations. The primary data sources of the study consisted of program learning outcomes from university MIS programs and expert opinions obtained from industry representatives. The primary data sources of the study are the program learning outcomes that all universities with MIS undergraduate programs in Türkiye provide to their students and expert opinions from sector representatives. All collected data were subjected to content analysis to identify the core competencies that MIS graduates are expected to possess.

Data Collection

The data collection process is based on two primary sources. Firstly, among the 83 universities in Türkiye offering undergraduate programs in Management Information Systems (MIS), the program learning outcomes of 64 universities those that publicly disclose such information were gathered through their official websites. A total of 777 program learning outcomes were compiled and structured to be suitable for the analysis process. The second data source consisted of expert opinions obtained from 22 individuals, including academics in the MIS field and representatives from the private sector who employ MIS graduates. Interviews conducted with these experts yielded a total of 289 competency statements.

Data Analysis

The collected program learning outcomes and expert opinions were subjected to content analysis using QDA Miner, a software tool widely used in qualitative data analysis. Six thematic approaches proposed by Laudon and Laudon (2020) for the MIS discipline were adopted as the main analytical themes prior to the coding process to enable systematic categorization of the data. These thematic areas include Computer Science, Operations Research, Management Science, Sociology, Economy, and Psychology. Under these six themes, 29 competency codes were developed to capture all data, as illustrated in Figure 1 comprehensively.

Figure 1. Themes and codes identified for qualitative analysis

The competencies identified in both data sets were listed and ranked during the analysis process. The ranking values of each competency from the respective lists were summed to establish a prioritization. Through this method, the most critical competency areas were identified based on both academic learning outcomes and industry expectations. This prioritization, presented in detail in the Findings section, reveals the relative importance of the competencies that MIS graduates are expected to possess.

Findings

This study analyzes the competencies derived from the program learning outcomes of Management Information Systems (MIS) programs in Türkiye, as well as expert opinions from professionals who employ MIS graduates in the industry. As a result of this analysis, the core competencies expected of MIS graduates were identified. These competencies were then compared in terms of their academic and industry-based priorities and are presented in Table 1.

Table 1. Qualitative analysis results

University Results		Sectoral Results	
1	Problem Solving	1	Project Management
2	Data Collection and Analysis	2	Business Processes
3	Project Management	3	Business Management
4	Business Management	4	Business Intelligence
5	Technology Adoption	5	Leadership
6	Ethics	6	Technology Adoption
7	Effective Communication	7	Algorithmic Thinking
8	Personal Development	8	Data Collection and Analysis
9	Foreign Language Skills	9	Personal Development
10	Business Processes	10	Programming
11	System Design and Management	11	Software Development Processes
12	Computer Hardware and Network Management	12	Problem Solving
13	Teamwork	13	Teamwork
14	Social Benefit	14	Cyber Security
15	Programming	15	Human Psychology
16	Database Management	16	Effective Communication
17	Leadership	17	System Design and Management
18	Decision Making	18	Computer Hardware and Network Management
19	Algorithmic Thinking	19	Foreign Language Skills
20	Business Intelligence	20	Decision Making
21	Software Development Processes	21	Reporting and Visualization
22	Human Computer Interaction	22	Digital Transformation
23	Reporting and Visualization	23	Social Benefit
24	Human Psychology	24	Ethics
25	Internet Applications	25	Internet Applications
26	Cyber Security	26	Database Management
27	Financial Management	27	Human Computer Interaction
28	Digital Transformation	28	Financial Management
29	Economic Development	29	Economic Development

According to Table 1, MIS qualifications have different levels of importance for the university and the sector. The competencies identified from the universities' program learning outcomes and those indicated by industry experts are presented separately in the table above. To integrate these two data sets, the ranking values of each competency from both tables were summed to obtain a total ranking score. This approach allowed comprehensive prioritization, and the combined ranking results are shown in Table 2.

As seen in Table 2, the competencies that MIS graduates should possess are ranked according to their level of importance. Within the scope of the bachelor's degree qualification at Level 6 of the TQF, not only professional skills but also personal skills are emphasized as critical. In this context, the key skills identified by the World Economic Forum (WEF) for the year 2025 were examined, and the resulting findings are presented in Figure 2.

A comparison between the key skills published by the World Economic Forum (WEF) and the competencies expected from MIS graduates, as identified in this study reveals a notable alignment. Subsequently, the competencies expected from MIS graduates were categorized into two groups: Professional Competencies and Personal Competencies. This classification is presented in Table 3.

Table 2. Combined competency results

Combined Competencies	Ranking Totals
Project Management	4
Business Management	7
Data Collection and Analysis	10
Technology Adoption	11
Business Processes	12
Problem Solving	13
Personal Development	17
Leadership	22
Effective Communication	23
Business Intelligence	24
Programming	25
Algorithmic Thinking	26
Teamwork	26
System Design and Management	28
Foreign Language Skills	28
Computer Hardware and Network Management	30
Ethics	30
Software Development Processes	32
Social Benefit	37
Decision Making	38
Human Psychology	39
Cyber Security	40
Database Management	42
Reporting and Visualization	44
Internet Applications	50
Digital Transformation	50
Financial Management	55
Economic Development	58

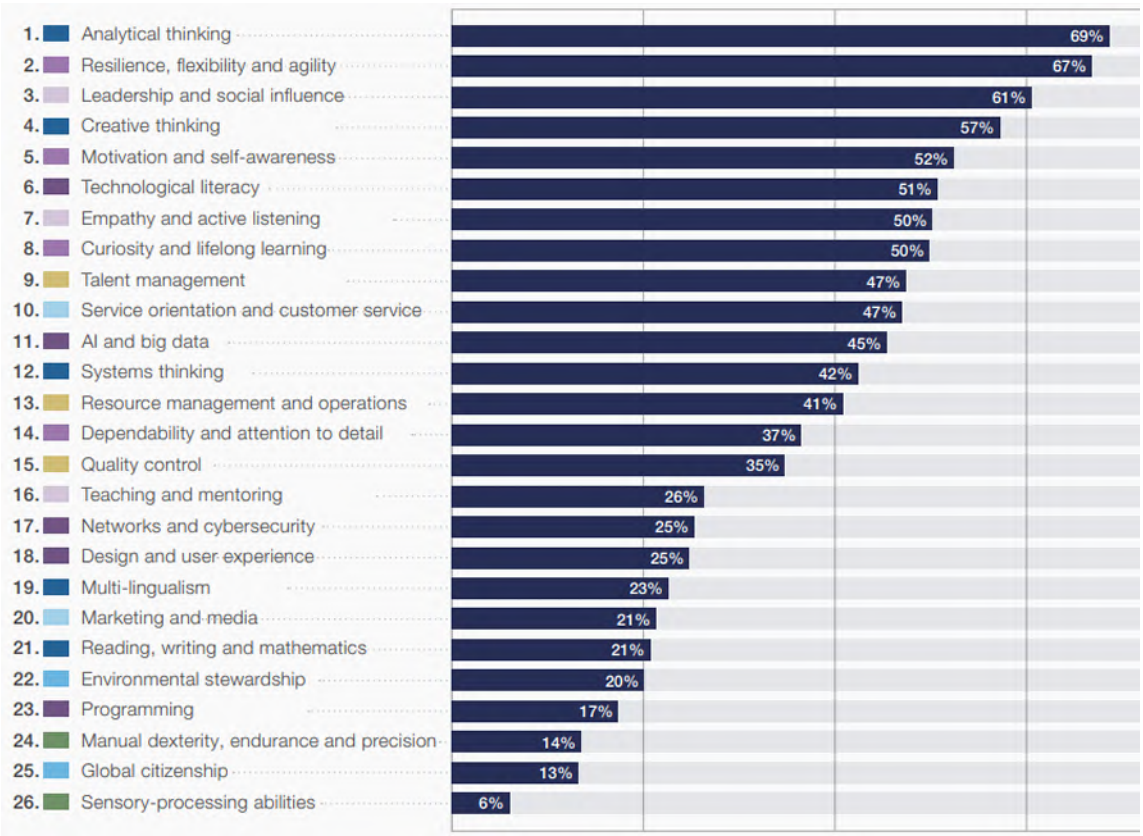

Figure 2. Core skills in 2025 – World Economic Forum

Table 3. Categorized competencies

Professional Competencies	Ranking Totals	Individual Competencies	Ranking Totals
Project Management	4	Technology Adoption	11
Business Management	7	Problem Solving	13
Data Collection and Analysis	10	Personal Development	17
Business Processes	12	Leadership	22
Business Intelligence	24	Effective Communication	23
System Design and Management	28	Programming	25
Computer Hardware and Network Management	30	Teamwork	26
Software Development Processes	32	Algorithmic Thinking	26
Cyber Security	40	Foreign Language Skills	28
Database Management	42	Ethics	30
Internet Applications	50	Social Benefit	37
Digital Transformation	50	Decision Making	38
Financial Management	55	Human Psychology	39
Economic Development	58	Reporting and Visualization	44

The table categorizes the competencies expected of MIS graduates into two main groups: professional and individual. Within the domain of professional competencies, project management, business management, and data collection and analysis are identified as the most significant. In terms of individual competencies, technology adoption, problem-solving, and personal development are particularly emphasized.

Conclusion

This study was conducted to identify the competencies that undergraduate Management Information Systems (MIS) programs in Türkiye aim to develop in their graduates and to compare these competencies with industry expectations. The findings indicate that university program learning outcomes place the greatest emphasis on competencies such as problem solving, data collection and analysis, and project management, while competencies like financial management, digital transformation, and economic development receive comparatively less attention. Moreover, according to industry experts, project management, business processes, and business management are considered the most critical competencies, whereas human-computer interaction, financial management, and economic development are the least emphasized.

The program learning outcomes of the 64 universities examined provide limited coverage of contemporary information technologies such as artificial intelligence and digital transformation. This situation poses a risk that graduates may lack the necessary competencies to meet the demands of today's rapidly evolving technological environment. The projections summarized in the World Economic Forum's Future of Jobs Report 2025 emphasize that by 2030, artificial intelligence, automation, and digital transformation processes will fundamentally reshape business practices, and employees' ability to adapt to these changes will be a decisive factor in gaining competitive advantage. The report also indicates that competencies such as technology adoption, complex problem solving, critical thinking, creativity, and digital literacy will become increasingly important within the workforce.

In this context, it is of great importance for MIS programs to update and restructure their curricula to address these emerging requirements. More effective integration of fields such as artificial intelligence, digital transformation, and automation into program outcomes will ensure that graduates are prepared not only for the current demands of the labor market but also for the uncertain and dynamic work environments of the coming decade. Furthermore, graduates equipped with these skills will be better positioned to leverage technology-driven opportunities in business processes.

In conclusion, MIS programs must be restructured to align more closely with industry expectations and to incorporate contemporary competencies that reflect ongoing technological transformations. To achieve this, it is essential to implement regular review and updating processes for program learning outcomes based on sectoral needs and technological advancements. Additionally, MIS departments should be encouraged to adopt continuous improvement mechanisms such as graduate tracer studies, alumni feedback systems, and industry advisory boards to systematically evaluate and revise their curricula. These efforts will ensure both academic quality and alignment with rapidly evolving industry demands.

Scientific Ethics Declaration

* The authors declare that the scientific ethical and legal responsibility of this article published in EPSTEM journal belongs to the authors.

Conflict of Interest

* The authors declare that they have no conflicts of interest

Funding

* This research received no specific grant from any funding agency in the public, commercial, or not-for-profit sectors.
.

Acknowledgements or Notes

* This study was presented as a poster presentation at the International Conference on Research in Engineering, Technology and Science (www.icrets.net) held in Peja/Kosovo on July 10-13, 2025.

References

AACSB. (2020). *2020 Guiding principles and standards for business accreditation*. Association to Advance Collegiate Schools of Business.

Aktas, B., Aktas, B. N., & Akbıyık, A. (2022). Management information systems awareness in the labor market: an evaluation based on job adverts in USA and Turkey. *Journal of Research in Business*, *7*, 60-89.

Ayvaz, B., Kusakci, A. O., & Borat, O. (2016). Quality assurance and accreditation processes. *İstanbul Ticaret Üniversitesi Mühendislik Fakültesi Endüstriyel Araştırma ve Gelişim Dergisi, 1*(1), 53–60.

Baser, S. H., & Bakirtas, H. (2023). Comparing business expectations with university programs: The case of Management Information Systems. *XX. IBANESS Congress Series on Economics, Business and Management* – Ohrid / Republic of North Macedonia.

Council of Higher Education (2023). *Universities with management information systems programs*. Retrieved from https://yokatlas.yok.gov.tr/lisans-bolum.php?b=10234

Davis, G. B. (1983). Evolution of information systems as an academic discipline. In *Proceedings of the 2nd Annual Information Systems Education Conference* (pp. 1–10). Chicago, IL.

Dickson, G.W. (1981). MIS – Quo Vadis? *Advances in Computers* 20.

Dogan, I. (1999). Eğitimde kalite ve akreditasyon sorunu: Eğitim fakülteleri üzerine bir deneme. *Kuram ve Uygulamada Eğitim Yönetimi*, *20*(20), 503-519.

George, J. F., & Hadidi, R. (2023). What's in a name? Central themes in MIS since the field's founding. *Journal of the Midwest Association for Information Systems* (JMWAIS), *2023*(1), 1.

Kılıcaslan, C. (2020). Accreditation in higher education. *Peyzaj – Education, Science, Culture and Art Journal 2020*(Special Issue), 10-18.

Henkoğlu, T., & Serefoglu, H. (2019). Evaluation of the department of management information systems curriculums from the perspective of information management. *Journal of Higher Education and Science 9*(3), 587-602.

Laudon, K. C., & Laudon, J. P. (2020). *Managing information systems: Managing the digital firm*. New York, NY: Pearson Education.

Sezgin, F., Kavgacı, H., & Kılınc, A. C. (2011). Self evaluations of educational administration and supervision graduate students in Turkey. *Journal of Higher Education and Science* (3), 161-169.

Turel, A., Altıntas, A. T. (2018). Benefits of AACSB accreditation and challenges of the accreditation process. *The Journal of International Social Research*, *11*(61), 1031-1038.

Ugur, N. G., Okursoy, A., & Turan, A. H. (2016). Management information systems education in Turkey and competency cluster assessment. *The Journal of Business Science*, *4*(1), 111-122.

Vural, M., & Turan, A. H. (2019). Knowledge, skills and competencies that must have of the graduates of management information systems. *The Journal of Business Science*, *7*(2), 357-388.

World Economic Forum (2025). Core skills in 2025. Retrieved from https://reports.weforum.org/docs/WEF_Future_of_Jobs_Report_2025.pdf

Author(s) Information

Ali Ucucu
Faculty of Economics and Administrative Sciences,
Management Information Systems, Ankara, Türkiye
Contact e-mail: ali.ucucu@*ostimteknik.edu.tr*

Basak Gok
Gazi University
Applied Science Faculty, Management Information Systems,
Gazi University, Ankara, Türkiye

Hadi Gokcen
Gazi University
Engineering Faculty, Industrial Engineering Department,
Ankara, Türkiye

To cite this article:

Ucucu, A., Gok, B., & Gokcen, H. (2025). Standardizing competencies in management information systems. *The Eurasia Proceedings of Science, Technology, Engineering and Mathematics (EPSTEM), 35,* 208-215.

ISRES Publishing

The Eurasia Proceedings of Science, Technology, Engineering & Mathematics (EPSTEM)
ISSN: 2602-3199

The Eurasia Proceedings of Science, Technology, Engineering and Mathematics (EPSTEM), 2025

Volume 35, Pages 216-220

ICRETS 2025: International Conference on Research in Engineering, Technology and Science

Effect of the Number of Images on the Normalized Noise Power Spectrum (NNPS) in Digital Mammography Detectors

Melike Kaya-Karaaslan
Sisli Hamidiye Etfal Research and Training Hospital

Abstract: The noise power spectrum (NPS) characterizes the noise properties of imaging systems in the frequency domain. In literature, a normalized NPS (NNPS) is given regardless of the linearization method. NNPS is typically measured from images acquired from the digital detector without the use of any test apparatus. However, there is no clear information about the number of images in the current standards. Furthermore, the number of images utilized in such assessments is either unspecified or varies across studies. This study aims to evaluate the influence of the number of images on NNPS calculations. Average NNPS values were computed using one, three, five, and six detector images acquired from two Fujifilm Amulet Innovality full-field digital mammography systems at selected spatial frequencies. The reference air kerma for the measurements ranged between 90 and 95µGy, and all results were computed in the radial direction. The x-ray spectrum utilized was 29kV with 2 mm of additional aluminum filtration. Statistical evaluation of the NNPS results was estimated using standard deviation and coefficient of variation (cov). For the first system, NNPS values at spatial frequencies of 0.5, 2.0, and 5.0mm^{-1} were $2.55\text{x}10^{-06} \pm 7.33\text{x}10^{-08}$ (cov=2.87%), $2.43\text{x}10^{-06} \pm 4.99\ \text{x}10^{-08}$ (cov=2.06 %) and $2.26\text{x}10^{-06} \pm 2.63\text{x}10^{-08}$ (cov= 1.16 %), respectively. Corresponding values for the second system were $2.63\ \text{x}10^{-06} \pm 3.74\text{x}10^{-08}$ (cov = 1.42 %), $2.3\ \text{x}10^{-06} \pm 4.76\text{x}10^{-08}$ (cov = 2.07 %) and $2.17\ \text{x}10^{-06} \pm 1.73\text{x}10^{-08}$ (cov=0.80 %), respectively. The findings indicate that the number of images used does not significantly impact the NNPS results particularly at higher spatial frequencies.

Keywords: Medical engineering, Digital mammography, Noise power spectrum, Image number

Introduction

In medical imaging, noise is unwanted signals unrelated to the imaged anatomical structure. Since these unwanted signals can make clinical diagnosis difficult, analyzing noise in the image is crucial. Besides, in mammography it is necessary to see very low contrast differences in the image, and noise can mask these differences. In this context, noise can be analyzed in the frequency domain with the noise power spectrum (NPS) (Bushberg et al., 2021). Many factors, such as the detector technology used, the air kerma in the detector, and the quality of the X-ray beam, affect the final result in NPS measurements, and careful analysis of the NPS will provide valuable information about the detector's performance (Marshall, 2009). Measurements of the NPS serve multiple purposes, including quality assurance, comparative evaluation of detectors, analysis of noise sources, and optimization of image processing techniques (Michael, 2017). The NPS is influenced by the signal transfer property (STP) used to linearize the original image data, as it represents a measure of absolute noise. Consequently, differences in linearization methods and/or exposure conditions prevent direct comparison of NPS values across systems. In scientific literature, a Normalized NPS (NNPS) is typically reported, independent of the linearization method.

The normalization aims to mitigate the influence of signal variations among images or regions of interest (ROIs) used in the NPS calculation, thereby facilitating more meaningful comparisons. The NNPS can be calculated by dividing NPS by the square of the Mean Pixel Values (MPV) within the ROI as shown in Equation (1)

(Ravaglia et al., 2009). It must be noted that while the NPS increases proportionally with radiation dose, the NNPS exhibits an inverse relationship with dose.

$$\text{NNPS (mm}^2\text{)} = \text{NPS}/(\text{MPV})^2 \quad (1)$$

Measurement methods for the Normalized Noise Power Spectrum (NNPS) are outlined in international standards such as the International Electrotechnical Commission (IEC, 2007), the Institute of Physics and Engineering in Medicine (IPEM, 2010), and European Guidelines for Quality Assurance in Mammography Screening (EUREF, 2013). Nevertheless, despite being conceptually well-defined, the experimental implementation of NNPS measurement remains challenging, and a universally accepted methodology has yet to be established. Moreover, current standards do not provide clear guidance on the number of images required for NNPS calculations. Furthermore, the number of images used in such evaluations is often unspecified or varies considerably across different studies (Dobbins et al., 2006), (Ravaglia et al., 2009), (Oberhofer et al., 2010), (Marshall et al., 2011), (Donini et al., 2014). Precise knowledge of the test conditions is essential, particularly when comparing different imaging systems, as measurement outcomes are highly dependent on the evaluation methods. This study aims to evaluate the influence of the number of images on NNPS calculations.

Method

Measurements were performed as recommended in the standards (IEC, 2007 and IPEM, 2010). The NNPS was calculated from the detector images at the reference air kerma (normal level between 90 and 95 μGy. Before determining the NNPS, a uniform 2mm Aluminum (Al) filter was placed on the collimator aperture (near the x-ray tube) to filter the mammography beam, and exposure was carried out without any test device (flat-field image) (Dobbinset al., 2006).

The tube voltage and anode/filter should be chosen to be representative of the factors used to acquire clinical images (29kVp/ W/Rh). To determine the effect of the number of images on NNPS, one, three, five, and six detector images were acquired from two Fujifilm Amulet Innovality full-field digital mammography systems (S1 and S2) at selected spatial frequencies (0.5, 2.0, and 5.0mm^{-1}).

There are many sources of software for the calculations of NNPS. ImageJ plug-in COQ was used to analyze NNPS. The calculated NNPS is a two-dimensional array, typically displayed as a one-dimensional graph. In this paper, the 1D NNPS was obtained from the 2D NNPS in the radial direction. Statistical evaluation of the NNPS results was estimated using standard deviation and coefficient of variation (cov).

Results and Discussion

Table 1 presents the average NNPS values obtained from one, three, five, and six detector images for the two examined systems at specified frequencies.

Table 1. The average NNPS values at selected frequencies

Frequency (mm^{-1})	NNPS (mm^2) for Fujifilm Amulet (S1)	NNPS (mm^2) for Fujifilm Amulet (S2)
0.5	$2.55\text{x}10^{-06}$±$7.33\text{x}10^{-08}$ (cov=2.87%)	$2.63\text{x}10^{-06}$ ± $3{,}74\text{x}10^{-08}$ (cov = 1.42 %)
2.0	$2.43\text{x}10^{-06}$± $4.99\ \text{x}10^{-08}$ (cov=2.06 %)	$2.3\ \text{x}10^{-06}$ ± $4{,}761\ \text{x}10^{-08}$ (cov = 2.07 %)
5.0	$2{,}26\ \text{x}10^{-06}$± $2{,}63\text{x}10^{-08}$ (cov= 1.16 %)	$2{,}17\ \text{x}10^{-06}$ ± $1{,}73\ \text{x}10^{-08}$ (cov=0.80 %)

Figures 1 and 2 present a comparative analysis of the outcomes for S1 and S2, derived from datasets comprising varying numbers of images (one, three, five, and six images), respectively.

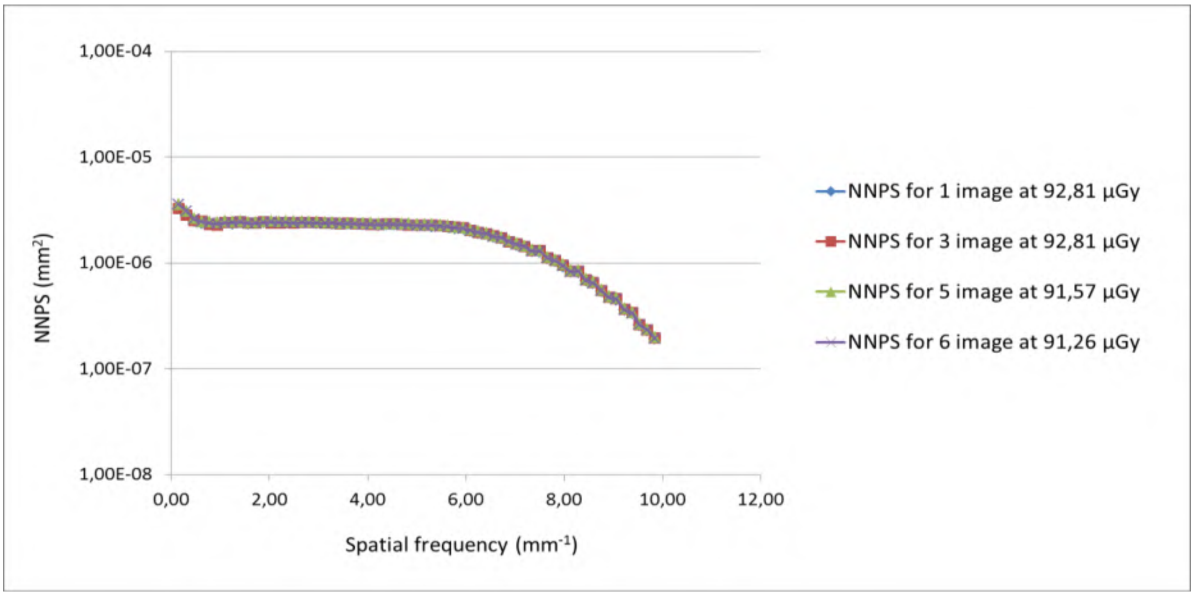

Figure 1. Radially averaged NNPSs for one, three, five and six images for S1

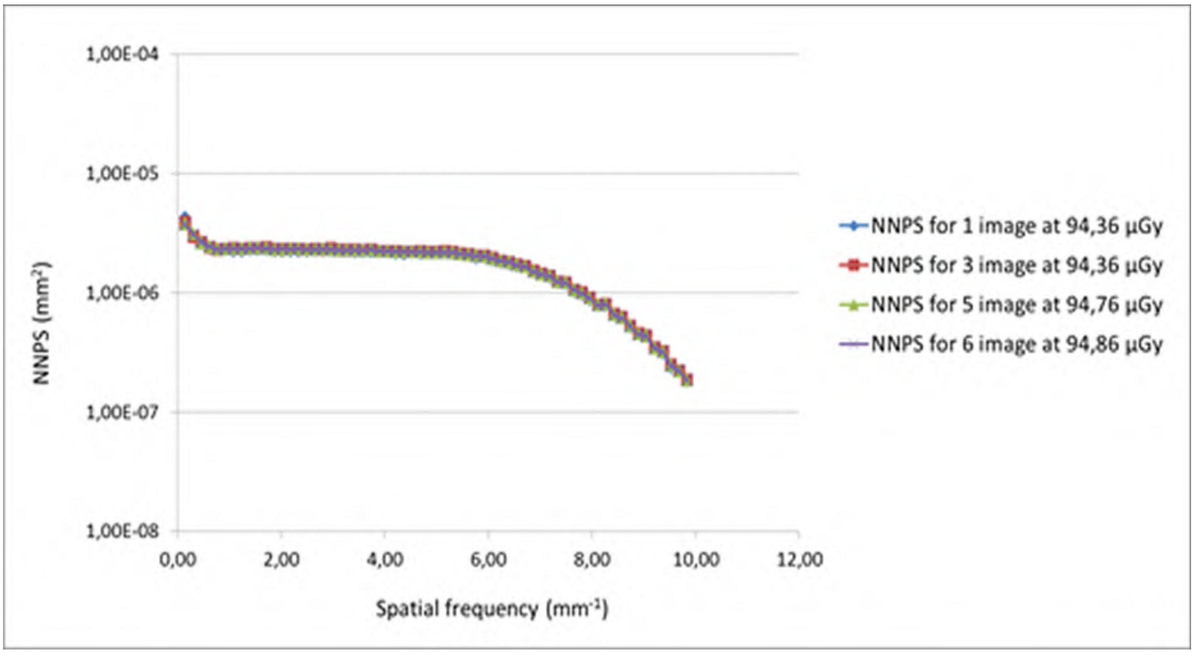

Figure 2. Radially averaged NNPSs for one, three, five and six images for S2

Figures 1 and 2 show that a high NNPS value at low spatial frequencies indicates the presence of large-scale intensity fluctuations, suggesting poor image homogeneity. In contrast, low NNPS at high spatial frequencies means that the imaging system exhibits less noise and better resolution in capturing fine details, resulting in higher image quality and clarity. As a result, the findings indicate that the number of images used does not significantly impact the NNPS results, particularly at higher spatial frequencies.

Conclusion

When performing the NNPS test, each image should have the same exposure parameters (kVp, mAs, filtering etc.), and there should be no difference in dose and exposure between images. An analysis of the NNPS results reveals that the highest relative difference, corresponding to the number of images, is observed at 0.5mm^{-1} spatial frequency, with a value of 2.87%. It is important to emphasize that the measured NNPS will relate to the appearance of the noise in the image. The NNPS measurements are inherently prone to inaccuracies due to the practical limitation on the number of images that can be acquired during data collection. The selection of the region of interest (ROI) size, sampling parameters, and the number of images used in the analysis represents a critical trade-off.

Recommendations

Although the results indicate that the number of images evaluated does not significantly affect the NNPS, it is important to recognize that noise is inherently a random variable. Therefore, increasing the number of images enhances statistical reliability and provides a more accurate estimation of the system's true average noise characteristics.

Scientific Ethics Declaration

* The author declares that the scientific ethical and legal responsibility of this article published in EPSTEM journal belongs to the author.

Conflict of Interest

* The authors declare that they have no conflicts of interest

Funding

* This research received no specific grant from any funding agency in the public, commercial, or not-for-profit sectors.

Acknowledgements or Notes

* This article was presented as an oral presentation at the International Conference on Research in Engineering, Technology and Science (www.icrets.net) held in Peja/Kosovo on July 10-13, 2025.

References

Bushberg, J.T., Seibert, J.A., Leidholdt, E.M., & Boone, J.M. (2021). *The essential physics of medical imaging* (4th ed.). Philadelphia: Lippincott Williams &Wilkins.

Dobbins, J.T. III, Samei, E., Ranger, N.T., & Chen, Y. (2006). Intercomparison of methods for image quality characterization: II. Noise power spectrum. *Med. Phys., 33*(5), 1466-1475.

Donini, B., Rivetti, S., Lanconelli. N., & Bertolini, M. (2014). Free software for performing physical analysis of systems for digital radiography and mammography. *Med. Phys., 41*(5), 051903.

European Commission. (2013). *European guidelines for quality assurance in breast cancer screening and diagnosis european guidelines for breast cancer screening* (EC, 4th ed. Supplement). Luxembourg.

International Electrotechnical Commission. (2007). *Medical electrical equipment- characteristics of digital x-ray image devices: Part 1-2 determination of the detective quantum efficiency-detectors used in mammography* (IEC 62220-1-2). Geneva.

Institute of Physics and Engineering in Medicine. (2010). *Measurement of the performance characteristics of diagnostic x-ray systems: Digital imaging systems* (IPEM Report 32-Part VII). New York.

Marshall, N. M. (2009). Detective quantum efficiency measured as a function of energy for two full-field digital mammography systems. *Phys. Med. Biol.,54*(9), 2845-2861.

Marshall, N. W., Monnin, P., Bosmans, H., Bochud, F. O., & Verdun, F. R. (2011). Image quality assessment in digital mammography: Part I technical characterization of the systems. *Phys. Med. Biol*., *56*(14), 4201–4220.

Michael, K. T. (2017). The application of quantitative data analysis for the assessment of flat panel x-ray detectors in digital radiography as part of a quality assurance programme. *Biomed. Phys. Eng. Express, 3*(3), 1-15.

Oberhofer, N., Fracchetti, A., Nassivera, E., Valentini, A., & Moroder, E. (2010). Comparison of two novel ffdm systems with different a-se detector technology: Physical characterization and phantom contrast detail evaluation in clinical conditions. *Digital Mammography 10th Int. Workshop, IWDM,* Girona, Spain, 16-18 June 2010.

Ravaglia, V., Bouwman, R. W., Young, K. C., Engen, van R., & Lazzari, B. (2009). Noise analysis of full field digital mammography systems. *SPIE Medical Imaging: Physics of Medical Imaging Proc. SPIE,* Florida, USA, 8-12 February 2009.

Author(s) Information

Melike Kaya-Karaaslan
Sisli Hamidiye Etfal Research and Training Hospital
Istanbul Health Directorate, Public Hospitals Precidency-4,
Biomedical Engineering Department
Halaskargazi Street, No:10, Sisli, Istanbul, Türkiye
Contact e-mail: *melikekaya08@gmail.com*

To cite this article:

Kaya-Karaaslan, M. (2025). Effect of the number of images on the normalized noise power spectrum (NNPS) in digital mammography detectors. *The Eurasia Proceedings of Science, Technology, Engineering and Mathematics (EPSTEM), 35,* 216-220.

The Eurasia Proceedings of Science, Technology, Engineering & Mathematics (EPSTEM)
ISSN: 2602-3199

The Eurasia Proceedings of Science, Technology, Engineering and Mathematics (EPSTEM), 2025

Volume 35, Pages 221-224

ICRETS 2025: International Conference on Research in Engineering, Technology and Science

Analysis of Inhibition of Proximal Tubule Sodium Reabsorption on Arterial Pressure by Using a Mathematical Model

Fatih Karaaslan
Health Sciences University

Abstract: Blood pressure in the human body is regulated by the nervous system, the renin-angiotensin-aldosteron system and the kidneys. While the nervous system regulates blood pressure by affecting arterial vascular resistance, the renin-angiotensin-aldosterone system adjusts blood pressure mainly by influencing water and sodium reabsorption from the kidneys.The kidneys mainly regulate blood pressure by adjusting blood volume.The proximal tubule is an effective part of the kidney for reabsorption of water and sodium.The blood pressure lowering effects of drugs that inhibite sodium and water reabsorption from the proximal tubule have been shown in several clinical studies. In order to analyze this effect, a mathematical model of the cardiovascular system including the kidneys, nervous system and renin-angiotensin-aldosterone hormones was used. In the model, when sodium intake was increased to twice the normal level, a decrease in proximal tubule sodium reabsorption and an increase in blood pressure, extracellular fluid volume and total body sodium were observed. However, in the model, when sodium intake is increased, it has been observed that arterial pressure increases further and more sodium accumulates in the body when proximal tubule sodium reabsorption is blocked at its normal value and its decrease is prevented. This simulation result supports the clinical evidence that drugs inhibiting sodium reabsorption from proximal tubule are effective in the treatment of hypertension.

Keywords: Proximal tubule, Sodium reabsorption, Mathematical model

Introduction

The nervous system, the renin-angiotensin-aldosterone system and the kidneys play a role in the regulation of arterial blood pressure. The nervous system controls arterial pressure by acting on arterial resistance. With the stimulation of the nervous system, the diameter of the arterial vessels decreases, that is, the vascular resistance increases. Therefore, arterial pressure increases. The renin-angiotensin-aldosterone hormone system increases the sodium and water reabsorption from the kidneys into the blood, causing an increase in blood volume. Thus blood pressure increases. In addition, angiotensin has an effect on increasing blood pressure by increasing arterial resistance. The effect on arterial pressure is observed within minutes after stimulation of the renin-angiotensin-aldosterone system. The kidneys affect arterial pressure by changing blood volume through urine excretion. The influence of the kidney on arterial pressure begins within a few hours.

Kidneys consist of functional units called nephrons. Each kidney contains 1 million nephrons. Blood coming from the renal artery to the nephron is filtered through the glomerular capillaries and then passes into the Bowman capsule. It then passes through the proximal tubule, distal tubule and collecting duct respectively, and is excreted as urine. In the tubules, water and sodium are reabsorbed into the blood. Angiotensin and aldosterone increase the reabsorption of water and sodium from the tubules into the blood. The renal sympathetic nerve activity also acts to increase water and sodium reabsorption from the kidneys. The proximal tubule has a powerful effect on water and sodium reabsorption.

Increased water and sodium reabsorption from the proximal tubule is known to increase blood volume and thus increase blood pressure. (Hall, 2011). Drugs that reduce water and sodium reabsorption from the proximal

- Selection and peer-review under responsibility of the Organizing Committee of the Conference

tubule have been clinically shown to lower blood pressure. In this study, this effect was tried to be analyzed by using the long term cardiovascular system mathematical model.

Method

The assumptions and equations of the long term cardiovascular system model used in this study are in related reference (Karaaslan et al., 2014). The model was established in Matlab/Simulink and the equations of the model were solved with the Runge-Kutta 4 numerical method. To analyze the effect of proximal tubule sodium reabsorption on arterial pressure, sodium intake was increased twofold for 12 days while proximal tubule sodium reabsorption was fixed at its normal value and proximal tubule sodium reabsorption responded normally. The variables and parameters of the model are as follows:

Effect of mean arterial pressure on renal sympathetic nerve activity; Effect of right atrial pressure on renal sympathetic nerve activity; Effect of renal sympathetic nerve activity on afferent arteriolar resistance; Effect of angiotensin II hormone concentration on fractional proximal sodium reabsorption; Effect of the filtered sodium load on fractional proximal sodium reabsorption; Effect of right atrial pressure on normalized antidiuretic hormone secretion rate; Effect of nitric oxide on the afferent arteriolar resistance; Autonomic multiplier effect; The effect of angiotensin II concentration on the efferent arteriolar resistance; Fractional collecting duct sodium reabsorption; Fractional distal tubule sodium reabsorption; Fractional proximal tubule sodium reabsorption; Effect of atrial natriuretic peptide on collecting duct sodium reabsorption rate; Effect of distal tubule sodium outflow on collecting duct sodium reabsorption rate; Effect of antidiuretic concentration on tubular water reabsorption rate; Effect of aldosterone concentration on tubular water reabsorption rate; Renin secretion rate as a function of macula densa sodium flow; Effect of renal sympathetic nerve activity on normalized renin secretion rate; Effect of angiotensin II hormone on normalized aldosterone secretion rate; Effect of potassium to sodium concentration ratio on normalized aldosterone secretion rate; Effect of mean arterial pressure on normalized aldosterone secretion rate; The effect of the angiotensin II concentration on the efferent arteriolar resistance; The effect of the myogenic response on the afferent arteriolar resistance; Tubuloglomerular feedback signal per kidney; Absolute collecting duct sodium reabsorption rate per kidney; Cardiac output; Distal tubule sodium outflow per kidney; Absolute distal tubule sodium reabsorption rate per kidney; Filtered sodium load per kidney; Glomerular filtration rate per kidney; Macula densa sodium flow per kidney; Absolute proximal tubular sodium reabsorption rate per kidney; The renal blood flow per kidney; Sodium intake; Tubular water reabsorption rate per kidney; Urine flow rate per kidney; Urine sodium flow per kidney; Venous return; Water intake; Effect of aldosterone concentration on fractional distal sodium reabsorption; Autonomus system activity; Baroreceptor activity; Chemoreceptor activity; Normalized antidiuretic hormone concentration; Antidiuretic hormone concentration; Normalized aldosterone concentration; Aldosterone concentration; Normalized atrial natriuretic peptide concentration; Angiotensin II concentration; Potassium concentration; Normalized renin concentration; Sodium concentration; Coefficient relating basic arterial resistance to vascularity; Glomerular capillary filtration coefficient per kidney; Vascularity destruction coefficient; Total amount of sodium; Normalized renal sympathetic nerve activity; Average afferent arteriolar pressure; Bowman hydrostatic pressure per kidney; Net filtration pressure; Glomerular hydrostatic pressure per kidney; Glomerular osmotic pressure per kidney; Mean arterial pressure; Mean filling pressure; Right atrial pressure; Arterial resistance; Afferent arteriolar resistance per kidney; Basic arterial resistance; Basic venous resistance; Efferent arteriolar resistance per kidney; Total peripheral resistance; Renal vascular resistance per kidney; Resistance to venous return; Renal sympathetic nerve activity; Normalized antidiuretic hormone secretion rate; Normalized aldosterone secretion rate; Renin secretion rate from a single kidney; Normalized renin secretion rate from both kidneys; Nitric oxide release from the afferent arteriole as a function of renal blood flow; Vascularity; Vascularity destruction rate; Vascularity formation rate; Blood volume; Extracellular fluid volume.

Results and Discussion

To analyze the effect of proximal tubule sodium reabsorption on arterial pressure, normal sodium intake is increased twofold for 12 days while proximal tubule sodium reabsorption is fixed at its normal value and proximal tubule sodium reabsorption responds normally. When sodium intake is increased (Figure 1.A), proximal tubule sodium reabsorption decreases (Figure 1.B). Therefore, urinary sodium flow increases (Figure 1.C). As the amount of sodium in the body increases (Figure 1.D), extracellular fluid volume increases (Figure 1.E) and, as a result, arterial pressure also increases (Figure 1.F). When sodium intake is increased (Figure 1.A) and proximal tubule sodium reabsorption is fixed at its normal value (Figure 1.B), urinary sodium flow increases less than with normal proximal sodium reabsorption (Figure 1.C). As a result, more sodium accumulates in the body (Figure 1.D). Thus, extracellular fluid volume (Figure 1.E) and arterial pressure (Figure 1.F) increase more than with normal proximal sodium reabsorption.

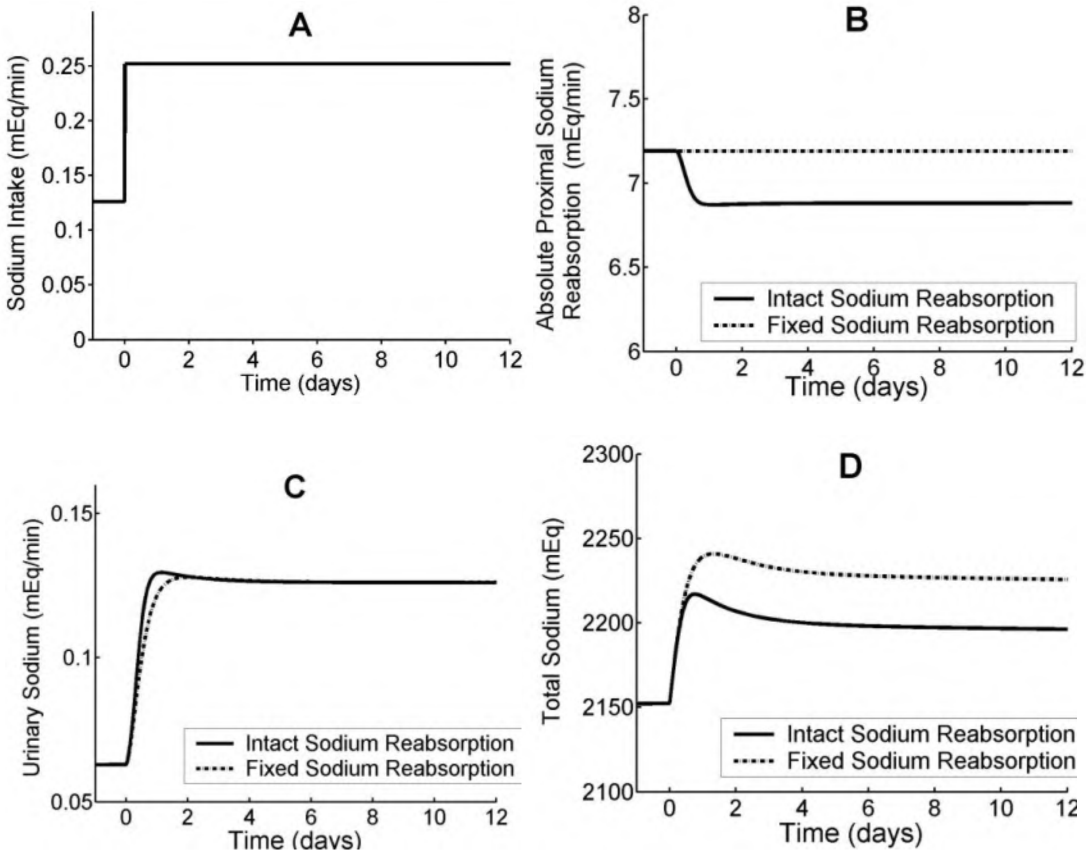

Figure 1. Model results when sodium intake is increased, proximal tubule sodium reabsorption is fixed at its normal value (dotted line) and proximal tubule sodium reabsorption responds normally (solid line). . A:sodium intake. B:Proximal tubule sodium reabsorption. C: Urinary sodium flow. D: Total sodium amount. E: Extracellular fluid volume. F:Mean arterial pressure

When sodium intake is increased, the preventing of the inhibition of proximal tubule sodium reabsorption results in a greater increase in arterial pressure, consistent with experimental and clinical studies (Leite et al., 2022), (Haaster et al., 2018), (Wang et al., 2009), (Windhager and Giebisch., 1976), (Dickstein et al., 1998)

Conclusion

When sodium intake is increased, it has been observed that arterial pressure increases further and more sodium accumulates in the body when proximal tubule sodium reabsorption is fixed at its normal value and its decrease is prevented. This simulation result supports the clinical evidence that drugs inhibiting sodium reabsorption from proximal tubule are effective in the treatment of hypertension.

Recommendations

Adding the effect of renal sympathetic nerve activity on tubular water reabsorption to the model may increase the model's closeness to reality.

Scientific Ethics Declaration

* The author declares that the scientific ethical and legal responsibility of this article published in EPSTEM journal belongs to the author.

Conflict of Interest

* The author declares that he has no conflicts of interest.

Funding

* This research received no specific grant from any funding agency in the public, commercial, or not-for-profit sectors.
.

Acknowledgements or Notes

* This article was presented as an oral presentation at the International Conference on Research in Engineering, Technology and Science (www.icrets.net) held in Peja/Kosovo on July 10-13, 2025.

References

Dickstein, K., Timmermans, P., & Segal, R. (1998). Losartan: a selective angiotensin II type 1 (AT_1) receptor antagonist for the treatment of heart failure. *Expert Opinion on Investigational Drugs,7*(11), 1897-914.

Haaster, M. C. V., McDonough A. A., Gurley, S. B. (2018). Blood pressure regulation by the angiotensin type 1 receptor in the proximal tubule. *Current Opinion in Nephrology and Hypertension, 27*(1), 1-7.

Hall, JE. (2011). *Guyton and hall textbook of medical physiology.* Philadelphia: Saunders Elsevier.

Karaaslan, F., Denizhan, Y., & Hester, RL. (2014). A mathematical model of long-term renal sympathetic nerve activity inhibition during an increase in sodium intake. *American Journal of Physiology-Regulatory Integrative and Comparative Physiology*, (306), 234-247.

Leite, A. P. O., Li, X. C., Wia, S. M., Hassan, R., & Zhuo, J. L. (2022). Angiotensin II and AT_{1a} receptors in the proximal tubules of the kidney: New roles in blood pressure control and hypertension. *International Journal of Molecular Sciences, 23*, 2402.

Wang, X., Armando I., Upadhygy, K., Pascua, A., Jose, P. A. (2009). The regulation of proximal tubular salt transport in hypertension: An update. *Current Opinion in Nephrology and Hypertension*, *18*, 412-420.

Windhager, E. E., & Giebisch, G. (1976). Proximal sodium and fluid transport. *Kidney International*, *9*, 121-133.

Author(s) Information

Fatih Karaaslan
Health Sciences University/Hamidiye Health Sciences
Institute/Medical Modelling and Simulation Department
Selimiye Mahallesi, Atölyeler Street,
Üsküdar,Istanbul,Türkiye.
Contact e-mail: fatih.karaaslan@*sbu.edu.tr*

To cite this article:

Karaaslan, F. (2025). Analysis of inhibition of proximal tubule sodium reabsorption on arterial pressure by using a mathematical model. *The Eurasia Proceedings of Science, Technology, Engineering and Mathematics (EPSTEM), 35,* 221-224.

The Eurasia Proceedings of Science, Technology, Engineering & Mathematics (EPSTEM)
ISSN: 2602-3199

The Eurasia Proceedings of Science, Technology, Engineering and Mathematics (EPSTEM), 2025

Volume 35, Pages 225-239

ICRETS 2025: International Conference on Research in Engineering, Technology and Science

Design and Implementation of Integrated RPL Protocol and Deep Learning for Energy-Aware Wireless Sensor Networks

Nashwa Rabah Abood
University of Baghdad

Anwar Qassim Al-Khateeb
University of Baghdad

Abstract: A wireless sensor network (WSN) represents a significant and contemporary technology that has recently emerged, playing a crucial role in enabling the Internet of Things (IoT) to bridge the gap between the physical environment and the digital domain. The major challenges facing WSNs include limited power, data security and reliability, and node failure, along with limitations in data storage, processing, analysis, power management, and security. WSNs with limited physical capabilities employ the low-power lossless routing (RPL) protocol, which employs various processes to simplify communications and network design. Despite its importance and effectiveness, the RPL protocol faces several challenges, including handling high traffic and load balancing, which can lead to service interruption. This paper proposes a machine learning model to address the challenges of energy consumption and efficiency in the RPL protocol. The proposed model is based on the use of Random Forest (RF) and Support Vector Machine (SVM) to identify the optimal path from source to interface, enhancing the network lifetime and delivering data packets in an energy-efficient manner. The model is implemented in two scenarios, one with uniformly distributed nodes and the other with randomly distributed nodes. The results demonstrate that the proposed system outperforms the standard RPL protocol and other protocols in terms of extending the network lifetime and enhancing energy efficiency.

Keywords: Wireless sensor networks, Machine learning, Random forest, Support vector machine, RPL, IOT

Introduction

As a result of the rapid development of information and communications technology, computer networks, the mobile phone industry and the emergence of IoT there has been significant advancement in daily life and smart cities. Wireless devices that support IoT play a crucial role in collecting, transmitting and processing data. Among these technologies, WSN is one of the most important and recent innovations for connecting the physical environment to the digital world. They are extensively utilized across a range of applications in multiple domains, such as environmental monitoring, healthcare, industrial automation, agriculture, and smart cities (Vlajic et al., 2011). A WSN consists of a collection of sensor nodes and actuators that interact with and control the physical environment and sensor nodes have limited energy storage capacity and low processing speed with limited communication bandwidth, which makes the design and maintenance of sensor networks difficult after energy consumption (Gaber et al., 2018). A WSN faces several challenges, including high power consumption, high bandwidth demand and data security concerns.

Furthermore, wireless communications are often subject to interference from other devices, resulting in poor data transmission quality. Among all these challenges, energy efficiency remains the most critical in WSN design. To overcome the above challenge inexpensive,low-power, multi-functional sensor nodes based on energy-efficient control protocols have been designed to ensure long-term operation and improve overall network performance by selecting protocols that contribute to reducing energy consumption, effectively improving data distribution and achieving excellent reliability (Dai et al., 2020).These protocols are either static or dynamic and are the backbone of the Internet of Things (IoT), the most important of which is the Routing

Protocol for Low Power Networks (RPL), which aims to improve overall network performance, and focuses on the use of low-power networks, and high loss rates due to its flexibility and suitability for different IoT, but it is not without limitations and drawbacks, especially in terms of service efficiency. Recently, machine learning (ML) and deep learning (DL) algorithms have been integrated with the RPL protocol to design hybrid systems to contribute to solving the shortcomings and problems (Zahra et al., 2022). This Study presents a methodology for WSNs based on the development of a low-power routing protocol (RPL) model that utilises machine learning. The target is to achieve energy efficiency by classifying available paths and determining the optimal path for delivering messages to a target with minimal energy consumption.

Literature Survey

Many studies have contributed to providing solutions to the challenges facing WSNs using different technologies. These efforts mainly focus on designing aggregation and routing protocols to reduce energy consumption, enhance security, and select the best path in the network, as detailed below:

Abdelhadi et al. (2019): A minimal hierarchical objective function (MRHOF) and zero-order objective function (OFO) evaluation scheme are proposed for large-area scenarios and realistic topologies, considering reliability in terms of packet delivery ratio, power consumption, average end-to-end delay, and radio activity ratio. COOJA is used as a wireless sensor network simulator, simulating the software and hardware levels of embedded nodes using Contiki OS. Based on the simulation results, it is concluded that the choice of the given objective function has an impact on PDR and delay and can achieve energy saving. Finally, the development of an objective function with hybridisation of more than one metric is proposed as future work to balance PDR and power consumption (Somula et al., 2022). The proposed method may not be ideal in some real-world large scenarios requiring a balance between PDR and power consumption may increase computation complexity.

Somula et al. (2021): A system based on the Seagull Optimisation Algorithm-based Energy Aware Cluster Routing (SOA-EACR) routing protocol and the (SEAGULL) optimisation algorithm was proposed. The system aims to extend the network lifetime and reduce the delay, as the network lifetime was improved by 20% with an increase in the packet delivery ratio from 2-5%. The simulation was performed using MATLAB 2019. The system performance was divided using similar optimisation algorithms based on the fitness function that takes into account the appropriate network parameters to choose the optimal channel among other nodes in the network (Gurram et al., 2022). The proposed method did not mention computational complexity or real-world applicability

Suliman et al. (2022): This study aims to propose the (EAFTC-RIS) technique which consists of three main processes which are (MFO), fault loading process and (SSO)-based routing to determine the communication channels and optimal paths towards the destination for efficiency and safety. The simulation results indicated that the technique is better compared to other methods and can be used as a skillful method to achieve maximum survivability of wireless sensor networks (Suliman et al., 2022). This research presents limited comparisons with other techniques and scalability concerns.

Nilabar et al. (2023): The authors proposed a system based on the SCORE BASED LINK DELAY AWARE ROUTING (SBLDAR) protocol and Modified Salp Swarm Optimisation (MSFO) algorithm to select the best routing path for secure data communication, distinguish between hostile and normal nodes, and allow collision-free data exchange. The results demonstrate that the protocol, used with a hybrid message authentication code (MAC) environment, reduces energy, improves network lifetime, and improves overall performance (Nilabar,et al, 2023). Different network conditions do not display the performance metrics in full detail.

Abubakar et al. (2024): This study proposed a system combining the RPL protocol with machine learning algorithms to enhance the security and quality of service (QOS) of RP networks in WSNs supporting IoT applications. The system results confirmed that the additional computational overhead is reasonable and acceptable, ensuring improved security and QoS without affecting the overall performance of WSNs. Thus, the system greatly enhances the QoS and secures the data transmission in WSNs supporting the IoT (Wakili et al., 2024). The proposed system has additional overhead that might impact resource-constrained nodes in large-scale networks.

Methods and Materials

This section presents a concise description of the material, protocol, algorithm, and network used in designing the proposed system.

Routing Protocol Low (RPL)

RPL is an IPv6-based protocol specifically designed for low-power and lossy networks (LLNs), facilitating routing across multiple layers (Hassani et al., 2019) and supports various modes such as store-and-no-store, transport and local repair (Culler et al., 2004). However, the protocol has several limitations and drawbacks concerning QoS,security, reliability, delay, jitter, packet loss, and power consumption (Porcus, et al., 2010). The primary objective of RPL is to establish optimal routing paths between multiple nodes and a single destination node or edge router, which serves as the gateway to the Internet. Unlike conventional routing protocols, RPL determines paths through an objective function that delineates a set of metrics and constraints for identifying the lowest-cost routes within a specific RPL instance. Despite certain limitations, RPL possesses several significant features, including support for automatic configuration via ICMPv6 messages, the ability to detect and prevent loops in the network by constructing multiple Directed Acyclic Graphs (DAGs) within a Destination-Oriented DAG (DODAG), and the utilization of rank values assigned by each node in the network. Additionally, RPL demonstrates the capability to adapt to changes in topology and effectively manage node failures. The following points outline the key aspects of the RPL protocol (Figure 1).

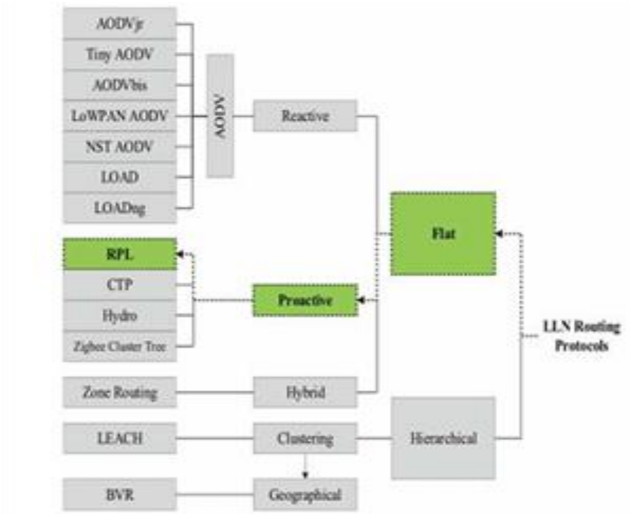

Figure 1. Classification of routing protocols for low-power and lossy networks.

We maintain DODAG by computing the rank of each node within the network and choosing its preferred parent. As illustrated in Figure 3, the rank of nodes decreases along paths leading to the root node. RPL employs Objective Functions (OFs) to determine the criteria for path selection, rank assignment, and parent selection. The process of constructing a DODAG using RPL is also represented in Figure 2.

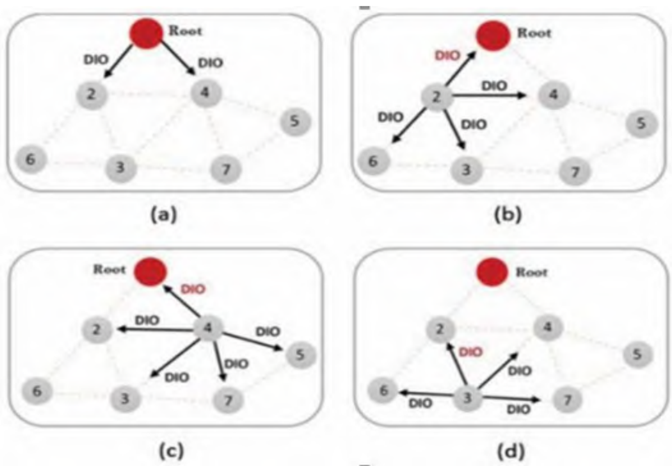

Figure 2. Structure of building DODAG with RPL

Designing an OF remains an active area of research to improve the performance of the routing protocol. In this context, the Routing Over Low Power and Lossy Networks (ROLL) working group designed two basic objective functions. The first one is OF0, which is based on the hop count metric that follows the philosophy of the famous algorithm of Dijkstra to select the nearest path first. The second one is MRHOF, which selects routes that minimize a metric relative to link paths. Figure 3. RPL utilizes OF, which outlines the process of selecting the computing path.

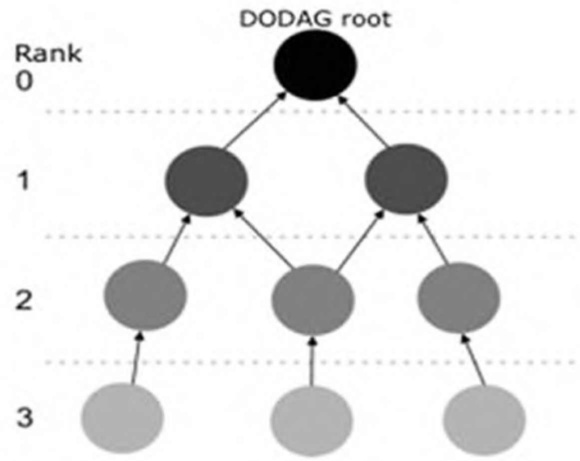

Figure 3. Ranks using DODAG.

Objective Function Zero (OF0)

OF0 is based on reducing hop count to ensure connectivity for a substantial number of nodes within the network and to facilitate the routing of data packets to the root. The overall path selection process initiates with the computation of a variable referred to as Rank Increase for each node, as defined in Eq. (1).

Rank node = Rank parent + Rank increase (1)

Where Rank parent refers to the rank of the preferred parent node, while the variable Rank increase is determined according to Eq (2).

Rank _increase = Min Hop Rank Increase *Step (2)

Where Step is a scalar value that indicates the magnitude of rank increment along a path within the DODAG, while Min Hop Rank Increase specifies the unit of rank increase.

Minimum Rank Hysteresis Objective Function (MRHOF)

The MRHOF is based on a standardised routing metric known as Expected Transmission Count (ETX) which represents the anticipated number of transmissions required for a node to successfully deliver a packet to its destination. The calculation of ETX for potential parent nodes is expressed in Eq. (3):

ETX = 1 / (Df * Dr) (3)

Where Df denotes the probability of packet reception by the neighbor, while Dr represents the acknowledgment probability for a successfully received packet. The rank of the node is subsequently computed using Eq (4):

Rank node = Rank parent + ETX (4)

Where Rank parent refers to the rank of the parent node and ETX indicates the expected transmission count to this parent node.

Machine Learning (ML)

ML is a subfield of artificial intelligence (AI) that enables systems of learning and analysing data (Dunkels et al., 2004) (Dimarco et al., 2010). It offers the flexibility to discover different network characteristics and determine optimal path solutions within a network (Santos et al., 2023). We have used machine learning (ML) techniques to solve wireless problems,ensuring timely and effective decision-making in complex situations. It also helps to enhance the efficiency of wireless sensor networks as well as reduce human intervention or reprogramming. This research has used Random Forest (RF) and Support Vector Machine (SVM) algorithms to design and implement the proposed system.

Support Vector Machine (SVM)

SVM is a non-probabilistic classifier that is formally characterized by a separating hyperplane. The training dataset is labeled through a supervised learning process,whereby the algorithm identifies an optimal hyperplane that maximizes the distance from the support vectors. In a two-dimensional space, this hyperplane manifests as a line that divides the plane into two distinct classes. The tuning parameters for the SVM classifier include epsilon, regularization and kernel parameters (Zidi et al., 2017) Figure 4 shows the technique of SVM.

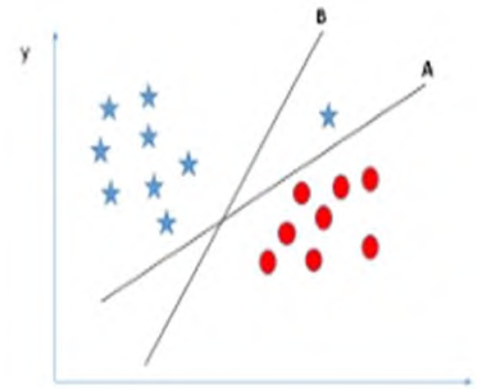

Figure 4. The SVM technique.

Random Forest (RF)

The Random Forest (RF) is an ensemble learning method used for classification, regression, and other predictive tasks. It operates by constructing decision trees during the training phase and producing a class based on the mean prediction of individual trees. In RF, there is a directly proportional relationship between the number of trees in the forest and the resulting accuracy. The RF algorithm consists of two main steps:
The first step is to create an RF tree, which involves five stages:

- Select K random features from the total features m, where K is less than the total number of features (m).
- Within the selected features, determine node d using the best split point.
- Distribute the nodes into daughter nodes through the best split.
- The first three steps are repeated until the number of nodes is obtained
- All of the above steps are repeated n times to achieve p number of trees, where n is not equal to p.

Next, we classify the data using the RF tree we created in the first step. It has the following stages:

- The rules created for each randomly formulated decision tree and test features,
- data are classified
- The votes are calculated for each target value.
- The highest voted prediction target is considered to be the final result of the RF algorithm (Zhang,et al,2018).

Figure 5 shows the RF algorithm.

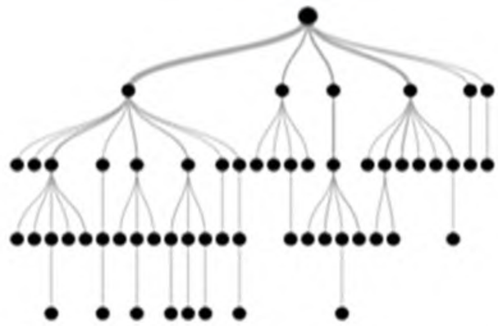

Figure 5. The RF technique.

Contributions of This Paper

Energy limitation is one of the most important challenges facing WSNs and is a major concern as the network expands. Therefore, we are developing key energy efficiency measures to manage energy consumption within the network effectively. This research contributes to addressing this issue.

- Development of a low-power routing protocol (RPL) based on machine learning in WSNs that support the IoT aimed to reduce energy consumption
- The proposed model classifies the available paths from the source node to the target based on the total energy consumption, ensuring that messages are delivered with the lowest possible energy usage.
- We used two models: one that used the RF algorithm and the other that used the SVM algorithm.

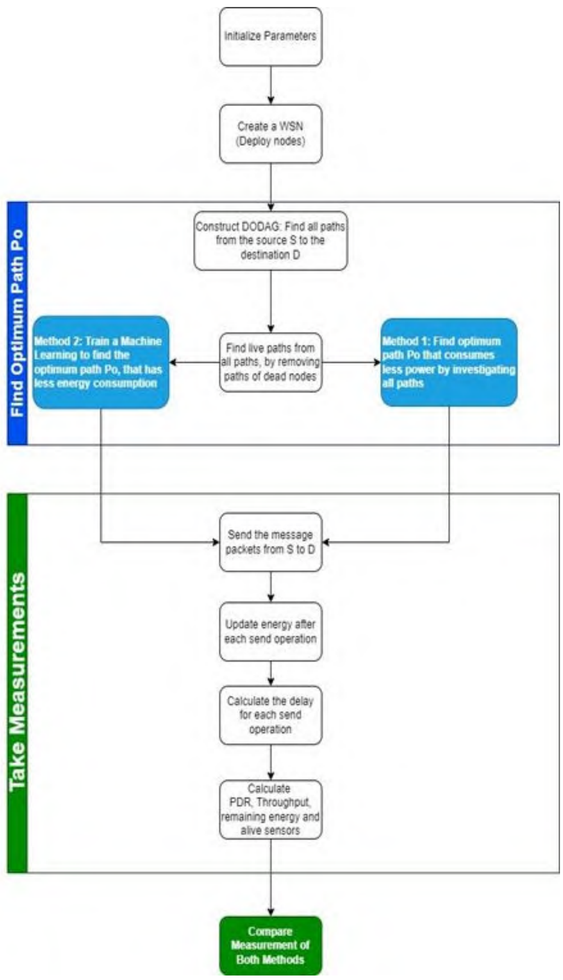

Figure 6. The framework of the proposed model.

The Proposed Model

This article presents a methodology for WSNs based on the development of a low-power routing protocol (RPL) model that utilises machine learning. The target is to achieve energy efficiency by classifying available paths and determining the optimal path for delivering messages to a target with minimal energy consumption. The proposed model divides into four stages, as depicted in Figure 6.

- Stage 1: Building the wireless sensor network and determining the initial parameters.
- Stage 2: Finding the optimal path.
- Stage 3: Implementing dependent measures.
- Stage 4: Conducting comparisons

Below is a detailed explanation of each stage along with subsequent partial steps.

Building the WSNs and Initial Parameters

This stage includes a brief overview of all the initial parameters selected for the simulation, which was implemented in two scenarios with different topologies. Choosing the parameters carefully ensures that the wireless sensor network performs well, as choosing the parameters of signal strength, data transfer rate and speed reduces energy consumption, increases the battery life of the nodes, improves the quality of the connection and the stability of the network, and reduces the failure rate, data transfer time, error rate, and the risk of hacking. Additional factors that contribute to ensuring acceptable network performance include the method used to select the network design scenarios and topologies. Figure 7 illustrates these factors, along with the simulation scenarios and scripts.

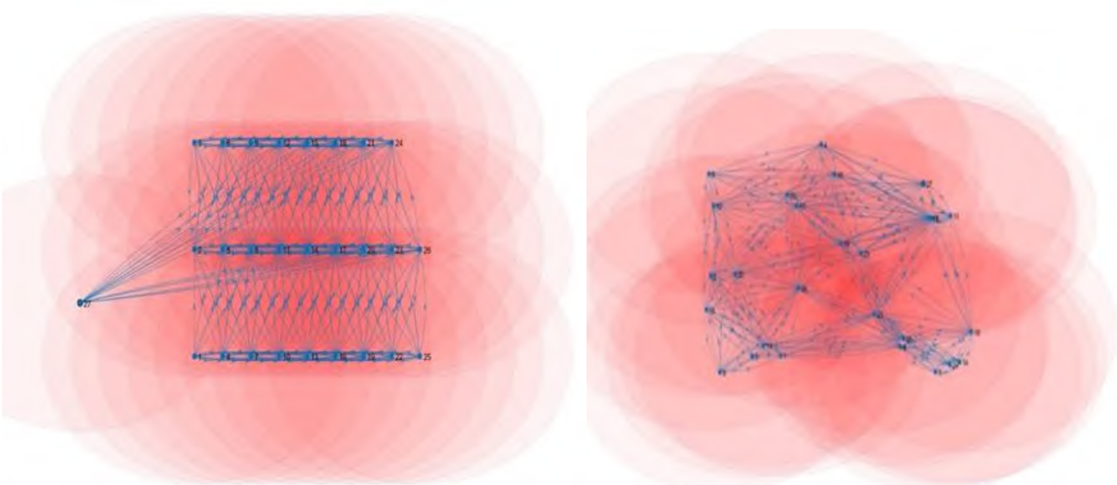

a) b)

Figure 7. a) Scenario 1: Uniform distribution. b) Scenario 2: Random distribution.

Send and Receive Packets

After initializing the WSN, the simulation starts sending data packets from the sender node to the receiver node. The packet may pass through many nodes till it reaches its destination. Between each pair of neighbouring nodes, the packet is transmitted through the channel by the transmitter, which consumes energy of E_TL Joules. The transmitter consumption loss energy E_TL is calculated based on the distance between them d as follows:

$$E_{TL} = \begin{cases} E_{Tx} + LRAEC \times PacketSize \times d^4 & if\ d > d_{th} \\ E_{Tx} + SRAEC \times d^2 & if\ d < d_{th} \end{cases} \quad (5)$$

where E_Tx is the initial energy consumption of the transmitter, d is the distance between the transmitter and the receiver. In any case, where the distance is less or greater than the threshold d_th, the receiver consumes the following energy:

$$E_{RL} = (E_{Rx} + EDA) \times PacketSize \qquad 6$$

where EDA is the Data Aggregation Energy, which is set in the initialization step.

Finding the Optimal Path Stage

After establishing the first stage by selecting the appropriate parameters, designing topology scenarios, and deploying the nodes, this stage involves identifying all paths from the source(s) to the interface (D) and determining the direct paths by eliminating the paths of neglected nodes through the construction of DODAG. The optimal path from the source to the interface is determined using two methods: the first uses the standard RPL protocol technology and uses the OF0 algorithm, while the second method involves ML techniques using the RF and SVM algorithms. Figure 8 shows the flowchart of this stage.

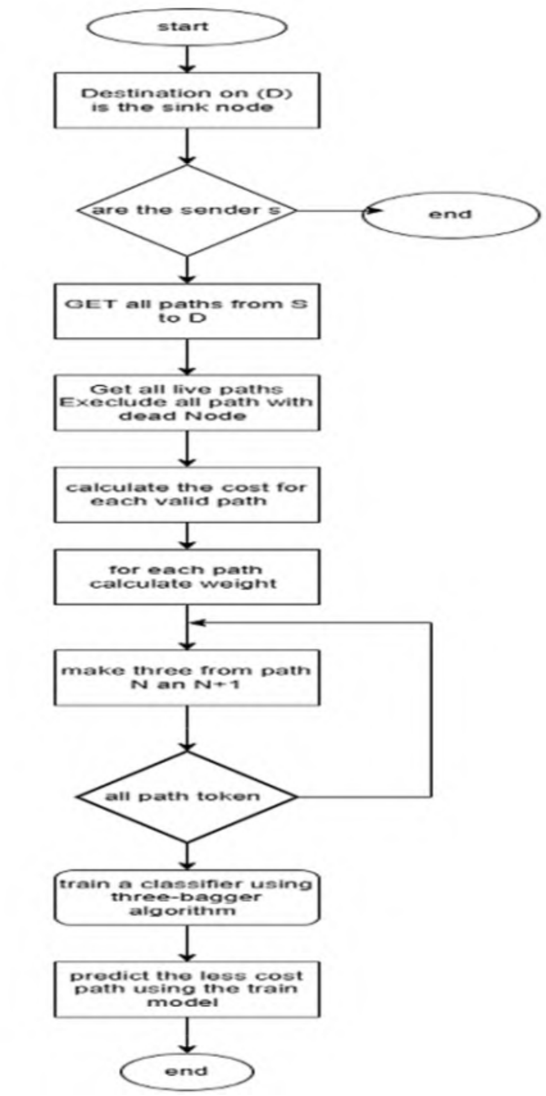

Figure 8. Flowchart of finding the optimal path.

Approach 1: The low-power lossless RPL protocol with the objective function OF0 determines the optimal path from the source to the interface in a WSN by identifying the immediate neighbour nodes, calculating the link cost between these neighbours, then constructing the tree for each node after identifying its immediate parent through the link quality. The objective function OF0 is calculated as follows:

OFO = min (Rank, Parent _ Rank) (7)

where Rank is the rank of the current node, and Parent Rank is the rank of its direct parent. After calculating the objective function OF0, the optimal path with the lowest cost is determined, and the tree is then cyclically checked to ensure that the optimal remains valid.

Approach 2: In this approach, the optimal path from the source to the interface is determined by combining machine learning models with the RPL protocol, using RF and SVM algorithms for comparison. When integrating either of the two algorithms into RPL, the process involves collecting and analysing data such as link quality, energy consumption, and data transmission time. Important features that affect the network performance are identified, and RF and SVM models are created based on these features. The models are trained using training datasets, optimising the path based on the trained model. This process is repeated multiple times to improve the network performance. Even the RF and SVM models have improved accuracy, still the SVM algorithm has limitations, including the complexity and time consumption of training data and determining the optimal parameters of the model.

Dependent Measures

Various measurements are collected, including the packet delivery ratio (PDR), power consumption, end-to-end delay (E2E Delay), and the percentage of time the radio is ON.

Comparisons

In the final stage of the proposed system, the overall performance of the network is compared among the RF algorithm, SVM, the standard RPL protocol with the objective function OF0 and the modified RPL protocol with Minimum Rank Hysteresis Objective Function (MRHOF).

Results and Discussion

In this section, we present the results of implementing the proposed model that aimed to improve energy consumption in WSNs.

Simulation Parameters

Table 1 shows the parameters used in simulating the proposed model

Table 1. Simulation parameters

Parameter	Value
Number of Nodes in the field	26, 50
Maximum number of rounds	300
WSN deployment Area	100
Radio Range	120
Maximum number of rounds (r max)	max Rounds
Data packet size (Packet Size)	400
Hello packet size (Hello Packet Size)	100
Number of Packets to be sent in steady-state phase (Num Packet)	100
Initial Energy in Joules (E_o)	0.5
Transmission and receiving energy consumption (E_x, E_r)	Ex=50×10−10E_x = 50 \times 10^{-10}, Er=50×10−10E_r = 50 \times 10^{-10}
Transmit Amplifier energy consumption (SRAEC)	10−1110^{-11} Joules
Long range Amplifier energy consumption (LRAEC)	13×10−1813 \times 10^{-18} Joules
Threshold distance (d_th)	877.0580 (unitless)

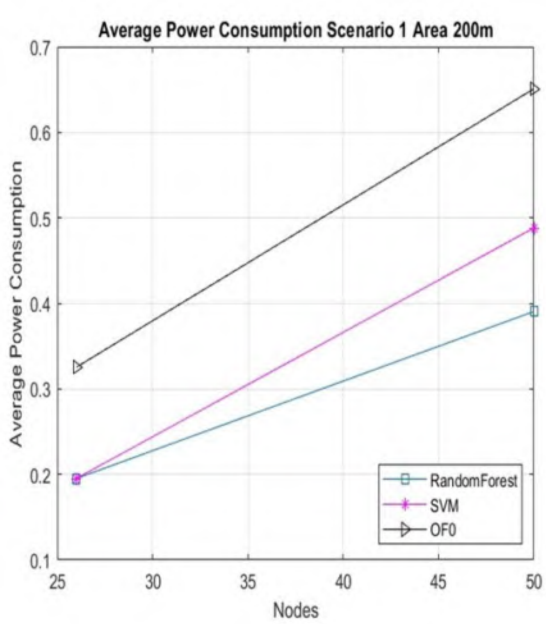

Figure 9. Average in scenario 1 with 26 nodes and a side area of 200 m.

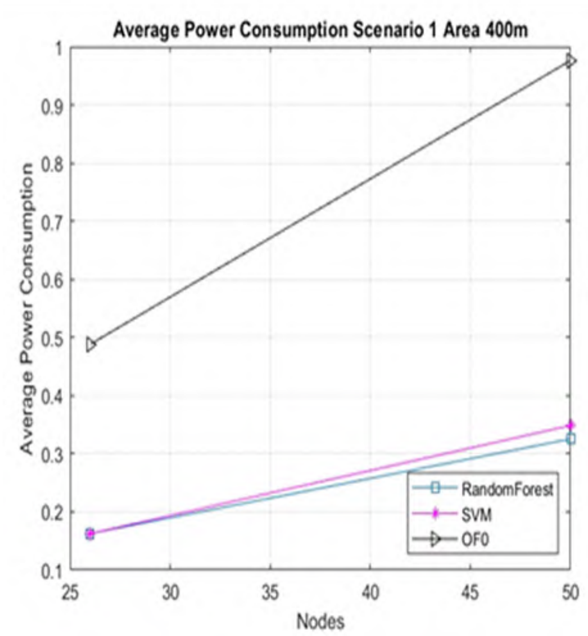

Figure 10. Average power consumpation scienario 1 area 400m

The Average Consumed Power

It is clear from figures (9-12) that the random forest algorithm is the best in terms of energy consumption for all scenarios, their topology, and components The reason is because the RF algorithm that the following advantages: Simple implementation, effective use of data, it work well when there's noise in the data, and work quickly in training.

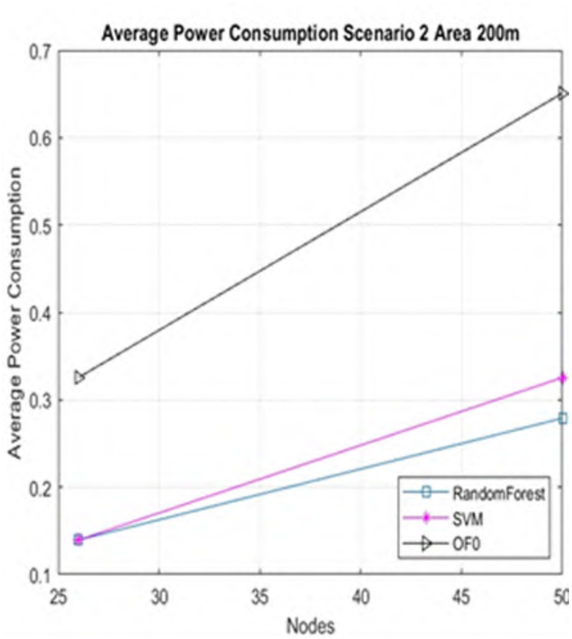

Figure 11. Average power consumption scenario 2, area 200m.

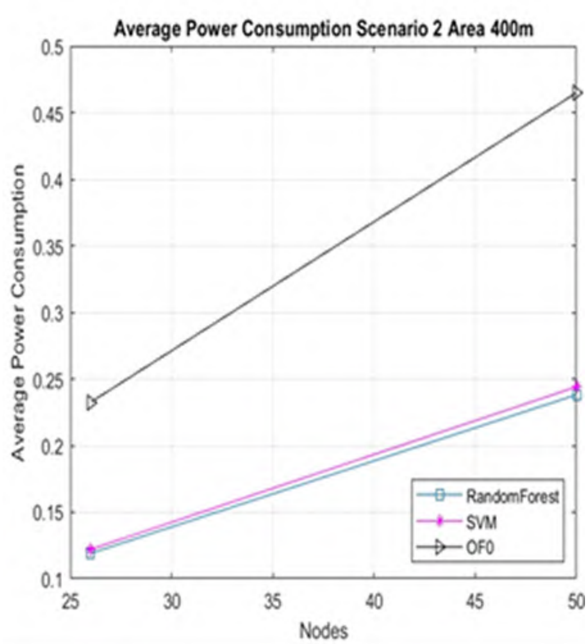

Figure 12. Average power consumption scenario 2 area 400m

Packet Delivery Ratio (PDR)

Figures (13-14) show that the RF algorithm is the best in terms of PDR in the two scenarios with an area of 200m. The reason is because the RF algorithm has the following advantages: Its ability to withstand data noise, rapid learning and dealing with non-linear, missing and heterogeneous data.

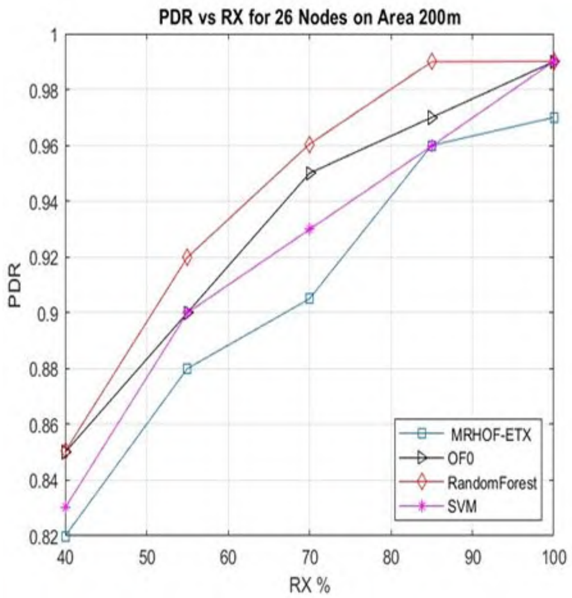

Figure 13. PDR vs RX in scenario 1 with 26 Nodes and side area 200m.

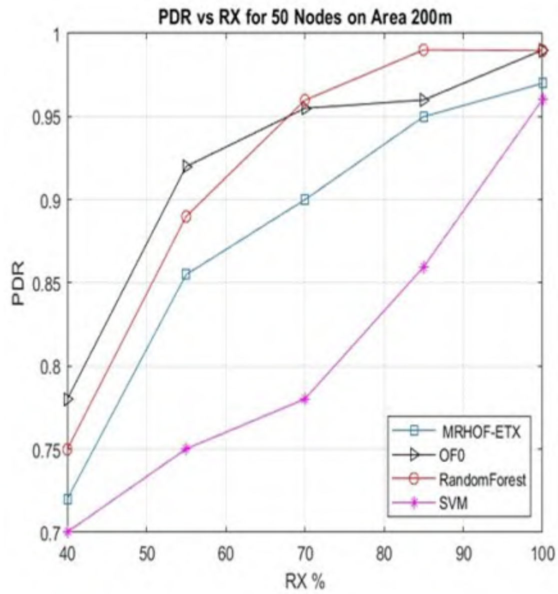

Figure 14.PDR vs RX in scenario 2 with 50 nodes and side area 200m.

The Percentage E2E Delay

Figures 15-18 show the percentage delay in data transmission from the source to the interface across the various simulation scenarios. The results indicate that delay increases proportionally with the number of nodes in the network. For both the RF and SVM algorithms, the observed delay percentages are relatively close, ranging between 10% and 50%, depending on the number of nodes deployed.

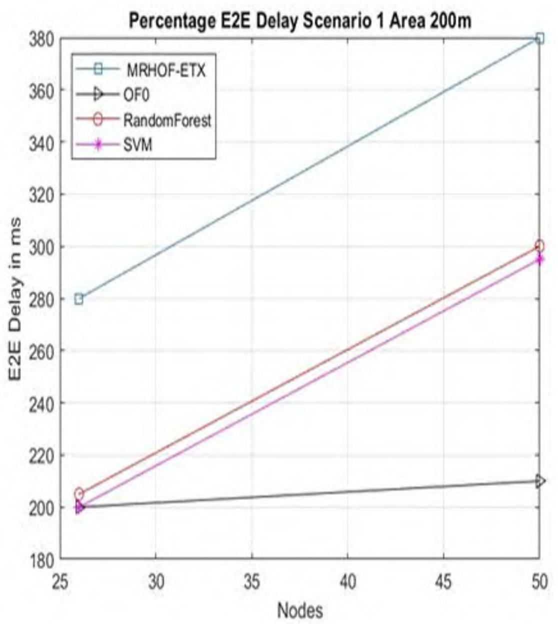

Figure 15. Percentage E2E delay scenario 1 area 200 m.

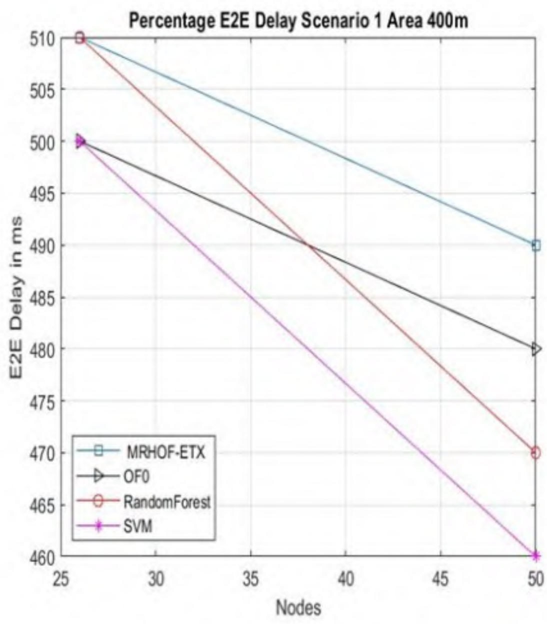

Figure 16. Percentage of E2E delay scenario 1 area 400m.

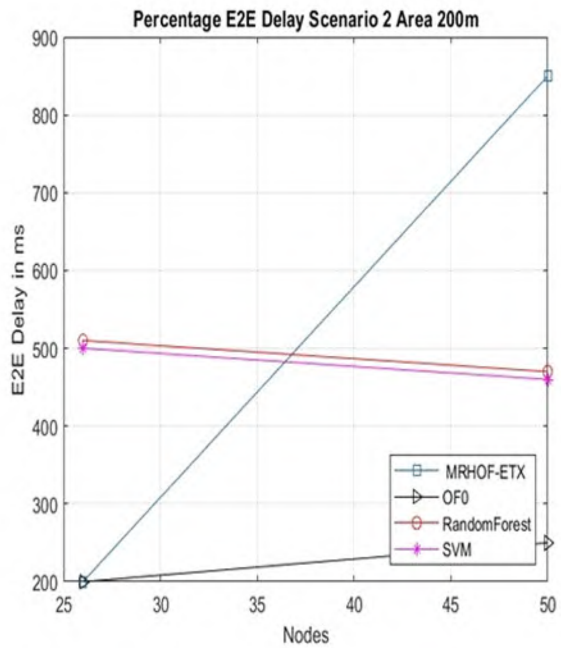

Figure 17. Percentage of E2E delay scenario 2 area 200m.

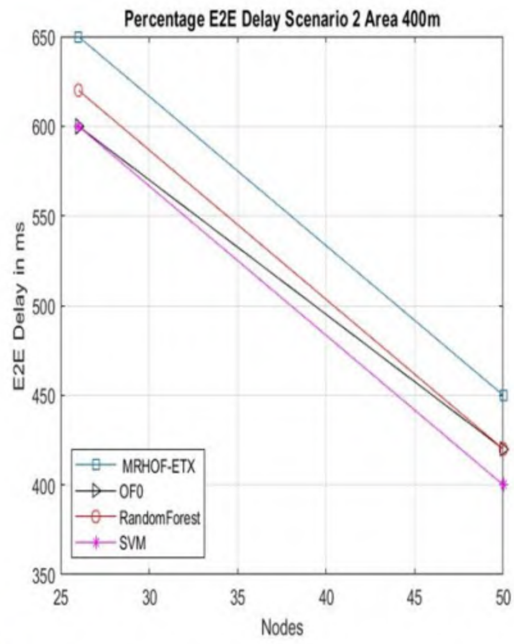

Figure 18. Percentage of E2E delay scenario 2 area 400m.

Percentage Radio ON

Figures (19-22) show the percentage of radio ON, which depends on the size of the network, the number of nodes and the link. In the RF algorithm, it ranges between 5% and 20%.

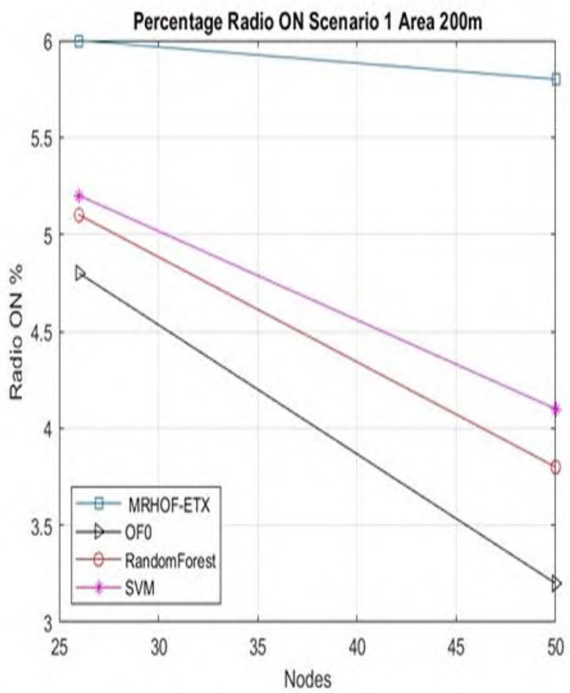

Figure 19. Percentage of radio ON scenario 1 area 200m.

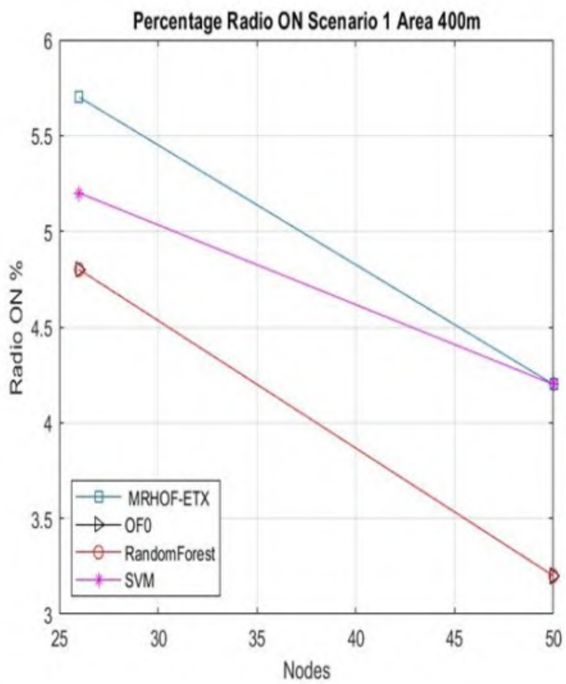

Figure 20. Percentage of radio ON scenario 1 area 400m.

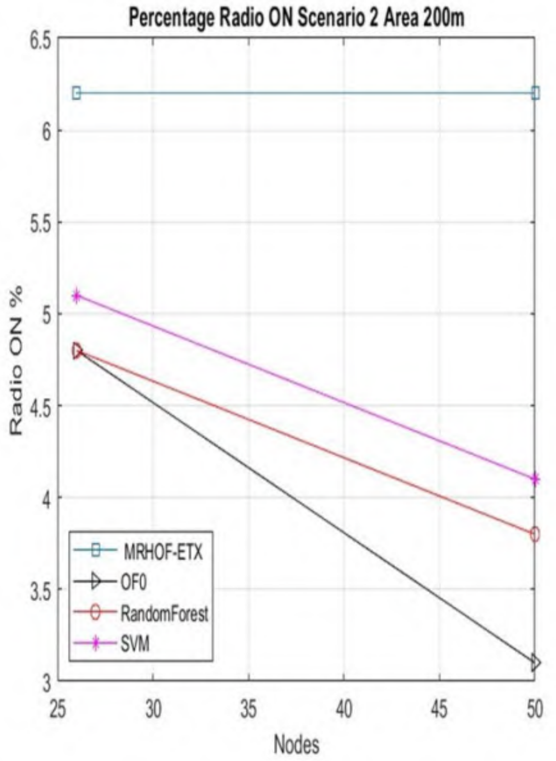

Figure 21. Percentage of radio on scenario area 400m.

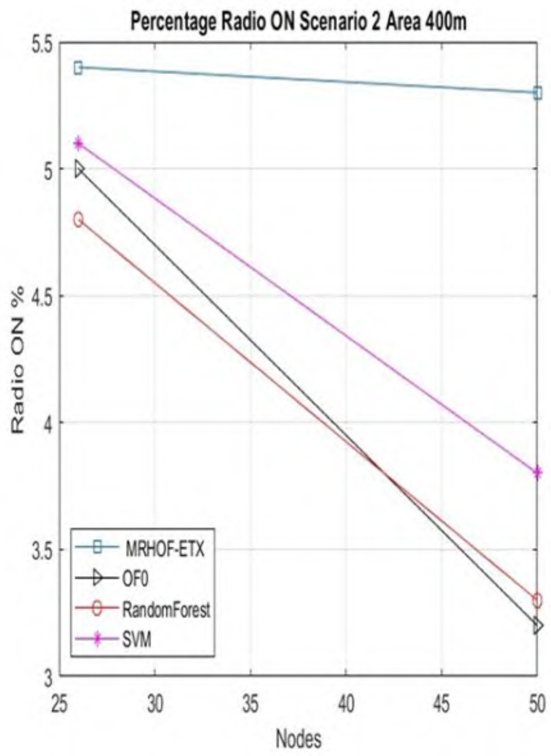

Figure 22. Percentage of radio ON scenario 2 area 400m

Conclusion

One of the most significant challenges facing the WSN is energy consumption, which plays an important and effective role in the network's performance and extending its life. Therefore, it is important to choose the appropriate nodes, protocols and technologies to ensure the lowest possible power consumption. The low-power lossy routing protocol (RPL) has many uses in WSNs due to its ability to reduce energy consumption and improve routine quality

This paper presents a model that combines machine learning techniques and the RPL protocol to improve the performance of standard RPL by identifying the best energy-efficient path for data transmission from the source node to the interface while maximising data delivery rate and minimising latency. Simulation results demonstrate that the RF algorithm achieved superior performance compared with the SVM algorithm and the FRIPL protocols using the OF0 and MRHOF-ETX objective functions.

Scientific Ethics Declaration

* The authors declare that the scientific ethical and legal responsibility of this article published in EPSTEM journal belongs to the authors.

Conflict of Interest

* The authors declare that they have no conflicts of interest.

Funding

* This research received no specific grant from any funding agency in the public, commercial, or not-for-profit sectors.

Acknowledgements or Notes

* This article was presented as an oral presentation at the International Conference on Research in Engineering, Technology and Science (www.icrets.net) held in Peja/Kosovo on July 10-13, 2025.

* The authors thank everyone who supported the work.

References

Culler, D., Estrin, D., & Srivastava, M. (2004). Guest editors' introduction: Overview of sensor networks. *Computer, 37*(8), 41-49.

Dai, H., Wu, X., Xu, L., & Chen, G. (2020). Practical scheduling for stochastic event capture in energy harvesting sensor networks. In *IEEE Wireless Communications and Networking Conference* (Vol. 18, pp. 85-100).

Dunkels, A., Gronnvall, B., & Voigt, T. (2004). Contiki- a lightweight and flexible operating system for tiny networked sensors. In *28th Annual IEEE International Conference on Local Computer Network*.

Gaber, T., Abdelwahab, S., Elhoseney, M., & Hassanien, E. (2018). Trust-based secure clustering in WSN-based intelligent transportation systems. *Computer.Network, 146*, 151-158.

Gurram, G. V., Stevanovic, D., & Spanogiannopoulos, G. (2022). Strategies for improving performance of IEEE 802.15.4/ZigBee WSNs with path-constrained mobile sink. *Computer Communication, 34*(6), 743-757.

Hassani, E., Sahel, A., & Badri, A. (2019). Assessment of a proactive routing protocol RPL in Ipv6 based wireless sensor networks. In *ICDS* (pp. 1-6).

Kundaliya, B., & Hadia, S. (2020). Enhancing network lifetime with an improved MOD-LEACH. *International Journal of Electrical and Computer Engineering, 9*(5), 3615-3622.

Kundaliya, B. L., & Hadia, S. K. (2020). Routing algorithms for wireless sensor networks: Analysed and compared. *Wireless Personal Communications, 110*(1), 85-107.

Nilabar, N. U., Manikandan, A., Venkataramanan, C., & Dhanapal, R. (2023). A score based link delay aware routing protocol to ımprove energy optimization in wireless sensor network. *Journal of Engineering Research, 11*, 192-219.

Ogundile, O., Balogun, M., Ijiga, O., & Falayi, E. (2019). Energy-balanced and energy-efficient clustering routing protocol for wireless sensor networks. *IET Communications, 13*(11), 1449-1457.

Park, P., Fischione, C., Bonivento, A., Johansson, K., & Sangiovanni-Vincent, A. (2011). Breath: An adaptive protocol for insutrial control applications using wireless sensor networks. *Mobile Computing, IEEE Transactions on, 10*(6), 821-838.

Santos, D. L. C., Mezher, M. A., Leon, A., Pabo, J., Cárdenas-Barrera, J., Guerra, E., & Meng, J. (2023). ML-RPL: Machine learning-based routing protocol for wireless smart grid network. *IEEE Access*, 57401-57414.

Sharma, R., Prakash, S., & Roy, P. (2020). Methodology, applications, and challenges of WSN-IoT. In *2020 International Conference on Electrical and Electronics Engineering (ICE3)* (pp. 502-507). IEEE.

Somula, R., Parvathala, B., Kolli, S., Pulipati, S., & Adita, S. S. T. (2021). SOA-EACR: Seagull optimization algorithm based energy aware cluster routing protocol for wireless sensor networks in the livestock industry. *Sustainable Computing Informatics and Systems, 33*.

Suliman, A. A., & Ahmed, J. O. (2022). High-quality clustering algorithm and optimal cluster head selection using fuzzy logic in wireless sensor networks. *Fuzzy Sets and Systems, 389*, 114-144.

Tahsien, S. M., Karimipour, H., & Spachos, P. (2020). Machine learning based solutions for security of ınternet of things (IoT): A survey. *Journal of Network and Computer Applications, 161*, 102630.

Vlajic, N., Stevanovic, D., & Spanogiannopoulos, G. (2011). Strategies for improving performance of ieee 802.15.4/zigbee wsn with path constrained mobile sink. *Computer Communication, 34*(6), 743-757.

Wakili, A. (2024). Machine learning for QoS and security enhancement of RPL in IoT-Enabled wireless sensors. *Wireless Networking Based Control*, 100289.

Zahra, F., Jhanjhi, N., Brohi, S. N., Khan, N. A., Masud, M., & AlZain, M. A. (2022). Rank and wormhole attack detection model for RPL-Based ınternet of things using machine learning. *Sensors, 22*(18).

Zhang, D., Qian, L., Mao, B., Huang, C., Huang, B., & Si, Y. (2018). A Data-driven design for fault detection of wind turbines using random forests and xg boost. *IEEE Access, 6*, 21020-21030.

Zidi, S., Moulahi, T., & Alaya, B. (2017). Fault detection in wireless sensor networks through SVM classifier. In *IEEE Sensors Journal, 18*(1), 340-347.

Author(s) Information

Nashwa Rabah Abood
University of Baghdad
Baghdad, Iraq
Contact email: *n.abood1020@coeng.uobaghdad.edu.iq*

Anwar Qassim Al-Khateeb
University of Baghdad
Baghdad, Iraq

To cite this article:

Abood, N. R., & Al-Khateeb, A. Q. (2025). Design and implementation of integrated RPL protocol and deep learning for energy-aware wireless sensor networks. *The Eurasia Proceedings of Science, Technology, Engineering and Mathematics (EPSTEM), 35,* 225-239.

The Eurasia Proceedings of Science, Technology, Engineering & Mathematics (EPSTEM)
ISSN: 2602-3199

The Eurasia Proceedings of Science, Technology, Engineering and Mathematics (EPSTEM), 2025

Volume 35, Pages 240-247

ICRETS 2025: International Conference on Research in Engineering, Technology and Science

Multicriteria Risk Assessment in Small and Medium-Sized Ship Repair Enterprises During the Repair of Ships Using Alternative Fuels

Yordan Denev
Technical University of Varna

Abstract: The article addresses the issue of risk assessment in small and medium-sized ship repair enterprises servicing ships that operate on alternative fuels. The characteristics and properties of the most commonly used alternative fuels in maritime transport—liquefied natural gas, petroleum gas, ammonia, hydrogen, and methanol—are presented. Various criteria have been developed depending on the type of fuel used and its specific features. A multicriteria analysis is used to assess the risk associated with different types of fuels. Using the TOPSIS method, three evaluation scenarios have been developed. Different weights have been assigned to certain criteria that directly impact humans and the risk of damage. It has been found that the lowest risk to crew members and the ship itself occurs when using liquefied natural gas and liquefied petroleum gas. The highest risk is associated with the use of ammonia and methanol. The use of hydrogen as an alternative fuel plays a relatively neutral role in risk assessment.

Keywords: Alternative fuels, Ship repair, Ammonia, Hydrogen, Multicriteria risk assessment

Introduction

With the introduction of requirements to reduce harmful emissions from shipping, the modernization of ship power plants began. A large number of existing ships underwent modernization. Fuel systems operating with alternative fuels were installed. In many cases, the newly installed fuel tanks are located on the main deck and in areas close to the ship's superstructures. This, to some extent, creates a precondition for accidents in the event of fuel leakage. Precisely because of this fact, it is advisable to carry out a risk assessment for ships operating with alternative fuels during periods when they are undergoing intermediate or class repairs.

Assessments and analyses of this type are finding increasingly wide application today and in the future in ship repair enterprises. This trend represents a new development in ship repair, and special attention should be given to ships that use alternative fuels. Some of these fuels are well known for their properties that affect human health and safety on board the vessel.

Alternative Fuels in Shipping

The use of alternative fuels in shipping, and consequently in shipbuilding and ship repair, is a response to the IMO's call for an intensive reduction of harmful gases in the atmosphere. At present, there are still challenges related to their storage, bunkering, and use from a safety perspective. Concepts for fueling ships with alternative fuels have been evaluated in terms of their reliability. The assessment considers the likelihood of failure and the severity of the consequences (Poop, 2021).

The use of green ammonia in shipping presents its challenges. It requires additional upgrades on board existing vessels, as well as significant additional port infrastructure for production, storage, and bunkering. To some

- Selection and peer-review under responsibility of the Organizing Committee of the Conference

extent, this will lead to accelerated modernization of ports, along with an increased risk of hazards. A comparative table of different fuels is presented in (Fullonton, 2025).

At the stages of ship design and selection of the power plant, it is advisable to assess the generated harmful emissions. This assessment would directly depend on the ship's deadweight, speed, and block coefficient. Over three years, nine bulk carriers were studied. Based on this, regression models for the assessment were developed using three different methods (Bilgili, 2018). The placement of fuel tanks and hazardous zones is of particular importance in risk assessment. In (Brouzas, 2025) such zones are presented, with attention also given to equipment, selection of insulation materials, safety valves, and the quality of the hydrogen. Legislative ambiguities have been identified regarding safety measures during the operation of ships using this type of fuel.

The use of ammonia as a marine fuel in dual-fuel power systems reduces the generation of harmful gases. Maintaining the ammonia content below 60% helps to lower the combustion temperature, which reduces NOx emissions. On the other hand, increasing the ammonia proportion leads to higher N_2O emissions, which offset the reduction in CO_2 emissions (Duong, 2025). For this reason, a precise balance of the fuel mixture in dual-fuel power systems using ammonia must be achieved. The specifics regarding the handling of ammonia as an alternative fuel are presented in detail in (DNV, 2021).

The use of alternative fuels such as ammonia, hydrogen, liquefied natural gas, liquefied petroleum gas, and methanol has its advantages and disadvantages. Some of these are thoroughly analyzed and presented in (Popek, 2024). The disadvantages are generally related to the lack of suitable bunkering infrastructure in ports, plants, and open sea locations. When using alternative fuels, the possibility of retrofitting the structure and the associated risks must be carefully analyzed and evaluated. Such an analysis, with proposed criteria, has been conducted in (Kolios, 2024). The criteria are largely focused on electric propulsion in shipping.

The transportation of natural gas can be carried out through the transport of gas hydrates, from which the gas can be extracted. Although the gas is not in a liquid or gaseous state, this method poses certain risks. A risk assessment for this mode of transportation is presented in (Kim, 2015). Criteria with different weightings have been defined, and the risk has been evaluated using a risk assessment matrix.

Evaluation Criteria

For the risk assessment, five criteria have been developed and proposed, each having a direct impact on the risk associated with ships using alternative fuels. Some of these criteria cover the physico-toxicological effects of the fuels, while others address the structural characteristics of the systems used for the transportation and storage of gases. They are:

- Flammability;
- Toxicity;
- Valve maintenance;
- Tank filling;
- Tank location;
- Tank material.

Each of the criteria has been assigned weighting coefficients. The values of these weighting coefficients have been selected to correspond closely to the actual likelihood of an accident occurring on board. They range from 0 to 20 in increments of five and have different meanings. For each of the various types of fuels, a risk matrix has been developed by introducing four values for each of the criteria. In the development of the risk matrix for each type of fuel, its specific characteristics were considered. Special attention was given to toxicity, flammability, and the method of fuel storage. These three characteristics are particularly important when the vessel is in a shipyard for dry dock or class repair. This necessitates the development of a multi-criteria risk assessment for ships in the modern commercial fleet that are in operation.

Multicriteria Risk Assessment During the Repair of Ships Using Alternative Fuels

There are various methods for multicriteria assessment. Depending on the desired solution to the problem, the methods can generally be divided into three main groups: methods that provide information on minimum and maximum values, weighting methods, and those that follow linear programming techniques, also known as preference analysis. Of all the methods for multi-criteria evaluation, the TOPSIS method, which belongs to the weighted methods group, has been chosen. To evaluate alternatives using this method, a rating matrix—also known as a decision matrix—is developed. It consists of m alternatives and n criteria with their corresponding x_{ij} elements, eq.1 (Shih. 2022).

$$D = \begin{array}{c c} & \begin{array}{ccccc} X_1 & X_2 & \cdots & X_j & \cdots & X_n \end{array} \\ \begin{array}{c} A_1 \\ A_2 \\ \vdots \\ A_i \\ \vdots \\ A_m \end{array} & \begin{bmatrix} x_{11} & x_{12} & \cdots & x_{1j} & \cdots & x_{1n} \\ x_{21} & x_{22} & \cdots & x_{2j} & \cdots & x_{2n} \\ \vdots & \vdots & \ldots & \vdots & \ldots & \vdots \\ x_{i1} & x_{i2} & \cdots & x_{ij} & \cdots & x_{in} \\ \vdots & \vdots & \ldots & \vdots & \ldots & \vdots \\ x_{m1} & x_{m2} & \cdots & x_{mj} & \cdots & x_{mn} \end{bmatrix}_{m \times n} \end{array} \tag{1}$$

After creating the evaluation matrix, a normalized rating matrix R is developed, eq.2.

$$R = \begin{array}{c c} & \begin{array}{ccccc} X_1 & X_2 & \cdots & X_j & \cdots & X_n \end{array} \\ \begin{array}{c} A_1 \\ A_2 \\ \vdots \\ A_i \\ \vdots \\ A_m \end{array} & \begin{bmatrix} r_{11} & r_{12} & \cdots & r_{1j} & \cdots & r_{1n} \\ r_{21} & r_{22} & \cdots & r_{2j} & \cdots & r_{2n} \\ \vdots & \vdots & \ldots & \vdots & \ldots & \vdots \\ r_{i1} & r_{i2} & \cdots & r_{ij} & \cdots & r_{in} \\ \vdots & \vdots & \ldots & \vdots & \ldots & \vdots \\ r_{m1} & r_{m2} & \cdots & r_{mj} & \cdots & r_{mn} \end{bmatrix}_{m \times n} \end{array} \tag{2}$$

The normalized matrix consists of m alternatives and n criteria with their corresponding r_{ij} elements, eq.3.

$$r_{ij} = \frac{x_{ij}}{\sqrt{\sum_{i=1}^{m} x_{ij}^2}} \tag{3}$$

A set of weights w=(w1,…,wn) where each weight wj>0 for j=1,…,nj, s assigned to the corresponding criterion Xj. These weights are normalized such that their sum equals 1. The weighted normalized matrix V=(wj,rij), eq.4 is then obtained by multiplying each element in column j of the normalized matrix R by its corresponding weight wj, for all j=1,…,nji.

$$V = \begin{array}{c c} & \begin{array}{ccccc} X_1 & X_2 & \cdots & X_j & \cdots & X_n \end{array} \\ \begin{array}{c} A_1 \\ A_2 \\ \vdots \\ A_i \\ \vdots \\ A_m \end{array} & \begin{bmatrix} v_{11} & v_{12} & \cdots & v_{1j} & \cdots & v_{1n} \\ v_{21} & v_{22} & \cdots & v_{2j} & \cdots & v_{2n} \\ \vdots & \vdots & \ldots & \vdots & \ldots & \vdots \\ v_{i1} & v_{i2} & \cdots & v_{ij} & \cdots & v_{in} \\ \vdots & \vdots & \ldots & \vdots & \ldots & \vdots \\ v_{m1} & v_{m2} & \cdots & v_{mj} & \cdots & v_{mn} \end{bmatrix}_{m \times n} \end{array} \tag{4}$$

From the completed weighted normalized evaluation matrix, the positive and negative ideal solutions are determined. The positive and negative ideal solutions are obtained based on the following conditions, eq.5 and eq.6:

V+={v1+,………………vn+}= {(max vij| j ϵ J), (min vij| j ϵ J)} (5)
V-={v1-,………………rn-}= {(min vij| j ϵ J), (max vij| j ϵ J)} (6)

Calculation of the separation measures between the alternatives A and the positive S+ and negative S- ideal solutions, eq.7 and eq.8.

$$S_i^+ = \sqrt{\sum_{j=1}^{n} (v_{ij} - v_j^+)^2} \tag{7}$$

$$S_i^- = \sqrt{\sum_{j=1}^{n} (v_{ij} - v_j^-)^2} \tag{8}$$

Determination of the relative closeness of the alternatives. The relative closeness or ranking index of alternative Ai, i = 1,…, m, is calculated by, eq.9:

$$C_i^* = \frac{S_i^-}{S_i^+ + S_i^-} \tag{9}$$

Where: 0≤Ci*≤1

The evaluation and ranking of alternatives using the TOPSIS method are based on their relative closeness. The alternative with the highest relative closeness value is ranked first. Three versions of multicriteria assessment have been developed, each with different weighting coefficients for the various criteria.

Variant 1

The considered option, based on the five criteria, which prioritizes toxicity and flammability, is presented in Figure 1. The results of the multi-criteria analysis are illustrated in Figure 2.

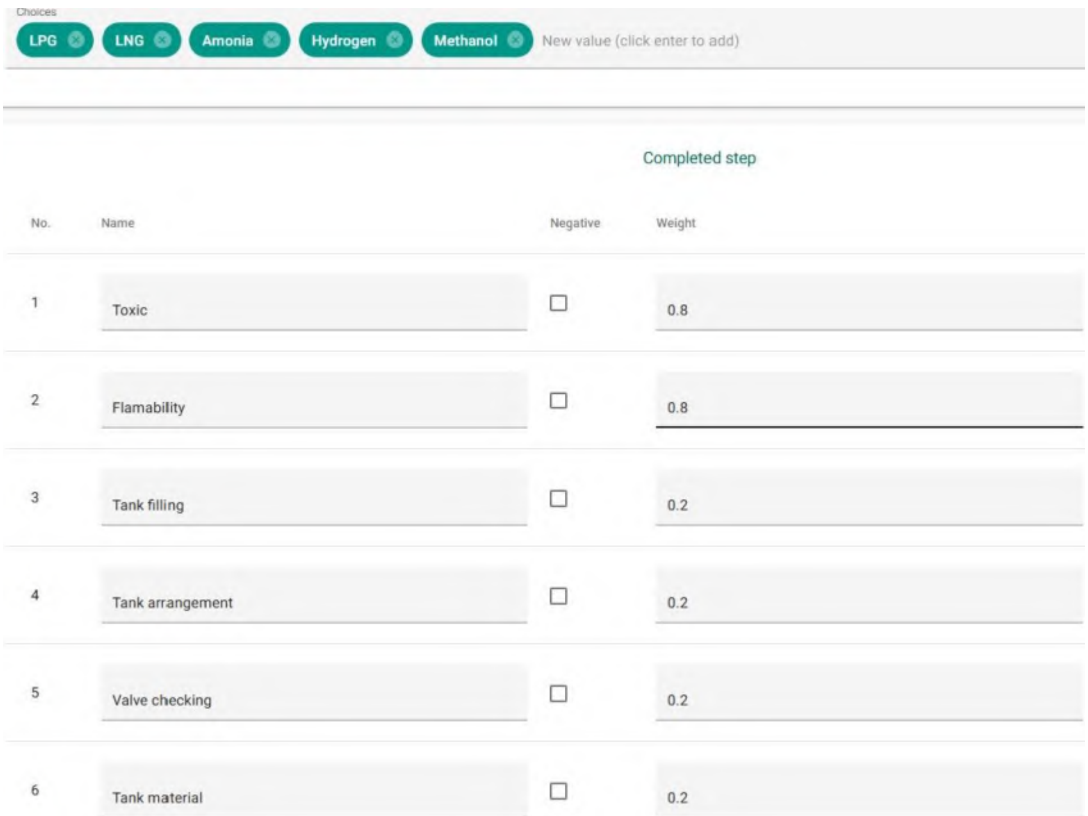

Figure1. Decision matrix with toxic and flammability criteria importance

From the results presented in Figure 2, it can be seen that the highest risk is associated with methanol, followed by ammonia and liquefied natural gas. This is due to the characteristics of the fuel types, given the assigned importance of the two criteria that are significant for human health.

Figure 2. Results from evaluation with variant 1

Variant 2

The second option analyzes the case in which importance is given to the location of the fuel storage tanks and their filling level, figure 3. The significance of these two criteria is driven by the fact that, on existing ships, fuel tank modernization is carried out or new tanks are installed on the main deck in areas with more available space. The filling level of the fuel tanks is also of great importance, as partial filling leads to the formation of vapors, which pose an explosion risk in the presence of a heat source.

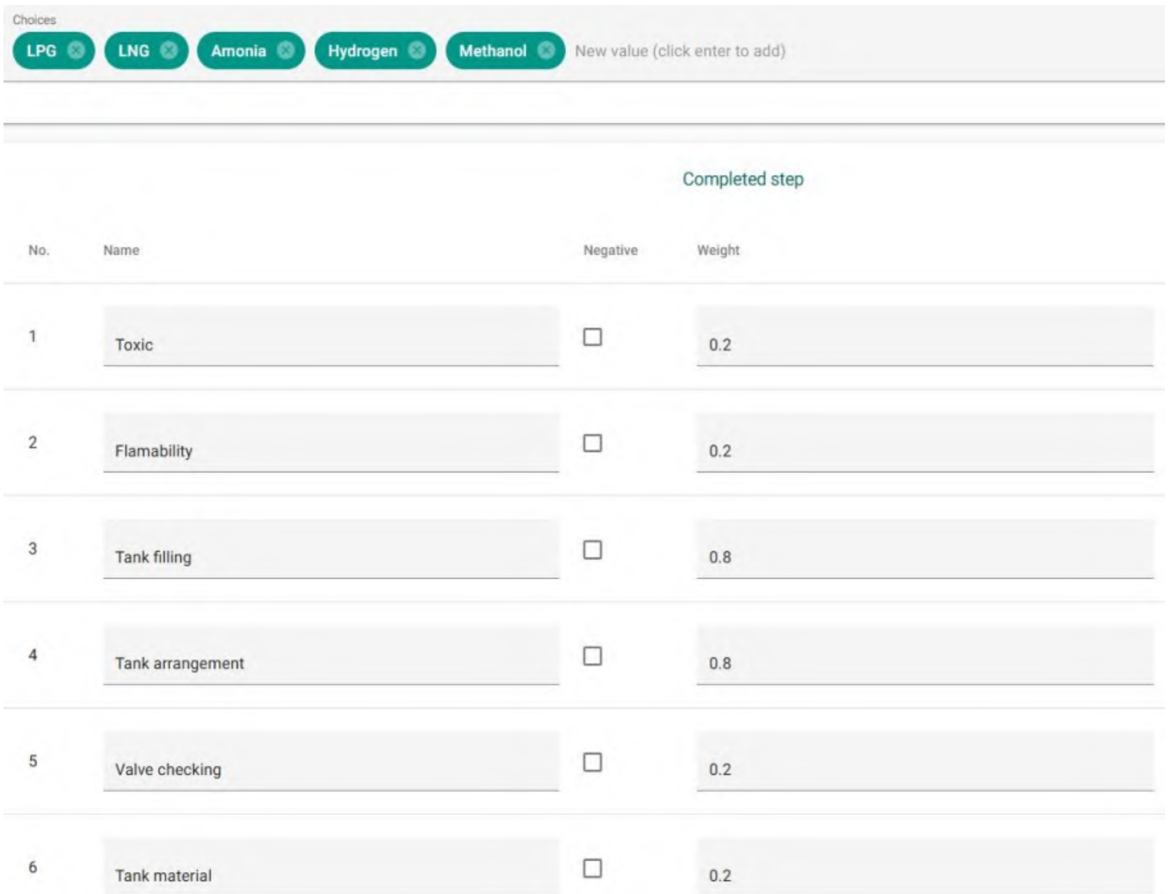

Figure 3. Decision matrix with tank filling and tank arrangement criteria importance,

From the results presented in figure 4, it becomes clear that methanol ranks first with the given weighting coefficients of the criteria. The results are similar to those of option one, but the final values are different.

Figure 4. Results from evaluation with variant 2

Variant 3

The third option analyzes and evaluates the case in which importance is given to the criteria of toxicity, tank placement, valve inspection, and the material from which the tank is made. Importance is given to the criteria related to the qualities of the fuels as well as the specifics of their transportation and storage systems, Figure 5.

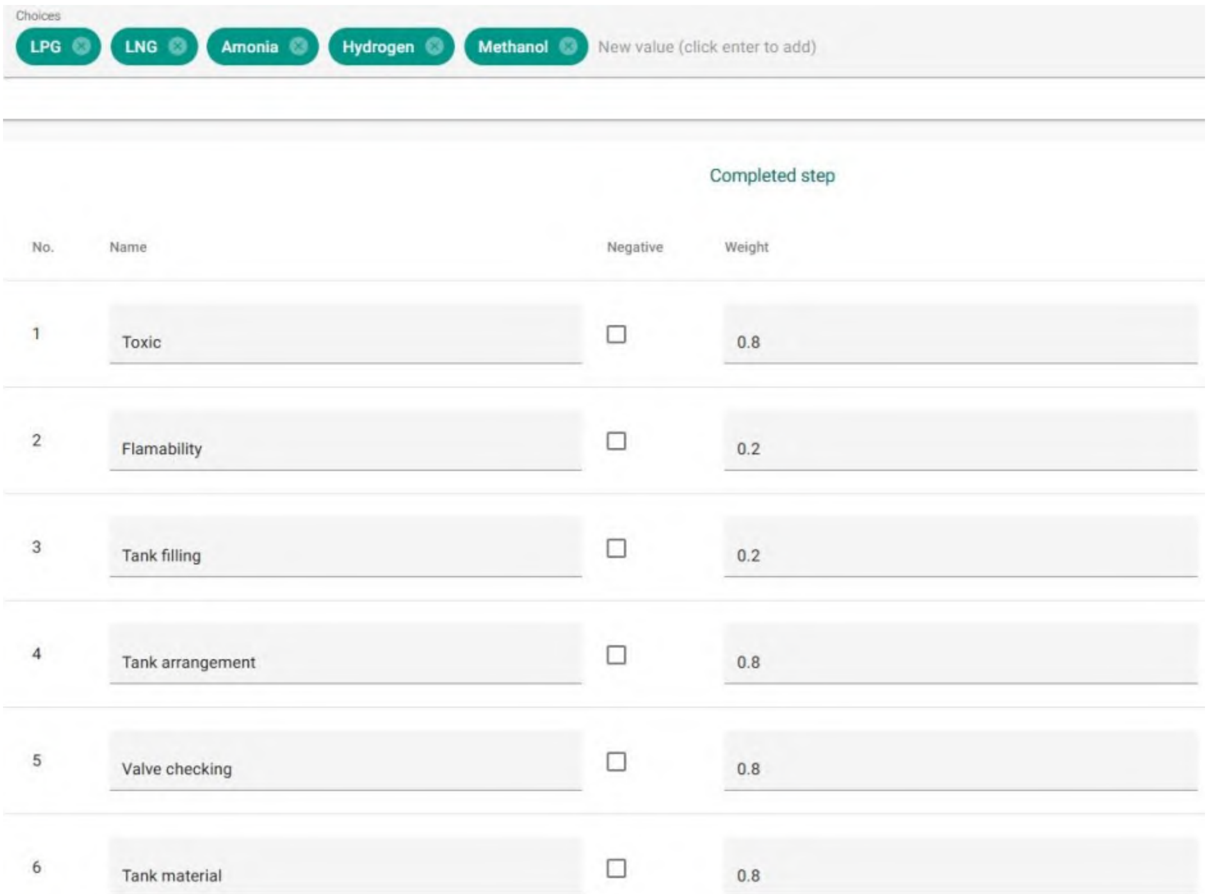

Figure 5. Decision matrix with toxic, tank arrangement, valve checking and tank material criteria importance

Based on the applied weighting coefficients of the different criteria from figure 5, the results are presented in figure 6 using the TOPSIS method.

Figure 6. Results from evaluation with variant three

Ammonia, followed by methanol and hydrogen, are in the top positions in this case. This is mainly due to the assigned weighting coefficients of the criteria directly ort he to the fuels and their properties.

Conclusions

In modern shipbuilding, navigation, and ship repair, the use of alternative fuels will become increasingly prevalent. This necessitates an assessment of the behavior of the most commonly used types of alternative fuels. This is especially important during periods when vessels from the modern commercial fleet are docked for repairs. The article examines and analyzes the risks and behavior of various alternative fuels used in shipping from the perspective of ship repair. Criteria for evaluation are proposed, directly related to the qualities and characteristics of the fuels, as well as to the locations and systems for their storage.

Based on the proposed criteria and point-based assessments of the likelihood of failure, three evaluation approaches have been developed. In the first approach, emphasis is placed on the properties of flammability and toxicity. The second approach analyzes risk with a focus on the criteria of tank filling and its location within the ship's hull. In the third approach, importance is assigned to toxicity, tank arrangement, tank material, and the inspection of valves in the fuel loading and storage system.

The evaluation was carried out using the TOPSIS multi-criteria assessment method. The results obtained for the different approaches vary. In the first approach, methanol and ammonia were found to be the most hazardous, which is to some extent justified by its properties and characteristics, followed by hydrogen and liquefied natural gas. Liquefied petroleum gas posed the lowest risk of failure. According to the assessment in the second approach, methanol was the most hazardous, followed by ammonia and hydrogen. Once again, liquefied petroleum gas had the lowest risk. In the third evaluated approach, the results were similar to those in the second approach, with differences only in the numerical values. Overall, the most hazardous alternative fuels from the perspective of ship repair are ammonia and methanol, while liquefied petroleum gas is considered the safest. The criteria and evaluation approaches developed in this study can be used by ship repair companies when servicing vessels that operate on alternative fuels.

Scientific Ethics Declaration

* The authors declare that the scientific ethical and legal responsibility of this article published in EPSTEM journal belongs to the authors.

Conflict of Interest

* The authors declare that they have no conflicts of interest.

Funding

* This research received no specific grant from any funding agency in the public, commercial, or not-for-profit sectors.

Acknowledgements or Notes

* This article was presented as an oral presentation at the International Conference on Research in Engineering, Technology and Science (www.icrets.net) held in Peja/Kosovo on July 10-13, 2025.

References

Bilgili, L., & Celebi, U. B. (2018). Developing a new green ship approach for flue gas emission estimation of bulk carriers. *Measurement*, *120*, 121–127.

Brouzas, S., Zadeh, M., & Lagemann, B. (2025). Essentials of hydrogen storage and power systems for green shipping. *International Journal of Hydrogen Energy*, *100*, 1543–1560.

DNV. (2021). *Green shipping programme, Amonia as a marine fuel safety handbook*. Green Shipping Programme.

Duong, P., & Kang, H. (2025). Amonia as a fuel for marine dual- fuel technology: A comprehensive review. *Fuel Processing Technology*, *275.*

Fullonton, A., Lea-Langton, A., Madugu, F., & Larkin, A. (2025). Green ammonia adoption in shipping: Opportunities and challenges across the fuel supply chain. *Marine Policy*, *171.*

Kim, K., Kang, H., & Kim, Y. (2015). Risk assessment for natural gas hydrate carriers: A hazard identification (HAZID) study. *Energies*, 3142–3164.

Kolios, A. (2024). Retrofitting ort he gies for eco-friendly ship structures: A risk analysis perspective. *Journal of Marine Science and Engineering*, *12*(4).

Poop, L., & Müller, K. (2021). Technical reliability of shipboard ort he gies ort he application of alternative fuels. *Energy, Sustainability and Society*, *11*(23).

Popek, M. (2024). Alternative fuels- prospects for shipping industry. *International Journal on Maritime Navigation and Safety of Sea Transportation*, *18,* 25–33.

Shih, H., & Olson, D. (2022). *TOPSIS and its extensions: A distance – based MCDM approach*. New York, NY: Springer.

Author(s) Information

Yordan Denev
Technical University of Varna
Varna, Bulgaria
Contact e-mail: *y.denev@tu-varna.bg*

To cite this article:

Denev, Y. (2025). Multicriteria risk assessment in small and medium-sized ship repair enterprises during the repair of ships using alternative fuels. *The Eurasia Proceedings of Science, Technology, Engineering and Mathematics (EPSTEM), 35,* 240-247.

The Eurasia Proceedings of Science, Technology, Engineering & Mathematics (EPSTEM)
ISSN: 2602-3199

The Eurasia Proceedings of Science, Technology, Engineering and Mathematics (EPSTEM), 2025

Volume 35, Pages 248-256

ICRETS 2025: International Conference on Research in Engineering, Technology and Science

From Monomer to Therapeutic Nanocarrier: Design, Characterization, and Anticancer Evaluation of Poly (Alpha-Lipoic Acid) Nanoparticles

Al-Hussein Abo El-Naga
Egypt-Japan University of Science and Technology(E-Just)

Mahmoud E. Soliman
Egypt-Japan University of Science and Technology(E-Just)

Amr A. Nassrallah
Egypt-Japan University of Science and Technology(E-Just)

Abstract: Nanotechnology has revolutionized drug delivery by enhancing therapeutic agent targeting, controlled release, and pharmacokinetics. Poly(α-lipoic acid) (PαLA), a biodegradable and redox-responsive polymer derived from α-lipoic acid (αLA), presents a promising nanocarrier system due to its biocompatibility and structural versatility. In this study, PαLA was synthesized via thermal ring-opening polymerization and subsequently formulated into nanoparticles (PαLA-NPs) using a modified nanoprecipitation method. The polymer and nanoparticles were characterized using UV-Vis spectroscopy, FTIR, dynamic light scattering (DLS), and transmission electron microscopy (TEM). The nanoparticles exhibited a spherical morphology with an average size of 70.98 nm, a polydispersity index (PDI) of 0.192, and a zeta potential of -20.4 mV, indicating good colloidal stability. Cytotoxicity assessment via MTT assay revealed that PαLA-NPs induced concentration-dependent cytotoxicity in human colorectal adenocarcinoma (HCT-116) cells while maintaining high biocompatibility with normal fibroblasts (BJ-1). Notably, at 50 µg/mL, PαLA-NPs reduced HCT-116 viability to ~65% but preserved over 90% viability in BJ-1 cells, demonstrating selective anticancer potential. These findings suggest that PαLA-NPs are a promising nanocarrier system for targeted cancer therapy with minimal off-target toxicity.

Keywords: Biocompatibility, Cancer therapy, Cytotoxicity, Nanoparticles, Poly(α-lipoic acid)

Introduction

Nanotechnology has become a significant platform for advancing drug delivery systems, providing improved targeting capabilities, controlled release profiles, and enhanced pharmacokinetics for therapeutic agents improved targeting capabilities, controlled release profiles, and enhanced pharmacokinetics for therapeutic agents (Panyam & Labhasetwar, 2003). Biodegradable polymers, as a category of nanomaterials, have attracted significant interest owing to their adjustable chemical properties, biocompatibility, and ability to reduce systemic toxicity (Danhier et al., 2012).

α-Lipoic acid (αLA) is a naturally occurring compound characterized by a five-membered disulfide ring (Figure 1). It is particularly intriguing in this context due to its potent antioxidant properties and recognized therapeutic advantages in conditions such as diabetes, neurological disorders, and cancer (Damnjanovic, 2019; Rochette et al., 2013; Shay et al., 2009; Smith et al., 2004; Zhang & Frei, 2001).

Although αLA exhibits therapeutic potential, its clinical application is hindered by poor water solubility, instability in biological fluids, and limited bioavailability (Pal et al., 2025). Recent advancements in polymer chemistry have facilitated the transformation of αLA into poly(α-lipoic acid) (PαLA), a biocompatible and redox-responsive polymer that preserves the advantageous properties of the monomer while providing improved structural and functional versatility (Liu et al., 2020; Yang et al., 2018). The thermal ring-opening polymerization (ROP) of αLA is a simple, initiator-free approach that maintains its intrinsic bioactivity and offers an appropriate framework for nanoparticle formation (Kisanuki et al., 2010).

In this study, we report the synthesis of PαLA via thermal polymerization and its subsequent formulation into nanoparticles using a modified nanoprecipitation method. The synthesized polymer and prepared nanoparticles were characterized. Finally, the cytotoxic potential of PαLA-NPs was assessed in vitro using MTT assays on human colorectal adenocarcinoma (HCT-116) cells and normal fibroblasts (BJ-1) to evaluate their selectivity and biocompatibility. This investigation aims to establish PαLA-NPs as a promising nanocarrier system for safe and selective cancer therapy.

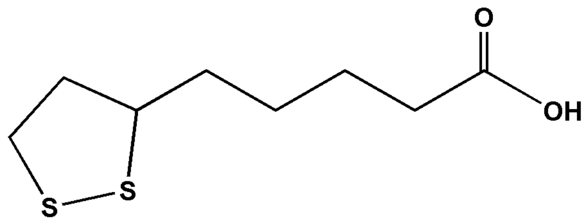

Figure 1. Chemical structure of αLA

Materials and Methods

Materials

αLA was generously gifted by EVA Pharma pharmaceutical company (Giza, Egypt). Acetone (HPLC grade, ≥99.9%) was obtained from SRL Chemicals, and acetonitrile (HPLC grade, ≥99.9%) was purchased from Fisher Chemical. Pluronic F-68 (Poloxamer 188) was purchased from BASF (Germany). MTT (3-[4,5-dimethylthiazol2yl]-2.5-diphenylterazolium bromide) was obtained from Sigma Aldrich company (St Louis, MO, USA). Fetal bovine serum (FBS), Dulbecco’s Modified Eagle Medium (DMEM)/high glucose, L-glutamine and penicillin/streptomycin were purchased from Gibco Inc. (NY, USA). Corning® 96-well clear flat-bottom polystyrene TC-treated Microplates, Corning® 75cm² U-Shaped canted neck cell culture flask with vent cap, Falcon® (15 and 50 ml) polystyrene centrifuge tubes and sterile individually-wrapped Stripette™ serological polystyrene pipettes were from Corning® USA. The human colorectal adenocarcinoma cells (HCT-116, CCL247™), and the noncancerous skin fibroblast (BJ-1, CRL-2522™) were brought from the American Type Culture Collection (ATCC, Manassas, VA, USA).

Synthesis of Poly (α-lipoic acid)

αLA was polymerized into PαLA by a thermal polymerization method with slight modification (Kisanuki et al., 2010). Briefly, 200 mg of αLA was added into a dry flask under vacuum and stirred at 85 °C for 3 hours. The resulting crude product was dissolved in acetone and gradually poured into an excess volume of acetonitrile to precipitate the polymer, which was subsequently washed three times with acetonitrile. The final polymer was freeze-dried, and the yield was quantified gravimetrically.

Characterization of Poly (α-lipoic acid)

Ultraviolet-Visible Spectrophotometric Analysis (UV-Vis)

αLA and synthesized PαLA were dissolved in tetrahydrofuran (THF), and the UV-Vis absorption spectra were measured by a NanoDrop™ 2000c spectrophotometer (Thermo Scientific, USA).

Fourier Transform Infrared Spectroscopic Analysis (FTIR)

The FTIR spectra of αLA and prepared PαLA were investigated using the KBr pellet technique on a Fourier transform infrared spectrophotometer (FTIR) (Shimadzu FTIR-8400 S, Japan) over a wavelength range of 400–4,000 cm-1.

Preparation of Poly (α-lipoic acid) Nanoparticles

PαLA-NPs were prepared by a nanoprecipitation method (Fessi et al., 1989), with modifications. Briefly, 10 mg of PαLA was dissolved in 1 ml of acetone. The organic phase was added dropwise into the aqueous phase containing 100 mg of Pluronic F-68 (Poloxamer 188) under moderate stirring at room temperature until the organic solvent was completely evaporated. The resulting nanoparticle suspension was filtered and stored at 4°C.

Characterization of Poly (α-lipoic acid) Nanoparticles

Particle size (PS) and Zeta Potential (ZP)

The average particle size (PS), polydispersity index (PDI), and zeta-potential (ZP) were measured using dynamic light scattering (DLS) with a Nano ZS (Malvern Instruments Ltd., Worcestershire, UK) after diluting the samples with deionized water at 25 °C.

Transmission Electron Microscopy (TEM)

The morphology and size of PαLA-NPs were studied using TEM (JEOL JEM-2100F, Japan) at 200 kV, utilizing Gatan digital micrograph software. Before analysis, a drop of nanoparticle dispersion was dropped onto a 200-mesh carbon-coated copper grid and dried at room temperature.

Cell Viability Assay

The cytotoxicity of PαLA-NPs and free αLA was evaluated using the MTT assay against human colorectal adenocarcinoma cells (HCT-116, ATCC® CCL-247™) and normal human fibroblasts (BJ-1, ATCC® CRL2522™). HCT-116 and BJ-1 cells were cultured in DMEM/high glucose supplemented with 2 mM L-glutamine, 10% FBS, and 1% penicillin/streptomycin, kept in a Corning® 75cm² U-Shaped canted neck cell culture flask with vent cap (Corning, New York, USA). Then, sub-confluent cultures (70–80%) were trypsinized (Trypsin 0.05%/0.53 mM EDTA) and split depending on the seeding ratio. Cells were seeded into 96-well microtiter plates (in triplicate) with 2x104 cells per well and incubated at 37°C under a humidified atmosphere of 5% CO2 for 24 hours. Following incubation, cells were treated with varying concentrations (0, 2.5, 5, 10, 25, and 50 µg/mL) of PαLA-NPs or free αLA and further incubated for 24 hours. After the treatment, the culture medium was replaced by medium containing 100 µL/well of MTT (0.5 mg/mL) in phosphate buffer saline (PBS) and incubated at 37°C for an additional 3 hours. The MTT solution was removed, and the purple formazan crystals formed at the bottom of the wells were dissolved using 100 µL isopropyl alcohol/well with shaking for 1 hour at room temperature. The absorbance was measured at 549 nm using a microplate reader (ELX 800; Bio-Tek Instruments, Winooski, VT, USA). Cell viability was calculated as a percentage relative to untreated control cells.

Results and Discussion

Synthesis of Poly (α-lipoic acid)

Thermal polymerization of αLA occurred efficiently above the melting point without any initiator. PαLA was synthesized via the ring-opening polymerization (ROP) of αLA monomer at 85 °C for 3 hours. The final product was a sticky solid with a mass of 90 mg and a yield of 45%. The characterization of the obtained product was performed to confirm the successful synthesis of PαLA.

Characterization of Poly (α-lipoic acid)

Ultraviolet-Visible Spectrophotometric Analysis (UV-Vis)

The polymerization of αLA into PαLA was successfully validated using UV-Vis spectroscopy. In the spectrum of the synthesized polymer (Figure 2), the characteristic absorption peak of dithiolane at 333 nm, which is indicative of the monomer αLA, is completely absent. This spectral change corresponds with the anticipated cleavage of the dithiolane ring, providing clear confirmation of complete ring-opening polymerization. The absence of residual monomeric signals provides additional evidence that the synthesis of a high-molecular-weight polymer was carried out successfully and with a high degree of purity.

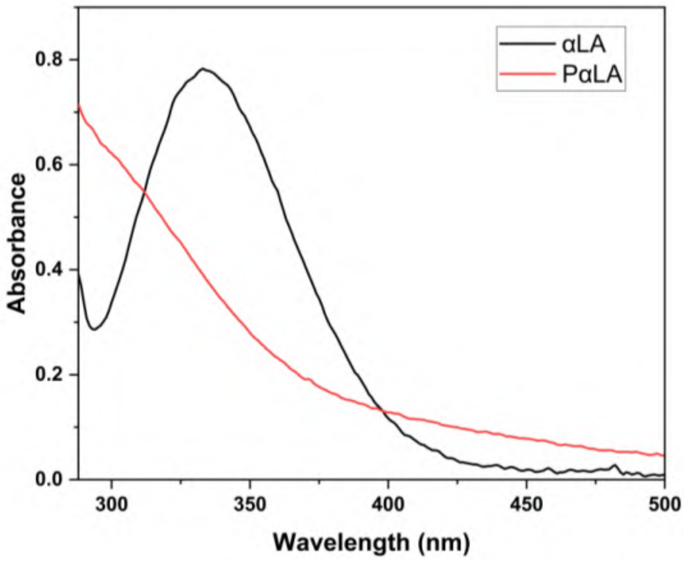

Figure 2. UV-Vis spectra of αLA and PαLA in THF

Fourier Transform Infrared Spectroscopic Analysis (FTIR)

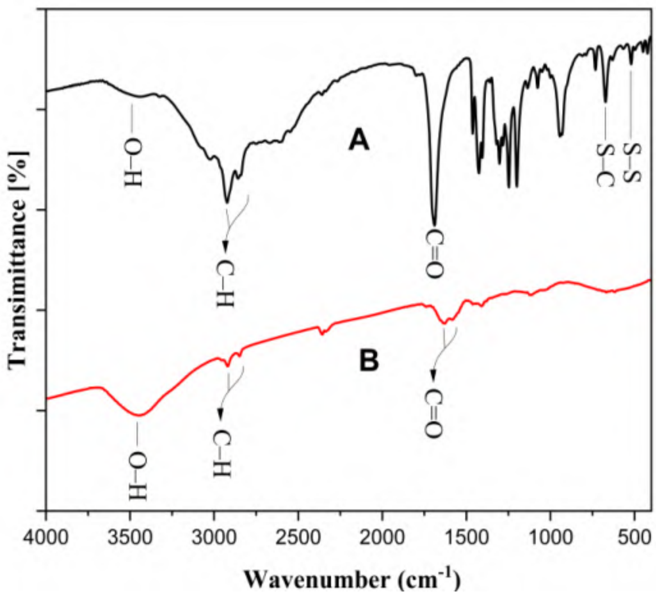

Figure 3. FTIR spectra of αLA (A) and PαLA (B)

FTIR spectroscopic analysis was performed to clarify the molecular transformation from the monomer (αLA) to the polymer (PαLA) (Figure 3). αLA spectra (Figure 3A) showed a broad absorption band at ~3470 cm^{-1} (O–H stretching), C–H stretching vibrations at ~2920 cm^{-1} and ~2850 cm^{-1}, and a prominent C=O stretching band about 1690 cm^{-1} (carboxylic group). Dithiolane ring structure was also indicated by fingerprint S–S and C–S stretching bands. These bands align with the recorded data (De Mello et al., 2025; Ikuta et al., 2014; Moyano et al., 2010; Rusu et al., 2022). In contrast, PαLA spectra (Figure 3B) exhibited a reduced S–S band intensity, with slight shifts in the O-H and C-H stretching bands. Furthermore, the carbonyl band (C=O) was downshifted to ~1635 cm^{-1}, reflecting changes in hydrogen bonding and the chemical environment after polymerization. These collective vibrational changes validate the successful structural transformation and polymerization of αLA into PαLA.

Preparation of Poly (α-lipoic acid) Nanoparticles

PαLA-NPs were effectively synthesized using a modified nanoprecipitation method. The gradual, dropwise addition of the polymer-acetone solution to an aqueous Pluronic F-68 solution led to the spontaneous formation of nanoparticles. The entire evaporation of the organic solvent, combined with the surfactant's stabilizing influence, yielded homogeneous and visually stable nanoparticles. This straightforward method facilitated efficient self-assembly of nanoparticles, rendering this approach appropriate for prospective biomedical applications. Additional characterizations of the synthesized nanoparticles were conducted to enhance understanding of their potential applications.

Characterization of Poly (α-lipoic acid) Nanoparticles

Particle Size (PS) and Zeta Potential (ZP)

DLS analysis (Figure 4) indicated the presence of monodisperse nanoparticles characterized by a narrow particle size distribution, exhibiting an average diameter of 70.98 nm and a polydispersity index (PDI) of 0.192, which demonstrates the high reproducibility of the nanoprecipitation technique. The low PDI reflects homogeneous particle formation, likely due to efficient solvent diffusion and stabilization by Pluronic F-68.

Figure 4. Size distribution of PαLA-NPs by intensity

The nanoparticles demonstrate a surface charge of -20.4 mV, as revealed by zeta potential measurements (Figure 5). The moderate negative charge improves the electrostatic stabilization of dispersion, suggesting advantageous colloidal stability under ambient conditions. The findings demonstrate the successful synthesis of precisely characterized, nanometric PαLA particles suitable for prospective biomedical applications.

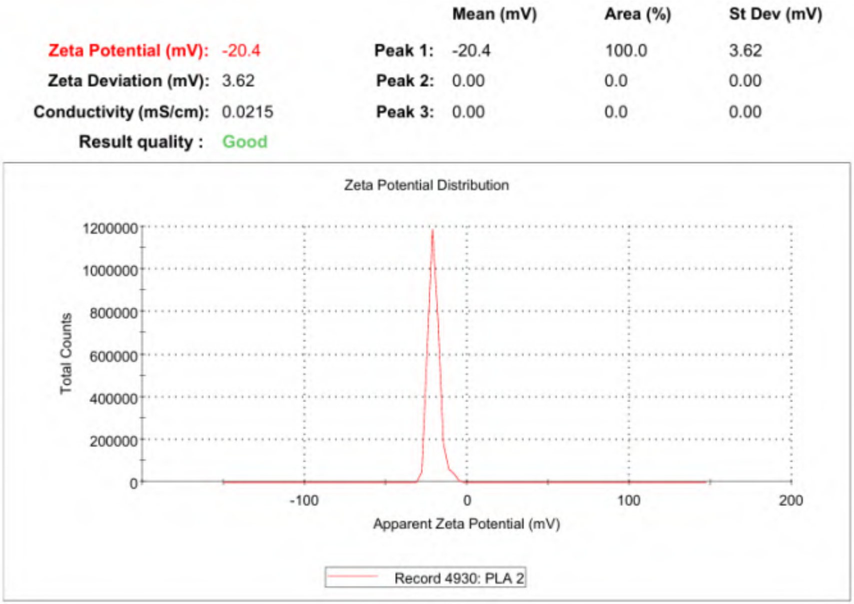

Figure 5. Zeta potential distribution of PαLA-NPs

Transmission Electron Microscopy (TEM)

TEM analysis (Figure 6) indicates that the prepared PαLA-NPs exhibit a spherical morphology characterized by distinct borders and a uniform size distribution. The nanoparticle sizes, which range from 70 to 100 nm, are consistent with the DLS data, indicating low aggregation and effective stabilization by Pluronic F-68. The homogeneous dispersion and smooth surface topology seen in TEM images further confirm the suitability of PαLA-NPs for biomedical applications, particularly in drug delivery.

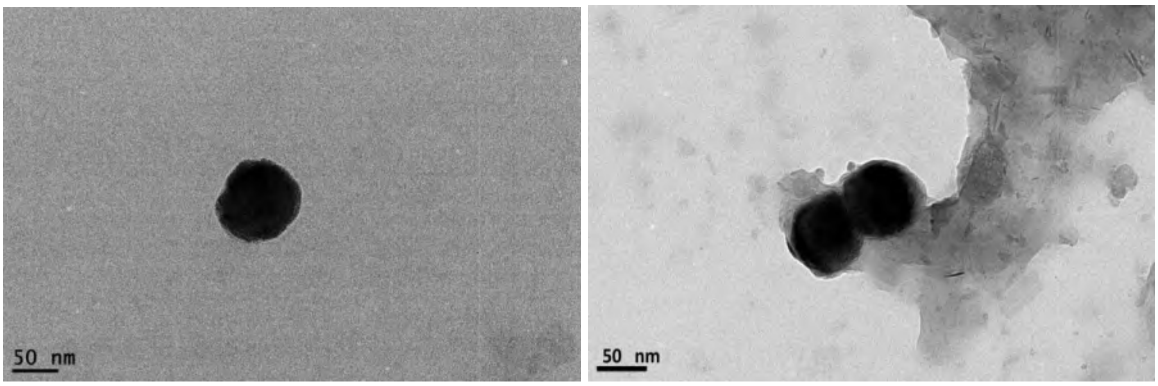

Figure 6. TEM images of PαLA-NPs

Cell Viability Assay

The Cytotoxicity of PαLA-NPs was obtained using MTT assays on human colorectal cancer (HCT-116) and normal fibroblast (BJ-1) cell lines at concentrations ranging from 0 to 50 µg/mL (Figure 7). In HCT-116 cells, as illustrated in Figure 7A, both PαLA-NPs and free αLA resulted in a concentration-dependent reduction in cell viability. At lower concentrations (2.5 µg/mL), minimal cytotoxicity was observed, with cell viability above 90% for both formulations. However, as the concentration increased, a more pronounced decrease in viability was recorded. At the highest dose (50 µg/mL), PαLA-NPs and free αLA reduced cell viability to approximately 65% and 62%, respectively, indicating a comparable but slightly stronger cytotoxic effect from the free form. This may be due to its unencapsulated form, which facilitates quicker cellular uptake and prompts immediate oxidative stress induction.

In contrast, BJ-1 normal fibroblasts (Figure 7B) exhibited over 90% viability for PαLA-NPs, which is significantly higher than the approximately 80% viability observed with free αLA at the same doses. This difference underscores the selective action of the nanoparticle system, potentially due to a more controlled release of αLA or reduced uptake by healthy cells. These findings suggest better biocompatibility of PαLA-NPs with non-cancerous cells and support their suitability as a drug delivery system with minimized off-target toxicity.

These results corroborate earlier studies (Ibrahim et al., 2022; Liu et al., 2019) demonstrating that nanoparticle encapsulation can influence drug release kinetics and enhance therapeutic indices through enhancing selectivity for tumor cells and preserving normal tissue. The selective cytotoxicity of PαLA-NPs, along with their favorable safety profile in normal cells, indicates their potential as a nanocarrier for cancer therapy.

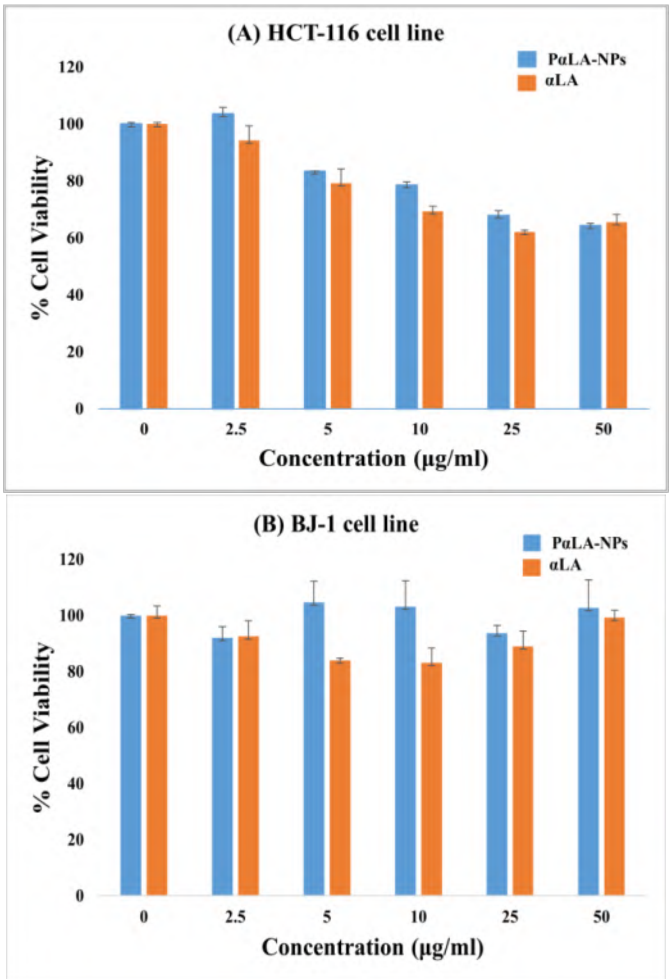

Figure 7. Cell viability of HCT-116 (A) and BJ-1 (B) cell lines after treatment with PαLA-NPs and αLA

Conclusion

This study demonstrates the successful synthesis of Poly(α-lipoic acid) through thermal polymerization and the subsequent creation of biocompatible nanoparticles utilizing a simple nanoprecipitation method. The PαLA-NPs produced were uniform in size, exhibited moderate charge, had a narrow size distribution, and exhibited excellent colloidal stability. Cytotoxicity studies indicated a concentration-dependent inhibitory effect on HCT116 cancer cells while exhibiting a significantly reduced impact on normal fibroblasts, thus demonstrating selective toxicity. These findings indicate that PαLA-NPs represent a promising nanocarrier platform for the targeted delivery of therapeutic agents in cancer treatment, necessitating further investigation into drug loading and in vivo studies.

Scientific Ethics Declaration

* The authors declares that the scientific ethical and legal responsibility of this article published in EPSTEM journal belongs to the authors.

Conflict of Interest

* The authors declare that they have no conflicts of interest

Funding

* This research received no specific grant from any funding agency in the public, commercial, or not-for-profit sectors.

Acknowledgements or Notes

* This article was presented as an oral presentation at the International Conference on Research in Engineering, Technology and Science (www.icrets.net) held in Peja/Kosovo on July 10-13, 2025.

References

Damnjanovic, I. (2019). Possible molecular mechanisms and pathways involved in bh3 mimetic activity of alpha-lipoic acid on human colon cancer cell line. *Farmacia*, *67*(2), 226–234.

Danhier, F., Ansorena, E., Silva, J. M., Coco, R., Le Breton, A., & Préat, V. (2012). PLGA-based nanoparticles: An overview of biomedical applications. *Journal of Controlled Release: Official Journal of the Controlled Release Society*, *161*(2), 505–522.

De Mello, L. R., Castelletto, V., Cavalcanti, L., Seitsonen, J., & Hamley, I. W. (2025). Self-assembly of a conjugate of lipoic acid with a collagen-stimulating pentapeptide showing cytocompatibility and wound healing properties, and chemical and photolytic disassembly. *Journal of Peptide Science*, *31*(3), e70002.

Fessi, H., Puisieux, F., Devissaguet, J. Ph., Ammoury, N., & Benita, S. (1989). Nanocapsule formation by interfacial polymer deposition following solvent displacement. *International Journal of Pharmaceutics*, *55*(1), 1-4.

Ibrahim, A., Khalil, I. A., & El-Sherbiny, I. M. (2022). Development and evaluation of core-shell nanocarrier system for enhancing the cytotoxicity of doxorubicin/metformin combination against breast cancer cell line. *Journal of Pharmaceutical Sciences*, *111*(9), 2581–2591.

Ikuta, N., Tanaka, A., Otsubo, A., Ogawa, N., Yamamoto, H., Mizukami, T., Arai, S., Okuno, M., Terao, K., & Matsugo, S. (2014). Spectroscopic studies of R(+)-α-lipoic acid—cyclodextrin complexes. *International Journal of Molecular Sciences*, *15*(11), 20469–20485.

Kisanuki, A., Kimpara, Y., Oikado, Y., Kado, N., Matsumoto, M., & Endo, K. (2010). Ring-opening polymerization of lipoic acid and characterization of the polymer. *Journal of Polymer Science Part A: Polymer Chemistry*, *48*(22), 5247–5253.

Liu, Z., Shen, N., Tang, Z., Zhang, D., Ma, L., Yang, C., & Chen, X. (2019). An eximious and affordable GSH stimulus-responsive poly(α-lipoic acid) nanocarrier bonding combretastatin A4 for tumor therapy. *Biomaterials Science*, *7*(7), 2803–2811.

Liu, Z., Tang, Z., Zhang, D., Wu, J., Si, X., Shen, N., & Chen, X. (2020). A novel GSH responsive poly(alpha-lipoic acid) nanocarrier bonding with the honokiol-DMXAA conjugate for combination therapy. *Science China Materials*, *63*(2), 307–315.

Moyano, M. A., Broussalis, A. M., & Segall, A. I. (2010). Thermal analysis of lipoic acid and evaluation of the compatibility with excipientes. *Journal of Thermal Analysis and Calorimetry*, *99*(2), 631–637.

Pal, S., Salzman, E. E., Ramirez, D., Chen, H., Perez, C. A., Dale, K., Ghosh, S. K., Lin, L., & Messersmith, P. B. (2025). Versatile solid-state medical superglue precursors of α-lipoic acid. *Journal of the American Chemical Society*, *147*(16), 13377–13384.

Panyam, J., & Labhasetwar, V. (2003). Biodegradable nanoparticles for drug and gene delivery to cells and tissue. *Advanced Drug Delivery Reviews*, *55*(3), 329–347.

Rochette, L., Ghibu, S., Richard, C., Zeller, M., Cottin, Y., & Vergely, C. (2013). Direct and indirect antioxidant properties of α-lipoic acid and therapeutic potential. *Molecular Nutrition & Food Research*, *57*(1), 114–125.

Rusu, E. A., Magyari, K., Baia, L., & Baia, M. (2022). Vibrational analysis of α-lipoic acid and its adsorption behavior study by SERS. *Journal of Molecular Structure*, *1248*, 131501.

Shay, K. P., Moreau, R. F., Smith, E. J., Smith, A. R., & Hagen, T. M. (2009). Alpha-lipoic acid as a dietary supplement: Molecular mechanisms and therapeutic potential. *Biochimica Et Biophysica Acta*, *1790*(10), 1149–1160.

Smith, A. R., Shenvi, S. V., Widlansky, M., Suh, J. H., & Hagen, T. M. (2004). Lipoic acid as a potential therapy for chronic diseases associated with oxidative stress. *Current Medicinal Chemistry*, *11*(9), 1135–1146.

Yang, H., Shen, W., Liu, W., Chen, L., Zhang, P., Xiao, C., & Chen, X. (2018). PEGylated poly(α-lipoic acid) loaded with doxorubicin as a pH and reduction dual responsive nanomedicine for breast cancer therapy. *Biomacromolecules*, *19*(11), 4492–4503.

Zhang, W. J., & Frei, B. (2001). Alpha-lipoic acid inhibits TNF-alpha-induced NF-kappaB activation and adhesion molecule expression in human aortic endothelial cells. *FASEB Journal: Official Publication of the Federation of American Societies for Experimental Biology*, *15*(13), 2423–2432.

Author(s) Information

Al-Hussein Abo El-Naga
Egypt-Japan University of Science and Technology (E-JUST), Biotechnology Program, Faculty of Basic and Applied Sciences, New Borg El-Arab City, Alexandria 21934, Egypt
Department of Zoology, Faculty of Science, Aswan University, Aswan 81528, Egypt
Contact e-mail: *alhussein.mekki@ejust.edu.eg*

Mahmoud E. Soliman
Egypt-Japan University of Science and Technology (E-JUST), PharmD Program, New Borg El-Arab City, Alexandria 21934, Egypt
Department of Pharmaceutics and Industrial Pharmacy, Faculty of Pharmacy, Ain Shams University, Cairo 11566, Egypt

Amr A. Nassrallah
Egypt-Japan University of Science and Technology (E-JUST), Biotechnology Program, Faculty of Basic and Applied Sciences, New Borg El-Arab City, Alexandria 21934, Egypt
Biochemistry Department, Cairo University Research Park, Cairo University, 12613 Giza, Egypt

To cite this article:

Abo El-Naga, A., Soliman, M. E., & Nassrallah, A. A. (2025). From monomer to therapeutic nanocarrier: Design, characterization, and anticancer evaluation of poly (alpha-lipoic acid) nanoparticles. *The Eurasia Proceedings of Science, Technology, Engineering and Mathematics (EPSTEM), 35,* 248-256.

The Eurasia Proceedings of Science, Technology, Engineering & Mathematics (EPSTEM)
ISSN: 2602-3199

The Eurasia Proceedings of Science, Technology, Engineering and Mathematics (EPSTEM), 2025

Volume 35, Pages 257-262

ICRETS 2025: International Conference on Research in Engineering, Technology and Science

Investigation of the Weldability of Copper-Magnesium Alloy Wire by Cold Pressure Welding After Wire Drawing

Volkan Akilli
Er-Bakır Electrolytic Copper Products Inc.

Orhan Akyuz
Er-Bakır Electrolytic Copper Products Inc.

Abstract: In the wire drawing industry, alloyed wires are widely used due to their superior mechanical properties, corrosion resistance, and wear resistance compared to pure copper wires. Although copper-magnesium alloys exhibit lower electrical conductivity than pure copper, they are frequently preferred in electrical and electronics, automotive, railway, and aerospace applications thanks to their excellent mechanical performance. These alloys also demonstrate good cold formability and drawability to fine diameters. In this study, the weldability of CuMg0.2 alloy copper wire, containing 0.12–0.20 wt.% magnesium and drawn cold with a deformation ratio of 99.99% to a diameter of 0.155 mm, was investigated using the cold pressure welding technique. The effects of process parameters in cold pressure welding on the mechanical and electrical properties of the CuMg0.2 wire were examined in detail. Experimental studies focused on the number of strokes and the waiting time between strokes. When comparing average measurements, the ultimate tensile strengths of welded and unwelded wires were found to be 738 MPa and 864 MPa, respectively. The elongations at break for welded and unwelded wires were measured as 1.4% and 2.7%, respectively. The electrical resistances were obtained as 1141.18 Ohm/km and 1123.40 Ohm/km, respectively. The results of this study indicate that the cold pressure welding technique is applicable to CuMg0.2 alloy copper wires that have undergone strain hardening during the wire drawing process. Considering both process efficiency and operator convenience, the optimum welding parameters were determined to be 15 strokes and a 2-second waiting time between strokes.

Keywords: Copper, Magnesium, Alloy, Cold pressure welding

Introduction

Among industrial metals, copper has the highest electrical conductivity. Due to its excellent thermal and electrical conductivity, good formability, and relatively high corrosion resistance, it is widely used in the conductor wire drawing industry. However, there are certain limitations regarding the weldability of fine-grained materials obtained through cold forming. In conventional welding techniques, localized increases in temperature can cause significant grain growth in the welding zone, which in turn leads to considerable changes in mechanical properties within the weld area. To eliminate these disadvantages, cold welding techniques have been employed in industry (Sato et al., 2003; Topic et al., 2009). Cold welding, also known as cold pressure welding or contact welding, is a solid-state process that joins two materials at room temperature by applying pressure. Scientifically, this method is referred to as solid-state diffusion bonding (Tylecote, 1968).

In this process, materials are joined under pressure at ambient temperatures. The advantages of this technique over conventional welding methods include the absence of secondary or tertiary phase formation, the elimination of thermal defects, and the prevention of material softening due to heat exposure. However, simply pressing two materials together is generally not sufficient for successful bonding, mainly due to the presence of oxide layers on their surfaces. Additionally, the materials to be joined must possess good plastic deformability,

- Selection and peer-review under responsibility of the Organizing Committee of the Conference

as permanent plastic deformation is essential for achieving a successful bond in cold welding (Kudo, Kikuchi, & Miyazaki, 1978). Prior to cold welding, a surface preparation step is necessary, where the oxide or barrier layer on the metal surface must be thoroughly cleaned (Zhang & Bay, 1992).

In CuMg0.2 production, wire breakage leads to a reduction in the amount of input wire, resulting in a shortfall in the quantity of the final product. In this study, cold pressure welding was applied to 7/0.155 mm CuMg0.2 wires, and their electrical and mechanical behavior was investigated. Two process parameters -number of strokes and waiting time between strokes- were evaluated. After determining the optimal welding parameters, the following results were obtained: the ultimate tensile strengths of welded and unwelded wires were 738 MPa and 864 MPa, respectively; elongations at break were 1.4% and 2.7%, respectively; electrical conductivity values were 47.06 and 47.44 m/(Ohm·mm²), and resistances were 1141.18 Ohm/km and 1123.40 Ohm/km, respectively.

Materials

In this study, high-purity copper cathode plates were used as the base material. The chemical composition of the copper sample obtained from these cathodes is presented in Table 1. As the alloying material, high-purity magnesium was used in the form of copper-coated magnesium powder wire on a spool. The ICP results of the produced magnesium alloyed copper wires are also presented in Table 2.

Table 1. Chemical analysis results of copper cathodes

Material	Cu	Ag	As	Fe	Ni	Pb	S	Sb	Se	Sn	Zn	Mn
Unit	%	ppm	ppm	ppm	ppm	ppm	ppm	ppm	ppm	ppm	ppm	ppm
Value	99.997	6.7	<0.3	0.3	<0.5	<0.3	2.6	<0.3	<0.3	<0.3	<0.3	<0.2

Table 2. ICP results of CuMg alloyed copper wires

Material	Cu	Ag	As	Fe	Ni	Pb	S	Sb	Se	Sn	Zn	Mn
Unit	%	ppm	ppm	ppm	ppm	ppm	ppm	ppm	ppm	ppm	ppm	ppm
Value	99.997	8.9	<0.4	0.8	0.6	<0.2	5.9	<0.5	<0.5	<0.2	0.2	<0.3

Method

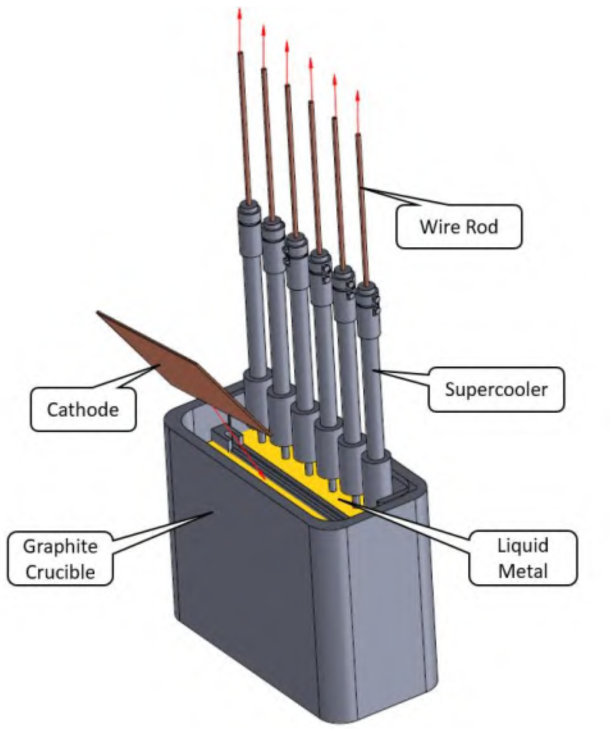

Figure 1. Schematic representation of up casting technique

The production of CuMg0.2 alloy copper rod was carried out using an RS-80 Up-Cast machine equipped with graphite crucible furnace technology. First, the crucible was heated to 1200 °C, and high-purity copper cathodes were added. In this technique, known as upward casting, water-cooled molds are immersed into the molten metal inside the graphite crucible, and the liquid metal is directed into the mold under metallostatic pressure. Through rapid solidification via water cooling, copper rods of the desired diameter are obtained. Figure 1 illustrates the schematic representation of the upward casting process.

The 20 mm CuMg0.2 rods obtained from casting were further processed using a continuous extrusion forming technique. In the continuous extrusion process, as the rod passes through the die, simultaneous extrusion deformation generates heat within the material, enabling warm/hot forming without external heating, thus producing an annealed-like microstructure. The schematic representation of the continuous extrusion process is shown in Figure 2.

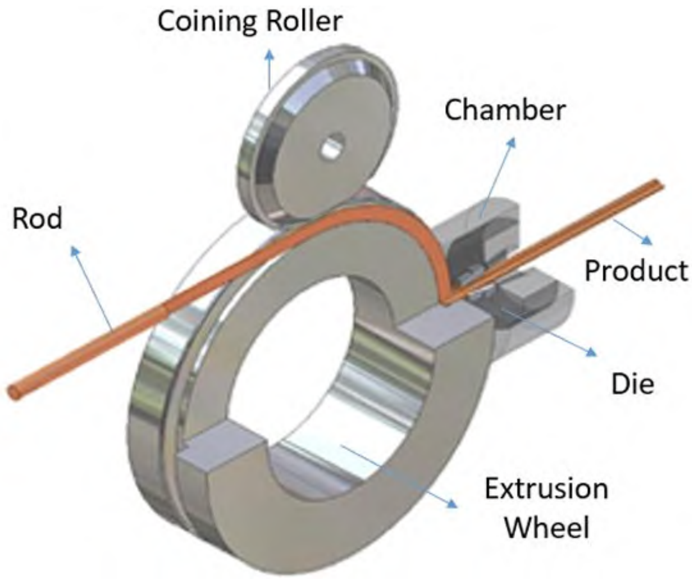

Figure 2. Schematic representation of the continuous extrusion process

The CuMg0.2 alloy rods were initially drawn without annealing using a draw-peeling machine and cold wire drawing technique. Subsequently, they were further cold drawn to a final 7/0.155 mm diameter—first through a single-wire drawing machine and then through a multi-wire drawing machine. The total applied deformation reached 99.99%. The formula used to calculate the deformation rate is given in Equation 1:

Figure 3. Cold welding machine

$$\varepsilon = [(Di^2 - Df^2) / Di^2] \times 100 \qquad (1)$$

Where:

- ε = Percentage Deformation
- **Df** = Final Diameter
- **Di** = Initial Diameter

For the welding of the 0.155 mm diameter wires, a cold pressure welding machine (Figure 3) was used. The wire ends were aligned face-to-face, and welding trials were conducted with stroke counts of 10, 15, 20, 25, 30, and 35, and with inter-stroke waiting times of 1 and 2 seconds.

Findings

The CuMg0.2 copper-magnesium alloy wires were produced using the upward casting method, subsequently processed by conform extrusion, and drawn to a final diameter of 7/0.155 mm with a total deformation of 99.99%. The mechanical and electrical properties of these wires are presented in Table 3.

Table 3. Mechanical and electrical properties of CuMg0.2 alloy wire with 0.155 mm diameter

Measurement	Resistance (Ohm/Km)	Diameter (mm)	Conductivity (m/(Ohm.mm²))	Elongation at Break (%)	Strength at Break (MPa)
1	1118,8	0,155	47,68	2,5	859
2	1109,5	0,155	47,77	3,3	884
3	1168,2	0,154	46,26	2,5	841
4	1092,0	0,156	47,91	2,1	855
5	1128,5	0,154	47,57	2,9	880
Average	1123,4	0,155	47,44	2,7	864

Welding Trials

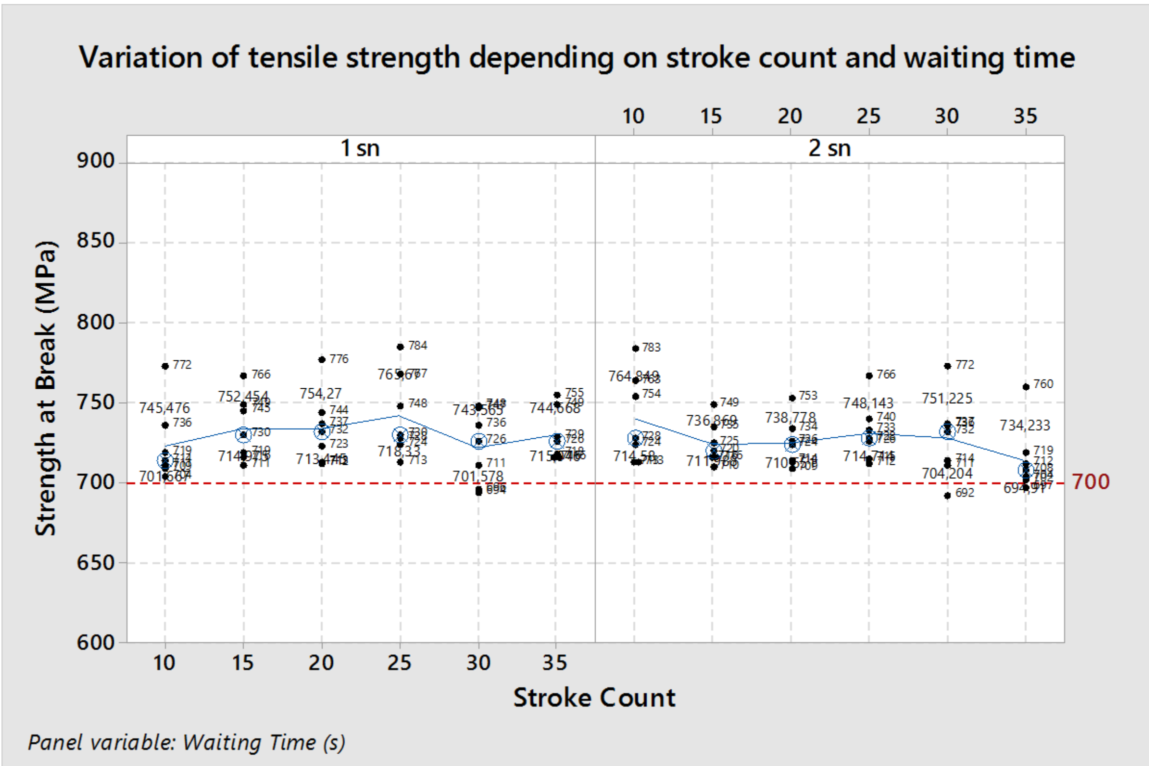

Figure 4. Variation of tensile strength depending on stroke count and waiting time

Welding experiments were initiated with 10 strokes and incremented by 5 strokes up to 35 strokes. Each of these experiments was conducted with two different inter-stroke waiting times. In the first set of experiments, the waiting time between strokes was set to 1 second, and in the second set, it was set to 2 seconds. The results of these experiments are shown in Figure 4. Upon examining the tensile-tested specimens, it was observed that fractures occurred outside the welded zone. Images of the fracture ends of the samples are shown in Figure 5.

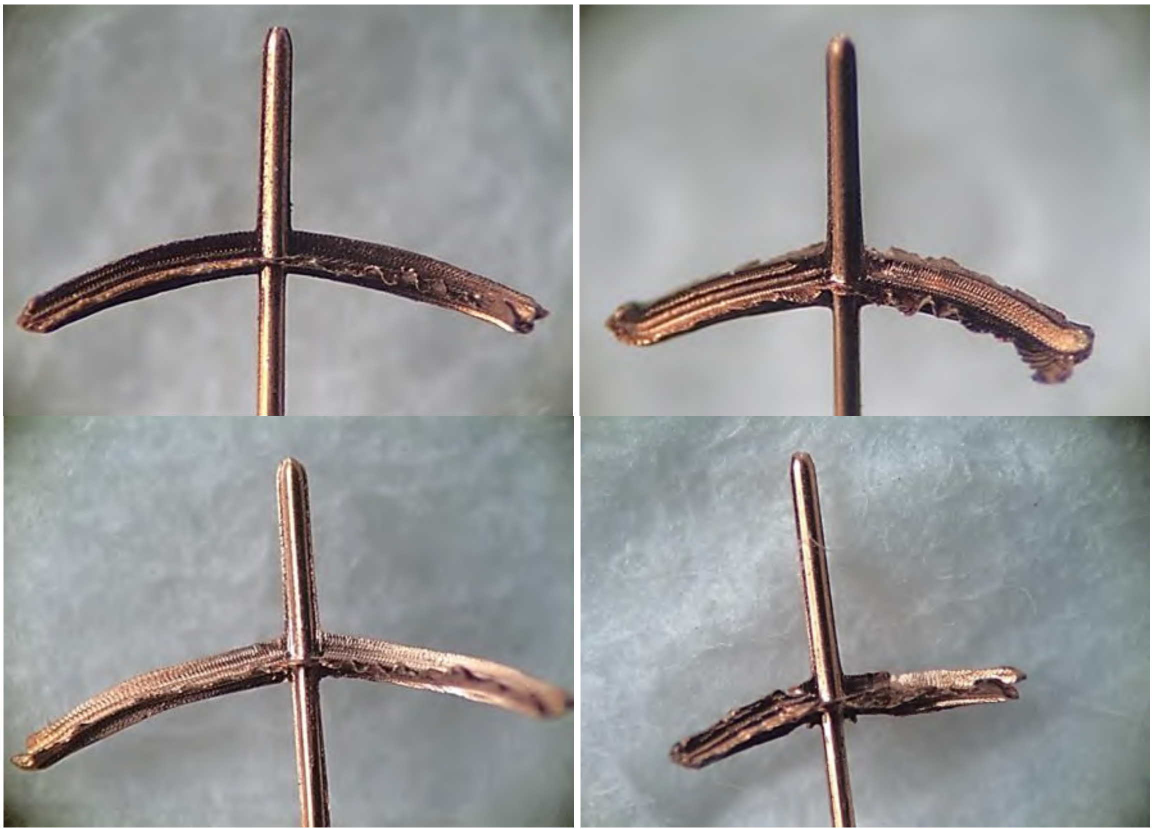

Figure 5. Fracture regions of tensile test samples

Mechanical and electrical properties of the welded wires were analyzed specifically for those welded with 15 strokes and a 2-second waiting time. The results are presented in Table 4.

Table 4. Mechanical and electrical properties of welded CuMg0.2 alloy wires with 0.155 mm diameter

Measurement	Resistance (Ohm/Km)	Diameter (mm)	Conductivity (m/(Ohm.mm²))	Elongation at Break (%)	Strength at Break (MPa)
1	1118,6	0,155	47,68	1,5	726
2	1140,1	0,154	47,40	1,3	736
3	1167,7	0,154	46,28	1,4	749
4	1168,1	0,154	46,26	1,2	748
5	1111,4	0,155	47,68	1,5	729
Average	1141,2	0,154	47,06	1,4	738

Results and Discussion

As a result of the welding trials conducted on CuMg0.2 alloy wires with a diameter of 0.155 mm:

- Considering the results obtained from Figure 1 and the ease of application for the operator, 15 strokes with a 2-second waiting time were determined to be the optimal welding condition.
- A comparison of the mechanical and electrical properties of welded and unwelded wires showed that the welded wires exhibited decreased tensile strength, elongation at break, and conductivity, while electrical resistance increased.
- Tensile test results indicated that fracture occurred outside the welded region, confirming the integrity of the weld.

- It was observed that the welding preparation process—including wire cutting angle, surface cleaning, and precise end-to-end alignment—can significantly influence welding performance.
- It was concluded that cold pressure welding is applicable to CuMg0.2 alloy wires with a diameter of 0.155 mm.

Scientific Ethics Declaration

* The authors declares that the scientific ethical and legal responsibility of this article published in EPSTEM journal belongs to the authors.

* This study has been conducted in accordance with the principles of scientific research and publication ethics. No unethical behavior such as plagiarism, fabrication, falsification, or duplicate publication has occurred during the preparation and execution of the study.

Conflict of Interest

* The authors declare that there is no conflict of interest regarding the publication of this paper.

Funding

* This research received no specific grant from any funding agency in the public, commercial, or not-for-profit sectors.

Acknowledgements or Notes

* This article was presented as an oral presentation at the International Conference on Research in Engineering, Technology and Science (www.icrets.net) held in Peja/Kosovo on July 10-13, 2025.

References

Kudo, H., Kikuchi, Y., & Miyazaki, K. (1978). Study of cold pressure welding by divergent extrusio. *CIRP, 27*(1), 165-170.

Sato, Y. S., Urata, M., Kokawa, H., & Ikeda, K. (2003). Hall–Petch relationship in friction stir welds of equal channel angular-pressed aluminium alloys. *Materials Science and Engineering: A, 354*(1–2), 298–305.

Topic, I., Hoppel, H. W., & Goken, M. (2009). Friction stir welding of accumulative roll-bonded commercial-purity aluminium AA1050 and aluminium alloy AA6016. *Materials Science and Engineering: A, 503*(1–2), 163–166.

Tylecote, R. F. (1968). *The solid phase welding of metals*. Edward Arnold Publishers Ltd.

Zhang, W., Bay, N., & Wanheim, T. (1992). Influence of hydrostatic pressure in cold-pressure welding. *CIRP Annals, 41*(1), 293–297.

Author(s) Information

Volkan Akilli	**Orhan Akyuz**
Er-Bakır Electrolytic Copper Products Inc.,	Er-Bakır Electrolytic Copper Products Inc.,
Denizli / Türkiye	Denizli / Türkiye
Contact e-mail: *vakilli@erbakir.com.tr*	

To cite this article:

Akilli, V., & Akyuz, O. (2025). Investigation of the weldability of copper-magnesium alloy wire by cold pressure welding after wire drawing. *The Eurasia Proceedings of Science, Technology, Engineering and Mathematics (EPSTEM), 35*, 257-262.

The Eurasia Proceedings of Science, Technology, Engineering & Mathematics (EPSTEM)
ISSN: 2602-3199

The Eurasia Proceedings of Science, Technology, Engineering and Mathematics (EPSTEM), 2025

Volume 35, Pages 263-270

ICRETS 2025: International Conference on Research in Engineering, Technology and Science

Assessing Market Preferences for a Health-Focused Ergonomic Lamp

Jose Marie Carrillo
Technological Institute of the Philippines

Carlos Nathaniel F. Dee
Technological Institute of the Philippines

John Lester B. Dela Paz
Technological Institute of the Philippines

Sarah Mae L. Galit
Technological Institute of the Philippines

Danica Angel S. Maquilan
Technological Institute of the Philippines

Jaypy T. Tenerife
Technological Institute of the Philippines

Abstract: The study explores the market viability of an ergonomic lamp within two rapidly urbanizing cities in the Philippines, Quezon City and Marikina City, which was evaluated based on the responses of 129 respondents. The study employed a mixed-methodology approach, which included the use of quantitative data from the seven-point Likert scale and qualitative data interpreted from the open-ended responses. Descriptive and multivariate analyses revealed consumer preferences and the relationship that could exist between different product characteristics and socio-demographic factors. The findings reflected a correlation between the adaptive lighting, automation, and health features that the users expect to find in the product. Aesthetic appeal and eye care functions were indicated as the primary drivers behind purchasing this product, with preference for these increasing with age. Market segmentation and targeting for marketing campaigns can be delineated for different groups of consumers based on lifestyle, age, and work setup. These results reflect a growing awareness among consumers of lighting ergonomics in hybrid and digital work environments. With lighting quality assuming ever greater importance for productivity and comfort, user-driven design will be paramount in shaping the successful innovations in product development. This study makes its contribution to marketing and consumer behavior by identifying all the psychological and functional attributes influencing purchasing decisions. Furthermore, it offers practical guidelines for matching product attributes with user requirements, improving brand positioning, and developing strategies for health-oriented, productivity-driven urban consumers. These findings provide valuable inputs to businesses entering emerging markets with user-centric innovations and targeted marketing within the Philippine market.

Keywords: Ergonomic lamp, Innovative technologies, Market analysis

Introduction

A study in 2025 by Kaur et al. and Agarwal et al. mentions that prolonged digital exposure can cause Digital Eye Strain (DES), leading to symptoms like headaches, dry eyes, and fatigue. This study promotes ocular health and explores the Pomodoro technique to enhance focus and reduce distractions (Santiago and Gurat, 2023). A mixed-method approach was used to assess user needs and market demand (Hassan, 2024), with data analyzed through descriptive statistics (Dong, 2023). The study is grounded in technology entrepreneurship and aligns innovation with market viability (Munoz, 2025; Belmonte et al., 2022), offering innovative, health-focused solutions that support productivity and well-being.

Figure 1. Product design

Figure 1 illustrates the design of FocusMoona, an ergonomic lamp developed to address eye strain and enhance user productivity.

Method

The study used a mixed research design combining qualitative and quantitative methods (Stoecker and Avila, 2025). The quantitative approach assigned numerical values through specific questions, while the qualitative method explored new perspectives and theories. Data were analyzed using descriptive statistics (Taherdoost, 2022), and qualitative data were examined through thematic analysis to identify supporting patterns and themes (Yardley, 2025). Multivariate analysis assessed relationships among variables (Branch, 2024), and correlation analysis explored connections between two or more variables (Xiang et al., 2021). The Kaiser-Meyer-Olkin (KMO) test confirmed data suitability for factor analysis, with a value above 0.7 as satisfactory (Shrestha, 2021); the study exceeded this threshold. Cronbach's Alpha, used to assess reliability, showed scores above 0.60, indicating acceptable reliability (Yee et al., 2021).

Participants

The study surveyed 129 respondents through convenience sampling in Marikina and Quezon City, selected for accessibility and demographic diversity (Golzar et al., 2022; Gray and Ocampo, 2017). Respondents were 50.4% female, 48.8% male, with a few undisclosed; the average age was 26. Most were single (64.3%), followed by those in a relationship (18.6%) and married (17.1%). Education levels included Bachelor's (59.7%), high school (28.7%), technical/vocational (6.2%), undergraduate (3.2%), Master's (1.6%), and Doctorate (0.8%). Employment included students (61.3%), employed (30.2%), self-employed (7%), and unemployed (1.6%). For work setup, 45.7% answered 'others,' 18.6% worked on-site, 13.2% had hybrid setups, and 11.6% worked from home. Income data showed 52.7% undisclosed, 20.9% earned below PHP 15,000, and only 1.6% earned above PHP 70,000.

Measures

Cognitive ergonomics was evaluated using a 7-point Likert scale covering cognitive performance, visual comfort, adaptability, emotional impact, and design functionality. The lamp was designed to enhance focus, reduce fatigue, and support productivity through Pomodoro timing and automated lighting adjustments. Customizable brightness and color temperature helped maintain a conducive environment, while the aesthetic design promoted calmness. Innovative features, like automation and the Pomodoro timer, support ergonomic sustainability. Respondents rated the lamp's effectiveness in addressing lighting discomfort, promoting eye health, and improving lighting habits. Data were analyzed using descriptive statistics (Peck and Olsen, 2025), with an online survey adapted from (Bluman, 2023) and structured based on the target market (Graham, 2023).

Table 1. Exploratory factor analysis (N=129)

Constructs	**Statements**	**Factor Loadings**
Multi-Functionality and Aesthetics (M-FA)	A moon phase lighting system would create a calming and soothing atmosphere in my space.	0.843
	I would like my lighting to mimic the moon's phases, changing its appearance throughout the day.	0.817
	I recommend purchasing a moon phase light as a decorative item for my home or office.	0.743
	Aesthetics are an essential factor when choosing lighting and home decor.	0.658
	A timer function is proper for automatically turning off lighting after a specific period.	0.605
	Adjustable brightness and color temperature help me stay focused and energized during work or study sessions.	0.575
Lighting Knowledge (LK)	I am aware of the appropriate intensity of light when doing tasks.	0.825
	I am aware of the effect of different wavelengths of light on the eyes	0.798
	I know the function of ambient lighting and task lighting.	0.731
	I know the importance of proper lighting when doing tasks.	0.731
	I know the appropriate placement and height of the lamp in the workplace	0.452
Eye-Care Purchase Behavior (EPB)	I am willing to allocate a portion of my monthly income to products that help reduce eye strain and improve productivity.	0.744
	I prefer checking social media advertisements as a good way to discover eye strain products.	0.635
	I am influenced by promotions from brands I see advertised on social media or by expert recommendations.	0.634
	I set a spending limit when purchasing ergonomic or eye strain-related products.	0.585
	Durability and long-term benefits are more important than price when purchasing ergonomic or eye-care products.	0.534
	I will spend more than usual on high-quality eye care or productivity-enhancing products.	0.532
	I am near-sighted.	0.488
Smart Tech Preference (STP)	I prioritize spending on other health-related items (e.g., vitamins, medical eye checkups) over eye-care products.	0.704
	I would like my lighting to turn on or off automatically using a motion sensor.	0.609
	I get sleepy while doing tasks for long periods.	0.535
	I often research and compare different brands before making a purchase related to eye strain and productivity products.	0.493
Adaptive Lighting Preference (ALP)	I find it helpful when lighting changes color temperature to match the time of day (e.g., warm light in the evening, cool light during the day).	0.652
	I prefer lighting that automatically adjusts brightness based on the ambient light in the room.	0.609
	I use the night light function of my devices.	0.595
	I frequently purchase low-cost alternatives instead of premium eye strain solutions.	0.562
Habit Building (HB)	I have a hard time setting healthy habits to protect my eye health.	0.799
	I get sleepy while doing tasks for extended periods.	0.620
	The lighting I have during tasks is either too much or too little.	0.547
	My eyes feel strained after working for long periods.	0.507

Data Collection Process

An online survey was administered via digital platforms (Andrade, 2020). Market needs were assessed using a mixed-method approach, combining qualitative and quantitative methods based on study objectives (Taherdoost, 2022). Convenience sampling was employed to reach accessible participants (Simkus, 2023). The questionnaire had five sections: Section 1 covered demographics, Sections 2–4 used Likert scales to examine behavior, experience, and spending habits (George, 2024), and Section 5 featured a narrative question for detailed qualitative responses (Taherdoost, 2022).

Data Analysis

Data were analyzed using IBM SPSS, a widely used tool in social science research (Rahman and Muktadir, 2021). The Kaiser-Meyer-Olkin (KMO) measure for sampling adequacy scored 0.796, indicating suitability for factor analysis (Astuti et al., 2024). An exploratory factor analysis using a rotated component matrix revealed no problematic variables. The acceptable loading coefficient was compressed to 0.47 (see Table 1).

To assess the reliability of the six identified factors (see Table 2), Cronbach's Alpha-a standard measure of internal consistency—was applied (Izah et al., 2024). Multi-Functionality (Factor 1) and Lighting Knowledge (Factor 2) showed high reliability, with scores of 0.864 and 0.829. Eye Care (Factor 3) scored 0.752, indicating relatively high reliability. Smart Tech Preference (Factor 4) scored 0.687, suggesting slightly lower consistency. Adaptive Lighting (Factor 5) and Habit Building (Factor 6) scored 0.628 and 0.631, both classified as moderately reliable (Izah et al., 2024).

Table 2. Descriptive statistics of the construct (N=129)

Constructs	Rank	Cronbach's Alpha	*Mean	Sd. Deviation
M-FA	1	.864	5.6408	1.08182
LK	2	.829	5.3907	1.20620
HB	3	.752	5.3372	0.96706
EPB	4	.687	5.1240	1.04405
ALP	5	.631	4.6860	1.17729
STP	6	.628	5.0271	1.13547

*Note: 1.00 - lowest; 7.00 - highest

Quantitative Analysis

Pearson correlation analysis (see Figure 2) revealed strong positive relationships between Multi-Functionality and Aesthetics with Smart Tech Preference (r = 0.572), and Smart Tech Preference with Eye Care Purchase Behavior (r = 0.542), indicating that visual appeal and wellness features influence consumer decisions more than utility alone (Shi et al., 2021). Lighting Knowledge and Habit Building were also correlated (r = 0.572), suggesting that knowledge must be paired with engaging design to sustain habits (Taylor et al., 2024). Multi-Functionality and Aesthetics further correlated with Lighting Knowledge (r = 0.429), and Eyecare Purchasing Behavior (r = .478).

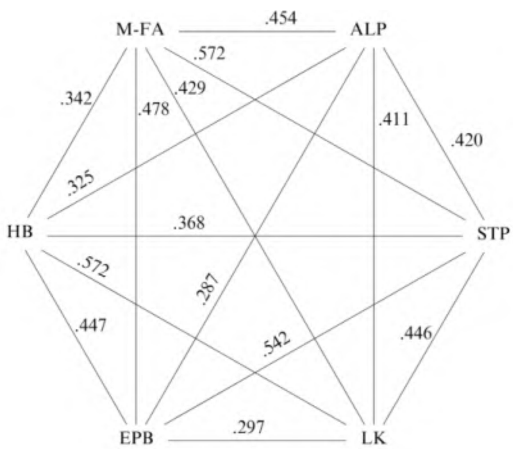

Figure 2. Product features path analysis

Purchase Behavior (r = 0.478), Adaptive Lighting Preference (r = 0.454), and Habit Building (r = 0.342), underscoring the value of adaptable, user-centered design (Lin and Chang, 2021). Lighting Knowledge correlated with Eye Care Purchase Behavior (r = 0.297), Smart Tech Preference (r = 0.446), and Adaptive Lighting Preference (r = 0.411), showing that information aids decision-making but has limited health impact (Shi et al., 2021; Lin and Chang, 2021). Eye Care Purchase Behavior correlated with Adaptive Lighting Preference (r = 0.287) and Habit Building (r = 0.447), highlighting the role of wellness features in sustained use (Lin et al., 2024), (Shao, 2025). Smart Tech Preference also correlated with Adaptive Lighting Preference (r = 0.420) and Habit Building (r = 0.368), reflecting the appeal of personalization (Zhao and Halabi, 2023), (Markannen, 2013). Lastly, Adaptive Lighting Preference and Habit Building were linked (r = 0.325), affirming adaptability's role in habit formation (Markannen, 2013).

Qualitative Analysis

Figure 3 illustrates the thematic analysis. For the first question, five sub-themes emerged on lighting challenges and productivity, which were grouped into two major themes: physical comfort and eye health, and productivity and mental well-being, both shaped by lighting conditions. For the second question, five sub-themes emerged: adjustability and customization, comfort and eye care, ease of use and convenience, innovative features, and aesthetic design. These formed two major themes: user comfort and functionality, and design innovation.

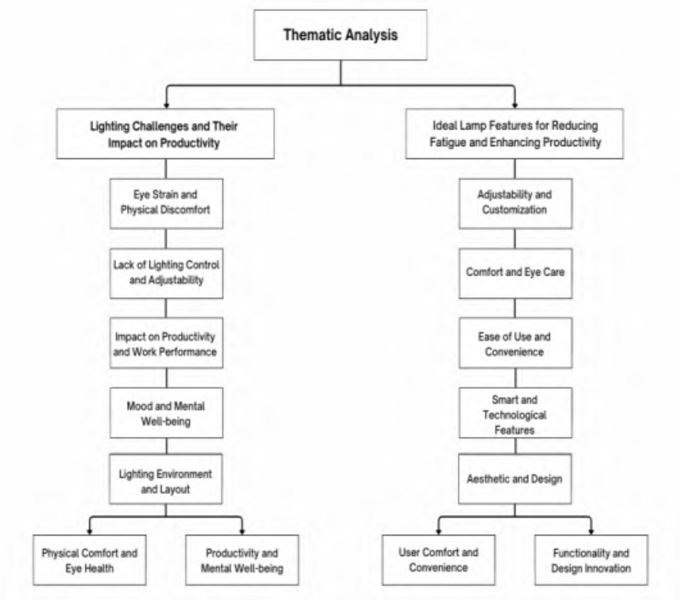

Figure 3. Thematic analysis

Results and Discussion

Findings from the data analyses were summarized, highlighting each construct's key characteristics and connection with other factors. The descriptive statistics of the constructs (see Table 2) highlighted key features and perceptions that the market perceived to use as a basis for product design and development. The thematic analysis (see Figure 3) provided new insights and feature characteristics that were based on the experiences of the market that could not be assessed by the quantitative analysis. The results are then further supplemented and strengthened by the narrative responses from the survey, adding weight and depth to the findings.

Findings showed that multifunctionality and aesthetics are foundational elements and can enhance other product features. The thematic analysis emphasized the constructs' role in functionality and design innovation. As one respondent shared, “My ideal lamp features an adjustable brightness and a flexible design. This helps by reducing eye strain and improving the productivity focus” (Gupta, 2017). Lighting awareness improved user experience but was most effective when combined with other features (Taylor et al., 2024). Appreciation for this feature increased with age, particularly among experienced users. This emerged as a core feature, strongly associated with quality-enhancing attributes. It was especially valued by older, married male users from Marikina. Thematic insights emphasized eye health and comfort: “My eyes more often than not start to hurt after long exposure to the screen. This prevents me from working proficiently, as I can no longer focus" (Lin et al., 2019). Integrating other features positively influenced Smart Tech Preference, encouraging health-conscious purchases. This trend was notable among older, married users in Marikina. Adaptive lighting correlated strongly with other features, enhancing convenience and comfort. Older users from Marikina particularly favored this. One respondent noted, "Smart features like automatic brightness adjustment or blue-light reduction would further enhance comfort, allowing me to work longer without fatigue and maintain high productivity levels" (Zhao and Halabi, 2023). The product should promote habit-building features to support sustained use and long-term health benefits. Additionally, the thematic analysis identified a seventh emerging feature—productivity support—driven by user demand for tools that improve focus and well-being. One respondent remarked, "I sometimes struggle with poor lighting... It can cause eye strain and make it harder to focus, which limits my productivity..." (Lin et al., 2019).

Conclusion

The researchers conclude that FocusMoona is a marketable product that addresses the needs of communities regarding eyestrain and productivity, with a particular focus on Marikina City. Using the results from the mixed methods analysis from the survey as inputs into the technological development of the product will improve the success rate of the product's marketing, emphasizing the product's multi-functionality and aesthetics, Eye Care Purchase Behavior, Lighting Knowledge, and proper habit building.

Recommendations

This study focused on eye health and productivity using an ergonomic lamp with IoT integration and a Pomodoro timer. Future work may explore broader ergonomic areas. In developing nations, limited progress in occupational, cognitive, and organizational ergonomics continues to affect performance (Koirala and Maharjan, 2023). Ergonomics plays a vital role in engagement and task efficiency (Koirala and Maharjan, 2023). Researchers are encouraged to examine IoT's potential in improving safety and well-being (McQuillen, 2024) and to explore other productivity frameworks like the Eisenhower Matrix, which aids in distinguishing urgent from important tasks (Kennedy and Porter, 2022).

Declaration of AI Usage

The authors also declare that artificial intelligence (AI) was used only to enhance readability and language and that no generative AI was used to develop ideas. The authors used Grammarly's AI to assist with grammatical adjustments. The authors still reviewed and edited these adjustments to ensure accuracy.

Scientific Ethics Declaration

* The authors declares that the scientific ethical and legal responsibility of this article published in EPSTEM journal belongs to the authors.

Conflict of Interest

* The authors declare no conflict of interest. Ethical standards were upheld throughout the study. Participants were informed of the study's purpose, provided informed consent, assured confidentiality, and received compensation.

Funding

* All funding of the project came from the personal funds of the researchers conducting the study.

Acknowledgements or Notes

* This article was presented as an oral presentation at the International Conference on Research in Engineering, Technology and Science (www.icrets.net) held in Peja/Kosovo, on July 10-13, 2025.

* The researchers express their gratitude to their adviser, Jaypy Tenerife, for his consistent support and guidance, and to all survey participants for their time and valuable contributions to the study.

References

Agarwal, R., Tripathi, A., Khan, I. A., & Agarwal, M. (2022). Effect of increased screen time on eyes during COVID-19 pandemic. *Journal of Family Medicine and Primary Care*, *11*(7), 3642–3647.

Andrade, C. (2020). The limitation of online surveys. *Indian Journal of Psychological Medicine*, *42*(6), 575-576.

Astuti, N. D., Hajaroh, M., Prihatni, Y., Setiawan, A., Setiawati, F. A., & Retnawati, H. (2024). Comparison of KMO results, eigen value, reliability, and standard error of measurement: Original & rescaling through summated rating scaling. *JP3I (Jurnal Pengukuran Psikologi dan Pendidikan Indonesia), 13*(2), 200-218.

Belmonte, Z.J. A., Cruz, C.S. C., De Castro, P.A. P., Estoesta, L., Mitra, E.J., & Lira, P.E.V. R. (2022). Factors influencing technopreneurial intention among undergraduate engineering students in the Philippines. *Journal of Engineering Education Transformations, 36*(1),148-157

Bluman, A. G. (2023). *Elemental statistics: a step-by-step approach*. McGraw Hill.

Branch, E. (March 23, 2024). *Multivariate analysis: an in-depth exploration in academic research*. Retrieved from https://tinyurl.com/yakcdter

Dong, Y. (2023). Descriptive statistics and its applications. *Highlights in Science, Engineering and Technology*, *47*(2023), 16-23.

George, E. (January 31, 2024). *What is a Likert scale? Definition, types, and examples*. Researcher Life. Retrieved from https://tinyurl.com/3aj2ycf6

Golzar, J., Noor, S., and Tajik, O. (2022). Convenience Sampling. *International Journal of Education & Language Studies*, *1*(2), 72-77.

Graham, N. (2023). *Project management for dummies-UK*. John Wiley & Sons

Gray, S. and Ocampo, M. A. (2017). Resilient edges: exploring a socio-ecological urban design approach in Metro Manila. *The Plan Journal 2* (2), 519-561.

Gupta, H., Noshin, L., & Sultana, N. (2017). Multipurpose table lamp: a functional improvement of a table lamp. *International Journal of Mechanical Engineering and Automation*, *4*, 138-148.

Hassan, M. (2024). Mixed-methods research - types & analysis. *Research Methods*. Retrieved from https://researchmethod.net/mixed-methods-research/

Izah, S. C., Sylva, L., & Hait, M. (2023). Cronbach's alpha: A cornerstone in ensuring reliability and validity in environmental health assessment. *ES Energy & Environment, 23*, 1057.

Kaur, K., Gurnani, B., Nayak, S., Deori, N., Kaur, S., Jethani, J., Singh, D., Agarkar, S., Hussaindeen, J. R., Sukhija, J., & Mishra, D. (2022). Digital eye strain - a comprehensive review. *Ophthalmol Ther, 11*, 1655–1680.

Kennedy, D. R., & Porter, A. L. (2022). The illusion of urgency. *American Journal of Pharmaceutical Education, 86*(7), 8914.

Koirala, R., & Maharjan, K. (2022). Cognitive ergonomics on employee wellbeing: a literature review. *The Journal of Economic Concerns, 13*(1), 93-106.

Lin, J., Hedekvist, P. O., Mylly, N., Bollen, M., Shen, J., Xiong, J., & Silfvenius, C. (2024). Human-centric and integrative lighting asset management in public libraries: qualitative insights and challenges from a Swedish field study. *IEEE Access, 12*, 40905-40921.

Lin, K. H., Su, C. C., Chen, Y. Y., & Chu, P. C. (2019). The effects of lighting problems on eye symptoms among cleanroom microscope workers. *International Journal of Environmental Research and Public Health, 16*(1), 101.

Lin, Y.-C., & Chang, C.-C. A. (2021). Influencing consumer responses to highly aesthetic products: The role of mindsets. *Journal of Retailing, 97*(3), 459–476.

Markkanen, P. (2013). *Intelligent and adaptive lighting in a retail environment* (master's thesis). University of Oulu Department of Architecture.

McQuillen, B. (August 20, 2024). *The impact of the internet of things (iot) on workplace safety and productivity*. IGNITE. Retrieved from https://tinyurl.com/33wufcx6

Munoz, J. M., & Terzidis, O. (Eds.). (2025). *Technology entrepreneurship in theory and practice: Perspectives in science and engineering.* Taylor & Francis.

Peck, R., and Olsen, C. (2025). *Introduction to statistics and data analysis*. Brooks & Cole.

Rahman, A., & Muktadir, M. G. (2021). SPSS: An imperative quantitative data analysis tool for social science research. *International Journal of Research and Innovation in Social Science, 5*(10), 300-302.

Santiago, C., & Gurat, M. (2023). The effect of the Pomodoro technique on student mastery of the concept of Mendelian genetics during synchronous remote learning. *International Research Journal of Management, IT and Social Sciences*, *10*(4), 233-243.

Shao, R. (2025). A study of healthy lighting for learning performance and visual fatigue in school-aged children with reading and writing tasks. *Light Engineering, 33*(1).

Shi, A. Q., Huo, F., & Hou, G. (2021). Effects of design aesthetics on the perceived value of a product. *Frontiers in Psychology, 12*, 670800.

Shrestha, N. (2021). Factor analysis as a tool for survey analysis. *American journal of Applied Mathematics and statistics*, *9*(1), 4-11.

Simkus, J. (July 31, 2023). *Convenience sampling: definition, method, and examples.* Simply Psychology. Retrieved from https://tinyurl.com/4v2n8e8y

Stoecker, R. and Avila, E. (2020). From mixed methods to strategic research design. *International Journal of Social Research Methodology*, *24*(6), 627-640.

Taherdoost, H. (2022). What are the different research approaches? Comprehensive review of qualitative, quantitative, and mixed methods research, their application, types, and limitations. *Journal of Management Science & Engineering Research*, *5*(1), 53-63.

Taylor, J. F., Beatty, S. E., & Roberto, K. J. (2024). Encouraging prolonged consumption through habit-boosting efforts: Conceptualization and research agenda. *Journal of Services Marketing, 38*(1), 28–42.

Xiang, M., Li, Y., Yang, J., Lei, K., Li, Y., Li, F., Zheng, D., Fang, X., & Cao, Y. (2021). Heavy metal contamination risk assessment and correlation analysis of heavy metal contents in soil and crops. *Environmental Pollution*, *278*, 116911.

Yardley, E. (2025). *Braun and Clarke's thematic analysis - how to do the six-step process for your qualitative research project*. Retrieved from: https://tinyurl.com/mpjskhua

Yee, K. W., Kee, P., and Radzi, N. M. M. (2022). Validity and reliability in psychological well-being, job satisfaction, and student-teacher relationship among preschool teachers. *Academy of Strategic Management Journal*, *21*, 1-5.

Zhao, H., & Halabi, K. N. M. (2023). A study on the relationship of smart light design characteristics with consumer behavior. *International Journal of Academic Research in Business and Social Sciences, 13*(12).

Author(s) Information

Jose Marie Carrillo
Technological Institute of the Philippines
938 Aurora Boulevard, Cubao, Quezon City, 1109, Philippines
Contact e-mail: *qjm-carrillo@tip.edu.ph*

Carlos Nathaniel F. Dee
Technological Institute of the Philippines
938 Aurora Boulevard, Cubao, Quezon City, 1109, Philippines

John Lester B. Dela Paz
Technological Institute of the Philippines
938 Aurora Boulevard, Cubao, Quezon City, 1109, Philippines

Sarah Mae L. Galit
Technological Institute of the Philippines
938 Aurora Boulevard, Cubao, Quezon City, 1109, Philippines

Danica Angel S. Maquilan
Technological Institute of the Philippines
938 Aurora Boulevard, Cubao, Quezon City, 1109, Philippines

Jaypy T. Tenerife
Technological Institute of the Philippines
938 Aurora Boulevard, Cubao, Quezon City, 1109, Philippines

To cite this article:

Carrillo, J. M., Dee, C.N.F., Dela Paz, J.L.B.., Galit, S.M.L., Maquilan, D.A.S., & Tenerife, J.T. (2025). Assessing market preferences for a health-focused ergonomic lamp. *The Eurasia Proceedings of Science, Technology, Engineering and Mathematics (EPSTEM), 35,* 263-270.

The Eurasia Proceedings of Science, Technology, Engineering & Mathematics (EPSTEM)
ISSN: 2602-3199

The Eurasia Proceedings of Science, Technology, Engineering and Mathematics (EPSTEM), 2025

Volume 35, Pages 271-283

ICRETS 2025: International Conference on Research in Engineering, Technology and Science

A Multi-Objective Optimization Model for Green Supply Chain Network Design Using Metaheuristic Algorithms

Farzad Zaare Tajabadi
Near East University

Abstract: Today, green supply chain managers in leading companies are trying to benefit from green logistics and improve their environmental performance throughout the supply chain as a strategic tool to gain sustainable competitive advantage by creating environmental desirability and satisfaction throughout the supply chain. The green supply chain has emerged as a new approach for companies to achieve profit and target market share by reducing risk and environmental impacts. Supplier selection is a complex decision-making problem in which a variety of evaluation criteria have different degrees of importance according to the supply chain strategy. In recent years, the relationship between supplier and consumer has received serious attention in manufacturing companies. When there is a long-term relationship between the two, the company's supply chain will be a serious and strong obstacle to competitors. Considering that a major part of the materials and components of products are supplied from external suppliers, paying attention to environmental criteria in the supply process is important. In this study, an integrated approach to distribution networks is presented to simultaneously address the location and allocation issues in the green supply chain. In this approach, decisions related to facility location, allocation, and customer demand satisfaction are made in a way that minimizes pollution. In this regard, a new mathematical model of multi-facility location-allocation is presented by considering several types of transportation to minimize the total environmental pollution, costs related to facility location and transportation costs and maximize the population coverage of demand. Also, non-dominated sorting genetic algorithms and non-dominated ranking genetic algorithms are used to solve the proposed model, and finally, the results of solving the model through each algorithm are compared with each other, and the necessary analyses are presented.

Keywords: Genetic algorithm, Green supply chain, Location-allocation, Supply chain

Introduction

In recent decades, environmental sustainability has become a key concern for supply chain managers worldwide (Srivastava, 2007). Organizations are under increasing pressure from governments, customers, and society to reduce the environmental impacts of their operations, particularly in logistics and distribution activities (Zhu & Sarkis, 2006). As a result, green supply chain management (GSCM) has emerged as a strategic approach to align economic objectives with environmental responsibility (Diabat & Govindan, 2011). Green logistics, as a core component of GSCM, seeks to improve environmental performance throughout the supply chain network while supporting the company's long-term competitiveness (Rodrigue et al., 2001).

One of the critical challenges in designing an effective green supply chain lies in optimizing the distribution network. Decisions regarding facility location, allocation of demand, and selection of transportation modes must be made in a way that balances cost efficiency with pollution reduction (Farahani et al., 2015). Supplier selection and the design of location-allocation networks are inherently complex multi-criteria decision-making problems, where various environmental, economic, and operational factors interact (Govindan et al., 2015). While prior studies have addressed facility location and transportation optimization individually, fewer efforts have integrated these decisions into a unified framework that explicitly minimizes environmental pollution across multiple transportation modes (Abdolazimi & Ghezavati, 2021).

In this study, after having a review of previous research and defining the gap, the study introducing a multi-objective mathematical model on the one hand to reduce environmental pollution and total cost, and on the other hand, increasing the customer coverage cat the same time by the specific constraint in demand satisfaction, facility capacity, and transportation limits. Then, with the help of two metaheuristic methods, NSAG-II and NRGA, we solve the proposed model and then compare the results. At the end, by applying the Pareto number of solutions (NOS) criteria on the mentioned algorithms and comparing the results, we will realize which of them has the better performance evaluation based on NOS criteria for the introduced mathematical model.

Literature Review

Background of Supply Chain

Supply chain management (SCM) is managing the flow of goods and services from the start point of the process till the final product reaches the customer. The mentioned chain includes with supplier, manufacturer, retailer, distributors, and end customers. Supply chain can be a complex network, and it needs an appropriate design to be able to work properly. To face this complexity, (Balinski, 1965) focused on the efficiency of the coordination of different parts in the supply chain and introduced an integer mathematical model for optimizing the facility location problems. Then, (Church & ReVelle, 1974; Church & Roberts, 1984) developed a mathematical model for service coverage. (Ball & Lin, 1993) Based on proposed models, they enhanced the efficiency in service reliability. (Melo et al., 2009) investigated the management of the capacity of facilities, which is fundamental to having a robust, cost-effective distribution network. By advancing the technology and increasing demand and market growth, speed in the supply chain and resiliency which is vital for customer satisfaction and stakeholders.

Background of Green Supply Chain

Green Supply Chain Management (GSCM) refers to a traditional supply chain with includes the environmental principles in the whole process from start to end. (Srivastava, 2007; Sarkis, 2006) emphasized the importance of evaluating the emissions, waste, and sustainability of the supply chain. In this regard (Min & Kim, 2012) and (Sarkis et al., 2011) introduced green practices like green purchase, green design, green manufacturing, green distribution, green packaging, green marketing, and reverse logistics. Recent research has presented comprehensive multi-objective mixed-integer programming models that aim to concurrently reduce both costs and emissions utilizing techniques like NSGA-II (Tavana et al., 2022; Rezaei & Kheirkhah, 2021; Barbosa-Póvoa et al., 2019). A comprehensive review (Al-Harkan et al., 2023) of 95 studies in sustainable supply chain logistics identified persistent gaps, particularly in integrating social sustainability and multi-modal transport decisions into optimization frameworks. The benchmark method has been applied using DEA standard models for enhancing efficiency in green supply chain management to pinpoint potentially efficient DMUs, with a slight modification aimed at changing these potentially efficient DMUs into efficient DMUs. Furthermore, the impact of different green principles on the efficiency values of DMUs is analyzed using Tobit regression both before and after this adjustment (Zaare Tajabdi & Daneshvar, 2023).

Background of Fixed-Cost Facility Location Model

The fixed-cost facility location problem is a cornerstone of operations research, balancing capital investment and operational efficiency. Initial models by (Balinski, 1965) set the stage for using mixed-integer formulations, Bender's decomposition further advanced network design strategies (Geoffrion & Graves, 1974). (Perl & Daskin, 1984) Integrated routing aspects, coupling location with vehicle assignment, while (Ghezavati et al., 2009) extended the problem to include service coverage considerations. These models form the basis for modern supply chain systems that must strategically balance infrastructure costs against transport and operational expenses in an environmentally conscious context.

Background of the Partial-Coverage Problem

The partial-coverage problem addresses facility placement under spatial-service constraints, where not all demand points need full coverage. (Church & ReVelle's., 1974) The maximal covering location model and its generalizations (Church & Roberts, 1984) are frequently applied in emergency service planning and logistics. (Karasakal & Karasakal, 2004) incorporated capacity constraints within partial coverage, demonstrating how allocating limited resources to maximize area served can shape efficient location strategies, especially when balancing coverage, cost, and environmental footprints in green logistics.

Background of the Sustainable Facility Location Problem

Sustainable facility location considers environmental, social, and economic criteria, beyond mere infrastructure placement. Studies like (Amiri, 2006) and (Sarkis, 2006) have proposed models combining environmental indicators with cost. (Ghezavati et al., 2009) proposed heuristic methods considering service levels and emissions. A recent study by (Li & Wang, 2025) embedded CO_2 emissions explicitly within location-allocation decisions, highlighting the need for frameworks that support resilience, carbon reduction, and stakeholder acceptability in high-impact sectors.

Background of Methods for Solving Multi-Objective Supply Chain Network Designs

By using multi-objective mathematical models in complex supply chain network design, we try to apply a balance between different objectives, like environmental factors, transportation, demand satisfaction, facility capacity, etc. In this case, some methods, such as the ε-constraint and weighted-sum techniques, often prove inefficient for complex supply chain problems due to their high computational requirements (Tavana et al., 2022). In this regard, metaheuristic algorithms have gained widespread popularity for use. Metaheuristic techniques like NRGA, NSGA-II, multi-objective particle swarm optimization (PSO), and hybrid models such as the equivalent circuit-controlled optimization (ECCO) have shown strong performance in solving multi-objective supply chain network design problems have been introduced over time by (Altiparmak et al., 2006; Cheng et al., 2022; Barbosa-Póvoa et al., 2019). An inductive study by (Kadziński et al., 2017) specified the trade-offs between convergence speed and solution diversity across different algorithms. (Tajabadi & Kazemi, 2016) developed an integer model for the green supply chain and solved it with two metaheuristic algorithms, such as NRGA and NSGA-II, and compared the results upon some performance evaluation criteria.

Background of Multi-Objective Evolutionary Algorithms

Multi-objective evolutionary algorithms have become vital for solving a complex supply chain network. The NSGA-II and the Strength Pareto Evolutionary Algorithm 2 (SPEA2) have been proposed by (Deb, 2001; Srinivas & Deb, 1994). (Zitzler & Thiele, 2001) effectively produce a diverse set of Pareto-optimal fronts while ensuring high-quality convergence. More recent variants, such as surrogate-assisted NSGA-II, have been implemented to expedite evaluations in environments where computation is costly (Stander et al., 2022). Moreover, some studies combined a graph-based surrogate model to increase optimality and hold the Pareto quality analysis while remarkably reducing the run times.

Method

Designing a sustainable supply chain network requires making decisions wisely and logically about the facilities, demand distribution, and the type of transportation to increase demand coverage, reduce both environmental effects and costs. In this research, a multi-faceted location-allocation issue is considered that reflects the essential compromises between economic objectives and environmental considerations. The model considers multiple facility types, customer demand zones, and transportation modes, each associated with specific pollution and cost factors.

Solving multi-objective optimization problems like the proposed green supply chain design model is challenging due to the conflicting objectives and the combinatorial nature of facility location and allocation decisions. Traditional exact optimization methods often become impractical for large-scale problems because of high computational complexity. To address this, metaheuristic algorithms offer efficient and flexible approaches for finding high-quality solutions within a reasonable computational time.

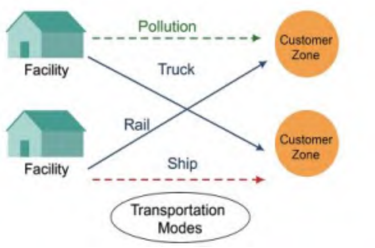

Figure 1. Illustrating the supply chain network and the model's key elements

The primary objectives of the model are:

- To minimize the total environmental pollution caused by transportation activities and facility operations,
- To minimize the combined costs of facility establishment and transportation,
- And to maximize the demand coverage, ensuring that as many customers as possible are served efficiently.

Notations

Sets and Indices

I: Set of potential facility locations, indexed by i.
J: Set of customer demand zones, indexed by j.
K: Set of transportation modes (e.g., truck, rail, ship), indexed by k.

Parameters

F_i: Fixed cost of establishing a facility at location i.

C_{ijk}: Transportation cost from facility i to demand zone j using mode k.

P_{ijk}: Environmental pollution emission (per unit transported) from i to j via mode k.

D_j: Demand quantity in demand zone j.

Cap_i: Capacity of facility i.

$MaxTrans_{ijk}$: Maximum transportation limit from i to j for mode k.

Decision Variables

x_{ijk}: Amount of product transported from facility i to demand zone j using transportation mode k.

y_i: Binary variable (1 if facility i is opened, 0 otherwise).

z_{ij} : Binary variable (1 if demand zone j is assigned to facility i, 0 otherwise).

Objective Functions

The problem is formulated as a multi-objective optimization with the following goals:

Minimize Environmental Pollution

$$minZ_1 = \sum_{i \in I} \sum_{j \in J} \sum_{k \in K} P_{ijk} \cdot x_{ijk}$$

where P_{ijk} represents the pollution emission rate for transportation from facility *i* to demand zone *j* using mode *k*.

Minimize Total Cost

$$minZ_2 = \sum_{i \in I} F_i . y_i + \sum_{i \in I} \sum_{j \in J} \sum_{k \in K} C_{ijk} . x_{ijk}$$

where F_i is the fixed cost of opening facility *i*, and C_{ijk} is the transportation cost.

Maximize Demand Coverage

$$MaxZ_3 = \sum_{j \in J} D_j . \sum_{i \in I} z_{ij}$$

where D_j is the demand of zone *j*.

Constraints

Demand Satisfaction

Ensure each demand zone's demand is satisfied:

$$\sum_{i \in I} \sum_{k \in K} x_{ijk} \geq D_j, \quad \forall_j \in J$$

Facility Capacity

Ensure that no facility exceeds its capacity:

$$\sum_{j \in J} \sum_{k \in K} x_{ijk} \leq Cap_i . y_i, \quad \forall_i \in I$$

Logical Link between Assignment and Flow

Only allow transportation if the demand zone is assigned to the facility:

$$\sum_{k \in K} x_{ijk} \leq M . z_{ij}, \quad \forall_i \in I, \forall_j \in J$$

(*M* is a large number for constraint relaxation.)

Transportation Mode Limits

Respect the transportation capacity for each mode:

$$x_{ijk} \leq MaxTrans_{ijk}, \quad \forall_i \in I, \forall_j \in J, \forall_k \in K$$

Binary and Non-negative Variables:

$$y_i \in \{0,1\}, \quad z_{ij} \in \{0,1\}, \quad x_{ijk} \geq 0$$

This approach leads to a mixed-integer linear programming problem with multiple objectives, in which certain variables are binary (decisions regarding facility openings) while others are continuous (quantities of transportation). Given the complexity of the problem, achieving exact optimization is often impractical for larger instances, prompting the adoption of metaheuristic algorithms to efficiently find solutions.

Non-dominated Sorting Genetic Algorithm (NSGA-II)

The Non-Dominated Sorting Genetic Algorithm (NSGA) was first presented by (Srinivas & Deb, 1994) and was later improved as NSGA-II by (Deb et al., 2000). NSGA-II is recognized as one of the most commonly utilized evolutionary algorithms for addressing multi-objective optimization challenges. The Non-Dominated Sorting Genetic Algorithm II (NSGA-II) is one of the most widely used evolutionary algorithms for solving multi-objective optimization problems. In this regard, NSGA-II develops a population of potential solutions toward the Pareto front, a set of optimal trade-off solutions where improving one objective would compromise another. Solutions based on their dominance level would be ranked by applying a non-dominating sorting process. The first Pareto front includes the best non-dominated solutions.

To ensure a diverse array of solutions, NSGA-II employs a crowding distance metric, promoting a well-dispersed set of trade-off alternatives. Its evolutionary approach incorporates standard genetic techniques like selection, crossover, and mutation, which facilitate effective exploration of the solution space. By integrating non-dominated sorting with the preservation of diversity, NSGA-II strikes a balance between converging on the optimal front and maintaining a wide variety of solutions, which makes it particularly effective for complex multi-objective challenges.

Non-dominated Ranking Genetic Algorithm (NRGA)

An alternative algorithm to solve the multi-objective optimization problems has been proposed by (Al Jaddan et al., 2005), justifying the process by which solutions are ranked and selected. By contrast, NSGA-II, which relies heavily on crowding distance to maintain diversity, the NRGA algorithm pursues a dominance-based ranking system combined with a tailored roulette wheel selection method. This strategy enhances both the convergence rate and the diversity of solutions across the Pareto front.

The NRGA algorithm distinguishes itself by assigning fitness based on a solution's non-dominance rank, allowing for a more structured and efficient exploration of the solution space. While it shares the goal of maintaining a diverse set of high-quality solutions with NSGA-II, its emphasis on rank-based selection often leads to improved performance in terms of speed and solution quality, particularly in complex or highly constrained problem settings. This makes NRGA a compelling alternative for tackling challenging multi-objective supply chain design problems.

Application to the Green Supply Chain Model

The metaheuristic algorithms NRGA and NSGA-II can both solve the complex multi-objective location and allocation problems with handling multiple objectives besides discrete decision variables. Because both are population-based search methods, it will enable the wide exploration of the solutions, and this will reduce the risk of being trapped in local optima. The performance of the mentioned algorithms can be evaluated by applying a comparative analysis, like Pareto fronts, as one of the performance evaluation criteria, between metaheuristic algorithms.

Results and Discussion

In this part, the proposed multi-objective model for green supply chain network design will be solved with NRGA and NSGA-II algorithms, and the performance evaluation between the mentioned algorithms will be investigated with the help of the Pareto number of solutions (NOS) criterion. Moreover, a 95% confidence interval will be applied to determine which of the algorithms has the better performance in diversity and stability of Pareto solutions.

Taguchi Experimental Design

In the late 1940s, Dr. Taguchi introduced innovative statistical principles that have since become essential tools in quality control and enhancement. Following this, numerous Japanese manufacturers have adopted this approach to elevate both product and process quality. The notable improvement in automobile quality produced in this country is closely linked to the extensive application of this approach. Unlike traditional and widely used quality engineering methods, the Taguchi method presents a distinct methodology. Taguchi's approach focuses on the importance of quality design during the stages of product and process development, whereas conventional methods rely on inspection and quality control during or after production. While Taguchi has utilized widely recognized statistical tools in his quality enhancement techniques, he has streamlined these processes by pinpointing a collection of effective solutions for designing experiments and interpreting results. The Taguchi method has proven to be quite successful in enhancing product quality in Japan. Recently, countries in the West have also adopted Taguchi's methodology as a straightforward and efficient means of improving product and process quality in their industries. Taguchi’s experimental design method has diverse applications across a variety of sectors. However, this approach is typically utilized for quality control in an "off-line" context. Dr. Taguchi categorized off-line quality control into three phases: system design, parameter design, and tolerance design. The primary focus of this review is "parameter design."

Steps to Perform Parameter Adjustment

In the first stage, appropriate experiments must be designed. For this purpose, first, controllable factors, uncontrollable factors, and performance measurement criteria are determined. Then, the levels related to each specific factor and appropriate orthogonal arrays are selected. Next, the designed experiments are performed, and the results obtained are analyzed. The signal-to-noise ratio is used to analyze the results. Analysis of variance is used to determine the most effective factors on the response variable, and the most effective factors on the response variable are determined. Finally, the optimal levels of each factor will be determined.

Determining Controllable Factors, Uncontrollable Factors, and Performance Measurement Criteria

When choosing a response variable, the researcher must ensure that the selected variable offers valuable insights into the process being investigated. Typically, either the mean or standard deviation (or sometimes both) will represent the characteristic of the response variable that is measured. It is also common to have multiple response variables. The effectiveness of the measurement tool is a crucial consideration as well. If the measurement tool is ineffective, the experiment will only detect substantial effects, or it may need to be conducted again.

Determining the Levels for Each Factor

Table 1. Controllable factors and their levels

Solution method	Parameters		Interval	Level 1	Level 2	Level 3
NSGA-II	*nPop*	Initial pop size	100-300	100	200	300
	P_c	Percent of crossover	0.75-0.95	0.75	0.85	0.95
	P_m	Percent of mutation	0.1-0.2	0.1	0.15	0.2
	Iteration	Number of generations	100-400	100	225	400
NRGA	*nPop*	Initial pop size	100-500	100	350	500
	P_c	Percent of crossover	0.7-0.9	0.7	0.8	0.9
	P_m	Percent of mutation	0.1-0.3	0.1	0.2	0.3
	Iteration	Number of generations	200-600	200	400	600

The experimenter needs to identify the factors to manipulate in the experiment, the variation ranges of these factors, and the specific levels to be used in the study. To accomplish this, a solid understanding and knowledge of the process are necessary. This understanding generally combines hands-on experience with theoretical insights. All factors that might significantly impact the experiment should be assessed to prevent overemphasizing those influenced by past experience, particularly in the initial stages of the experiment or when dealing with a relatively novel process. When the goal is to screen factors or analyze the process, it is often advisable to limit the number of factor levels being examined to a small number (three levels are commonly utilized). (Table 1) presents the search ranges for the input parameter levels of the two algorithms.

Choosing Appropriate Orthogonal Arrays

The Taguchi method aims to enhance the quality of products and processes where system performance is largely influenced by various factors. In the design of experiments and strategy development, straightforward logic is typically employed to create all potential combinations of factors along with acceptable ranges for each relevant factor. However, in engineering projects with numerous influencing factors, the number of possible combinations can become exceedingly large. Additionally, for specialized projects, it may be necessary to take into account interactions between the influencing factors. The traditional approach to minimize the number of experimental combinations is to utilize partial factorial experiments. Taguchi has introduced a unique set of general designs for factorial experiments that address most applications. Orthogonal arrays are included within this collection of designs. The use of these arrays assists in identifying the minimum number of experiments needed for a specified set of factors. The structure of the designed arrays and the results of the experiments for the NSGA-II and NRGA algorithms are given in Table 2.

Table 2. Orthogonal arrays and NOS values

Exp No.					*NSGA-II*	*NRGA*
	nPop	P_c	P_m	Iteration	NOS	NOS
1	1	1	1	1	35	24
2	1	1	1	1	41	31
3	1	1	1	1	49	35
4	1	2	2	2	129	104
5	1	2	2	2	98	79
6	1	2	2	2	70	54
7	1	3	3	3	83	61
8	1	3	3	3	83	63
9	1	3	3	3	77	60
10	2	1	2	3	96	82
11	2	1	2	3	109	88
12	2	1	2	3	71	54
13	2	2	3	1	64	59
14	2	2	3	1	74	59
15	2	2	3	1	157	144
16	2	3	1	2	79	60
17	2	3	1	2	104	89
18	2	3	1	2	106	84
19	3	1	3	2	84	74
20	3	1	3	2	86	68
21	3	1	3	2	79	58
22	3	2	1	3	102	84
23	3	2	1	3	100	84
24	3	2	1	3	99	78
25	3	3	2	1	69	54
26	3	3	2	1	109	83
27	3	3	2	1	84	68

It is noted that the response variable considered in order to solve the proposed model is the number of solutions in the first row of the algorithms. Some of the features of the design presented for this problem are as follows:

1. In this design, only main effects are estimated.
2. To estimate the main effects of the three-level factors, two degrees of freedom are required, as well as one degree of freedom to estimate the total mean. Therefore, we need at least one degree of freedom for each degree of freedom, so the minimum number of experiments required is nine experiments. The design presented here has 27 experiments, which is 18 more experiments. If the minimum number of experiments is used, we will naturally have less information compared to the presented design.
3. The main effects estimates can be used to predict the response of any combination of factor levels. The optimal design is one whose prediction error variance is the same as the factorial design.

Determining Optimal Levels and Analyzing Data Using the Signal-to-Noise Ratio

The characteristics in the problem under consideration are continuous variables. Here, the goal of these experiments is to find a combination of control factor levels such that for the quantitative variable of the objective function, the mean value is maximized as much as possible, while the standard deviation for the above response variable is minimized. The above topic is known as optimizing the combination of control factor levels. To achieve the above goal, the performance criterion presented by Taguchi, namely the S/N ratio, is considered as the response variable. The response variable should be as large as possible, so the variable associated with it corresponds to the "bigger is better" condition. Considering these materials, the S/N ratio for the above variable will be as follows:

$$\eta = \left(\frac{S}{N}\right) = -10\, log \left(\frac{1}{n}\right) \sum_{i} \left(1/{y_i}^2\right)$$

Figures 2 and 3 show how the S/N index values change at different levels of the algorithms. Similarly, the following are the graph forms of the parameter tuning results, as well as the tables of the tuning parameter values related to the NSGA-II method.

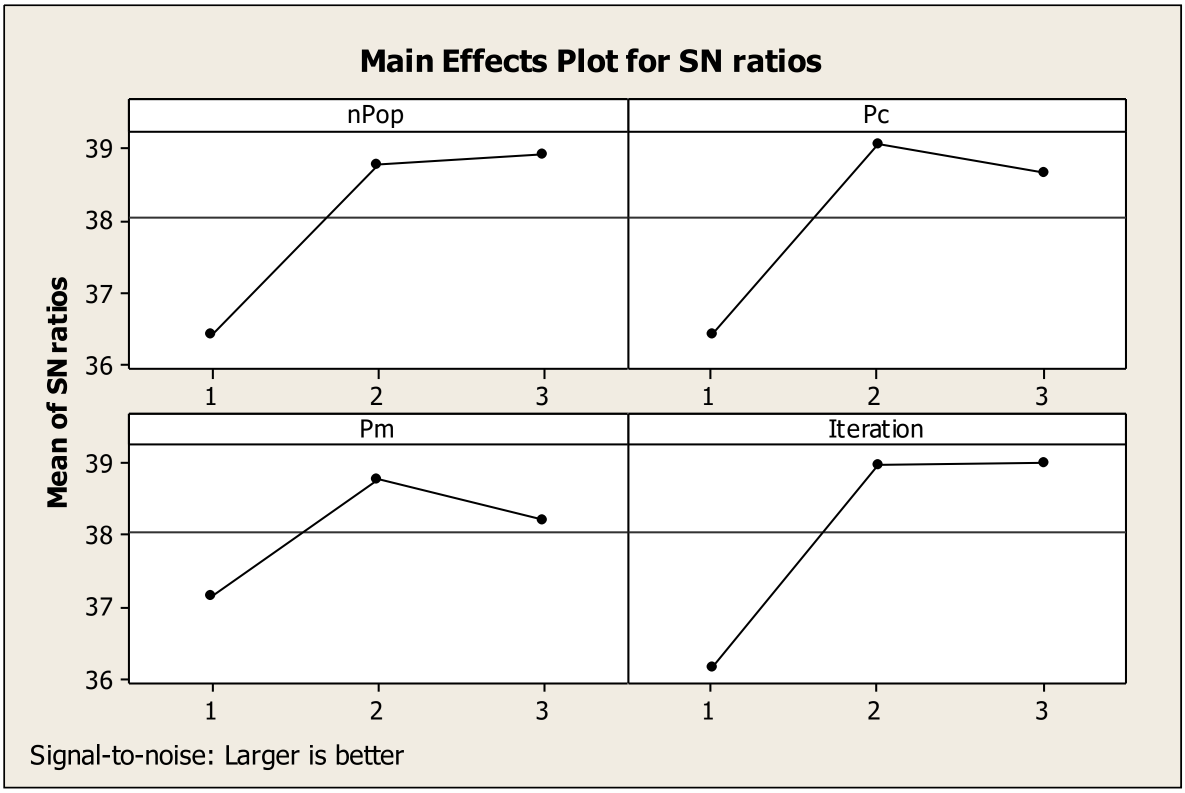

Figure 2. How to change the S/N index values at different levels of the NRGA algorithm

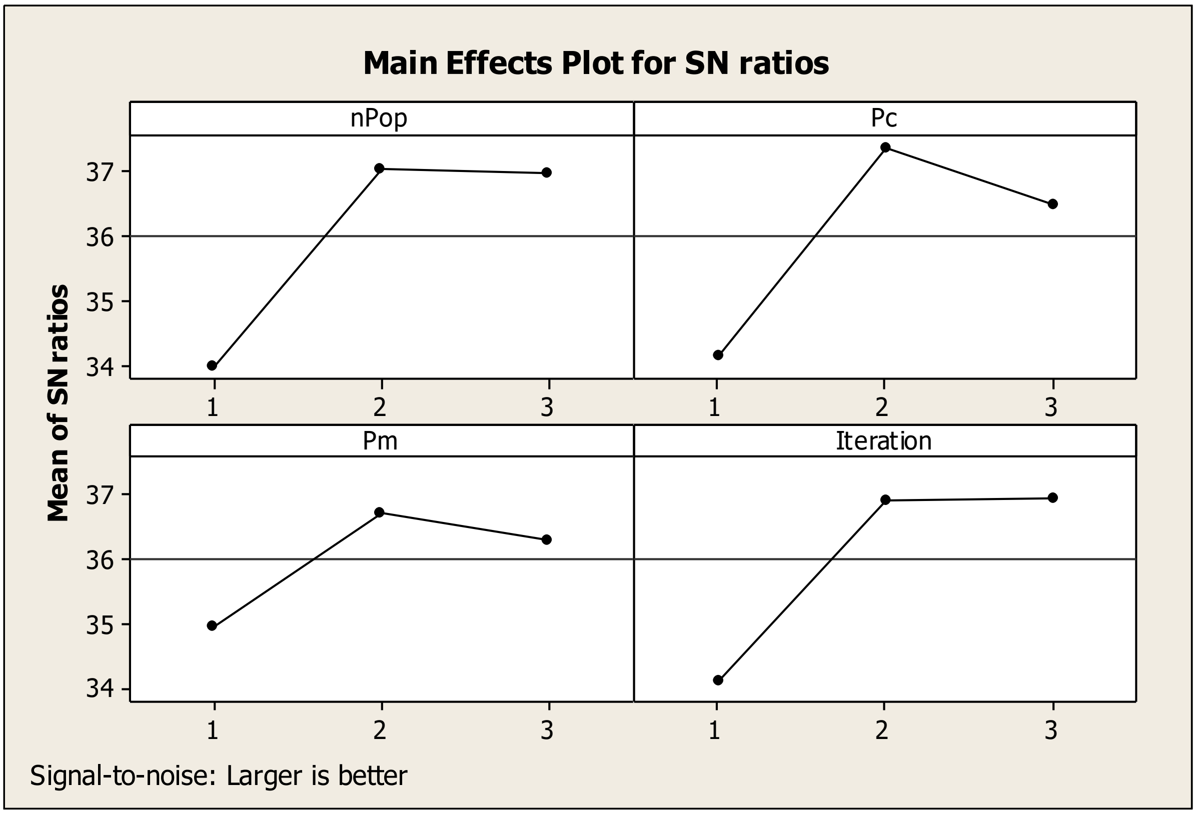

Figure 3. How to change the S/N index values at different levels of the NSGA-II algorithm

Performance Evaluation Indicators of Multi-Objective Algorithms

As mentioned, the proposed multi-objective algorithms search and work based on Pareto. On the other hand, we know that the final Pareto found by the algorithms must have two properties of good convergence and diversification. For this purpose, it is necessary to examine different indicators to obtain a comprehensive understanding of the performance of a multi-objective algorithm. In this section, we will mention one example of these criteria.

Pareto Number of Solutions (NOS) Criterion

The main performance metric utilized in this research was the Pareto Number of Solutions (NOS) achieved in the last generation. NOS reflects the diversity and abundance of the Pareto front, illustrating the algorithm's effectiveness in navigating the solution landscape. An increased NOS value implies superior performance in producing a broader range of trade-off solutions, which is essential in multi-objective decision-making.

Following the execution of 30 independent trials for both NSGA-II and NRGA using the same problem parameters, the Number of Pareto Solutions (NOS) achieved in each trial was documented and assessed. Table 3 below provides a summary of the average, highest (maximum), and standard deviation of the NOS for both algorithms.

Table 3. The summary of the average, the best (maximum), and the standard deviation of the NOS

Algorithms	Average	Best	St.Dv.
NSGA-II	48	55	3.2
NRGA	54	60	2.9

A two-sample *t*-test was performed to evaluate the significance of the difference in NOS between the two algorithms. The obtained *p*-value was lower than 0.05, suggesting that the difference is statistically significant at the 95% confidence level. Figure 4 illustrates the result.

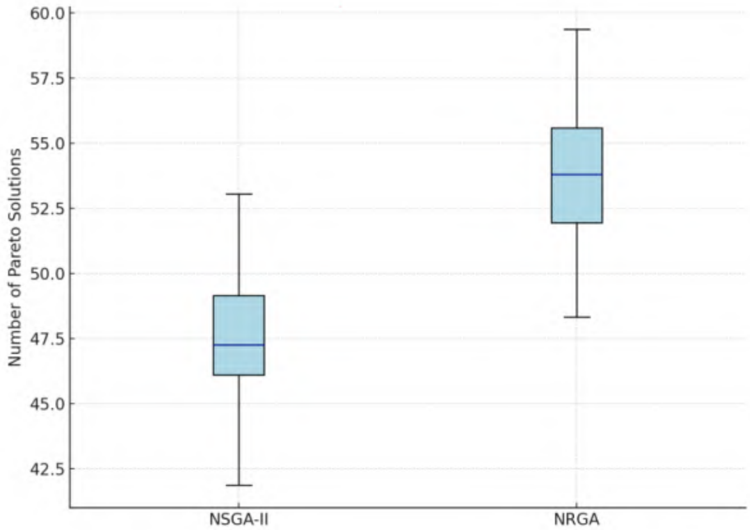

Figure 4. Comparison of the number of pareto solutions

The findings indicate that although both algorithms can address the formulated multi-objective green supply chain network design challenge, NRGA exhibits enhanced performance regarding the diversity and stability of Pareto solutions. This advantage is due to its ranking-based selection approach, which more effectively encourages exploration within the solution space.

Conclusion

In this study, a general multi-objective mathematical model for green supply chain network design with the focus on minimizing environmental effects and total operational cost on one hand and maximizing the demand coverage for customers concerning demand satisfaction, facility capacity, and transformation limit constraints has been proposed. To solve the introduced model, two metaheuristic algorithms, NRGA and NSGA-II, have been applied, and the results are compared. The results illustrated that both algorithms are well-suitable for solving our model. For evaluating the performance of the algorithms mentioned, the Pareto number of solutions (NOS) criterion has been applied. The results revealed that the NRGA algorithm slightly outperformed the NSGA-II algorithm in minimizing environmental effects and improving demand coverage, but with a slight increase in total cost, which was expected. Likewise, a 95% confidence interval by using a *t*-test has been applied, and the results showed that the NRGA algorithm has a larger number of Pareto solutions and boosted performance according to the diversity and stability.

For future work, it is suggested to use real-world case studies and industry-based data to validate the proposed model in a practical study. Also, additional environmental factors like carbon footprint, waste, etc, can be added to the model for application. Moreover, for the uncertainty in some parameters like demand, emission, and cost, stochastic or robust optimization can be used to have flexibility in the decision-making process upon an unexpected situation. Moreover, other performance evaluation criteria like diversity, time, and spacing can also be applied and compared in multi-objective algorithms. Overall, the proposed model and solution approaches contribute to the growing field of green logistics by offering decision-makers tools to design environmentally responsible and economically viable supply chain networks.

Scientific Ethics Declaration

* The author declares that the scientific ethical and legal responsibility of this article published in EPSTEM journal belongs to the author.

Conflict of Interest

* The authors declare that they have no conflicts of interest

Funding

* This research received no specific grant from any funding agency in the public, commercial, or not-for-profit sectors.

Acknowledgements or Notes

* This article was presented as an oral presentation at the International Conference on Research in Engineering, Technology and Science (www.icrets.net) held in Peja/Kosovo, on July 10-13, 2025.

References

Abdolazimi, O., & Ghezavati, V. R. (2021). A bi-objective robust possibilistic programming approach for a green closed-loop supply chain network design problem. *Journal of Cleaner Production, 280*, 124501.

Al-Harkan, I. M., Beirami, A., & Tavana, M. (2023). Multi-objective optimization in sustainable supply chain logistics: A comprehensive review. *Sustainability, 15*(5), 12790.

Altiparmak, F., Gen, M., Lin, L., & Paksoy, T. (2006). A genetic algorithm approach for multi-objective optimization of supply chain networks. *Computers & Industrial Engineering, 51*(1), 196–215.

Amiri, A. (2006). Designing a distribution network in a supply chain system: Formulation and efficient solution procedure. *European Journal of Operational Research, 171*(2), 567–576.

Balinski, M. L. (1965). Integer programming: Methods, uses, computation. *Management Science, 12*(3), 253–273.

Ball, M. O., & Lin, F. L. (1993). A reliability model applied to emergency service vehicle location. *Operations Research, 41*(1), 18–36.

Barbosa-Póvoa, A. P., Tautenhain, C., & Mota, B. (2019). An efficient Lagrangian-based heuristic to solve a multi-objective sustainable supply chain problem. *Expert Systems with Applications, 233*, 113–133.

Cheng, P., Ji, G., Zhang, G., & Shi, Y. (2022). Closed-loop supply chain network considering low-carbon preference under cap-and-trade regulation. *Sustainable Production and Consumption, 29*, 614–635.

Church, R. L., & ReVelle, C. (1974). The maximal covering location problem. *Papers of the Regional Science Association, 32*(1), 101–118.

Church, R. L., & Roberts, K. L. (1984). Generalized coverage models and public facility location. *Papers of the Regional Science Association, 53*, 117–135.

Deb, K. (2001). *Multi-objective optimization using evolutionary algorithms*. Wiley.

Diabat, A., & Govindan, K. (2011). An analysis of the drivers affecting the implementation of green supply chain management. *Resources, Conservation and Recycling, 55*(6), 659–667.

Farahani, R. Z., Asgari, N., & Davarzani, H. (2015). *Supply chain and logistics in national, international and governmental environment: Concepts and models*. Springer.

Geoffrion, A. M., & Graves, G. W. (1974). Multicommodity distribution system design by Benders decomposition. *Management Science, 20*(5), 822–834.

Ghezavati, V. R., Jabal-Ameli, M. S., & Makui, A. (2009). A new heuristic method for distribution networks considering service level constraints and coverage radius. *Expert Systems with Applications, 36*(3), 5620–5629.

Govindan, K., Rajendran, S., Sarkis, J., & Murugesan, P. (2015). Multi-criteria decision making approaches for green supplier evaluation and selection: A literature review. *Journal of Cleaner Production, 98*, 66–83.

Hoboken. Zitzler, E. (1999). *Evolutionary algorithms for multiobjective optimization: Methods and applications.* ETH.

Horn, J., Nafpliotis, N., & Goldberg, D. E. (1994). A niched Pareto genetic algorithm for multi-objective optimization. In *Proceedings of the First IEEE Conference on Evolutionary Computation* (pp. 82–87).

Kadziński, M., Tervonen, T., Tomczyk, M. K., & Dekker, R. (2017). Evaluation of multi-objective optimization approaches for solving environmentally conscious supply chain design problems. *Omega, 68*, 168–184.

Karasakal, O., & Karasakal, K. K. (2004). A maximal covering location model in the presence of partial coverage. *Computers & Operations Research, 31*(9), 1515–1526.

Li, J., & Wang, L. (2025). A sustainable facility location problem with vehicle allocation to minimize CO_2 emissions. *Journal of Transportation Systems, 12*(1), 45–60.

Melo, M. T., Nickel, S., & Saldanha-da-Gama, F. (2009). Facility location and supply chain management – A review. *European Journal of Operational Research, 196*(2), 401–430.

Min, H., & Kim, I. (2012). Green supply chain research: Past, present, and future. *Logistics Research, 3*(1), 39–47.

Perl, J., & Daskin, M. S. (1984). A unified warehouse location-routing methodology. *Journal of Business Logistics, 5*, 92–111.

Rezaei, S., & Behnamian, J. (2021). Strategic supplier selection based on modified sandcone theory and alignment principle. *Sustainable Production and Consumption, 26*, 256-274.

Rodrigue, J. P., Slack, B., & Comtois, C. (2001). Green logistics. In J-P. Rodrigue (Ed.), *The Geography of Transport Systems.* Routledge.

Sarkis, J. (2006). The adoption of environmental and risk management practices: Relationships to environmental performance. *Annals of Operations Research, 145*(1), 367–381.

Sarkis, J., Zhu, Q., & Lai, K. H. (2011). An organizational theoretic review of green supply chain management literature. *International Journal of Production Economics, 130*(1), 1-15.

Srinivas, N., & Deb, K. (1994). Multi-objective optimization using nondominated sorting in genetic algorithms. *Evolutionary Computation, 2*(3), 221–248.

Srivastava, S. K. (2007). Green supply-chain management: A state-of-the-art literature review. *International Journal of Management Reviews, 9*(1), 53–80.

Stander, L., Woolway, M., & Van Zyl, T. L. (2022). Surrogate assisted evolutionary multi-objective optimisation for pressure swing adsorption systems. *Chemical Engineering Research and Design, 180*, 13–25.

Tajabadi, F. Z., & Kazemi, A. (2016). To develop an integrated model for green supply chain. *Journal of Fundamental and Applied Sciences, 8*(3), 1340-1365.

Tavana, M., Kian, H., Nasr, A. K., Govindan, K., & Mina, H. (2022). A comprehensive framework for sustainable closed-loop supply chain network design. *Journal of Cleaner Production, 332*, 129777.

Zaare Tajabadi, F., & Daneshvar, S. (2023). Benchmark approach for efficiency improvement in green supply chain management with DEA models. *Sustainability, 15*(5), 4433.

Zhu, Q., & Sarkis, J. (2006). An inter-sectoral comparison of green supply chain management in China: Drivers and practices. *Journal of Cleaner Production, 14*(5), 472–486.

Zitzler, E., & Thiele, L. (1998, September). Multiobjective optimization using evolutionary algorithms-a comparative case study. *International Conference on Parallel Problem Solving from Nature* (pp. 292-301). Berlin, Heidelberg: Springer Berlin Heidelberg.

Author(s) Information

Farzad Zaare Tajabadi
Department of Industrial Engineering, Faculty of
Engineering, Near East University
Near East Boulevard, ZIP: 99138, Nicosia, Northern Cyprus
via Mersin 10 – Türkiye
Contact e-mail: *farzad.zaare@neu.edu.tr*

To cite this article:

Tajabadi, F. Z. (2025). A multi-objective optimization model for green supply chain network design using metaheuristic algorithms. *The Eurasia Proceedings of Science, Technology, Engineering and Mathematics (EPSTEM), 35,* 271-283.

The Eurasia Proceedings of Science, Technology,
Engineering & Mathematics (EPSTEM)
ISSN: 2602-3199

The Eurasia Proceedings of Science, Technology, Engineering and Mathematics (EPSTEM), 2025

Volume 35, Pages 284-296

ICRETS 2025: International Conference on Research in Engineering, Technology and Science

Investigation of the Adsorptive Performance of Chitosan/Halloysite Nanotube/Green Mold Biocomposite Beads for Methylene Blue Removal

Serife Parlayici
Konya Technical University

Erol Pehlivan
Konya Technical University

Abstract: In this study, chitosan-based composite hydrogel beads were successfully synthesized using halloysite nanotubes and green mold derived from grapefruit (*Citrus paradisi*) peel. The efficiency of these novel composites in removing methylene blue (MB) from aqueous solutions was evaluated under batch conditions. Comprehensive characterization of the hydrogel beads was carried out using Scanning Electron Microscopy (SEM) and Fourier Transform Infrared Spectroscopy (FT-IR). The effects of various operational parameters including contact time, pH, initial dye concentration, adsorbent dosage, and temperature on the adsorption performance were systematically investigated. Optimal adsorption conditions were identified as 2.5 g/L adsorbent dosage, 100 mg/L initial dye concentration, pH 7, contact time of 120 minutes, stirring speed of 200 rpm, and a temperature of 25 °C. Adsorption isotherm studies revealed that the Langmuir model best fit the experimental data, suggesting monolayer adsorption with a maximum adsorption capacity of 67.11 mg/g. Kinetic modeling demonstrated that the adsorption process followed the pseudo-second-order model. The primary adsorption mechanisms between MB and the composite are reduction, electrostatic interaction, and chemisorption. Furthermore, thermodynamic analysis confirmed that the adsorption process was spontaneous and exothermic in nature. These findings highlight the potential of the synthesized biocomposite hydrogel beads as an effective and sustainable adsorbent for dye removal from wastewater.

Keywords: Chitosan, Halloysite nanotube, Green mold, Methylene blue, Composite

Introduction

A major environmental issue resulting from a variety of industrial activities, including textiles, paper, and plastics, is dye pollution in water streams. Methylene Blue (MB), a widely used cationic dye, is a notable water contaminant that is well known for being highly visible, long-lasting, and potentially harmful to aquatic life and human health. Due to their toxicity, carcinogenicity, and non-biodegradability, the increasing discharge of synthetic dyes into water bodies, especially from the textile, paper, and plastics industries, presents a significant threat to the environment and human health (Al-Asadi et al., 2025; El-Kousy et al., 2020; Liu et al. 2018). Because synthetic dyes are resistant to traditional wastewater treatment methods, novel, effective, and environmentally beneficial ways must be devised to 284ors ix of them from water solutions. The majority of traditional wastewater treatment techniques are unable to effectively eliminate such dyes, necessitating the development of more effective, cost-effective, and environmentally beneficial solutions. Given its simplicity, efficiency, and versatility in treating different kinds of pollutants, adsorption has become a promising method in this situation.

Due to their biodegradability, abundance, and low cost, natural polymers and agricultural waste materials have gained more attention in the search for efficient and sustainable adsorbents (Zhang et al., 2023). Chitosan, a biopolymer derived from chitin, is considered highly attractive due to its abundance, biodegradability, and non-toxicity. Its chemical structure contains amino and hydroxyl functional groups, which provide active binding sites for pollutants, making it particularly effective for environmental applications such as pollutant removal (Pehlivan & Parlayıcı, 2021; Teshemo et al., 2020). However, 285ors chitosan has limitations such as poor mechanical strength and a propensity for dissolving in acidic media, which may restrict its use as an adsorbent. Due to their exceptional tubular structures, high surface area, and good mechanical qualities, naturally occurring aluminosilicate clay minerals like halloysite nanotubes (HNTs) are ideal for strengthening chitosan matrices. The closed formula for the member of the natural alumina silicate clay family, HNT, is $Al_2Si_2O_5(OH)_4 \cdot nH_2O$ (Moeinpour et al., 2019; Pirhaji et al., 2020). HNTs are inorganic clay structures that are 12 µm long and 30–50 nm in diameter. They are cheap, hollow, tubular, biocompatible, and environmentally safe (Pietraszek et al., 2019). Using agricultural waste materials complies with the tenets of sustainability and a circular economy. The grapefruit peel, a prevalent waste product of the fruit processing sector, is rich in a variety of organic substances, such as cellulose, lignin, and 285ors i (Chaudhary & Singh, 2025, Dubinin & Singh, 2024)). Furthermore, the integration of grapefruit peel-derived green mold biomass is an innovative way to introduce more functional groups for dye binding and enhance biocompatibility (Parlayıcı & Pehlivan, 2024a). Due to their inherent nontoxicity and high aspect ratio, the resulting composites may have higher stability and adsorption capacity.

This research presents a unique method for creating composite hydrogel beads made of chitosan that contain green mold taken from grapefruit peel as well as halloysite nanotubes. It is thought that the synergistic interaction of these materials will result in an efficient and potent MB adsorbent. By optimizing the overall performance of the composite beads, the distinct characteristics of each component are predicted to contribute to improved mechanical stability, a larger surface area, and a higher concentration of active adsorption sites.

285ors ix adsorption of MB from aqueous solutions, this study is on the creation and assessment of a novel composite (Cht/HNT/GM) hydrogel bead made of chitosan, halloysite nanotubes, and green mold. By utilizing the synergistic effects of grapefruit-derived green mold, chitosan, and HNTs, the goal is to create an effective, environmentally beneficial, and affordable adsorbent. To investigate the impact of key parameters including contact time, pH, temperature, dye concentration, and adsorbent dosage comprehensive material characterization and batch adsorption experiments were conducted. This study intends to offer significant understanding of the viability of employing nanocomposite materials for dye removal in actual wastewater treatment applications by examining thermodynamic behavior, isotherms, and adsorption kinetics. The following sections of this work will explore a thorough examination of the adsorptive capabilities of these produced composite hydrogel beads. This includes a thorough description of their morphological and chemical characteristics, a systematic examination of the numerous operational factors that affect adsorption, and a comprehensive examination of the underlying adsorption mechanisms using isotherm, kinetic, and thermodynamic modeling.

Method

Materials and Experimentation

The supplier of the chitosan (degree of deacetylation, DD = 75–85%) was Sigma-Aldrich. The HNTs, which were ~20–40 nm in diameter and 98% pure, were provided by the Eczacıbaşı Group ESAN Company. The acetic acid, HCl, and NaOH were provided by the Merck Company. The company selling methylene blue was Acros Organics. All relevant chemicals used in the experiments were of analytical grade. In the preparation of the composite adsorbent, an IKAMAG-RO15 model mechanical stirrer, a GFL 3033 model thermostatic shaker, and a pH meter with glass electrodes (Orion 900S2) were used. A UV-visible spectrophotometer (Schmadzu UV-1700) was used 285ors ix determination of MB (λmax: 664 nm). The FT-IR spectrum was recorded on a Bruker VERTEX 70 FT-IR spectrometer. The microstructure of the adsorbent was examined using scanning electron microscopy (SEM, Nova Nano SEM 200, FEI Company).

Synthesis of Adsorbent

The 3 g of Cht was mixed in an acetic acid solution (2% v/v) for 24 hours, at which point gelation took place. The Cht solution was then combined with 1 g of HNT and 1 g of GM and mixed for 5 hours to achieve a uniform suspension. The mixture was added drop by drop to a sodium hydroxide solution (600 mL methanol, 400 mL water, and 120 g of NaOH) using a burette to produce composite spheres. They were maintained in the NaOH bath overnight. The spheres were then filtered and rinsed to neutrality in order to 285ors ix of the extra acetic acid. The beads were agitated 285ors ix hours at 50 °C in 0.1 M epichlorohydrin in order to induce ionic crosslinking. The composite spheres were filtered and rinsed with deionized water numerous times after the reaction, then dried at 60 °C and stored until use.

Batch Adsorption Experiments

To assess the adsorption efficiency of MB removal from aqueous solutions using Cht/HNT/GM composite beads, batch adsorption experiments were carried out. To determine the influence of various operational parameters on the adsorption efficiency and capacity of the composite, experiments were systematically conducted by varying factors such as initial dye concentration, temperature, pH, contact time, and adsorbent dosage. The composite were mixed in MB solutions with known concentrations and stirred under regulated circumstances to guarantee uniformity. The remaining MB was determined by UV-Vis. Spectrophotometry after samples were taken, filtered, and analyzed at set intervals. The variations between the initial and final dye concentrations were used to compute the adsorption capacity (q_e, mg/g) and removal effectiveness (%). According to these batch experiments, the composite has a strong affinity for MB dye, which is affected by the synergistic interaction between the amino groups of Cht, the tubular structure of HNT, which offers a vast surface area, and the sorption capability of the GM.

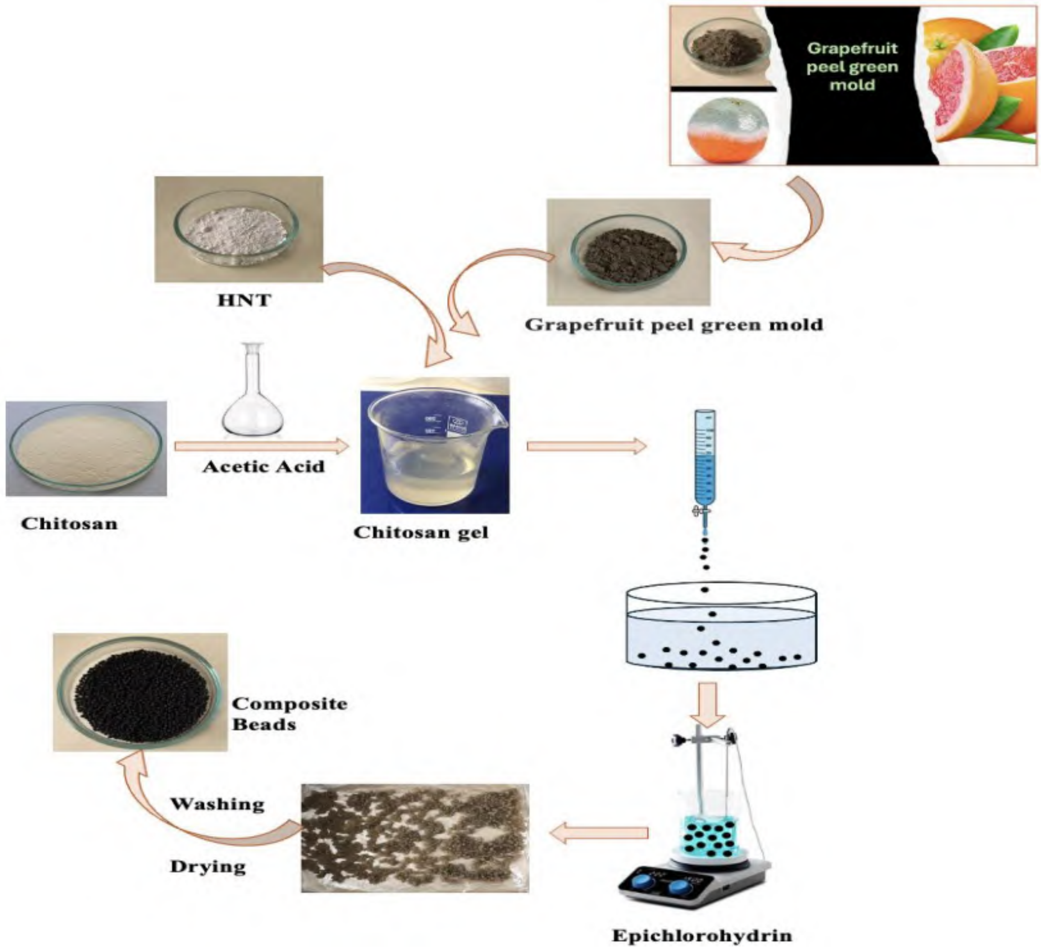

Figure 1. Schematic steps of composite (Cht/HNT/GM) beads synthesis

Results and Discussion

Results of Characterization for the Composite Materials

Figure 2 presents the FT-IR spectra of both the individual components and the final composite beads. The FT-IR analysis identifies key functional groups, providing insight into molecular interactions within the composite and highlighting the potential active sites responsible for MB adsorption. The FT-IR spectrum of Cht displays characteristic peaks indicating the presence of amino ($–NH_2$) and hydroxyl (–OH) functional groups. Specifically, the broad band around 3350 cm^{-1} is attributed to the O–H stretching vibrations, while the peak near 1659 cm^{-1} and $–NH_2$ bending bands at 1560 cm^{-1}correspond to the amide band, associated with C=O stretching (Far et al., 2023). The absorption bands at around 2919 and 2867 cm^{-1} can be attributed to C-H symmetric and asymmetric stretching, respectively (Teshome et al., 2024; Far et al., 2024). The peak seen around 1375 cm^{-1} belongs to acetyl (–CH_3) groups. Around 1026 cm^{-1}, there is a peak of the C–O–C symmetrical tension (Parlayıcı & Pehlivan, 2024b). These bands are characteristics typical of polysaccharide and are found in other polysaccharide spectra, such as xylan, glucans and carrageenans. These features confirm that Cht is rich in amino groups, which play a crucial role in its adsorption capabilities.

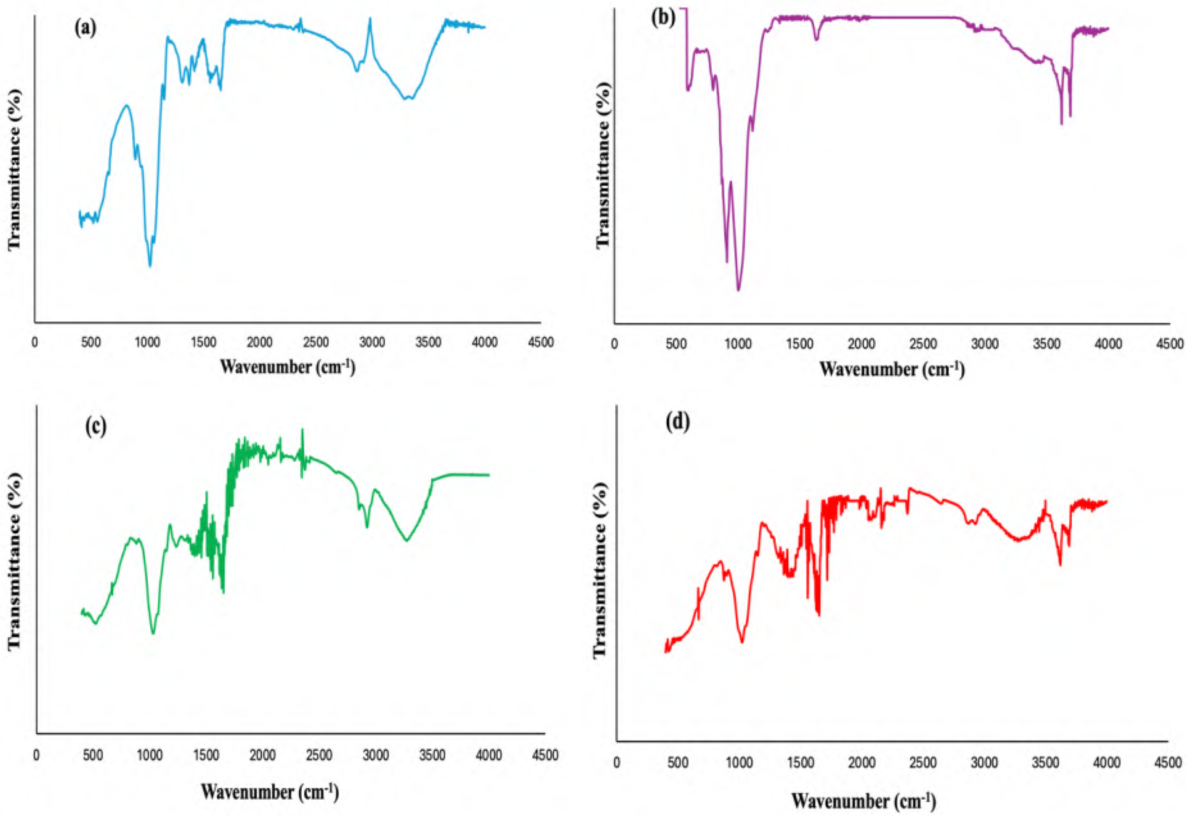

Figure 2. FT-IR diagram of Chitosan (a), Halloysite nanotubes (b), Grapefruit peel green mold (c) and Cht/HNT/GM composite (d)

The FT-IR spectrum of HNTs exhibits typical silicate characteristics, such as the distinctive band at around 1000 cm^{-1}, which is attributable to the Si-O stretching vibrations. The stretching of the hydroxyl (–OH) groups caused by the Al–OH bond on the interior surface of the HNT can be observed at 3694 and 3622 cm^{-1}. The hygroscopic nature of halloysite is demonstrated by the peak at 3445 cm^{-1}, which is related to OH stretching (Jiang et al. , 2024). It is described as the stretching of hydroxyl groups in the interlayer and surface water molecules. Due to the stretching vibration (Veghari Atigh & Shaki, 2025), the Si-O bond stretches at 1002 cm^{-1}. The O-H deformation peak of the inner Al-OH groups of HNT is observed at 910 cm^{-1}. The FT-IR spectrum of the GM displays prominent peaks indicative of organic acids, phenolic compounds, and polysaccharides. Absorption bands observed between 1400 and 1600 cm^{-1} suggest the presence of aromatic rings and phenolic functional groups, while the distinct band near 1060 cm^{-1} is attributed to C–O stretching vibrations, characteristic of polysaccharide structures. These functional groups contribute to the material's potential in adsorption processes.

The characteristics of Cht/HNT/GM composite are combined in the FT-IR spectrum of the composite bead. Significant changes in peak positions and intensities, particularly the broadening of the peak around 3400 cm^{-1}, point to hydrogen bonding interactions between the constituents. The silicarelated peak at 1000 cm^{-1} exhibits only minor changes, which demonstrates the successful integration of the individual materials into a useful composite. In the composite structure, the stretching of hydroxyl (–OH) groups that start from the AlOH bond on the HNT surface is seen at 3692 and 3620 cm^{-1}. Various C-H stretching at 2920 cm^{-1}, C=H bond stretching (carbonyl group) at 2371 cm^{-1}, amide I vibration band at 1640-1735 cm^{-1}, amide II vibration band at 1550 cm^{-1} ,various C-C-H, C-O-C, C-C-O bendings and C-C, C-O stretching vibrations between 1800-1500 cm^{-1} were observed in the FT-IR spectrum (Gumsel et al., 2024; Ünlü et al., 2018). The peaks at 1725, 1659, 1551, 1417, and 1150 cm^{-1} were assigned to the presence of aliphatic amines (C=O stretch), amines (N-H bend), and carboxylic acids (C-H bend, C-N stretch) (Preethi et al., 2020). Furthermore, the peaks at 1026 cm^{-1} correspond to the C-O-C stretch and the peaks at 670 cm^{-1} correspond to the C-H bend planar vibrations of alkynes.

Figure 3 displays scanning electron microscope (SEM) images of a substance known as Cht/HNT/GM composite, showing two distinct phases: (a) Prior to MB adsorption: The substance before it absorbs MB is seen in the first set of photographs. The SEM images reveal a surface with noticeable rough features, and close-up views emphasize the material's exquisite texture. The SEM images captured prior to MB adsorption reveal a rough, irregular, and porous surface morphology. These structural features are indicative of a high surface area, which is favorable for adsorption processes. The textured surface provides numerous active sites for dye attachment, which is critical for effective interaction with MB molecules. (b) Following MB absorption: The identical material following MB adsorption is seen in the second set of images. Due to the interaction and uptake of MB molecules, the surface structure of photographs shows obvious changes. The once rough and porous surface now seems smoother and denser, indicating that MB molecules have either successfully bonded to or blocked the pores. The diminished visibility of tiny structural features seen previously demonstrates the surface coverage by MB.

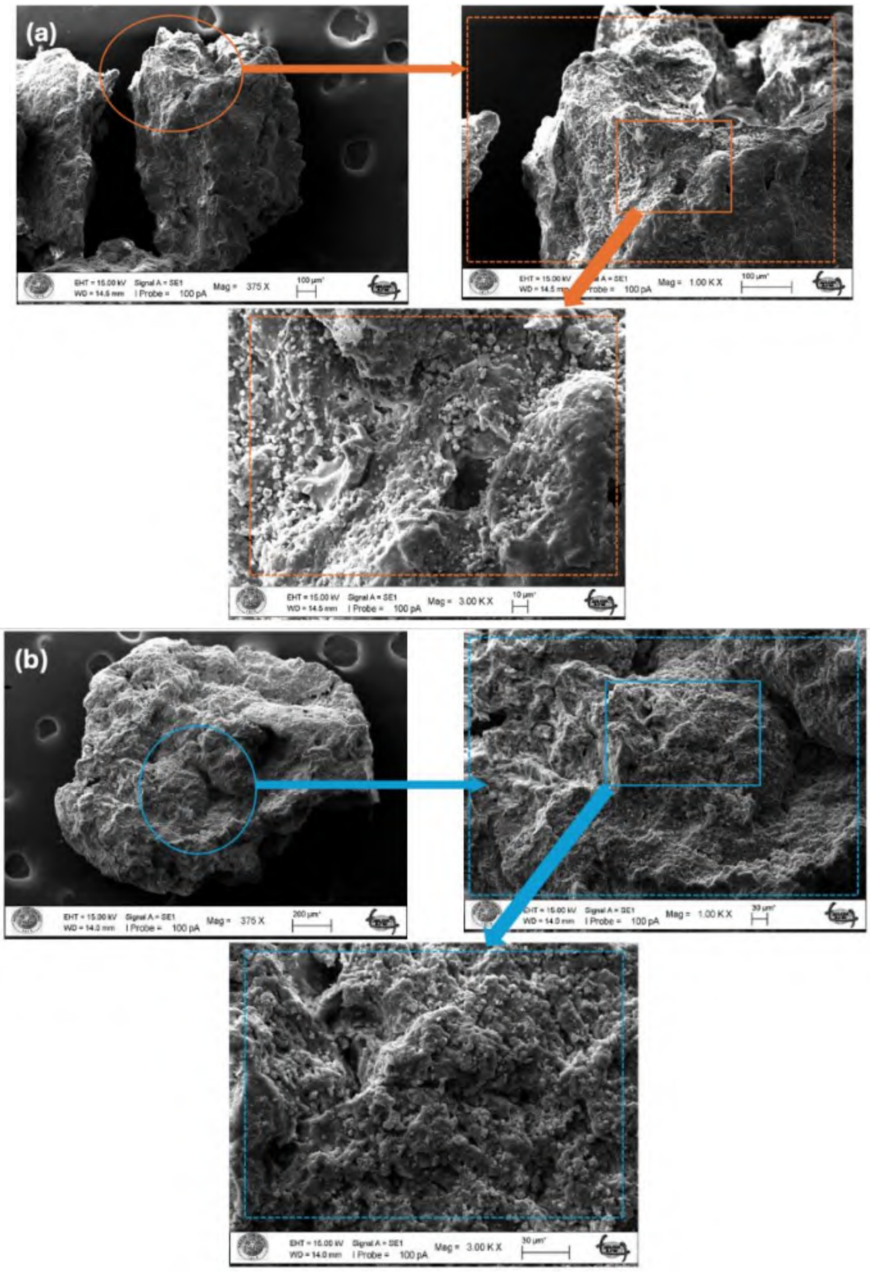

Figure 3. SEM image of (a) Cht/HNT/GM before MB adsorption (b) Cht/HNT/GM composite after MB adsorption

Results of the Batch Adsorption Experiments

Effect of pH

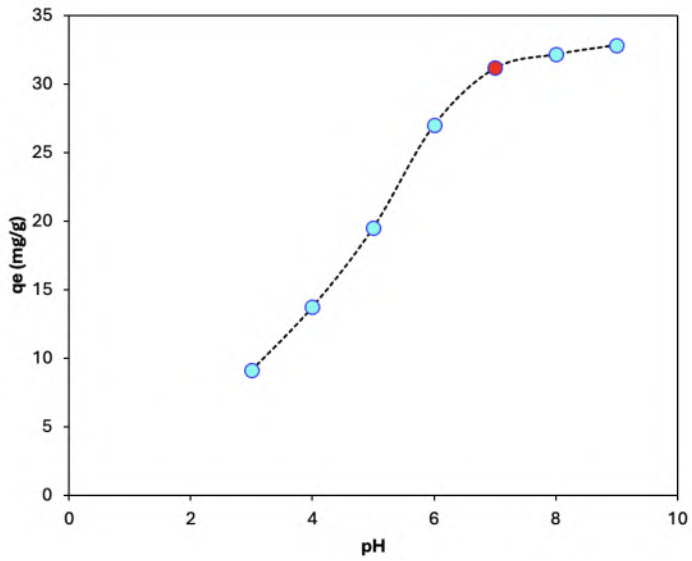

Figure 4. The effect of pH on MB adsorption.

The link between the pH and adsorption capacity (q_e, mg/g) of Cht/HNT/GM composite for MB removal is shown in the graph in Figure 4. pH is a key factor in determining the adsorption efficacy of dyes across a range of adsorbents, according to earlier research (Türkeş et al. ,2020). The data clearly show that the adsorption capacity increases gradually as the pH of the solution rises from 3 to around 9, and then it levels out around pH 7 and 8. The composite beads do not improve the removal efficiency of MB at higher pH levels, as seen by the fact that the adsorption does not significantly increase beyond this pH 9. The surface of the Cht/HNT/GM composite may be protonated at lower pH values, which would cause a repulsion between the positively charged MB molecules and the beads, decreasing the adsorption ability.

The electrostatic interactions between the negatively charged bead surface and the positively charged MB molecules increase as the pH rises, which promotes adsorption by deprotonating the surface. The significant rise in adsorption capacity between pH 4 and pH 7 indicates that the composite has an ideal pH range for adsorbing the MB. The surface of the beads now has a balance of charge interaction, allowing 289ort he most efficient adsorption of MB molecules. It seems that the system reaches a saturation level beyond pH 8, at which point further increases in pH do not have a significant impact on the adsorption process. This could be because the Cht/HNT/GM composite may become excessively deprotonated at higher pH levels or may experience competitive adsorption from other ionic species in the solution, which would lower its ability to adsorb MB.

Effect of nHNT-Cht/GM Dosage

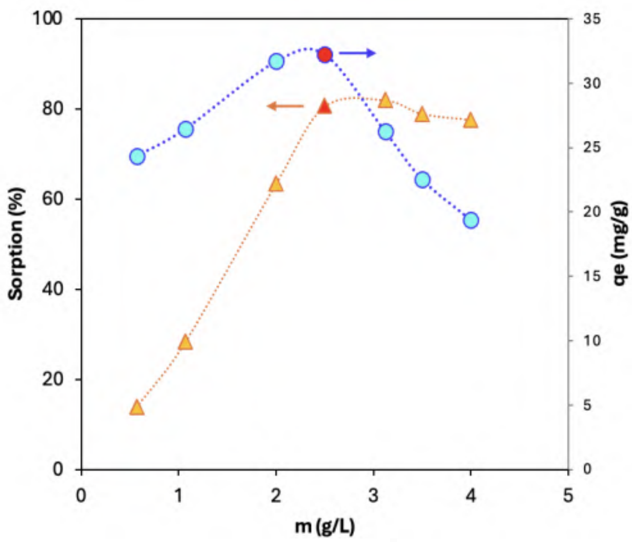

Figure 5. Effect of Cht/HNT/GM composite dosage

Figure 5 illustrates that the sorption percentage initially increases with the composite dosage, reaching a maximum of about 2.5 g/L before gradually falling. In addition, the quantity of MB adsorbed per unit mass of adsorbent (q_e) also increases with dosage, indicating that there is an optimal dosage for maximizing both the overall removal efficiency and the adsorption capacity of the composite.

Effect of Contact Time and Kinetic Studies

Contact time has a major impact on the adsorption behavior of composite made of Cht/HNT/GM, as shown in Figure 6. Particularly during the first 50 minutes, MB was absorbed quickly, suggesting a strong interaction between the dye molecules and the adsorbing surface. The composite surface's high concentration of active sites, which facilitate rapid dye diffusion and binding, is what causes this early stage. Following this dramatic rise, the rate of adsorption began to fall gradually until it reached equilibrium, at which point there was no further noticeable improvement in dye removal. The plateau phase indicates that the material has reached its maximum adsorption capability by saturating binding sites (Peng et al., 2015). Further insights into the adsorption process are provided by the time-dependent kinetic analysis, as shown in Figure 7 and Table 1.

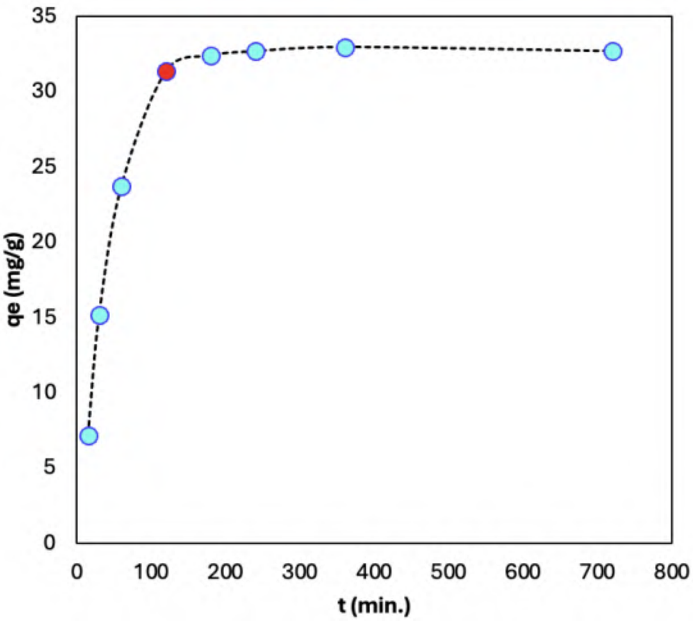

Figure 6. Effect of contact time on adsorption.

Pseudo-first-order

Pseudo-second-order

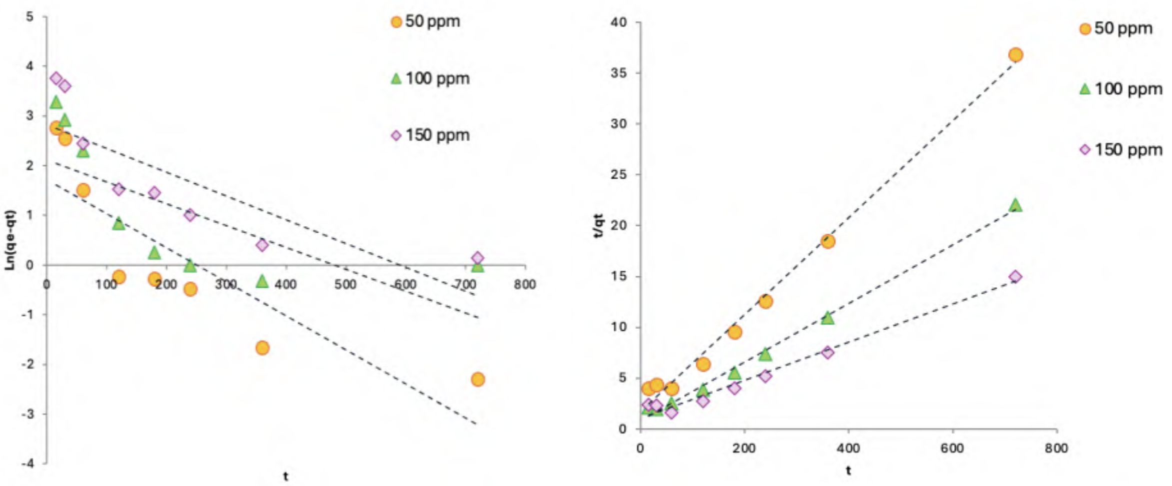

Figure 7. Kinetics for MB adsorption onto Cht/HNT/GM composite.

Table 1. Comparison of the pseudo-first-order, pseudo-second-order adsorption rate constants and calculated and experimental q_e values obtained at at various starting MB concentrations.

		Pseudo First-order			Pseudo Second- order		
C_o(ppm)	q_e exp	k_1	q_e	R^2	k_2	q_e	R^2
50	19.66	0.0068	5.55	0.743	0.0013	20.96	0.992
100	33.66	0.0044	8.22	0.509	0.0010	34.60	0.995
150	49.21	0.0048	16.87	0.681	0.0003	53.48	0.979

Higher R^2 values (≥ 0.992) demonstrate that the pseudo-second-order model better matched the experimental data across various MB concentrations than the pseudo-first-order model. This suggests that chemisorption, in which the rate-limiting step is the sharing or exchange of electrons between the MB molecules and functional groups on the Cht/HNT/GM surface, is the main factor driving the adsorption process. The time it took to reach equilibrium remained relatively consistent across concentrations, indicating that the interaction dynamics and necessary contact time for saturation remained effectively stable, even if the amount of dye adsorbed increases with concentration.

Effect of Initial Concentration of MB and Isotherm Studies

The adsorption capacity was assessed by varying the MB initial concentration (25, 50, 100, 150, 200, 250 and 300 ppm) in Figure 8. The influence of the starting dye concentration on the adsorption capability of MB onto Cht/HNT/GM composite is a key consideration in assessing adsorption performance. The adsorption capacity increases with increasing initial MB concentrations, as shown in Figure 8(a), suggesting that a larger concentration gradient improves mass transport between the dye molecules and the adsorbent surface.

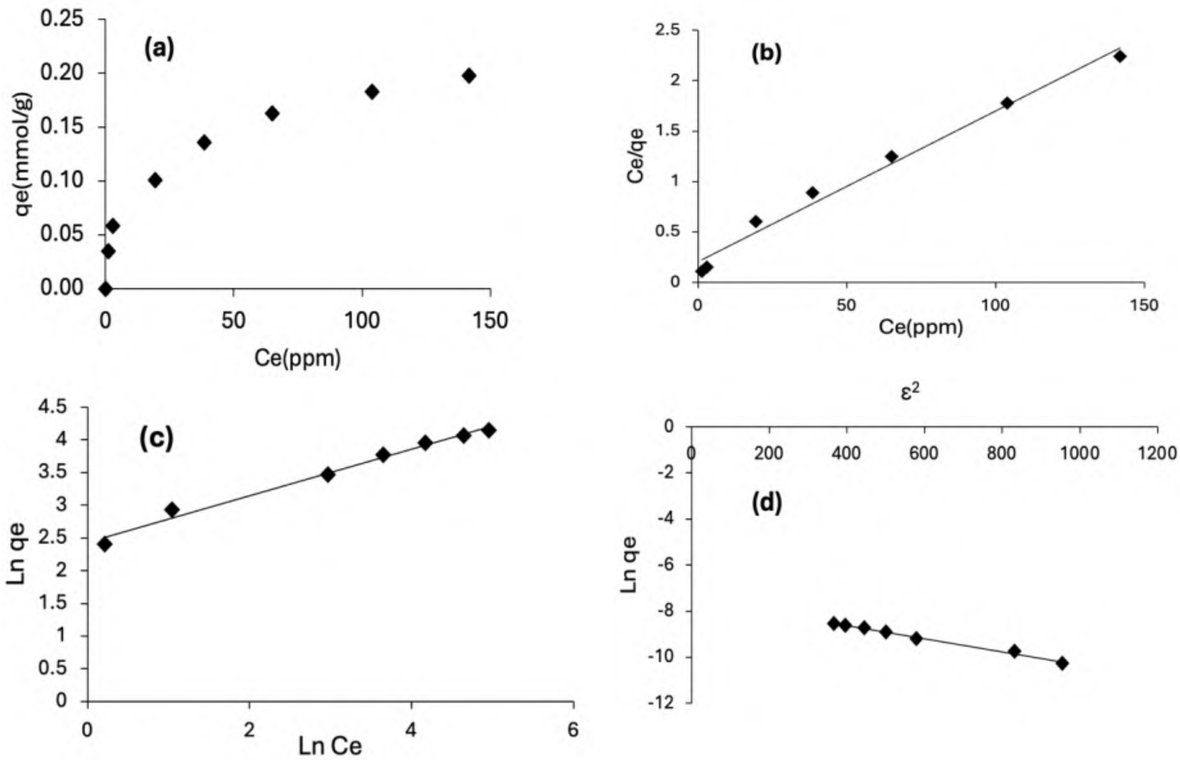

Figure 8. Effect of initial concentration (a), result of fitting isotherms data of MB adsorption onto nHNT-Cht/GM beads with Langmuir (b), Freundlich (c), Dubinin–Radushkevich (d).

This trend implies that the adsorption process is concentration-dependent, with a greater number of MB molecules available to fill the active sites on the composite. Greater absorption occurs until a saturation point is reached, probably because the increased driving force at higher concentrations overcomes resistance to MB uptake.

Additional information about the adsorption process may be gleaned from the isotherm data shown in Figure 8(b-d) and Table 2.

Table 2. Parameters for the adsorption isotherm of MB removal.

Model	Equation	Parameters for dye			
Langmuir (Langmuir, 1917)	$\frac{C_e}{q_e} = \frac{C_e}{A_s} + \frac{1}{K_b A_s}$	q_e 67.11	K_b 0.0716	R^2 0.985	R_L 0.123
Freundlich (Freundlich, 1906)	$\ln q_e = \ln K_f + \frac{1}{n} \ln C_e$	K_f 11.41	n 2.81	R^2 0.975	
D-R (Dubinin & Radushkevic 1947)	$\text{In } q_e = \ln q_m - \beta\, \varepsilon^2$	X_m 0.00057	K 0.0029	E 13.13	R^2 0.991

The Langmuir model (R^2=0.985) is the best fit for the experimental data, showing monolayer coverage of MB molecules on the uniform surface of the Cht/HNT/GM. The composite' high adsorption potential is highlighted by the computed maximum adsorption capacity (q_e) of 67. 11 mg/g. The Langmuir constant (K_b=0.0716 L/mg) further supports the favorable nature of adsorption, while the R_L value (0.123) falls between 0 and 1, confirming that the process is favorable at the concentrations studied. Conversely, with an R^2 value of 0.975, the Freundlich model suggests a little surface heterogeneity and multilayer adsorption, even if it does not explain the system as well as the Langmuir model. The Dubinin–Radushkevich (D–R) model offers details about how adsorption works. The calculated mean adsorption energy (E=13.13 kJ/mol) implies that the adsorption is mostly chemical in character (chemisorption). The high q_e value, in addition to this energy value, backs up the notion that the Cht/HNT/GM composite have a strong binding affinity for MB molecules, even at high starting concentrations. The data, in general, show that the initial dye concentration has a major impact on the adsorption process, with the Langmuir-type monolayer adsorption model prevailing and the composite demonstrating excellent MB removal effectiveness.

Influence of Thermodynamic Studies and Temperature

Important information about the nature of the adsorption process is provided by the thermodynamic analysis of MB adsorption onto the Cht/HNT/GM composite, as shown in the Figure 9. The plot of ln Kc vs. 1/T is linear, with a high correlation coefficient (R^2=0.976), which implies that the adsorption process adheres to a consistent thermodynamic pattern and lends credence to the thermodynamic parameters that were computed.

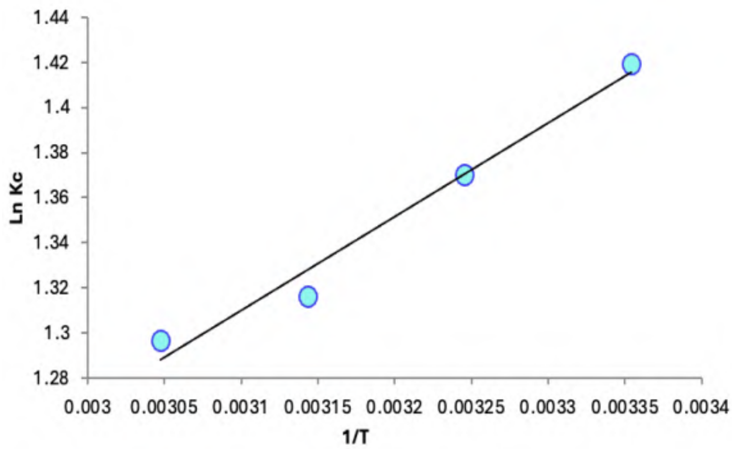

Figure 9. The impact of temperature on MB adsorption in the temperature range of 25°C, 35°C, 45°C, and 55°C.

The spontaneous nature of MB adsorption is supported by the negative values of Gibbs free energy change (ΔG°) across all examined temperatures. Additionally, the modest rise in the value of ΔG° with increasing temperature implies that thermal energy somewhat increases the spontaneity and the adsorption feasibility decreases at elevated temperatures, which points to a temperature-favorable process (Yu et al.,2021; Kanani-Jazi et al., 2021).

Furthermore, the adsorption process is exothermic in nature, as indicated by the negative enthalpy change (ΔH°=3463.02 J/mol). This indicates that the adsorption of MB onto the Cht/HNT/GM composite may be dominated by physical adsorption mechanisms such as van der Waals forces or hydrogen bonding. The positive entropy change (ΔS°=0.192 J/K·mol) implies an increase in randomness at the solid-liquid interface during the adsorption process, possibly as a result of the displacement of water molecules by MB dye molecules on the adsorbent surface. In conclusion, these thermodynamic findings support the biocomposite beads' ability to efficiently remove MB dye via a spontaneous, exothermic, and entropy-driven mechanism, highlighting their potential use.

Table 3. Thermodynamic characteristics of MB adsorption.

ΔS°	**ΔH°**	**ΔG° (J mol^{-1})**				
(J K^{-1} mol^{-1})	J mol^{-1}	T=298.15K	T=308.15K	T=318.15K	T=328.15K	R^2
0.192	-3463.02	-3520.21	-3522.13	-3524.05	-3525.97	0.976

MB Adsorption Mechanism

Reduction, electrostatic interaction (Zhang et al., 2024), and chemical interaction (Zain et al., 2023) together or some of them are active on the adsorption of the MB. The Cht/HNT/GM composite has negatively charged functional groups in a basic environment, which facilitates electrostatic interactions with the positively charged groups of MB dye molecules. By interacting with nitrogen atoms in the MB structure, hydrogen atoms on the composite surface likely play a key role in facilitating adsorption.

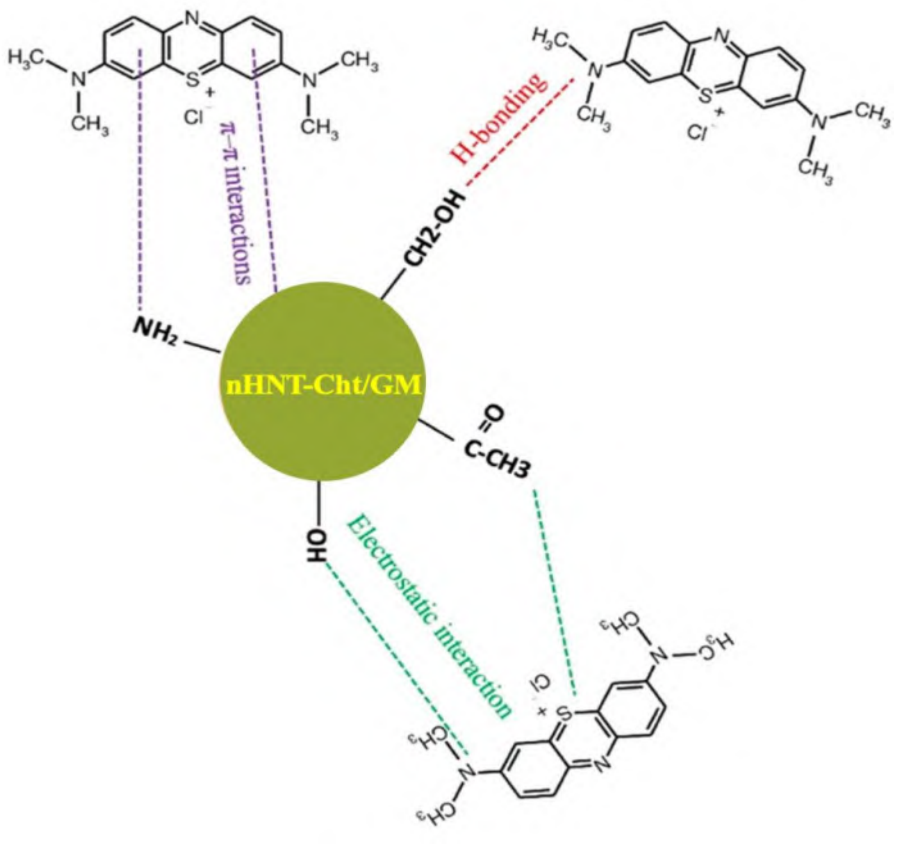

Figure 10. Schematic illustration of the adsorption mechanism between methylene blue (MB) and the Cht/HNT/GM composite

Furthermore, the connection is strengthened by the hydrogen bonding between the hydroxyl (-OH) groups on the composite surface and the nitrogen and sulfur atoms in the MB molecules. The composite's porous structure, as well as π-π stacking interactions between the aromatic rings of MB and those of the Cts framework, are also major contributors to the adsorption process. The aromatic structure of MB is well-aligned with the aromatic moieties in the composite, which facilitates these stacking interactions.

Conclusion

This study successfully developed a unique composite hydrogel bead and demonstrated its effectiveness in removing MB from aqueous solutions. The porous structure essential for improved adsorption and the successful integration of functional groups were confirmed by the thorough FT-IR and SEM characterization. Batch adsorption experiments showed that the ideal conditions for removal were a temperature of 25°C, a contact period of 120 minutes, an adsorbent dose of 2.5 g/L, an initial dye concentration of 100 mg/L, and a pH of 7. Kinetic modeling matched with the pseudo-second-order model, suggesting a chemisorption-driven process, whereas the Langmuir isotherm best fit the data, indicating monolayer adsorption with a maximum capacity of 67.11 mg/g. The thermodynamics investigation also revealed that the MB absorption onto the composite was spontaneous, exothermic, and accompanied by an increase in entropy, indicating a good adsorption mechanism and strong molecular interactions. In general, the synergistic combination of Cht, HNT, and GE provides an environmentally acceptable, low-cost, and sustainable method for treating wastewater contaminated with dyes. A number of processes, such as electrostatic interactions, reduction, hydrogen bonding, and surface complexation, all had a substantial impact on the composite's adsorption capabilities, which in turn led to its greater binding affinity for MB molecules. The novel application of naturally occurring nano-clay, chitosan and agricultural waste biomass (green mold) in the composite form (Cht/HNT/GM) improves adsorption efficiency and adheres to the concepts of green chemistry and a circular economy. This study offers a potential basis for the creation of scalable composite adsorbents and promotes additional research into multifunctional biobased materials for environmental cleanliness by highlighting their practical use in the treatment of industrial wastewater.

Scientific Ethics Declaration

* The authors declare that the scientific ethical and legal responsibility of this article published in EPSTEM journal belongs to the authors.

Conflict of Interest

* The authors declare that they have no conflicts of interest

Funding

* This research received no specific grant from any funding agency in the public, commercial, or not-for-profit sectors.

Acknowledgements or Notes

* This article was presented as an oral presentation at the International Conference on Research in Engineering, Technology and Science (www.icrets.net) held in Peja/Kosovo, on July 10-13, 2025.

References

Al-Asadi, S. T., Mussa, Z. H., Al-Qaim, F. F., Kamyab, H., Al-Saedi, H. F. S., Deyab, I. F., & Kadhim, N. J. (2025). A comprehensive review of methylene blue dye adsorption on activated carbon from edible fruit seeds: A case study on kinetics and adsorption models. *Carbon Trends*, *20*, 100507.

Chaudhary, S., & Singh, B. (2024). Grapefruit peel waste: unlocking the potential for industrial applications in the circular economy. *Food Science and Biotechnology*, *34,* 2131–2155.

Dubinin M. M., & Radushkevic L. V. (1947). Equation of the characteristic curve of activated charcoal. *Proceeding of the Academy of Sciences of USSR: Physical Chemistry Section 55*, 331–333.

El-Kousy, S. M., El-Shorbagy, H. G., & Abd El-Ghaffar, M. A. (2020). Chitosan/montmorillonite composites for fast removal of methylene blue from aqueous solutions. *Materials Chemistry and Physics*, *254*, 123236.

Far, B. F., Naimi-Jamal, M. R., Jahanbakhshi, M., Rostamani, H., Karimi, M., & Keihankhadiv, S. (2023). Synthesis and characterization of chitosan/collagen/polycaprolactone hydrogel films with enhanced biocompatibility and hydrophilicity for artificial tendon applications. *International Journal of Biological Macromolecules*, *253*, 127448.

Far, B. F., Naimi-Jamal, M. R., Jahanbakhshi, M., Keihankhadiv, S., & Baradarbarjastehbaf, F. (2024). Enhanced methylene blue adsorption using single-walled carbon nanotubes/chitosan-graft-gelatin nanocomposite hydrogels. *Scientific Reports*, *14*(1), 19217.

Freundlich, H. M. F. (1906). Uber die adsorption in lasungen. *Journal of Physical Chemistry 57*, 385–470.

Gumsel, E., Bulut, S., & Okur, M. (2024). Investigation of adsorption potential of acid violet 90 dye with chitosan/halloysite/boron nitride composite materials. *International Journal of Biological Macromolecules*, *264*, 130531.

Jiang, J., Deng, S., Kuang, W., Wang, L., Chen, D., Ma, Y., & Yang, W. (2024). Highly carboxylate functionalized halloysite nanotube as an efficient and recyclable adsorbent for methylene blue. *Applied Clay Science*, *250*, 107292.

Kanani-Jazi, M. H., & Akbari, S. (2021). Amino-dendritic and carboxyl functionalized halloysite nanotubes for highly efficient removal of cationic and anionic dyes: Kinetic, isotherm, and thermodynamic studies. *Journal of Environmental Chemical Engineering*, *9*(3), 105214.

Langmuir I. (1917). The constitution and fundamental properties of solids and liquids. *Journal of the Franklin Institute, 183* (1), 102–105.

Liu, C., Omer, A. M., & Ouyang, X. K. (2018). Adsorptive removal of cationic methylene blue dye using carboxymethyl cellulose/k-carrageenan/activated montmorillonite composite beads: Isotherm and kinetic studies. *International Journal of Biological Macromolecules*, *106*, 823-833.

Moeinpour, F., Soofivand, F., & Mohseni-Shahri, F. S. (2019). Controlled release of losartan from acid-and heat-treated halloysite nanotubes. *Medicinal Chemistry Research*, *28*(2), 160-168.

Parlayıcı, S., & Pehlivan, E. (2024a). Removal of Hazardous Methylene Blue from Aqueous Solutions by Green Citrus Mold (Penicillium digitatum)@ Chitosan Hydrogel Beads. *Pharmata*, *4*(4), 89-101.

Parlayıcı, S., & Pehlivan, E. (2024b). Methylene blue removal using nano-TiO2/MWCNT/Chitosan hydrogel composite beads in aqueous medium. *Chemosphere*, *365*, 143244.

Pehlivan, E., & Parlayıcı, S. (2021). Fabrication of a novel biopolymer-based nanocomposite (nanoTiO2-chitosan-plum kernel shell) and adsorption of cationic dyes. *Journal of Chemical Technology & Biotechnology*, *96*(12), 3378-3387.

Peng, Q., Liu, M., Zheng, J., & Zhou, C. (2015). Adsorption of dyes in aqueous solutions by chitosan–halloysite nanotubes composite hydrogel beads. *Microporous and Mesoporous Materials*, *201*, 190-201.

Pietraszek, A., Karewicz, A., Widnic, M., Lachowicz, D., Gajewska, M., Bernasik, A., & Nowakowska, M. (2019). Halloysite-alkaline phosphatase system-A potential bioactive component of scaffold for bone tissue engineering. *Colloids and Surfaces B: Biointerfaces*, *173*, 1-8.

Pirhaji, J. Z., Moeinpour, F., Dehabadi, A. M., & Ardakani, S. A. Y. (2020). Synthesis and characterization of halloysite/graphene quantum dots magnetic nanocomposite as a new adsorbent for Pb (II) removal from water. *Journal of Molecular Liquids*, *300*, 112345.

Preethi, S., Abarna, K., Nithyasri, M., Kishore, P., Deepika, K., Ranjithkumar, R.,Bhuvaneshwari, V., & Bharathi, D. (2020). Synthesis and characterization of chitosan/zinc oxide nanocomposite for antibacterial activity onto cotton fabrics and dye degradation applications. *International Journal of Biological Macromolecules*, *164*, 2779-2787.

Teshome, S., Kassahun, S. K., & Tiruneh, S. N. (2024). Response surface statistical modeling for optimization of methylene blue adsorption from aqueous solution using chitosan/graphite composites: Isotherm and kinetics studies. *Separation Science and Technology*, *59*(2), 205-223.

Turkes, E., & Sag Acikel, Y. E. S. I. M. (2020). Synthesis and characterization of magnetic halloysite–chitosan nanocomposites: use in the removal of methylene blue in wastewaters. *International Journal of Environmental Science and Technology*, *17*(3), 1281-1294.

Unlu, C. H., Pollet, E., & Avérous, L. (2018). Original macromolecular architectures based on poly (ε-caprolactone) and poly (ε-thiocaprolactone) grafted onto chitosan backbone. *International Journal of Molecular Sciences*, *19*(12), 3799.

Veghari Atigh, F., & Shaki, H. (2025). Cost-effective removal of methylene blue dye from wastewater using polyacrylamide/sodium carboxymethyl cellulose/magnetic halloysite nanotube hydrogel. *International Journal of Environmental Science and Technology*, *22,* 9849–9876.

Yu, C. X., Chen, J., Zhang, Y., Song, W. B., Li, X. Q., Chen, F. J., ... & Liu, L. L. (2021). Highly efficient and selective removal of anionic dyes from aqueous solution by using a protonated metal-organic framework. *Journal of Alloys and Compounds*, *853*, 157383.

Zain, Z. M., Abdulhameed, A. S., Jawad, A. H., ALOthman, Z. A., & Yaseen, Z. M. (2023). A pH-sensitive surface of chitosan/sepiolite clay/algae biocomposite for the removal of malachite green and remazol brilliant blue R dyes: optimization and adsorption mechanism study. *Journal of Polymers and the Environment*, *31*(2), 501-518.

Zhang, S., Fan, X., & Xue, J. (2023). A novel magnetic manganese oxide halloysite composite by one-pot synthesis for the removal of methylene blue from aqueous solution. *Journal of Alloys and Compounds*, *930*, 167050.

Zhang, L. L., Zaoui, A., & Sekkal, W. (2024). Adsorption efficiency of highly methylene blue dye concentrations with multilayer chitosan-modified clays for a precise nanofiltration performance of polluted water. *Journal of Water Process Engineering*, *57*, 104651.

Author(s) Information

Şerife Parlayici
Konya Technical University, Faculty of Engineering and Natural Sciences, Department of Chemical Engineering, Rauf Orbay Street. 42250, Selcuklu/Konya, Türkiye.

Erol Pehlivan
Konya Technical University
Faculty of Engineering and Natural Sciences
Department of Chemical Engineering
Rauf Orbay Street. 42250, Selcuklu/Konya, Türkiye
Contact e-mail: *erolpehlivan@gmail.com*

To cite this article:

Parlayici S., & Pehlivan E. (2025). Investigation of the adsorptive performance of chitosan/halloysite nanotube/green mold biocomposite beads for methylene blue removal. *The Eurasia Proceedings of Science, Technology, Engineering and Mathematics (EPSTEM), 35,* 284-296.

The Eurasia Proceedings of Science, Technology, Engineering & Mathematics (EPSTEM)
ISSN: 2602-3199

The Eurasia Proceedings of Science, Technology, Engineering and Mathematics (EPSTEM), 2025

Volume 35, Pages 297-301

ICRETS 2025: International Conference on Research in Engineering, Technology and Science

Synthesis of Piperazine Functionalized Calix[4]Arene-1,8-Naphthalimidine Derivatives and Preparation of Antimicrobial Transparent Biofilms

Mustafa Yilmaz
Selcuk University

Ayse Yildirim
Selcuk University

Ahmet Uysal
Selcuk University

Abstract: In supramolecular chemistry, calix[n]arenes, known as the “third generation” host molecules after crown ethers and cyclodextrins, are important macrocyclic compounds (Neri et al., 2016). Calix[n]arenes are macrocyclic molecules containing phenolic rings bridged by methylene groups and are known for their ability to form inclusion complexes or act as molecular scaffolds (Fateh et al., 2021; Migliore et al., 2021). In recent years, it has been proven by various studies that some calix[n]arene derivatives are suitable for bioactivity studies. In this study, three new fluorescent calix[4]arene derivatives were formed and characterized by reacting calix[4]arene with 4-bromo-1,8-naphthalanhydride and then replacing the bromine in the naphthyl groups with piperase derivatives. These synthesized fluorescent compounds were reacted with hyaluronic acid to form transparent biofilm, and FE-SEM and EDX analyses were performed to determine the surface profiles of these prepared antimicrobial transparent biofilms. Among the synthesized compounds, compound number **7** showed significant antimicrobial activity on Sarcian lutea at a dose of 0.097 mg/ml and also, this MIC value was reported as the lowest value recorded in the entire study.

Keywords: Calixarene, Fluorescent, Antimicrobial

Introduction

Calix[n]arenes, the "third generation" host molecules in supramolecular chemistry after crown ethers and cyclodextrins, are important macrocyclic compounds obtained by the condensation of p-substituted phenols with formaldehyde, usually in the presence of inorganic bases (Neri et al., 2016). Calix[n]arenes are macrocyclic molecules containing phenolic rings bridged by methylene groups, known for their ability to form inclusion complexes or serve as molecular scaffolds (Sayin et al, 2011; Consoli et al., 2018). The calix[n]arene family presents a variety of oligomers that differ in the number of phenolic units in the macrocycle. The number given in parentheses varies between 4 and 20. The most studied oligomers are calyx[4,5,6,8]arenes formed by 4, 5, 6, or 8 phenolic units linked by methylene bridges in the o-position to phenolic OH groups (Ortolan et al., 2018). The calixarene structure is characterized by a "p-position of phenolic units," a "Phenolic-O region," and a central ring. Both edges can be easily functionalized to design advanced functional molecules. Rotation of the phenolic ring "across the ring" produces a variety of conformers in solution (Neri et al., 2016). While the wide ring makes calixarene conformationally mobile, in calixarene, where tert-butyl rotation across the ring is hindered, functionalization of the -OH groups with substituents larger than ethyl can block rotation and produce four different conformers. One of the important properties of calixarenes is their wide variety of conformations in solution. Unsubstituted calixarenes generally exhibit variable and mobile conformations at room temperature and in solution. Calixarenes acquire these conformations due to the up- or down-orientation of the aryl rings in

- Selection and peer-review under responsibility of the Organizing Committee of the Conference

their structures. Calixarenes have four different conformations: cone, partial cone, 1,3-altrnate, and 1,2- altrnate (Gutsche, 1989). The differences between the conformations and the specific conformation of a calixarene can be understood by examining the signals of the Ar-CH_2-Ar protons in the ^{1}H-NMR spectrum. In calixarenes, increasing the number of aryl groups also increases the number of conformations.

Calix[n]arenes have a wide range of applications due to their ease of derivatization via both the p-position and the phenolic -OH, their hydrophobic cavity that can interact with many guest molecules, their tunable conformations, and their versatile complexation properties (Yilmaz et al,2007;Yilmaz & Erdemir, 2013). Some of the applications of calixarenes are described under various headings. Sensor studies, As molecule/ion carriers, Enzyme immobilization studies, Catalyst studies, Anticancer studies, Antimicrobial studies.

In this study, we will focus on the antimicrobial properties of calixarenes. In this study, a novel polycationic macrocyclic compound carrying four circularly arranged N-methyldiethanol ammonium groups clustered around a calix[4]arene skeleton was designed and synthesized. The in vitro activity of compound 2 was evaluated alone and in combination with known antibiotics (ofloxacin, chloramphenicol or tetracycline) against Staphylococcus aureus (ATCC 6538 and methicillin-resistant isolate), S. epidermidis (ATCC 35984 and methicillin-resistant isolate), and Pseudomonas aeruginosa (ATCC 9027 and antibiotic-resistant isolate) strains (Consoli et al., 2018). In a study conducted by Chandio and colleagues, calix[4]arene-based silver nanoparticles Calix-AgNPs were synthesized and used in antimicrobial studies. The minimum inhibitory value for Calix-AgNPs against selected microorganisms was found to be 0.62 µg/mL (Kayhan et al, 2023; Chandio et al., 2024).

In this study, calix[4]arene is first converted to diester derivative and then reacted with hydrazine to form dihydrazine derivatives and then with 4-bromo-1,8-naphthylanhydride to form a fluorescent structure. Then, this compound is replaced with bromine by different piperazine groups (1-methylpiperazine, 1-phenylpiperazine, 1-(2-pyrimidyl)piperazine). Compound **5** was synthesized with 1-methylpiperazine, compound **6** with 1-phenylpiperazine and compound **7** with 1-(2-pyrimidyl)piperazine.

Method

Synthesis

In Figure 1, compound 8 was obtained by reacting the calix[4]arene dihydrazide derivative with 4-bromo-1,8-naphthylanhydride. Then, in order to make this structure antimicrobial, molecules (1-methylpiperazine, 1-phenylpiperazine, 1-(2-pyrimidyl)piperazine), which have antimicrobial effects in the literature (Jalageri et al., 2021), were attached by replacing –Br in the naphthyl group, and a transparent biofilm was prepared by interacting each compound with HA.

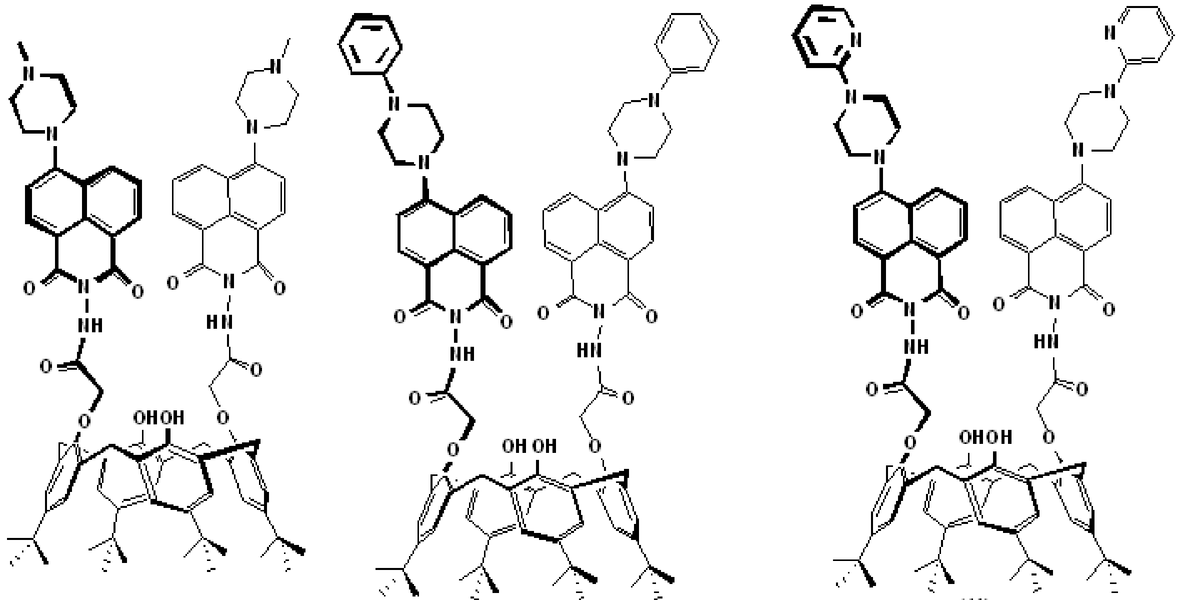

(9) (10) (11)

Figure 1. Synthesized antimicrobial compounds

Results and Discussion

In this study, the minimum inhibitory concentration (MIC) values of the tested compounds against various pathogenic bacteria were evaluated. Among the tested compounds, compound **7** exhibited the most notable antibacterial activity. Specifically, it showed a MIC value of 0.097 mg/mL against *Sarcina lutea* ATCC 9341, indicating a high level of antibacterial efficacy. In addition, compound **7** demonstrated activity against *Pseudomonas aeruginosa* ATCC 27853 with a MIC value of 0.781 mg/mL, and also showed moderate activity against *Staphylococcus aureus (MRSA) ATCC 43300* and *Escherichia coli ATCC 25922* with MIC values of 1.562 mg/mL. Compound **5** displayed consistent and moderate antibacterial activity with a MIC value of 1.562 mg/mL against four bacterial strains (E. coli, P. aeruginosa, *K. pneumoniae*, and *S. lutea*). Similarly, compound **6** exhibited limited antibacterial potential, particularly against *P. aeruginosa* and *S. aureus (MRSA)*, with MIC values ranging from 1.562 to 3.125 mg/mL. In contrast, compound **4** showed no antibacterial activity against any of the tested bacterial strains.

Table 1. MIC values of chemicals against pathogen bacteria and fungi (mg/mL)

Strains	4	7	HA-4Ag	HA-7Ag	Gentamicin (µg/mL)
Escherichia coli ATCC 25922	-	-	0.097	0.195	1.95
Staphylococcus aureus (MRSA)ATCC 43300	3.125	-	0.097	0.781	1.95
Sarcina lutea ATCC 9341	-	-	0.012	0.097	1.95
Bacillus cereus ATTC 11778	-	-	0.024	0.195	1.95
Candida albicans NRRL Y-417	1.562	1.562	0.097	0.390	7.81

When compared to the control antibiotic gentamicin, the MIC values of the tested compounds were generally higher, indicating weaker antibacterial activity. For instance, gentamicin exhibited a MIC value of <0.97 µg/mL against *P. aeruginosa*, while the tested compounds required higher concentrations in the mg/mL range. Nevertheless, the significant activity of compound **7** against *S. lutea* and *P. aeruginosa* suggests that this compound may have potential as a novel antibacterial agent. In conclusion, compound **7** demonstrated notable antibacterial activity particularly against Gram-positive bacteria, and it may be considered a promising candidate for further pharmacological investigations as a potential antimicrobial agent.

Antimicrobial Biofilm Studies

In this study, compound **7** was identified as the most effective antimicrobial agent among the synthesized compounds **5**, **6**, and **7**. To develop an antimicrobial biofilm incorporating this compound, HA:CEL:SP and the ionic liquid $BMIm^+Cl^-$ were utilized. The resulting gel films were visually evaluated under daylight and UV illumination, as shown in Figure 2**.** Two distinct biofilm formulations were prepared using different ratios of HA, CEL, and SP: **HA:CEL:SP (2:1:1)-7** and **HA:CEL:SP (2:2:1)-7**. According to the visual and functional assessment, the **HA:CEL:SP (2:2:1)-7** formulation was identified as the most suitable for antimicrobial biofilm applications, demonstrating enhanced structural integrity and potential activity.

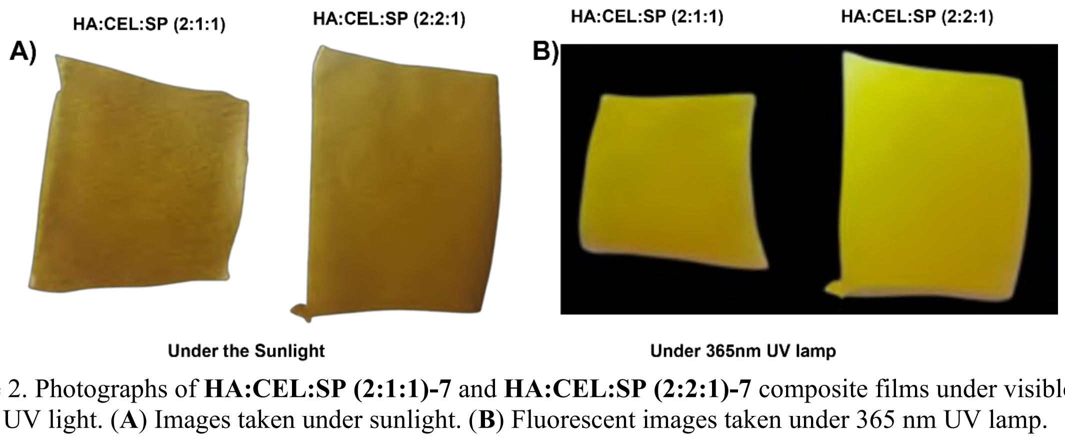

Figure 2. Photographs of **HA:CEL:SP (2:1:1)-7** and **HA:CEL:SP (2:2:1)-7** composite films under visible and UV light. (**A**) Images taken under sunlight. (**B**) Fluorescent images taken under 365 nm UV lamp.

SEM and EDX analyses were conducted to examine the surface morphology and elemental composition of the biofilms prepared using **HA:CEL:SP (2:1:1)-7** and **HA:CEL:SP (2:2:1)-7** formulations. The results revealed that compound 7 was homogeneously distributed within the biofilm matrix of both compositions. Moreover, EDX analysis (**Figure 3. A** and **B**) confirmed the presence of essential elements, including carbon (C), oxygen (O), nitrogen (N), and sodium (Na).

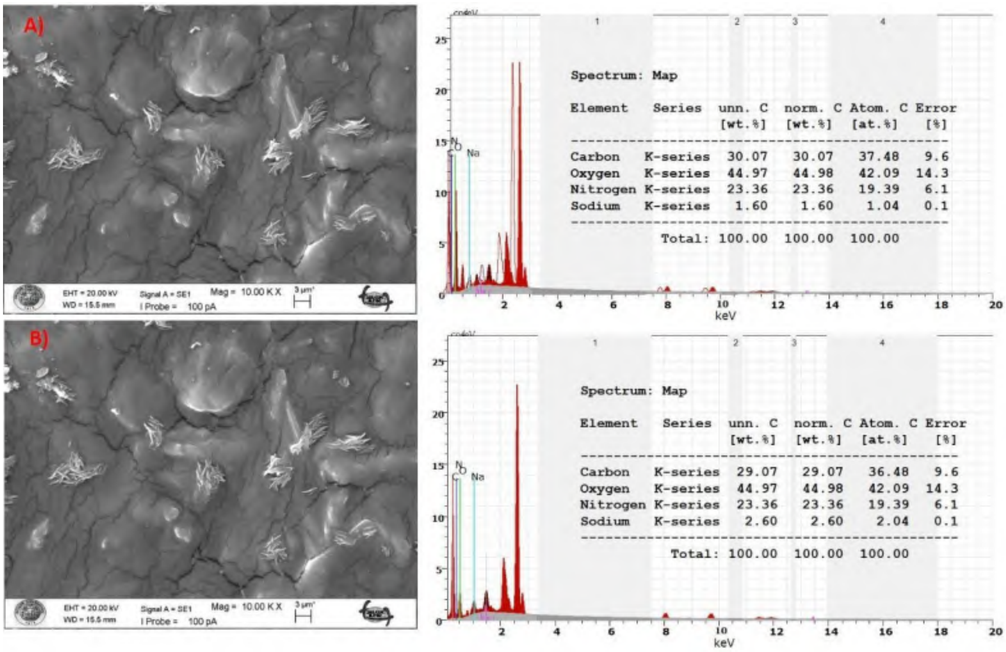

Figure 3. SEM images and EDX analyses of biofilms prepared with compound **7**: A) **HA:CEL:SP (2:2:1)-7**, B) **HA:CEL:SP (2:1:1)-7**

Conclusion

In this study, calix[4]arene was interacted with 4-bromo-1,8-naphthalic anhydride at the phenolic-O position. Three new antimicrobial compounds were then synthesized by interacting with piperazine derivatives under appropriate conditions. The synthesized and prepared compounds were subjected to antimicrobial testing against Gram-positive and Gram-negative bacteria and fungi. Biofilms were also prepared using these antimicrobial compounds, including hyaluronic acid, cellulose, and sporopollenin.

Recommendations

In conclusion, the materials synthesized in this thesis demonstrated efficacy in antimicrobial studies. A number of new and alternative antimicrobial agents can be used as examples for future studies in this field.

Scientific Ethics Declaration

* The authors declare that the scientific ethical and legal responsibility of this article published in EPSTEM journal belongs to the authors.

Conflict of Interest

* The authors declare that they have no conflicts of interest

Funding

* This research received no specific grant from any funding agency in the public, commercial, or not-for-profit sectors.

Acknowledgements or Notes

* This article was presented as an oral presentation at the International Conference on Research in Engineering, Technology, and Science (www.icrets.net) held in Peja/Kosovo, on July 10-13, 2025.

References

Chandio, A. A., Memon, S., Otho, A., Khalid, A., Alotaibi, B. S., Balouch, A., Brohi, N. A., Memon, F. N., Memon, A. A., & Thebo, K. H. (2024). Supramolecular structural-based fabrication of silver nanoparticles using diamide derivative of calix [4] arene: an efficient antimicrobial agent. *Chemical Papers*, *78*(7), 4593-4603.

Consoli, G. M., Granata, G., & Geraci, C. (2018). Calixarene-based micelles: properties and applications. In A. M. Grumezescu (Ed.), *Design and Development of New Nanocarriers* (pp. 89-143). Elsevier.

Fateh, F., Yildirim, A., Bhatti, A. A., & Yilmaz, M. (2021). A New benzothiazin-functionalized calix [4] arene-based fluorescent chemosensor for the selective detection of Co2+ Ion. *Journal of Fluorescence*, *31*(4), 1075-1083.

Kayhan, E. Y. Yildirim, A., Kocer, M. B., Uysal, A., & Yilmaz, M. (2023). A cellulose-based material as a fluorescent sensor for Cr (VI) detection and investigation of antimicrobial properties of its encapsulated form in two different MOFs. *International Journal of Biological Macromolecules, 240*, 124426

Migliore, R., Granata, G., Rivoli, A., Consoli, G. M. L., & Sgarlata, C. (2021). Binding affinity and driving forces for the interaction of calixarene-based micellar aggregates with model antibiotics in neutral aqueous solution. *Frontiers in Chemistry*, *8*, 626467.

Neri, P., Sessler, J. L., & Wang, M.-X. (2016). *Calixarenes and beyond*. Springer.

Ortolan, A. O., Øestrøm, I., Caramori, G. F., Parreira, R. L., Munoz-Castro, A., & Bickelhaupt, F. M. (2018). Anion recognition by organometallic calixarenes: analysis from relativistic DFT calculations. *Organometallics*, *37*(13), 2167-2176.

Sayin, S., Yilmaz, M., & Tavasli, M. (2011). Syntheses of two diamine substituted 1, 3-distal calix [4] arene-based magnetite nanoparticles for extraction of dichromate, arsenate and uranyl ions. *Tetrahedron, 67*(20), 3743-3753.

Yilmaz, M., & Erdemir, S. (2013). Calixarene-based receptors for molecular recognition. *Turkish Journal of Chemistry*, *37*(4), 558-585.

Yilmaz, A., Tabakci, B., Akceylan, E., & Yilmaz, M. (2007). Synthesis and dichromate anion extraction ability of p-tert-butylcalix [4] arene diamide derivatives with different binding sites. *Tetrahedron*, *63*(23), 5000-5005.

Author(s) Information

Mustafa Yilmaz
Selcuk University
Department of Chemistry, Konya/Türkiye
Contact e-mail: *myilmaz42@yahoo.com*

Ayse Yildirim
Selcuk University
Department of Chemistry, Konya/Türkiye

Ahmet Uysal
Selcuk University
Department of Chemistry, Konya/Türkiye

To cite this article:

Yilmaz, M. Yildirim, A., & Uysal, A. (2025). Synthesis of piperazine functionalized calix[4]arene-1,8-naphthalimidine derivatives and preparation of antimicrobial transparent biofilms. *The Eurasia Proceedings of Science, Technology, Engineering and Mathematics (EPSTEM), 35,* 297-301.

The Eurasia Proceedings of Science, Technology, Engineering & Mathematics (EPSTEM)
ISSN: 2602-3199

The Eurasia Proceedings of Science, Technology, Engineering and Mathematics (EPSTEM), 2025

Volume 35, Pages 302-313

ICRETS 2025: International Conference on Research in Engineering, Technology and Science

Image-Based Air Pollution Classification Using Deep Learning Techniques

Fatma Ozge Ozkok
Erciyes University
FOMOTECH R&D

Abstract: Air pollution is a considerable threat to human health and environmental sustainability. Traditional monitoring techniques involve sensor networks, which can be expensive, spatially constrained, and time-consuming to scale. This paper aims to examine a deep learning-based image classification technique to analyze air pollution levels using environmental imagery. A labelled dataset with varying levels of pollution intensity was used to train convolutional neural networks (CNNs) on visual indicators such as haze density, sky colour, and visibility. Several well-known architectures were assessed, namely: ResNet50, AlexNet, VGG16, VGG19, Xception, and InceptionV3. The findings indicate that the best model, which is invariant and accurate, was the model called Xception. To improve generalisation and robustness, regularisation techniques such as dropout, batch normalisation, and data augmentation were applied. Model performance was assessed using accuracy, F1-score, precision, and recall. The highest results were achieved by Xception, with 90.45% (test), 90.21% (train), and 88.31% (validation). VGG16 and VGG19 were the next highest performing models. Conversely, ResNet50 demonstrated the poorest performance across all metrics These findings highlight the potential of advanced CNN architectures as a cost-effective and scalable alternative to traditional sensor-based monitoring, providing valuable insights for smart city applications and sustainable urban planning.

Keywords: Air pollution, Deep learning, CNN, Image classification, Smart cities

Introduction

Air pollution is one of the most significant global issues with a negative impact on human health. Exposure to airborne particulate matter, ozone and other pollutants has been linked to higher rates of mortality and hospital admissions for cardiovascular, respiratory and neurological diseases. Major sources of air pollution include energy production, industry, traffic, domestic heating, and agriculture, and the effects are observed even at very low exposure levels. The impacts of air pollution affect multiple organ systems, emphasizing the need for comprehensive disease burden assessments to guide effective prevention strategies (Sigsgaard & Hoffmann, 2024)

Accurate and continuous monitoring of air quality remains challenging due to limitations in measurement infrastructure, restricted geographical coverage and high operational costs. Pollution levels fluctuate significantly depending on meteorological conditions, geographical features and human activities, which makes prediction and monitoring complex. While traditional measurement methods are precise, they are often time-consuming, costly, and unsuitable for large-scale or real-time applications (Marć, et al, 2015). The monitoring and detection of air quality has increasingly incorporated the use of images. The analysis of satellite imagery or aerial photographs can facilitate the drawing of conclusions regarding pollution levels, thereby enabling effective monitoring of large areas. However, due to the sheer volume of data, the use of automated systems is imperative for efficient processing (Pritt et al., 2017).

Deep learning methods have been employed to develop automated systems that have been successfully implemented in various fields for image and signal analysis. These methods have been used in a variety of fields, including healthcare (Pacal & Kılıcarslan, 2023), agriculture (Pacal, et al., 2024), and security (Elmaci, et al., 2024). In particular, CNN-based methods, which essentially imitate the human visual mechanism, have been shown to effectively accomplish those tasks of identifying and classifying objects. Convolutional Neural Networks (CNNs) are used in this study with images related to air quality. Some of the most popular CNN-based architectures were compared, including ResNet50, AlexNet, VGG16, VGG19, Xception, and InceptionV3, as reported in the literature. The performance of the models was evaluated based on the metrics of F1 score, accuracy, recall, and sensitivity.

This study is organized into 5 sections. Section 2 is a review of the literature. Section 3 describes the CNN methods used in this study which are ResNet50, AlexNet, VGG16, VGG19, Xception, and InceptionV3, and the datasets used. Section 4 shows, discusses, and including model performance the experimental results. Section 5 summarises the conclusion and recommendations of the study.

Related Works

Air pollution remains a global challenge and the Air Quality Index (AQI) is often used to quantify it. A range of data sources has been used in the literature to monitor and predict air quality. These include IoT sensors, mobile sensor measurements of gases and particulates, weather data, data on traffic and industrial activity, and satellite/image data. (Tahir Bahadur et al., 2024).

Air quality monitoring using IoT and mobile sensors is ubiquitous. The data collected can be analyzed using a variety of machine learning and deep learning models such as Long Short-Term Memory (LSTM), Convolution Neural Network (CNN), Recurrent Neural Network (RNN), Support Vector Machines (SVM), Random Forest, Gradient Boosting, among other ensemble or statistical methods to predict air pollution with a higher degree of accuracy (Malleswari & Mohana, 2022). Other parameters of air quality measurement, including important meteorological parameters such as temperature, windspeed and humidity, provide useful information for concept models of air quality. These parameters have shown significant correlation factor with air pollutant concentrations, primarily ozone concentrations. By including these parameters in predictive and estimation models, further value can be added in terms of the reliability and validity of air pollution forecasts. This additional value contributes to additional vigilance and monitoring of air pollution to support potential management decisions (McNider & Pour-Biazar 2020).

Air pollution is an emerging pollutant newly developed from the environmental impact of vehicle usage, and industry effects on anthropogenic air pollution. There are potential health consequences with air pollution exposure, with concern related to lung cancer and other infectious diseases being most significant. Our concern around exposure is immediate acute health impact from ultrafine particles in diesel exhaust, volatile organic compounds (VOCs), and other hazardous gases (Forehead & Huynh, 2018).

Air quality can be assessed and measured using either satellite images or aerial images. Both methods can provide large area data on concentrations of pollutants. For satellite systems, pollutants (e.g., PM2.5 and NO2) can be assessed due to scattering and/or absorption of sunlight or emitted radiant flux from various spectral bands (Holloway et al., 2021). An example of this is a scalable deep transfer learning method from satellite imagery, where transfer learning from high-income cities was used to estimate air quality in low-and-middle income cities (Yadav et al., 2022). The methodology focused on Accra, Ghana, where monitoring networks were limited. In another example, Kaushal et al. (2024) classified air quality into good, moderate, and severe categories. They determined the performance of the VGG-19 and ResNet-50 deep learning models for this classification task.

This study utilized CNN-based deep learning methods to classify images of air quality from India and Nepal. The images were classified as Good, Moderate, Unhealthy for Sensitive Groups, Unhealthy, Very Unhealthy and Hazardous/Severe based on the Air Quality Index (AQI). The images were passed through the deep learning models (ResNet50, AlexNet, VGG16, VGG19, Xception, InceptionV3). The methods produced very good results.

Method

In this study, the air images were classed in respect to air quality using deep learning algorithms. As a result, Convolutional Neural Network based algorithms such as ResNet50, AlexNet, VGG16, VGG19, Xception, and

InceptionV3, are used in this study. The dataset is publically available and can be found on Kaggle. The following section describes the dataset and algorithms in detail.

Dataset

The dataset used in this study, titled Air Pollution Image Dataset from India and Nepal, is publicly available and was obtained from Kaggle. It comprises images depicting air pollution conditions across various cities in India and Nepal, totalling 12,240 images, each resized to 224×224 pixels. According to the Air Quality Index (AQI), air quality is classified into six levels: Good (0–50), indicating satisfactory air quality with minimal risk; Moderate (51–100), where air quality is generally acceptable but may pose moderate health concerns for highly sensitive individuals; Unhealthy for Sensitive Groups (101–150), affecting primarily sensitive groups; Unhealthy (151–200), which may impact the general population with more pronounced effects on sensitive groups; Very Unhealthy (201–300), signaling a health alert for everyone; and Hazardous/Severe (301–500), indicating emergency conditions with heightened health risks for all individuals (Rouniyar et al, 2023).

Figure 1 shows one representative image from each Air Quality Index (AQI) category in the dataset The images show a variety of air conditions, ranging from Good to Severe. The set of images shows all six levels of the pollution spectrums.

Figure 1. Sample images from the dataset (Utomo et al, 2023)

Algorithms

In this section, a detailed explanation of the use of the following algorithms ResNet50, AlexNet, VGG16, VGG19, Xception, and InceptionV3 will be provided.

Resnet50

"ResNet" is an abbreviation of "Residual Networks." The ResNet architecture relies on skip connections. They allow for training very deep architectures and improve the vanishing gradient structure of ResNet models. Several versions of ResNet architecture are available, including ResNet18, ResNet34, ResNet50, and ResNet101. ResNet-50 was chosen in this study because it is one of the most widely used and successful ResNet architectures.

ResNet-50 is a deep convolutional neural network (CNN) with a total of 50 layers (48 convolutional and two pooling layers). The structure organizes the layers into bottleneck blocks, which helps maintain performance and keep computation optimal. Using the ResNet-50 architecture allows the model to learn detailed feature maps contained in images and address complex classification problems (He et al., 2016). This research study used ResNet-50 to enhance the accuracy and consistency of classifying air pollution based on images. Figure 2 illustrates the layout of the ResNet-50 architecture. The input for ResNet-50 is a 224×224 RGB image. The image first rotates through a convolutional layer before the first pooling layer. The convolutional layer has 64 filters of 7×7. The first pooling layer is a 3×3 max-pooling layer. ResNet-50 has four identity groups, a 7×7 average-pooling layer, fully connected layers, and a softmax classifier at the output end. The first, second, and third identity group has 3, 4, and 3 identity blocks, consequently.

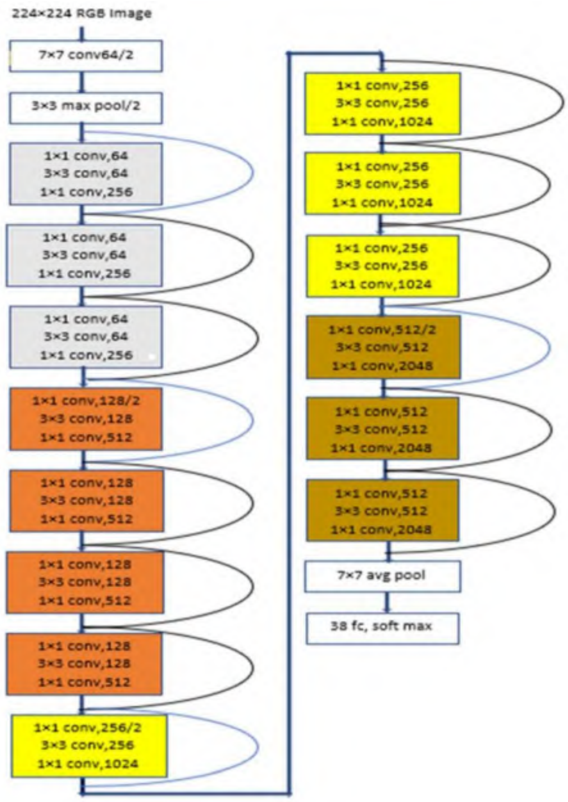

Figure 2. Architecture of ResNet50 (Mukti & Biswas, 2009)

AlexNet

AlexNet was a acquired attention when it won the ImageNet challenge in 2012(Krizhevsky et al., 2012). It set a new standard for image recognition and has since been used in areas like healthcare, farming, self-driving cars, and industrial checks. (Tang et al., 2023; Alom et al., 2020). The architecture of AlexNet is shown in Figure 4. AlexNet takes a 227 × 227 RGB image as input, consists of five convolutional layers and some of the convolutional layers include max-pooling layers, followed by three fully connected layers and a softmax classifier to finish the architecture.

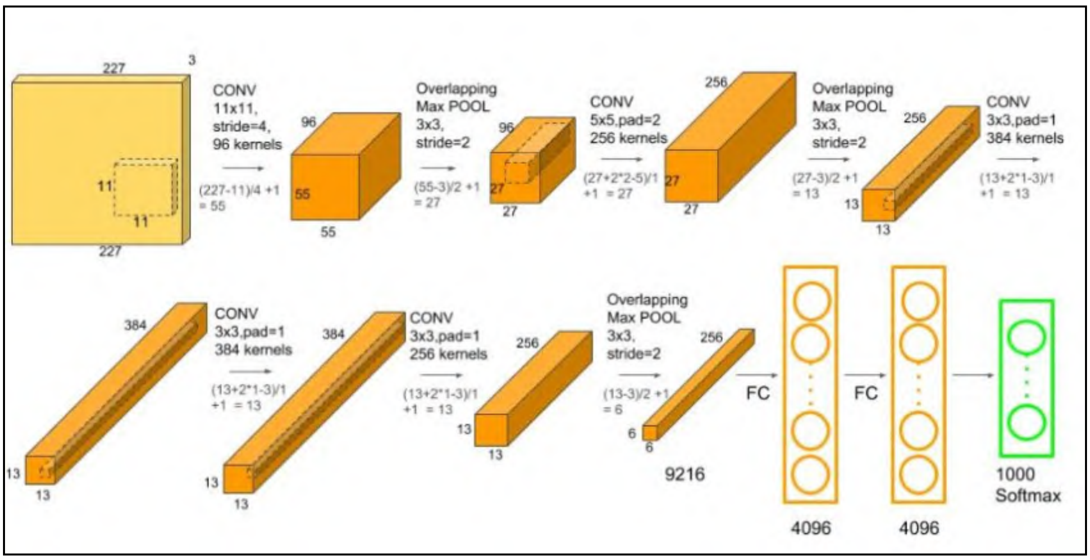

Figure 3. Architecture of AlexNet (Mathivanan et al., 2024)

Visual Geometry Group (VGG)

VGG16 and VGG19, made by the Visual Geometry Group at Oxford. They are made up of 16 and 19 layers and are known for their simple, consistent construction. This architecture uses small (3×3) convolutional filters, and the trend has been to increase depth in networks, as greater depth increases accuracy on large-scale image classification. In the ImageNet Challenge 2014, VGG took first and second place for localization and classification, respectively, and their learned representations generalize well to other datasets, demonstrating state-of-the-art performance (Simonyan & Zisserman, 2014).

The architecture of VGG16 is shown in Figure 4. VGG16 takes a 224×224 RGB image and is made up of thirteen convolutional layers, separated into five blocks of convolutional layers with a max-pooling layer after each block, followed by three fully connected layers and a final softmax classifier.

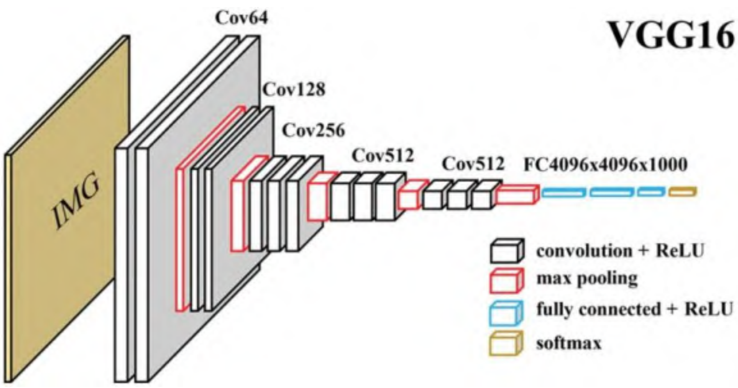

Figure 4. Architecture of VGG16 (Mangalmurti & Wattanapongsakorn, 2022)

The architecture of VGG19 is illustrated in Figure 5. VGG19 takes an RGB input image of 224×224 and has sixteen convolutional layers distributed into five different convolutional blocks, each with a max-pooling layer. It also has three fully connected layers and a final softmax classifier.

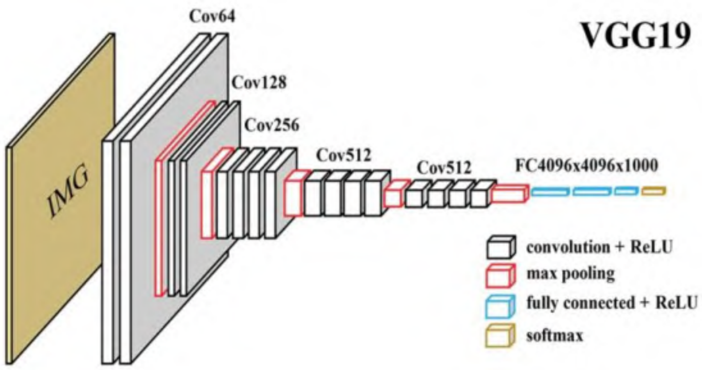

Figure 5. Architecture of VGG16 (Mangalmurti & Wattanapongsakorn, 2022)

InceptionV3

InceptionV3, released in 2016, is an advanced version of earlier Inception models. This version applies factorized convolutions, which improve total accuracy and therefore increase computational efficiency (Szegedy et al., 2016). InceptionV3 has been widely used in computer vision as it captures multi-scale features while minimizing the number of parameters.

InceptionV3 architecture is illustrated in Figure 6. The network receives a 299×299 RGB image as input. The network has a convolutional block made of five convolutional layers, two max-pooling layers, 11 Inception modules, an average pooling layer, and fully connected layers.

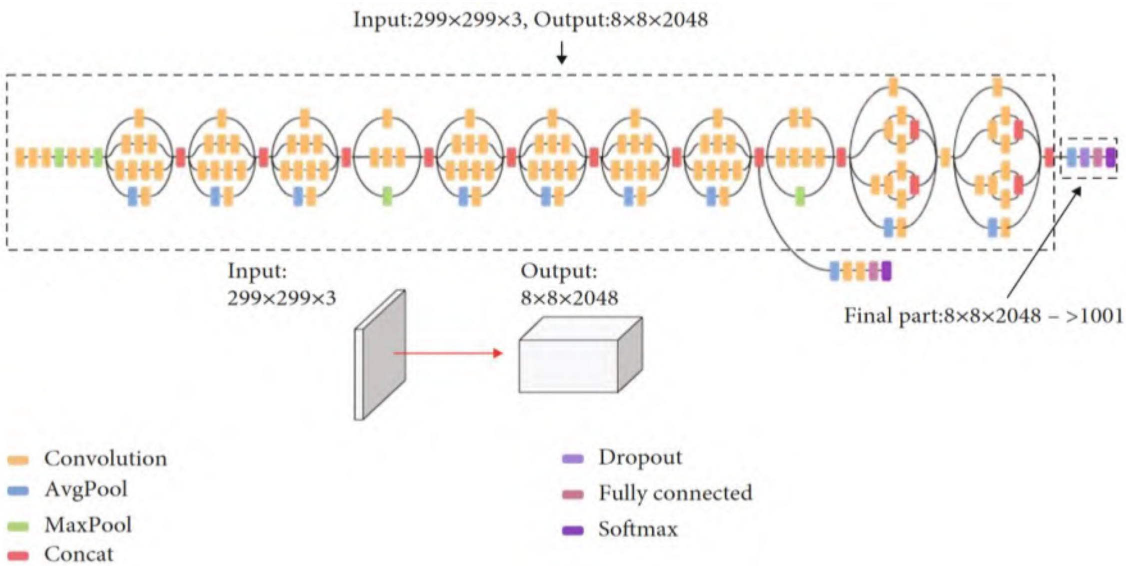

Figure 6. The architecture of InceptionV3 (Ramaneswaran et al., 2021)

Xception

The Xception architecture is an extension of the Inception architecture which François Chollet introduced (Chollet, 2017). This architecture consists of a series of depthwise separable convolution (DWSC) layers interconnect with residual links. The architecture aims to minimize computation and memory consumption (Yang et al., 2020; Gulmez, 2023).

Figure 7 presents the representation of Xception architecture. It accepts a 299×299 RGB image input. The model consists of three parts: entry flow, middle flow, and exit flow. The architecture consists of 36 depthwise separable convolutional layers; However, it can extract features from spatial feature in addition to cross-channel feature. The entry flow is intended for the initial feature extraction and downsampling, the middle flow incorporates a deeper representation and complexity, and the exit flow gathers for classification tasks.

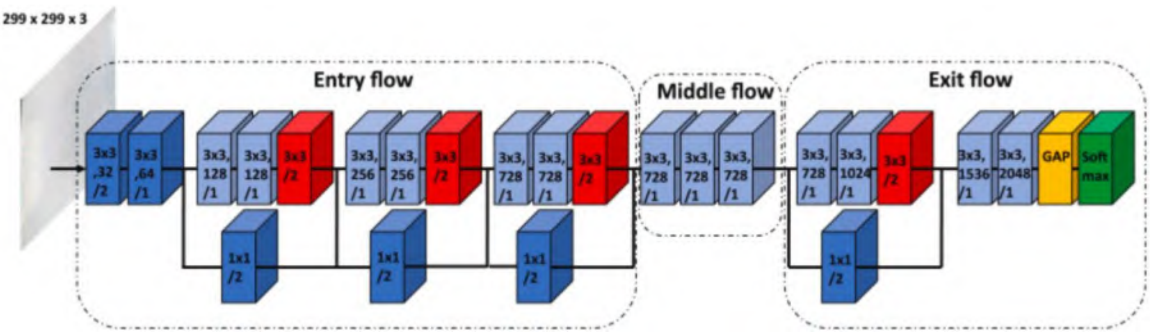

Figure 7. Architecture of Xception (Westphal & Seitz, 2021)

Results and Discussion

In this study, the level of air pollution was predicted using six separate convolutional neural network (CNN) architectures, including ResNet50, AlexNet, VGG16, VGG19, Xception, and InceptionV3. Each model was implemented individually in Google Colab using an NVIDIA A100 GPU. The dataset, comprising environmental images from India and Nepal, was meticulously divided into training (70%), validation (10%), and test (10%) sets, ensuring balanced class distribution through a custom balanced generator. In the context of transfer learning models, the initial layers were subjected to a process of freezing, while the final 10 layers underwent a process of fine-tuning. In contrast, AlexNet was trained from the beginning. The application of data augmentation techniques, encompassing rotation, shifting, shearing, zooming, and horizontal flipping, was employed to enhance the generalisation capabilities of the model. All models were trained for 15 epochs with a batch size of 16 and a learning rate of 1e^{-4} using the Adam optimiser. The training process of all models over 15 epochs is illustrated in Figure 8.

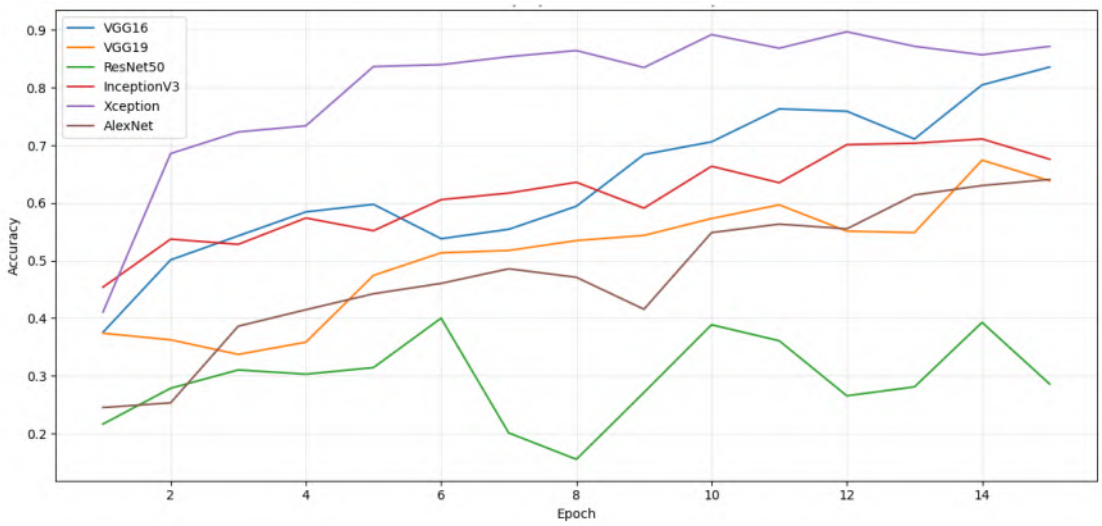

Figure 8. Training process of models

The confusion matrix is a statistical tool that plots model predictions on the x-axis, with the true classes represented on the y-axis. Within each cell, the number of samples allocated to a specific prediction-true class pair is indicated. The values in each cell represent the number of samples that are classified into the predicted-true classes pair. The darker blue shade indicates a greater number of samples that are correctly or incorrectly classified, i.e. a larger congruence of predicted and true classes (Markoulidakis et al., 2021).

The confusion matrix of the ResNet50 model is presented in Figure 9. The model displayed an inability to accurately categorise instances within the Unhealthy_for_Sensitive Groups class. However, it demonstrated a comparatively superior capacity to differentiate the Very-Unhealthy class compared to the other categories. In summary, the other classes showed weaker classification performance.

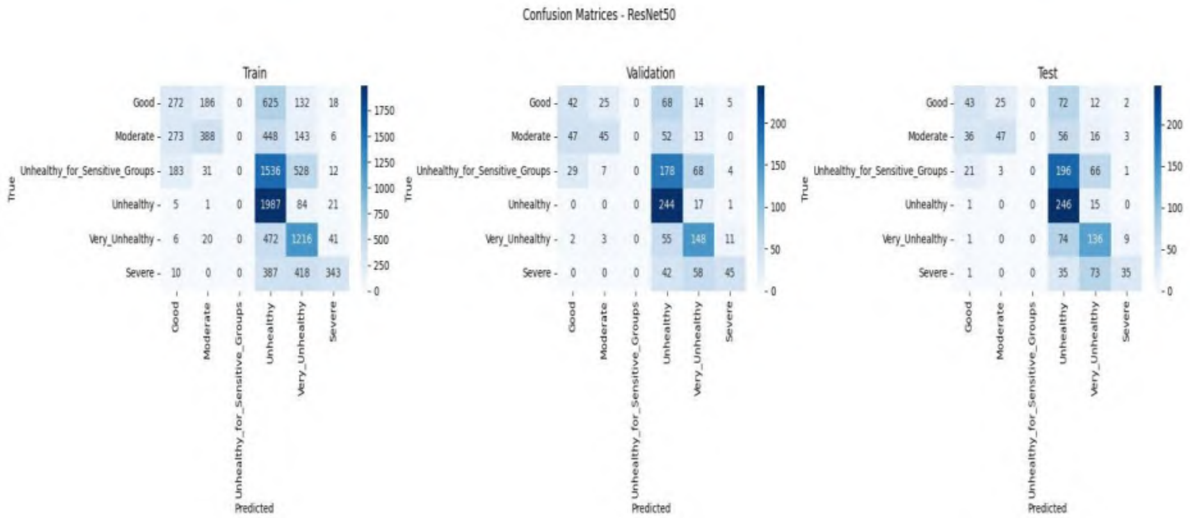

Figure 9. Confusion matrices of Resnet50

The confusion matrix of the AlexNet model is presented in Figure 10. In general, it was demonstrated that AlexNet exhibited superior classification performance in comparison to ResNet50. The model demonstrated higher efficacy in the Unhealthy_for_Sensitive_Groups class. The highest levels of accuracy were achieved in the Severe class. While AlexNet outperformed ResNet50 in distinguishing between distant classes, such as Good–Severe, it still failed to accurately differentiate between closer classes, such as Good–Moderate or Severe–Very Unhealthy.

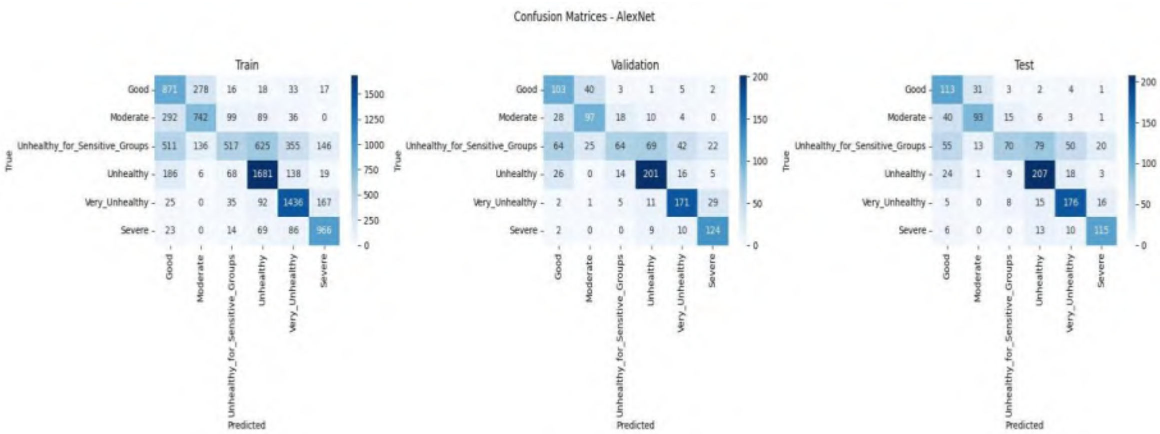

Figure 10. Confusion matrices of AlexNet

The confusion matrix of the VGG16 model is presented in Figure 11. Although the Unhealthy_for_Sensitive_Groups class was the most challenging, the model generally showed strong classification performance. The Unhealthy_for_Sensitive_Groups class is often confused with the Unhealthy and Very_Unhealthy classes, whereas the Unhealthy class itself is correctly classified with good accuracy.

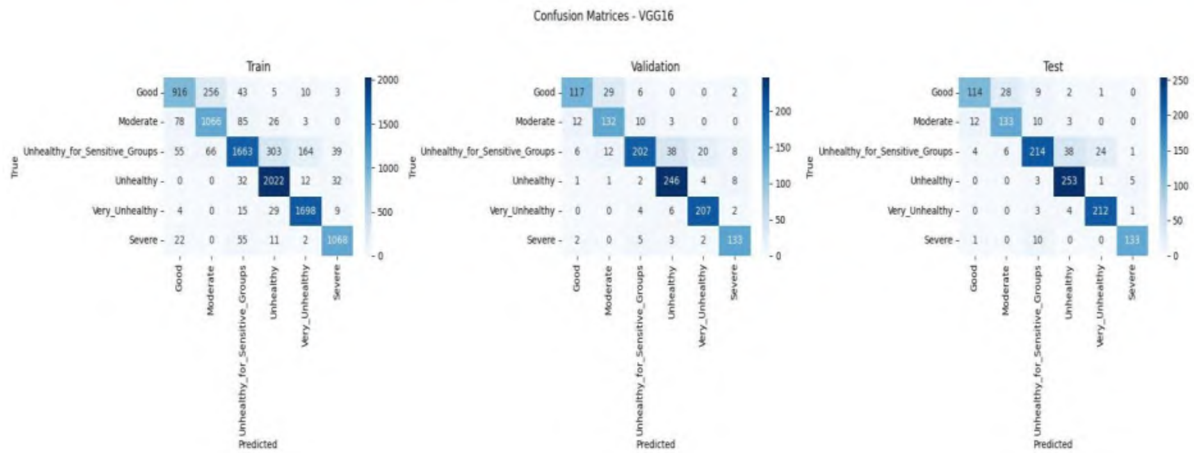

Figure 11. Confusion matrices of VGG16

The confusion matrix of the VGG19 model is presented in Figure 12. Although VGG19 performed better than ResNet50 and AlexNet, it showed lower performance compared to VGG16. The highest accuracy was achieved in the Moderate class, while the lowest performance was observed in the Unhealthy_for_Sensitive_Groups class.

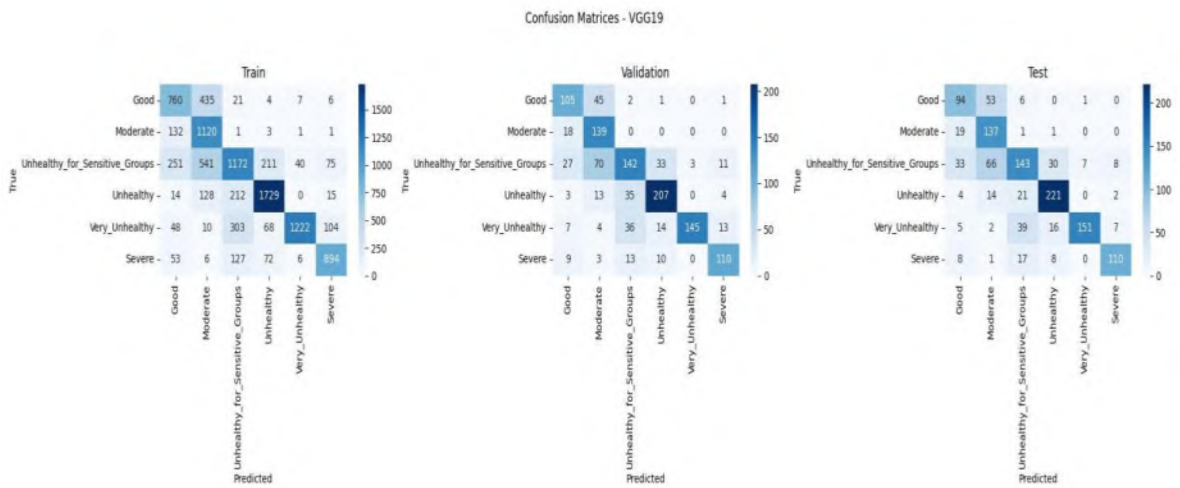

Figure 12. Confusion matrices of VGG19

The confusion matrix of the InceptionV3 model is presented in Figure 13. For the InceptionV3 model, the lowest performance is observed in the Unhealthy for Sensitive Groups class, while the highest accuracy is achieved in the Unhealthy class. The performance of the model in question can be characterised as moderate. Its performance is inferior to that of VGG19, though superior to that of AlexNet and ResNet50.

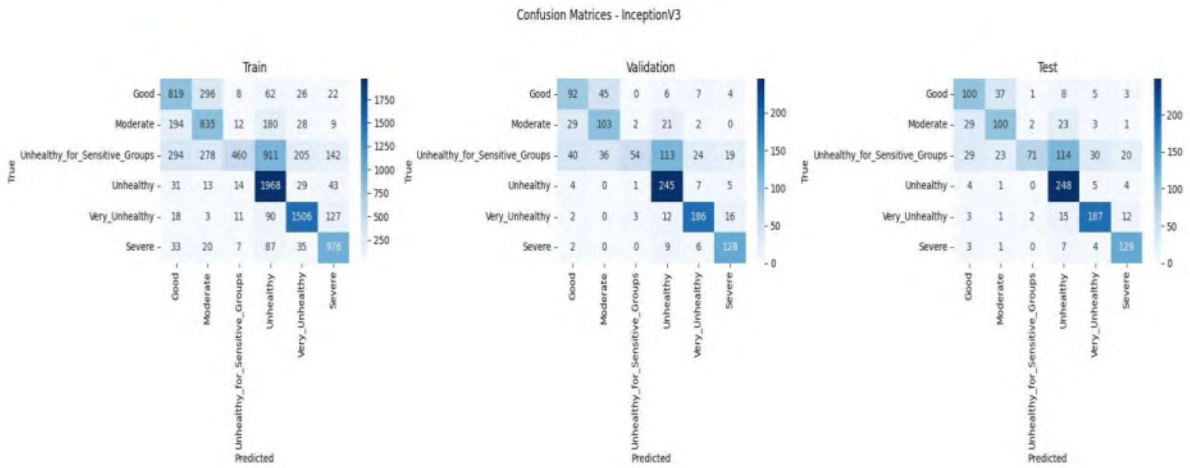

Figure 13. Confusion matrices of InceptionV3

The confusion matrix of the Xception model is presented in Figure 14. Xception demonstrates high performance across nearly all classes and outperforms all other algorithms, including VGG models. The highest accuracy is achieved in the Severe class, while the lowest performance is observed in the Unhealthy for Sensitive Groups class.

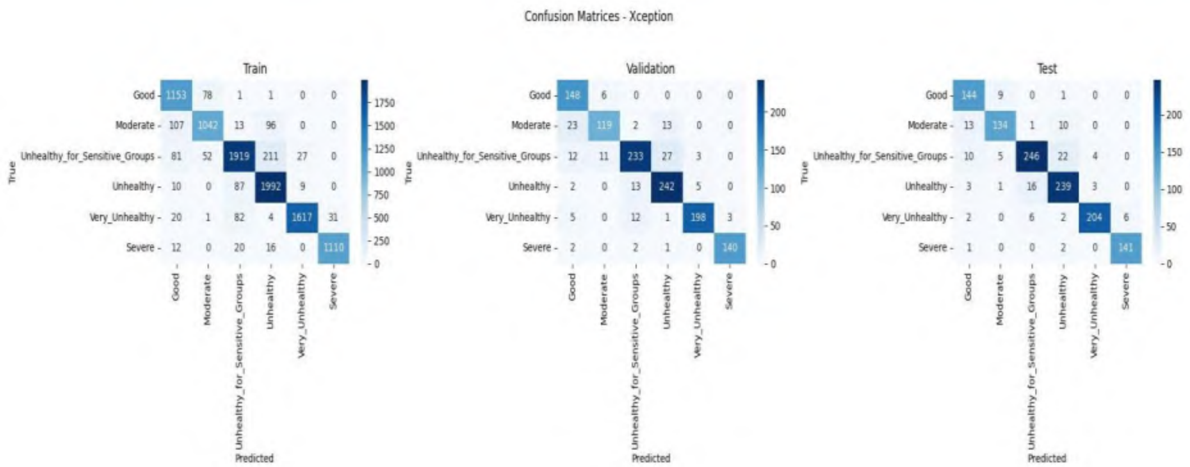

Figure 14. Confusion matrices of Xception

F1-score, precision, and recall are widely accepted metrics for the evaluation of classification performance (Ozcan, 2021; Vakili et al, 2022; Tasyurek & Gul, 2023). Precision is defined as the number of true positives divided by the sum of true positives and false positives. The recall is defined as the number of true positives divided by the sum of true positives and false negatives. The F1-score is considered the harmonic mean of precision and recall. It is one of the methods to characterize model performance in the context of imbalanced classes of the predicted outputs (Yacouby & Axman, 2020; Reddy & Karthikeyan, 2022; Houten et al., 2010).

The classification performance of the models is shown in Table 1, exhibited by accuracy, F1-score, precision, and recall. Based on the evaluation of accuracy, Xception produced the best performance with 90.45% (test), 90.21% (train), and 88.31% (validation). Next came VGG16 with 86.45% (test), 86.12% (train), and 84.79% (validation). Following VGG16, the VGG19 model took third place with 84.79% (test), 70.44% (train), and 69.88% (validation). The InceptionV3 model then came next, producing accuracy estimates of 68.16% (test), 67.03% (train), and 66.07% (validation). The AlexNet model appeared to perform relatively the weakest with 63.45% (test), 63.18% (train), and 62.14% (validation). Lastly, the ResNet50 model produced the weakest results for all accuracy estimates: 42.95% (test), 42.85% (train), and 41.39% (validation). All models illustrated that accuracy measure estimates across training, validation, and test were similar, signifying that there is no evidence of significant overfitting.

Table 1. Performance of models

Model	Accuracy (%)	F1 Score	Precision	Recall
Xception - Test	90.45	0.90	0.91	0.90
Xception - Train	90.21	0.90	0.90	0.90
Xception - Validation	88.31	0.88	0.89	0.88
VGG16 - Test	86.45	0.86	0.87	0.86
VGG16 - Train	86.12	0.86	0.86	0.86
VGG16 - Validation	84.79	0.85	0.85	0.85
VGG19 - Train	70.44	0.71	0.74	0.70
VGG19 - Test	69.88	0.70	0.73	0.70
VGG19 - Validation	69.34	0.70	0.73	0.
InceptionV3 - Test	68.16	0.65	0.73	0.68
InceptionV3 - Train	67.03	0.63	0.72	0.67
InceptionV3 - Validation	66.07	0.62	0.71	0.66
AlexNet - Train	63.45	0.61	0.65	0.63
AlexNet - Test	63.18	0.61	0.65	0.63
AlexNet - Validation	62.14	0.60	0.63	0.62
ResNet50 - Train	42.95	0.35	0.38	0.43
ResNet50 - Validation	42.85	0.35	0.36	0.43
ResNet50 - Test	41.39	0.34	0.37	0.41

Conclusion

The present study focused on the detection and classification of air pollution based on a number of deep learning techniques. Continued concrete evidence of air quality degradation is essential for public health and environmental management. Results from the experiments presented indicate that CNN-based techniques provided robust results, and we found that Xception was the most successful model, ultimately achieving accuracy values of 90.45% (testing), 90.21% (training), and 88.31% (validation). The model overall performed well across most classes, with the most difficult class being the Unhealthy for Sensitive Groups class, which had a lower-than-average classification accuracy compared to the total performance across the other classes. The next best models were VGG16, followed by VGG19, InceptionV3, AlexNet, and finally ResNet50. Moreover, we found that the results across training, validation, and testing were similar across all models, meaning there was no significant evidence of overfitting. The proposed method provides a significant contribution to air quality assessment and could, furthermore, be integrated within autonomous systems and smart city implementations. Future work could improve the performance of the models by combining sensor data with image data. There is also the option to create new deep learning models designed to identify various kinds of pollution. Furthermore, these models can be enhanced in terms of their architecture and training approach, thereby leading to improvements in the accuracy of the models with respect to air quality. In this setting, multimodal data (sensor measurements, meteorological factors, and images) are expected to provide enhanced predictive capabilities. In the interim, transformer-based architecture has the potential to offer enhanced feature extraction capabilities. In addition, the utilisation of approaches to explainable AI is recommended for the purpose of visualising and elucidating model decisions. This approach is expected to result in an enhancement of transparency and confidence in the system's predictions.

Scientific Ethics Declaration

* The author declares that the scientific ethical and legal responsibility of this article published in EPSTEM journal belongs to the author.

Conflict of Interest

* The authors declare that they have no conflicts of interest

Funding

* This study is supported by the Scientific and Technological Research Council of Turkey (TUBITAK) with the 2224-A program.

Acknowledgements or Notes

* This article was presented as an oral presentation at the International Conference on Research in Engineering, Technology and Science (www.icrets.net) held in Peja/Kosovo on July 10-13, 2025.

References

Alom, M. Z., Taha, T. M., Yakopcic, C., Westberg, S., Sidike, P., Nasrin, M. S., ... & Asari, V. K. (2018). The history began from alexnet: A comprehensive survey on deep learning approaches. *arXiv preprint arXiv:1803.01164*.

Chollet, F. (2017). Xception: Deep learning with depthwise separable convolutions. *Proceedings of the IEEE conference on computer vision and pattern recognition* (pp. 1251-1258).

Elmaci, M., Toprak, A. N., & Aslantas, V. (2024). Detection of background forgery using a two-stream convolutional neural network architecture. *Multimedia Tools and Applications, 83*(12), 36739–36766.

Forehead, H., & Huynh, N. (2018). Review of modelling air pollution from traffic at street-level: The state of the science. *Environmental Pollution, 241*, 775–786.

Gulmez, B. (2023). A novel deep neural network model based Xception and genetic algorithm for detection of COVID-19 from X-ray images. *Annals of Operations Research*, *328*(1), 617-641.

He, K., Zhang, X., Ren, S., & Sun, J. (2016). Deep residual learning for image recognition. *Proceedings of the IEEE Conference on Computer Vision and Pattern Recognition* (pp. 770–778).

Holloway, T., Miller, D., Anenberg, S., Diao, M., Duncan, B., Fiore, A. M., … & Zondlo, M. A. (2021). Satellite monitoring for air quality and health. *Annual Review of Biomedical Data Science, 4*(1), 417–447.

Houten, W., Geradts, Z., Franke, K., Veenman, C. (2010). Verification of video source camera competition (CAMCOM 2010). In D. Unay, Z. Çataltepe, S. Aksoy (eds.), *Recognizing patterns in signals, speech, ımages and videos*. Springer, Berlin, Heidelberg.

Kaushal, R. K., Pandey, H., Kalaiarasi, G., Arya, S., & Rawat, D. (2024). Evaluation of deep learning approaches for air quality analysis using an image dataset. *2024 Second International Conference on Intelligent Cyber Physical Systems and Internet of Things (ICoICI)* (pp. 1378–1383). IEEE.

Koonce, B. (2021). ResNet 50. In *Convolutional neural networks with swift for tensorflow: image recognition and dataset categorization* (pp. 63–72). Berkeley, CA: Apress.

Krizhevsky, A., Sutskever, I., & Hinton, G. E. (2012). ImageNet classification with deep convolutional neural networks. *Advances in Neural Information Processing Systems, 25*. https://proceedings.neurips.cc/paper/2012/file/c399862d3b9d6b76c8436e924a68c45b-Paper.pdf

Marć, M., Tobiszewski, M., Zabiegała, B., de la Guardia, M., & Namieśnik, J. (2015). Current air quality analytics and monitoring: A review. *Analytica Chimica Acta, 853*, 116–126.

Mangalmurti, Y., & Wattanapongsakorn, N. (2022). Practical machine learning techniques for COVID-19 detection using chest X-ray images. *Intelligent Automation & Soft Computing, 34*(2), 733-752.

Mathivanan, S. K., Francis, D., Srinivasan, S., Khatavkar, V., P, K., & Shah, M. A. (2024). Enhancing cervical cancer detection and robust classification through a fusion of deep learning models. *Scientific Reports, 14*(1), 10812.

Malleswari, S. M. S. D., & Mohana, T. K. (2022). Air pollution monitoring system using IoT devices. *Materials Today: Proceedings, 51*, 1147–1150.

Markoulidakis, I., Kopsiaftis, G., Rallis, I., & Georgoulas, I. (2021, June). Multi-class confusion matrix reduction method and its application on net promoter score classification problem. *Proceedings of the 14th PErvasive technologies related to assistive environments conference* (pp. 412-419).

McNider, R. T., & Pour-Biazar, A. (2020). Meteorological modeling relevant to mesoscale and regional air quality applications: A review. *Journal of the Air & Waste Management Association, 70*(1), 2–43.

Mukti, I. Z., & Biswas, D. (2019, December). Transfer learning based plant diseases detection using ResNet50. *2019 4th International Conference on Electrical Information and Communication Technology (EICT)* (pp. 1–6). IEEE.

Ozcan, T. (2021). A new composite approach for COVID-19 detection in X-ray images using deep features. *Applied Soft Computing*, *111*, 107669.

Pacal, I., Kunduracioglu, I., Alma, M. H., Deveci, M., Kadry, S., Nedoma, J., … & Martinek, R. (2024). A systematic review of deep learning techniques for plant diseases. *Artificial Intelligence Review, 57*(11), 304.

Pacal, I., & Kılıcarslan, S. (2023). Deep learning-based approaches for robust classification of cervical cancer. *Neural Computing and Applications, 35*(25), 18813–18828.

Pritt, M., & Chern, G. (2017, October). Satellite image classification with deep learning. In *2017 IEEE Applied Imagery Pattern Recognition Workshop (AIPR)* (pp. 1–7). IEEE.

Ramaneswaran, S., Srinivasan, K., Vincent, P. D. R., & Chang, C. Y. (2021). Hybrid inception v3 XGBoost model for acute lymphoblastic leukemia classification. *Computational and Mathematical Methods in Medicine*, *2021*(1), 2577375.

Reddy, B. H., & Karthikeyan, P. R. (2022, November). Classification of fire and smoke images using decision tree algorithm in comparison with logistic regression to measure accuracy, precision, recall, F-score. *2022 14th International Conference on Mathematics, Actuarial Science, Computer Science and Statistics (MACS)* (pp. 1-5). IEEE.

Rouniyar, A., Utomo, S., A. J., & Hsiung, P.-A. (2023). *Air pollution image dataset from India and Nepal (Data set). Kaggle*. Retrieved from https://doi.org/10.34740/kaggle/ds/3152196

Simonyan, K., & Zisserman, A. (2014). Very deep convolutional networks for large-scale image recognition. *arXiv preprint arXiv:1409.1556*.

Tahir Bahadur, F., Rasool Shah, S., & Rao Nidamanuri, R. (2024). Air pollution monitoring and modelling: An overview. *Environmental Forensics, 25*(5), 309–336.

Tang, W., Sun, J., Wang, S., & Zhang, Y. (2023). Review of AlexNet for medical image classification. *arXiv preprint arXiv:2311.08655*.

Tasyurek, M., & Gul, E. (2023). A new deep learning approach based on grayscale conversion and DWT for object detection on adversarial attacked images. *The Journal of Supercomputing*, *79*(18), 20383-20416.

Utomo, S., Rouniyar, A., Jiang, G. H., Chang, C. H., Tang, K. C., Hsu, H. C., & Hsiung, P. A. (2023, September). Eff-AQI: An efficient CNN-based model for air pollution estimation: A study case in India. *Proceedings of the 2023 ACM Conference on Information Technology for Social Good* (pp. 165–172).

Vakili, M., Ghamsari, M., & Rezaei, M. (2020). Performance analysis and comparison of machine and deep learning algorithms for IoT data classification. *arXiv preprint arXiv:2001.09636*.

Yacouby, R., & Axman, D. (2020). Probabilistic extension of precision, recall, and f1 score for more thorough evaluation of classification models. *Proceedings of the first workshop on evaluation and comparison of NLP systems* (pp. 79-91).

Yadav, N., Sorek-Hamer, M., Von Pohle, M., Asanjan, A. A., Sahasrabhojanee, A., Suel, E., … & Ganguly, A. R. (2022). Deep transfer learning on satellite imagery improves air quality estimates in developing nations. *arXiv preprint arXiv:2202.08890.*

Yang, L., Tao, L., Chen, X., & Gu, X. (2020). Multi-scale semantic feature fusion and data augmentation for acoustic scene classification. *Applied Acoustics*, *163*, 107238.

Szegedy, C., Vanhoucke, V., Ioffe, S., Shlens, J., & Wojna, Z. (2016). Rethinking the inception architecture for computer vision. *Proceedings of the IEEE conference on computer vision and pattern recognition* (pp. 2818-2826).

Sigsgaard, T., & Hoffmann, B. (2024). Assessing the health burden from air pollution. *Science, 384*(6691), 33–34.

Westphal, E., & Seitz, H. (2021). A machine learning method for defect detection and visualization in selective laser sintering based on convolutional neural networks. *Additive Manufacturing*, *41*, 101965.

Author(s) Information

Fatma Ozge Ozkok
Erciyes Univesity, Department of Computer Engineering, Turkiye
FOMOTECH R&D, Erciyes Technopark, Turkiye
Contact e-mail: fozgeozkok@*erciyes.edu.tr*

To cite this article:

Ozkok, F. O. (2025). Image-based air pollution classification using deep learning techniques. *The Eurasia Proceedings of Science, Technology, Engineering and Mathematics (EPSTEM), 35,* 302-313.

The Eurasia Proceedings of Science, Technology, Engineering and Mathematics (EPSTEM), 2025

Volume 35, Pages 314-322

ICRETS 2025: International Conference on Research in Engineering, Technology and Science

Scheduling in Flexible Flow Shop Environments with Re-Entrant Jobs and Heterogeneous Workers

Seyma Bekli
Abdullah Gul University

Betul Kayisoglu
Abdullah Gul University

Abstract: In many industries, manufacturing is organized as a flexible flow shop (FFS), which has gotten the researchers' attention. The scheduling studies, particularly those on FFS scheduling, are concerned with homogeneous workers with the same skill set or heterogeneous workers who can only perform one specific type of operation on the production lines. Moreover, jobs are mainly assumed to go through an operation once. Yet, in real-life production, workers might have different skill sets with varying processing times. Furthermore, certain jobs may require revisiting the same machine multiple times, i.e., re-entrant jobs. We study an FFS environment with re-entrant jobs, considering worker flexibility. We propose a mixed integer linear programming model to find the optimal sequences of jobs to be processed by the multiskilled workers assigned to the production system, ensuring each re-entrant job waits for a predefined time window before reprocessing on the same operation. The objective of the model is to minimize makespan. We tested the proposed model on a dataset taken from a real production system of a PVC windows and doors production facility.

Keywords: Production scheduling, Re-entrant scheduling, Sustainable manufacturing, Integer programming model, Multiskilled labour assignment

Introduction

Scheduling the manufacturing operations aims to set the timing and the order of manufacturing activities while achieving production goals. Scheduling increases efficiency, resource utilization, customer satisfaction, and business competitiveness; therefore, optimizing schedules is crucial for businesses. Researchers have widely studied scheduling since the study of Johnson (1954). It remains a focus for researchers owing to new manufacturing techniques, different requirements of resources and jobs, and the complexity of the problem. Among the different scheduling settings, flow shop environments have been broadly studied due to their widespread industrial and economic applications (Komaki et al., 2019). In flow shops, the jobs are processed at the machines in the same predefined order, following a fixed linear structure. Flexible flow shops extend the flow shop by allowing parallel machines in at least one of the stages of production.

A particular variant of flexible flow shop systems, re-entrant flexible flow shops, requires some jobs to go through certain processes more than once, making it more complex than standard flow shop systems. Such systems are often observed in semiconductor wafer manufacturing, mirror manufacturing, construction, dyeing processes, and panel line manufacturing (El-Khouly et al., 2009; Kayisoglu et al., 2024). Systems involving re-entrant components present further considerations and require attention to the duration between successive visits to the machine and the timing and sequencing of these re-entry processes.

Another aspect that highly affects the schedules is the competencies of the workers within the flexible flow shop production lines. Worker allocation of a multiskilled heterogeneous workforce impacts the overall performance

- Selection and peer-review under responsibility of the Organizing Committee of the Conference

of the production system and resource utilization (Costa et al., 2014). Instead of waiting for the jobs and work to arrive at a station, multiskilled workers can effectively rotate between the processes in which they are experts. Although this situation results in fewer workers being needed in the production area, having a multiskilled workforce will increase the complexity of work schedules as it requires resolving conflicts in task assignments - challenges not seen in systems where homogeneous workers are present and work at only one workstation/machine.

In this study, we focused on a flexible flow shop system in which jobs may revisit certain machines multiple times. Moreover, the machine operators are assumed to operate multiple machines. This study proposes a mathematical model that examines the re-entrant requirements of particular jobs while effectively leveraging the heterogeneity of multiskilled workers.

The structure of the paper is as follows. First, we review related literature in the next section. Second, we present the problem and a mixed integer linear programming model for the re-entrant flexible flow shop scheduling considering a multiskilled workforce. This is followed by a real-life case from a PVC Windows and Doors production facility that represents the problem. We report the results in the Computational Experiments section. Finally, we provide concluding remarks and highlights for future directions.

Related Literature

The flow shop scheduling problem has been the focus of a considerable number of studies in the literature. The readers are referred to Ruiz and Vázquez-Rodríguez (2010) for a review on hybrid flow shop scheduling, to Rossit et al. (2018) for an in-depth analysis of non-permutation flow shop scheduling, to Nasser et al. (2021) for a review on permutation flow shop scheduling, and to Komaki et al. (2019) for a literature review on flow shop scheduling with a focus on assembly operations.

Here, we first briefly introduce the literature on flow shop scheduling with re-entrant jobs. Graves et al. (1983) introduced the concept of re-entrant jobs in a flow shop environment. A heuristic algorithm is developed to create schedules and tested at an integrated circuit chip fabrication plant. Wang et al. (1993) showed that minimizing makespan in a re-entrant flow shop environment is NP-hard even in very restricted settings. Chen et al. (2008) studied minimizing the makespan in re-entrant flow shops and proposed hybrid genetic algorithms. They have demonstrated that hybrid genetic algorithms work well in finding near-optimal solutions. (Hassanpour et al., 2015) studied the re-entrant no-wait flow shop scheduling problem, where a job is processed continuously from the initiation of the first process to the completion of the last. A mathematical model and three heuristic algorithms, based on simulated annealing, genetic algorithm, and bottleneck heuristic, respectively, were proposed. It is concluded that, simulated annealing type heuristic outperforms the other two heuristic algorithms. Chamnanlor et al. (2017) studied the re-entrant hybrid flow shop systems with the consideration of time windows. It is considered that a job's start time of the first operation and end time of the last operation should fall into a certain time window. A mixed integer linear programming model was constructed in order to minimize the makespan. As a solution algorithm for large-sized problems, the ant colony algorithm was embedded in a genetic algorithm, which outperforms both simple genetic and ant colony algorithms. Geng et al. (2022) studied re-entrant hybrid flow shop systems with sequence-dependent setup times and factory eligibility considerations. They assumed that available machinery may vary from one factory to another, or some jobs may not be produced at certain factories. This mimics real-life conditions, leading to the consideration of factory eligibility. They proposed an artificial bee colony algorithm to minimize makespan and total energy consumption.

Next, we examine the related literature on a multiskilled workforce in flow shop environments. Liu and Yang (2019) worked in a hybrid flow shop to schedule multi-skilled worker assignments. They have formulated a bi-objective mixed integer linear model to minimize makespan and total flow time and solved it through the epsilon-constraint method. Costa et al. (2014) studied the flow shop sequence dependent group scheduling problem with the consideration of skilled workforce assignment. First, a mixed integer linear programming model that aims to minimize the makespan is created, and then a genetic algorithm-based heuristic is proposed. It is concluded that, with a higher number of machines, multiskilled worker assignments have a greater impact on minimizing the makespan. Fekri et al. (2024) examined a flexible flow shop environment with multiple skilled workers. Like Liu and Yang (2019), they have created a bi-objective mixed integer linear programming model, in which the objectives are minimizing total idle time of the workers and minimizing the makespan. A genetic algorithm and a simulated annealing algorithm are proposed as heuristic algorithms for the given problem. It is concluded that the genetic algorithm outperforms the simulated annealing algorithm in terms of performance at the large-scale instances.

Chu et al. (2018) examined both re-entrant jobs and workers with different abilities in flow shop environments. They have proposed a mixed integer linear programming model that minimizes the number of tardy jobs. A hill-climbing algorithm and a genetic algorithm are developed as solution algorithms to the given problem. The algorithms were tested on a generated dataset, and the results demonstrate that the genetic algorithm provides better solutions.

Similar to Chu et al. (2018), our study investigates re-entrant jobs and multiskilled workers but within the context of a flexible flow shop environment. Our study aims to minimize the makespan of the system. We have provided a mixed integer linear programming model that incorporates both assignments of the jobs (including re-entrant and non-reentrant) and multiskilled labour to the machines. This study reflects real-world production challenges in re-entrant flow shops where multiple competencies among the workers are observed.

Problem Definition and Proposed Mathematical Model

An extension of the traditional Flexible Flow Shop Scheduling Problem (FFSSP) involves incorporating worker capabilities such as skill levels, efficiency, and processing speeds. Ozpacaci et al. (2025) refer to FFSSP with worker capabilities as the Flexible Flow Shop Scheduling Problem with Heterogeneous Worker Assignment (FFSSP_HWA). In this study, similarly, we address FFSSP by considering worker heterogeneity in terms of both worker capability to perform the operations and the variability in processing times that reflects processing efficiencies of workers. Additionally, we introduce re-entrant jobs, where certain jobs require repeated processing at specific operations after a waiting period, such as a drying phase, before proceeding to the remaining operations. As a result, we focus on an advanced version of FFSSP_HWA, which we refer to as the Re-entrant Flexible Flow Shop Scheduling Problem with Heterogeneous Worker Assignment (RFFSSP_HWA). We modify the modeling framework proposed by Ozpacaci et al. (2025) for the FFSSP_HWA and extend it to include re-entrant jobs.

We use the same sets, parameters, and decision variables as those defined by Ozpacaci et al. (2025) and moreover introduce additional elements to extend their model. Let J denote the set of jobs, where $j, j' \in J$. Each job j may consist of a different number of orders, represented by n_j. Jobs are composed of a sequence of operations performed in a specific order. Let I be the set of operations, where $i, i' \in I$. A precedence relationship exists among operations, ensuring that each job follows its designated operation sequence. Furthermore, once an operation for a given job has started, no subsequent operation from the same job can begin until the current operation is fully completed for all n_j units. The variables X_{ij} and C_{ij} represent the start and completion times of operation i for job j, respectively.

In this problem, we also have re-entrant jobs for certain operations. That is, a job is processed by a certain operation, and after a waiting period, it re-enters the same operation for a second processing. When a job is processed a second time on the operation i, we denote this re-entrant operation as $\hat{\imath}$ where $\hat{\imath} \in I$. After this re-entrant step and an additional waiting period, the job is processed for the remaining subsequent operations as usual. If job j has a re-entrant operation i, we define the pair $(i, j) \in R$. This is all to say, the set R includes all (i, j) pairs for which job j must undergo a second processing on operation i. If pair $(i, j) \in R$, then job j has a waiting period after its processing on operation i. We represent this waiting time by the parameter b_{ij}. On the contrary, if pair $(i, j) \notin R$, then $b_{ij} = 0$, showing that no waiting period is required.

In RFFSSP_HWA, the scheduling environment involves workers with heterogeneous skill levels. Let W be the set of workers. Each worker may only be capable of performing certain operations, which is denoted by the binary parameter a_{iw}: it takes the value 1 if worker w is qualified to perform operation i, and 0 otherwise. Moreover, differences in experience and efficiency of workers are reflected in their processing speed for each operation. To account for this, the parameter p_{ijw} represents the processing time required to complete a single order of job j at operation i when assigned to worker w. Worker assignments are represented by the binary variable O_{ijw}, which is equal to 1 if worker w is assigned to operation i of job j. Since the assigned worker determines the actual processing time of operations, P_{ij} is a decision variable to represent the total processing time of job j for operation i. The model also includes a precedence variable $Y_{ii'jj'}$ that takes the value 1 if operation i of job j is scheduled to start before operation i' of job j', and 0 otherwise. The objective in RFFSSP_HWA is to minimize the makespan, denoted by C_{max}, that corresponds to the completion time of the last job in the schedule.

Sets, Parameters, and Decision Variables for RFFSSP_HWA

Sets

I	$Set\ of\ operations\ where\ i, i', \hat{\imath} \in\ I$
J	$Set\ of\ jobs$ where $j, j' \in\ J$
W	$Set\ of\ workers$
R	$Set\ of\ re-entrant\ (i,j)\ pairs$

Parameters

a_{iw}	$1\ if\ worker\ w\ is\ capable\ of\ performing\ operation\ i, 0\ otherwise$
p_{ijw}	$Processing\ time\ of\ job\ j\ for\ operation\ i\ done\ by\ worker\ w$
n_j	$Number\ of\ orders\ of\ job\ j$
b_{ij}	$Waiting\ period\ of\ job\ j\ after\ its\ processing\ on\ operation\ i$
M	$Arbitrary\ large\ number$

Decision Variables

C_{max}	$Makespan\ (the\ time\ at\ which\ the\ last\ job\ finishes\ processing)$
X_{ij}	$Start\ time\ of\ operation\ i\ for\ job\ j$
C_{ij}	$Completion\ time\ of\ operation\ i\ for\ job\ j$
P_{ij}	$Processing\ time\ of\ operation\ i\ for\ job\ j$
O_{ijw}	$1, if\ worker\ w\ is\ assigned\ to\ operation\ i\ of\ job\ j, \quad 0\ otherwise.$
$Y_{ii'jj'}$	$1, if\ operation\ i\ of\ job\ j\ starts\ before\ operation\ \ i'\ of\ job\ j', \quad 0\ otherwise.$

Based on the above definitions, the mathematical formulation for RFFSSP_HWA is presented below*:*

$$Z = \text{Min } C_{max} \tag{1}$$

s.t.

$$C_{ij} \leq C_{max} \qquad \forall i \in I, \forall j \in\ J \tag{2}$$

$$C_{ij} = X_{ij} + P_{ij} \qquad \forall i \in I, \forall j \in\ J \tag{3}$$

$$\sum_{w} O_{ijw} = 1 \qquad \forall i \in I, \forall j \in\ J \tag{4}$$

$$X_{ij} + P_{ij} \leq X_{i+1,j} \qquad \forall i \in I\ and\ i \neq |I|, \forall j \in\ J, \forall\ \text{ij} \notin R \tag{5}$$

$$X_{ij} + P_{ij} + b_{ij} \leq X_{\hat{\imath}j} \qquad \forall i \in I\ and\ i \neq |I|, \forall j \in\ J, \forall\ \text{ij} \in R \tag{6}$$

$$X_{\hat{\imath}j} + P_{\hat{\imath}j} +\ b_{ij} \leq X_{i+1,j} \qquad \forall i \in I\ and\ i \neq |I|, \forall j \in\ J, \forall\ \text{ij}\ \in R \tag{7}$$

$$X_{\hat{\imath}j} = 0 \qquad \forall\ \text{ij} \notin R \tag{8}$$

$$C_{\hat{\imath}j} = 0 \qquad \forall\ ij \notin R \qquad (9)$$

$$X_{ij} + P_{ij} \leq X_{i'j} + M\big(1 - Y_{ii'jj}\big) \qquad \forall i, i' \in I, \forall j \in J \qquad (10)$$

$$X_{ij} \leq X_{i'j'} + M\big(1 - Y_{ii'jj'}\big) \qquad \forall i, i' \in I, \forall j, j' \in J \qquad (11)$$

$$X_{ij} + P_{ij} \leq X_{i'j'} + M\big(3 - Y_{ii'jj'} - O_{ijw} - O_{i'j'w}\big) \qquad \forall i, i' \in I, \forall j, j' \in J, \forall w \in W \qquad (12)$$

$$O_{ijw} \leq a_{iw} \qquad \forall i \in I, \forall j \in J, \forall w \in W \qquad (13)$$

$$Y_{ii'jj'} + Y_{i'ij'j} = 1 \qquad \forall i, i' \in I \text{ and } i \neq i', \forall j, j' \in J \text{ and } j \neq j' \qquad (14)$$

$$P_{ij} = \textstyle\sum_w p_{ijw}\, n_j\, O_{ijw} \qquad \forall i \in I, \forall j \in J \qquad (15)$$

$$P_{ij}, X_{ij}, C_{ij} \geq 0 \qquad \forall i \in I, \forall j \in J \qquad (16)$$

$$Y_{ii'jj'} \in \{0,1\} \qquad \forall i, i' \in I, \forall j, j' \in J \qquad (17)$$

$$O_{ijw} \in \{0,1\} \qquad \forall i \in I, \forall j \in J, \forall w \in W \qquad (18)$$

Objective function (1) minimizes makespan, i.e., the completion time of the final job in the schedule. Constraints (2) enforce the makespan to be no less than the completion time of any job in the system. Constraints (3) compute the completion time for each job operation by summing its start time and the corresponding processing duration. Constraints (4) ensure that each operation is assigned to exactly one worker. Constraints (5) enforce that the start time of any operation must follow the completion time of its immediate predecessor for non-re-entrant jobs. Constraints (6) ensure that for each re-entrant pair $(i, j) \in R$, job j re-enters operation i denoted as $\hat{\imath}$ only after the given waiting time has elapsed after its completion at operation i. Constraints (7) control the flow of re-entrant jobs by ensuring that, for every pair $(i, j) \in R$, job j continues its subsequent operations only after completing the re-entrant step at operation $\hat{\imath}$ and the associated waiting period. Constraints (8) and (9) respectively enforce that the start and end times of the re-entrant operation $\hat{\imath}$ are set to zero for jobs that do not require re-entry at operation i. Constraints (10) find the order of operations for each job and define the corresponding values of the precedence variable $Y_{ii'jj}$. Constraints (11) ensure that if $Y_{ii'jj'}$=1, then operation i of job j must begin before operation i' of job j'. Constraints (12) prevent scheduling conflicts by coordinating the order of operations across all jobs and ensuring that no worker is assigned to more than one operation at the same time. Constraints (13) allow assignments only where a worker is capable of performing the given operation. Constraints (14) ensure that either operation i of job j starts before operation i' of job j', or vice versa. Constraints (15) determine the processing time of operation i for job j based on the assigned worker w, accounting for worker-specific efficiency. Finally, Constraints (16) through (18) define the decision variables.

Case Study in a PVC Window and Door Manufacturing System

We consider a real-world case study from a company manufacturing PVC windows and doors to evaluate the applicability of the proposed RFFSSP_HWA (Re-entrant Flexible Flow Shop Scheduling Problem with Heterogeneous Worker Assignment) model. The company has a make-to-order production system, fulfilling large-scale orders for entire buildings. These orders are diverse, varying in terms of color, dimensions, opening mechanisms, glass specifications, and component configurations. In our study, each order is referred to as a job that must undergo a fixed sequence of 14 operations. These operations ranging from initial lamination of PVC profiles to packaging are mandatory for all the jobs and follow a strict precedence relationship illustrated in Figure 1. Once the processing of a job starts on an operation, it must be completed without interruption, i.e., no preemption is allowed. Furthermore, the subsequent operation for a job can only begin once the current operation has been fully completed for the entire job quantity.

A typical feature of this case is the presence of re-entrant jobs, specifically for the first operation (lamination). Some orders have different colors on the interior and exterior sides of the profile, requiring lamination twice. In such cases, the exterior or interior side is laminated first. The profile must then wait for a certain time to allow the adhesive material to dry before re-entering lamination for the side not laminated. After this second lamination process, the job can proceed to the subsequent operations.

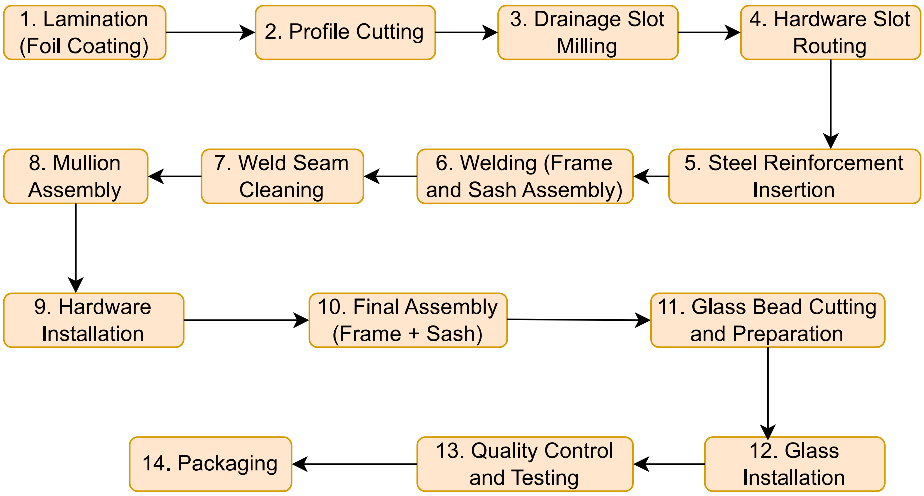

Figure 1. Operation sequence with precedence relationships for PVC window manufacturing

The company employs 10 workers, each with varying skills and experience. As a result, processing times vary, influenced by worker efficiency and familiarity with each specific operation. Every operation requires the assignment of one worker, and worker capabilities significantly affect the total processing time. Currently, for each planning horizon, the company manually prepares the production schedule and assigns workers to operations based on capability and experience. However, this manual scheduling often leads to several challenges, including inefficient resource utilization, scheduling conflicts, and production delays. To address these inefficiencies, the proposed RFFSSP_HWA model is applied to generate a schedule that minimizes the makespan without scheduling conflicts.

For this case study, we consider a one-week planning horizon with five working days, each consisting of an 9-hour shift, resulting in a total available production time of 45 hours. The company has received five different orders for this planning horizon, each with varying order quantities. Among these, Job 1, Job 2, and Job 4 require dual-color lamination and are therefore re-entrant for lamination operation. At the beginning of the planning horizon, all machines and workers are assumed to be available, and no job prioritization is considered. With the proposed model for RFFSSP_HWA, for this case study, we will be able to get the production schedule and assign workers to operations automatically without scheduling conflicts. Since we minimize the makespan, we will also avoid inefficient use of resources and delays in production.

Computational Experiments with the Mathematical Model for RFFSSP_HWA

The case study, which focuses on a real-world PVC window and door manufacturing system, was solved using the proposed RFFSSP_HWA model. The optimal solution was successfully obtained using IBM ILOG CPLEX. The resulting objective function value, corresponding to the makespan, is 2,396 minutes. This outcome confirms that the entire production schedule is possible within the specified planning horizon of 45 hours (i.e., 2,700 minutes).

A detailed visualization of the obtained schedule is illustrated in Figure 2, which shows the Gantt chart of all jobs and their corresponding operations. The Gantt chart clearly indicates that all precedence constraints are satisfied, as each job's operations are executed in the correct order without any violations. The makespan is determined by the completion time of the final operation in Job 4.

The most distinctive feature of the RFFSSP_HWA that differentiates it from the classical FFSSP is its ability to handle re-entrant jobs, i.e., jobs that revisit a particular operation more than once. In this case study, three jobs, namely Job 1, Job 2, and Job 4 require dual-color lamination and as a result, they re-enter into the lamination process (Operation 1). As shown in the Gantt chart, this second process is represented by an additional operation, denoted as $\hat{1}$. Furthermore, the model incorporates a predefined waiting time of 4 hours after each lamination process to account for drying. The schedule explicitly reflects this requirement: a visible 4-hour idle period follows the initial and second lamination processes, thereby validating that the model appropriately integrates re-entrant behavior.

Figure 2. Gantt chart illustrating job schedules

In addition, the RFFSSP_HWA model also includes the heterogeneity of workers, which is another essential extension beyond classical formulations. In our case, the system consists of ten workers with varying skill sets, each qualified to perform specific operations. Furthermore, the processing speeds of workers differ depending on the operation due to variations in experience and proficiency. When we analyze the solution, it is observed that each operation is assigned to a worker who is both qualified and efficient. In other words, workers are frequently assigned to tasks for which their processing times are relatively shorter, suggesting that the solution effectively exploits worker-specific efficiencies. The model also imposes a strict constraint preventing simultaneous assignment of a worker to more than one operation. The resulting schedule satisfies this constraint, with each worker assigned to at most one operation at any given time.

The results demonstrate that the proposed RFFSSP_HWA model successfully captures the complexities of re-entrant job flows and worker heterogeneity in a flexible flow shop scheduling environment. The solution satisfies all realistic requirements and operational constraints, confirming that the model is valid and effective for real-world scheduling scenarios.

Concluding Remarks and Future Research Directions

This study addresses the Re-entrant Flexible Flow Shop Scheduling Problem with Heterogeneous Worker Assignment (RFFSSP_HWA), a complex scheduling scenario in real-world manufacturing systems. The problem environment is characterized by two primary sources of complexity: (1) the presence of re-entrant jobs that revisit certain operations more than once with predefined waiting period between passes, e.g., for drying, and (2) worker heterogeneity, where employees have different skill sets and processing efficiency depending on the operation assigned. Traditional models often do not include these dimensions, limiting their applicability to realistic production settings.

To address these limitations, we develop an integer programming model that schedules jobs and assigns workers based on their individual capabilities. The objective of the model is to minimize the makespan while satisfying precedence constraints, respecting re-entrant processing requirements, and assigning each operation to a suitable worker. The model prevents workers from being assigned to multiple tasks simultaneously and satisfies waiting time requirements in re-entrant processes.

The model was validated using a real-world case study from a company manufacturing PVC windows and doors. The case involves scheduling five jobs with varying quantities, including three jobs with re-entrant operations. The problem was successfully solved to optimality using IBM ILOG CPLEX. The solution shows that the model not only respects all operational constraints but also effectively incorporates re-entrant jobs and heterogeneous worker capabilities. In the optimal solution, each operation is assigned to a worker who is both eligible and efficient, reflecting the model's ability to impose workforce flexibility. Furthermore, the Gantt chart analysis confirmed the correct sequencing of operations, appropriate waiting times between re-entrant stages, and worker utilization without conflicts. The results highlight the model's potential for use in complex production systems where both job re-entry and worker heterogeneity must be considered. Besides producing optimal schedules, the model can also serve as a decision-support tool for workforce planning, identifying opportunities to improve operational efficiency.

Future research could extend this work in several directions. One area is the integration of workload balancing among workers, ensuring not only efficiency but also equity and fairness among workers. Another is the application of the model to larger-scale instances, where computational complexity may limit to reach optimal solutions. In such cases, the development of heuristic algorithms is possible for generating high-quality solutions within reasonable computational times. Lastly, industry-specific constraints, such as machine eligibility, shift schedules, and job priorities, could be incorporated to enhance the model's applicability across various manufacturing environments.

Scientific Ethics Declaration

* The authors declare that the scientific ethical and legal responsibility of this article published in EPSTEM journal belongs to the authors.

Conflict of Interest

* The authors declare that they have no conflicts of interest

Funding

* This research received no specific grant from any funding agency in the public, commercial, or not-for-profit sectors.

Acknowledgements or Notes

* This article was presented as an oral presentation at the International Conference on Research in Engineering, Technology and Science (www.icrets.net) held in Peja/Kosovo on July 10-13, 2025.

References

Chamnanlor, C., Sethanan, K., Gen, M., & Chien, C. F. (2017). Embedding ant system in genetic algorithm for re-entrant hybrid flow shop scheduling problems with time window constraints. *Journal of Intelligent Manufacturing*, *28*(8), 1915–1931.

Chen, J. S., Pan, J. C. H., & Lin, C. M. (2008). A hybrid genetic algorithm for the re-entrant flow-shop scheduling problem. *Expert Systems with Applications*, *34*(1), 570–577.

Chu, F., Liu, M., Liu, X., Chu, C., & Jiang, J. (2018). Reentrant Flow Shop Scheduling considering Multiresource Qualification Matching. *Scientific Programming*, *2018,* 2615096.

Costa, A., Cappadonna, F. A., & Fichera, S. (2014). Joint optimization of a flow-shop group scheduling with sequence dependent set-up times and skilled workforce assignment. *International Journal of Production Research*, *52*(9), 2696–2728.

Fekri, M., Heydari, M., & Mahdavi Mazdeh, M. (2024). Bi-objective optimization of flexible flow shop scheduling problem with multi-skilled human resources. *Engineering Applications of Artificial Intelligence*, *133*, 108094.

Geng, K., Liu, L., & Wu, Z. (2022). Energy-efficient distributed heterogeneous re-entrant hybrid flow shop scheduling problem with sequence dependent setup times considering factory eligibility constraints. *Scientific Reports*, *12*(1), 18741.

Graves, S. C., Meal, H. C., Stefek, D., & Zeghmi, A. H. (1983). Scheduling of re-entrant flow shops. *Journal of Operations Management, 3*(4), 197–207.

El-Khouly, I. A., El-Kilany, K. S., & El-Sayed, A. E. (2009). Modelling and simulation of re-entrant flow shop scheduling: An application in semiconductor manufacturing. *2009 International Conference on Computers & Industrial Engineering*, 211–216.

Johnson, S. M. (1954). Optimal two- and three-stage production schedules with setup times included. *Naval Research Logistics Quarterly*, *1*(1), 61–68.

Kayisoglu, B., Bekli, S., Sahin, A. S., Akyurek, G. G., Aydinli, R., Copur, S. N., & Ekinci, T. (2024). Parallel machine scheduling with re-entrant jobs with consideration of set up times. *Technology, Engineering & Mathematics (EPSTEM)*, *32*, 311–319.

Komaki, G. M., Sheikh, S., & Malakooti, B. (2019). Flow shop scheduling problems with assembly operations: a review and new trends. *International Journal of Production Research*, *57*(10), 2926–2955.

Liu, M., & Yang, X. (2019). Bi-objective optimization for scheduling and multi-skilled worker assignments in the hybrid flow shop. *IFAC-PapersOnLine*, *52*(13), 2128–2133.

Nasser, A., Zaied, H., Ismail, M. M., & Mohamed, S. S. (2021). Permutation flow shop scheduling problem with makespan criterion: Literature review. *Journal of Theoretical and Applied Information Technology*, *99*(4), 830-848.

Ozpacaci, K., Bekli, S., & Kayisoglu, B. (2025). Incorporating worker heterogeneity in flexible flow shop environment. *Technology, Engineering & Mathematics (EPSTEM)*, *34*, 359-368.

Rossit, D. A., Tohmé, F., & Frutos, M. (2018). The non-permutation flow-shop scheduling problem: A literature review. *Omega, 77*, 143–153.

Ruiz, R., & Vázquez-Rodríguez, J. A. (2010). The hybrid flow shop scheduling problem. *European Journal of Operational Research, 205*(1), 1–18.

Hassanpour, S. T., Naseri, M. A., & Nahavandi, N. (2015). Solving re-entrant no-wait flow shop scheduling problem. *International Journal of Engineering-Transactions C: Aspects*, *28*(6), 903-912.

Wang, M. Y., Sethi, S. P., & van de Velde, S. L. (1997). Minimizing makespan in a class of reentrant shops. *Operations Research, 45*(5), 702-712.

Author(s) Information

Seyma Bekli
Abdullah Gul University, Kayseri, Türkiye
Contact e-mail: *seyma.bekli@agu.edu.tr*

Betul Kayisoglu
Abdullah Gul University, Kayseri, Türkiye

To cite this article:

Bekli, S., & Kayisoglu, B. (2025). Scheduling in flexible flow shop environments with re-entrant jobs and heterogeneous workers. *The Eurasia Proceedings of Science, Technology, Engineering and Mathematics (EPSTEM), 35,* 314-322.

The Eurasia Proceedings of Science, Technology, Engineering & Mathematics (EPSTEM)
ISSN: 2602-3199

The Eurasia Proceedings of Science, Technology, Engineering and Mathematics (EPSTEM), 2025

Volume 35, Pages 323-345

ICRETS 2025: International Conference on Research in Engineering, Technology and Science

Neutrosophic λ-Compactness, λ-Connectedness, and λ-Separation Axioms in Neutrosophic Topological Spaces

Raja Mohammad Latif
Prince Mohammad Bin Fahd University

Abstract: Real-life structures always include indeterminacy. The Mathematical tool, which is well known in dealing with indeterminacy, is neutrosophic. Neutrosophic sets deal with uncertain data. The notion of a neutrosophic set is generally referred to as the generalization of an intuitionistic fuzzy set. In 2025, Shivangi Tyagi and Mridul Kumar Gupta introduced the concept of neutrosophic λ-closed $\left(\text{briefly}, N_{eu}\lambda\text{-closed}\right)$ sets and $N_{eu}\lambda$-open sets and investigated their fundamental properties. In this chapter, we introduce the notions of $N_{eu}\lambda$-compact spaces, $N_{eu}\lambda$-Lindelof space, countably $N_{eu}\lambda$-compact spaces, $N_{eu}\lambda$-connected spaces, $N_{eu}\lambda$-separated sets, N_{eu}-Super-λ-connected spaces, N_{eu}-Extremely-λ-disconnected spaces, and N_{eu}-Strongly-λ-connected spaces, $N_{eu}\lambda$-Regular spaces, strongly $N_{eu}\lambda$-Regular spaces, $N_{eu}\lambda$-Normal spaces, and strongly $N_{eu}\lambda$-Normal spaces by using $N_{eu}\lambda$-open sets and $N_{eu}\lambda$-closed sets in Neutrosophic topological spaces. We study the basic properties and fundamental characteristics of these spaces in Neurosophic topological spaces.

Keywords: $N_{eu}\lambda$-Top-Space, $N_{eu}\lambda$-open set, $N_{eu}\lambda$-closed set, $N_{eu}\lambda$-continuous function

Introduction

Many real-life problems in Business, Finance, Medical Sciences, Engineering, and Social Sciences deal with uncertainties. There are difficulties in solving the uncertainties in data by traditional mathematical models. There are approaches such as fuzzy sets, intuitionistic fuzzy sets, vague sets, and rough sets, which can be treated as mathematical tools to avert obstacles when dealing with ambiguous data. But all these approaches have their implicit crisis in solving the problems involving indeterminant and inconsistent data due to the inadequacy of parameterization tools. Smarandache studies neutrosophic sets as an approach for solving issues that cover unreliable, indeterminacy, and persistent data. Topology is an important and major area of mathematics, and it can give many relationships between other scientific areas and mathematical models. Recently, many scientists have studied the neutrosophic set theory, which was initiated by Molodtsov and easily applied to many problems having uncertainties from social life. In the present work, we have continued to study the properties of neutrosophic topological spaces. Applications of neutrosophic topology depend upon the properties of neutrosophic closed sets, neutrosophic interior operator, and neutrosophic open sets. In 2025, Shivangi Tyagi and Mridul Kumar Gupta introduced the concept of neutrosophic λ-closed $\left(\text{briefly}, N_{eu}\lambda\text{-closed}\right)$ sets and $N_{eu}\lambda$-open sets and investigated their fundamental properties. In this paper, we introduce the notions of $N_{eu}\lambda$-compact spaces, $N_{eu}\lambda$-Lindelof spaces, countably $N_{eu}\lambda$-compact spaces, $N_{eu}\lambda$-connected spaces, $N_{eu}\lambda$-separated sets, N_{eu}-Super-λ-connected spaces, N_{eu}-Extremely-λ-disconnected spaces, and N_{eu}-Strongly-λ-connected spaces,

$N_{eu}\lambda-$Regular spaces, strongly $N_{eu}\lambda-$Regular spaces, $N_{eu}\lambda-$Normal spaces, and strongly $N_{eu}\lambda-$Normal spaces by using $N_{eu}\lambda-$open sets and $N_{eu}\lambda-$closed sets in Neutrosophic topological spaces. We study their basic properties and fundamental characteristics of these spaces in Neurosophic topological spaces.

2. Preliminaries

We recall basic definitions and operations of neutrosophic sets and neutrosophic topological spaces.

Definition 2.1. Let X be a non-empty fixed set. A $N_{eu}\lambda-$set P is an object having the form $P=\left\{\left\langle x,\mu_P(x),\sigma_P(x),\gamma_P(x)\right\rangle : x\in X\right\}$, where $\mu_P(x)$- represents the degree of membership, $\sigma_P(x)$- represents the degree of indeterminacy, and $\gamma_P(x)$- represents the degree of non-membership.
The class of all neutrosophic sets of X is denoted by $N_{eu}(X)$.

Definition 2.2. Let X be a non-empty set and let $P=\left\{\left\langle x,\mu_P(x),\sigma_P(x),\gamma_P(x)\right\rangle : x\in X\right\}$ and $Q=\left\{\left\langle x,\mu_Q(x),\sigma_Q(x),\gamma_Q(x)\right\rangle : x\in X\right\}$ be two $N_{eu}-$Spaces., Then $N_{eu}-$Top$-$Spaces.

1. $(Empty\ set)$ $0_N=\langle x,0,0,1\rangle$ is called the $N_{eu}-$empty set,

2. $(Universal\ set)$ $1_N=\langle x,1,1,0\rangle$ is called the $N_{eu}-$universal set,

3. (Inclusion): $P\subseteq Q$ if and only if $\mu_P(x)\le\mu_Q(x)$, $\sigma_P(x)\le\sigma_Q(x)$ and $\gamma_P(x)\ge\gamma_Q(x)$: $x\in X$,

4. (Equality): $P=Q$ if and only if $P\subseteq Q$ and $Q\subseteq P$, 5. $(Complement)$ $P^C=1_N-P=\left\{\left\langle x,\gamma_P(x),1-\sigma_P(x),\mu_P(x)\right\rangle : x\in X\right\}$,

5. $(Union)$ $P\bigcup Q=\left\{\left\langle x,\max\left(\mu_P(x),\mu_Q(x)\right),\max\left(\sigma_P(x),\sigma_Q(x)\right),\min\left(\gamma_P(x),\gamma_Q(x)\right)\right\rangle : x\in X\right\}$.

6. $(Intersection)$ $P\bigcap Q=\left\{\left\langle x,\min\left(\mu_P(x),\mu_Q(x)\right),\min\left(\sigma_P(x),\sigma_Q(x)\right),\max\left(\gamma_P(x),\gamma_Q(x)\right)\right\rangle : x\in X\right\}$.

Definition 2.3. A $N_{eu}-$pooint $x_{(\alpha,\beta,\gamma)}$ is said to be in the $N_{eu}-$set A- in symbols $x_{(\alpha,\beta,\gamma)}\in A$ if and only if $\alpha<\mu_A(x)$, $\beta<\sigma_A(x)$ and $\gamma>\gamma_A(x)$.

Definition 2.4. A $N_{eu}-$Topology on a non-empty set X is a family T_N of $N_{eu}-$subsets of X satisfying (i) $0_N, 1_N\in T_N$. (ii) $G\bigcap H\in T_N$, for every $G, H\in T_N$. (iii) $\bigcup_{j\in J}G_j\in T_N$ for every $\left\{G_j : j\in J\right\}\subseteq\tau_N$,
Then the pair (X,T_N) is called a $N_{eu}-$Top$-$Space. The elements of T_N are called $N_{eu}-$open sets in X. A $N_{eu}-$set A is called a $N_{eu}-$closed set if and only if its complement A^C is a $N_{eu}-$open set.

Definition 2.5. Let (X,T_N) be a $N_{eu}-$Top$-$Space and A be a $N_{eu}-$set. Then
(i) The neutrosophic interior of A denoted by $N_{eu}Int(A)$ is the union of all $N_{eu}-$open sets contained in A. Clearly $N_{eu}Int(A)$ is the biggest $N_{eu}-$open subset of X contained in A.
(ii) The neutrosophic closure of A denoted by $N_{eu}Cl(A)$ is the intersection of all $N_{eu}-$closed sets containing A. $N_{eu}Cl(A)$ is the smallest $N_{eu}-$closed set which contains A.

Definition 2.6. A N_{eu}-set A in a N_{eu}-Top-Space (X, T_N) is called $N_{eu}\lambda$-closed if $N_{eu}\text{-Cl}(O) \subseteq A$ for each N_{eu}-open O in X, satisfying $O \subseteq A$. The complement of $N_{eu}\lambda$-closed set is called $N_{eu}\lambda$-open set in X. The collection of all $N_{eu}\lambda$-open sets $(\text{resp. } N_{eu}\lambda\text{-closed})$ is represented by the symbol $N_{eu}\lambda\text{-O}(X, \tau)$ $(\text{resp. } N_{eu}\lambda\text{-C}(X, \tau))$.

Definition 2.7. Let A be a subset of a N_{eu}-Top-Space (X, T_N). Then $N_{eu}\lambda$-closure of A and $N_{eu}\lambda$-interior of A are denoted and defined by: $N_{eu}\lambda\text{-}Cl(A) = \bigcap\{G : G \text{ is a } N_{eu}\lambda\text{-closed set in } X \text{ and } A \subseteq G\}$ and $N_{eu}\lambda\text{-}Int(A) = \bigcup\{G : G \text{ is a } N_{eu}\lambda\text{-open set in } X \text{ and } G \subseteq A\}$ respectively.

Theorem 2.8. Every N_{eu}-closed $(\text{resp. } N_{eu}\text{-open})$ set is $N_{eu}\lambda$-closed $(\text{resp. } N_{eu}\lambda\text{-open})$ set in X.

Theorem 2.9. The union (resp. intersection) of two $N_{eu}\lambda$-open $(\text{resp. } N_{eu}\lambda\text{-closed})$ sets is $N_{eu}\lambda$-open $(\text{resp. } N_{eu}\lambda\text{-closed})$ in a N_{eu}-Top-Space (X, T_N).

Definition 2.10. Let $f : (X, T_N) \to (Y, \sigma_N)$ be a mapping. Then f is called a N_{eu}-continuous mapping if $f^{-1}(V)$ is a N_{eu}-open $(\text{resp. } N_{eu}\text{-closed})$ set in X for every N_{eu}-open $(\text{resp. } N_{eu}\text{-closed})$ set V in Y.

Definition 2.11. Let $f : (X, T_N) \to (Y, \sigma_N)$ be a mapping. Then f is called a $N_{eu}\lambda$-continuous mapping if $f^{-1}(V)$ is a $N_{eu}\lambda$-open $(\text{resp. } N_{eu}\lambda\text{-closed})$ set in X for every N_{eu}-open $(\text{resp. } N_{eu}\text{-closed})$ set V in Y.

Definition 2.12. Let $f : (X, T_N) \to (Y, \sigma_N)$ be a mapping. Then f is called a $N_{eu}\lambda$-irresolute mapping if $f^{-1}(V)$ is a $N_{eu}\lambda$-open $(\text{resp. } N_{eu}\lambda\text{-closed})$ set in X for every $N_{eu}\lambda$-open $(\text{resp. } N_{eu}\lambda\text{-closed})$ set V in Y.

Definition 2.13. Let $f : (X, T_N) \to (Y, \sigma_N)$ be a mapping. Then f is called a N_{eu}-open $(\text{resp. } N_{eu}\text{-closed})$ mapping if $f(U)$ is a N_{eu}-open $(\text{resp. } N_{eu}\text{-closed})$ set in Y for every N_{eu}-open $(\text{resp. } N_{eu}\text{-closed})$ set U in X.

Definition 2.14. Let $f : (X, T_N) \to (Y, \sigma_N)$ be a mapping. Then f is called a $N_{eu}\lambda$-open $(\text{resp. } N_{eu}\lambda\text{-closed})$ mapping if $f(U)$ is a $N_{eu}\lambda$-open $(\text{resp. } N_{eu}\lambda\text{-closed})$ set in Y for every N_{eu}-open $(\text{resp. } N_{eu}\text{-closed})$ set U in X.

3 Neutrosophic λ-Compact Spaces

In this section, we introduce $N_{eu}\lambda$-compact space, $N_{eu}\lambda$-Lindelof space, and countably $N_{eu}\lambda$-compact space and investigate their basic properties and characterizations.

Definition 3.1. A collection $\{A_i : i \in I\}$ of N_{eu} -open (resp. $N_{eu}\lambda$ -open) sets in a N_{eu} -Top -Space (X, T_N) is called a N_{eu} -open (resp. $N_{eu}\lambda$ -open) cover of a subset B of X if $B \subseteq \bigcup\{A_i : i \in I\}$ holds.

Definition 3.2. A subset B of a N_{eu} -Top -Space (X, T_N) is said to be N_{eu} -compact (resp. $N_{eu}\lambda$ -compact) relative to (X, T_N), if for every collections $\{A_i : i \in I\}$ of N_{eu} -open (resp. $N_{eu}\lambda$ -open) subsets of (X, T_N) such that $B \subseteq \bigcup\{A_i : i \in I\}$ there exists a finite subset I_0 of I such that $B \subseteq \bigcup\{A_i : i \in I_0\}$.

Definition 3.3. A subset B of a N_{eu} -Top -Space (X, T_N) is called N_{eu} -compact (resp $N_{eu}\lambda$ -compact) if B is N_{eu} -compact (resp. $N_{eu}\lambda$ -compact) as a subspace of X.

Theorem 3.4. A $N_{eu}\lambda$ -closed subset of a $N_{eu}\lambda$ -compact (X, T_N) is $N_{eu}\lambda$ -compact relative to (X, T_N).

Proof. Let A be a $N_{eu}\lambda$ -closed subset of a $N_{eu}\lambda$ -compact space (X, T_N). Then A^C is $N_{eu}\lambda$ -open in (X, T_N). Let $S = \{A_i : i \in I\}$ be a $N_{eu}\lambda$ -open cover of A by $N_{eu}\lambda$ -open subsets of (X, T_N). Then $S^* = S \bigcup\{A^C\}$ is a $N_{eu}\lambda$ -open cover of (X, T_N). That is $X = \left(\bigcup_{i \in I} A_i\right) \bigcup A^C$. By hypothesis (X, T_N) is $N_{eu}\lambda$ -compact and hence S^* is reducible to a finite subcover of (X, T_N) say $X = A_{i_1} \bigcup A_{i_2} \ldots\ldots \bigcup A_{i_n} \bigcup A^C$, $A_{i_k} \in S \subseteq S^*$. Then $A = A_{i_1} \bigcup A_{i_2} \ldots\ldots \bigcup A_{i_n}$. Thus a $N_{eu}\lambda$ -open cover S of A contains a finite subcover. Hence A is $N_{eu}\lambda$ -compact relative to (X, T_N).

Theorem 3.5. A N_{eu} -Top -Space (X, T_N) is $N_{eu}\lambda$ -compact if and only if every family of $N_{eu}\lambda$ -closed sets of (X, T_N) having a finite intersection property has a non-empty intersection.

Proof. Suppose (X, T_N) is $N_{eu}\lambda$ -compact. Let $\{A_i : i \in I\}$ be a family of $N_{eu}\lambda$ -closed sets with finite intersection property. Suppose $\bigcap_{i \in I} A_i = \phi$. Then $X - \bigcap_{i \in I} A_i = X$. This implies $\bigcup_{i \in I}(X - A_i) = X$. Thus the cover $\{X - A_i : i \in I\}$ is a $N_{eu}\lambda$ -open cover of (X, T_N). Then the $N_{eu}\lambda$ -open cover $\{X - A_i : i \in I\}$ has a finite subcover, say $\{X - A_i : i \in I_0\}$ for some finite subset I_0 of I. This implies $X = \bigcup_{i \in I_0}(X - A_i)$, which implies $X - \bigcup_{i \in I_0}(X - A_i) = \phi$ which implies $\bigcap_{i \in I_0} A_i = \phi$. This contradicts the assumption. Hence $\bigcap_{i \in I} A_i \neq \phi$. Conversely, suppose (X, T_N) is not $N_{eu}\lambda$ -compact. Then there exists a $N_{eu}\lambda$ -open cover of (X, T_N) say $\{G_i : i \in I\}$ having no finite subcover. This implies that for any finite subfamily $\{G_i : i = 1, 2, \ldots, n\}$ of $\{G_i : i \in I\}$, we have $\bigcup_{i=1}^{n} G_i \neq X$, which implies $X - \bigcup_{i=1}^{n} G_i \neq X - X$, which implies $\bigcap_{i=1}^{n}(X - G_i) \neq \phi$. Then the family $\{X - G_i : i \in I\}$ of $N_{eu}\lambda$ -closed sets has a finite intersection property. Also, by assumption $\bigcap_{i \in I}(X - G_i) \neq \phi$ which implies $X - \bigcup_{i \in I} G_i \neq \phi$ so that $\bigcup_{i \in I} G_i \neq X$. This implies $\{G_i : i \in I\}$ is not a cover for (X, T_N). This contradicts the fact $\{G_i : i \in I\}$ is a cover for (X, T_N). Therefore a $N_{eu}\lambda$ -open cover $\{G_i : i \in I\}$ of (X, T_N) has a finite subcover $\{G_i : i = 1, 2, \ldots, n\}$. Hence (X, T_N) is a $N_{eu}\lambda$ -compact.

Theorem 3.6. The image of a $N_{eu}\lambda-$compact space under a $N_{eu}\lambda-$irresolute mapping is $N_{eu}\lambda-$compact.

Proof. Let $f:(X,T_N)\to(Y,\sigma_N)$ be a $N_{eu}\lambda-$irresolute mapping from a $N_{eu}\lambda-$compact space (X,T_N) onto a $N_{eu}-$Top$-$Space (Y,σ_N). Let $\{A_i : i\in I\}$ be a $N_{eu}\lambda-$open cover of (Y,σ_N). Then $\{f^{-1}(A_i): i\in I\}$ is a $N_{eu}\lambda-$open cover of (X,T_N), since f is $N_{eu}\lambda-$irresolute. As (X,T_N) is $N_{eu}\lambda-$compact, the $N_{eu}\lambda-$open cover $\{f^{-1}(A_i): i\in I\}$ of (X,T_N) has a finite subcover $\{f^{-1}(A_i): i=1,2,...,n\}$. Therefore $X=\bigcup_{i=1}^{n} f^{-1}(A_i)$. Then $f(X)=\bigcup_{i=1}^{n} A_i$, that is $Y=\bigcup_{i=1}^{n} A_i$. Then $\{A_1,A_2,...,A_n\}$ is a finite subcover of $\{A_i : i\in I\}$ for (Y,σ_N). So Y is a $N_{eu}\lambda-$compact space.

Definition 3.7. A $N_{eu}-$Top$-$Space (X,T_N) is countably $N_{eu}\lambda-$compact if every countable $N_{eu}\lambda-$open cover of (X,T_N) has a finite subcover.

Definition 3.8. A $N_{eu}-$Top$-$Space (X,T_N) is said to be $N_{eu}\lambda-$Hausdorff if whenever $x_{(\alpha,\beta,\gamma)}$ and $y_{(r,s,t)}$ are distinct points of (X,T_N), there exist disjoint $N_{eu}\lambda-$open sets A and B of X such that $x_{(\alpha,\beta,\gamma)}\in A$ and $y_{(r,s,t)}\in B$.

Theorem 3.9. Let (X,T_N) be a $N_{eu}-$Top$-$Space and (Y,σ_N) be a $N_{eu}\lambda-$Hausdorff space. If $f:(X,T_N)\to(Y,\sigma_N)$ is $N_{eu}\lambda-$irresolute injective mapping, then (X,T_N) is $N_{eu}\lambda-$Hausdorff.

Proof. Let $x_{(\alpha,\beta,\gamma)}$ and $y_{(r,s,t)}$ be any two distinct $N_{eu}-$points of (X,T_N). Then $f\left(x_{(\alpha,\beta,\gamma)}\right)$ and $f\left(y_{(r,s,t)}\right)$ are distinct $N_{eu}-$points of (Y,σ_N), because f is injective. Since (Y,σ_N) is $N_{eu}\lambda-$Hausdorff, there are disjoint $N_{eu}\lambda-$open sets G and H in (Y,σ_N) containing $f\left(x_{(\alpha,\beta,\gamma)}\right)$ and $f\left(y_{(r,s,t)}\right)$ respectively. Since f is $N_{eu}\lambda-$irresolute and $G\cap H=\phi$, we have $f^{-1}(G)$ and $f^{-1}(H)$ are disjoint $N_{eu}\lambda-$open sets in (X,T_N) such that $x_{(\alpha,\beta,\gamma)}\in f^{-1}(G)$ and $y_{(r,s,t)}\in f^{-1}(H)$. Hence (X,T_N) is $N_{eu}\lambda-$Hausdorff.

Theorem 3.10. If $f:(X,T_N)\to(Y,\sigma_N)$ is $N_{eu}\lambda-$irresolute and bijective and if X is $N_{eu}\lambda-$compact and Y is $N_{eu}\lambda-$Hausdorff, then f is a $N_{eu}\lambda-$homeomorphism.

Proof. We have to show that the inverse function g of f is $N_{eu}\lambda-$irresolute. For this we show that if A is $N_{eu}\lambda-$open in (X,T_N), then the pre-image $g^{-1}(A)$ is $N_{eu}\lambda-$open in (Y,σ_N). Since the $N_{eu}\lambda-$open (or $N_{eu}\lambda-$closed) sets are just the complements of $N_{eu}\lambda-$closed (resp. $N_{eu}\lambda-$open) subsets, and $g^{-1}(X-A)=Y-g^{-1}(A)$. We see that the $N_{eu}\lambda-$irresolute mapping of g is equivalent to: if B is $N_{eu}\lambda-$closed in (X,T_N) then the pre-image $g^{-1}(B)$ is $N_{eu}\lambda-$closed in Y. To prove this, let B be a $N_{eu}\lambda-$closed subset of X. Since g is the inverse of f, we have $g^{-1}(B)=f(B)$, hence we have to show that $f(B)$ is a $N_{eu}\lambda-$closed set in Y. By theorem 3.4, B is $N_{eu}\lambda-$compact. By Theorem 3.6, it implies that $f(B)$ is $\mathrm{N}_{eu}\lambda-$copmpact. Since Y is $\mathrm{N}_{eu}\lambda-$Hausdorff space implies that $f(B)$ is $\mathrm{N}_{eu}\lambda-$closed in (Y,σ_N).

Definition 3.11. A $\mathrm{N}_{eu}-$Top$-$Space (X,T_N) is said to be $\mathrm{N}_{eu}\lambda-$Lindelof space if every $\mathrm{N}_{eu}\lambda-$open cover of (X,T_N) has a countable subcover.

Theorem 3.12. Every $\mathrm{N}_{eu}\lambda-$compact space is a $\mathrm{N}_{eu}\lambda-$Lindelof space.

Proof. Let (X,T_N) be $\mathrm{N}_{eu}\lambda-$compact. Let $\{A_i : i\in I\}$ be a $\mathrm{N}_{eu}\lambda-$open cover of (X,T_N). Then $\{A_i : i\in I\}$ has a finite subcover $\{A_i : i=1,2,...,n\}$, since (X,T_N) is $\mathrm{N}_{eu}\lambda-$copmpact. Since every finite subcover is always a countable subcover and therefore, $\{A_i : i=1.2,...,n\}$ is a countable subcover of $\{A_i : i\in I\}$ for (X,T_N). Hence (X,T_N) is $\mathrm{N}_{eu}\lambda-$Lindelof space.

Theorem 3.13. The image of a $\mathrm{N}_{eu}\lambda-$Lindelof space under a $\mathrm{N}_{eu}\lambda-$irresolute mapping is $\mathrm{N}_{eu}\lambda-$Lindelof.

Proof. Let $f:(X,\mathrm{T}_N)\to(Y,\sigma_N)$ be a $\mathrm{N}_{eu}\lambda-$irresolute mapping from a $\mathrm{N}_{eu}\lambda-$Lindelof space (X,T_N) onto a $\mathrm{N}_{eu}-$Top$-$Space (Y,σ_N). Let $\{A_i : i\in I\}$ be a $\mathrm{N}_{eu}\lambda-$open cover of (Y,σ_N). Then $\{f^{-1}(A_i) : i\in I\}$ is a $\mathrm{N}_{eu}\lambda-$open cover of (X,T_N), since f is $\mathrm{N}_{eu}\lambda-$irresolute. As (X,T_N) is $\mathrm{N}_{eu}\lambda-$Lindelof, the $\mathrm{N}_{eu}\lambda-$open cover $\{f^{-1}(A_i) : i\in I\}$ of (X,T_N) has a countable subcover $\{f^{-1}(A_i) : i\in I_0\}$ for some countable subset I_0 of I. Therefore $X=\bigcup_{i\in I_0} f^{-1}(A_i)$ which implies $f(X)=Y=\bigcup_{i\in I_0} A_i$, that is $\{A_i : i\in I_0\}$ is a countable subcover of $\{A_i : i\in I\}$ for (Y,σ_N). Hence (Y,σ_N) is $\mathrm{N}_{eu}\lambda-$Lindelof space.

Theorem 3.14. Let (X,T_N) be $\mathrm{N}_{eu}\lambda-$Lindelof and countably $\mathrm{N}_{eu}\lambda-$copmpact space. Then (X,T_N) is $\mathrm{N}_{eu}\lambda-$copmpact.

Proof. Let $\{A_i : i\in I\}$ be a $\mathrm{N}_{eu}\lambda-$open cover of (X,T_N). Since (X,T_N) is $\mathrm{N}_{eu}\lambda-$Lindelof space. Hence $\{A_i : i\in I\}$ has a countable subcover $\{A_{i_n} : n\in \mathrm{N}\}$. Therefore, $\{A_{i_n} : n\in \mathrm{N}\}$ is a countable subcover of (X,T_N) and $\{A_{i_n} : n\in \mathrm{N}\}$ is a subfamily of $\{A_i : i\in I\}$ and so $\{A_{i_n} : n\in \mathrm{N}\}$ is a countable $\mathrm{N}_{eu}\lambda-$open cover of (X,T_N). Again since (X,T_N) is countably $\mathrm{N}_{eu}\lambda-$copmpact, $\{A_{i_n} : n\in \mathrm{N}\}$ has a finite subcover $\{A_{i_k} : k=1,2,...,n\}$. Thus $\{A_{i_k} : k=1,2,...,n\}$ is a finite subcover of $\{A_i : i\in I\}$ for (X,T_N). Hence (X,T_N) is $\mathrm{N}_{eu}\lambda-$copmpact space.

Theorem 3.15. A $\mathrm{N}_{eu}-$Top$-$Space (X,T_N) is $\mathrm{N}_{eu}\lambda-$copmpact if and only if every basic $\mathrm{N}_{eu}\lambda-$open cover of (X,T_N) has a finite subcover.

Proof. Let (X,T_N) be $\mathrm{N}_{eu}\lambda-$copmpact. Then every $\mathrm{N}_{eu}\lambda-$open cover of (X,T_N) has a finite subcover. Conversely, suppose that every basic $\mathrm{N}_{eu}\lambda-$open cover of (X,T_N) has a finite subcover and let $\mathrm{C}=\{G_\lambda : \lambda\in\Lambda\}$ be any $\mathrm{N}_{eu}\lambda-$open cover of (X,T_N). If $\mathrm{B}=\{D_\alpha : \alpha\in\Delta\}$ is any $\mathrm{N}_{eu}\lambda-$open base for

(X, T_N), then each G_λ is union of some members of $\mathcal{B}$ and the totality of all such members of $\mathcal{B}$ evidently a basic $N_{eu}\lambda-$open cover of (X, T_N). By hypothesis this collection of members of $\mathcal{B}$ has a finite subcover, $\{D_{\alpha_i} : i = 1, 2, ..., n\}$. For each D_{α_i} in this finite subcover, we can select a G_{λ_i} from $\mathcal{C}$ such that $D_{\alpha_i} \subseteq G_{\lambda_i}$. It follows that the finite subcollection $\{G_{\lambda_i} : i = 1, 2, ..., n\}$, which arises in this way is a subcover of $\mathcal{C}$. Hence (X, T_N) is $N_{eu}\lambda-$copmpact.

4 Neutrosophic λ –Connected Spaces

In this section, we introduce and study the notions of $N_{eu}\lambda-$connected spaces, $N_{eu}\lambda-$separated sets, $N_{eu}-$Super$-\lambda-$connected spaces, $N_{eu}-$Extremely$-\lambda-$disconnected spaces and $N_{eu}-$Strongly$-\lambda-$connected spaces in $N_{eu}-$Top$-$Spaces.

Definition 4.1. A $N_{eu}-$Top$-$Space (X, T_N) is $N_{eu}\lambda-$disconnected if there exist $N_{eu}\lambda-$open sets A, B in X, $A \neq 0_N$, $B \neq 0_N$ such that $A \bigcup B = 1_N$ and $A \bigcap B = 0_N$. If (X, T_N) is not $N_{eu}\lambda-$disconnected then it is said to be $N_{eu}\lambda-$connected.

Theorem 4.2. A $N_{eu}-$Top$-$Space (X, T_N) is $N_{eu}\lambda-$connected space if and only if there exists no nonempty $N_{eu}\lambda-$open sets U and V in (X, T_N) such that $U = V^C$.

Proof. **Necessity:** Let U and V be two $N_{eu}\lambda-$open sets in (X, T_N) such that $U \neq 0_N, V \neq 0_N$ and $U = V^C$. Therefore V^C is a $N_{eu}\lambda-$closed set. Since $U \neq 0_N, V \neq 1_N$. This implies V is a proper $N_{eu}-$subset which is both $N_{eu}\lambda-$open set and $N_{eu}\lambda-$closed set in X. Hence X is not a $N_{eu}\lambda-$connected space. But this is a contradiction to our hypothesis. Thus, there exists no nonempty $N_{eu}\lambda-$open sets U and V in X, such that $U = V^C$.

Sufficiency: Let U be both $N_{eu}\lambda-$open and $N_{eu}\lambda-$closed set of X such that $U \neq 0_N, U \neq 1_N$. Now let $V = U^C$. Then V is a $N_{eu}\lambda-$open set and $V \neq 1_N$. This implies $U^C = V \neq 0_N$, which is a contradiction to our hypothesis. Therefore X is $N_{eu}\lambda-$connected space.

Theorem 4.3. A $N_{eu}-$Top$-$Space (X, T_N) is $N_{eu}\lambda-$connected space if and only if there do not exist nonempty $N_{eu}-$subsets U and V in X such that $U = V^C$, $V = \left[N_{eu}\lambda-Cl(U)\right]^C$ and $U = \left[N_{eu}\lambda-Cl(V)\right]^C$.

Proof. **Necessity:** Let U and V be two $N_{eu}-$subsets of (X, T_N) such that $U \neq 0_N, V \neq 0_N$ and $U = V^C$, $V = \left[N_{eu}\lambda-Cl(U)\right]^C$ and $U = \left[N_{eu}\lambda-Cl(V)\right]^C$. Since $\left[N_{eu}\lambda-Cl(U)\right]^C$ and $\left[N_{eu}\lambda-Cl(V)\right]^C$ are $N_{eu}\lambda-$open sets in X, so U and V are $N_{eu}\lambda-$open sets in X. This implies X is not a $N_{eu}\lambda-$connected space, which is a contradiction. Therefore, there exist no nonempty $N_{eu}\lambda-$open sets U and V in X, such that $U = V^C$, $V = \left[N_{eu}\lambda-Cl(U)\right]^C$ and $U = \left[N_{eu}\lambda-Cl(V)\right]^C$.

Sufficiency: Let U be both $N_{eu}\lambda-$open and $N_{eu}\lambda-$closed set in X such that $U \neq 0_N$, $U \neq 1_N$. Now by taking $V = U^C$ we obtain a contradiction to our hypothesis. Hence X is $N_{eu}\lambda-$connected space.

Theorem 4.4. Let $f:(X,\mathrm{T}_N)\rightarrow(Y,\sigma_N)$ be a $\mathrm{N}_{eu}\lambda-$irresolure surjection and X be $\mathrm{N}_{eu}\lambda-$connected. Then Y is $\mathrm{N}_{eu}\lambda-$connected.

Proof. Assume that Y is not $\mathrm{N}_{eu}\lambda-$connected, then there exist nonempty $\mathrm{N}_{eu}\lambda-$open sets U and V in Y such that $U\bigcup V=1_N$ and $U\bigcap V=0_N$. Since f is $\mathrm{N}_{eu}\lambda-$irresolure mapping, $A=f^{-1}(U)\neq 0_N$, $B=f^{-1}(V)\neq 0_N$, which are $\mathrm{N}_{eu}\lambda-$open sets in X and $f^{-1}(U)\bigcup f^{-1}(V)=f^{-1}(1_N)=1_N$, which implies $A\bigcup B=1_N$. Also $f^{-1}(U)\bigcap f^{-1}(V)=f^{-1}(0_N)=0_N$, which implies $A\bigcap B=0_N$. Thus, X is $\mathrm{N}_{eu}\lambda-$disconnected, which is a contradiction to our hypothesis. Hence Y is $\mathrm{N}_{eu}\lambda-$connected.

Definition 4.5. Let A and B be nonempty $\mathrm{N}_{eu}-$subsets in a $\mathrm{N}_{eu}-$Top$-$Space (X,T_N). Then A and B are said to be $\mathrm{N}_{eu}\lambda-$separated if $\mathrm{N}_{eu}\lambda-Cl(A)\bigcap B=A\bigcap \mathrm{N}_{eu}\lambda-Cl(B)=0_N$.

Remark 4.6. Any two disjoint non-empty $\mathrm{N}_{eu}\lambda-$closed sets are $\mathrm{N}_{eu}\lambda-$separated.

Proof. Suppose A and B are disjoint non-empty $\mathrm{N}_{eu}\lambda-$closed sets. Then $\mathrm{N}_{eu}\lambda-Cl(A)\bigcap B=A\bigcap \mathrm{N}_{eu}\lambda-Cl(B)=A\bigcap B=0_N$. This shows that A and B are $\mathrm{N}_{eu}\lambda-$separated.

Theorem 4.7. (i) Let A and B be two $\mathrm{N}_{eu}\lambda-$separated subsets of a $\mathrm{N}_{eu}-$Top$-$Space (X,T_N) and $C\subseteq A$, $D\subseteq B$. Then C and D are also $\mathrm{N}_{eu}\lambda-$separated.
(ii) Let A and B be both $\mathrm{N}_{eu}\lambda-$separated subsets of a $\mathrm{N}_{eu}-$Top$-$Space (X,T_N) and let $H=A\bigcap B^C$ and $G=B\bigcap A^C$. Then H and G are also $\mathrm{N}_{eu}\lambda-$separated.

Proof. (i) Let A and B be two $\mathrm{N}_{eu}\lambda-$separated sets in $\mathrm{N}_{eu}-$Top$-$Space (X,T_N). Then $\mathrm{N}_{eu}\lambda-Cl(A)\bigcap B=0_N=A\bigcap \mathrm{N}_{eu}\lambda-Cl(B)$. Since $C\subseteq A$ and $D\subseteq B$, then $\mathrm{N}_{eu}\lambda-Cl(C)\subseteq \mathrm{N}_{eu}\lambda-Cl(A)$ and $\mathrm{N}_{eu}\lambda-Cl(D)\subseteq \mathrm{N}_{eu}\lambda-Cl(B)$. This implies that, $\mathrm{N}_{eu}\lambda-Cl(C)\bigcap D\subseteq \mathrm{N}_{eu}\lambda-Cl(A)\bigcap B=0_N$ and hence $\mathrm{N}_{eu}\lambda-Cl(C)\bigcap D=0_N$. Similarly $\mathrm{N}_{eu}\lambda-Cl(D)\bigcap C\subseteq \mathrm{N}_{eu}\lambda-Cl(B)\bigcap A=0_N$ and so $\mathrm{N}_{eu}\lambda-Cl(D)\bigcap C=0_N$. Therefore C and D are $\mathrm{N}_{eu}\lambda-$separated.
(ii) Let A and B be both $\mathrm{N}_{eu}\lambda-$open subsets of X. Then A^C and B^C are $\mathrm{N}_{eu}\lambda-$closed sets. Since $H\subseteq B^C$, then $\mathrm{N}_{eu}\lambda-Cl(H)\subseteq \mathrm{N}_{eu}\lambda-Cl(B^C)=B^C$ and so $\mathrm{N}_{eu}\lambda-Cl(H)\bigcap B=0_N$. Since $G\subseteq B$, then $\mathrm{N}_{eu}\lambda-Cl(H)\bigcap G\subseteq \mathrm{N}_{eu}\lambda-Cl(H)\bigcap B=0_N$. Thus, we have $\mathrm{N}_{eu}\lambda-Cl(H)\bigcap G=0_N$. Similarly, $\mathrm{N}_{eu}\lambda-Cl(G)\bigcap H=0_N$. Hence H and G are $\mathrm{N}_{eu}\lambda-$separated.

Theorem 4.8. Two $\mathrm{N}_{eu}-$subsets A and B of a $\mathrm{N}_{eu}-$Top$-$Space (X,T_N) are $\mathrm{N}_{eu}\lambda-$separated if and only if there exist $\mathrm{N}_{eu}\lambda-$open sets U and V in X such that $A\subseteq U$, $B\subseteq V$ and $A\bigcap V=0_N$ and $B\bigcap U=0_N$.

Proof. Let A and B be $\mathrm{N}_{eu}\lambda-$separated. Then $A\bigcap \mathrm{N}_{eu}\lambda-Cl(B)=0_N=B\bigcap \mathrm{N}_{eu}\lambda-Cl(A)$. Take $V=(\mathrm{N}_{eu}\lambda-Cl(A))^C$ and $U=(\mathrm{N}_{eu}\lambda-Cl(B))^C$. Then U and V are $\mathrm{N}_{eu}\lambda-$open sets in X such that $A\subseteq U$, $B\subseteq V$ and $A\bigcap V=0_N$ and $B\bigcap U=0_N$.

Conversely, let U and V be $\mathrm{N}_{eu}\lambda-$open sets such that $A\subseteq U$, $B\subseteq V$ and $A\bigcap V=0_N$, $B\bigcap U=0_N$. Then $A\subseteq V^C$, $B\subseteq U^C$, V^C and U^C are $\mathrm{N}_{eu}\lambda-$closed. This implies that $\mathrm{N}_{eu}\lambda-Cl(A)\subseteq$

$N_{eu}\lambda-Cl(V^C)=V^C\subseteq B^C$ and $N_{eu}\lambda-Cl(B)\subseteq N_{eu}\lambda-Cl(U^C)=U^C\subseteq A^C$. Thus, $N_{eu}\lambda-Cl(A)\subseteq B^C$ and $N_{eu}\lambda-Cl(B)\subseteq A^C$. Therefore $A\cap N_{eu}\lambda-Cl(B)=0_N=N_{eu}\lambda-Cl(A)\cap B$. Hence A and B are $N_{eu}\lambda-$separated.

Theorem 4.9. Each two $N_{eu}\lambda-$separated sets are always disjoint.

Proof. Let A and B be $N_{eu}\lambda-$separated. Then $A\cap N_{eu}\lambda-Cl(B)=0_N=N_{eu}\lambda-Cl(A)\cap B$. Now, $A\cap B\subseteq A\cap N_{eu}\lambda-Cl(B)=0_N$. Therefore $A\cap B=0_N$ and hence A and B are disjoint.

Theorem 4.10. A $N_{eu}-$Top$-$Space (X,T_N) is $N_{eu}\lambda-$connected if and only if $A\cup B\neq 1_N$, where A and B are $N_{eu}\lambda-$separated sets.

Proof. Assume that (X,T_N) is $N_{eu}\lambda-$connected space. Suppose $A\cup B=1_N$, where A and B are $N_{eu}\lambda-$separated sets. Then $N_{eu}\lambda-Cl(A)\cap B=A\cap N_{eu}\lambda-Cl(B)=0_N$. Since $A\subseteq N_{eu}\lambda-Cl(A)$, we have $A\cap B\subseteq N_{eu}\lambda-Cl(A)\cap B=0_N$. Therefore $N_{eu}\lambda-Cl(A)\subseteq B^C=A$ and $N_{eu}\lambda-Cl(B)\subseteq A^C=B$. Hence $A=N_{eu}\lambda-Cl(A)$ and $B=N_{eu}\lambda-Cl(B)$. Therefore A and B are $N_{eu}\lambda-$closed sets and hence $A=B^C$ and $B=A^C$ are disjoint $N_{eu}\lambda-$open sets. Thus $A\neq 0_N$, $B\neq 0_N$ such that $A\cup B=1_N$ and $A\cap B=0_N$, A and B are $N_{eu}\lambda-$open sets. That is X is not $N_{eu}\lambda-$connected, which is a contradiction to X is a $N_{eu}\lambda-$connected space. Hence 1_N is not the union of any two $N_{eu}\lambda-$separated sets.
Conversely, assume that 1_N is not the union of any two $N_{eu}\lambda-$separated sets. Suppose X is not $N_{eu}\lambda-$connected. Then $A\cup B=1_N$, where $A\neq 0_N$, $B\neq 0_N$ such that $A\cap B=0_N$, A and B are $N_{eu}\lambda-$open sets in X. Since $A\subseteq B^C$ and $B\subseteq A^C$, $N_{eu}\lambda-Cl(A)\cap B\subseteq B^C\cap B=0_N$ and $A\cap N_{eu}\lambda-Cl(B)\subseteq A\cap A^C=0_N$. That is A and B are $N_{eu}\lambda-$separated sets. This is a contradiction. Therefore X is $N_{eu}\lambda-$connected.

Definition 4.11. A $N_{eu}-$Top$-$Space (X,T_N) is $N_{eu}-$Super$-\lambda-$disconnected if there exists a $N_{eu}-$Regular$-\lambda-$open set A in X such that $A\neq 0_N$ and $A\neq 1_N$. A $N_{eu}-$Top$-$Space (X,T_N) is called $N_{eu}-$Super$-\lambda-$connected if X is not $N_{eu}-$Super$-\lambda-$disconnected.

Theorem 4.12. Let (X,T_N) be a $N_{eu}-$Top$-$Space. Then the following assertions are equivalent:

(i) X is $N_{eu}-$Super$-\lambda-$connected.

(ii) For each $N_{eu}\lambda-$open set $U\neq 0_N$ in X, we have $N_{eu}\lambda-Cl(U)=1_N$.

(iii) For each $N_{eu}\lambda-$closed set $U\neq 1_N$ in X, we have $N_{eu}\lambda-Int(U)=0_N$.

(iv) There do not exist $N_{eu}\lambda-$open subsets U and V in (X,T_N), such that $U\neq 0_N$, $V\neq 0_N$ and $U\subseteq V^C$.

(v) There do not exist $N_{eu}\lambda-$open subsets U and V in (X,T_N), such that $U\neq 0_N$, $V\neq 0_N$, $V=(N_{eu}\lambda-Cl(U))^C$ and $U=(N_{eu}\lambda-Cl(V))^C$.

(vi) There do not exist $N_{eu}\lambda-$closed subsets U and V in (X,T_N), such that $U\neq 1_N$, $V\neq 1_N$, $V=(N_{eu}\lambda-Int(U))^C$ and $U=(N_{eu}\lambda-Int(V))^C$.

Proof. $(\mathrm{i})\Rightarrow(\mathrm{ii})$: Assume that there exists a $N_{eu}\lambda$-open set $A\neq 0_N$ such that $N_{eu}\lambda-Cl(A)\neq 1_N$. Now take $B=N_{eu}\lambda-Int[N_{eu}\lambda-Cl(A)]$. Then B is a proper N_{eu}-Regular-λ-open set in X which contradicts that X is N_{eu}-Super-λ-connected. Therefore $N_{eu}\lambda-Cl(A)=1_N$.

$(\mathrm{ii})\Rightarrow(\mathrm{iii})$: Let $A\neq 1_N$ be a $N_{eu}\lambda$-closed set in X. Then A^C is $N_{eu}\lambda$-open set in X and $A^C\neq 0_N$. Hence by hypothesis, $N_{eu}\lambda-Cl(A^C)=1_N$, and so $N_{eu}\lambda-Cl(A^C)=(N_{eu}\lambda-Int(A))^C=1_N$. This implies that $N_{eu}\lambda-Int(A)=0_N$.

$(\mathrm{iii})\Rightarrow(\mathrm{iv})$: Let A and B be $N_{eu}\lambda$-open sets in X such that $A\neq 0_N\neq B$ and $A\subseteq B^C$. Since B^C is $N_{eu}\lambda$-closed set in X and $B\neq 0_N$ implies $B^C\neq 1_N$, we obtain $N_{eu}\lambda-Int(B^C)=0_N$. But, from $A\subseteq B^C$, $0_N\neq A=N_{eu}\lambda-Int(A)\subseteq N_{eu}\lambda-Int(B^C)=0_N$, which is a contradiction.

$(\mathrm{iv})\Rightarrow(\mathrm{i})$: Let $0_N\neq A\neq 1_N$ be N_{eu}-Regular-λ-open set in X. Let $B=(N_{eu}\lambda-Cl(A))^C$. Since $N_{eu}\lambda-Int[N_{eu}\lambda-Cl(B)]=N_{eu}\lambda-Int\left[N_{eu}\lambda-Cl\left(N_{eu}\lambda-Cl(A)\right)^C\right]$

$=N_{eu}\lambda-Int\left[N_{eu}\lambda-Int\left(N_{eu}\lambda-Cl(A)\right)\right]^C=N_{eu}\lambda-Int(A^C)=[N_{eu}\lambda-Cl(A)]^C=B.$ Also we get $B\neq 0_N$, since otherwise, we have $B=0_N$ and this implies $(N_{eu}\lambda-Cl(A))^C=0_N$. That implies $N_{eu}\lambda-Cl(A)=1_N$. That shows that $A=N_{eu}\lambda-Int[N_{eu}\lambda-Cl(A)]=N_{eu}\lambda-Int(1_N)=1_N$. That is $A=1_N$, which is a contradiction. Therefore $B\neq 0_N$ and $A\subseteq B^C$. But this is a contradiction to (iv). Therefore (X,T_N) is N_{eu}-Super-λ-connected space.

$(\mathrm{i})\Rightarrow(\mathrm{v})$: Let A and B be $N_{eu}\lambda$-open sets in (X,T_N) such that $A\neq 0_N\neq B$, $B=[N_{eu}\lambda-Cl(A)]^C$, $A=[N_{eu}\lambda-Cl(B)]^C$. Now $N_{eu}\lambda-Int[N_{eu}\lambda-Cl(A)]=N_{eu}\lambda-Int(B^C)=[N_{eu}\lambda-Cl(B)]^C=A$, $A\neq 0_N$ and $A\neq 1_N$, since if $A=1_N$, then $1_N=[N_{eu}\lambda-Cl(B)]^C$. This implies $N_{eu}\lambda-Cl(B)=0_N$. But $B\neq 0_N$. Therefore $A\neq 1_N$ implies that A is proper N_{eu}-Regular-λ-open set in (X,T_N), which is a contradiction to (i). Hence (v) is true.

$(\mathrm{v})\Rightarrow(\mathrm{i})$: Let A be N_{eu}-Regular-λ-open set in (X,T_N) such that $A=N_{eu}\lambda-Int[N_{eu}\lambda-Cl(A)]$ and $0_N\neq A\neq 1_N$. Now take $B=[N_{eu}\lambda-Cl(A)]^C$. In this case we get $B\neq 0_N$ and B is N_{eu}-Regular-λ-open set in (X,T_N). $B=[N_{eu}\lambda-Cl(A)]^C$ and $[N_{eu}\lambda-Cl(B)]^C=\left[N_{eu}\lambda-Cl\left(N_{eu}\lambda-Cl(A)\right)^C\right]^C=N_{eu}\lambda-Int\left[\left(N_{eu}\lambda-Cl(A)\right)^C\right]^C=$ $N_{eu}\lambda-Int\left[\left(N_{eu}\lambda-Cl(A)\right)\right]=A.$ But this is a contradiction. Therefore (X,T_N) is N_{eu}-Super-λ-connected space.

$(\mathrm{v})\Rightarrow(\mathrm{vi})$: Let A and B be two N_{eu}-Regular-λ-closed sets in (X,T_N) such that $A\neq 1_N\neq B$, $B=[N_{eu}\lambda-Int(A)]^C$, $A=[N_{eu}\lambda-Int(B)]^C$. Take $C=A^C$ and $D=B^C$, C and D become N_{eu}-Regular-λ-open sets in (X,T_N) with $C\neq 0_N\neq D$, $D=[N_{eu}\lambda-Int(C)]^C$, $C=[N_{eu}\lambda-Int(D)]^C$, which is a contradiction to (v). Hence (vi) is true.

$(\mathrm{vi})\Rightarrow(\mathrm{v})$: It can be easily proved by the similar way as in $(\mathrm{v})\Rightarrow(\mathrm{vi})$.

Definition 4.13. A N_{eu} -Top-Space (X,T_N) is said to be N_{eu}-Extremely-λ-disconnected if the $N_{eu}\lambda$-closure of every $N_{eu}\lambda$-open set in (X,T_N) is $N_{eu}\lambda$-open set in X.

Theorem 4.14. Let (X,T_N) be a N_{eu}-Top-Space. Then the following statements are equivalent.

(i) X is N_{eu}-Extremely-λ-disconnected space.

(ii) For each $N_{eu}\lambda$-closed set A, $N_{eu}\lambda-Int(A)$ is $N_{eu}\lambda$-closed set.

(iii) For each $N_{eu}\lambda$-open set A, $N_{eu}\lambda-Cl(A)=\left[N_{eu}\lambda-Cl\left(N_{eu}\lambda-Cl(A)\right)^C\right]^C$.

(iv) For each $N_{eu}\lambda$-open sets A and B with $N_{eu}\lambda-Cl(A)=B^C$, $N_{eu}\lambda-Cl(A)=\left[N_{eu}\lambda-Cl(B)\right]^C$.

Proof. (i)$\Rightarrow$(ii): Let A be any $N_{eu}\lambda$-closed set in (X,T_N). Then A^C is $N_{eu}\lambda$-open set. So (i) implies that $N_{eu}\lambda-Cl\left(A^C\right)=\left[N_{eu}\lambda-Int(A)\right]^C$ is $N_{eu}\lambda$-open set. Thus $N_{eu}\lambda-Int(A)$ is $N_{eu}\lambda$-closed set in (X,T_N).

(ii)$\Rightarrow$(iii): Let A be $N_{eu}\lambda$-open set. Then we have $\left[N_{eu}\lambda-Cl\left(N_{eu}\lambda-Cl(A)\right)^C\right]^C=\left[N_{eu}\lambda-Cl\left(N_{eu}\lambda-Int\left(A^C\right)\right)\right]^C$. Since A is $N_{eu}\lambda$-open set. Then A^C is $N_{eu}\lambda$-closed set. So, by (ii) $N_{eu}\lambda-Int\left(A^C\right)$ is $N_{eu}\lambda$-closed set. That is $N_{eu}\lambda-Cl\left[N_{eu}\lambda-Int\left(A^C\right)\right]=N_{eu}\lambda-Int\left(A^C\right)$. Hence we obtain $\left[N_{eu}\lambda-Cl\left(N_{eu}\lambda-Cl(A)\right)^C\right]^C=\left[N_{eu}\lambda-Cl\left(N_{eu}\lambda-Int\left(A^C\right)\right)\right]^C=\left[N_{eu}\lambda-Int\left(A^C\right)\right]^C=$ $N_{eu}\lambda-Cl(A)$ which implies that $N_{eu}\lambda-Cl(A)=\left[N_{eu}\lambda-Cl\left(N_{eu}\lambda-Cl(A)\right)^C\right]^C$.

(iii)$\Rightarrow$(iv): Let A and B be any two $N_{eu}\lambda$-open sets in (X,T_N) such that $N_{eu}\lambda-Cl(A)=B^C$. Then (iii)$\Rightarrow$ $N_{eu}\lambda-Cl(A)=\left[N_{eu}\lambda-Cl\left(N_{eu}\lambda-Cl(A)\right)^C\right]^C=\left[N_{eu}\lambda-Cl\left(B^C\right)^C\right]^C=\left[N_{eu}\lambda-Cl(B)\right]^C$.

(iv)$\Rightarrow$(i): Let A be any $N_{eu}\lambda$-open set in (X,T_N). Let $B=\left[N_{eu}\lambda-Cl(A)\right]^C$. Then $N_{eu}\lambda-Cl(A)=B^C$. Then (iv) implies $N_{eu}\lambda-Cl(A)=\left[N_{eu}\lambda-Cl(B)\right]^C$. Since $N_{eu}\lambda-Cl(B)$ is $N_{eu}\lambda$-closed set, this implies that $N_{eu}\lambda-Cl(A)$ is $N_{eu}\lambda$-open set. This implies that (X,T_N) is N_{eu}-Extremely-λ-disconnected space.

Definition 4.15. A N_{eu}-Top-Space. (X,T_N) is N_{eu}-Strongly-λ-connected, if there does not exist any nonempty $N_{eu}\lambda$-closed sets A and B in X such that $A\cap B=0_N$.

Theorem 4.16. Let $f:(X,T_N)\to(Y,\sigma_N)$ be a $N_{eu}\lambda$-irresolute surjection and X be a N_{eu}-Strongly-λ-connected space. Then Y is N_{eu}-Strongly-λ-connected.

Proof. Assume that Y is not N_{eu}-Strongly-λ-connected, then there exist nonempty $N_{eu}\lambda$-closed sets U and V in Y such that $U\neq 0_N$, $V\neq 0_N$, and $U\cap V=0_N$. Since f is $N_{eu}\lambda$-irresolute mapping, $A=f^{-1}(U)\neq 0_N$, $B=f^{-1}(V)\neq 0_N$, which are $N_{eu}gs\alpha*$-closed sets in X and $f^{-1}(U)\cap f^{-1}(V)=f^{-1}(0_N)=0_N$, which implies $A\cap B=0_N$. Thus, X is not

N_{eu} $-$Strongly$-\lambda-$connected, which is a N_{eu} $-$Strongly$-\lambda-$connected. Hence this is a contradiction to our hypothesis. Therefore, Y is N_{eu} $-$Strongly$-\lambda-$connected.

5 Neutrosophic $\lambda-$Regular Spaces

In this section, we define $N_{eu}\lambda-$Regular spaces and Strongly$-N_{eu}\lambda-$Regular spaces by using $N_{eu}\lambda-$open sets and $N_{eu}\lambda-$closed sets in $N_{eu}-$Top$-$Spaces. We study their basic properties and characterizations.

Definition 5.1. A $N_{eu}-$Top$-$Space (X,τ_N) is said to be $N_{eu}\lambda-$Regular if for each $N_{eu}\lambda-$closed set A and a $N_{eu}-$point $x_{(\alpha,\beta,\gamma)}\notin A,$ there exist disjoint $N_{eu}\lambda-$open sets U and V such that $A\subseteq U,\ x_{(\alpha,\beta,\gamma)}\in V.$

Theorem 5.2. Let (X,τ_N) be a $N_{eu}-$Top$-$Space. Then the following statements are equivalent:

(i) X is $N_{eu}\lambda-$Regular.

(ii) For every $x_{(\alpha,\beta,\gamma)}\in X$ and every $N_{eu}\lambda-$open set G containing $x_{(\alpha,\beta,\gamma)},$ there exists a $N_{eu}\lambda-$open set U such that $x_{(\alpha,\beta,\gamma)}\in U\subseteq N_{eu}\lambda-Cl(U)\subseteq G.$

(iii) For every $N_{eu}\lambda-$closed set $F,$ the intersection of all $N_{eu}\lambda-$closed $N_{eu}\lambda-$neighbourhoods of F is exactly $F.$

(iv) For any $N_{eu}-$set A and a $N_{eu}\lambda-$open set B such that $A\cap B\neq 0_N,$ there exists a $N_{eu}\lambda-$open set U such that $A\cap U\neq 0_N$ and $N_{eu}\lambda-Cl(U)\subseteq B.$

(v) For every non-empty $N_{eu}-$set A and $N_{eu}\lambda-$closed set B such that $A\cap B=0_N,$ there exist disjoint $N_{eu}\lambda-$open sets U and V such that $A\cap U\neq 0_N$ and $B\subseteq V.$

Proof. $(\mathrm{i})\Rightarrow(\mathrm{ii})$: Suppose X is $N_{eu}\lambda-$Regular. Let $x_{(\alpha,\beta,\gamma)}\in X$ and let G be a $N_{eu}\lambda-$open set containing $x_{(\alpha,\beta,\gamma)}.$ Then $x_{(\alpha,\beta,\gamma)}\notin G^C$ and G^C is $N_{eu}\lambda-$closed. Since X is $N_{eu}\lambda-$Regular, there exist $N_{eu}\lambda-$open sets U and V such that $U\cap V=0_N$ and $x_{(\alpha,\beta,\gamma)}\in U,\ G^C\subseteq V.$ It follows that $U\subseteq V^C\subseteq G$ and hence $N_{eu}\lambda-Cl(U)\subseteq N_{eu}\lambda-Cl(V^C)=V^C\subseteq G.$ That is $x_{(\alpha,\beta,\gamma)}\in U\subseteq N_{eu}\lambda-Cl(U)\subseteq G.$

$(\mathrm{ii})\Rightarrow(\mathrm{iii})$: Let F be any $N_{eu}\lambda-$closed set and $x_{(\alpha,\beta,\gamma)}\notin F.$ Then F^C is $N_{eu}\lambda-$open and $x_{(\alpha,\beta,\gamma)}\in F^C.$ By assumption, there exists a $N_{eu}\lambda-$open set U such that $x_{(\alpha,\beta,\gamma)}\in U\subseteq N_{eu}\lambda-Cl(U)\subseteq F^C.$ Thus $F\subseteq\left(N_{eu}\lambda-Cl(U)\right)^C\subseteq U^C.$ Now U^C is $N_{eu}\lambda-$closed and $N_{eu}\lambda-$neighbourhood of F which does not contain $x_{(\alpha,\beta,\gamma)}.$ So, we get the intersection of all $N_{eu}\lambda-$closed $N_{eu}\lambda-$neighbourhoods of F to be exactly equal to $F.$

$(\mathrm{iii})\Rightarrow(\mathrm{iv})$: Suppose $A\cap B\neq 0_N$ and B is $N_{eu}\lambda-$open set. Let $x_{(\alpha,\beta,\gamma)}\in A\cap B.$ Since B is $N_{eu}\lambda-$open, B^C is $N_{eu}\lambda-$closed and $x_{(\alpha,\beta,\gamma)}\notin B^C.$ By using $(\mathrm{iii}),$ there exists a $N_{eu}\lambda-$closed, $N_{eu}\lambda-$neighbourhood V of B^C such that $x_{(\alpha,\beta,\gamma)}\notin V.$ Now for the $N_{eu}\lambda-$neighbourhood V of $B^C,$ there exists a $N_{eu}\lambda-$open set G such that $B^C\subseteq G\subseteq V.$ Take $U=V^C.$ Thus U is a $N_{eu}\lambda-$open set containing $x_{(\alpha,\beta,\gamma)}.$ Also $A\cap U\neq 0_N$ and $N_{eu}\lambda-Cl(U)\subseteq G^C\subseteq B.$

$(\text{iv}) \Rightarrow (\text{v})$: Suppose A is a non-empty set and B is a $\mathrm{N}_{eu}\lambda-$closed set such that $A \cap B = 0_N$. Then B^C is $\mathrm{N}_{eu}\lambda-$open set and $A \cap B^C \neq 0_N$. By our assumption, there exists a $\mathrm{N}_{eu}\lambda-$open U such that $A \cap U \neq 0_N$ and $\mathrm{N}_{eu}\lambda-Cl(U) \subseteq B^C$. Take $V = (\mathrm{N}_{eu}\lambda-Cl(U))^C$. Since $\mathrm{N}_{eu}\lambda-Cl(U)$ is $\mathrm{N}_{eu}\lambda-$closed, V is $\mathrm{N}_{eu}\lambda-$open. Also $B \subseteq V$ and $U \cap V \subseteq \mathrm{N}_{eu}\lambda-Cl(U) \cap (\mathrm{N}_{eu}\lambda-Cl(U))^C = 0_N$.

$(\text{v}) \Rightarrow (\text{i})$: Let S be $\mathrm{N}_{eu}\lambda-$closed set and $x_{(\alpha,\beta,\gamma)} \notin S$. Then $S \cap \{x_{(\alpha,\beta,\gamma)}\} = 0_N$. By (v), there exist disjoint $\mathrm{N}_{eu}\lambda-$open sets U and V such that $U \cap \{x_{(\alpha,\beta,\gamma)}\} \neq 0_N$ and $S \subseteq V$. That is U and V are disjoint $\mathrm{N}_{eu}\lambda-$open sets containing $x_{(\alpha,\beta,\gamma)}$ and S respectively. This proves that (X, τ_N) is $\mathrm{N}_{eu}\lambda-\mathrm{R}$egular.

Corollary 5.3. Let (X, τ_N) be a $\mathrm{N}_{eu}-$Top$-$Space. Then the following statements are equivalent:

(i) X is $\mathrm{N}_{eu}\lambda-\mathrm{R}$egular.

(ii) For every $x_{(\alpha,\beta,\gamma)} \in X$ and every $\mathrm{N}_{eu}\lambda-$open set G containing $x_{(\alpha,\beta,\gamma)}$, there exists a $\mathrm{N}_{eu}\lambda-$open set U such that $x_{(\alpha,\beta,\gamma)} \in U \subseteq \mathrm{N}_{eu}\lambda-Cl(U) \subseteq G$.

(iii) For every $\mathrm{N}_{eu}\lambda-$closed F, the intersection of all $\mathrm{N}_{eu}-$closed neighbourhoods of F is exactly F.

(iv) For any $\mathrm{N}_{eu}-$set A and a $\mathrm{N}_{eu}-$open set B such that $A \cap B \neq 0_N$, there exists a $\mathrm{N}_{eu}\lambda-$open set U such that $A \cap U \neq 0_N$ and $\mathrm{N}_{eu}\lambda-Cl(U) \subseteq B$.

(v) For every non-empty $\mathrm{N}_{eu}-$set A and a $\mathrm{N}_{eu}-$closed set B such that $A \cap B = 0_N$, there exist disjoint $\mathrm{N}_{eu}\lambda-$open sets U and V such that $A \cap U \neq 0_N$ and $B \subseteq V$.

Proof. Since every $\mathrm{N}_{eu}-$open set is $\mathrm{N}_{eu}\lambda-$open and follows from Theorem 5.2.

Theorem 5.4. A $\mathrm{N}_{eu}-$Top$-$Space (X, τ_N) is $\mathrm{N}_{eu}\lambda-\mathrm{R}$egular if and only if every $x_{(\alpha,\beta,\gamma)} \in X$ and every $\mathrm{N}_{eu}\lambda-$neighbourhood N containing $x_{(\alpha,\beta,\gamma)}$, there exists a $\mathrm{N}_{eu}\lambda-$open set V such that $x_{(\alpha,\beta,\gamma)} \in V \subseteq \mathrm{N}_{eu}\lambda-Cl(V) \subseteq N$.

Proof. Let X be a $\mathrm{N}_{eu}\lambda-\mathrm{R}$egular space. Let N be any $\mathrm{N}_{eu}\lambda-$neighbourhood of $x_{(\alpha,\beta,\gamma)}$. Then there exists a $\mathrm{N}_{eu}\lambda-$open set G such that $x_{(\alpha,\beta,\gamma)} \in G \subseteq N$. Since G^C is $\mathrm{N}_{eu}\lambda-$closed set and $x_{(\alpha,\beta,\gamma)} \notin G^C$, by definition there exist $\mathrm{N}_{eu}\lambda-$open sets U and V such $G^C \subseteq U$ and $x_{(\alpha,\beta,\gamma)} \in V$ and $U \cap V = 0_N$ so that $V \subseteq U^C$. It follows that $\mathrm{N}_{eu}\lambda-Cl(V) \subseteq \mathrm{N}_{eu}\lambda-Cl(U^C) = U^C$. Also $G^C \subseteq U$ implies $U^C \subseteq G \subseteq N$. Hence $x_{(\alpha,\beta,\gamma)} \in V \subseteq \mathrm{N}_{eu}\lambda-Cl(V) \subseteq N$. Conversely, suppose for every $x_{(\alpha,\beta,\gamma)} \in X$ and every $\mathrm{N}_{eu}\lambda-$neighbourhood N containing $x_{(\alpha,\beta,\gamma)}$, there exists a $\mathrm{N}_{eu}\lambda-$open set V such that $x_{(\alpha,\beta,\gamma)} \in V \subseteq \mathrm{N}_{eu}\lambda-Cl(V) \subseteq N$. Let F be any $\mathrm{N}_{eu}\lambda-$closed set and $x_{(\alpha,\beta,\gamma)} \notin F$. Then $x_{(\alpha,\beta,\gamma)} \in F^C$. Since F^C is $\mathrm{N}_{eu}\lambda-$open set, F^C is $\mathrm{N}_{eu}\lambda-$neighbourhood containing $x_{(\alpha,\beta,\gamma)}$. By hypothesis there exists a $\mathrm{N}_{eu}\lambda-$open set V such that $x_{(\alpha,\beta,\gamma)} \in V$ and $\mathrm{N}_{eu}\lambda-Cl(V) \subseteq F^C$. This implies that $F \subseteq (\mathrm{N}_{eu}\lambda-Cl(V))^C$. Then $(\mathrm{N}_{eu}\lambda-Cl(V))^C$ is a $\mathrm{N}_{eu}\lambda-$open set containing F. Also $V \cap (\mathrm{N}_{eu}\lambda-Cl(V))^C = 0_N$. Hence (X, τ_N) is $\mathrm{N}_{eu}\lambda-\mathrm{R}$egular.

Theorem 5.5. A N_{eu} $-$Top$-$Space (X,τ_N) is $N_{eu}\lambda-$Regular if and only if for each $N_{eu}\lambda-$closed set F of X and each $x_{(\alpha,\beta,\gamma)}\in F^C$, there exist $N_{eu}\lambda-$open sets U and V of X such that $x_{(\alpha,\beta,\gamma)}\in U$ and $F\subseteq V$ and $N_{eu}\lambda-Cl(U)\cap N_{eu}\lambda-Cl(V)=0_N$.

Proof. Suppose (X,τ_N) is $N_{eu}\lambda-$Regular. Let F be a $N_{eu}\lambda-$closed set in X and $x_{(\alpha,\beta,\gamma)}\notin F$. Then there exist $N_{eu}\lambda-$open sets $U_{x_{(\alpha,\beta,\gamma)}}$ and V such that $x_{(\alpha,\beta,\gamma)}\in U_{x_{(\alpha,\beta,\gamma)}}$, $F\subseteq V$ and $U_{x_{(\alpha,\beta,\gamma)}}\cap V=0_N$. This implies that $U_{\left(x_{(\alpha,\beta,\gamma)}\right)}\cap N_{eu}\lambda-Cl(V)=0_N$. Also $N_{eu}\lambda-Cl(V)$ is a $N_{eu}\lambda-$closed set and $x_{(\alpha,\beta,\gamma)}\notin N_{eu}\lambda-Cl(V)$. Since (X,τ_N) is $N_{eu}\lambda-$Regular, there exist $N_{eu}\lambda-$open sets G and H of X such that $x_{(\alpha,\beta,\gamma)}\in G$, $N_{eu}\lambda-Cl(V)\subseteq H$ and $G\cap V=0_N$. This implies $N_{eu}\lambda-Cl(G)\cap H\subseteq N_{eu}\lambda-Cl(H^C)\cap H=H^C\cap H=0_N$. Take $U=G$. Now U and V are $N_{eu}\lambda-$open sets in X such that $x_{(\alpha,\beta,\gamma)}\in U$ and $F\subseteq V$. Also $N_{eu}\lambda-Cl(U)\cap N_{eu}\lambda-Cl(V)\subseteq N_{eu}\lambda-Cl(G)\cap H=0_N$.
Conversely, suppose for each $N_{eu}\lambda-$closed set F of X and each $x_{(\alpha,\beta,\gamma)}\in F^C$, there exist $N_{eu}\lambda-$open sets U and V of X such that $x_{(\alpha,\beta,\gamma)}\in U$ and $F\subseteq V$ and $N_{eu}\lambda-Cl(U)\cap N_{eu}\lambda-Cl(V)=0_N$. Now $U\cap V\subseteq N_{eu}\lambda-Cl(U)\cap N_{eu}\lambda-Cl(V)=0_N$. Therefore $U\cap V=0_N$. This proves that (X,τ_N) is $N_{eu}\lambda-$Regular.

Theorem 5.6. Let $f:(X,\tau_N)\to(Y,\sigma_N)$ be a bijective function. If f is $N_{eu}\lambda-$irresolute, $N_{eu}\lambda-$open and X is $N_{eu}\lambda-$Regular, then Y is $N_{eu}\lambda-$Regular.

Proof. Suppose (X,τ_N) is $N_{eu}\lambda-$Regular. Let S be any $N_{eu}\lambda-$closed set in Y such that $y_{(r,t,s)}\notin S$. Since f is $N_{eu}\lambda-$irresolute, $f^{-1}(S)$ is $N_{eu}\lambda-$closed set in X. Since f is onto, there exists $x_{(\alpha,\beta,\gamma)}\in X$ such that $y_{(r,t,s)}=f\left(x_{(\alpha,\beta,\gamma)}\right)$. Now $f\left(x_{(\alpha,\beta,\gamma)}\right)=y_{(r,t,s)}\notin S$ implies that $x_{(\alpha,\beta,\gamma)}\notin f^{-1}(S)$. Since X is $N_{eu}\lambda-$Regular, there exist $N_{eu}\lambda-$open sets U and V in X such that $x_{(\alpha,\beta,\gamma)}\in U$, $f^{-1}(S)\subseteq V$ and $U\cap V=0_N$. Now $x_{(\alpha,\beta,\gamma)}\in U$ implies that $f\left(x_{(\alpha,\beta,\gamma)}\right)\in f(U)$ and $f^{-1}(S)\subseteq V$ implies that $S\subseteq f(V)$. Also $U\cap V=0_N$ implies that $f(U\cap V)=0_N$ which implies that $f(U)\cap f(V)=0_N$. Since f is a $N_{eu}\lambda-$open mapping, $f(U)$ and $f(V)$ are disjoint $N_{eu}\lambda-$open sets in Y containing $y_{(r,t,s)}$ and S respectively. Thus Y is $N_{eu}\lambda-$Regular.

Theorem 5.7. Let (X,τ_N) be a $N_{eu}\lambda-$Regular space. Then
(i) Every $N_{eu}\lambda-$open set in X is a union of $N_{eu}\lambda-$closed sets.
(ii) Every $N_{eu}\lambda-$closed set in X is an intersection of $N_{eu}\lambda-$open sets.

Proof. (i) Suppose X is $N_{eu}\lambda-$Regular. Let G be a $N_{eu}\lambda-$open set and $x_{(\alpha,\beta,\gamma)}\in G$. Then $F=G^C$ is $N_{eu}\lambda-$closed set and $x_{(\alpha,\beta,\gamma)}\notin F$. Since X is $N_{eu}\lambda-$Regular, there exist disjoint $N_{eu}\lambda-$open sets $U_{x_{(\alpha,\beta,\gamma)}}$ and V in X such that $x_{(\alpha,\beta,\gamma)}\in U_{x_{(\alpha,\beta,\gamma)}}$ and $F\subseteq V$. Since $U_{x_{(\alpha,\beta,\gamma)}}\cap F\subseteq U_{x_{(\alpha,\beta,\gamma)}}\cap V=0_N$, we have $U_{x_{(\alpha,\beta,\gamma)}}\subseteq F^C=G$. Take $V_{\left(x_{(\alpha,\beta,\gamma)}\right)}=N_{eu}\lambda-Cl\left(U_{x_{(\alpha,\beta,\gamma)}}\right)$. Then $V_{x_{(\alpha,\beta,\gamma)}}$ is $N_{eu}\lambda-$closed set and $V_{x_{(\alpha,\beta,\gamma)}}\cap V=0_N$. Now $F\subseteq V$ implies that $V_{x_{(\alpha,\beta,\gamma)}}\cap F\subseteq V_{x_{(\alpha,\beta,\gamma)}}\cap V=0_N$. It follows that

$x_{(\alpha,\beta,\gamma)} \in V_{x_{(\alpha,\beta,\gamma)}} \subseteq F^C = G$. This proves that $G = \bigcup\left\{V_{x_{(\alpha,\beta,\gamma)}} : x_{(\alpha,\beta,\gamma)} \in G\right\}$. Thus G is a union of $N_{eu}\lambda$-closed sets. (ii) Follows from (i) by using set-theoretic properties.

Theorem 5.8. Let $f:(X,\tau_N) \to (Y,\sigma_N)$ be a $N_{eu}\lambda$-continuous and N_{eu}-closed injection from a N_{eu}-Top-Space (X,τ_N) into a N_{eu}-Regular. space (Y,σ_N). If every $N_{eu}\lambda$-closed set in X is N_{eu}-closed, then X is $N_{eu}\lambda$-Regular.

Proof. Let $x_{(\alpha,\beta,\gamma)} \in X$ and A be a $N_{eu}\lambda$-closed set in X such that $x_{(\alpha,\beta,\gamma)} \notin A$. Then by assumption, A is N_{eu}-closed in X. Since f is N_{eu}-closed, $f(A)$ is a N_{eu}-closed set in Y such that $f\left(x_{(\alpha,\beta,\gamma)}\right) \notin f(A)$. Since Y is N_{eu}-Regular, there exist disjoint N_{eu}-open sets G and H in Y such that $f\left(x_{(\alpha,\beta,\gamma)}\right) \in G$ and $f(A) \subseteq H$. Since f is $N_{eu}\lambda$-continuous, $f^{-1}(G)$ and $f^{-1}(H)$ are disjoint $N_{eu}\lambda$-open sets in X containing $x_{(\alpha,\beta,\gamma)}$ and A respectively. Hence X is $N_{eu}\lambda$-Regular.

Theorem 5.9. Let $f:(X,\tau_N) \to (Y,\sigma_N)$ be a N_{eu}-continuous, $N_{eu}\lambda$-open bijection of a N_{eu}-Regular space X into a N_{eu}-space Y and if every $N_{eu}\lambda$-closed set in Y is N_{eu}-closed, then Y is $N_{eu}\lambda$-Regular.

Proof. Let $y_{(r,t,s)} \in Y$ and B be a $N_{eu}\lambda$-closed set in Y such that $y_{(r,t,s)} \notin B$. Since f is a bijection. So there exists a unique point $x_{(\alpha,\beta,\gamma)} \in X$ such that $f\left(x_{(\alpha,\beta,\gamma)}\right) = y_{(r,t,s)}$. Then by assumption, B is N_{eu}-closed in Y. Since f is a N_{eu}-continuous bijection, $f^{-1}(B)$ is a N_{eu}-closed set in X such that $x_{(\alpha,\beta,\gamma)} \notin f^{-1}(B)$. Since X is N_{eu}-Regular, there exist disjoint N_{eu}-open sets G and H in X such that $x_{(\alpha,\beta,\gamma)} \in G$ and $f^{-1}(B) \subseteq H$. Since f is $N_{eu}\lambda$-open, $f(G)$ and $f(H)$ are disjoint $N_{eu}\lambda$-open sets in Y such that $f\left(x_{(\alpha,\beta,\gamma)}\right) = y_{(r,t,s)} \in f(G)$ and $B \subseteq f(H)$. Hence Y is $N_{eu}\lambda$-Regular.

Definition 5.10. A N_{eu}-Top-Space (X,τ_N) is said to be strongly $N_{eu}\lambda$-Regular if for each $N_{eu}\lambda$-closed set A and a point $x_{(\alpha,\beta,\gamma)} \notin A$, there exist disjoint N_{eu}-open sets U and V such that $A \subseteq U$ and $x_{(\alpha,\beta,\gamma)} \in V$.

Proposition 5.11. (i) Every strongly $N_{eu}\lambda$-Regular space is $N_{eu}\lambda$-Regular.
(ii) Every strongly $N_{eu}\lambda$-Regular space is strongly N_{eu}-Regular.

Proof. (i) Suppose (X,τ_N) is strongly $N_{eu}\lambda$-Regular. Let F be a $N_{eu}\lambda$-closed set and $x_{(\alpha,\beta,\gamma)} \notin F$. Since X is strongly $N_{eu}\lambda$-Regular, there exist disjoint N_{eu}-open sets U and V such that $x_{(\alpha,\beta,\gamma)} \in U$ and $F \subseteq V$. Since every N_{eu}-open set is $N_{eu}\lambda$-open, so U and V are $N_{eu}\lambda$-open sets. This implies that X is $N_{eu}\lambda$-Regular.
(ii) This can be proved similarly as (i).

Definition 5.12. A N_{eu}-Top-Space (X,τ_N) is said to be strongly* $N_{eu}\lambda$-Regular. if for each N_{eu}-closed set A and a point $x_{(\alpha,\beta,\gamma)} \notin A$, there exist disjoint $N_{eu}\lambda$-open sets U and V such that $A \subseteq U$, $x_{(\alpha,\beta,\gamma)} \in V$.

Proposition 5.13. Every $\mathrm{N}_{eu}\lambda-\mathrm{R}$egular $\mathrm{N}_{eu}-$Top$-$Space (X,τ_N) is strongly* $\mathrm{N}_{eu}\lambda-\mathrm{R}$egular.

Proof. Suppose (X,τ_N) is $\mathrm{N}_{eu}\lambda-\mathrm{R}$egular. Let F be a $\mathrm{N}_{eu}-$closed set and $x_{(\alpha,\beta,\gamma)}\notin F.$ Then F is $\mathrm{N}_{eu}\lambda-$closed. Since X is $\mathrm{N}_{eu}\lambda-\mathrm{R}$egular, there exist disjoint $\mathrm{N}_{eu}\lambda-$open sets U and V such that $x_{(\alpha,\beta,\gamma)}\in U$ and $F\subseteq V.$ This implies that X is strongly* $\mathrm{N}_{eu}\lambda-\mathrm{R}$egular.

Theorem 5.14. Let (X,τ_N) be a $\mathrm{N}_{eu}-$Top$-$Space. Then the following statements are equivalent:

(i) X is strongly $\mathrm{N}_{eu}\lambda-\mathrm{R}$egular.

(ii) For every $x_{(\alpha,\beta,\gamma)}\in X$ and every $\mathrm{N}_{eu}\lambda-$open set G containing $x_{(\alpha,\beta,\gamma)}$, there exists a $\mathrm{N}_{eu}-$open set U such that $x_{(\alpha,\beta,\gamma)}\in U\subseteq \mathrm{N}_{eu}Cl(U)\subseteq G.$

(iii) For every $\mathrm{N}_{eu}\lambda-$closed set $F,$ the intersection of all $\mathrm{N}_{eu}-$closed, $\mathrm{N}_{eu}-$neighbourhoods of F is exactly $F.$

(iv) For any $\mathrm{N}_{eu}-$set A and a $\mathrm{N}_{eu}\lambda-$open set B such that $A\cap B\neq 0_N$, there exists a $\mathrm{N}_{eu}-$open set U such that $A\cap U\neq 0_N$ and $\mathrm{N}_{eu}-Cl(U)\subseteq B.$

(v) For every non-empty $\mathrm{N}_{eu}-$set A and $\mathrm{N}_{eu}\lambda-$closed set B such that $A\cap B=0_N$, there exist disjoint $\mathrm{N}_{eu}-$open sets U and V such that $A\cap U\neq 0_N$ and $B\subseteq V.$

Proof. $(\mathrm{i})\Rightarrow(\mathrm{ii})$: Suppose X is strongly $\mathrm{N}_{eu}\lambda-\mathrm{R}$egular. Let $x_{(\alpha,\beta,\gamma)}\in X$ and let G be a $\mathrm{N}_{eu}\lambda-$open set containing $x_{(\alpha,\beta,\gamma)}$. Then $x_{(\alpha,\beta,\gamma)}\notin G^C$ and G^C is $\mathrm{N}_{eu}\lambda-$closed. Since X is $\mathrm{N}_{eu}\lambda-\mathrm{R}$egular, there exist $\mathrm{N}_{eu}-$open sets U and V such that $U\cap V=0_N$ and $x_{(\alpha,\beta,\gamma)}\in U,$ $G^C\subseteq V.$ It follows that $U\subseteq V^C\subseteq G$ and hence $\mathrm{N}_{eu}-Cl(U)\subseteq \mathrm{N}_{eu}-Cl(V^C)=V^C\subseteq G.$ That is $x_{(\alpha,\beta,\gamma)}\in U\subseteq \mathrm{N}_{eu}-Cl(U)\subseteq G.$

$(\mathrm{ii})\Rightarrow(\mathrm{iii})$: Let F be a $\mathrm{N}_{eu}\lambda-$closed set and $x_{(\alpha,\beta,\gamma)}\notin F.$ Then F^C is $\mathrm{N}_{eu}\lambda-$open set and $x_{(\alpha,\beta,\gamma)}\in F^C.$ By assumption, there exists a $\mathrm{N}_{eu}-$open set U such that $x_{(\alpha,\beta,\gamma)}\in U\subseteq \mathrm{N}_{eu}-Cl(U)\subseteq F^C.$ Thus $F\subseteq(\mathrm{N}_{eu}-Cl(U))^C\subseteq U^C.$ Now U^C is $\mathrm{N}_{eu}-$closed, $\mathrm{N}_{eu}-$oneighbourhoods of F which does not contain $x_{(\alpha,\beta,\gamma)}$. So, the intersection of all $\mathrm{N}_{eu}-$closed, $\mathrm{N}_{eu}-$oneighbourhoods of F is exactly $F.$

$(\mathrm{iii})\Rightarrow(\mathrm{iv})$: Suppose $A\cap B\neq 0_N$ and B is $\mathrm{N}_{eu}\lambda-$open set. Let $x_{(\alpha,\beta,\gamma)}\in A\cap B.$ Since B is $\mathrm{N}_{eu}\lambda-$open, B^C is $\mathrm{N}_{eu}\lambda-$closed and $x_{(\alpha,\beta,\gamma)}\notin B^C.$ By using (iii), there exists a $\mathrm{N}_{eu}-$closed, $\mathrm{N}_{eu}-$oneighbourhood V of B^C such that $x_{(\alpha,\beta,\gamma)}\notin V.$ Now for the $\mathrm{N}_{eu}-$oneighbourhood V of B^C, there exists a $\mathrm{N}_{eu}-$open set G such that $B^C\subseteq G\subseteq V.$ Take $U=V^C.$ Thus U is a $\mathrm{N}_{eu}-$open set containing $x_{(\alpha,\beta,\gamma)}$. Also $A\cap U\neq 0_N$ and $\mathrm{N}_{eu}-Cl(U)\subseteq G^C\subseteq B.$

$(\mathrm{iv})\Rightarrow(\mathrm{v})$: Suppose A is a non-empty set and B is $\mathrm{N}_{eu}\lambda-$closed set such that $A\cap B=0_N.$ Then B^C is $\mathrm{N}_{eu}\lambda-$open set and $A\cap B^C\neq 0_N.$ By our assumption, there exists a $\mathrm{N}_{eu}-$open set U such that $A\cap U\neq 0_N$ and $\mathrm{N}_{eu}-Cl(U)\subseteq B^C.$ Take $V=(\mathrm{N}_{eu}-Cl(U))^C.$ Since $\mathrm{N}_{eu}-Cl(U)$ is neutrosophic closed, V is $\mathrm{N}_{eu}-$open. Also $B\subseteq V$ and $U\cap V\subseteq \mathrm{N}_{eu}-Cl(U)\cap(\mathrm{N}_{eu}-Cl(U))^C=0_N.$

$(\mathrm{v})\Rightarrow(\mathrm{i})$: Let S be $\mathrm{N}_{eu}\lambda-$closed set and $x_{(\alpha,\beta,\gamma)}\notin S.$ Then $S\cap\{x_{(\alpha,\beta,\gamma)}\}=0_N.$ By (v), there exist disjoint $\mathrm{N}_{eu}-$open sets U and V such that $U\cap\{x_{(\alpha,\beta,\gamma)}\}\neq 0_N$ and $S\subseteq V.$ That is U and V are disjoint

N_{eu} −open sets containing $x_{(\alpha,\beta,\gamma)}$ and S respectively. This proves that (X,τ_N) is strongly $N_{eu}\lambda$ −Regular.

Theorem 5.15. A N_{eu} −Top −Space. (X,τ_N) is $N_{eu}\lambda$ −Regular if and only if for each $N_{eu}\lambda$ −closed set F of X and each $x_{(\alpha,\beta,\gamma)} \in F^C$, there exist N_{eu} −open sets U and V of X such that $x_{(\alpha,\beta,\gamma)} \in U$ and $F \subseteq V$ and $N_{eu}-Cl(U) \cap N_{eu}-Cl(V) = 0_N$.

Proof. Suppose (X,τ_N) is strongly $N_{eu}\lambda$ −Regular. Let F be a $N_{eu}\lambda$ −closed set in X and $x_{(\alpha,\beta,\gamma)} \notin F$. Then there exist N_{eu} −open sets $U_{x_{(\alpha,\beta,\gamma)}}$ and V such that $x_{(\alpha,\beta,\gamma)} \in U_{x_{(\alpha,\beta,\gamma)}}$, $F \subseteq V$ and $U_{x_{(\alpha,\beta,\gamma)}} \cap V = 0_N$. This implies that $U_{\left(x_{(\alpha,\beta,\gamma)}\right)} \cap N_{eu}-Cl(V) = 0_N$. Also $N_{eu}-Cl(V)$ is a N_{eu} −closed set and $x_{(\alpha,\beta,\gamma)} \notin N_{eu}-Cl(V)$. Since (X,τ_N) is strongly $N_{eu}\lambda$ −Regular, there exist N_{eu} −open sets G and H of X such that $x_{(\alpha,\beta,\gamma)} \in G$, $N_{eu}-Cl(V) \subseteq H$ and $G \cap V = 0_N$. This implies $N_{eu}-Cl(G) \cap H \subseteq N_{eu}-Cl(H^C) \cap H = H^C \cap H = 0_N$. Take $U = G$. Now U and V are N_{eu} −open sets in X such that $x_{(\alpha,\beta,\gamma)} \in U$ and $F \subseteq V$. Also $N_{eu}-Cl(U) \cap N_{eu}-Cl(V) \subseteq N_{eu}-Cl(G) \cap H = 0_N$. Thus $N_{eu}-Cl(U) \cap N_{eu}-Cl(V) = 0_N$.
Conversely, suppose for each $N_{eu}\lambda$ −closed set F of X and each $x_{(\alpha,\beta,\gamma)} \in F^C$, there exist N_{eu} −open sets U and V of X such that $x_{(\alpha,\beta,\gamma)} \in U$ and $F \subseteq V$ and $N_{eu}-Cl(U) \cap N_{eu}-Cl(V) = 0_N$. Now $U \cap V \subseteq N_{eu}-Cl(U) \cap N_{eu}-Cl(V) = 0_N$. Therefore $U \cap V = 0_N$. This proves that (X,τ_N) is strongly $N_{eu}\lambda$ −Regular.

Theorem 5.16. A N_{eu} −Top −Space. (X,τ_N) is strongly $N_{eu}\lambda$ −Regular if and only if every pair consisting of a N_{eu} −compact set and a disjoint $N_{eu}\lambda$ −closed set can be separated by N_{eu} −open sets.

Proof. Let (X,τ_N) be strongly $N_{eu}\lambda$ −Regular and let A be a N_{eu} −compact set, and B be a $N_{eu}\lambda$ −closed set such that $A \cap B = 0_N$. Since X is strongly $N_{eu}\lambda$ −Regular, for each $x_{(\alpha,\beta,\gamma)} \in A$, there exist disjoint N_{eu} −open sets $U_{x_{(\alpha,\beta,\gamma)}}$ and $V_{x_{(\alpha,\beta,\gamma)}}$ such that $x_{(\alpha,\beta,\gamma)} \in U_{x_{(\alpha,\beta,\gamma)}}$, $B \subseteq V_{x_{(\alpha,\beta,\gamma)}}$. Obviously, $\left\{U_{x_{(\alpha,\beta,\gamma)}} : x_{(\alpha,\beta,\gamma)} \in A\right\}$ is a N_{eu} −open covering of A. Since A is N_{eu} −compact, there exists a finite set $F \subseteq A$ such that $A \subseteq \bigcup\left\{U_{x_{(\alpha,\beta,\gamma)}} : x_{(\alpha,\beta,\gamma)} \in F\right\}$ and $B \subseteq \bigcap\left\{V_{x_{(\alpha,\beta,\gamma)}} : x_{(\alpha,\beta,\gamma)} \in F\right\}$. Put $U = \bigcup\left\{U_{x_{(\alpha,\beta,\gamma)}} : x_{(\alpha,\beta,\gamma)} \in F\right\}$ and $V = \bigcap\left\{V_{x_{(\alpha,\beta,\gamma)}} : x_{(\alpha,\beta,\gamma)} \in F\right\}$. Then U and V are N_{eu} −open sets in X. Also $U \cap V = 0_N$. Otherwise, if $x_{(\alpha,\beta,\gamma)} \in U \cap V$, then $x_{(\alpha,\beta,\gamma)} \in U_{(r,s,t)}$ for some $x_{(r,s,t)} \in F$ and $x_{(\alpha,\beta,\gamma)} \in V \subseteq V_{(r,s,t)}$. This implies that $x_{(\alpha,\beta,\gamma)} \in U_{x_{(r,s,t)}} \cap V_{x_{(r,s,t)}}$, which is a contradiction to $U_{x_{(r,s,t)}} \cap V_{x_{(r,s,t)}} = \phi$. Thus U and V are disjoint N_{eu} −open sets containing A and B respectively. Conversely, suppose every pair consisting of a N_{eu} −compact set and a disjoint $N_{eu}\lambda$ −closed set can be separated by N_{eu} −open sets. Let F be a $N_{eu}\lambda$ −closed set and $x_{(\alpha,\beta,\gamma)} \notin F$. Then $\left\{x_{(\alpha,\beta,\gamma)}\right\}$ is N_{eu} −compact set of X and $\left\{x_{(\alpha,\beta,\gamma)}\right\} \cap F = 0_N$. By our assumption, there exist disjoint N_{eu} −open sets U and V such that $x_{(\alpha,\beta,\gamma)} \in U$ and $F \subseteq V$. This proves that X is strongly $N_{eu}\lambda$ −Regular.

Corollary 5.17. If X is a strongly $N_{eu}\lambda-$Regular space, A is a $N_{eu}-$compact subset of X and B is a $N_{eu}\lambda-$open set containing A, then there exists a $N_{eu}-$regular open set V such that $A \subseteq V \subseteq N_{eu}-Cl(V) \subseteq B$.

Proof. Let X be strongly $N_{eu}\lambda-$Regular and let A be a $N_{eu}-$compact set, and B be $N_{eu}\lambda-$open set with $A \subseteq B$. Then B^C is $N_{eu}\lambda-$closed set such that $B^C \cap A = 0_N$. Since X is a strongly $N_{eu}\lambda-$Regular space, then there exist disjoint $N_{eu}-$open sets G and H such that $A \subseteq G$ and $B^C \subseteq H$. Take $V = N_{eu}-Int\left[N_{eu}-Cl(G)\right]$. Then $N_{eu}-Cl(V) = N_{eu}-Cl\left[N_{eu}-Int\left(N_{eu}-Cl(G)\right)\right] \subseteq N_{eu}-Cl\left[N_{eu}-Cl(G)\right] = N_{eu}-Cl(G)$. Since G is a $N_{eu}-$open set and $G \subseteq N_{eu}-Cl(G)$, we have $G = N_{eu}-Int(G) \subseteq N_{eu}-Int\left[N_{eu}-Cl(G)\right] = V$. This implies that $N_{eu}-Cl(G) \subseteq N_{eu}-Cl(V)$. It follows that $N_{eu}-Cl(V) = N_{eu}-Cl(G)$ and $N_{eu}-Int\left[N_{eu}-_{eu}Cl(V)\right] = N_{eu}-Int\left[N_{eu}-Cl(G)\right] = V$. Thus V is $N_{eu}-$regular open. Now $A \subseteq G = N_{eu}-Int(G) \subseteq N_{eu}-Int\left[\left(N_{eu}-Cl(G)\right)\right] = V$. This implies that $A \subseteq V$ and $N_{eu}-Cl(V) = N_{eu}-Cl(G) \subseteq H^C \subseteq B$ implies that $A \subseteq V \subseteq N_{eu}-Cl(V) \subseteq B$.

Theorem 5.18. Let $f:(X,\tau_N) \to (Y,\sigma_N)$ be a bijective function. If f is $N_{eu}\lambda-$irresolute, $N_{eu}-$open and X is strongly $N_{eu}\lambda-$Regular, then Y is strongly $N_{eu}\lambda-$Regular.

Proof. Suppose (X,τ_N) is strongly $N_{eu}\lambda-$Regular. Let S be a $N_{eu}\lambda-$closed set in Y such that $y_{(r,t,s)} \notin S$. Since f is $N_{eu}\lambda-$irresolute, $f^{-1}(S)$ is $N_{eu}\lambda-$closed set in X. Since f is onto, there exists $x_{(\alpha,\beta,\gamma)} \in X$ such that $y_{(r,t,s)} = f\left(x_{(\alpha,\beta,\gamma)}\right)$. Now $f\left(x_{(\alpha,\beta,\gamma)}\right) = y_{(r,t,s)} \notin S$ implies that $x_{(\alpha,\beta,\gamma)} \notin f^{-1}(S)$. Since X is strongly $N_{eu}\lambda-$Regular. there exist $N_{eu}-$open sets U and V in X such that $x_{(\alpha,\beta,\gamma)} \in U$, $f^{-1}(S) \subseteq V$ and $U \cap V = 0_N$. Now $x_{(\alpha,\beta,\gamma)} \in U$ implies that $f\left(x_{(\alpha,\beta,\gamma)}\right) \in f(U)$ and $f^{-1}(S) \subseteq V$ implies that $S \subseteq f(V)$. Also $U \cap V = 0_N$ implies that $f(U \cap V) = 0_N$ which implies that $f(U) \cap f(V) = 0_N$. Since f is a $N_{eu}-$open mapping, $f(U)$ and $f(V)$ are disjoint $N_{eu}-$open sets in Y containing $y_{(r,t,s)}$ and S respectively. Thus Y is strongly $N_{eu}\lambda-$Regular.

6 Neutrosophic λ –Normal Spaces

In this section, we introduce $N_{eu}\lambda-$Normal and strongly $N_{eu}\lambda-$Normal spaces and study their properties and characteristics.

Definition 6.1. A $N_{eu}-$Top$-$Space (X,T_N) is said to be $N_{eu}\lambda-$Normal if for any two disjoint $N_{eu}\lambda-$closed sets A and B, there exist disjoint $N_{eu}\lambda-$open sets U and V such that $A \subseteq U$ and $B \subseteq V$.

Theorem 6.2. Let (X,T_N) be a $N_{eu}-$Top$-$Space. Then the following statements are equivalent:

(a) X is $N_{eu}\lambda-$Normal.

(b) For every $N_{eu}\lambda-$closed set A in X and every $N_{eu}\lambda-$open set U containing A, there exists a $N_{eu}\lambda-$open set V containing A such that $N_{eu}\lambda-Cl(V) \subseteq U$.

(c) For each pair of disjoint $N_{eu}\lambda$-closed sets A and B in X, there exists a $N_{eu}\lambda$-open set U containing A such that $N_{eu}\lambda\text{-}Cl(U)\cap B = 0_N$.
(d) For each pair of disjoint $N_{eu}\lambda$-closed sets A and B in X, there exist $N_{eu}\lambda$-open sets U and V containing A and B respectively such that $N_{eu}\lambda\text{-}Cl(U)\cap N_{eu}\lambda\text{-}Cl(V) = 0_N$.

Proof. $(a)\Rightarrow(b)$: Let U be a $N_{eu}\lambda$-open set containing the $N_{eu}\lambda$-closed set A. Then $B = U^C$ is a $N_{eu}\lambda$-closed set disjoint from A. Since X is $N_{eu}\lambda$-Normal, there exist disjoint $N_{eu}\lambda$-open sets V and W containing A and B respectively. Then $N_{eu}\lambda\text{-}Cl(V)$ is disjoint from B. Since if $y_{(r,t,s)} \in B$, the set W is a $N_{eu}\lambda$-open set containing $y_{(r,t,s)} \in B$ disjoint from V. Hence $N_{eu}\lambda\text{-}Cl(V) \subseteq U$.
$(b)\Rightarrow(c)$: Let A and B be disjoint $N_{eu}\lambda$-closed sets in X. Then B^C is a $N_{eu}\lambda$-open set containing A. By (b), there exists a $N_{eu}\lambda$-open set U containing A such that $N_{eu}\lambda\text{-}Cl(U) \subseteq B^C$. Hence $N_{eu}\lambda\text{-}Cl(U)\cap B = 0_N$. This proves (c).
$(c)\Rightarrow(d)$: Let A and B be disjoint $N_{eu}\lambda$-closed sets in X. Then by (c), there exists a $N_{eu}\lambda$-open set U containing A such that $N_{eu}\lambda\text{-}Cl(U)\cap B = 0_N$. Since $N_{eu}\lambda\text{-}Cl(U)$ is $N_{eu}\lambda$-closed, B and $N_{eu}\lambda\text{-}Cl(U)$ are disjoint $N_{eu}\lambda$-closed sets in X. Again by (c), there exists a $N_{eu}\lambda$-open set V containing B such that $N_{eu}\lambda\text{-}Cl(U)\cap N_{eu}\lambda\text{-}Cl(V) = 0_N$. This proves (d).
$(d)\Rightarrow(a)$: Let A and B be disjoint $N_{eu}\lambda$-closed sets in X. By (d), there exist $N_{eu}\lambda$-open sets U and V containing A and B respectively such that $N_{eu}\lambda\text{-}Cl(U)\cap N_{eu}\lambda\text{-}Cl(V) = 0_N$. Since $U\cap V \subseteq N_{eu}\lambda\text{-}Cl(U)\cap N_{eu}\lambda\text{-}Cl(V)$, U and V are disjoint $N_{eu}\lambda$-open sets containing A and B respectively. Hence the result of (a) follows.

Theorem 6.3. A N_{eu}-Top-Space (X, T_N) is $N_{eu}\lambda$-Normal if and only if for every $N_{eu}\lambda$-closed set F and $N_{eu}\lambda$-open set W containing F, there exists a $N_{eu}\lambda$-open set U such that $F \subseteq U \subseteq N_{eu}\lambda\text{-}Cl(U) \subseteq W$.

Proof. Let (X, T_N) be $N_{eu}\lambda$-Normal. Let F be a $N_{eu}\lambda$-closed set and let W be a $N_{eu}\lambda$-open set containing F. Then F and W^C are disjoint $N_{eu}\lambda$-closed sets. Since X is $N_{eu}\lambda$-Normal, there exist disjoint $N_{eu}\lambda$-open sets U and V such that $F \subseteq U$ and $W^C \subseteq V$. Thus $F \subseteq U \subseteq V^C \subseteq W$. Since V^C is $N_{eu}\lambda$-closed, so $N_{eu}\lambda\text{-}Cl(U) \subseteq N_{eu}\lambda\text{-}Cl(V^C) = V^C \subseteq W$. Thus $F \subseteq U \subseteq N_{eu}\lambda\text{-}Cl(U) \subseteq W$.
Conversely, suppose the condition holds. Let G and H be two disjoint $N_{eu}\lambda$-closed sets in X. Then H^C is a $N_{eu}\lambda$-open set containing G. By assumption, there exists a $N_{eu}\lambda$-open set U such that $G \subseteq U \subseteq N_{eu}\lambda\text{-}Cl(U) \subseteq H^C$. Since U is $N_{eu}\lambda$-open and $N_{eu}\lambda\text{-}Cl(U)$ is $N_{eu}\lambda$-closed. Then $(N_{eu}\lambda\text{-}Cl(U))^C$ is $N_{eu}\lambda$-open. Now $N_{eu}\lambda\text{-}Cl(U) \subseteq H^C$ implies that $H \subseteq (N_{eu}\lambda\text{-}Cl(U))^C$. Also $U\cap(N_{eu}\lambda\text{-}Cl(U))^C \subseteq N_{eu}\lambda\text{-}Cl(U)\cap(N_{eu}\lambda\text{-}Cl(U))^C = 0_N$. That is U and $(N_{eu}\lambda\text{-}Cl(U))^C$ are disjoint $N_{eu}\lambda$-open sets containing G and H respectively. This shows that (X, T_N) is $N_{eu}\lambda$-Normal.

Theorem 6.4. Let (X, T_N) be a N_{eu}-Top-Space. Then the following statements are equivalent:
(a) X is $N_{eu}\lambda$-Normal.

(b) For any two $N_{eu}\lambda$-open sets U and V whose union is 1_N, there exist $N_{eu}\lambda$-closed subsets A of U and B of V such that $A \bigcup B = 1_N$.

Proof. $(a) \Rightarrow (b)$: Let U and V be two $N_{eu}\lambda$-open sets in a $N_{eu}\lambda$-Normal space X such that $U \bigcup V = 1_N$. Then U^C and V^C are disjoint $N_{eu}\lambda$-closed sets. Since X is $N_{eu}\lambda$-Normal, then there exist disjoint $N_{eu}\lambda$-open sets G and H such that $U^C \subseteq G$ and $V^C \subseteq H$. Let $A = G^C$ and $B = H^C$. Then A and B are $N_{eu}\lambda$-closed subsets of U and V respectively such that $A \bigcup B = 1_N$. This proves (b).
$(b) \Rightarrow (a)$: Let A and B be disjoint $N_{eu}\lambda$-closed sets in X. Then A^C and B^C are $N_{eu}\lambda$-open sets whose union is 1_N. By (b), there exist $N_{eu}\lambda$-closed sets E and F such that $E \subseteq A^C$, $F \subseteq B^C$ and $E \bigcup F = 1_N$. Then E^C and F^C are disjoint $N_{eu}\lambda$-open sets containing A and B respectively. Therefore X is $N_{eu}\lambda$-Normal.

Definition 6.5. A N_{eu}-Top-Space (X, T_N) is said to be strongly $N_{eu}\lambda$-Normal if for every pair of disjoint N_{eu}-closed sets A and B in X, there are disjoint $N_{eu}\lambda$-open sets U and V in X containing A and B respectively.

Theorem 6.6. Every $N_{eu}\lambda$-Normal space is strongly $N_{eu}\lambda$-Normal.

Proof. Suppose X is $N_{eu}\lambda$-Normal. Let A and B be disjoint N_{eu}-closed sets in X. Then A and B are $N_{eu}\lambda$-closed in X. Since X is $N_{eu}\lambda$-Normal, there exist disjoint N_{eu}-open sets U and V containing A and B respectively. Since every N_{eu}-open set is $N_{eu}\lambda$-open set. Therefore U and V are $N_{eu}\lambda$-open sets in X. This implies that X is strongly $N_{eu}\lambda$-Normal.

Theorem 6.7. Let (X, T_N) be a N_{eu}-Top-Space. Then the following statements are equivalent:
(a) X is strongly $N_{eu}\lambda$-Normal.
(b) For every N_{eu}-closed set F in X and every N_{eu}-open set U containing F, there exists a $N_{eu}\lambda$-open set V containing F such that $N_{eu}\lambda\text{-}Cl(V) \subseteq U$.
(c) For each pair of disjoint N_{eu}-closed sets A and B in X, there exists a $N_{eu}\lambda$-open set U containing A such that $N_{eu}\lambda\text{-}Cl(U) \bigcap B = 0_N$.

Proof. $(a) \Rightarrow (b)$: Let U be a N_{eu}-open set containing N_{eu}-closed set F. Then $H = U^C$ is a N_{eu}-closed set disjoint from F. Since X is strongly $N_{eu}\lambda$-Normal, there exist disjoint $N_{eu}\lambda$-open sets V and W containing F and H respectively. Then $N_{eu}\lambda\text{-}Cl(V)$ is disjoint from H, since if $y_{(r,t,s)} \in H$, the set W is a $N_{eu}\lambda$-open set containing $y_{(r,t,s)}$ disjoint from V. Hence $N_{eu}\lambda\text{-}Cl(V) \subseteq U$.
$(b) \Rightarrow (c)$: Let A and B be disjoint N_{eu}-closed sets in X. Then B^C is a N_{eu}-open set containing A. By (b), there exists a $N_{eu}\lambda$-open set U containing A such that $N_{eu}\lambda\text{-}Cl(U) \subseteq B^C$. Hence $N_{eu}\lambda\text{-}Cl(U) \bigcap B = 0_N$. This proves (c).
$(c) \Rightarrow (a)$: Let A and B be disjoint $N_{eu}\lambda$-closed sets in X. By (c), there exists a $N_{eu}\lambda$-open set U containing A such that $N_{eu}\lambda\text{-}Cl(U) \bigcap B = 0_N$. Take $V = \left(N_{eu}\lambda\text{-}Cl(U)\right)^C$. Then U and V are disjoint $N_{eu}\lambda$-open sets containing A and B respectively. Thus X is strongly $N_{eu}\lambda$-Normal.

Theorem 6.8. Let (X, T_N) be a N_{eu} −Top −Space. Then the following statements are equivalent:
(a) X is strongly $N_{eu}\lambda$ −Normal.
(b) For any two N_{eu} −open sets U and V whose union is 1_N, there exist $N_{eu}\lambda$ −closed subsets A of U and B of V such that $A \bigcup B = 1_N$.

Proof. (a)$\Rightarrow$(b): Let U and V be two N_{eu} −open sets in a strongly $N_{eu}\lambda$ −Normal space X such that $U \bigcup V = 1_N$. Then U^C and V^C are disjoint N_{eu} −closed sets. Since X is strongly $N_{eu}\lambda$ −Normal, then there exist disjoint $N_{eu}\lambda$ −open sets G and H such that $U^C \subseteq G$ and $V^C \subseteq H$. Let $A = G^C$ and $B = H^C$. Then A and B are $N_{eu}\lambda$ −closed subsets of U and V respectively such that $A \bigcup B = 1_N$.
(b)$\Rightarrow$(a): Let A and B be disjoint N_{eu} −closed sets in X. Then A^C and B^C are N_{eu} −open sets such that $A^C \bigcup B^C = 1_N$. By (b), there exist $N_{eu}\lambda$ −closed sets G and H such that $G \subseteq A^C$, $H \subseteq B^C$ and $G \bigcup H = 1_N$. Then G^C and H^C are disjoint $N_{eu}\lambda$ −open sets containing A and B respectively. Therefore, X is strongly $N_{eu}\lambda$ −Normal.

Conclusion

We have introduced the idea of new types of neutrosophic compactness, neutrosophic connectedness, neutrosophic regular spaces, and neutrosophic normal spaces defined in terms of neutrosophic λ-open sets and neutrosophic λ-closed sets in a neutrosophic topological space (X, T_N) namely, $N_{eu}\lambda$ −compact spaces, $N_{eu}\lambda$ −Lindelof spaces, countably $N_{eu}\lambda$ −compact spaces, $N_{eu}\lambda$ −connected spaces, $N_{eu}\lambda$ −separated sets, N_{eu} −Super−λ −connected spaces, N_{eu} −Extremely−λ −disconnected spaces, and N_{eu} −Strongly−λ −connected spaces, $N_{eu}\lambda$ −Regular spaces, strongly $N_{eu}\lambda$ −Regular spaces, $N_{eu}\lambda$ −Normal spaces, and strongly $N_{eu}\lambda$ −Normal spaces.

Also, several of their topological properties are investigated. Finally, some effects of various kinds of neutrosophic functions on them are studied. and have established several interesting properties. Because there exist compact connections between neutrosophic sets and information systems, we can use the results deduced from the studies on neutrosophic topological spaces to improve these kinds of connections. We see that this paper will help researchers enhance and promote further study on neutrosophic topology to carry out a general framework for their applications in practical life.

Scientific Ethics Declaration

* The author declares that the scientific ethical and legal responsibility of this article published in EPSTEM journal belongs to the author.

Conflict of Interest

* The author declares that he has no conflicts of interest.

Funding

* This research received no specific grant from any funding agency in the public, commercial, or not-for-profit sectors.
.

Acknowledgements or Notes

* This article was presented as an oral presentation at the International Conference on Research in Engineering, Technology and Science (www.icrets.net) held in Peja/Kosovo on July 10-13, 2025.

* The author is highly and gratefully indebted to Prince Mohammad Bin Fahd University Al Khobar Saudi Arabia, for providing excellent research facilities during the preparation of this research paper.

References

Acikegoz, A., & Esenbel, F. (2020). An approach to pre-separation axioms in neutrosophic soft topological spaces. *Communications Faculty of Sciences University of Ankara Series A1 Mathematics and Statistics, 69*(2), 1389–1404.

Al-Nafee, A. B., Al-Hamido, R. K., & Smarandache, F. (2019). Separation axioms in neutrosophic crisp topological spaces. *Neutrosophic Sets and Systems, 25*, 25–32.

Al-Shami, T. M., Mhemdi, A., Rawshdeh, A. A., & Al-Jarrah, H. H. (2021). Soft version of compact and Lindelöf spaces using soft somewhere dense sets. *AIMS Mathematics, 6*(8), 8064–8077.

Amarendra, B. V., & Aswini, J. (2021). Separation axioms in supra-neutrosophic crisp topological spaces. *Advances and Applications in Mathematical Sciences, 20*(6), 1115–1128.

Bageerathi, K., & Puvaneswari, P. J. (2019). Neutrosophic feebly connectedness and compactness. *IOSR Journal of Polymer and Textile Engineering (IOSR-JPTE), 6*(3), 07–13.

Benchalli, S. S., Patil, P. G., & Dodamani, A. S. (2017). Some properties of soft β-compact and related soft topological spaces. *Italian Journal of Pure and Applied Mathematics, 38*, 487–496.

Dhavaseelan, R., & Jafari, S. (2017). Generalized neutrosophic closed sets. *New Trends in Neutrosophic Theory and Applications, 2*, 261–273.

Evanzalin, E. P., Jude, I. H., & Bazil, W. C. (2018). On neutrosophic b-open sets in neutrosophic topological space. *International Conference on Applied and Computational Mathematics, IOP Conference Series: Journal of Physics*, 1–5.

Imran, H. Q., Smarandache, F., Al-Hamido, R. K., & Dhavaseelan, R. (2017). On neutrosophic semi alpha open sets. *Neutrosophic Sets and Systems, 18*, 37–42.

Jeevitha, R., Parimala, M., & Udhaya Kumar, R. (2019). Nano Aψ-connectedness and compactness in nano topological spaces. *International Journal of Research Technology and Engineering, 8*(2).

Krishnaprakash, S., Ramesh, R., & Suresh, R. (2018). Nano-compactness in nano topological space. *International Journal of Pure and Applied Mathematics, 119*(13), 107–115.

Krshnaprakashi, K., & Chandrasekar, S. (2020). Neutrosophic bg-closed sets and its continuity. *Neutrosophic Sets and Systems, 36*, 108–120.

Maheshwari, B. C., & Chandrasekar, S. (2019). Neutrosophic gb-closed sets and neutrosophic gb-continuity. *Neutrosophic Sets and Systems, 29*, 89–100.

Mary, M. A., & Trinita, P. M. (2018). Neutrosophic vague generalized pre-connectedness in neutrosophic vague topological space. *International Journal of Mathematics Trends and Technology (IJMTT), 58*(2), 85–93.

Mehmood, A., Nadeem, F., Nordo, G., Zamir, M., Park, C., Kalsoom, H., Jabeen, S., & Khan, M. I. (2020). Generalized neutrosophic separation axioms in neutrosophic soft topological spaces. *Neutrosophic Sets and Systems, 32*, 38–51.

Molodtsov, D. A. (1999). Soft set theory—first results. *Computers & Mathematics with Applications, 37*, 19–31.

Rodrigo, P. A., & Maheswari, S. (2021). Neutrosophic generalized semi alpha atar closed sets in neutrosophic topological spaces. *Journal of Human University (Natural Sciences), 48*(11), 1156–1175.

Salama, A. A., & Alblowi, S. A. (2012). Neutrosophic sets and neutrosophic topological spaces. *IOSR Journal of Mathematics, 3*(4), 31–35.

Salama, A. A., Smarandache, F., & Kromov, V. (2014). Neutrosophic closed set and neutrosophic continuous functions. *Neutrosophic Sets and Systems, 4*, 4–8.

Smarandache, F. (2002). Neutrosophy and neutrosophic logic. *First International Conference on Neutrosophy, Neutrosophic Logic, Set, Probability, and Statistics*, University of New Mexico, Gallup, NM 87301, USA.

Turnali, N., & Coker, D. (2000). Fuzzy connectedness in intuitionistic fuzzy topological spaces. *Fuzzy Sets and Systems, 116*, 369–375.

Tyagi, S., & Gupta, M. K. (2025). Neutrosophic λ-closed set and related mappings in neutrosophic topological spaces. *Neutrosophic Sets and Systems, 82*, 911–923.

Zadeh, L. A. (1965). Fuzzy sets. *Information and Control, 8*, 338–353.

Author(s) Information

Raja Mohammad Latif
Department of Mathematics and Natural Sciences
Prince Mohammad Bin Fahd University
Al Khobar, Kingdom of Saudi Arabia
Contact e-mail: *rlatif@pmu.edu.sa*

To cite this article:
Latif, M. R. (2025). Neutrosophic λ-compactness, λ-connectedness, and λ-separation axioms in neutrosophic topological spaces. *The Eurasia Proceedings of Science, Technology, Engineering and Mathematics (EPSTEM), 35,* 323-345.